



*B.V. Korvin Kroukovsky's*

# HYDRODYNAMIC DESIGN OF SEAPLANES

## GRADUATE SCHOOL COURSE NOTES

Third Edition, 2024  
Michael G. Morabito, Editor  
United States Naval Academy

*Davidson Laboratory  
Stevens Institute of Technology  
Hoboken, New Jersey*





## TABLE OF CONTENTS

### PART 1: HYDRODYNAMICS

1. General Description and Terminology
2. Buoyancy and Static Stability
3. Planing and Resistance
4. Towing Tests and Take-off
5. Dynamic Stability - Porpoising and Skipping
6. Directional Stability and Control
7. Spray
8. Impact

### PART 2: DESIGN

9. Full Scale Trials
10. Early-Stage Sizing
11. Hull Standard Series
12. Lines Design
13. Tip Floats
14. High L/B Prediction Method
15. Weights

### PART 3: FURTHER STUDY

16. Stability Theory

### APPENDICES

APPENDIX 1. Seaplane Operations Manual - FAA

APPENDIX 2. Seaplane Design Regulations - CFR Title 14

### STANDARD SERIES CHARTS

- 1947 - Strumpf - Martin Mars Series
- 1947 - Hugli - Consolidated Coronado Series
- 1947 - Locke - Misc. Flying Boats (Editor Selected a Few)
- 1951 - Hugli - Small Flying Boats and Amphibians Series
- 1952 - Haar - High L/B Series

## INTRODUCTION

M.G. Morabito, 2024

### 1. Davidson Laboratory

These course notes have been formed using text and materials developed primarily at Stevens Institute of Technology over a span of approximately 90 years. The "Experimental Towing Tank" (Later known as Davidson Laboratory) was started in the mid-1930s by Professor Kenneth S.M. Davidson. Davidson pioneered the use of small model testing by applying turbulence stimulation to scale models. He performed towing tank tests on the 1936 America's Cup J-Boat Ranger, and sailed on the boat as navigator to defend the cup. Having flown for the U.S. during World War I, he applied the aerodynamic principles of lift and drag to sailing yacht design, and to steering of ships. He wrote the Resistance section for the first edition of Principles of Naval Architecture in 1939. The Society of Naval Architects and Marine Engineers continues to award the "Davidson Medal" for technical achievement.

With the urgency of World War II, Davidson directed the research efforts toward the problem of hydrodynamic development of seaplanes. Working with the National Advisory Committee for Aeronautics, the Navy's Bureau of Aeronautics, and prominent engineers from the aviation industry, Davidson and his team tested hundreds of seaplane models. They developed methods for investigating dynamic instabilities, take-off resistance, spray and impact loads. This research continued at a steady pace into the early 1960s.

Today, the High-Speed Towing Tank at Stevens Institute of Technology is used for many different purposes, but the Davidson Laboratory still remains a center of excellence for seaplane model testing.

### 2. Seaplane Notes

These notes are comprised of three parts; Hydrodynamics, Design and Further Study. Wherever possible, original text from a variety of authors at Davidson Lab has been used. Where applicable, the author and

approximate year for various sections are listed. The editor takes responsibility for any errors, omissions, or misinterpretations, as much of this material was originally produced decades ago and the original authors are no longer with us. In some cases, it was necessary to edit material for length, content, style, or recent technological developments.

"Part 1 - Hydrodynamics" comprises 8 chapters of notes primarily written by Boris V. Korvin-Kroukovsky, for the first of a two-semester graduate course in hydrodynamic design of seaplanes, offered by Stevens Institute of Technology in the late 1940s and 1950s. These notes have stood up to multiple generations of academic and industry scrutiny, and prepare a firm foundation for study. Where necessary, supplementary material was substituted. For historical interest, the original notes can be made available by contacting Davidson Lab.

"Part 2 - Design" includes chapters or subsections written by a variety of authors. This material was included to address the types of questions that were coming from industry. The decision for what to include in this section was made on the basis of its usefulness and its rarity in the public domain.

"Part 3 - Further Study," comprises material of a very technical nature that does not necessarily belong with the first two parts. In addition to the notes, design charts from the original Stevens Institute Standard Series are included.

### 3. Previous Editions

1<sup>st</sup> Edition. The first edition of these notes was written in the 1948-1950 time frame. The course was offered in close cooperation with the U.S. Navy, and some Naval Officers attended Stevens for graduate school and specialized in seaplanes. In the early 1960s, the Hydrodynamic Design of Seaplanes course was evolved into the Hydrodynamic Design of Planing Hulls course by Dr. Daniel Savitsky. This course is still offered at Stevens, by Dr. Raju Datla.

2<sup>nd</sup> Edition. The second edition was prepared in 2011 in support of a combined undergraduate / graduate course on Seaplane Design at Stevens. Daniel Savitsky, who had taught the course half a century earlier, offered guidance on which material was relevant. A variety of

modern predictive methods, especially for spray, bottom pressures, and computerized analysis were included. The undergraduate students completed design projects, and the graduate students each had a small research project, either analytical or doing towing tank tests.

3<sup>rd</sup> Edition. This was prepared in 2024, for midshipmen at the U.S. Naval Academy. In the intervening years since the second edition, we were able to see which portions of the notes were the most useful. Some of the 2011 material did not get much use and was omitted. Additional questions from industry were addressed in the section on design. At this time, we had a better understanding of the standard series, and efforts were taken to carefully scan and present them.

### 3. About the Authors

Boris V. Korvin-Kroukovsky was a pilot in the Russian Air Force during World War I, taught as a professor of Aerodynamics at the Russian Military Aviation School, and then emigrated to the United States in 1918. From 1925 through the end of World War II, he served as the chief engineer of EDO Aircraft Corporation, a leading manufacturer of seaplane floats. After taking a position at Stevens Institute, he led fundamental research on planing craft, and then later developed the linear strip theory of seakeeping.

Dr. Daniel Savitsky joined the staff at the Davidson Laboratory in 1947, after working at EDO Aircraft Corporation and the N.A.C.A. impact basin during World War II. He began his Master's at the same time and earned a degree in fluid mechanics and naval architecture, advised by Korvin-Kroukovsky. During the late 1950s he took over teaching the Seaplane Design course. In 1964, he wrote the paper Hydrodynamic Design of Planing Hulls, in which much of the methodology previously developed for seaplanes was adapted to create a performance prediction of planing craft. In 1984 he became director of the Davidson Laboratory. In 1989 he retired, but actively continued research as professor emeritus. His last published paper was on planing boat accelerations, at the age of 94. He passed away at age 98 in 2020. Dr. Savitsky has contributed to sections on design

characteristics of seaplanes, as well as the comprehensive prediction method for high length-to-beam ratio seaplanes.

Dr. Michael Morabito is a former research engineer at Davidson Lab. He is currently the Director of the Naval Architecture and Marine Engineering Program at the United States Naval Academy in Annapolis, MD.

Wilfred C. Hugli, Jr. worked at Stevens during the 1940s and into the mid 1950s. He was responsible for much of the development for the seaplane standard series. During World War II, he met his wife, Cynthia, who an employee at the towing tank. Hugli's reports on the development of the hull designs for the standard series are the primary source for the chapter on Lines Design.

Bob Van Dyck worked at Davidson Laboratory from the early 1950s to the late 1980s. Early projects included the development of seakeeping test methodologies for seaplanes, including a servo-controlled towing carriage for constant force towing. He contributed significantly to the development of Surface Effect Ships, hydrofoil craft and amphibious vehicles. Van Dyck's reports on the tip float standard series provide the primary reference for the chapter on float design.

Kenneth E. Ward worked at the National Advisory Committee for Aeronautics during the 1930s, and performed early seaplane model tests in the N.A.C.A. towing tank. In the early 1940s, he worked at Consolidated Aircraft Corp. Ward wrote the dynamic stability chapter as a guest lecture for a 1943 course in seaplane design, offered by Ernest G. Stout, of Consolidated. This was one of a series of courses offered by the University of California system to support engineering for the war effort. Stout provided industry guidance for the seaplane research efforts and standard series tested at Stevens during and after the war.

F.W.S. Locke, Jr. earned his masters of engineering at Stevens Institute. He joined the Naval Bureau of Aeronautics during World War II, where he became assistant director of the Research Division. He

later became the Assistant Director of Advanced Systems Division of the Bureau of Naval Weapons and served as the Head of the Aircraft Branch of the Advanced Concepts Division, Naval Air Systems Command. Locke had a profound influence on seaplane research in the United States. Many of the graphs in these notes were developed by Locke.

## General Description and Terminology

### CHAPTER 1 GENERAL DESCRIPTION AND TERMINOLOGY

B.V. Korvin-Kroukovsky, 1948

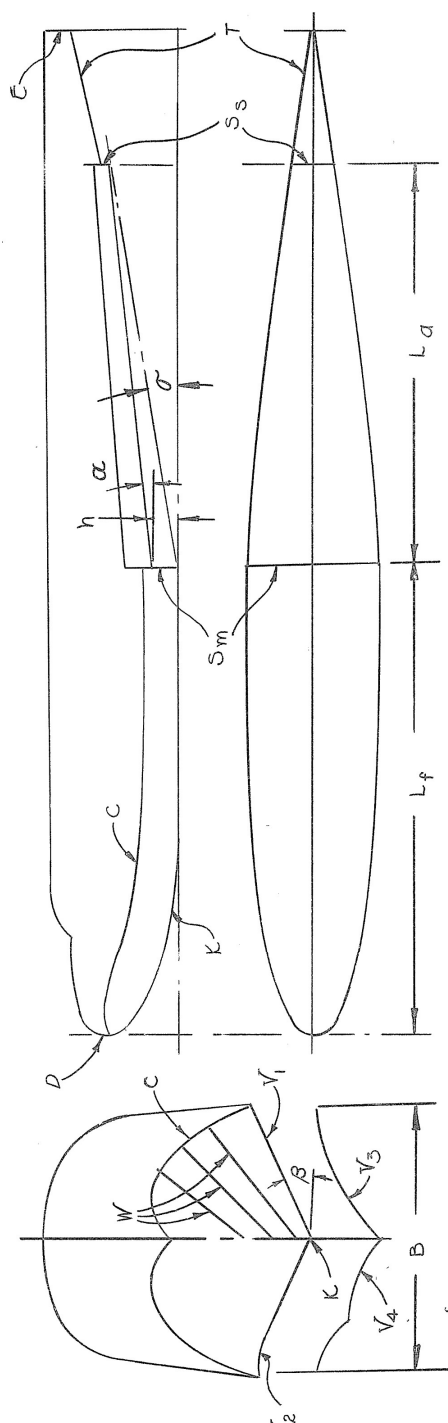
The term "Seaplane" defines any type of an airplane capable of resting on, taking off from, and alighting on the surface of water. In the "float seaplane" this ability is obtained by the use of floats, the sole function of which is to provide the flotation and the planing area. In the "flying boat" the body provides the flotation and the planing areas and is used also as an integral part of the air frame, supporting the wings and the tail surfaces, and as a housing for the crew, the equipment, and the useful load. The "amphibian" is a flying boat or a float seaplane equipped with wheels in addition to the flotation and planing body, making it capable of alighting on either land or water (Figure 1.1). Most of the material in this book will apply equally to all types of seaplane, and only occasionally it will be necessary to discuss the features specific to a float seaplane, or to a flying boat. The term "planing" signifies the motion on the water surface with such a speed, and in such an attitude, that the weight of the aircraft is supported primarily by dynamic pressures, rather than by buoyant forces. The "planing area" or "planing bottom" is that part of the hull surface which is shaped so as to permit such a motion with the minimum of drag, and which has sufficient structural strength to withstand the forces involved. The conventional form of the hull with such a planing bottom is shown on Fig 1.2, with letters designating each of the elements.



## General Description and Terminology



Figure 1.1: Flying Boats, Floatplanes and Amphibians (Taken from FAA, 2004)



- |                |                        |                |   |
|----------------|------------------------|----------------|---|
| D              | - Bow                  | σ              | - Sternpost Angle                                     |
| E              | - Stern                | V <sub>1</sub> | - Straight Vee Bottom                                 |
| K              | - Keel                 | V <sub>2</sub> | - Vee Bottom with the Chine Flare                     |
| C              | - Chine                | V <sub>3</sub> | - Concave Vee Bottom                                  |
| S <sub>m</sub> | - Main Step            | V <sub>4</sub> | - Scalloped Vee Bottom                                |
| S <sub>s</sub> | - Second Step          | β              | - Angle of Deadrise                                   |
| T              | - Tail Cone            | W              | - Warp, i.e. the change of the deadrise β with length |
| L <sub>f</sub> | - Forebody Length      |                |   |
| L <sub>a</sub> | - Afterbody Length     |                |   |
| h              | - Main Step Height     |                |   |
| OC             | - Afterbody Keel Angle |                |   |

Figure 1.2: The Elements of the Hull of Float Lines - Straight Steps.

## General Description and Terminology

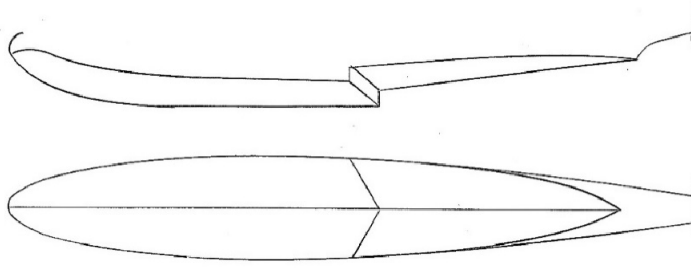


Figure 1.3: Vee Main Step and Pointed Second Step.

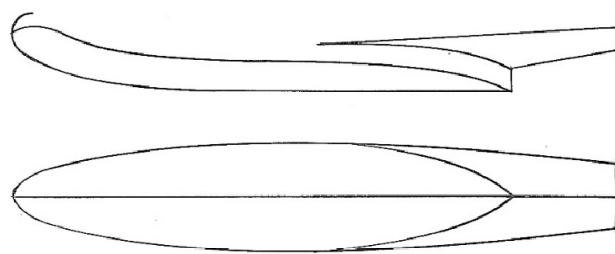


Figure 1.4: Pointed Main Step

Figure 1.2 showed the hull with transverse steps. Figure 1.3 shows the Vee main step, and the pointed second step. Figure 1.4 shows the pointed main step. The variety of the pointed main step hull in which the height, the step is large and the afterbody is long, so that the stern E serves as a second step Ss is called the "planing-tail hull".

While the hull is designed to be as perfect a streamline body as possible, certain deviations and sacrifices are necessary to insure satisfactory water planing action. The water in motion clings to, and exerts suction on any convex surface which comes in contact with it. This is the most important fact which the seaplane designer must constantly and vividly keep in mind. It is impossible to avoid the use of convex faces at the bow, but these are in water only at low speeds, and are raised above it even at moderate speeds. The lines of the bottom

Formed by the intersection of it with the vertical planes parallel to the hull centerline plane are called the "buttock lines". Aft of approximately the midpoint of the forebody length these lines must be straight in order to avoid the harmful suction, and to permit the dynamic pressure to be generated efficiently. These lines must terminate at their aft ends in discontinuities called "steps", as any upward change of direction of the continuous line would cause the suction to be generated.

## General Description and Terminology

The drawing giving all details of the external shape of a hull or a float is called the lines drawing. Such a drawing in a somewhat, simplified form is shown on Figure 1.4 for a seaplane float. The part of the line drawing showing the front or rear elevations with the contours of all stations is known as the "body plan". The notes "1.71 buttock" and "3.43 buttock" designate the lines formed by the intersection of the planing bottom with the vertical planes spaced at a distance of 1.71 and 3.43 inches from the centerline plane of the float. In this case they are used to supply the additional information about the bottom shape only. Quite frequently they are used in the same way for the upper part of the float as well. The "table of offsets", such as Table 1.1 also forms an integral part of a line drawing. The line drawing contains only a few fundamental dimensions on the drawing itself, while all dimensions defining the contours of all stations are collected in the table of offsets.

## General Description and Terminology

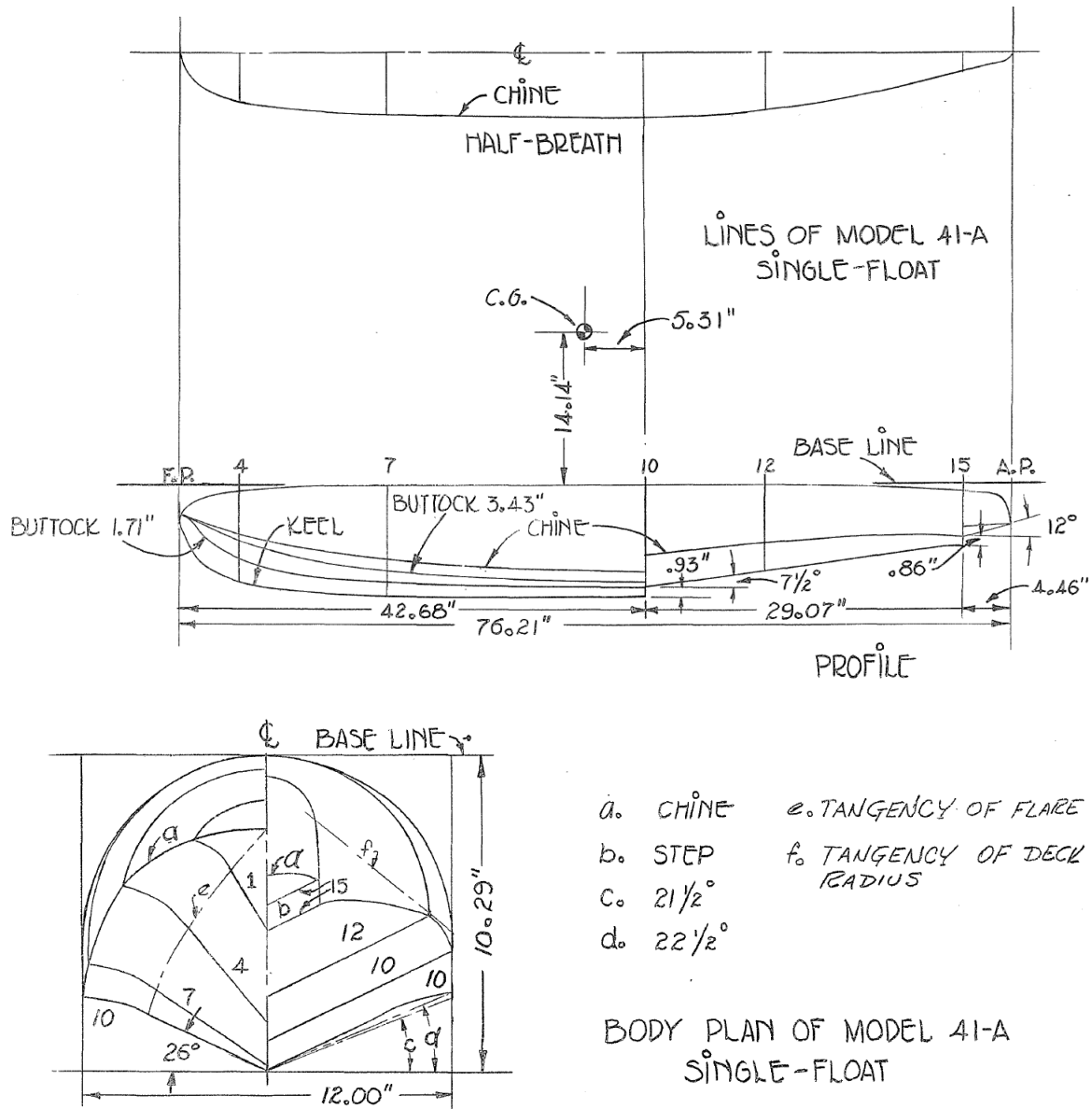


Figure 1.4: Line Drawing of NACA Model 4-A Single Float (Navy Mark V Float)

### References for Chapter 1

FAA "Seaplane, Skiplane and Float/Ski Equipped Helicopter Operations Handbook", U.S. Department of Transportation, Federal Aviation Administration, Flight Standards Service, 2004.

## Buoyancy and Static Stability

### CHAPTER 2. BUOYANCY AND STATIC STABILITY

B.V. Korvin-Kroukovsky, 1948

2.1 Submerged Displacement, Normal Flotation and the Center of Buoyancy

2.2 Static Stability Metacentric Height Application to Twin-Float Seaplanes

2.3 Lateral Stability of Flying Boats and of Single Float Seaplanes

#### 2.1 Submerged Displacement, Normal Flotation and the Center of Buoyancy

Seaplane floats are built as entirely watertight structures, with exception of the small air vent holes, usually incorporated in the handhole covers. The float will retain therefore its buoyancy even when completely submerged, and this buoyancy is called the "Submerged Displacement". The excess of the submerged displacement over the normal flotation, expressed in per cent of the latter, is called the "Reserve Buoyancy" and represents the most common measure of the adequacy of the float for the airplane it has to support. For instance, if the float completely submerged has the buoyancy of 3800 pounds, and in normal flotation has to support the load of 2000 pounds, the reserve buoyancy is

$$100 \frac{3800 - 2000}{2000} = 90\%$$

As a common and good practice in float design the reserve buoyancy of 100% is recommended, i.e. the submerged displacement is made equal to twice the normal displacement. 90% is the minimum permitted by the Civil Aeronautics Administration\*\*\* as, low as 65% and as high as 130% was used by Military Services on special occasions

In order to determine the submerged displacements, the cross-sectional areas of the float are measured at each station of the line drawing, and are plotted against the float length as shown by the curve "submerged displacement" on Figure 1. On this plot the abscissae are the distances of a given station from the bow of the float. The station numbers are also marked for the convenience of reference. It is a common practice, however, to use

## Buoyancy and Static Stability

the distance from some reference line as a station number, thus avoiding the confusion of two numbering systems. The ordinates are the sectional areas of the float stations in square inches. The area under the curve thus plotted on Figure 1 is again integrated giving the total displacement. Let A be the scale of ordinates, such for instance as 1" = 400 sq. in. and L the scale of abscissae, such as 1" = 30" of float length. The scale of the area of the diagram is then 1 sq.in. = A x L, in this case 400 x 30 = 12,000 cu.in. The total area under the curve of figure 1, as measured in square inches, is multiplied by this scale, divided by 1,728 (12 in/ft cubed) to convert into cubic feet, and multiplied by 62.4 or 64 to convert into the pounds of displacement of both fresh or salt water respectively. Thus, in the example cited in connection with Figure 1, the submerged displacement in salt water is:

$$S.D. = 35 \times 12,000 \times 64 / 1728 = 15,500 \text{ pounds.}$$

If the stations of the line drawing are spaced so that the length of the float is divided into an even number of equal spaces the volume can be obtained by Simpson's rule:

$$\text{Volume} = \frac{1}{3} \frac{L}{n} (a_1 + a_2/4 + a_3/2 + a_4/4 + \dots + a_{n-2}/2 + a_{n-1}/4 + a_n)$$

where L is the length of the float, n - the number of spaces, and a<sub>1</sub>, a<sub>2</sub> ... a<sub>n</sub> are the sectional areas of the float sections.

The preliminary estimates of the float, size can be made on the basis of the "block coefficient", i.e. the ratio of the float volume to the volume of the rectangular block, the length, width and height of which are equal to these of the float. The average value of 0.45 can be assumed for this coefficient.

Example:

A seaplane float has a length of 21 feet, a beam of 3 feet and a depth of 2 feet. The probable submerged displacement is:

$$.45 \times 2 \times 3 \times 21 = 56.7 \text{ cu. ft.}$$

or, in sea water at 64 lb./cu.ft.:

$$64 \times 56.7 = 3630 \text{ lb.}$$

## Buoyancy and Static Stability

In order to determine the "normal flotation", the estimated position of the water line is drawn on the side elevation of the float or hull, the intersection of this water line with each of the hull stations is measured, and the water line of each station is drawn on the front elevation of the line drawing, known as the "body plan". The sectional area below this line is measured for each station, and the same procedure is followed as described previously for the submerged displacement. The first estimate of the position of the waterline and of the normal flotation is facilitated by computing the draft on the basis of the block coefficient, based in this case on the length of the waterline, the maximum beam, and the draft. In this case 0.38 can be taken as the average value of the coefficient. If the normal displacement is found to be larger or smaller than the weight of the aircraft, the waterline is lowered or raised, and the procedure repeated until the displacement is exactly equal to the weight.

Next, it is necessary to check the position of the center of buoyancy, i.e. of the center of gravity of the displaced water. For this purpose, the sectional areas below the water line are multiplied by the distance from the main step, and the resultant area moments are plotted, as shown by the curves "forebody moment" and "afterbody moment" on Figure 1. The distance  $x$  from the step to the center of buoyancy is determined as:

$$x = \frac{\left( \begin{array}{c} \text{Area under the forebody} \\ \text{moment curve} \end{array} \right) - \left( \begin{array}{c} \text{Area under the afterbody} \\ \text{moment curve} \end{array} \right)}{\left( \begin{array}{c} \text{Area under the curve of the normal flotation} \end{array} \right)}$$

$x$  is taken, of course, to the scale of abscissae of Figure 1

In the example used above:

Scale of the displacement area . . . 1" = 12,000 cu.in.

Scale of the moment area . . . 1" = 20,000x30 = 600,000 in.<sup>4</sup>

$$x = \frac{600,000 (15 - 5)}{12,000 \times 17.5} = 28.6 \text{ inches.}$$

The vertical position of the center of buoyancy is seldom computed; and can be taken with sufficient accuracy to be located between 35 and 40 per cent of the draft below waterline. The line passing through the center of buoyancy and drawn normal to the waterline must pass through the center of



# Buoyancy and Static Stability

gravity of the seaplane. If it passes forward of it, it means that there is too much buoyancy in the forward part of the hull, and too little in the aft part. The assumed waterline is then tilted, so as to reduce the draft of the bow sections, and to increase the draft of the stern sections. Several trials and adjustments are usually needed. The change of the trim will affect the buoyancy, and the changes of draft, made to correct the buoyancy will affect the trim. Therefore, both sets of computations must be carried out concurrently, and the results tabulated to permit the interpolation between trials.

Table 1: Sample Table of Offsets

Taken from N.A.C.A. Technical Note No. 563

| Offsets for N.A.C.A. Model 41-A Single Float (Inches) |                               |                         |       |      |                             |                    |                             |                       |                      |
|---|-------------------------------|-------------------------|-------|------|-----------------------------|--------------------|-----------------------------|-----------------------|----------------------|
| Sta-<br>tion  | Dis-<br>tance<br>from<br>F.P. | Distance from base line |       |      | Half-breadths               |                    |                             | Radius<br>of<br>flare | Radius<br>of<br>deck |
|   |                               | Keel                    | Chine | Deck | Tan-<br>gent<br>of<br>flare | Chine              | Tan-<br>gent<br>of<br>flare |                       |                      |
| F.P.  | 0.00                          | 2.43                    | 2.43  | 2.43 |                             | Tangent<br>to F.P. |                             |                       |                      |
| 1   | 1.00                          | 5.72                    | 2.79  | 1.50 | 3.75                        | 2.46               | 1.13                        | 1.92                  | 2.96                 |
| 2   | 2.13                          | 7.06                    | 3.25  | 1.00 | 4.43                        | 3.36               | 1.72                        | 2.78                  | 3.63                 |
| 3   | 3.25                          | 7.86                    | 3.63  | .74  | 4.86                        | 3.93               | 2.06                        | 2.98                  | 4.12                 |
| 4   | 5.50                          | 8.79                    | 4.29  | .47  | 5.57                        | 4.64               | 2.57                        | 3.65                  | 4.74                 |
| 5   | 10.00                         | 9.68                    | 5.32  | .22  | 6.54                        | 5.32               | 3.15                        | 4.71                  | 5.31                 |
| 6   | 14.46                         | 10.00                   | 6.14  | .11  | 7.14                        | 5.61               | 3.43                        | 4.62                  | 5.61                 |
| 7   | 19.03                         | 10.16                   | 6.74  | .03  | 7.61                        | 5.78               | 3.61                        | 5.16                  | 5.78                 |
| 7-1/2   | 23.52                         | 10.25                   | 7.15  | .00  | 7.91                        | 5.88               | 3.73                        | 5.59                  | 5.88                 |
| 8   | 28.00                         | 10.29                   | 7.40  | ↑    | 8.13                        | 5.93               | 3.80                        | 6.02                  | 5.93                 |
| 8-1/2   | 32.50                         | ↑                       | 7.55  | ↓    | 8.27                        | 5.98               | 3.84                        | 7.29                  | 5.98                 |
| 9   | 37.00                         | ↑                       | 7.68  | ↓    | 8.36                        | 5.99               | 3.86                        | 7.34                  | 5.99                 |
| 10,F.   | 42.68                         | 10.29                   | 7.81  | ↓    | 8.43                        | 6.00               | 3.86                        | 6.97                  | 6.00                 |
| 10,A.   | 42.68                         | 9.36                    | 6.44  |      |                             |                    |                             |                       |                      |
| 11  | 46.00                         | ↑                       | 6.04  | .00  |                             | 5.90               |                             |                       | 5.90                 |
| 12  | 53.68                         | ↑                       | 5.35  | .02  |                             | 5.25               |                             |                       | 5.25                 |
| 13  | 61.36                         | ↑                       | 4.93  | .15  |                             | 4.05               |                             |                       | 4.05                 |
| 14  | 69.04                         | 5.90                    | 4.73  | .54  |                             | 2.39               |                             |                       | 2.39                 |
| 15,F.   | 71.75                         | 5.73                    | 4.91  | .72  |                             | 1.68               |                             |                       | 1.68                 |
| 15,A.   | 71.75                         | 4.88                    | 4.06  |      |                             |                    |                             |                       |                      |
| 16  | 74.29                         | ↓                       | 3.85  | .97  |                             | 1.00               |                             |                       | 1.00                 |
| A.P.  | 76.21                         | 3.93                    | 3.93  |      |                             |                    |                             |                       |                      |

# Buoyancy and Static Stability

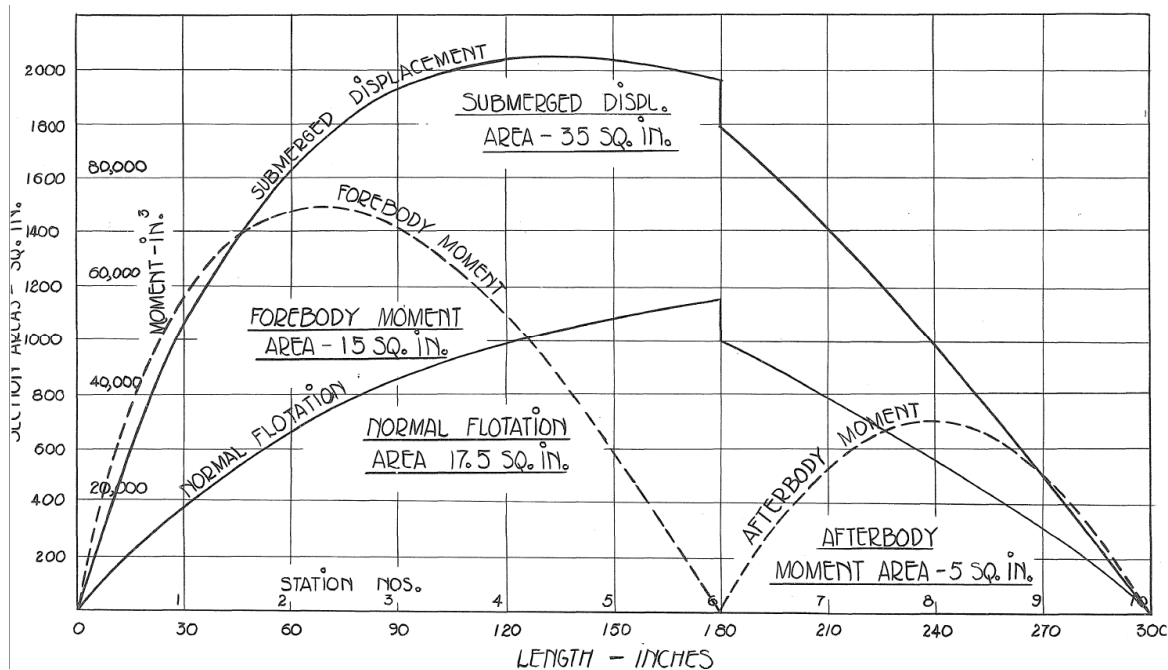


Figure 1: Typical Set of Curves used in Buoyancy Calculations

## 2.2 Static Stability Metacentric Height Application to Twin-Float Seaplanes

We will consider now the principles of static stability for a body floating on water. Assume Figure 2 to represent a cross section of a boat's hull, or more precisely a slice of a hull between two transverse planes spaced by the distance  $dx$ . Assume the hull to be inclined by a small angle, so that the triangular area  $g_1$  is emerged, and the area  $g_2$  is immersed, shifting the center of buoyancy from  $B$  to  $B_1$ . The vertical force of buoyancy now passing through  $B$  will intersect the centerline plane at the point  $M$ , called "metacenter". If  $G$  is the center of gravity, we evidently have the stabilizing moment formed by the couple of the weight and buoyancy forces equal to:

$$W \times MG \times \theta$$

The location of the metacenter  $M$  generally depends on the angle of heel, but it is reasonably constant for small values of  $\theta$  say up to 15-degrees. When the metacenter is referred to, it usually means the initial metacenter for the infinitely small angle  $\theta$ .

The moment due to the transfer of the buoyancy of the emerged triangle having its center of gravity at  $g_1$  to the immersed one  $g_2$  is

$$2 \times \frac{2}{3} y \times \frac{y^2 \theta}{2} = \frac{2}{3} y^3 \theta dx$$

or integrating for the length  $L$  of the hull:

$$\frac{2}{3} \int_0^L y^3 dx$$

This moment is evidently equal to the moment produced by the entire submerged volume of the hull  $V$  times the displacement of the center of buoyancy  $BB_1$ , or

$$BB_1 \times V = \frac{2}{3} \theta \int_0^L y^3 dx$$

Substituting  $BB_0 = BM\theta$ , cancelling  $\theta$  and transposing:

$$BM = \frac{\frac{2}{3} \int_0^L y^3 dx}{V}$$

the numerator of this expression is recognized as the moment of inertia of the waterplane, and the expression is rewritten therefore as

$$BM = \frac{I}{V}$$

Flying-boat hulls, and the floats of single float seaplanes are usually long enough to give the satisfactory longitudinal stability, so that special calculations are not needed. The floats of twin-float seaplanes must be checked for the longitudinal as well as lateral stability by the method described above. If I is the moment of inertia of the waterplanes and D is the displacement in cubic feet of both floats:

$$I = 2(I_0 + AB^2)$$

where  $I_0$  is the moment of inertia of the waterplane of each float about its own centerline, and A is the area of the waterplane, i.e. of the intersection of the water surface with the float. b is the distance of the float centerline from the plane of symmetry, i.e. the half spacing of two floats.  $I_0$  is quite small compared to  $Ab^2$  and usually can be neglected, assuming  $I = 2Ab^2$

Since the distance BG is known from the design data, we get:

$$MG = MB - BG$$

The minimum spacing of the floats is determined by the requirement of the Civil Aeronautics Administration [Editor unable to verify this reference. Possibly this is a Canadian requirement] for the minimum metacentric height

$$MG = 4\sqrt[3]{V}$$

Where,  $V$  is the total displacement of the seaplane in cubic feet or cubic meters, based on the gross weight.

The same expression  $MB = I/\Delta$  is used for checking the longitudinal stability, but in this case I is the longitudinal moment of inertia of the waterplane of two floats:

## Buoyancy and Static Stability

$$I = \frac{2}{3} \int_0^L yx^2 dx$$

where y is the breadth of the waterplane, and x is the distance of the particular station from the centroid of the area. The outline of the waterplane is drawn by measuring the half breadth at each waterline on the body plan, and by plotting it against the length of the float. The waterplane area is either measured by the planimeters or is computed by Simpson's Rule. The products  $yx^2$  are tabulated, and are plotted on the length basis. The longitudinal moment of inertia of one float is obtained as the area under the curve. This is found by integration (either graphically or by Simpson's rule). As before,  $MG = MB - BG$ , but in this case the CAA regulations [Reference needed] require that:

$$\text{Longitudinal MG} = 6\sqrt[3]{\nabla}$$

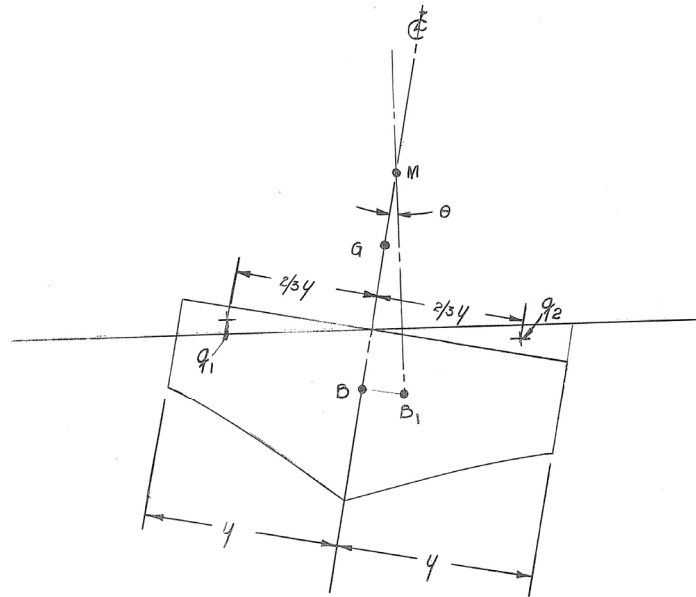
Where,  $\nabla$  is the total displacement of the seaplane in cubic feet or cubic meters, based on the gross weight.

[Diehl (1924) provided a study of existing seaplanes up to that time and found that in general the longitudinal MG can be estimated with the following equation, which is a bit of a shortcut relative to integrating.

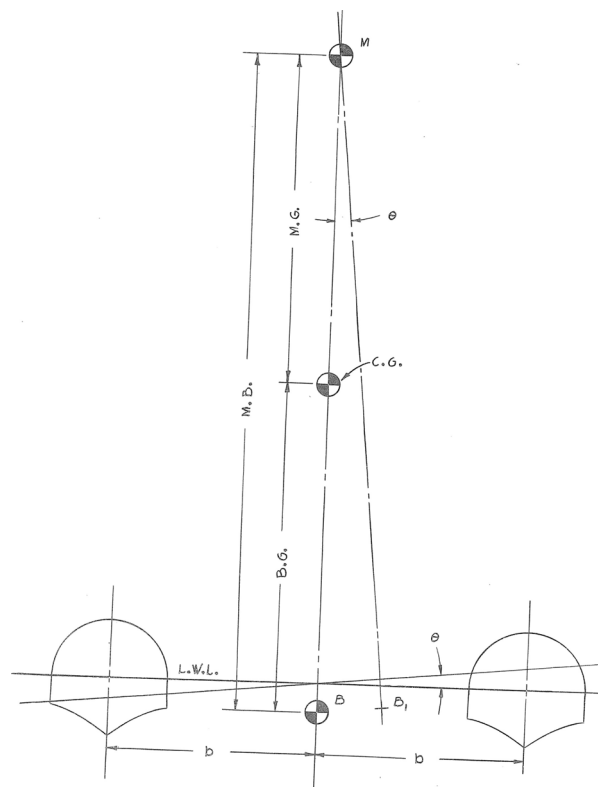
$$\text{Longitudinal MG} = \frac{KnBL^3}{\Delta}$$

Where n is the number of floats, B is the beam of each float, L is the overall length of each float,  $\Delta$  is the gross weight of the seaplane, in pounds. K is a constant varying from 1.9 to 2.4 with an average value of 2.1.]

# Buoyancy and Static Stability



a. Single Float or Flying Boat



b. Twin Float

Figure 2: Definition of the Metacenter  $M$ , and the Metacentric Height  $MG$

### 2.3 Lateral Stability of Flying Boats and of Single Float Seaplanes

The narrowness of flying-boat hulls and of single floats, and the resulting small moment of inertia of the waterplane area results in the transverse metacenter  $M$  being located below the center of gravity, i.e. the metacentric height,  $MG$  is negative. This indicates the lateral instability, which must be corrected by auxiliary means. Figure 3 (top) shows the "stubs" or "sponsons" introduced by Dornier (Germany), and used in this country by Boeing. By providing larger breadth and therefore larger lateral moment of inertia of the waterplane, the stubs provide positive  $MG$ , and permit to attain the practical amount of stability. This arrangement is mostly abandoned because of the weight and the added water resistance during take-offs, but it has appeared on some small seaplanes, such as the Icon A5 (2012), and the Dornier Seastar(1984).

Figure 3 (bottom) shows the use of two auxiliary floats located near the main hull, and so disposed as to have sufficient waterplane area and moment of inertia to provide the necessary amount of stability. This arrangement was introduced by Rohrbach (Germany), and was used in this country by Sikorsky. This arrangement has been abandoned in favor of auxiliary floats of small size located near wing tips, as shown on Figure 4. The floats, known as "auxiliary floats" or "wing tip floats" are so located vertically that they about touch the water surface, sometimes immersed an inch or two, sometimes a few inches above water level. The flying boat is permitted to list a certain amount before sufficient buoyancy is developed in the auxiliary float for equilibrium.

Figure 5 shows a typical curve of heeling moment for a flying boat. The dashed line is the upsetting moment, calculated by running large angle stability calculations, assuming there are no tip floats. This moment is destabilizing. The solid line is the righting moment, due to the tip floats. There is no righting moment until the float becomes immersed, around 1 degree of heel. Above this angle, the float provides a large, increasing righting moment. Once the float is fully immersed (above 8 degrees on the diagram), there is very little change in righting moment until the wing becomes immersed. The tip floats must provide enough righting moment, with enough margin for bad conditions. Two previous standards have existed that can aid in initial design.

## Buoyancy and Static Stability

14 CFR § 23.757 - Auxiliary floats (Removed 2017)

"Auxiliary floats must be arranged so that, when completely submerged in fresh water, they provide a righting moment of at least 1.5 times the upsetting moment caused by the seaplane or amphibian being tilted."

This ratio can be determined from Figure 5 by comparing the upsetting moment and righting moment at 8 degrees.

The factor of 1.5 is a simplification that includes the effects of wind heeling moments and the margin of safety. For large seaplanes, it may be necessary to exceed this value. Nelson, 1934 suggests that values as high as 3.0 to 3.5 can be used.

U.S. Navy (SR-59)

Carter (1947) shows a comparison of various transverse stability standards for flying boats, and compares the standards with the opinion of the operators on how satisfactory the design is. The paper shows that the following guideline provides satisfactory tip float sizing (equation only works in U.S. customary units):

$$\Delta_T = \frac{\Delta_o}{\ell} \left( h_e \sin \phi_1 + \frac{0.10b}{(\Delta_o/S)} + 0.06\sqrt{\Delta_o} \right)$$

Where,

$\Delta_o$  is the static weight of the seaplane (lbf)

$\Delta_T$  is the weight displacement of the tip float (lbf)

$\ell$  is the distance from the center of the tip float to the centerline of the seaplane (ft)

$\phi_1$  is the heel angle required to submerge the float

$b$  is the wingspan (ft)

$S$  is the wing area (sq. ft)

$h_e$  is the absolute value of the negative metacentric height at zero heel (ft)



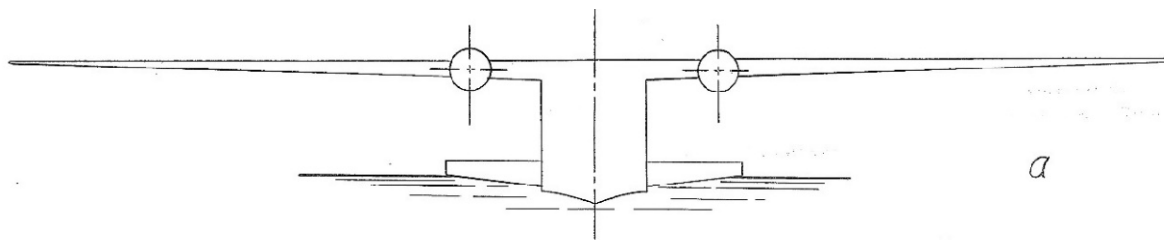
## Buoyancy and Static Stability

"First term within brackets is the result of the inherent upsetting moment caused by the effective destabilizing height of C.G.; second term is result of the effect of wind on wings; and third term represents a reasonable excess restoring moment based on accumulated experience" (Stout, 1947). It is noted that in the second term the upsetting moment due to the side wind is taken to be proportional to the span and to the area of wings, since displacement  $\Delta_0$  in the denominator is cancelled by  $\Delta_0$  in front of brackets

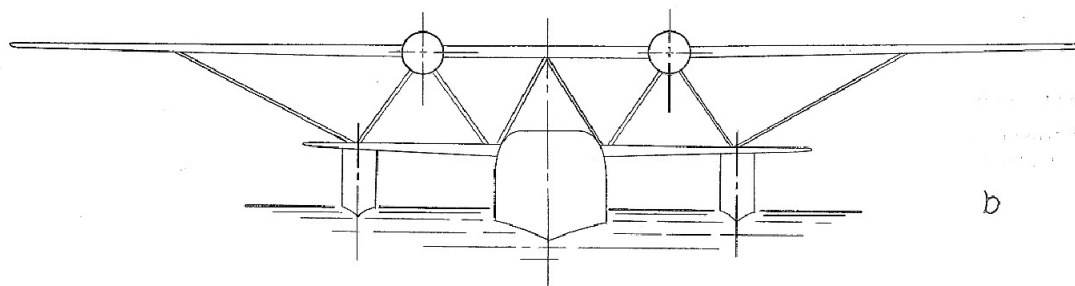
It is evident from the above that required size of the auxiliary float increases as the float is moved inboard, and increases with the angle of list  $\theta$  needed to submerge the float. For this reason, the floats are placed as low as possible, and as far outboard, as the strength of the wing permits. If the floats are located too low, they cause additional drag during take-off, and are more exposed to the danger of the damage during landing, so that making the keel of the float just touch the surface, or to be submerged only an inch or two appears to be the best compromise.

While only the buoyancy was treated in the above discussions it is equally important for the float to have a satisfactory planing bottom to furnish dynamic lift at high speed. The general shape of the float, must be such as to continue to generate the lift force when moving through water in fully submerged condition. Some streamline shapes suffer the rapid reduction of the lift force, or even change to the downward suction if submerged while moving forward at sufficient speed. Figure 6 gives the outline of the float which was used on naval float, seaplanes.

## Buoyancy and Static Stability



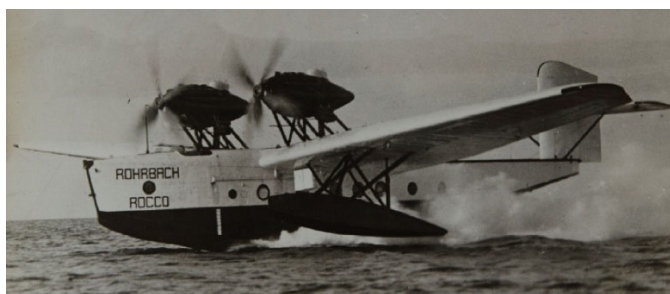
Sponsons



Inboard Auxiliary Floats



Dornier DO-24



Rohrbach Ro-V "Rocco"

Figure 3: Sponsons and Inboard Floats for Lateral Stability.

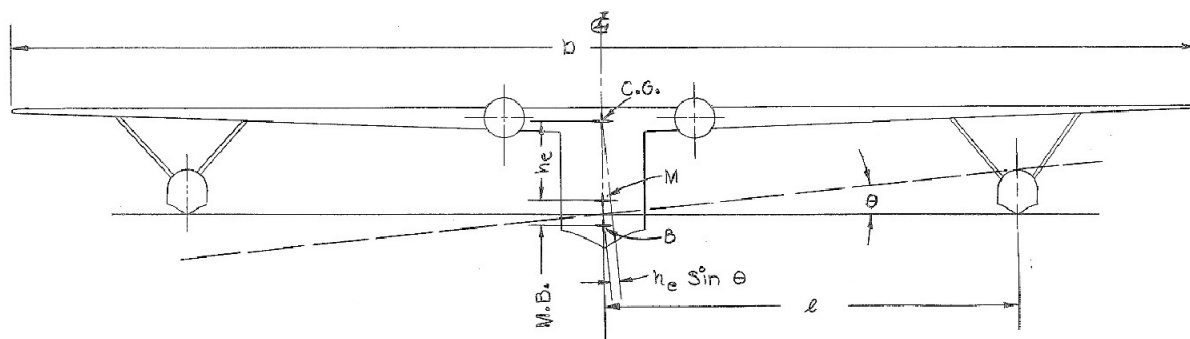


Figure 4: Wing Tip Floats for Lateral Stability.

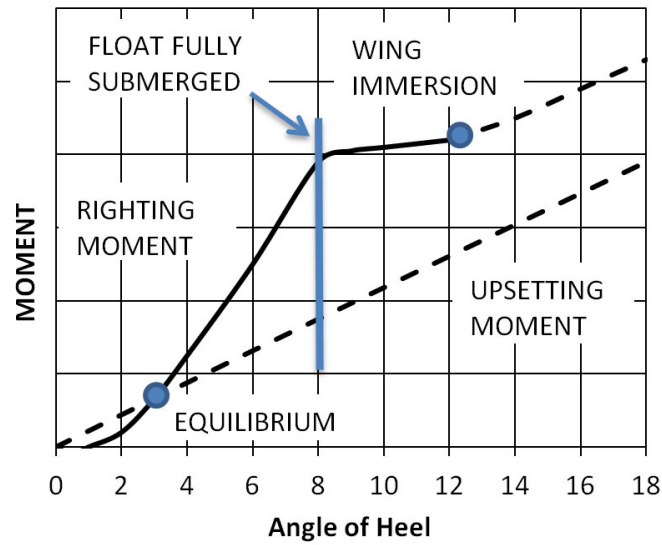


Figure 5: Heeling Moments versus Angle of Heel (Adapted from Diehl, 1986)

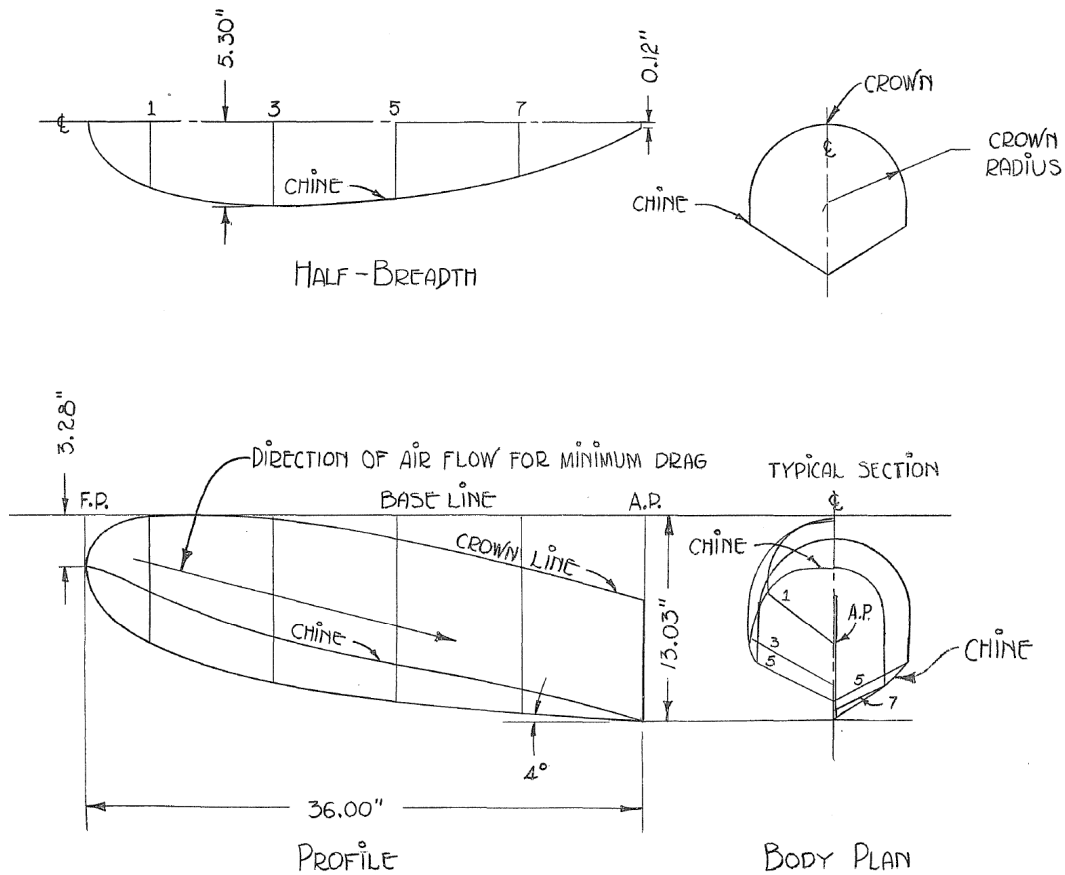


Figure 6: Lines of NACA Model 51-B Wing Tip Float.

References for Chapter 2

Anon. Airplane Airworthiness. Pt 04 of Civil Aero. Manual, CAA, U.S. Dept. Commerce, Feb 1, 1941.

Carter, A.W. Comparison of Design Specifications with the Actual Static Transverse Stability of 25 Seaplanes. N.A.C.A. Technical Note No. 1253. April 1947.

Diehl, W.S. Static Stability of Seaplane Floats and Hulls. Bureau of Aeronautics, U.S. Navy. NACA TN-183. March, 1924.

Diehl, W.S. Engineering Aerodynamics. Revised Edition. David W. Taylor Naval Ship Research and Development Center. Bethesda, Maryland. 2<sup>nd</sup> Edition 1936. Reprint 1986.

Ernest G. Stout, "Static Stability Analysis for Flying Boats and Seaplanes", Aviation, February, 1947.

Nelson, W. "Seaplane Design." First Edition. McGraw-Hill Book Company, inc. New York. 1934.



CHAPTER 3. PLANING AND RESISTANCE

B.V. Korvin Kroukovsky, 1948

3.1 General Considerations

3.2 General Expression of Hydrodynamic Force

3.3 The Lift Force

3.4 Resistance of Prismatic Planing Surfaces

3.5 Ratio of Resistance to Lift

3.6 The Attitude and Balance of the Planing Seaplane Hull in Two-Step Planing

3.1 General Considerations

Figure 1 shows a flat surface of the beam B planing at the angle of trim  $\tau$  and wetted length  $\ell$ . At the trailing edge the water breaks away forming a wave in the wake of the surface. It also breaks away cleanly on two sides leaving the upper part of the planing body dry. The exact speed at which this condition occurs is indetermined [varies with quite a few parameters], and in this course we will generally consider speeds corresponding to  $C_v$  (to be defined in the following paragraph)  $\geq 2.5$ . In front of the planing surface the water surface rises first gently, then makes a quick turn up and forward, forming a thin sheet of water flowing forward. The streamline, separating the part of the water eventually directed forward from that flowing aft, meets the surface at the point called "stagnation point". At this point the maximum water pressure on the surface is developed. Forward of this point the pressure drops sharply, aft of it the pressure drops more rapidly at first, then more gradually towards the trailing edge. The drop of the pressure aft of the stagnation point occurs more rapidly at small angles of trim  $\tau$  and less rapidly at large angles. The region of rapidly curving water surface and in the vicinity of the stagnation point is given the name "spray root" by H. Wagner, who formulated the theory of its formation (Wagner, 1931). It was first observed experimentally by W. Sottorf (1937/1944).

Figure 2 shows a vee planing surface. At the point B, where the keel meets the water surface, there is no discernible rise of the surface, and this point can be assumed to lie on the undisturbed water surface. Aft of this point the water surface rises forming the "spray root", so that wetted area at chines is at the point C, above and forward of the intersection with undisturbed water at D. Wagner established the relation  $b_1/b_2 = \pi/2$ , from which it follows that  $L_1/L_2 = 2/\pi$ . If we denote by  $\lambda$  the ratio of the wetted length  $\ell$  to the beam B, we obtain the expressions,

$$\text{Wetted length of keel} = B (\lambda + \tan \beta / 2\pi \tan \tau)$$

$$\text{Wetted length of chine} = B (\lambda - \tan \beta / 2\pi \tan \tau)$$

These deductions are demonstrated to agree well with experimental data (pages 12, 13 and 14 of Korvin-Kroukovsky, Savitsky and Lehman, 1949)

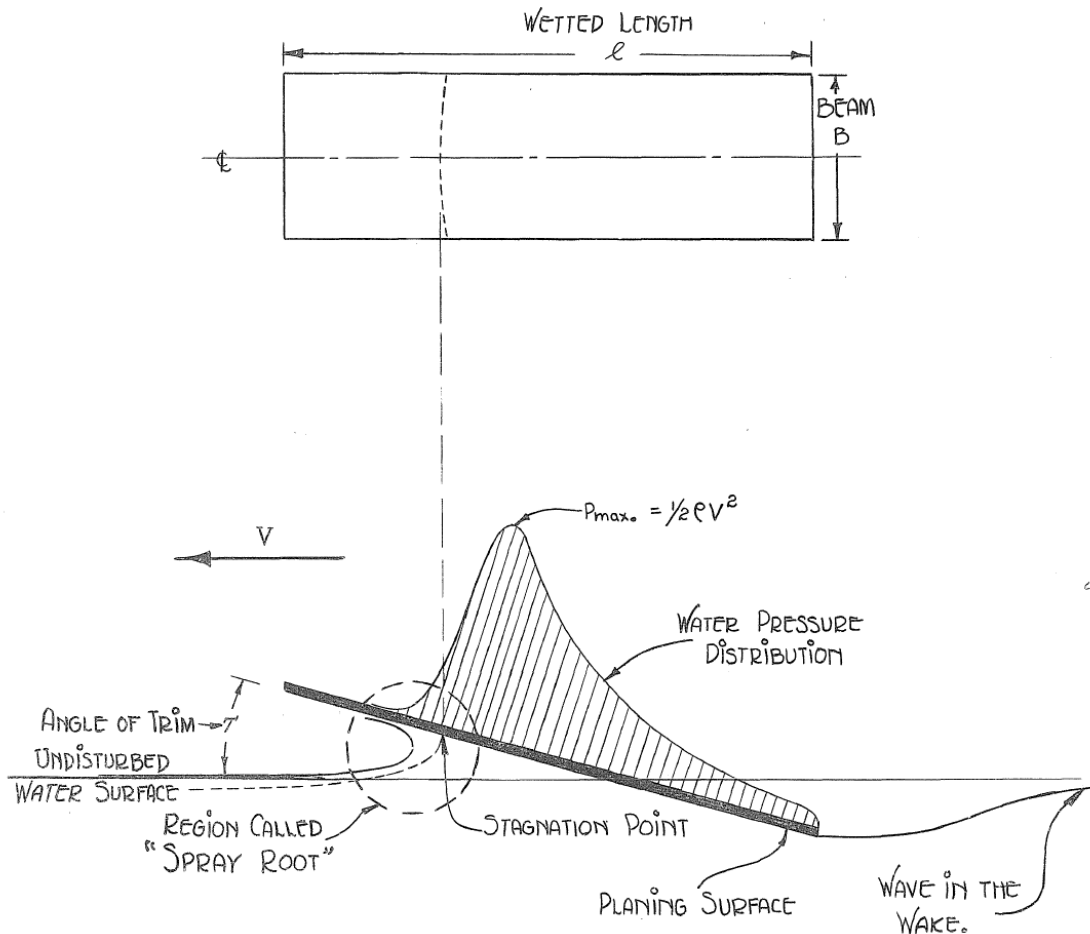


Figure 1: Flat Planing Surface

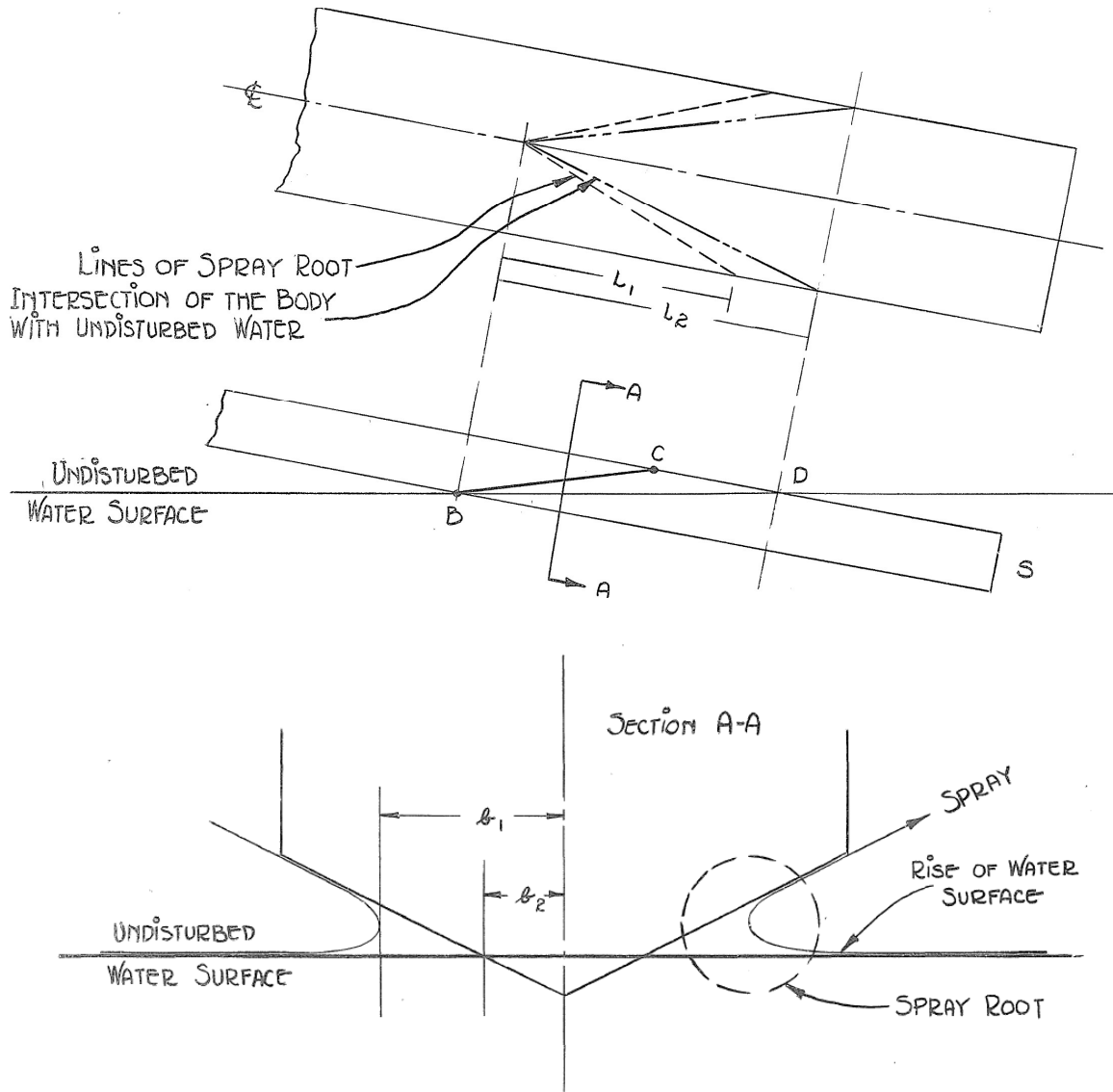


Figure 2: Vee Planing Surface



### 3.2 General Expression of Hydrodynamic Force

It is shown by dimensional analysis that a hydrodynamic force acting on a submerged body, located far away from any boundaries, has the form

$$\text{Force} = k \times \frac{1}{2} \rho V^2 L^2 f\left(\frac{VL}{\nu}\right) \quad (\text{Eq. 1})$$

Where:

$\rho$  is the density of water in mass units

$V$  - velocity in feet per second

$L$  - any characteristic linear dimension of body

$k$  - a non-dimensional constant

$\nu$  - kinematic viscosity, defined as  $\mu/\rho$ , where  $\mu$  is the viscosity

the ratio  $VL/\nu$  is known as Reynolds number, and is frequently denoted by  $R_e$ .

$f(VL/\nu) = f(R_e)$  is an unknown function of the Reynolds number.

In the case of a body moving on water surface, the force acting on the body is further affected by the gravity (resulting from the wave making), and by the surface tension of water, which resists the distortion of the initially flat surface. The expression for the force then takes the form:

$$\text{Force} = k \times \frac{1}{2} \rho V^2 L^2 f\left(\frac{VL}{\nu}\right) F\left(\frac{V}{\sqrt{gL}}\right) \varphi\left(\frac{V^2 L}{\sigma/\rho}\right) \quad (\text{Eq. 2})$$

where:  $g$  is the acceleration of gravity

$\sigma$  is the surface tension of water

$F$  and  $\varphi$  denote unknown forms of the functions.

The ratio  $\frac{V}{\sqrt{gL}}$  is known as Froude number. If this number is squared, the ratio takes the form  $V^2/gL$ . Since for a given mass  $V^2$  is proportional to dynamic

pressure, while  $gL$  is proportional to the force of gravity, the Froude number indicates the ratio of dynamic forces to the force of gravity. The ratio  $V^2L/(\sigma/\rho)$ , known as the Weber number, likewise indicates the ratio of dynamic forces to the forces of surface tension. The detail treatment of the dimensional theory by which Eq. (2) is derived, as well as of the boundary layer theory and laws of skin friction, to be discussed later, is beyond the scope of these notes.

It is not always necessary to consider all three of the functions  $f$ ,  $F$  and  $\phi$ . Thus, the influence of the Weber number is felt only at low speed and in case of very small models, and in our study of planing we can consider it as constant equal to unity, i.e. we can disregard it. The Reynolds and Froude numbers will be considered separately in the problems involving the lift force and the drag force.

### 3.3 The Lift Force

The vertical component of the forces acting on a body is called the lift force, and will be designated by  $L$ . It is known from experience that Reynolds number has very little influence on the lift, and that only the Froude number need be considered. In the study of the planing process it became customary to take the beam  $B$  as the characteristic length, and in such case give the Froude number the special term "speed coefficient", and to designate it by  $C_v$ . Thus

$$C_v = V/\sqrt{gB} \quad (\text{Eq. 3})$$

Disregarding Reynolds and Weber numbers, and including the  $F(C_v)$  into the non-dimensional lift coefficient  $C_L$ , we can rewrite (Eq. 2) as

$$\begin{aligned} \text{Lift} &= C_L \times \frac{1}{2} \rho V^2 B^2 \\ \text{where } C_L &= f(\tau, \lambda, C_v, \beta) \end{aligned} \quad (\text{Eq. 4})$$

It has not been possible to evaluate the coefficient  $CL$  analytically, and the value of it is established by the empirical analysis of the test data. It is found convenient to separate the effect of the deadrise  $\beta$  from the effect of  $\tau$ ,  $\lambda$  and  $C_v$ , and to define first the lift coefficient  $CL_0$  of a flat planing surface.

L. Sedov (1939) gave the following expression for the value of  $CL=f(\tau, \lambda, C_v)$

$$C_{L_0} = \tau \left[ \frac{0.7\lambda}{1+1.4\lambda} + \lambda(0.92\lambda - 0.38)/C_v^2 \right] \quad (\text{Eq. 5})$$

At the Experimental Towing Tank (Korvin-Kroukovsky, Savitsky and Lehman, 1949), this expression was simplified, and was written:

$$C_{L_0} = \tau^{1/4} \left[ 0.0120 \lambda^{1/2} + 0.0095 (\lambda/C_v)^2 \right] \quad (\text{Eq. 6})$$

[2024 note - this is slightly different from the equation that appears in the Savitsky, 1964 paper]

The first of these two expressions is particularly interesting in indicating the proportionality of  $CL$  with  $\tau$ , which is only slightly modified by the second expression. The second expression is slightly more accurate for the range of  $C_v$  used in seaplane design, and brings out more clearly the significance of  $\lambda$  and of  $C_v$ .

The lift coefficient  $CL$  of a prismatic Vee planing surface is given in terms of a flat surface (Korvin-Kroukovsky, Savitsky and Lehman, 1949) as,

$$C_{L\beta} = C_{L_0} - 0.0065\beta C_{L_0}^{0.6} \quad (\text{Eq. 7})$$

For convenience of use the expressions (6) and (7) are given in the form of charts on Figure 3, taken from Korvin-Kroukovsky, Savitsky and Lehman (1949)

Example: 1. Find the lift  $\Delta$  of a flat surface 1 foot wide planing at the angle of trim  $\tau$  of 5 degrees at the speed of 20 feet per second on fresh water with the mean wetted length of 2 feet.

$$\tau' = 5.87 \quad \lambda = \ell/B = 2.0$$

$$C_v = V/\sqrt{gB} = 20/\sqrt{32.2 \times 1} = 3.5$$

$$C_L = 5.87 [.0120 \times 2^{1/2} + .0095 (2/3.5)^2] =$$

$$5.87 (.0170 + .0031) = .118$$

$$\Delta = .118 (62.5/2 \times 32.2) \times 20^2 \times 1^2 = 46 \text{ lbs.}$$

2. Find the lift of the above surface assuming that it has a Vee shape with the angle of deadrise  $\beta$  of 20 degrees.

$$C_{L\beta} = .118 - .0065 \times 20 \times .118^{.6} = .082$$

$$\Delta = .082 \times (62.5/2 \times 32.2) \times 20^2 \times 1^2 = 31.8 \text{ lbs.}$$

All of the expressions were given in the form  $\Delta = f(\lambda)$ , since it is not practical to give Eqs. (6 and 7) in the inverse form  $\lambda = \Phi(\Delta)$ . In the actual work it is the latter relation that is usually required, and can be easily obtained from the chart on Fig. 3 [or by iteration in a computer program]. In the usual statement of a problem  $B$ ,  $\beta$ ,  $\Delta$  and  $V$  are given. The trim  $\tau$  is taken as a parameter, and the  $\lambda$  and  $\ell$  are determined. In case of the aerodynamic analysis of an airplane, the wing area is fixed, and the computations are arranged so as to determine the lift coefficient and the angle of attack. In the case of a planing surface the wetted area (i.e. the  $\lambda$ ) is variable, so the angle of trim  $\tau$  is taken as a parameter, and the computations are arranged so as to determine  $\lambda$ . Conversely, if the resultant

force is to pass through the center of gravity of a seaplane, the wetted length must be held constant, and the angle of trim is the variable to be determined.

The knowledge of the wetted length for every speed and trim angle during the take-off run of a seaplane will prevent many errors in the design. For instance were too small a beam  $B$  assumed, the calculations would immediately show excessive wetted length, with wetting of the curved areas of the bottom near the bow, and with resultant increase of the resistance and spray. For all planing conditions the wetted area must be confined to the region in which the buttock lines are straight, and the forward area of the bottom where the buttock lines are curved must remain above water. In the same way the computations of the wetted length  $\ell = \lambda B$  will indicate the maximum load  $\Delta$  which can be used for a given  $B$  and  $\tau$ , or the minimum value of the angle of trim  $\tau$  which can be used for a given load  $\Delta$ . It should be particularly emphasized that the important first term of Eq.6 shows that wetted length varies as the square of the loading, and inversely as the square of the beam.

# LIFT OF PLANING SURFACES

LIFT COEFFICIENT IS DEFINED AS:

$$C_L = \Delta / \frac{1}{2} \rho V^2 b^2 = 2C_{L0} / C_V^2$$

FOR A FLAT PLATE - DEADRISE ZERO:

$$C_{L0} = T^{1.1} (.0120 \lambda^{1/2} + .0095 \lambda^2 / C_V^2)$$

FOR A VEE SURFACE OF DEADRISE  $\beta$ :

$$C_{L\beta} = C_{L0} - .0065 \beta C_{L0}^{.6}$$

$\Delta$  - LOAD LB.

V - VELOCITY IN FEET PER SEC.

$\lambda$  - RATIO OF MEAN WETTED

$\rho$  - WATER DENSITY

T - ANGLE OF TRIM IN DEGREES

LENGTH TO BEAM

b - BEAM IN FEET

$\beta$  - DEADRISE IN DEGREES

$C_V$  - SPEED COEFF. =  $V / \sqrt{gb}$

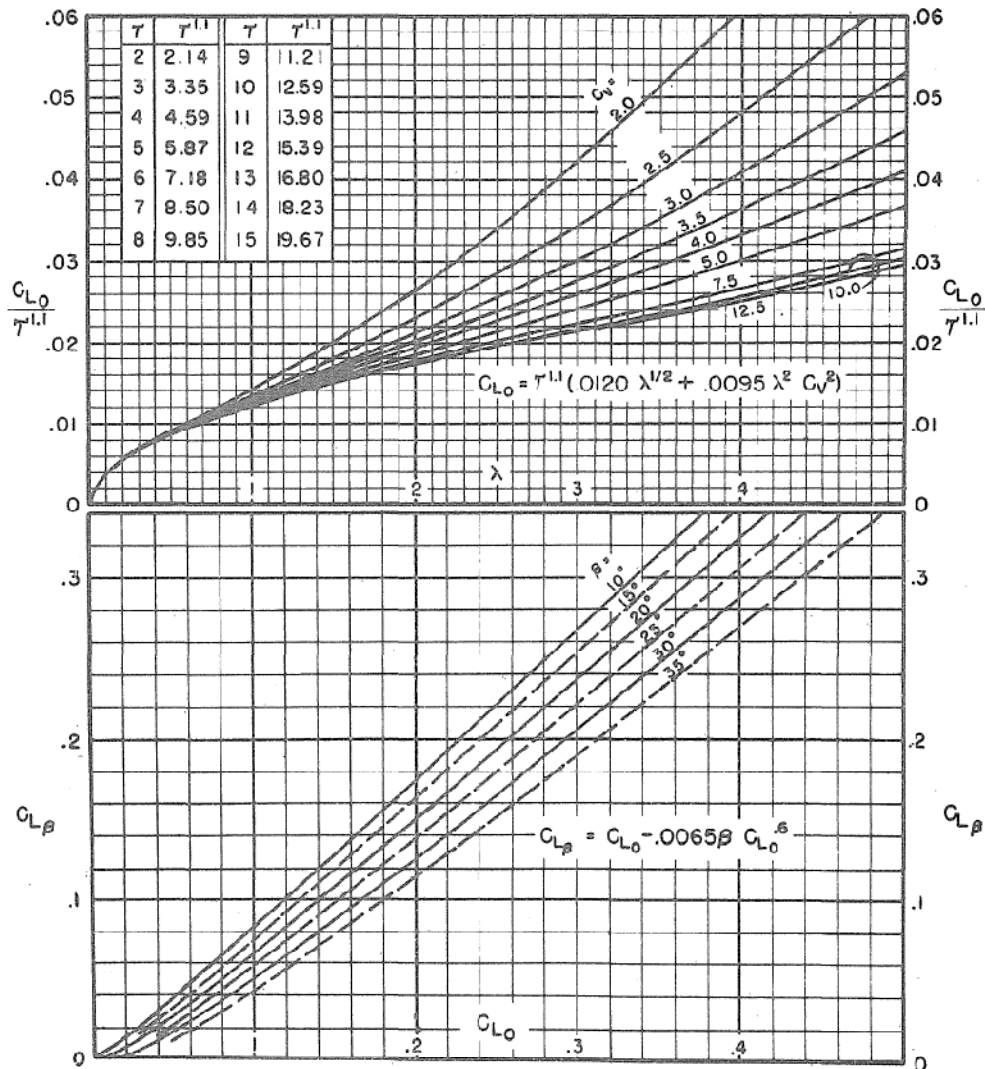


Figure 3: Lift of Planing Surfaces

(Taken from Korvin-Kroukovsky, Savitsky and Lehman 1949)

### 3.4 Resistance of Prismatic Planing Surfaces

The resistance of a planing surface is found to depend both on the Froude number and the Reynolds number and for this case Eq. (2) is rewritten as,

$$\text{Resistance} = k \times \frac{1}{2} \rho V^2 B^2 F\left(\frac{V}{\sqrt{gB}}\right) f\left(\frac{VL}{D}\right) \quad (\text{Eq. 8})$$

It was assumed, and subsequently verified experimentally that effects of the Froude number and of the Reynolds number can be separated and Eq. (8) can be rewritten as:

$$C_D = \frac{\text{Resistance}}{\frac{1}{2} \rho V^2 B^2} = k_1 F(C_v) + k_2 f(Re) \quad (\text{Eq. 9})$$

Thus, total resistance  $R$  can be considered as the sum of two distinct parts: the resistance which is due to the normal pressures on the surface, which would exist even in frictionless fluid, and one due to tangential, or frictional force.

Normal pressures acting on a surface produce the lift, as well as the drag, and for a prismatic surface two are connected by simple relations resulting from Figure 4

$$R = \Delta \tan \tau$$

and, dividing by  $\frac{1}{2} \rho V^2 B^2$ , and denoting the dynamic drag coefficient by  $C_{dd}$

$$C_{dd} = C_L \tan \tau$$

The effect of  $C_v$  is here already included in  $C_L$  obtained from Eqs. 6 and 7.

Friction drag coefficient, resulting from  $f(Re)$ , and proportional to the wetted area, can be estimated on the basis of Schoenherr's Formula:

$$\frac{0.242}{V C_f} = \log_{10} (Re \cdot C_f) \quad (\text{Eq. 10})$$

2024 Note - Most today would use the ITTC 1957 line, which is identical to the Schoenherr curve at high Reynolds numbers:

$$C_F = \frac{0.075}{(\log_{10}(Re) - 2)^2}$$

The Schoenherr line is a recursive formula that can be computed by assuming a value of  $C_f = 0.003$  and then iterating 5-6 times until it converges. Values  $C_f$  prior to computers were published in large tables.

The plot of  $C_f$  obtained by Schoenherr's Formula vs.  $Re$  given by the curve (144) on Figure 5a. The value of Schoenherr's Formula lies in its applicability to a wide range of values of Reynold's number. If the Reynold's number does not exceed  $2 \times 10^7$ , the simpler Prandtl-Karman formula can be used :

$$C_f = .074 (VL/D)^{-0.2} \quad (\text{Eq. 11})$$

While for  $10^6 < Re < 10^8$  Schoenherr's formula agrees closely with Schlichting's formula

$$C_f = \frac{0.455}{(\log_{10} Re)^{2.58}} \quad (\text{Eq. 12})$$

In Eqs. 10, 11 and 12 the coefficient  $C_f$  is referred to the actual wetted area, i.e. is determined as

$$C_f = \frac{\text{Frictional Resistance}}{\frac{1}{2} \rho V^2 (\text{Wetted Area})} \quad (\text{Eq. 13})$$

For use in Eq. 9 it must be converted to beam squared basis, i.e. it must be multiplied by  $\lambda$  and by  $\sec \beta$  ( $\sec \beta = 1/\cos \beta$ ) so that we have finally

$$C_D = C_L \tan \tau + C_f \lambda \sec \beta \quad (\text{Eq. 14})$$



The above equations refer to the turbulent boundary layer, which can be assumed to exist on the full-scale floats and hulls. In the testing of the small models the turbulent layer can be assumed to exist only if special measures are taken to induce it, as for instance, towing of a vertical wire in front of the model. Without such a precaution, the boundary layer will be often turbulent with laminar approach (Figure 5b), and the value of the frictional drag will be lower and the data will be less consistent.

2024 Note - Savitsky and Ross (1952) made a good study on the effectiveness of turbulence-inducing struts. It was found that regardless of strut position, when the Reynolds number exceeded  $2 \times 10^6$ , the flow was turbulent on the planing models. See Figure 6.

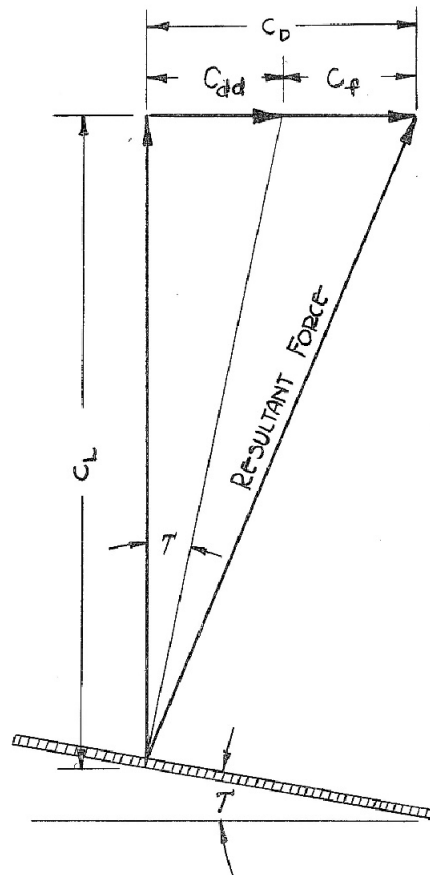


Figure 4: The Diagram Showing the Total Drag as the Sum of the Dynamic Drag and the Friction Drag.

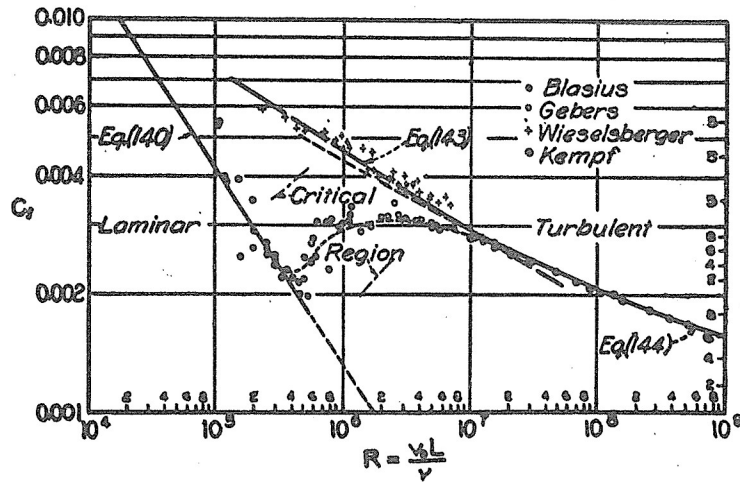


Figure 5a: Friction Coefficient vs. Reynolds Number

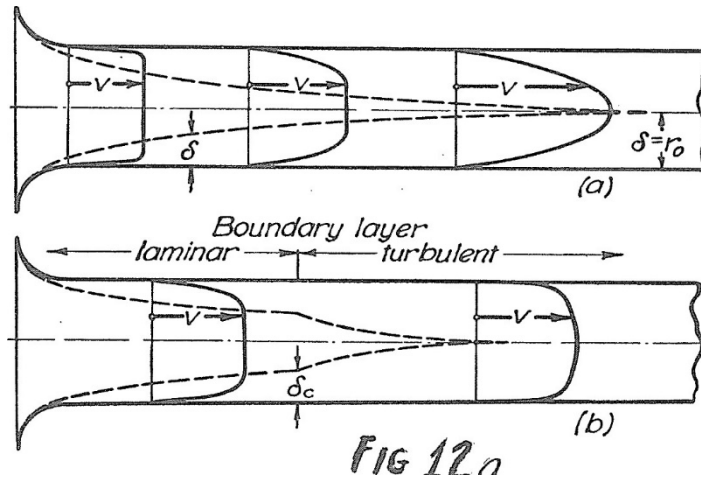


Figure 5b: Laminar Transition (Taken from Sottorf, 1934)

# Planing and Resistance

## EFFECT ON FRICTION COEFFICIENT AND STATE OF BOUNDARY LAYER OF VARIOUS LONGITUDINAL POSITIONS OF A .040" DIAMETER TURBULENCE STRUT

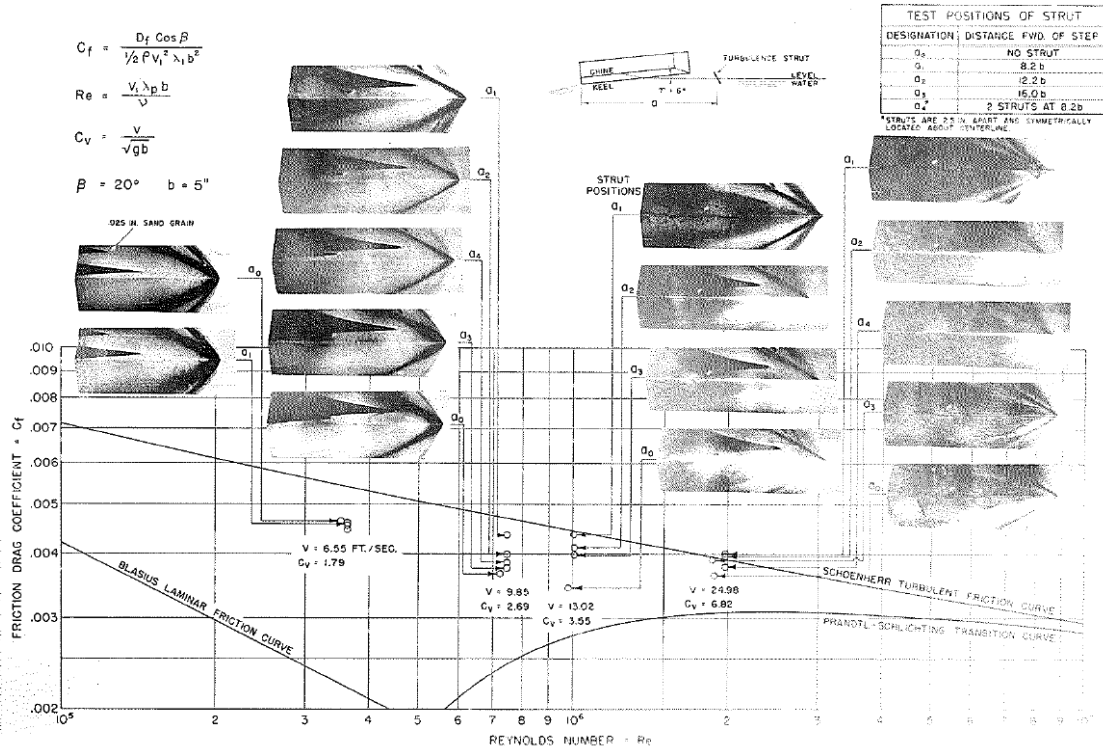


Figure 6: Effectiveness of Turbulence Strut (Taken from Savitsky and Ross, 1952)

3.5. Ratio of Resistance to Lift

The ratio of the resistance to lift  $R/\Delta$  is often designated by  $\epsilon$  and called the "Planing Coefficient". In the previous discussion the lift and drag coefficients were referred to the square of the beam as the characteristic dimension, and were designated as  $C_L$  and  $C_D$ . For the following discussion it will be more convenient to refer them to the bottom area  $BL$ , i.e. to  $\lambda B^2$ , and in this form we will designate them as  $C_l$  and  $C_d$ . In this form Eq. (9) becomes:

$$C_d = C_e \tan \tau + C_f \sec \beta \quad (\text{Eq. 15})$$

and

$$\epsilon = \frac{C_d}{C_l} = \frac{C_e \tan \tau + C_f \sec \beta}{C_l} \quad (\text{Eq. 16})$$

On the basis of Equation 5 (Sedov's lift equation), the lift coefficient  $C_l$  can be assumed to be approximately proportional to  $\tan \tau$ , i.e.

$C_l = K \tan \tau$ , and Equation 16 takes the form:

$$\epsilon = \frac{\tan^2 \tau + \text{Const.}}{\tan \tau} \quad (\text{Eq. 17})$$

The form of this function is shown by Figure 7, which represents the plot of the experimental data of Sottorf (1934), obtained from tests on the planing surfaces 30 cm wide at the speed of 6 m/sec., or  $C_v$  of about 3.5. This diagram is very useful in understanding the influence of the angle of trim  $\tau$ . It is noted that minimum resistance for Vee surface occurs at the angle of trim of approximately 6 degrees, and the seaplanes are usually maintained at this attitude at high speeds when the pilot has the control power to do so. At smaller angles of trim the drag rises rapidly, due to the predominance of the second (friction) term, with  $\tan \tau$  in the denominator being small. At the larger angles the first term predominates, and the curves approach asymptotically the line  $\epsilon = \tan \tau$  indicating relatively unimportant effect of the friction. It should be emphasized that these curves apply to the prismatic Vee planing surface of sufficient length. In the actual

seaplanes the prismatic section cannot be made to support the load at, or slightly above the hump speed at the angle of the minimum drag, and the drag increases rapidly as the curved, upswept part of the bottom is wetted. In this case the angle of the minimum drag becomes much larger, usually between, 9 and 12 degrees, and the drag is correspondingly large. In analyzing the hull performance it is always necessary to keep in mind these two factors: the angle of trim, and the corresponding wetted length.

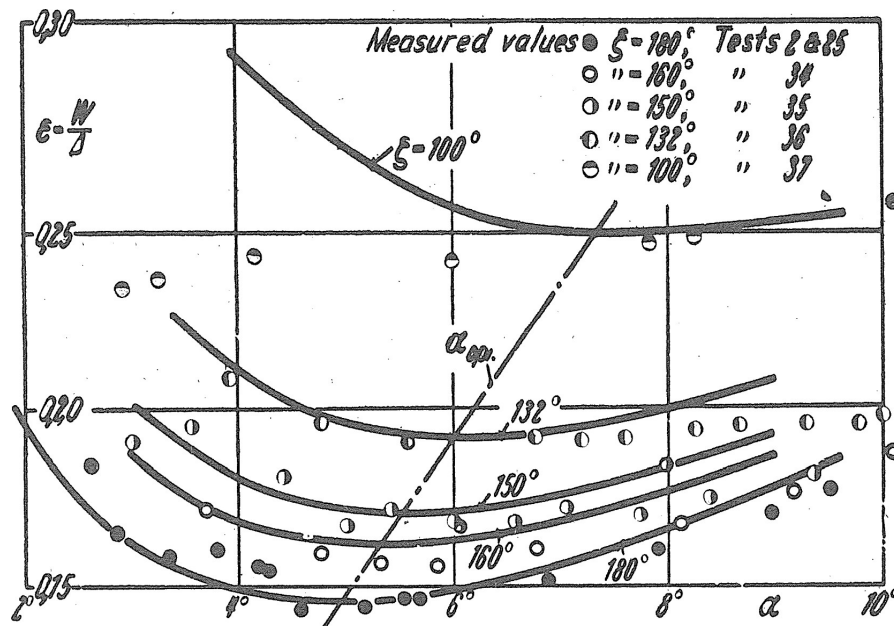


Figure 7: The Variation of the Planing Coefficient  $\epsilon$  with the Angle of Trim  $\alpha$  for the constant  $\Delta$ , and with  $\lambda$  Variable (Taken from Sottorf, 1934)

### 3.6 The Attitude and Balance of the Planing Seaplane Hull in Two-Step Planing

Figure 8 shows the seaplane hull in the planing condition approximately at the hump speed. The hull is supported by water pressures on the forebody, the resultant of which is  $\Delta - \delta$  and by the pressures on the afterbody near the second step, the resultant of which is  $\delta$ . At a given angle of trim and a given speed, a certain wetted length  $L$  is required to support the load, and this can be determined from the lift formulae for prismatic planing surfaces (section 3.3). In supporting the load the forebody deflects the water surface, forming the wave. The second step usually rides on the forward slope of the wave, somewhat below the level of undisturbed water. For the afterbodies of the length commonly used it can be assumed that  $\tau$  at hump speed is equal to  $1.2\sigma$  with  $1.1\sigma$  for very long afterbodies, and  $1.3\sigma$  for very short ones (where  $\sigma$  is the sternpost angle). A more accurate check on the estimated value of  $\delta$  can be made by use of the data on the wave contours in the wake of planing surfaces given by Korvn-Kroukovsky, Savitsky and Lehman (1949), and also provided in Figure 9. Since this angle of inclination is not large we can assume the cosine of it to be equal to one, and can consider the resultant to be equal to  $\Delta - \delta$ . Then we have the positive pitching moment due to the forebody of  $a(\Delta - \delta)$ , from which the stern load is found to be:

$$\delta = \Delta a / (a + b)$$

It appears to be most advantageous to locate the center of gravity so that  $\delta$  is 5% to 10% of  $\Delta$  at the hump speed. With this load the hull is stably supported by the forebody and the afterbody forces. If the stern load is much lighter it will disappear with very small increase of speed, leaving the hull supported in complete balance by the forebody alone, with the probability of the low limit porpoising. If the stern load is much heavier, the variation of it will produce significant changes in the forebody load, and in the resultant wave form. This may lead to the high limit porpoising.

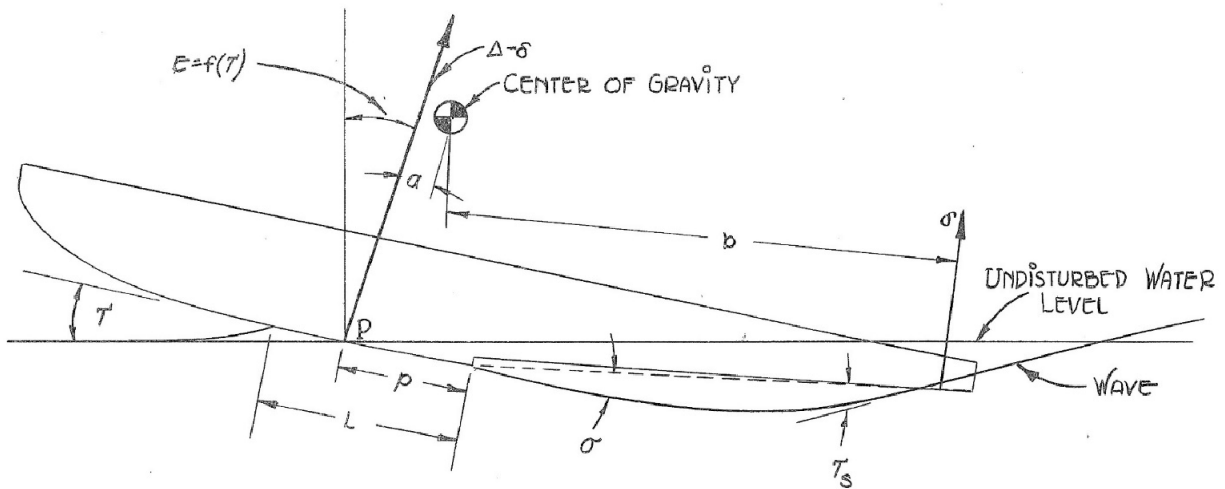
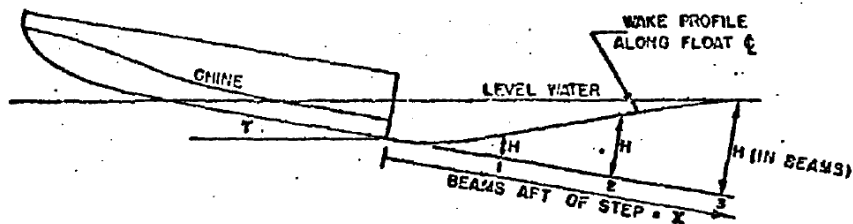


Figure 8: The Balance of the Forces and Moments in Two Step Planing.

LONGITUDINAL CENTERLINE PROFILE THROUGH WAKE OF  
PRISMATIC PLANING SURFACES  
( $10^\circ \leq \beta \leq 30^\circ$ )



$$H = \underbrace{.02064 \left[ \frac{X}{C_V^{.60}} \gamma^{.70} \right]^2}_{H_0} - \underbrace{.00448 \left[ \frac{X}{C_V^{.60}} \gamma^{.70} \right]^{2.44} + .0108 \lambda \gamma^{.34} X}_{H_A}$$

EXAMPLE

$$\gamma = 12^\circ$$

$$C_V = 4.25$$

$$\lambda = 2.00$$

| X              | 1   | 2   | 3   | 4   | 5    | 6    |
|----------------|-----|-----|-----|-----|------|------|
| H <sub>0</sub> | .08 | .27 | .52 | .77 | 1.04 | 1.27 |
| H <sub>A</sub> | .07 | .10 | .15 | .20 | .25  | .30  |
| H              | .15 | .37 | .67 | .97 | 1.29 | 1.57 |

Figure 9 - Longitudinal Centerline Wake Profile (Taken from Korvin-Koukovsky, Savitsky and Lehman, 1949)

References for Chapter 3

Korvin-Kroukovsky, B.V., Savitsky, Daniel and Lehman, William F. "Wake Profile of a Vee Planing Surface, Including Test Data on a 30-degree Deadrise Surface" Experimental Towing Tank of Stevens Institute of Technology Report No 339, April 1949, Sherman Fairchild Publication Fund Paper No 229, Institute of the Aeronautical Sciences, New York.

Korvin-Kroukovsky, B.V., Savitsky, Daniel and Lehman, William F. "Wetted Area and Center of Pressure of Planing Surfaces" Experimental Towing Tank of Stevens Institute of Technology Report No 360, August 1949, Sherman Fairchild Fund Publication No. 244. Institute of the Aeronautical Sciences.

Pierson, John D. and Burghardt, Joseph R. "A Specific Chart for Flying Boat Take-off Performance", Journal of the Aeronautical Sciences, April 1945.

Sedov, "Scale Effect and Optimum Relations for Sea Surface Planing", NACA TM No. 1097, February 1947 (originally Report No. 439 of the Central Aero-Hydrodynamic Institute, Moscow, 1939)

Sottorf, "Analysis of Experimental Investigations of the Planing Process on the Surface of Water" N.A.C.A. T.M. No. 1061, March 1944 (originally Jahrbuch 1937 der Deutschen Luftfahrtforschung).

Sottorf, "Scale Effect of Model in Seaplane-Float Investigations" , NACA TM No. 704 April, 1933

Sottorf, "Experiments with Planing Surfaces", NACA TM No. 739, March 1934

Stout, Ernest G., "Take-off Analysis for Flying Boats and Seaplanes", Aviation, August and September, 1944.

Wagner, H. "Landing of Seaplanes" N.A.C.A. T.M. No. 622, 1931





CHAPTER 4. TANK TESTING AND TAKE-OFF CALCULATION

4.1 Specific Test

4.2 General Tank Test

4.3 Stevens Collapsed Data Test

4.4 Turbulence Control and Correction of Frictional Drag

4.5 Take-off Calculations

The primary purpose of the previous articles is to expose the basic principles involved in the process of planing, and to give the reader the understanding and the means of judging test data. The art of predicting the performance of a hull on the basis of its design characteristics is in its infancy, and in practice the design is laid out on the basis of the designer's experience, and usually is subjected to tests in the towing tank.

There are three systems of planning the test, and of presenting the test data:

- a. Specific Test
- b. N.A.C.A. General Test
- c. Experimental Towing Tank of the Stevens Institute of Technology Collapsed Data Set

4.1 Specific Test

The "specific test" is made to verify, and to present by graphs the characteristics of a specific designs at a specific initial load, and the specific take-off speed. It is the simplest test, and it gives the data usable directly with the minimum amount of calculations. Since the form of the function of the speed coefficient  $F(C_V) = F\left(\frac{V}{\sqrt{gb}}\right)$  or  $F\left(\frac{V}{\sqrt{gL}}\right)$  in Eq. 8 of the last chapter, is unknown, the model and the full-scale prototype can be compared only at identical values of the speed coefficient  $C_V$ . Therefore the speed of the test is related to the size of the model by the Froude law of similarity:.

$$V_m/V_{fs} = \sqrt{L_m/L_{fs}} = \lambda^{\frac{1}{2}}$$

where the subscript m denotes the model, the subscript fs denotes the full scale, and  $\lambda$  is the scale, i.e. the ratio of any linear dimension of the model to that of the full scale [not to be confused with wetted length-to-beam ratio  $\lambda$  discussed earlier in Planing theory]. The size of the model is

## Tank Testing and Take-off Calculation

chosen, after consultation with the test tank staff, to be as large as the capacity of the towing equipment permits in regards both to the weight and the speed, with the latter being usually the critical limit. The model is supported by the pivoted connection placed at the point corresponding to the location of the center of gravity of the complete seaplane. The center of gravity of the model is brought to this point by a system of counterweights. The weight of the model is also brought to the correct weight  $W$ :

$$W_m = \Delta_m = \lambda^3 W_{fs}$$

If the model is too light, the weights are added to it. If it is too heavy, it is counterbalanced, or "unloaded" by the means provided in the design of the towing carriage. Various features of the test are best explained by the reference to Figure 1, showing the form in which the results are usually reported. The "load" curve gives the weight supported by the hull at any speed. The initial loading is equal to the weight of the seaplane to the proper scale, or otherwise to the displacement at rest  $\Delta_0$ . The wings are assumed to remain at a constant angle of attacks so that at any speed  $V$  the load on water is:

$$\Delta = \Delta_0 (1 - V^2/V_0^2)$$

where  $V_0$  is the take-off, or getaway speed at which the load on water  $\Delta=0$ . This relation is referred to as the "parabolic unloading curve". Such an unloading is achieved in the test by either suitable adjustment of the model loading, or by a hydrofoil immersed in waters and adjusted so as to balance fully the weight of the model at the getaway speed.

With the model "free to trim", i.e. to assume any attitude solely under the action of the water forces, the following quantities are measured:

- a. Vertical displacement of the model with respect to its position at rest, referred to as the change of draft", "heave" or "rise".
- b. The angle of trim the model assumes.
- c. The resistance.

All of these quantities are plotted against the speed as shown on Figure 1. These tests are made for the series of speeds from the start to the highest speed at which the test can be safely performed. At too high a speed the model may develop the tendency to dive, endangering both the model and the apparatus. Usually, the test can be carried to the speed at which the angle of trim, diminishing with it, drops to about 5 degrees. If the model tends to

## Tank Testing and Take-off Calculation

oscillate, this is eliminated by connecting it with a dashpot giving sufficient damping.

The hull design may be such that the model left to itself assumes the angle of trim different from the one desired for the best performance. To check this, certain test runs are repeated with the model restrained from pitching, i.e. are run at a "fixed trim", and the following quantities are measured

- a. The change of draft.
- b. Pitching moment exerted by the model.
- c. Resistance.

The range of these tests usually covers the most probable attitudes of the seaplane, i.e. the large trim angles at the hump, and the low trim angles at higher speed; so as to furnish additional data not obtained in the free-to-trim test. On Figure 1 the corresponding curves are distinguished by the indication of the angle of trim.

Now certain features of the test curves can be pointed. It is noted that both the "change of draft" and the "angle of trim" curves show a slight dip at (A) at very low speed, shortly after the start of the take-off run. This is primarily due to the suction generated by the water flow around curved bow sections of the hull.

In the satisfactory hulls this feature is of no importance. In certain hulls, however, the excessive curvature of the lines at the bow, combined with excessive draft at the bow, makes this small dip to develop into the complete diving.

The next point of importance is the maximum in the resistance curve at (B) usually referred to as the "hump" This is the critical point which often will determine the ability of the seaplane to take off, as this is described in the section on take-off calculations.

The hump in the resistance curve is usually associated with the maximum in the angle of trim curve although often it may occur at a somewhat lower or higher speed. As can be seen from Figure 7, the higher the trim of the hull at the hump, the higher will be its resistance. To reduce the resistance, it is necessary to reduce the angle of trim, and this can be achieved by either reduction of the sternpost angle, or by increasing the afterbody length. The reduction of the trim angle will decrease the resistance only if the region in which the buttock lines are straight is long enough to accommodate the increased wetted length resulting from the decrease of the angle of trim. Because of these considerations, it is highly desirable that during the test,

## Tank Testing and Take-off Calculation

the wetted length be observed with respect to the suitable markings on the model.

After passing the hump speed, the slight break in the trim curve at (C) corresponds to the rise of the stern from water, and to the beginning of the planing on the forebody alone. As the hump the speed is low, the wetted area is large, and the stern load  $\delta$  is therefore also large. The orientation of the force vector  $\delta$  is such, however, that it does not contribute to the total drag, which therefore corresponds to the load  $\Delta - \delta$  rather than  $\Delta$ . The increase of the planing speed above the hump causes the decrease of the wetted length, although the rate of this decrease is tempered by the simultaneous decrease of the angle of trim. Eventually the wetted length is shortened to such an extent that the resultant force acting on the forebody passes through the center of gravity, becomes zero, and the second step leaves the water surface. The angle of trim between the hump and the point (C) of Figure 10 is determined by the sternpost angle and the wake configuration, giving a broad low peak of the resistance curve. Were the sternpost angle increased so that the trim  $\tau$  would become much larger, the wetted length would become shorter, the sternpost load  $\delta$  at hump would become light, and a very small increase of the speed would reduce it to zero. The points B and C would almost coincide. If no external moments were applied, the resultant of the forebody pressure would have to remain thereafter in one position determined by the position of the C.G. This means that the wetted length would have to remain essentially constant, and the increase of the speed would have to be compensated by the decrease of the angle of trim  $\tau$ . The trim, too high at the hump, would tend to become too low at the high speed. The resistance curve would display a high and sharp peak at the hump, with the tendency to rise again at high speed.

# Tank Testing and Take-off Calculation

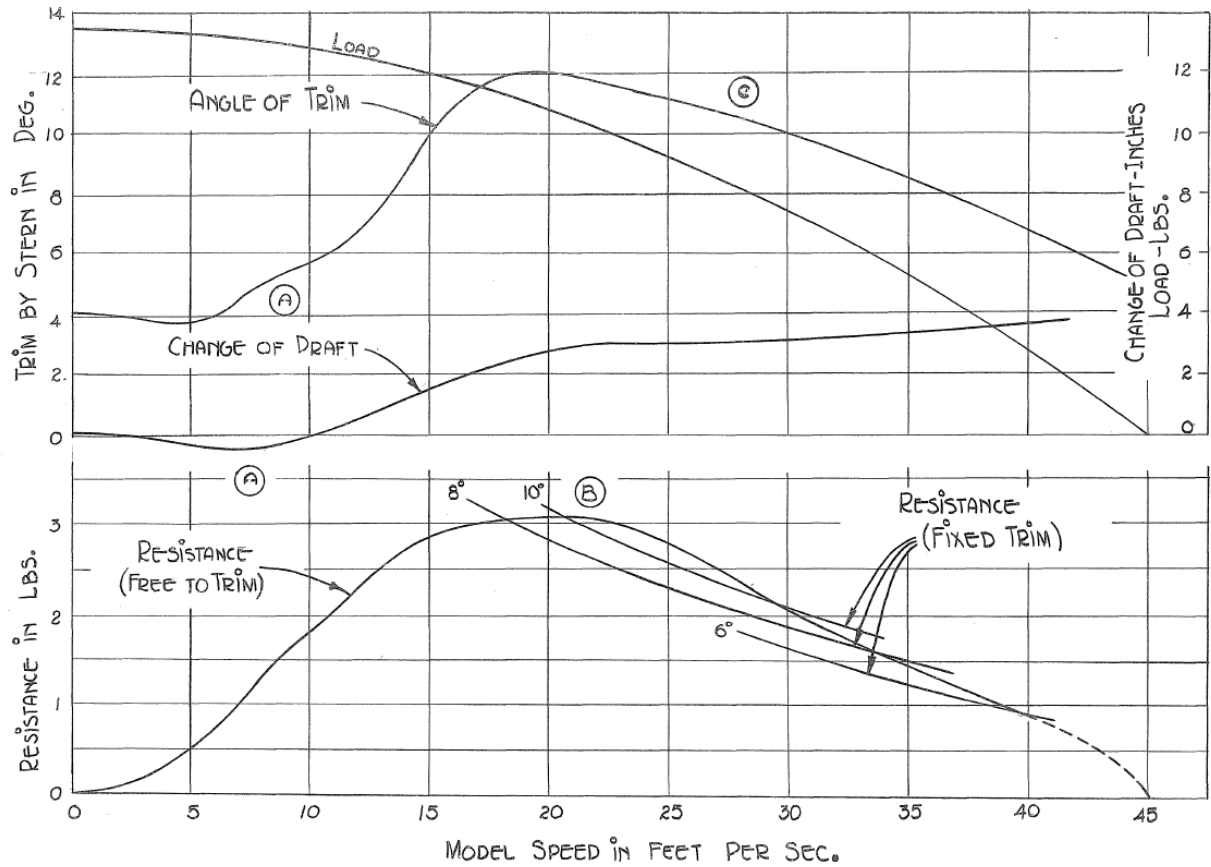


Figure 1: The Typical Set of the Resistance, Trim and Heave Curves from the Specific Test of a Model.

#### 4.2 General Tank Test

The drawback of the specific test is found in the lack of means of using the data for the speeds and loads other than those used in the test. The N.A.C.A. "General Tank Test" was devised to give the data which can be used for the wide range of loads, speeds, and hull sizes. For this purpose, all test data are put into the form of non-dimensional coefficients:

$$\text{Load Coefficient } C_{\Delta} = \Delta / wb^3$$

$$\text{Resistance Coefficient } C_R = R / wb^3$$

$$\text{Speed Coefficient } C_v = V / \sqrt{gb}$$

$$\text{Trimming Moment Coefficient } C_M = M / wb^4$$

$$\text{Draft Coefficient } C_d = d / b$$

where:

$\Delta$  displacement in units of weight.

$w$  weight of water per unit volume.

$b$  beam.

$d$  draft.

$V$  speed.

$M$  pitching moment about c.g. of the seaplane.

$g$  acceleration of gravity.

any consistent system of units can be used such as pound-foot-second, or metric ton-meter-second.

$C_R$  and  $C_M$  are determined by test, and are plotted against  $C_v$ , with  $C_{\Delta}$  as a parameter. A separate plot is made for each value of the trim angle  $\tau$ . Figure 2, taken from Dawson(1938) gives the data for  $\tau=7$  degrees. This particular report covered the values of  $\tau=3, 5, 7, 9$  and 11 degrees.

The drawback of the plot shown on Figure 2 is that it is impossible to judge where the best value of  $R/\Delta$  is. For this purpose, the alternate way of presenting the general test data is shown on Figure 3, also taken from Dawson(1938) The resistance coefficient  $C_R$  is plotted against the angle of trim  $\tau$  with  $C_{\Delta}$  and  $C_M$  as parameters. Thus for a given trim angle and loading, the resistance, and the pitching moment are readily read from the chart. A

## Tank Testing and Take-off Calculation

separate chart is prepared for each value of  $C_v$ , and two such charts for  $C_v$  of 3.5 and 4.0 are included on Figure 3.

Attention is called to the wide range of values of  $C_\Delta$  used, so that, every conceivable condition occurring during the take-off run of a seaplane is represented. This is very important advantage for N.A.C.A. reports, which are used by many designers for many problems. The disadvantage is in that the plots do not convey directly the picture of the take-off performance and the data have to be read from the general test charts, and put into the form of the specific test for the analysis of the specific problem. While very large and expensive test schedule is needed to cover the broad field, for which the data are intended, the number of points which can be obtained for a specific problem is rather small, and there may be some difficulty in the precise definition of the specific curve.

Example: Assume a flying boat to which the data given by Figure 2 apply, with the beam of 10 feet, the gross weight of 64,000 pounds, and the getaway speed of 100 ft. per sec. operating in sea water. Find the resistance and the pitching moment occurring at 60 ft. per sec.

$$C_{\Delta_0} = 64,000/64 \times 10^3 = 1.00$$

$$C_\Delta = 1.00 [1 - (60/100)^2] = .64$$

$$C_v = 60/\sqrt{32.2 \times 10^3} = 3.34$$

From Figure 2  $CR = 0.117$  and  $CM = +0.06$

$$\text{Resistance} = .117 \times 64 \times 10^3 = 7480 \text{ pounds.}$$

$$\text{Moment} = .06 \times 64 \times 10^4 = 40,300 \text{ ft.lbs.}$$

The computations of this type can be readily arranged in a tabular form to cover a number of values of  $V$  throughout, the speed range, thus furnishing the data for the plot of the resistance and moment curves. Making the computations for the several values of the angle of trim will indicate the most favorable attitude of the boat for any speed. The use of plots of the type shown on Figure 3 will save some labor, since the best values of trim are directly indicated.



# Tank Testing and Take-off Calculation

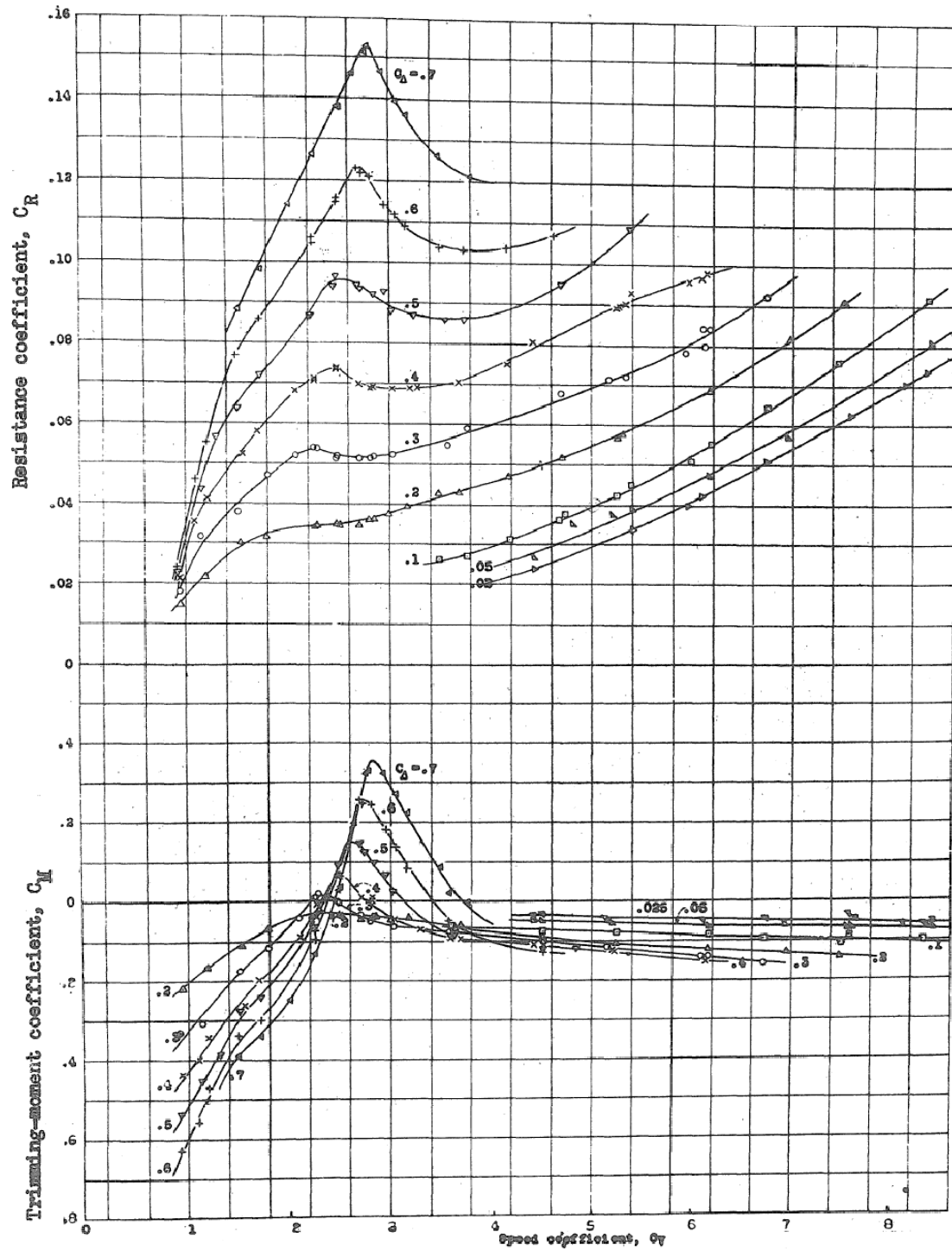


Figure 2: The Plot of the General Tank Test Data for trim  $\tau = 7$ -degrees  
(Taken from N.A.C.A. Tec. Note No. 681 Dawson, 1938)

4-9

#### 4.3 Stevens Collapsed Data Test

The method of plotting the data, originated at the Stevens Institute of Technology, and described in Locke (1944), aims at giving the data of the General Test type with lesser number of test points, and in a more compact form. It, also demonstrates more clearly how satisfactory test data can be obtained from a model which is too large for the available tank capacity to permit, the straightforward specific test shown on Figure 1. It is the direct outcome of trying to get greater usefulness of test, tanks which are much smaller than the tanks of N.A.C.A. The seaplane hull performance is considered in two separate parts -- below and above the hump speed. Below the hump speed the attitude of the hull is determined by the hull interaction with the wave it creates, and very large moments would be needed to modify this natural angle of trim. The effect of aerodynamic controls is therefore weak, and to the first approximation can be neglected. The hull therefore is tested free to trim, and the angle of trim and the resistance are recorded. Below the hump, i.e. in the displacement range, the resistance coefficient is a function of the Froude Number:

$$R/\frac{1}{2}\rho V^2 L^2 = f(V^2/gL)$$

where L is any characteristic dimension. Defining L as proportional to cube root of length

$$L = \left(\frac{\Delta}{w}\right)^{\frac{1}{3}} = \left(\frac{\Delta}{\rho g}\right)^{\frac{1}{3}} = (V)^{\frac{1}{3}}$$

and substituting the N.A.C.A. coefficients puts the above expression into the form:

$$\frac{C_R}{C_{\Delta}^{2/3} C_V^2} = f\left(\frac{C_V^2}{C_{\Delta}^{1/3}}\right)$$

[Note, the speed term is a version of the Volumetric Froude number used for planing craft]

The typical free-to-trim test, curve expressing the above relation is shown in the middle section of Figure 4. Considerable range of the hull loadings  $C_{\Delta}$  of a given hull is found to give the same curve, and conversely one curve can be taken to represent considerable range of loadings, so that

it is not necessary to test actually for many loadings. The overloading may give, however a somewhat higher resistance and a higher trim angle, and therefore tests should be made for this condition. With the general shape of the curve well established, relatively few check points are needed for this.

Above the hump speed and particularly at the important range near take-off or getaway speed the aerodynamic controls are effective and a pilot is usually able to keep the hull at any attitude he chooses. Therefore, the tests for the planing range above hump are made at a series of fixed trims. In this range the resistance can be assumed to be approximately independent of the Froude Number, and for a given angle of trim, dependent on the loading only. This statement is essentially equivalent to neglecting the second term in square brackets in Eq. (6) and in Eq. (14) of the last chapter, neglecting the variation of  $C_f$  with Reynolds Number. The neglect of the effect of these variables permits to write in the coefficient form:

$$\frac{\text{Resistance}}{\frac{1}{2} \rho V^2 L^2} = f\left(\frac{\Delta}{\frac{1}{2} \rho V^2 L^2}\right)$$

or substituting the N.A.C.A. coefficients:

$$\frac{\sqrt{C_R}}{C_v} = f\left(\frac{\sqrt{C_\Delta}}{C_v}\right)$$

Test results are computed, and the above relation is plotted as on Figure 5 giving a curve for each angle of trim. By cross plotting the curves of the trim vs.  $C_R/C_v$  with the  $C_\Delta/C_v$  as parameter are finally obtained. These are shown separately on Figure 6, and as a part of the lower diagram on Figure 4.

Example: Assume the hull shown on Figure 4 to be used with the beam of 8 feet, gross weight of 27,000 pounds, and getaway speed of 90 ft. per sec., assuming the parabolic unloading curve. Find the resistance:

# Tank Testing and Take-off Calculation

$$C_v = 70 / \sqrt{32.2 \times 8} = 4.37$$

$$C_{\Delta_0} = 27,000 / 64 \times 8^3 = .82$$

$$C_{\Delta} = .82 \left[ 1 - (70/90)^2 \right] = .32$$

$$\sqrt{C_{\Delta}} / C_v = .13$$

From the lower chart of Figure 4:

$\sqrt{C_R} / C_v = .0625$  at the angle of trim of 9 degrees  
at which the pitching moment coefficient  $C_M$  is  
zero.

The Ratio

$$\left[ \sqrt{C_R} / C_v \right] \div \left[ \sqrt{C_{\Delta}} / C_v \right] = \sqrt{C_R / C_{\Delta}} = .0625 / .13 = .48$$

$$\underline{C_R / C_{\Delta} = .23} \quad C_R = .23 \times .32 = .0737$$

Resistance

$$.0737 \times 64 \times 8^3 = 2420 \text{ lbs.}$$

The resistance can be reduced by applying a nose-down moment by means  
of elevators so that angle of trim be reduced from 9 degrees to 6 1/2  
degrees, at which  $\sqrt{C_R} / C_v$  of .0575 is obtained, or  $R/\Delta = 0.195$

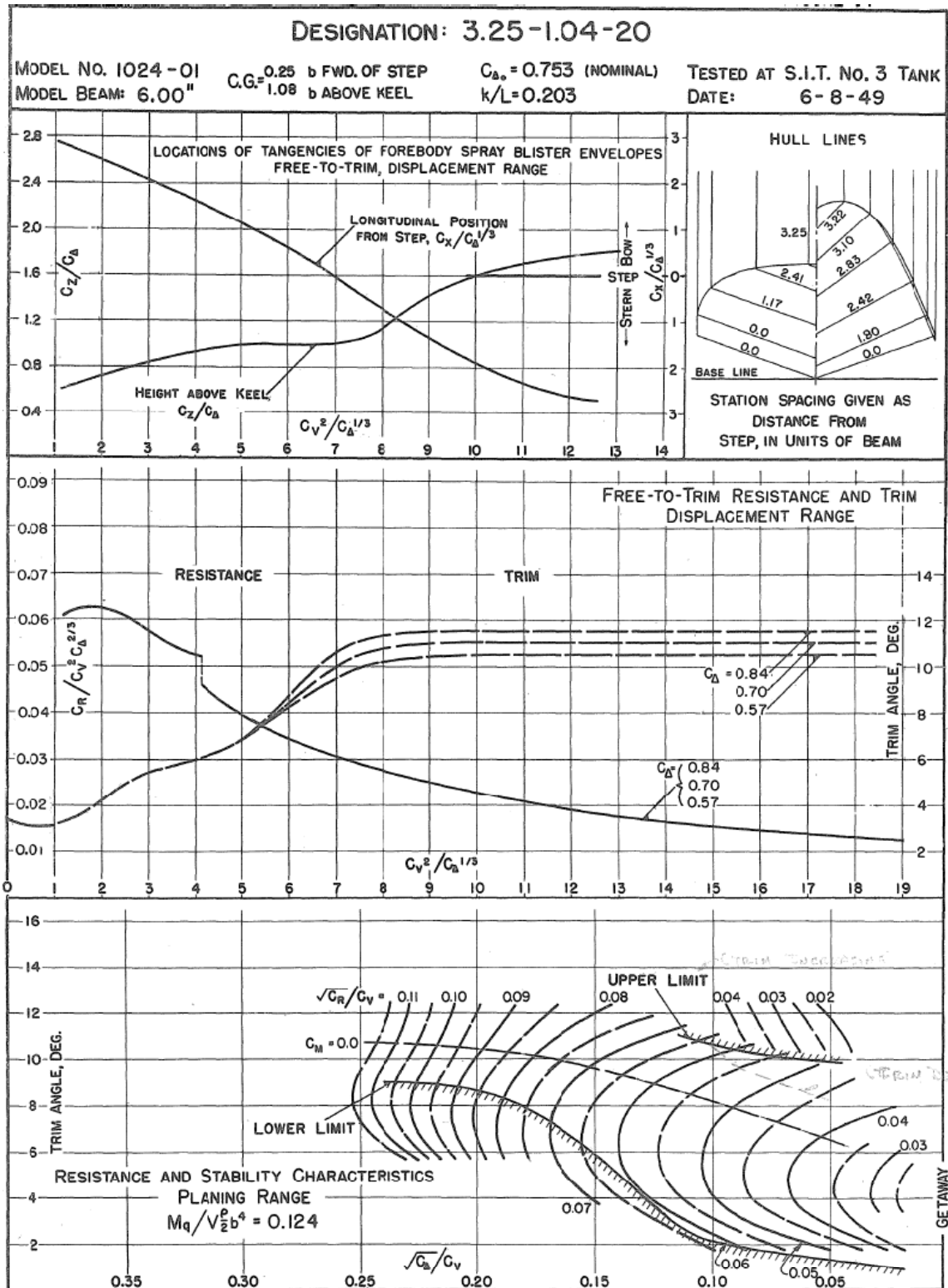


Figure 4: Typical Collapsed Summary Chart of the General Tank Test Data  
 (Taken from N.A.C.A. Tech. Note No. 1182.)

# Tank Testing and Take-off Calculation

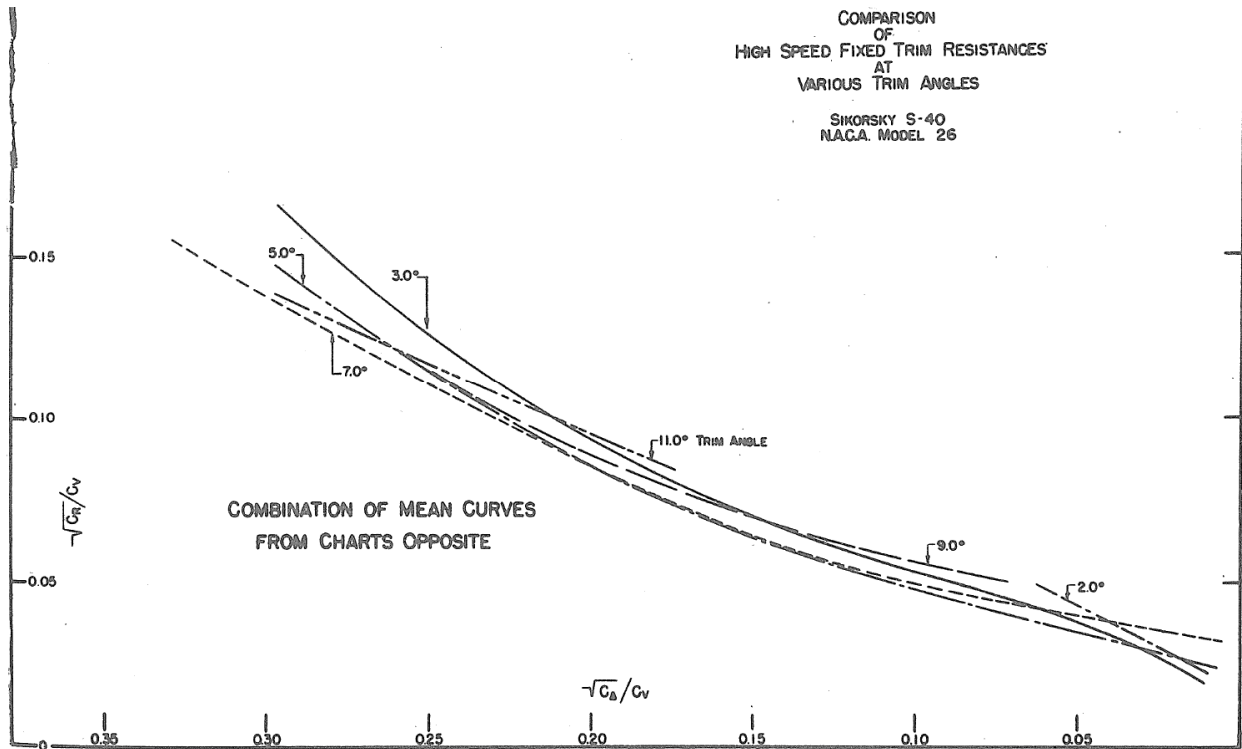


Figure 5: Plot of  $\sqrt{C_R}/C_V$  vs.  $\sqrt{C_D}/C_V$  for the Fixed Trim Resistance Tests (from N.A.C.A. Wartime Report No. W-70)

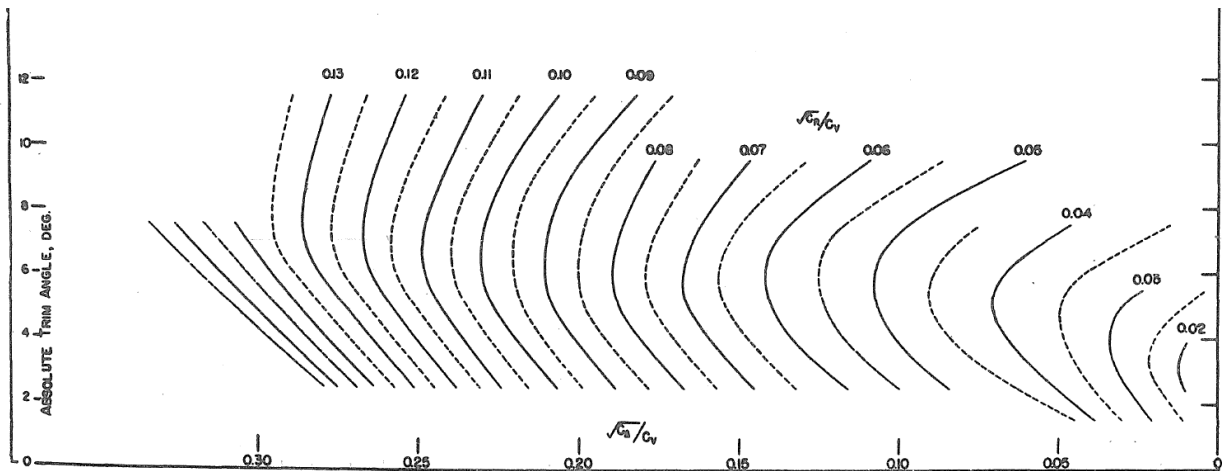


Figure 6: The Angle of Trim vs.  $\sqrt{C_D}/C_V$  with  $\sqrt{C_R}/C_V$  as a Parameter by Cross Plotting the Data of Figure 5 (Taken from N.A.C.A. Wartime Report No. W-70)

#### 4.4 Turbulence Control and Correction of Frictional Drag for Changes in Reynolds Number

A small model tested in a towing tank at low speed may have a partly laminar flows, so that friction drag coefficient may be anywhere between the laminar and the turbulent (Schoenherr's) drag coefficient curves. In order to avoid the uncertainty in  $C_f$  value, the turbulence may be introduced by means of towing an approximately vertical piece of round rod or wire in front of the model and close to it. The turbulent wake of the rod induces the turbulence in the boundary layers [2024 note - sometimes, not always] and raises the  $C_f$  value to the Schoenherr's curve, the use of which permits the recalculation of it from the Reynold's number of the test model to that of the full-scale prototype. The measurements of wetted areas needed for direct application of friction drag formulae are very seldom made [2024 note - Much more common now, given the availability of underwater photos]. However, a simple method of correction can be devised by using the ratio of Reynolds numbers  $Re_m/Re_s$  where subscripts m and s designate the model and the full-size prototype. Using the exponential form of expression for  $C_f$ , such for instance as Prandtl-Von Karman formula, we can write:

$$\frac{C_{fs}}{C_{fm}} = \left(\frac{Re_m}{Re_s}\right)^{0.2} = \left(\frac{V_m L_m}{V_s L_s}\right)^{0.2} = \left(\lambda^{\frac{1}{2}} \cdot \lambda\right)^{0.2} = \lambda^{0.3}$$

For the range of values of  $Re > 2 \times 10^6$  where the Prandtl-Von Karman formula does not, apply directly it can be made to approximate Schoenherr's line at  $Re_m$  and  $Re_s$  by replacing the exponent 0.2 by another suitable value. Since the specific test is made on the basis of identical Froude Number for the model and the full-scale prototypes the wave formation of the model is identical with that of the prototype, and the distribution of wetted area is identical. The friction resistance is therefore proportional to  $C_f$ . The procedure of making the correction, therefore, is as follows:

$$\begin{array}{rcl} \text{Total measured resistance at the} & & \\ \text{angle of trim } \tau & \text{---} & = \text{ say A} \\ \text{Resistance due to load } \Delta = \Delta \tan \tau & \text{---} & = \text{ say B} \\ \hline \text{Frictional Resistance} & \text{---} & = A-B \\ \\ \text{Corrected Frictional Resistance } (A-B)\lambda^{0.3} & \text{---} & = C \\ \text{Total Corrected Resistance} & \text{---} & = B + C \end{array}$$



Care should be taken to define  $\tau$  as the true mean inclination of the planing area and not as a nominal figure referred to an arbitrary reference line.

#### 4.5 Take-off Calculations

In the problem of making the take-off calculations, the initial load and the getaway speed are determined by the design of the seaplane. Since the minimum drag of the hull at high speed occurs at the angle of trim of about 6 degrees, this angle of the keel is assumed, and corresponding angle of incidence of wings is taken in computation of the take-off speed. The flaps are found usually beneficial when lowered for the take off to the angle of approximately half of that used for landing. The lift coefficient obtained on this basis is further increased by the ground effect, by the slipstream of the propeller, and by the vertical component of the propeller thrust. As a rough rule it is suggested that lift coefficient be increased by 25% to account for these factors.

The parabolic unloading curve can be usually assumed. For a given speed, the loading is read from this curve, the  $C_v$  and  $C_A$  are computed, and from these  $C_v^2/C_A^{1/3}$  and  $\frac{\sqrt{C_A}}{C_v}$ . The corresponding values of  $C_R$  and of the trim  $\tau$  are then determined from a suitable data report, such for instance as Locke (1947). These are used to construct the curves, similar to the ones which are given directly by the specific test. Computations based on the general test data can be carried out directly in terms of the full-size seaplane, as this has been done in two examples above. The data of a specific test usually refer to the model of a certain scale  $\lambda$  and have to be scaled up to the full size by the relations:

$$\begin{aligned} V_{fs} &= V_m / \lambda^{1/2} \\ R_{fs} &= R_m / \lambda^3 \end{aligned}$$

The angles of trim of the model and of the full-size seaplane correspond directly.

On Figure 7 the curve "hull drag" represents the sample plot of such a scaled-up drag. The aerodynamic drag is also plotted, and the two are added to form the total drag. The aerodynamic drag is computed for the attitude of the seaplane corresponding to the getaway angle of incidence, or approximately that of the steep climb. The increase of the drag due to the

propeller slipstream is taken into account. The propeller thrust is computed by the methods given in various courses and data books on aerodynamics, and the curve of thrust vs. scale is plotted. The difference between the propeller thrust and the total drag represents the force available for the acceleration. Since this force varies with speed, the acceleration has to be integrated over the entire speed range. This is accomplished most conveniently by the following graphical construction: compute the velocity reached in the first second  $a = g \times \text{thrust/weight}$ , where  $g$  is the acceleration of gravity = 32.2 ft./sec.<sup>2</sup>, convert it into m.p.h., plot on the speed axis of Figure 7, and draw the lines b-c and b-d which make the angle  $\pm \alpha$  with the vertical axis. The increment of speed  $a'$  gained in any of the following seconds is defined as  $a' = a \times (\text{thrust less drag})/(\text{initial thrust})$ , i.e. the increments of speed are proportional to the accelerating force. All that is needed, therefore, is to draw two series of the parallel strokes filling the space between the thrust curve and the total drag curve, each stroke inclined at the same angle  $\pm \alpha$  to the vertical, where  $\alpha$  is the angle of inclination of the initial stroke b-c. The number of strokes gives the number of seconds consumed in the process of take off. The zig-zag pattern of inclined strokes of Figure 7 permits to read off, and to plot the speed  $V$  versus time counted from the start. The take-off distance

$S = \int_0^t V dt$  is determined as the area under such a curve. The take-off time can be calculated also by an alternate method of integration. writing formally:

$$t = \int_0^{V_0} dt \quad (\text{Eq. 1})$$

substitute

$$dt = \frac{1}{a'} dV \quad (\text{Eq. 2})$$

## Tank Testing and Take-off Calculation

where:

$a'$  is the acceleration at a given instant defined as  $\frac{(T-R)g}{W}$   
 (T-R) is the effective net thrust, i.e. the difference between the propeller thrust and the total resistance (in pounds) as given on Figure 7.

$G = 32.2 \text{ ft/s}^2$  the acceleration of gravity

$V$  is the speed at any given instant

$V_0$  the getaway speed

$W$  - the gross weight

Substituting equation 2 into equation 1:

$$t = \int_0^{V_0} \frac{W}{(T-R)g} dV \quad (\text{Eq. 3})$$

The values of  $\frac{W}{(T-R)g}$  are computed for a series of values of  $V$  from 0 to  $V_0$ , preferably using uniform and even number of steps or increments  $\Delta V$ . The integral can be evaluated then by Simpson's Rule.

For more detailed discussion of the take-off computations consult Locke (1948), Pierson (1945), Wood (1947) and Diehl (1940).

It will be noted that there are two minima of acceleration: at the hump, and near getaway speed. The relative importance of these varies with the value of  $C_v$  at getaway. Large flying boats usually have low  $C_v = \frac{V}{\sqrt{gb}}$ , even if  $V$  is large, because of the large value of  $b$ . The hump speed is usually critical in such a case, while at the getaway speed ample excess thrust is available for the acceleration. Relatively small sternpost angles, producing relatively low trim angles are, therefore, in order. On the other hand, a small twin-float seaplane may have low  $V$ , but  $b$  is so small that resultant  $C_v$  is large. In such a case the total drag near getaway speed may approach the available thrusts leaving only a small margin for acceleration. The high speed range now has to be favored, the sternpost angle has to be large to avoid afterbody interference, even at the expense of the increased trim and the drag at hump speed. By varying the beam or the sternpost angle, the best compromise between the hump and the high speed range is achieved.

# Tank Testing and Take-off Calculation

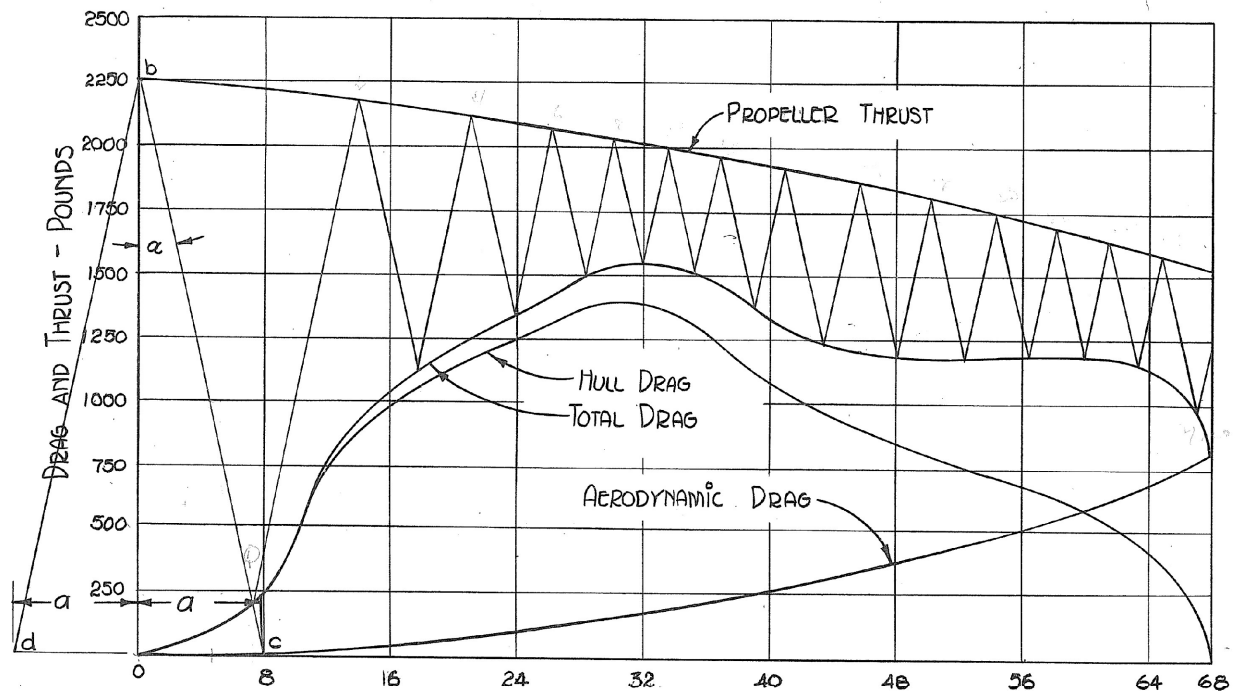


Figure 7: The Typical Set of Curves for Calculation of Take-Off Time

## Tank Testing and Take-off Calculation

### References for Chapter 4

Dawson, John R. "A General Tank Test of a Model of the Hull of the P3M-1 Flying Boat Including a Special Working Chart for the Determination of Hull Performance" NACA TN No. 681. 1938.

Diehl, Walter Stuart, "Engineering Aerodynamics" The Ronald Press Company, New York, Revised Edition, Fourth Printing, July 1940, pp 498-505

Locke, F.W.S. "General Resistance Tests on Flying-Boat Hull Models", NACA Wartime Report No W-70 (Originally ARR No.4B19). 1944

Locke, F.W.S. "A Collection of the Collapsed Results of General Tank Tests of Miscellaneous Flying-boat hull models." Naca Technical Note 1182. 1947.

Locke, F.W.S. Jr, "A Graphical Method for Interpolation of Hydrodynamic Characteristics of Specific Flying Boats from Collapsed Results of General Tests of Models", NACA TN No. 1259. January 1948.

Pierson, John D. and Burghardt, Joseph R. "A Specific Chart for Flying Boat Take-off Performance", Journal of the Aeronautical Sciences, April 1945.

Wood, Karl D., "Technical Aerodynamics", McGraw-Hill Book Company, New York, Second Edition, 1947, PPO 290-308.

### CHAPTER 5. LONGITUDINAL DYNAMIC STABILITY - PORPOISING AND SKIPPING

M.G. Morabito, 2024

- 5.1 Definitions
- 5.2 Stability of Single Planing Surfaces
- 5.3 Porpoising of Seaplanes
- 5.4 Skipping of Seaplanes
- 5.5 Stability Theory

#### 5.1 Definitions

Porpoising is a coupled oscillation in pitch and heave that can damage aircraft structures and make it impossible to achieve take-off. Figure 1 shows a typical diagram of porpoising. In the diagram, the seaplane enters an uncontrollable oscillatory motion with increasing amplitude, leading to an accident. Porpoising is a high-speed dynamic instability that is predicted by the lift coefficient of the planing surface, as well as the trim angle, as shown by Savitsky (1964) and confirmed by Celano (1998). Seaplane porpoising can result from the hydrodynamic characteristics of the forebody alone, as well as forebody-afterbody interactions. Whereas a planing hull has only one porpoising limit - an upper limit of trim above which porpoising will occur at a given speed -- a seaplane has two limits and must stay between them to prevent porpoising.

Figure 2 shows a typical plot of seaplane porpoising stability limits. The horizontal axis shows speed, and the vertical axis shows trim angle. It is necessary to stay between the two porpoising limits to prevent dangerous oscillations. The pilot has aerodynamic control at high speeds and can orient the seaplane between the limits if they are sufficiently separated. Poor designs have a very small stable region or none at all.

Skipping is an oscillation in heave (constant trim) that typically occurs during landings, but has been observed during take-off and also in steady speed towing tank tests. During a skip, the hull at high speeds will first be pulled downward into the water, and then suddenly jump out of the water, sometimes causing a loss of control. Studies by Locke (1946) Olson

## Porpoising and Skipping

(1948) and Lorio, Morabito and Pavkov (2015) indicate that it is related to afterbody angle, step height and step ventilation. However, tests by Sedov (1940) showed that it can occur in certain conditions with a simple flat planing surface and no afterbody.



Figure 1: Diagram of Floatplane Porpoising (Anon, 2004)

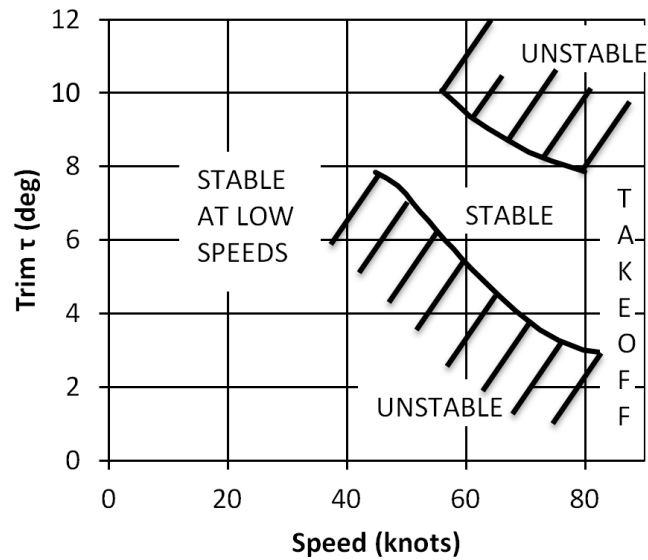


Figure 2: Example Trim Limits of Stability for a Seaplane

### 5.2 Stability of Single Planing Surfaces

Porpoising is a result of large hydrodynamic forces combined with insufficient damping. In the case of planing hulls, this occurs at high speeds (low lift coefficients) and high trim angles, where a very small wetted area of hull generates a very large amount of lift.

Figure 3 shows a graph for estimating the porpoising limits for a planing boat. The boat is stable at low trim angles and speeds. It is unstable at high trim angles and high speeds.

Figure 4 shows tests of a flat-bottom planing surface, extended to unusually high trim angles, with a pivot located farther aft and higher than in a typical planing boat.

- The planing surface is stable at low trim angles. Increasing trim enters an unstable “upper limit” like in planing craft.
- Further increases in trim angles (beyond typical planing boats), it become stable. This is where the seaplane forebody operates.
- The planing surface has another unstable range at very high trim angles. Sedov hypothesized this was related to “Skipping” and confirmed this by repeating the tests fixed-in-trim and finding the same limit.

The theory of stability for single planing surfaces has been explored extensively (See for instance Martin, 1970, Sun and Faltinson, 2011, and many others)



# Porpoising and Skipping

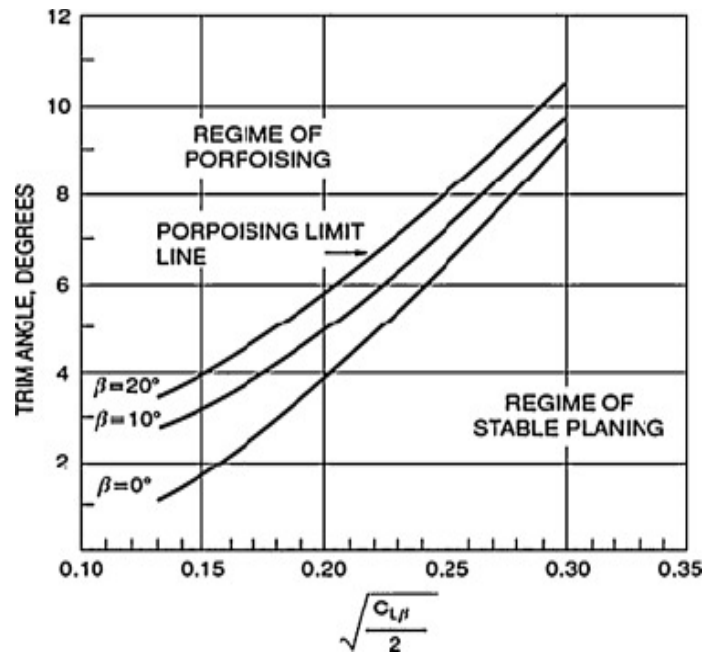


Figure 3: Day and Haag Porpoising Criteria (Taken from Savitsky, 1964) Note:  
Higher Speeds are to the Left,

## Porpoising and Skipping

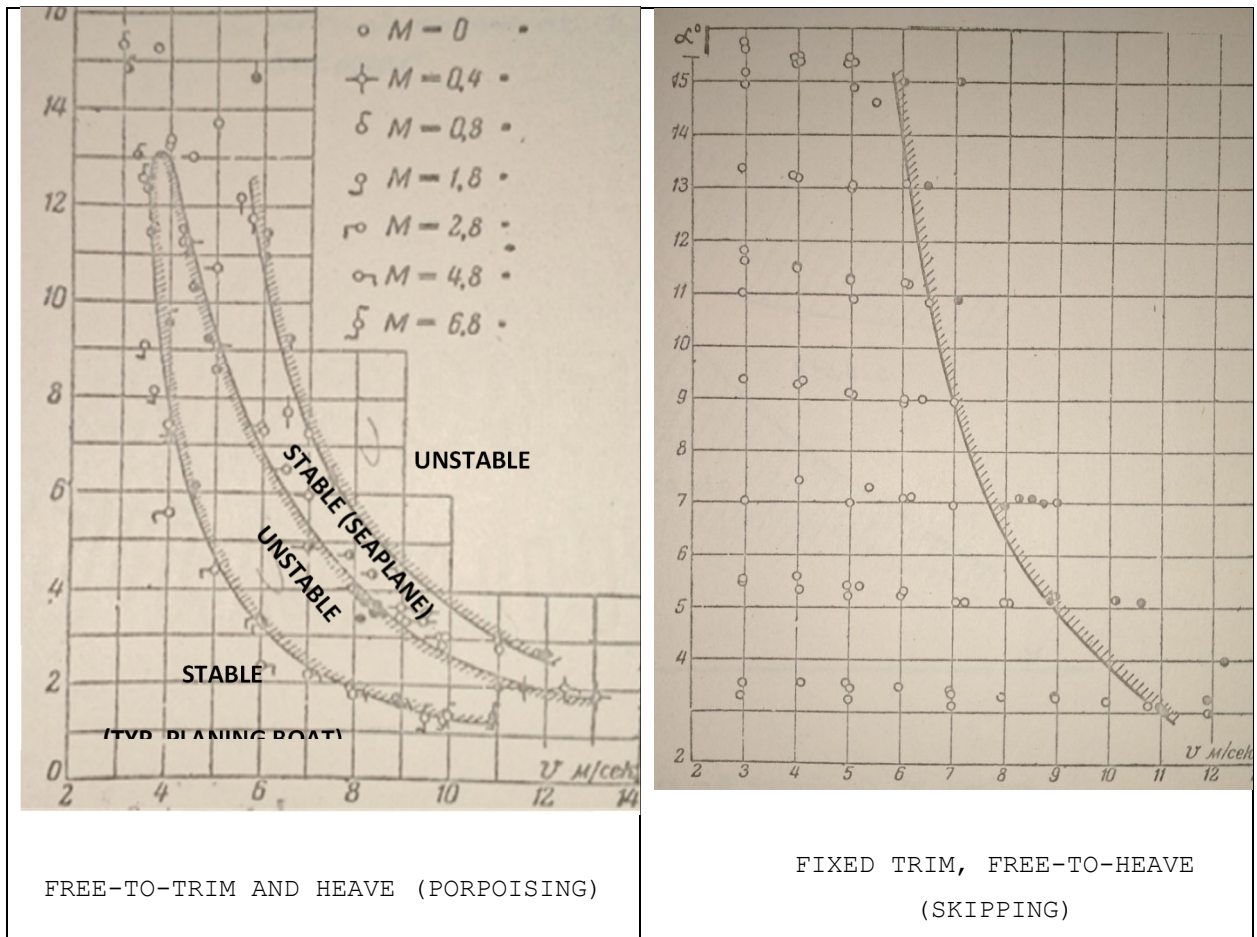


Figure 4: Porpoising Limits of Flat Planing Surface (Sedov, 1940)  
 Notes: X-Axis is Speed, Y-Axis is Trim. Pivot located 0.4 beams forward of trailing edge and 1 beam above plate. Load is 10kg on 0.3m beam.

### 5.3 Porpoising of Seaplanes

Figure 5 shows a picture of the seaplane in two-step planing. The dynamic stability is more complicated because of the interaction between afterbody and forebody.

Figure 6 summarizes the principal findings of an extensive series of tests by Davidson and Locke (1943) on the factors that affect porpoising, including afterbody geometries and loading.

- The forebody on its own is unstable below a certain trim angle for each speed. This can be predicted with the stability derivatives or test data made on the forebodies of seaplanes.
- Afterbody contact with the water stabilizes the hull. This is important at hump speed.
  - Lower sternpost angles (smaller step heights or afterbody angles) permit the seaplane to operate at lower trim angles, because it keeps the afterbody in the water.
- Near take-off, it is possible to plane on the afterbody alone, which is often unstable. This is the upper limit.
  - Lower sternpost angles put more load on the afterbody, and lower the "upper limit"
- There is a region of instability caused by improper ventilation of the afterbody at high speeds and trim angles. This is usually mitigated by incorporating enough step height.
- When the forebody and afterbody are BOTH in contact with the water, the seaplane is usually stable.
- Porpoising was shown to be a function of the lift coefficient, so a variety of speeds and loadings collapse on the same set of curves. The porpoising coefficient is identical to shown in Figure 3 for planing boats.

Figure 7 shows the experimental evidence for Davidson's summary diagram. It consists of a model tested with many different afterbody angles, step heights, and even without the afterbody. The envelope curve of all of the lower porpoising limits is the "Forebody Alone" curve.

## Porpoising and Skipping

- Lower sternpost angles (lower step height or afterbody angle) suppress the lower stability limit of the forebody because the afterbody is in contact with the water.
- Lower sternpost angles also lower the upper stability limit because it is more likely to be planing on the afterbody.

In actual landings and tests with powered models, a secondary upper limit has been shown. Once the seaplane begins experiencing upper limit porpoising, it must be trimmed to a much lower trim than the one needed to start it. The resultant new limit is known as "upper limit, trim decreasing," as opposed to the "upper limit, trim increasing" seen in most model tests. This is important when landing at high trim angles, which can initiate the instability.

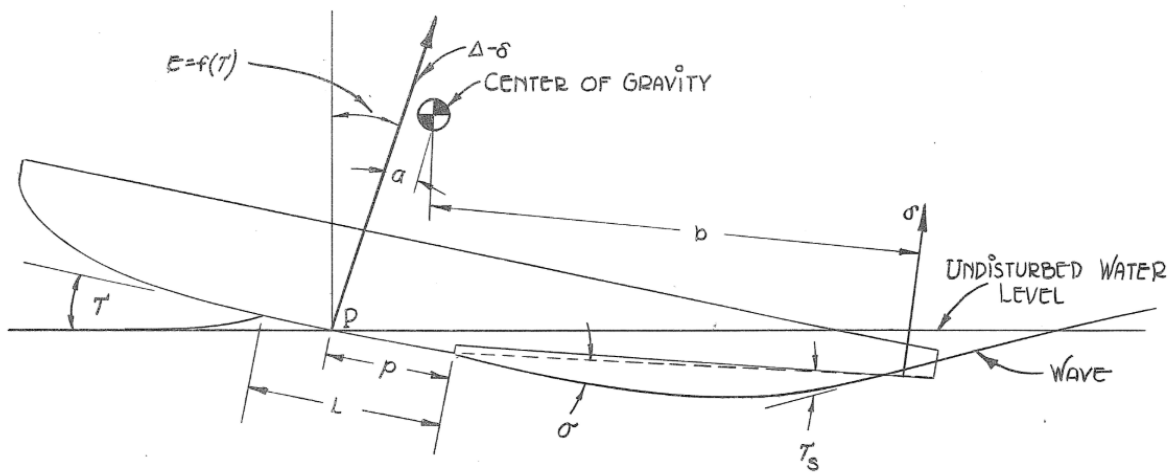


Figure 5: The Balance of Forces and Moments in Two-Step Planing (Taken from Stevens Seaplane Design Course Notes, B.V. Korvin-Kroukovsky 1950s)

# Porpoising and Skipping

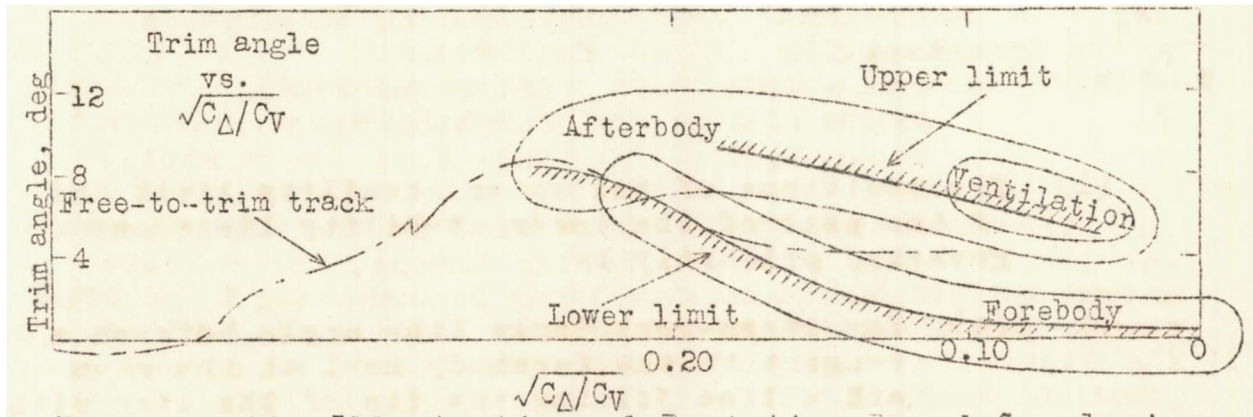


Figure 6: Broad Conclusions Regarding Porpoising, Showing the Regions Influenced by the Forebody, by the Afterbody and by Ventilation (Davidson and Locke, 1943)

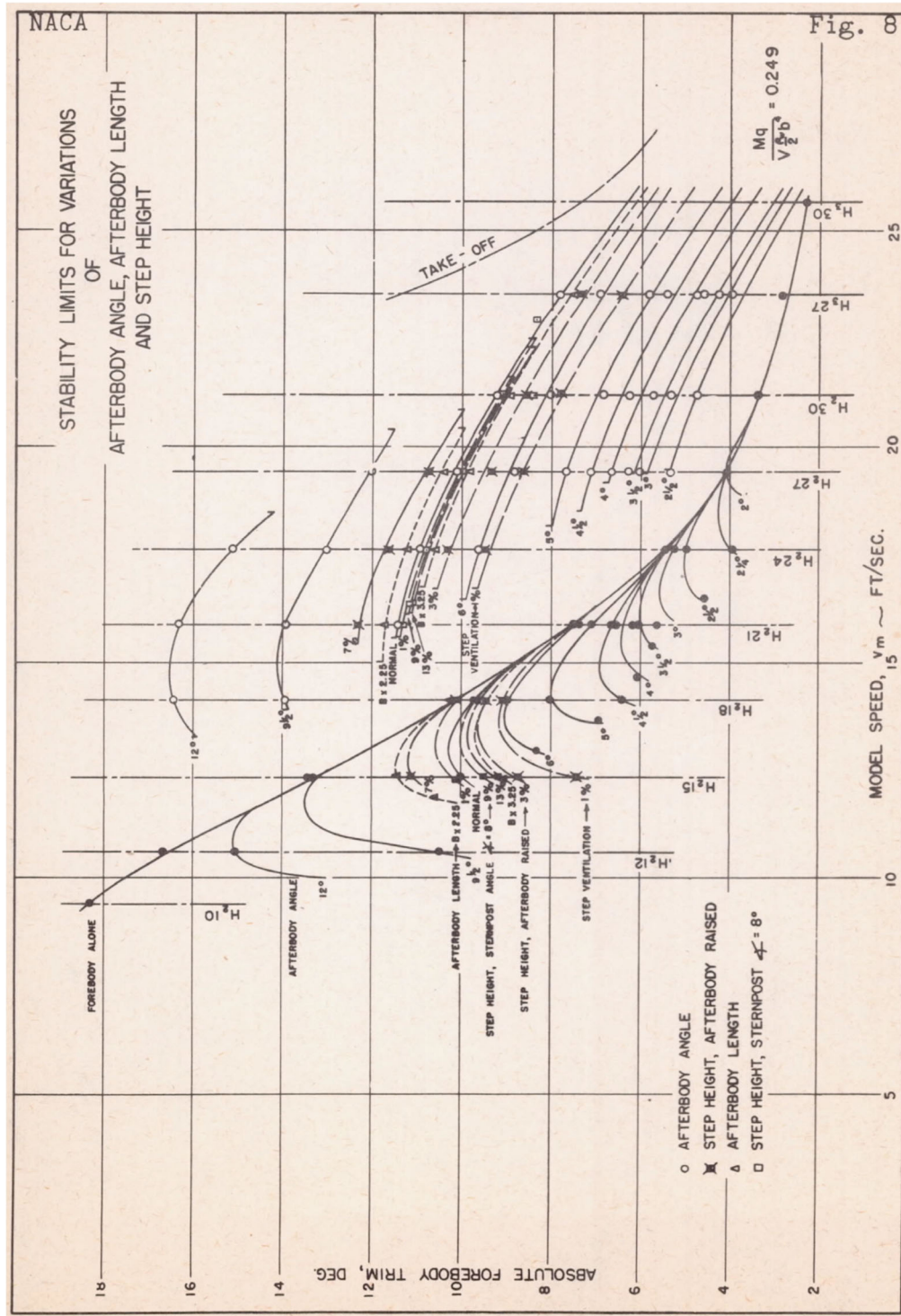


Figure 7: Stability Limits for Variations of Afterbody Angle, Afterbody Length and Step Height (Davidson and Locke, 1943)

#### 5.4 Skipping of Seaplanes

[Korvin-Kroukovsky, 1948] The term "skipping" is applied to describe the phenomenon of the seaplane leaving water upon landing, or bouncing even after a good landing. One or several skips may occur in landing. The skipping may be manifested also in take-off as a jump take-off, rather than a smooth transition from the water-borne planing to the air-borne flight. To quote from Locke (1946): "Skipping is associated with conditions whereby the forebody carries most of the water borne load and at the same time a large amount of water is washing over the afterbody bottom."

Prior to the contact with water, there exists the established air flow over the forebody, step and afterbody. At the instant of the contact this flow of air is interrupted at the step, while the inertia of the air moving along the afterbody, and the entrainment of this air by the water moving in close proximity to the afterbody generate the suction. The suction force distributed over the large area of the afterbody produces the downward force and the stalling moment. The downward force causes greater submergence, and brings into action greater wetted area than is required to support the small part of the seaplane weight which is not supported by wings. Subsequently the water surface in the rapidly developing wake is deflected downwards, greater clearance is created under the afterbody, and the suction is broken. The excessive life of the forebody, caused by the excessive submergence, as well as by the increase of the trim, accelerates the seaplane upwards, throwing it out of the water. These events occur in such a rapid sequence that the period of time from the first contact with water to the emergence of it is a fraction of a second for a dynamic model, and is found to be about one second for a certain 8000-pound flying boat (see Parkinson, 1943).

The primary remedy against skipping is the adequate ventilation of the step, which is achieved best by making it deep enough. The hull exhibiting unsatisfactory skipping characteristics due to the insufficient depth of step may be corrected by addition of ventilating ducts extending from the keel to not over half beam in breadth, and having the sectional area of about  $0.02(\text{beam})^2$ . The supply of air is

## Porpoising and Skipping

needed instantaneously at the time of the contact with water and therefore it is not necessary to extend ducts through the deck, but is sufficient to have them open to the interior of the hull. It is important however to guard against any constriction, or other impediment to the air flow, which is large for an instant in time.

The skipping is tested in towing tanks by using dynamic models and simulating landing by means of gradual deceleration of the towing carriage. Noting the number of skips per landing provides a simple means of comparison.

[Morabito, 2024] The ratio of step height to sternpost angle is useful to compare skipping results between hulls. Locke (1946) investigated the skipping characteristics of full-scale seaplanes, based on pilot input, and found that increased step height, reduced beam loading and reduced sternpost angle  $\sigma$  all tend to improve performance for hulls. Figure 8 shows a graph that may be useful in design. Olson and Land (1948) extended this work to higher L/B with model tests, arriving at a higher step height than predicted by Locke. Their formula can be expressed as:

$$h_{\%b} \geq 0.59 \frac{L_a}{b} AA$$

Where,

$h_{\%b}$  is step height in a percentage of beam

$L_a$  is the length of the afterbody (meters)

$b$  is the beam of the planing surface (meters)

$AA$  is the afterbody angle (degrees)

(this equation can use meters or feet since they cancel)

*Step Height Example:*

*Estimate the minimum step height for the following seaplane using Olson and Land's (1948) criteria*

$L_a = 12.8m$     $b = 3m$     $AA = 5.5$  degrees    $\sigma = 7.3$  degrees    $\Delta_0 = 56,000$  kg

*Ans:*

$$h_{\%b} \geq 0.59 \frac{L_a}{b} AA \geq 0.59 \frac{12.8m}{3m} 5.5 \text{ deg} = 13.8\%$$



## Porpoising and Skipping

Although Sedov (1940) showed that skipping can occur at very high trim angles on single planing surfaces, skipping is usually the result of low step heights and poor afterbody ventilation. To confirm some of the potential causes of skipping, experiments were conducted by Lorio, Morabito and Pavkov (2015) to isolate skipping (pure heave) from porpoising (heave and pitch) and rebound (an impact phenomena). This was done by fixing the model in trim and running it in calm water, eliminating wave impact, rebound or porpoising as possibilities.

Figure 9 shows a photograph of the skipping tests. The model was accelerated to a constant towing speed during the start of the run. As the model reached full speed, the stagnation line approached and then crossed the step. Once the stagnation line crossed the step, the following was observed, illustrated in Figure 10:

1. As the stagnation line crossed the step, the flow of air behind step was blocked by spray and solid water. The pressure taps recorded strong negative pressures.
2. The hull moved downward, deeper into the water, increasing the wetted area of the forebody. The large increase in area increases the hydrodynamic lift force on the forebody, while the negative pressures on the afterbody continue to pull the hull deeper into the water.
3. The suction broke on the afterbody and the hull accelerated upward.
4. The hull left the surface of the water and upon its return, repeated steps 1-4.

Further tests were made on the effects of variations in trim angle and step ventilation. Step ventilation eliminated the skipping tendency of this particular seaplane. These experiments seem to confirm Korvin-Kroukovsky's description.

An interesting solution to skipping is the planing tail seaplane shown in Figure 11. The step height very large and the afterbody provides very little hydrostatic support. The planing tail seaplane does not usually suffer from upper limit porpoising or skipping

(Suydam, 1952). While unsuitable for cargo aircraft due to diminished internal volume, they are very popular today for light one or two passenger recreational aircraft (Figure 12), where cargo carrying capacity is not important. They are also an excellent choice for unmanned aerial vehicles.

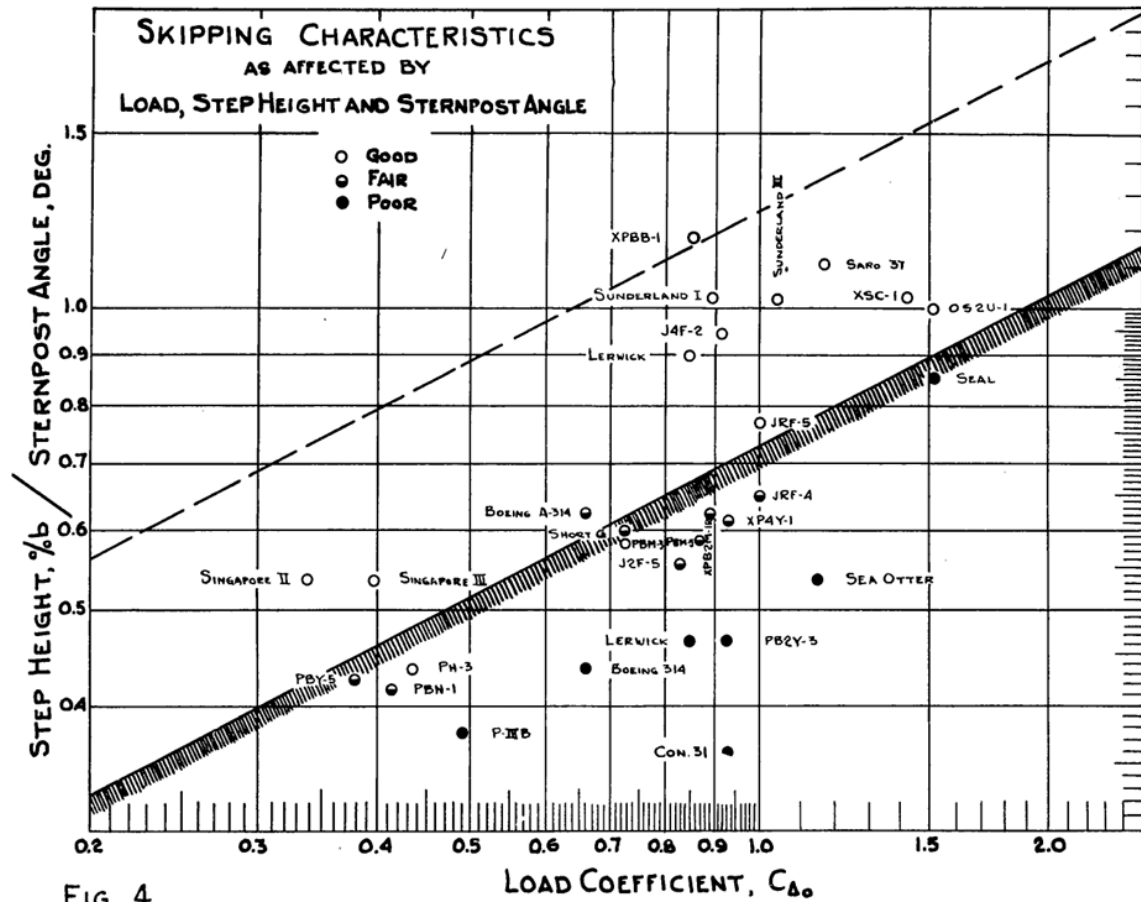


FIG 4

Figure 8: Skipping of Full-Sized Flying Boats (Locke, 1946) Note: All of the hulls in this study had a relatively small L/B from 4-7, and the results do not hold for higher L/B.

## Porpoising and Skipping

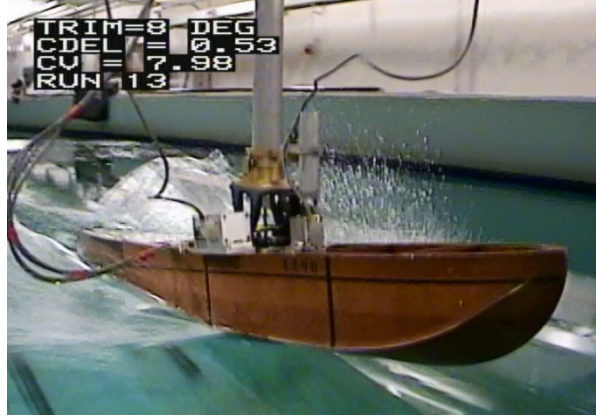


Figure 9: Photograph of Skipping Test (Lorio, Morabito, Pavkov 2015)

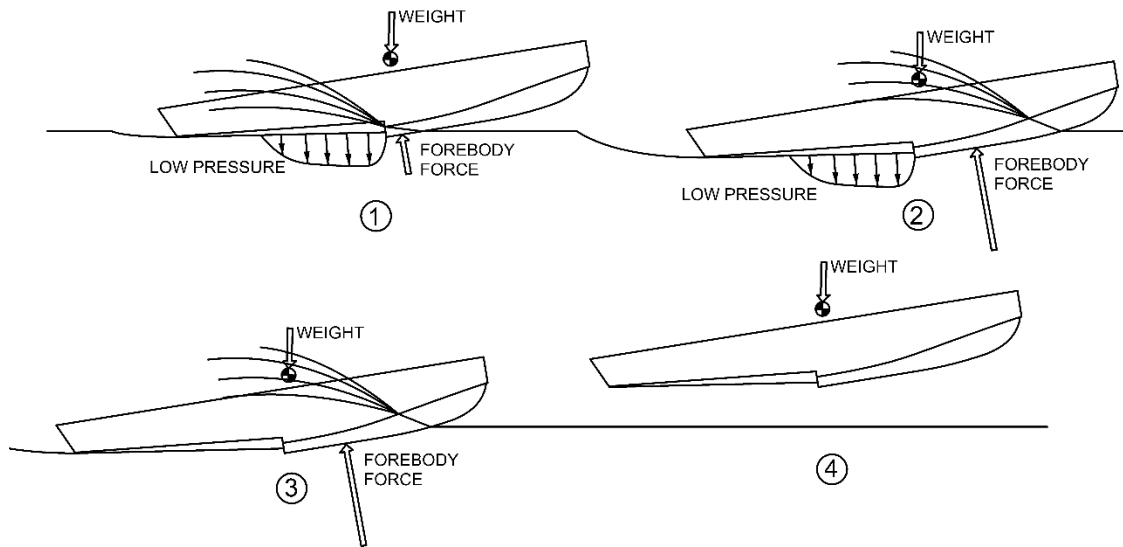


Figure 10: Illustration of Skipping (Lorio, Morabito, Pavkov, 2015)

## Porpoising and Skipping

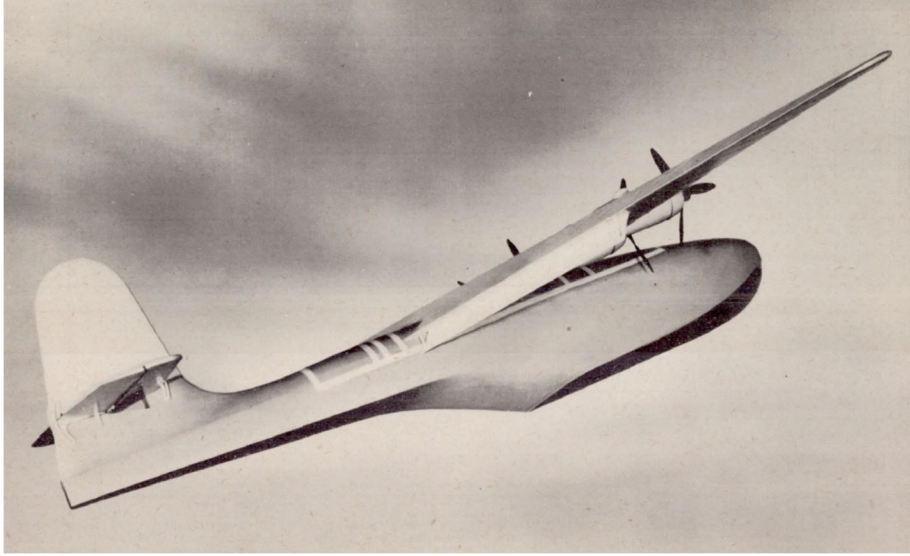


Figure 11: Planing Tail Seaplane (Suydam, 1952)



Figure 12: Icon A5 Seaplane (Taken from CNN.com)

### 5.5 Stability Theory

Perring and Glauert (1933) suggested that the porpoising stability of a seaplane could be estimated by use of linearized equations of motion in pitch and heave, and the "Routh Stability Criterion." This follows, to some extent, the process of determining stability in aircraft, but with the addition of the hydrodynamic force and moment derivatives. This method has lead to innumerable research papers on stability theory applied to planing boats or seaplanes. (See Davidson, Locke and Suarez 1943, Benson and Friehofner 1943, Martin 1976, Faltison 2005, Sun and Faltinson 2011, and many others)

The use of stability equations provides a means to estimate the effects of mass and pitch inertia; however, the overall process is difficult to implement in practice. For each combination of loading, speed and trim, there are four hydrodynamic stiffness derivatives that can be estimated from partially captive model tests, the Savitsky (1964) method or other planing force estimates.

Change in lift with change in draft  
Change in lift with change in trim angle  
Change in pitch moment with change in draft  
Change in pitch moment with change in trim angle

Figures 13 and 14 are an attempt to clarify each of these effects for the forebody alone, and also the forebody-afterbody combination. The figures are confusing and unhelpful because, based on different locations of center of gravity, wetted lengths, center of pressure, and strength of the afterbody, the signs on the terms can change. While not particularly helpful, they show how a hull could transition from stable to unstable depending on differences in loading, speed or trim. The complexity is frustrating.

In addition to the stiffness terms, there are four more hydrodynamic damping terms. These are related to the heave velocity and the pitch velocity. The velocity terms require assumptions such as how to treat the vertical velocity (Is it an effective increase or decrease in trim angle? Can it be treated as an increase in the

## Porpoising and Skipping

equivalent planing velocity?) and how to estimate the derivatives involving pitch (Where is the point of rotation taken about? The step? The forward extent of the wetted surface? The center of gravity? another location?) Added to these are all the aerodynamic terms.

Additional terms are included in some methods, such as Faltinson (2005) and Sun and Faltinson (2011), such as added mass terms that can be theoretically derived from strip theory, or experimentally measured with oscillating model tests. Faltinson (2005) shows the sensitivity of the method to the estimates of the added mass terms.

Given the complexity, the large number of assumptions, and the high probability of error, it is expedient to simply run the porpoising tests with a model, rather than try to determine all the terms in the equations of motion.

# Porpoising and Skipping

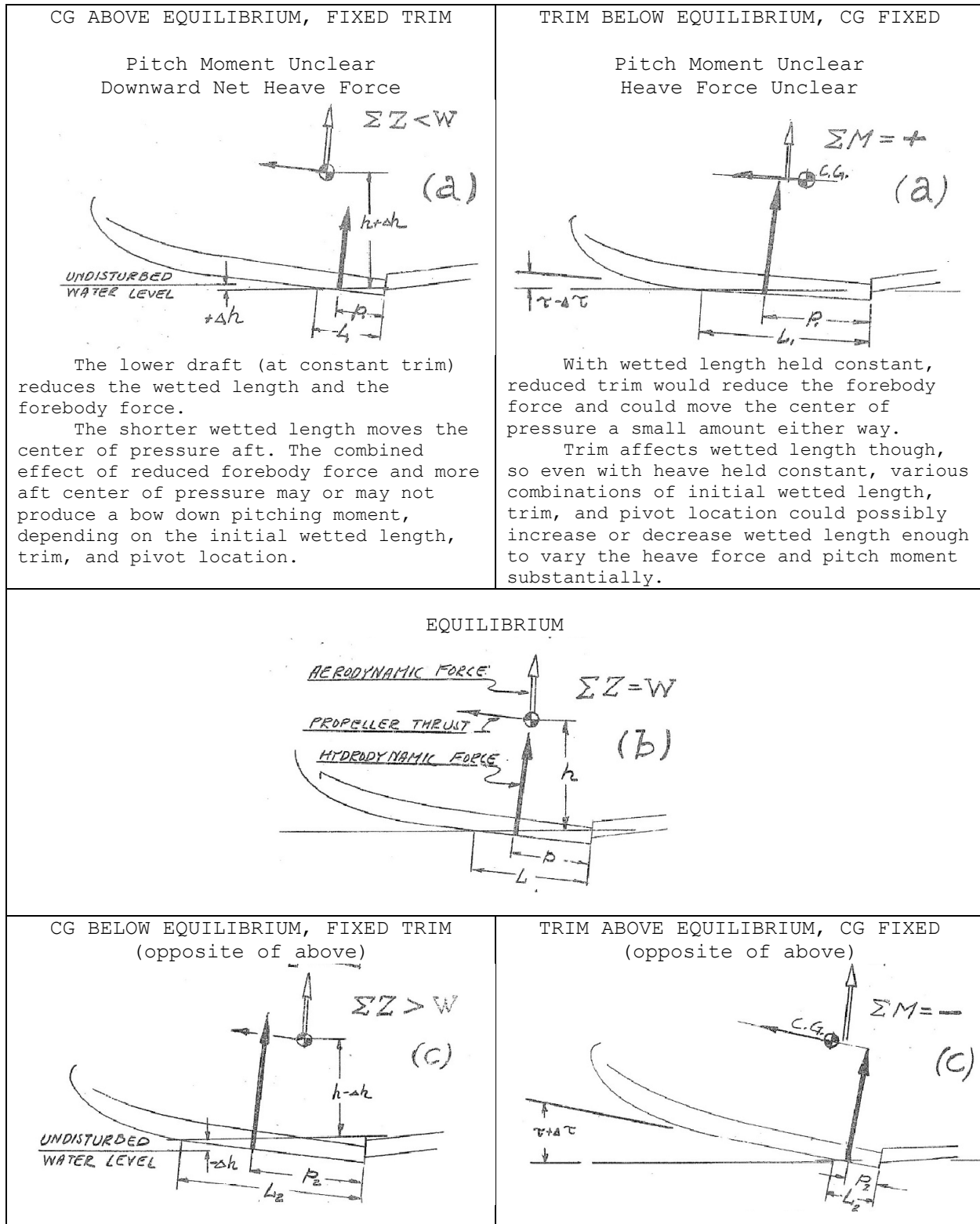


Figure 13: Effects of Heave and Trim in Single-Step Planing

# Porpoising and Skipping

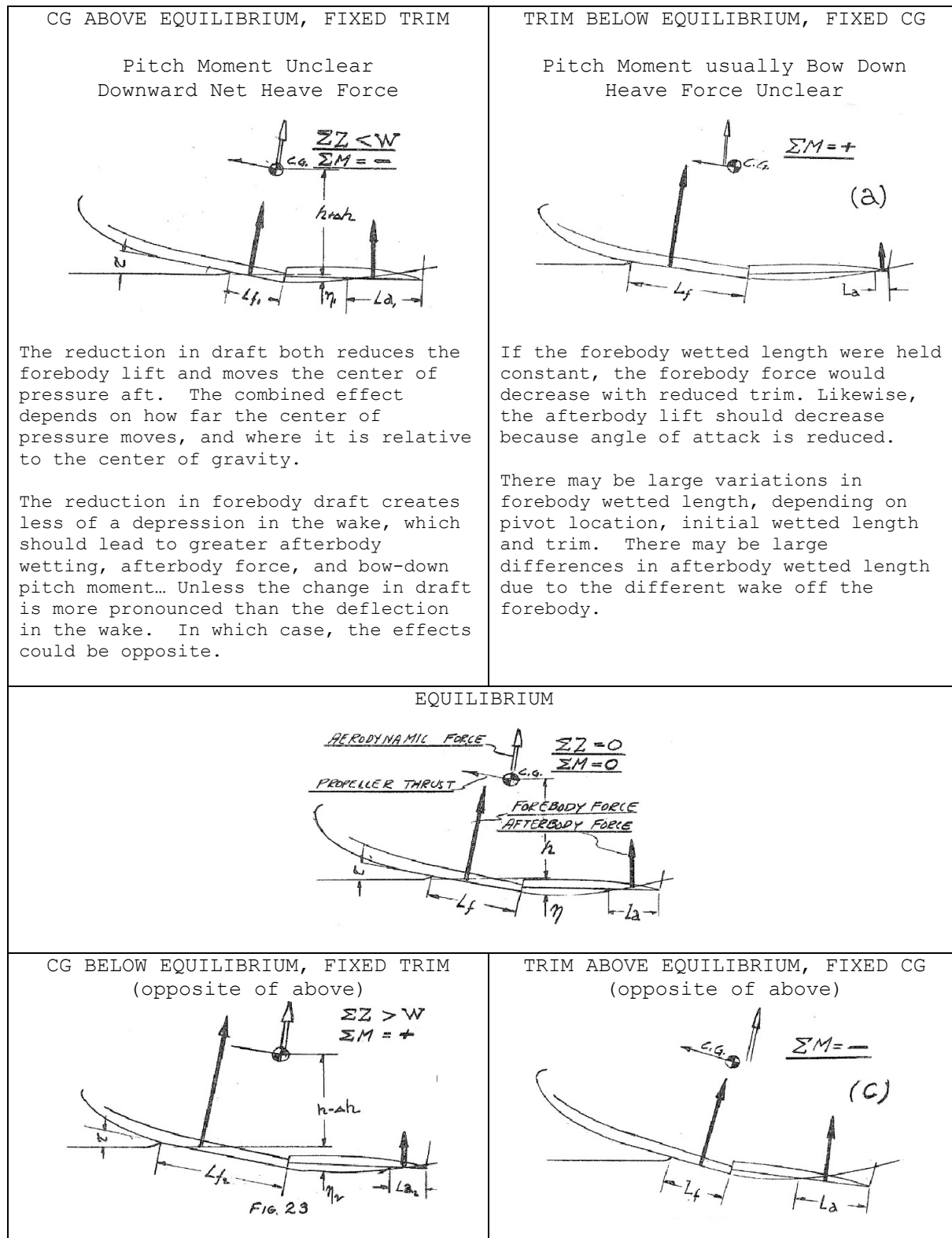


Figure 14: Effects of Heave and Trim in Two-Step Planing



## Porpoising and Skipping

### References for Chapter 5

Benson, J.M. and Lina, L.J. "The Effect of Dead Rise Upon the Low-Angle Type of Porpoising" NACA Wartime Report L-610 Advance Restricted Report ARR Oct. 1942

Benson, J.M. and Friehofner, A. Methods and Charts for Computing Stability Derivatives of a V-Bottom Planing Surface. NACA Wartime Report L-349. Originally issued December 1943 as Advanced Restricted Report 3L08

Davidson, K.S.M, Locke, F.W.S., and Suarez, A. "Porpoising, a comparison of theory with experiment" NACA Wartime Report W-65. Originally issued July 1943 as Advanced Restricted Report 3G07

Davidson, K.S.M. and Locke, F.W.S. Some Analyses of Systematic Model Experiments on the Porpoising Characteristics of Flying Boat Hulls. NACA Wartime Report W-68. Originally Issued September 1943 as Advance Restricted Report 3I06.

Faltinson, O.M. Hydrodynamics of High-Speed Marine Vehicles. 2005. Cambridge University Press

Locke, F.W.S., and Davidson, K.S.M. Some Systematic Model Experiments on the Porpoising Characteristics of Flying Boat Hulls. NACA Wartime Report W-67. Originally Issued June 1943 as Advance Restricted Report 3F12.

Locke, F.W.S. An Analysis of the Skipping Characteristics of Some Full-Size Flying Boats. N.A.C.A. Wartime Report W-104. 1946.

Lorio, J, Morabito, M.G. and Pavkov, M.E., Exploratory Towing Tests of Seaplane Skipping. 13<sup>th</sup> International Conference on Fast Sea Transportation, FAST. Washington, D.C., September 2015.

Martin, M. Theoretical Determination of Porpoising Instability of High-Speed Planing Boats. David Taylor Naval Ship Research and Development Center. Report 76-0052. April 1970.

## Porpoising and Skipping

Olson, R.E. and Land, N.S., Effect of Afterbody Length and Keel Angle on Minimum Depth of Step for Landing Stability and on Take-Off Stability of a Flying Boat. N.A.C.A. Technical Note No. 1571. September, 1948.

Parkinson, J.B. "Notes on the Skipping of Seaplanes", N.A.C.A. RB No. 3I27 September, 1943.

Perring, W.G.A., and Glauert, H. "The Stability on the Water of a Seaplane in the Planing Condition." R. & M. No. 1493, British A.R.C., 1933

Savitsky, D. Hydrodynamic Design of Planing Hulls. Marine Technology, Volume 1. 1964.

Sedow (Sedov?), L.I. Planing on a Water Surface. R.T.P. Translation No. 2506. Translated by F/LT. K.M. Tomaszewski. Inz. lotn. (Warsaw) Seaplane Tank, R.A.E. T.W.F., No.4-5. 194

Sun, H. and Faltinson, O.M. Predictions of porpoising inception for planing vessels. J Mar Sci Technol (2011) 16:270-282  
DOI 10.1007/s00773-011-0125-2

Suydam, H.B. Hydrodynamic Characteristics of a Low-Drag Planing-Tail Flying-Boat Hull. N.A.C.A. Technical Note 2481. January 1952.



CHAPTER 6. DIRECTIONAL STABILITY AND CONTROL

6.1 Directional Stability

6.2 Piloting and Design Mitigation Strategies

6.1 Directional Stability (B. V. Korvin-Kroukovsky, 1948)

The directional characteristics of Seaplanes are considered under two headings;

- a. Directional control in taxiing
- b. Directional stability during take-off,

At the low speed of taxiing the hull is acting as a displacement vessel, with rather deep draft in forebody sections, and a small draft and small side area of the submerged portion at the stern. In case of a small yaw, say due to side Wind, the resultant reaction of water acts forward of the center of gravity, increasing the initial yaw, i.e. making the hull unstable in yaw. Due to the presence of the vertical tail surface the side wind force acts aft of the center of gravity. Thus, the couple formed by the side wind force and the water reaction tends to turn the seaplane into the wind, i.e. makes it, "weathercock". At the low speed and the small engine power used for taxiing the air velocity over the rudder is small, and the rudder often does not have sufficient power to overcome this weathercocking couple. In order to gain the necessary control under these conditions, the single engine seaplanes are usually equipped with water rudders placed at the stern of the float, or aft of the second step of flying boats. The area of the rudder should be equal approximately 4% of the side area of the submerged part of the hull or float, and the rudder should extend as far as possible into the undisturbed water, i.e., appreciable area of it should be placed below the afterbody keel. The rudders of small height, located at water surface, and rudders located wholly in the wake of the stern are not efficient. The multi-engine flying boats usually depend on the unbalanced engine thrust, and are not equipped with rudders. The engine thrust may be controlled by manipulation of throttles, but greatly superior control is obtained by the use of reversible pitch propellers.

## Directional Stability and Control

The stability of the hull during take-off run is easily tested in the towing tank by placing the model at the angle of yaw  $\Psi$ , and measuring the yawing moment acting on it by means of the calibrated spring (Figure 1) [Or other suitable instrumentation to measure yawing moments]. The moment coefficient,  $CM_{\Psi}$  is defined as  $M_{\Psi}/wb^4$ , where  $M_{\Psi}$  is the yawing moment in pound-foot units at the angle of yaw  $\Psi$ ,  $w$  is the weight of water per cubic foot =  $\rho g$  and  $b$  is the beam in feet. The moment coefficient is plotted against yaw angle, as shown on Figure 2. The top of Figure 2 shows the conditions of a certain flying boat [XPB2M-1 Martin "Mars" prototype, shown in Figure 3] at  $C_v = 1.04$ , at which the hull is in displacement condition, as shown by the small values of trim  $\tau$  and the negative value of the heave coefficient  $h/b$ . As was described above, the hull is distinctly unstable in this condition, and this is shown by the positive slope of the moment coefficient curve.

The middle graph on Figure 2 refers to the higher speed at  $C_v 2.17$ . This is still far from the planing condition, but the dynamic forces are sufficient to cause certain increase of the heave coefficient  $h/b$  and the angle of trim  $\tau$ . The fin area forward of the center of gravity is thereby reduced, and that at the stern is increased. The negative slope of the curve in the range  $\Psi = \pm 2$ -degrees indicates the positive stability, and outside of this limited range the stability is essentially neutral.

The bottom graph on Figure 2, a slightly higher speed with  $C_v=2.33$ , illustrates the condition termed "hooking instability". There are two stable branches of the curve at the yaw larger than 3 degrees, with a highly unstable range between. It appears that this small increase of the speed changed the conditions of the wake at the second step, reducing the effective fin area at stern, and making the second step to plane in a middle of a wave hollow in the unstable condition. A small yaw brings the stern into contact with sides of the hollow, opposing further increase of the yaw, i.e. producing a stable branch of the curve on the plot. Three plots of test data discussed above illustrate the complex conditions governing the directional stability of the flying boat in the pre-hump region: they start at low speed with the natural instability of a displacement vessel, are modified by changes of trim as the speed increases, and then become dependent on the shape of the wake, which is rapidly changing with the speed and in the process of transition from the displacement to the planing condition. The conditions producing instability are further aggravated by details of the

## Directional Stability and Control

water flow at the stern of the boat, particularly by the suction generated at any convex curved surface. At a pre-hump speed large areas on the sides of the boat at stern are wetted. The curvature of these sides in the plan view of a pointed second step produces suction forces which often cause large unstable yawing moments to appear. Likewise, the water flow clinging to the rounded tail cone aft of the second step is the frequent cause of instability.

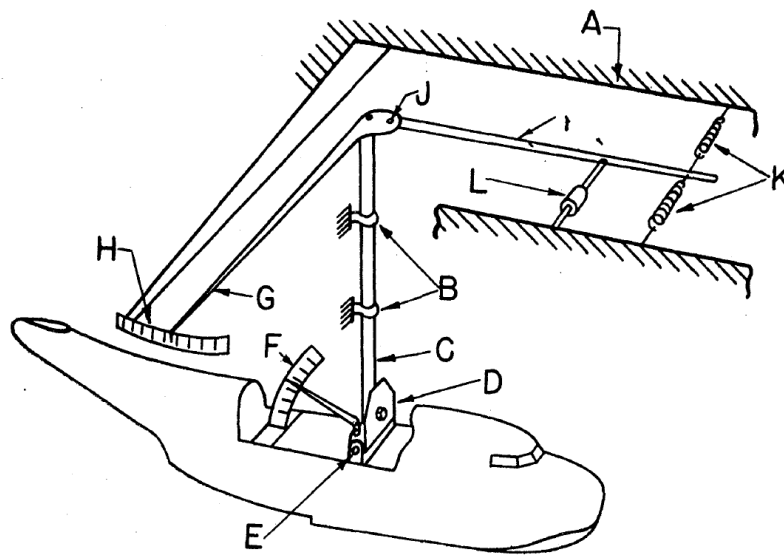
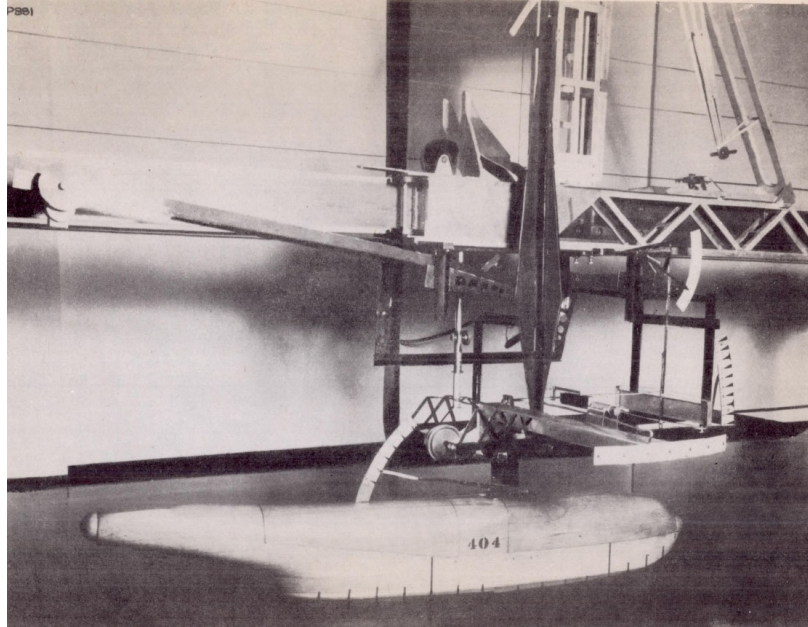
The seaplane float has a simpler shape than a typical flying-boat hull, has much smaller area of sides near stern, and has no structure to interfere with water aft of the second step. The difficulties with the directional stability in float seaplanes therefore occur but seldom.

In a flying boat the difficulties due to directional instability are confined to the "displacement" or the "pre-hump" region. At the planing speed the wetted area forward of C.G. is small, the aerodynamic stability is significant, and with the increase of speed, and the slip stream of the propeller, the rudder acquires ample power for the control.

The above discussion points to the nature of the problem of the directional stability, and to the towing tank tests by means of which the stability can be measured, and quantitatively described. No criterion exists, however, to indicate whether the degree of the instability of the particular model is acceptable for the practical use or not. The behavior of the actual flying boat, the model of which gave the plots illustrated by Figure 2, is described by the following quotation from Locke (1943):

" . . . at speeds below the hump, constant attention must be given to keep the flying boat headed very close to the course, and unbalanced power must be applied rapidly to check any deviation from the course. If corrective moment is not applied rapidly to check the first sign of yawing, the boat may become unmanageable. Cross-wind taxiing may be very nearly impossible, even with maximum unbalanced power."

## Directional Stability and Control



- A - Main towing gate (free vertically)
- B - Strut bearings attached to frame (A)
- C - Model support tube (free to rotate about vertical axis)
- D - Heel angle adjustment
- E - Pivot Points, model attachment (freedom in pitch)
- F - Trim scale on model
- G - Yaw angle indicator fastened to tube ©
- H - Yaw angle scale fastened to (A)
- I - Torque arm pivoted at axis of © clamped to (G)
- J - Yaw angle adjustment
- K - Spring restraining yaw
- L - Dashpot, Yaw Damper

Figure 1: Photo and Sketch of Apparatus for Yaw Tests (Locke, 1943)

# Directional Stability and Control

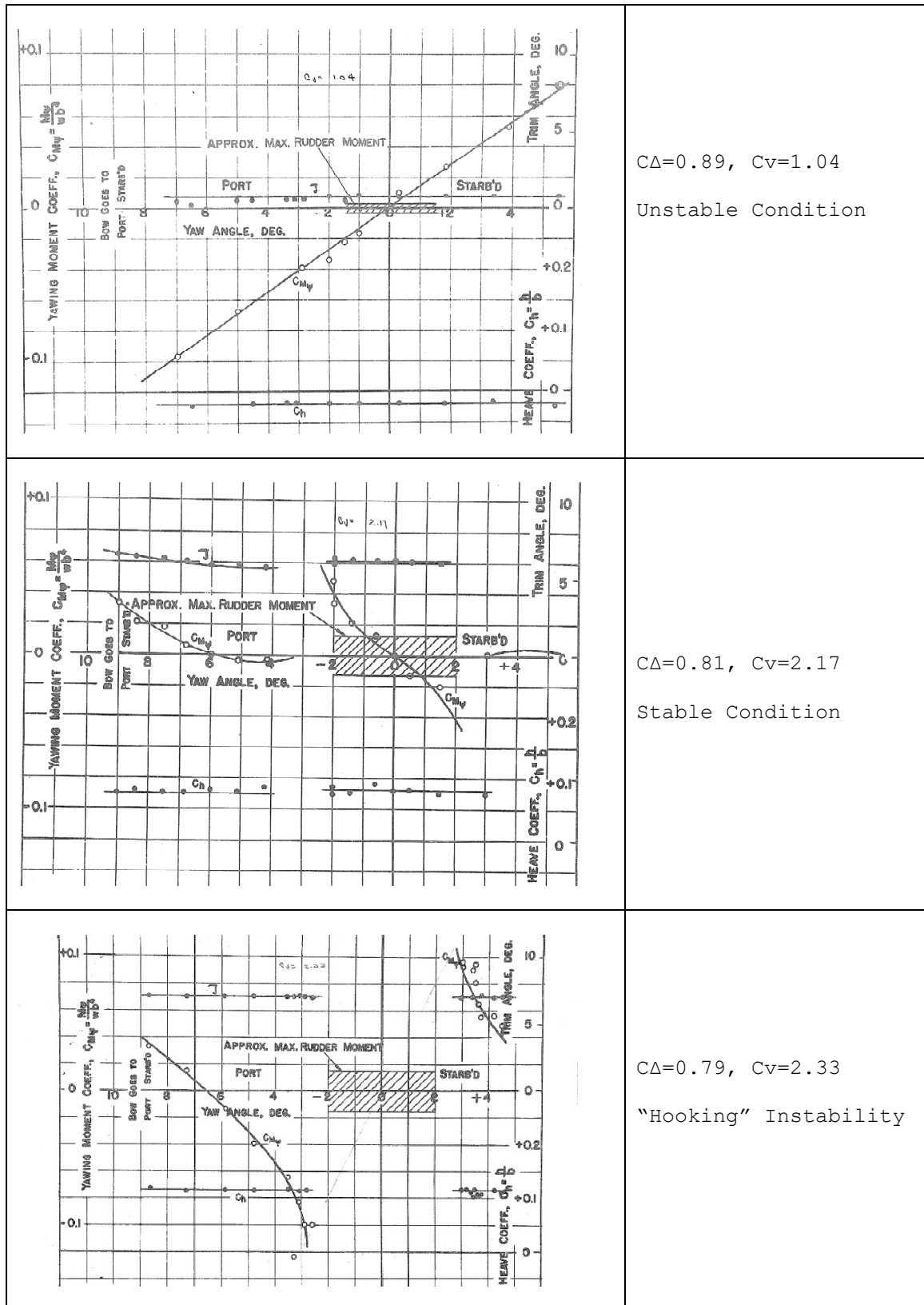


Figure 2: Curves of the yawing Moment Coefficient vs. the Yaw Angle  $\Psi$  for Three Conditions (Taken from Locke 1943)



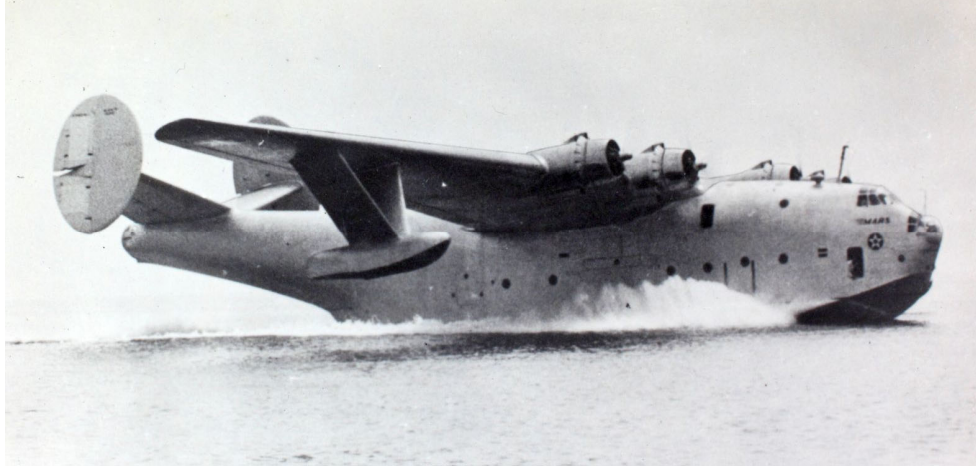


Figure 3: XPB2M-1 Martin Mars Prototype

## 6.2 Piloting and Design Mitigation Strategies (M.G. Morabito, 2024)

Pierson (1944) provides some additional information on the yaw tests discussed above, including description of piloting strategies and means to mitigate the problems.

As shown above, the seaplane can transition into and out of unstable regimes as it accelerates up to speed. The pilot can keep a directionally unstable seaplane on course with the rudder and/or unbalanced power. So long as it doesn't start turning. Large seaplanes, with a minimum excess thrust at hump speed (Figure 4) may not have enough available thrust to use unbalanced power effectively.

The cross-wind taxiing condition shown in Figure 5 is challenging. The wind acts on the projected area of the hull, causing it to heel downwind onto the leeward float. The heel causes additional projected area. The combined effect of wind forces and forces due to leeway through the water is to turn the seaplane into the wind. In strong enough winds, the pilot will not have the control to prevent this. Once the yawing has started, a directionally unstable hull may rapidly turn. The only recourse is to reduce power and try again.

There are a few engineering solutions that can be applied. The skeg can be especially effective. For instance, Brown (1953) commented in his report of water handling trials of a small seaplane that the hull was originally directionally unstable, even in winds less than 5 knots. After the addition of the small skeg shown in Figure 6, it showed no directional instability and

## Directional Stability and Control

required no asymmetric power in 80 take-offs and landings at different weight, power, wind speed and flap settings.

The hull studied by Pierson (1944) and Locke (1943) had issues with water flowing around the afterbody. As water clung to the side, it developed a low pressure, which tended to pull the stern farther off center. The proposed solutions (Figure 7) all involved trying to prevent the flow from coming up the sides or around the rounded area aft of the second step and toward the tail of the aircraft.

- The skeg was used to prevent water from flowing under the rounded portions of the stern of the model. This was effective for the hull with the deeper afterbody; however, not needed for another design variant that had a less full stern.
- The chine strips were used to prevent water from clinging to the side of the hull. These were effective at low loads; however, at heavier loading the water clung to the sides anyway.
- The side step was also used to prevent water from clinging to the side of the hull. These were very effective at a variety of speeds and load cases. A cap was put on the side step to prevent water from running further up the side step.

Presentation of directional stability tests is difficult due to the multitude of charts. Figure 8 is a fairly compact format. It shows stability results for a range of speeds (horizontal) and trim angles (vertical), identifying regions of instability, hooking, neutral stability and positive stability. The inset curves are the stability test results at each condition tested.

Figure 9 has a similar format, only this time it is free-to-trim with load case on the vertical. The region of instability is highlighted. Comparison of the top and bottom charts shows that the addition of side steps greatly reduced the region of instability.

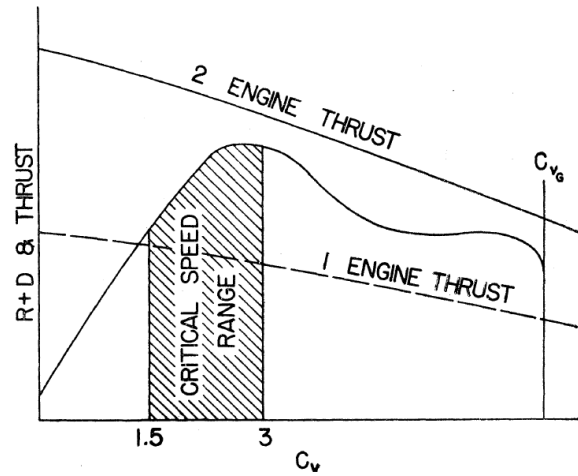


Figure 4: Typical Drag vs Thrust Curve for a Highly Loaded, Twin-Engine flying Boat (Pierson, 1944)

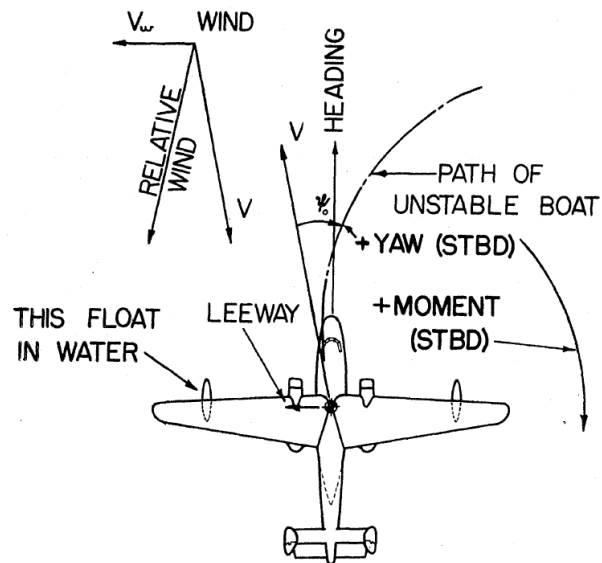


Figure 5: Cross-Wind Taxiing Condition

## Directional Stability and Control

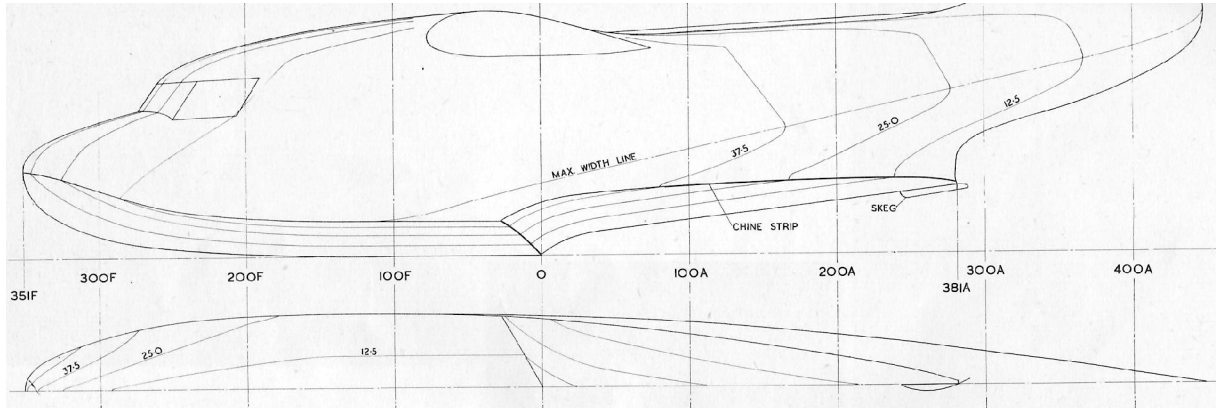


Figure 6: Showing Small, but Effective Skeg (Brown, 1953)

Figure Notes: This hull was directionally unstable, even in winds less than 5 knots. After the addition of the small skeg, it showed no directional instability in 80 take-offs and landings at different weight, power, wind speed and flap settings.

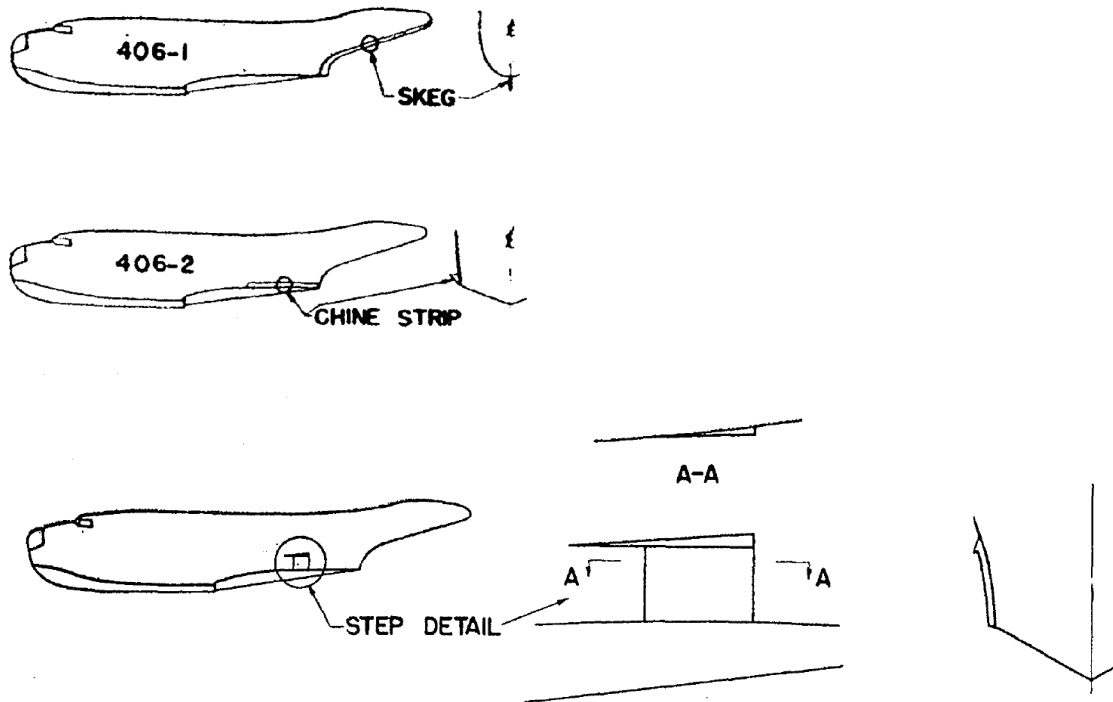


Figure 7: Mitigation Methods (Pierson, 1944)

# Directional Stability and Control

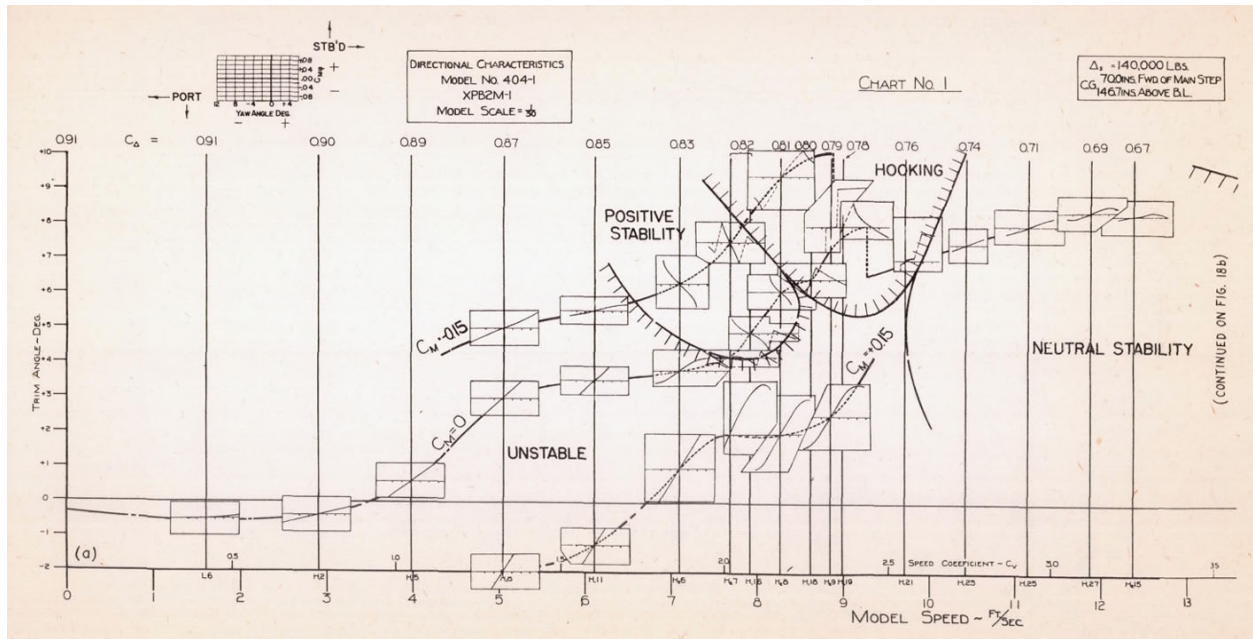


Figure 8: Presentation of Directional Stability Data (Locke, 1943)

# Directional Stability and Control

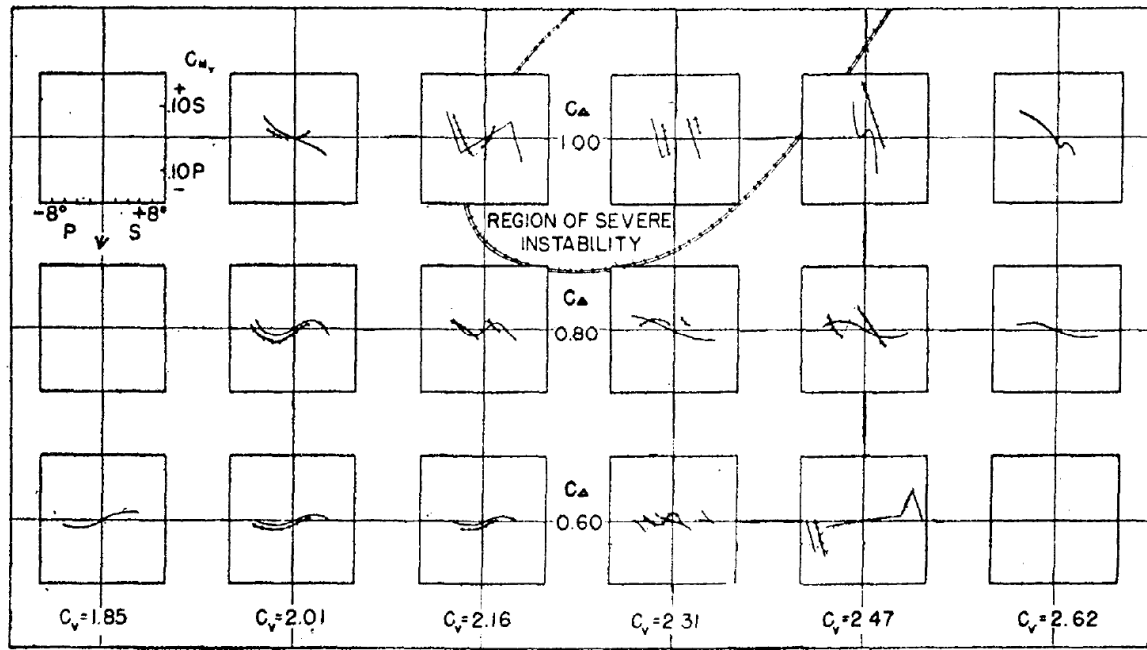
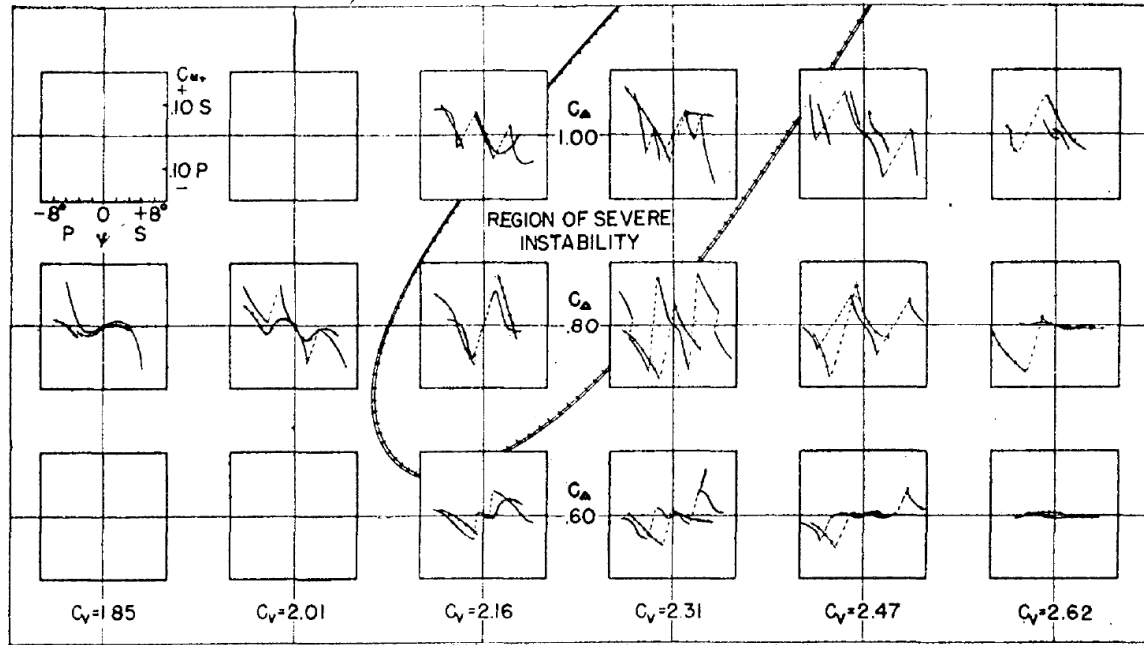


Figure 9: Comparison of Directional Stability Data. (Pierson, 1944)

Figure Notes: Horizontal is speed, Vertical is load. Small graphs show the results of stability tests at each condition tested. The region of

instability is highlighted. Bottom chart shows that the hull with side steps has a smaller unstable region.

References for Chapter 6

Brown, P. Ward. "Brief Water Handling Trials of the Short SA6 Sealand Amphibian. Short Brothers & Harland Limited Hydrodynamics Report No. 135. Jul7 1953.

Locke, F.W.S., Jr. "Some Yawing Tests of a 1/30-Scale Model of the XPB2M-1 Flying Boat", NACA Wartime Report W-66 (Originally ARR No. 3G06). 1943.

Pierson, J.D. "Directional Stability of Flying Boat Hulls During Taxiing." Journal of the Aeronautical Sciences. Volume 11, No. 3, July, 1944.

CHAPTER 7. SPRAY

7.1 Physical Description (Savitsky and Morabito, 2010)

A typical spray formation associated with planing hulls is shown on Figure 1. Two distinct spray patterns are evident in this photograph. One is the so-called "whisker" spray and the other is called the main spray. Characteristically, the whisker spray is a thin, light, spray consisting of droplets of water that are projected outboard of the chine at a trajectory angle essentially equal to the local hull deadrise angle. The main spray is a discharge of water in the form of a cone whose apex is in the vicinity of the stagnation line intersection with the chine and whose outboard trajectory is elevated significantly relative to that of the whisker spray. While distinctly different in appearance, both spray patterns are a consequence of the same hydrodynamic phenomenon.

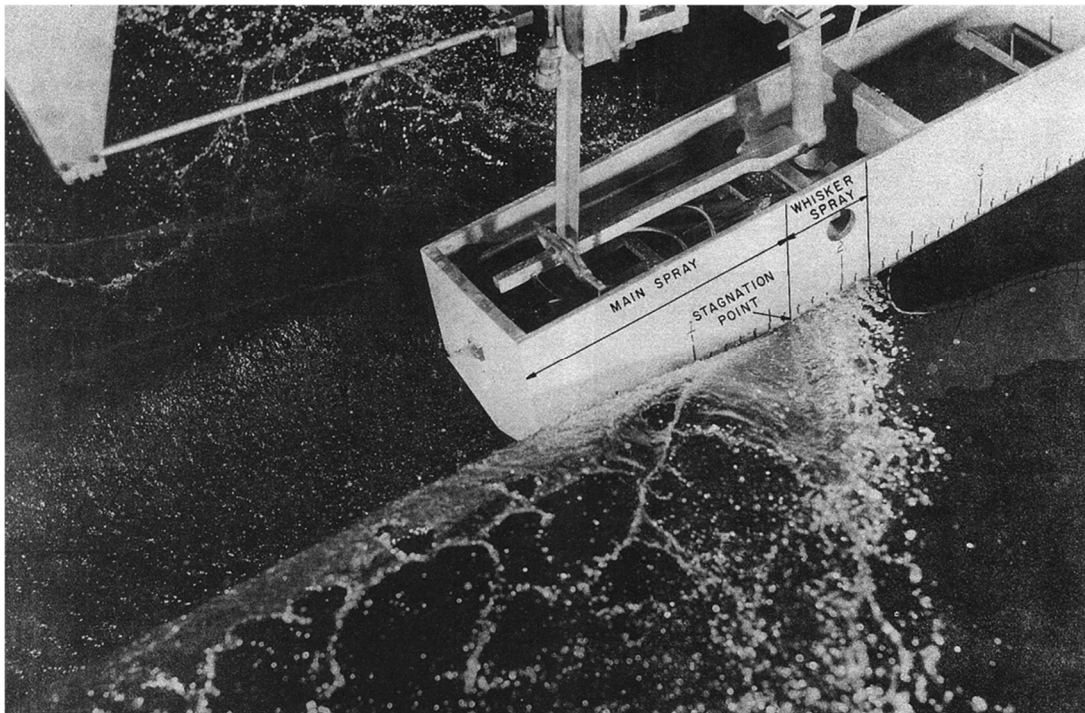


Figure 1: Typical Spray Formation for a Prismatic Planing Surface ( $\beta = 20$  deg,  $\tau = 8$  deg,  $C_v = 4.00$ ) Taken from Savitsky and Breslin, 1958



## Spray

In order to describe the origin of the two basic spray forms associated with high speed planing hulls it is first necessary to describe the free water surface intersections with the hull as shown on the sketches in Figure 2. At pre-planing speeds the spray patterns do not develop but rather a small bow wave originates at the chine intersection with the water surface. As the speed increases, droplets of whisker spray and a small main spray blister appear slightly outboard of the crest of the bow wave. At high planing speeds the whisker and main spray formations become higher and larger so that they dominate and completely obscure the bow wave. For all speeds, the height of bow wave crest is relatively small. These characteristics are demonstrated by a series of photographs taken by Savitsky and Breslin (1958).

While many of the notations in Figure 2 are self-explanatory, it is important to define the stagnation line and the spray root line. Specifically, the stagnation line is a locus of points on the bottom along which the flow is divided into forward and aft components and on which the pressure is a maximum and is developed from bringing to rest the component of free stream velocity normal to this line. Just forward of the stagnation line is the so-called spray root line. This defines the forward extent of the wetted bottom area when planing. According to theoretical (Wagner, 1932) and experimental (typically Savitsky and Neidinger, 1954) results, the actual wetted width at any cross section through the bottom is essentially  $\pi/2$  times the wetted width defined by the level water line intersection with the bottom. This is referred to as the "wave-rise" factor. The angle of the spray root line,  $\alpha$ , relative to the keel measured in a plane normal to the hull centerline and along the keel can be established from a knowledge of the deadrise, trim and  $\pi/2$  wave rise factor. Thus, it can be shown that:

$$\alpha = \tan^{-1} \left( \frac{\pi \tan \tau}{2 \tan \beta} \right)$$

Because the stagnation line and the spray root line are very close to each other, the  $\pi/2$  wave rise factor is often applied to both lines. Also shown on Figure 2 is the forward extent of the whisker spray area. This spray area gives rise to additional viscous resistance (Savitsky, Delorme and Datla, 2007).

Figures 3 and 4 show the results of tests of four constant deadrise hulls towed behind a wind screen to define the geometry of the main spray

## Spray

(prior to its breakup into intense droplets) as a function of hull deadrise angle, trim angle, and speed coefficient. The important findings are that the spray originates from a short length along the chine intersection with the stagnation line, and wetted length does not affect the spray dimensions, if measurements are taken from the spray origin.

The theory of spray formation for prismatic planing hulls (constant deadrise cross-section without bow curvature) is discussed in great detail by Savitsky and Morabito (2010), but it is not directly applicable to the design of seaplanes because the most important spray that wets the windshield, or enters the propellers or flaps, originates from the curved bow sections. Efforts have been made to correlate the prismatic planing hull spray by using effective deadrise and trim; however, it is usually more accurate to use existing test data.

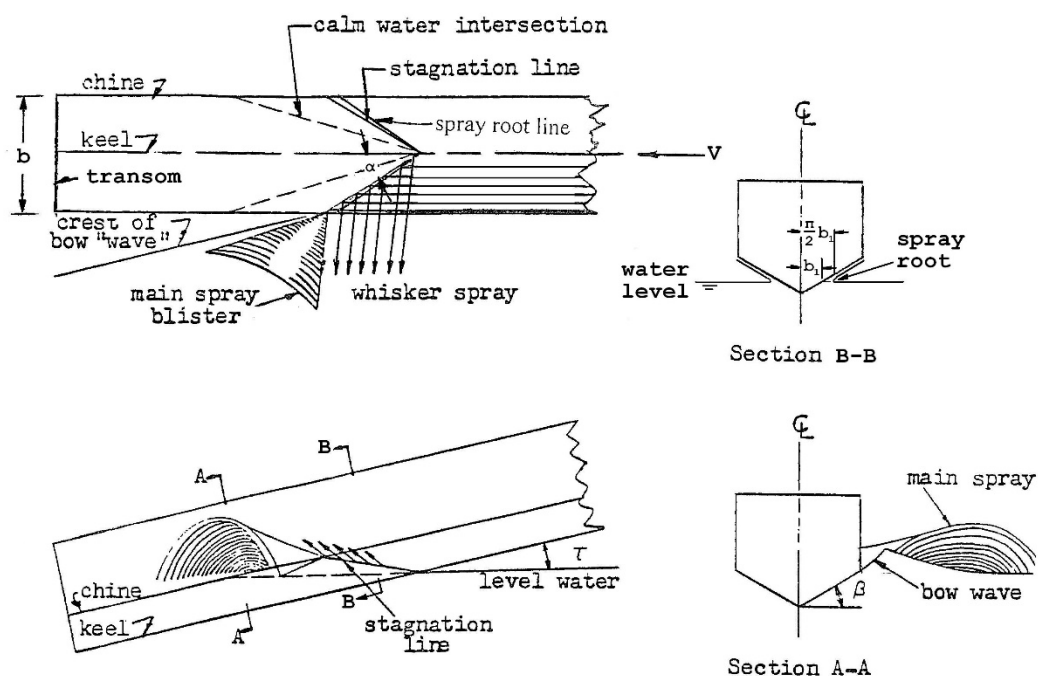


Figure 2: Graphical Representation of Spray Components (Taken from Savitsky and Breslin, 1958)

VARIATION OF MAXIMUM HEIGHT OF MAIN SPRAY BLISTER  
WITH TRIM AND DEADRISE  
FOR  $C_V > 1.50$

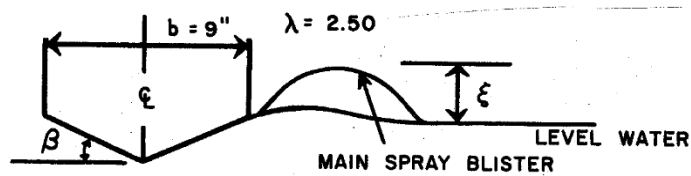
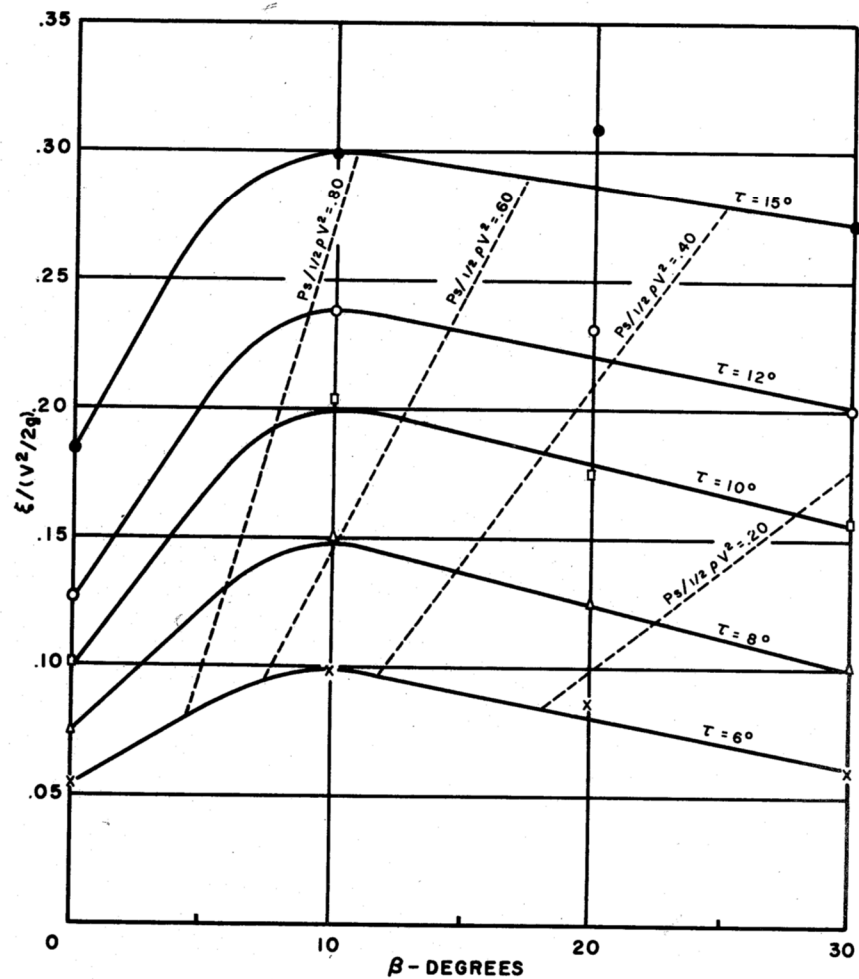


Figure 3: Vertical Measurements of Intact Spray Blister Apex (Savitsky and Breslin, 1958)

FIGURE 10  
VARIATION OF LATERAL POSITION OF MAXIMUM SPRAY HEIGHT  
WITH TRIM AND DEADRISE  
(MAXIMUM LATERAL POSITIONS TAKEN FROM FIGURE 12)

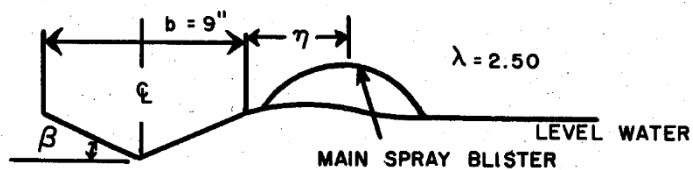
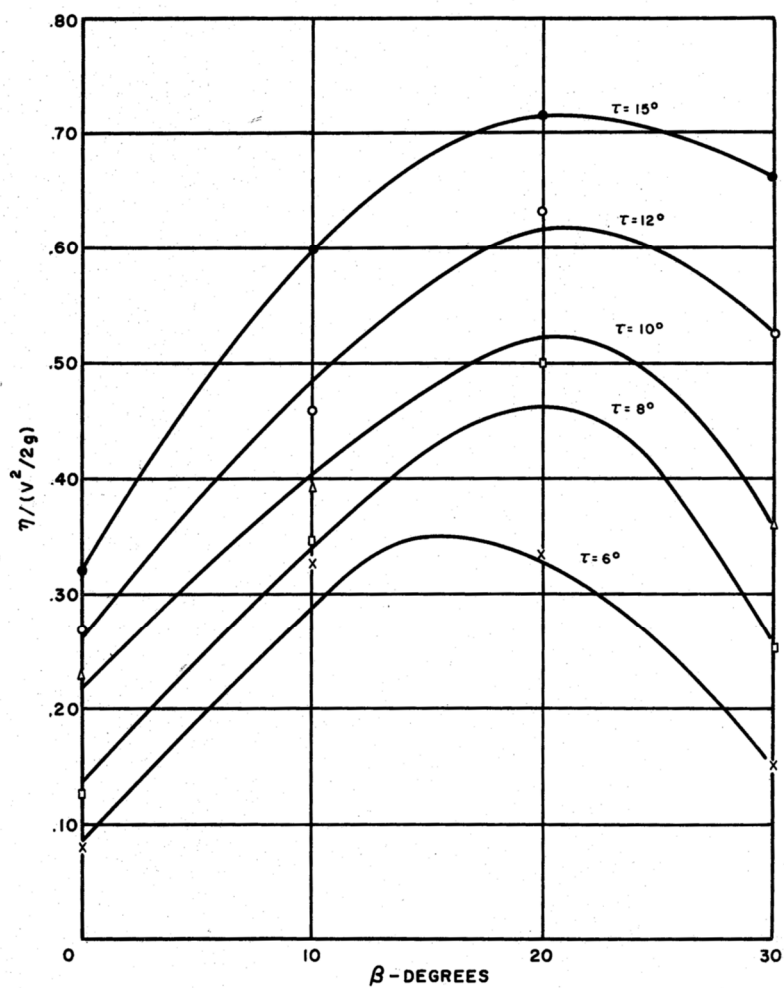


Figure 4: Lateral Measurements of Intact Spray Blister Apex (Taken from Savitsky and Breslin, 1958)

### 7.2 Seaplane Spray (Korvin-Kroukovsky, 1955)

Between the start of the take-off run and the hump speed, there is very little change in heave and draft, but the resistance rapidly increases. Reference to Figure 1 of Chapter 4 shows this at about 10 ft./sec. in this case, there is hardly any change in the draft, and only a small change in trim, yet the resistance is already about 2/3 of the maximum. The water surface meets the hull bottom not far aft of the bow at large angles of incidence, producing high local pressures. These pressures cause some of the water to flow in a thin sheet along the bottom of the hull in the outward and aft directions. This sheet of water breaks away at the chine, forming the spray blister. In a small model this blister has the form of a dome of thin water sheet, on a full-size hull the sheet breaks into a mass of water drops without changing the general form of the blister.

Figure 5 shows the contour map of a typical spray blister. In a flying boat the spray interferes with propellers, and impinges on wing flaps, often causing structural damage. The spray therefore is one of the important factors determining the seaworthiness of the boat, and the experimental quantitative measurement of it represents an important phase of the towing tank testing. For this purpose, the grid of the vertical and horizontal lines is painted on the side of the hull, and the side view of the spray is photographed against this grid. Simultaneously the photographs of the plan and front views are also taken (See Figure 6 for tank-side photo of the spray test setup, and . When the spray blister contours for several speeds of the seaplane are superimposed, the conical surface can be drawn tangent to all blisters, i.e. enveloping all individual blister plots. The points of tangency of the blister to this envelope for each speed is defined by dimensions X, Y and Z, as shown on Fig 5.

Figure 7 are photos showing the effect of speed on the spray patterns, and Figure 8 shows the effect of load. Work has been undertaken to express the spray measurements in a non-dimensional format that can be used for design, while occupying a minimum number of charts. For the beam of the hull b, the coefficients are defined (Locke and Bott, 1943 and Locke, 1943):

## Spray

|                                |             |
|--------------------------------|-------------|
| Longitudinal Spray Coefficient | $C_x = X/b$ |
| Lateral Spray Coefficient      | $C_y = Y/b$ |
| Vertical Spray Coefficient     | $C_z = Z/b$ |

Spray can be considered as a form of the wave so these coefficients can be presumed to be functions of the Froude Number. If the cube root of the volume is used as the characteristic length, instead of waterline length or beam, then the "Volumetric Froude number" can be used.  $F_V = \frac{V}{\sqrt{gV^{1/3}}}$  where V is the forward speed, g is the acceleration due to gravity and  $\nabla$  is the submerged underwater volume  $\nabla = \Delta / (\rho g)$ . The square of the volumetric Froude number is  $\frac{V^2}{gV^{1/3}}$ , which using NACA coefficients is  $C_V^2 / C_\Delta^{1/3}$ .

Furthermore, the use of coefficients X/b, Y/b and Z/b would be sufficient for the hulls differing in size but geometrically similar form. To make coefficients applicable to hulls of the different length/beam ratio, they are divided by functions of  $C_\Delta$ , finally expressing the relationships to be plotted as:

$$\begin{aligned} C_X / C_\Delta^{1/3} &= \phi_1 (C_V^2 / C_\Delta^{1/3}) && \text{for longitudinal position} \\ C_Y / C_\Delta^{1/3} &= \phi_2 (C_V^2 / C_\Delta^{1/3}) && \text{for lateral position} \\ C_Z / C_\Delta &= \phi_3 (C_V^2 / C_\Delta^{1/3}) && \text{for vertical position} \end{aligned}$$

The X and Y dimensions collapse with the cube root of the load coefficient. The difference for the vertical coefficient was, "pure empiricism" (Locke, 1943), as the data plotted better using this format.

The plot of the first of these relationships, defining  $C_x$ , is shown on Figure 9. It is observed that spray characteristics for a wide range of loadings for a flying-boat hull are well represented by a single curve. Equally good agreement is shown in Reference ?? for second and third relationships, defining  $C_y$  and  $C_z$ . Three curves describing the height and position of the spray blister are therefore included in the summary sheet of hull characteristics, as shown by the upper section of the Stevens Collapsed Data Set (Figure 4, Chapter 4).

At speeds above the hump, the bow sections of the hull are clear of water, and the spray coming off the main planing bottom is located further

## Spray

aft, and is of low height, so that it does not strike any part of the seaplane, and therefore is of no interest to the designer.

The spray described above is usually referred to as the "main spray". In addition to this the bow spray has to be considered. At very low speed, say about 5 ft/sec, on Figure 1 of Chapter 4, both the heave and the pitch are below these of the static flotation. The hull settled in water, and trimmed by the bow. This causes water at the bow either to break into spray, or to envelope the bow in a thin sheet of water clinging to the surface, eventually breaking into spray at the upper part of the hull bow. These conditions are very much aggravated during operation in waves, when the bow plunges into the oncoming wave. The bow spray is important in that it wets the windshield, thereby temporarily obscuring pilot's vision, and also leaves the deposit of salt, thus impairing the visibility for the entire duration of flight. In single engine, twin float seaplanes the bow spray of floats is primarily responsible for the wear of the propeller.

The bow spray in calm water and in waves is studied in towing tanks, and results are reported qualitatively by a series of photographs. Extensive study of the bow spray, as it is affected by the bow shape, is given by Locke (1945). Quoting from this reference: "... the height and the volume of spray at the windshield can be reduced by (1) increasing the hull length and especially the forebody length, (2) increasing the "sharpness" of the bow lines below the chine, (3) increasing the static trim when the bow form is such that relatively bad spray otherwise occurs, and (4) decreasing the waterborne load. These changes are listed approximately in the order of their importance from the point of view of reducing spray". As a corollary to the item (3) above, the piloting technique for reducing the bow spray calls for the use of the full-up elevator at the start as the throttle is opened until the bow comes up, or for the entire duration of the low-speed taxiing. Moreover, the taxiing at the speed of the bad spray should be reduced to the minimum; it is usually possible to taxi at either lower or higher speed.

## Spray

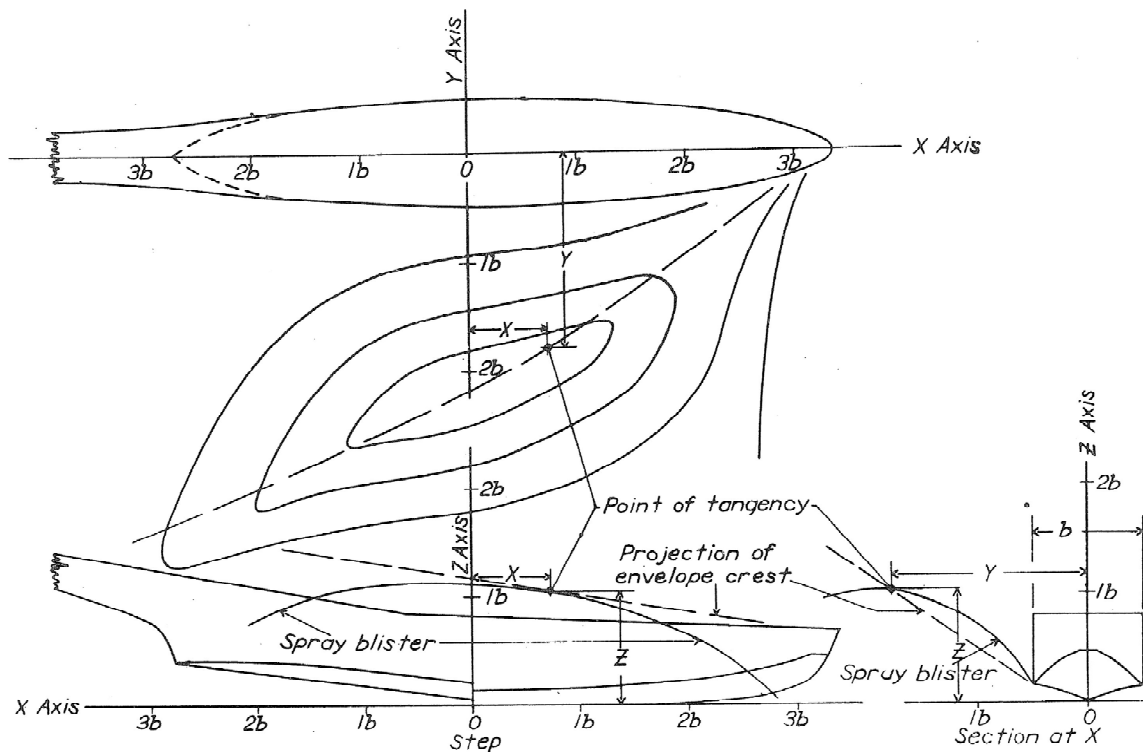


Figure 5: Diagram showing the Contours of the Main Spray blister, and the Location of its Point of Tangency to Spray Envelope. (Taken from Locke, 1943)

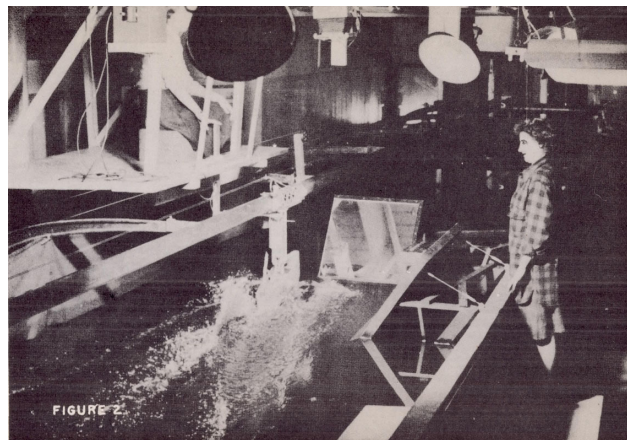
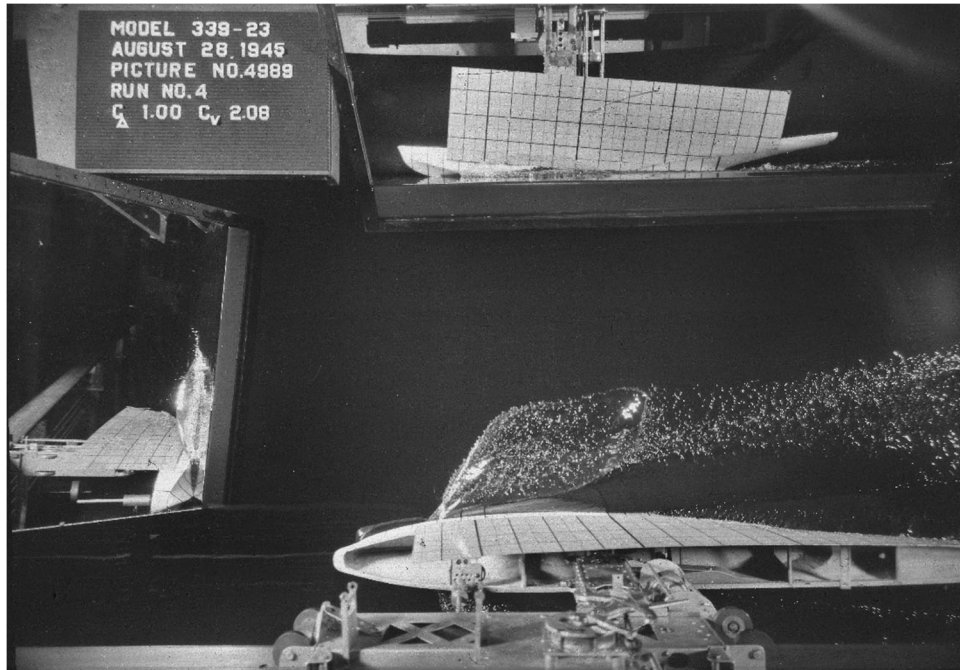


Figure 6: Spray Experiment Setup (Taken from Locke and Bott, 1943)



## Spray



$C_V = 2.08$



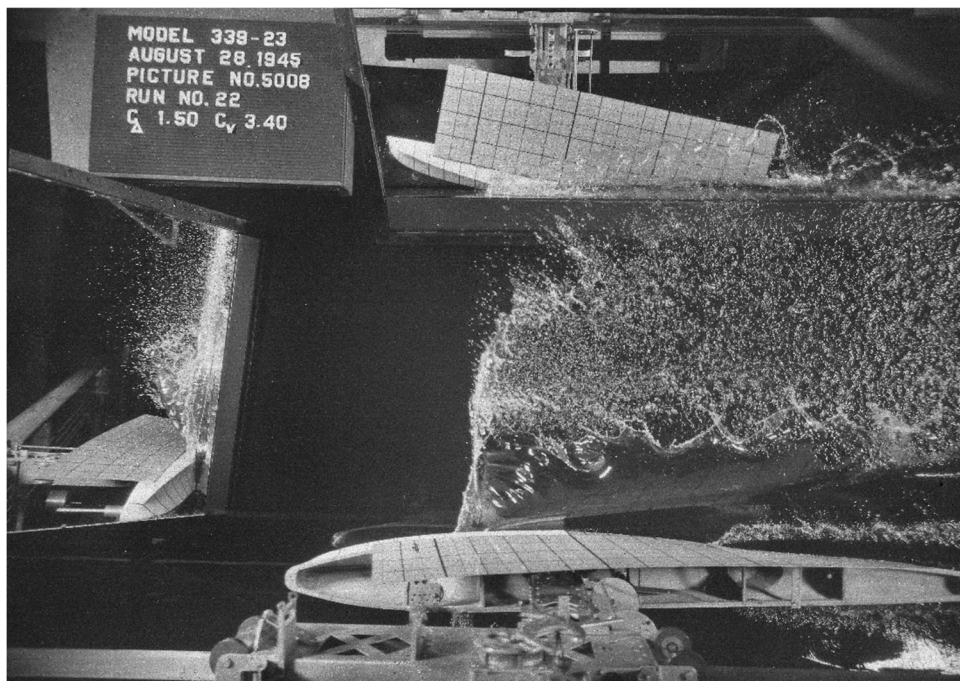
$C_V = 2.83$

Figure 7: Effect of Speed on Spray

## Spray



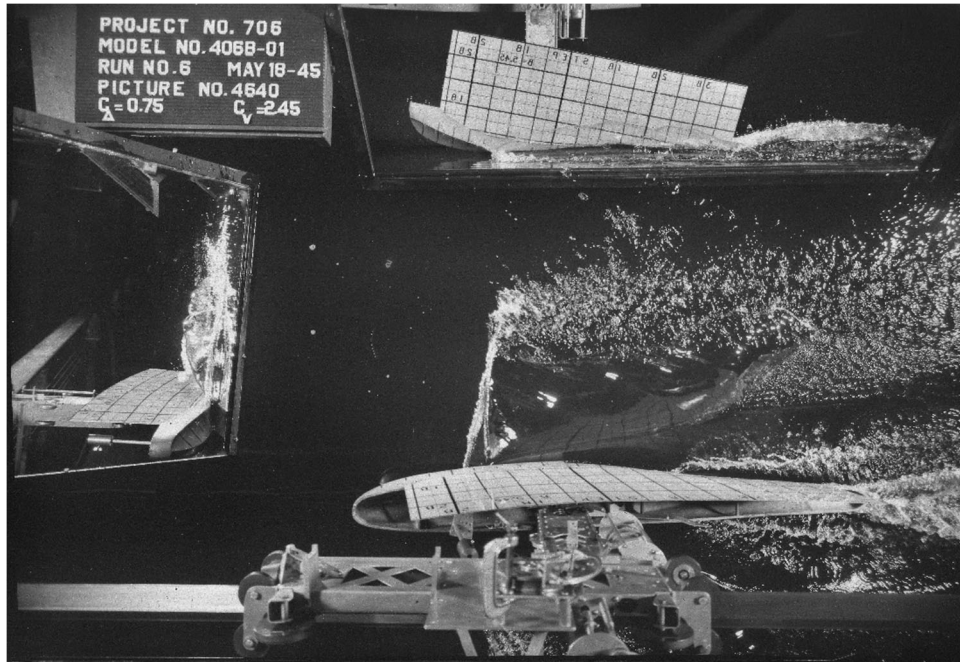
$C_v = 3.21$



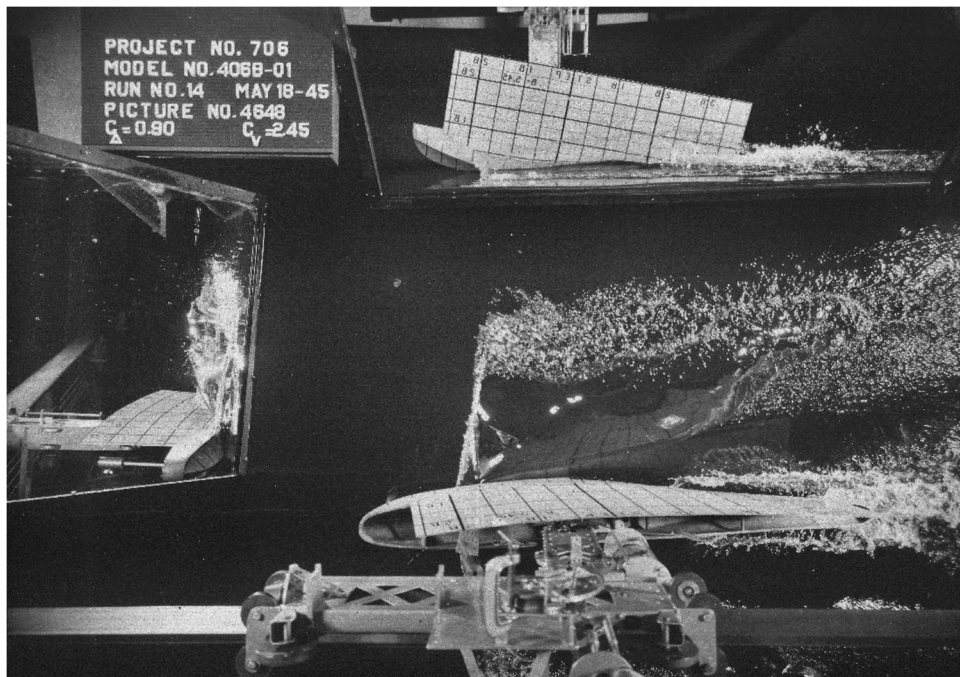
$C_v = 3.40$

Figure 7 (cont.): Effect of Speed on Spray

## Spray



$$C_D = 0.75$$



$$C_D = 0.90$$

Figure 8: Effect of Load on Spray

## Spray

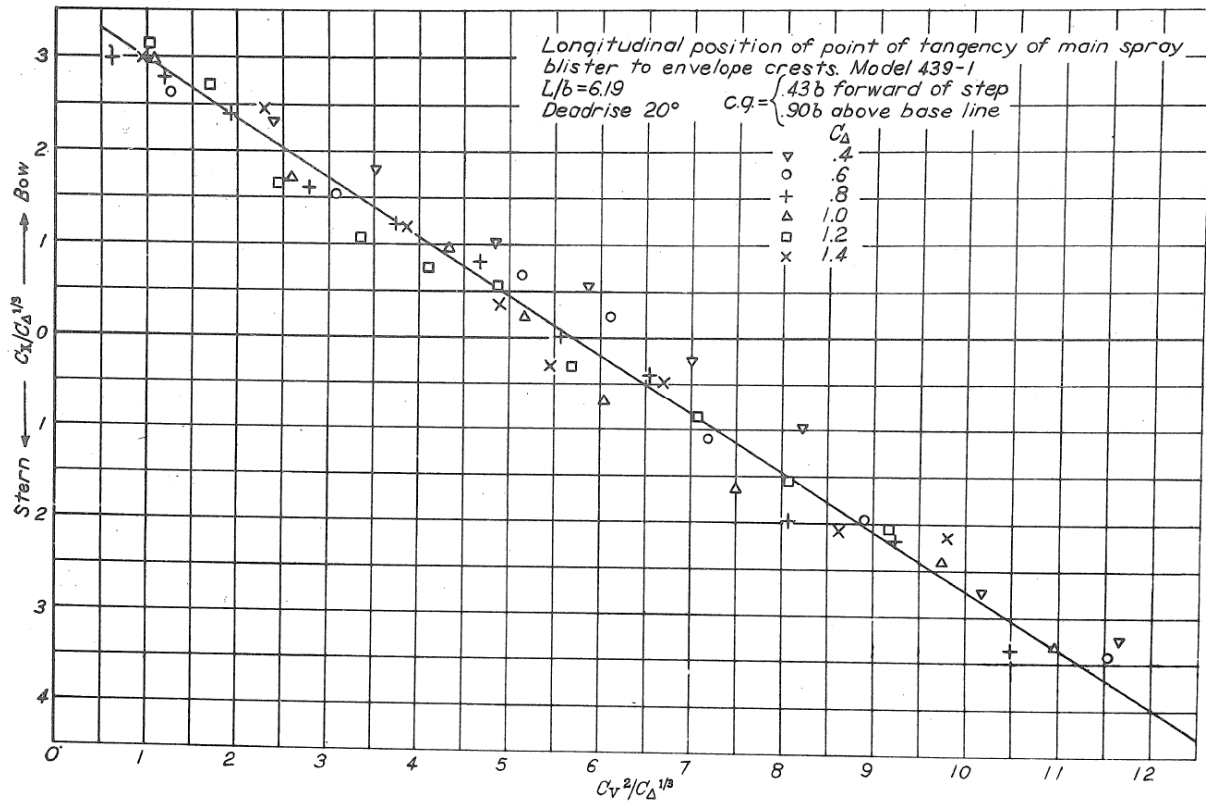


Figure 9: The Plot Showing the Longitudinal Position of the Point of Tangency of the Main Spray Blister to Envelope Crests. (Taken from Locke, 1943)

### References for Chapter 7

Locke, F.W.S., Jr. and Bott, Helen, L. "A method for Making Quantitative Studies of the Main Spray Characteristics of Flying-Boat Hull Models", NACA Wartime Report W-69. (Originally ARR No. 3K11). 1943.

Locke, F.W.S., Jr. "Some Systematic Model Experiments of the Bow Spray Characteristics of Flying-Boat Hulls Operating at Low Speed in Waves", NACA Wartime Report W-71. (Originally ARR No. 3L04). 1943.

Locke, F.W.S., Jr. "General Main-Spray Tests of Flying-Boat Models in the Displacement Range", NACA Wartime Report W-72. (Originally ARR No. 5A02). 1945

Savitsky, D. Breslin, J. "On the Main Spray Generated by Planing Surfaces." Stevens Institute of Technology Experimental Towing Tank Report 678. 1958

## Spray

Savitsky, Daniel, Delorme, M. F., and Datla, R. (2007). "Inclusion of Whisker Spray Drag in Performance Prediction Method for High Speed Planing Hulls" SNAME Marine Technology, Vol.44, No.1, January, 2007

Savitsky, Daniel and Morabito, M.G. 2010. "Origin and Characteristics of the Spray Patterns Generated by Planing Hulls." Davidson Laboratory Technical Report No. 2882. Journal of Ship Design and Production SNAME, 2011.

CHAPTER 8. IMPACT

B.V. Korvin-Kroukovsky, 1948

- 8.1 Introduction, Statement of the Problem
- 8.2 Theory and Tests Pertaining to the Impact in Smooth Water
- 8.3 Three-Dimensional Case of Oblique Impact
- 8.4 Impact Basin
- 8.5 Landing on Waves
- 8.6 Pressures Acting on the Hull Bottom
- 8.7 Effect of the Elasticity of Supporting Structure
- 8.8 Waves

8.1 Introduction, Statement of the Problem

When a seaplane makes a perfect landing on smooth water, the series of events are similar to the ones occurring during take-off, but taken in the reverse order: after flare-out of the glide, the velocity becomes practically tangential to the water surface, which is penetrated without any shock. With engines throttled the seaplane decelerates under action of the air and water drag, and, as the speed is decreased the hull wetted area and the angle of trim increase, with constant increase of the drag. The hump speed, i.e. the speed of the maximum resistance is reached, after which the planing ceases, and the seaplane settles to the displacement phase, and finally to static flotation. Often, however, the flare-out of the glide is far from being perfect, and the flight path at the instant of the contact with the water surface is inclined at the angle  $\gamma_0$ , as this is shown on Figure 1. It is convenient to trace the subsequent motion of the seaplane by reference to the keel at step - point 0 on figure 1. This motion is shown on Figure 2(a). The downward component of the velocity is gradually decreased by the reaction of water, then is reversed in sign accelerating the seaplane upward till it leaves the water at a certain point P. The water reaction is shown on Figure 2(b). At the point of entry 0 the velocity is high, but the wetted area is nil. Subsequently a point is reached where the remaining velocity and the wetted area of the bottom are such that maximum reaction is produced, and

finally the reaction becomes zero again at the point of exit P. The maximum reaction usually occurs somewhat before the maximum draft is reached, and before the chine becomes wetted. Indeed, in the case of flying boats the entire cycle of the impact-rebound often occurs without wetting of chines, so that in theoretical study it is possible to assume a Vee shape of infinite width. Furthermore the duration of time from the entry to exit is so short that angle of trim does not change appreciably, and in the conditions preceding the impact can be described by three parameters: velocity  $V_0$ , the glide path angle  $\gamma_0$ , and the angle of trim  $\tau$ . Here the subscript zero indicates conditions at the first contact with water, both  $V$  and  $\gamma$  varying subsequently under the action of water forces, while  $\tau$  remains sensibly constant.

Since the force of the impact determines the strength which the hull must possess, the theoretical and experimental study of it received a good deal of attention, beginning with the work of G. H. Bottomley (1919). This study has three basic objectives:

- a. The determination of the total force of the water reaction, and of its variation with the time and submergence.
- b. The intensity of the water pressure on the bottom plating and its distribution.
- c. The effect of elasticity in the structure connecting the planing bottom with the masses of the seaplane.

Theoretical and experimental studies of the impact establish the form of relationship between the impact force, three approach parameters mentioned above, the mass of the seaplane and such parameters of its shape as the deadrise  $\beta$  or curvature of the bottom. The actual magnitude of impact forces, however, is determined statistically from the analysis of the operational practice. Furthermore it is always possible to imagine conditions severe enough to break any seaplane hull. The most unfavorable combination of the parameters, indicating the maximum strength to be provided in the hull, is limited, therefore by the weight which can be tolerated in the aircraft. The final outcome of all these considerations takes the form of regulation established by the Bureau of Aeronautics for the seaplanes procured by the U. S. Navy, or by the Civil Aeronautics Board for the seaplanes to be licensed for civilian uses. The object of this chapter, therefore, is to give the reader the understanding of the phenomena of the

## Impact

impact, and to improve thereby his ability to interpret and to supplement the regulations, rather than to give any direct design data or instructions.

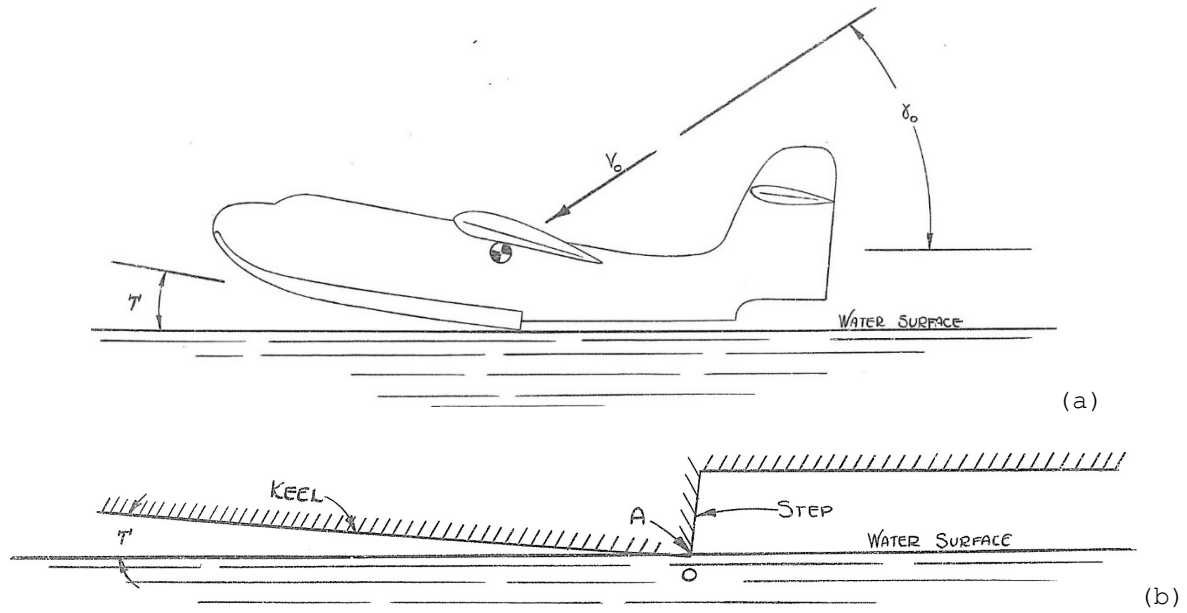


Figure 1: Seaplane at Instant of Entry into Water (taken from Benscoter, 1947)



## Impact

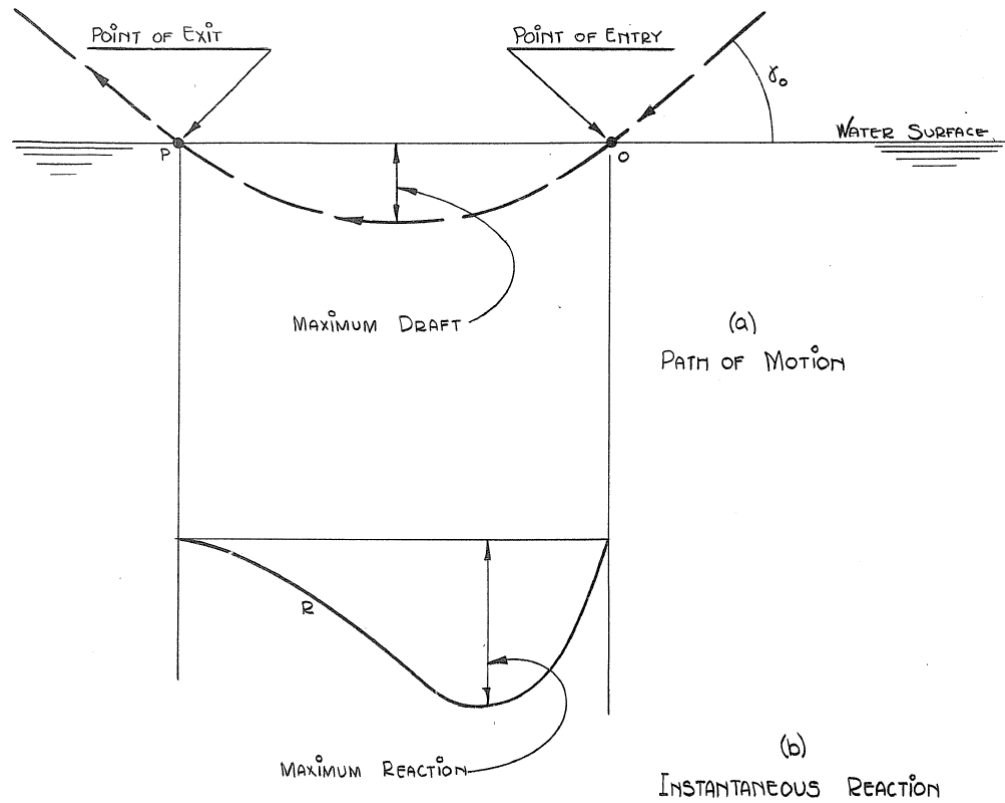


Figure 2: Trajectory of the Step Point and Reaction during Impact Period  
(taken from Benscoter, 1947)

## 8.2 Theory and Tests Pertaining to the Impact in Smooth Water

Theory of the impact of the wedge dropped onto water vertically was originated by Th. von Karman (1929) - who established the concept that momentum of the wedge plus the momentum of the added mass of entrained water must be equal to all times to the initial momentum of the wedge, i.e.:

$$MVo = MV + mV \quad (\text{Eq. 1} = 25)$$

where:  $M$  - mass of the wedge.

$m$  - added mass of the entrained water.

$Vo$  - velocity of the wedge at the instant of the contact.

$V$  - vertical velocity of the wedge at any instant during immersion.

The movement of a body in the fluid causes various fluid particles to move in many paths with various velocities and various momenta. It is possible to imagine a certain mass of the fluid as moving with the same velocity as the body, and possessing the momentum equal to the sum of momenta of all fluid particles involved. Such a hypothetical mass of the fluid is known as the "additional mass". In case of the fluid flowing around a flat strip of a certain width  $2C$  and of infinite length, the additional mass is shown by the hydrodynamic theory to be equal to the mass of the cylinder of the diameter  $2C$ , i.e.  $m = \rho\pi C^2$ , where  $\rho$  is the mass density of the fluid, in this case of water. The case of the wedge penetrating the water surface - as on Figure 3(a) - was compared by Th. von Karman to the flat plate having water on one side of it, i.e. was associated with additional mass of water equal to one half of the cylinder, or  $\rho\pi C^2/2$ . In the process of immersion of the wedge the half breadth  $C$  is continuously increasing, and the additional mass  $m$  is also continuously increasing, so that both  $V$  and  $m$  in Equation 1 are considered as variables.

Using the concept of virtual mass described above, equations of motion will be developed defining the impact process for the case of a vertical drop of an infinitely long prismatic section at zero trim angle. For this condition of vertical drop the fluid flow over the bottom is a two-dimensional nature and the flow can be considered as being in planes normal to the keel.

## Impact

### Two-Dimensional Case

The action of a unit slice of the wedge and a unit slice of the fluid is considered herein. The momentum of the fluid is equal to the product of the "additional mass"  $m$  and the instantaneous velocity of the float  $\dot{z}$ . The impact force is equal to the time rate of change of the momentum. The displacements, velocities, and accelerations are considered positive downward, and the effects of buoyancy and viscosity are assumed negligible. Also, it is assumed that the wedge has a 1 g lift force acting on it which corresponds to the wing lift of an actual seaplane hull.

$$F = \frac{d}{dt} (m\dot{z}) = m\ddot{z} + \dot{m}\dot{z}$$

$$\text{also: } F = -M\ddot{z}$$

$$\text{Therefore: } M\ddot{z} + m\ddot{z} + \dot{m}\dot{z} = 0$$

$$\text{Let } m = Kz^2$$

$$\dot{m} = 2Kz\dot{z} = \frac{2m\dot{z}}{z}$$

(Eq. 2)

Substituting for  $\dot{m}$  and dividing by  $M$ :

$$\ddot{z} \left(1 + \frac{m}{M}\right) + \frac{2\frac{m}{M}\dot{z}^2}{z} = 0$$

$$\text{Let } \frac{m}{M} = R$$

$$\ddot{z}(1+R) + \frac{2R\dot{z}^2}{z} = 0$$

(Eq. 3)

This equation defines  $\ddot{z}$  in terms of the unknown instantaneous values of  $\dot{z}$  and  $z$ . The analysis will now proceed with an evaluation of the relation between  $\dot{z}$  and  $z$ . From Equation 2,

$$\frac{dR}{dt} = \frac{2R\dot{z}}{z}$$

$$R = \frac{dR}{dt} \frac{z}{2\dot{z}}$$

Thus, Equation 2 becomes

## Impact

$$\frac{d\dot{z}}{dt}(1+R) + \frac{z}{2} \frac{dR}{dt} \frac{3}{z} \frac{1}{z} \dot{z}^2 = 0$$

$$\frac{d\dot{z}}{\dot{z}} + \frac{dR}{(1+R)} = 0$$

(Eq. 4)

Now integrating:

$$\log \dot{z} + \log(1+R) = \log c$$

To solve for the constant of integration, substitute the conditions just prior to impact:

$$t = 0; z = 0; R = 0; \dot{z} = \dot{z}_0 = \text{initial contact velocity.}$$

$$\text{Thus: } \log \dot{z}_0 = \log c$$

$$\text{and } \dot{z} = \frac{\dot{z}_0}{(1 + \frac{m}{M})} = \text{Vertical Velocity}$$

(Eq. 5)

Solving the vertical velocity equation for acceleration gives,

$$\ddot{z} = \frac{-2 \frac{m}{M} \dot{z}_0^2}{z(1 + \frac{m}{M})^3}$$

(Eq. 6)

By differentiating the acceleration equation with respect to  $z$  and setting the quantity equal to zero, it can be shown that the maximum acceleration for the two-dimensional case occurs then the ratio  $\frac{m}{M} = \frac{1}{5}$ .

Although the two-dimensional analysis is of small practical value for design it serves to illustrate the fundamentals of the impact theory and is extremely useful in the development of the three-dimensional case of the more practical case of the oblique impact.

# Impact

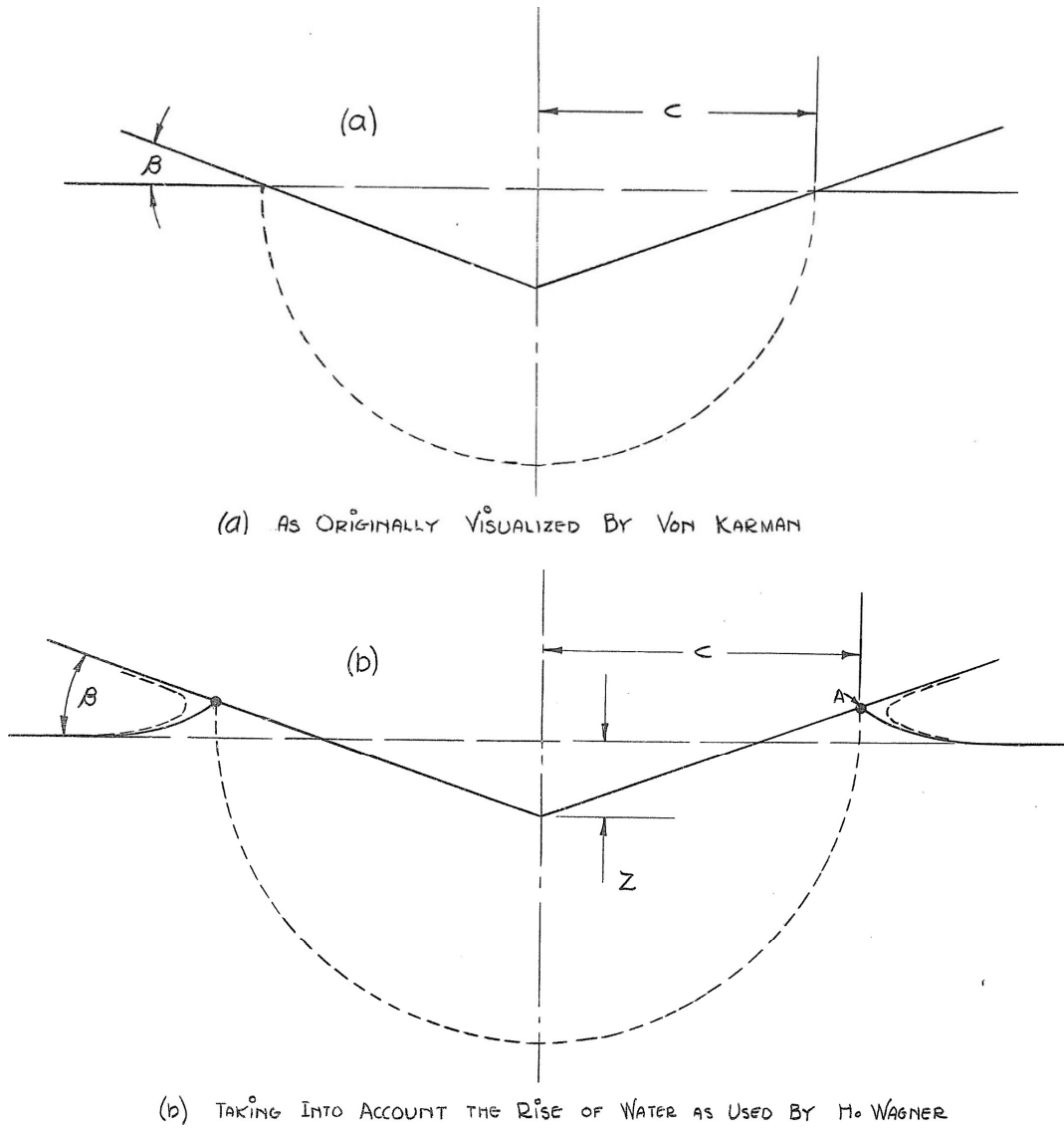


Figure 3: Half Cylinder of Water the Mass of which is Added to the Mass of the Wedge in Impact, a) as originally visualized by von Karman, and b) taking into account the rise of water as used by H. Wagner.

### 8.3 Three-Dimensional Case of Oblique Impact

In an actual seaplane landing, the hull usually penetrates the water surface with a definite trim angle and with a resultant velocity which is not normal to the keel of the hull. Also, the forebody of the hull has a definite length terminating at the step that results in certain end flow losses at the step which must be considered. The three-dimensional analysis will be made for an ideal prismatic float with no afterbody. The float is assumed to maintain a constant trim and horizontal velocity throughout the impact period. In Figure 4 an ideal float is shown immersed in the water after having travelled along a path of motion indicated by the dotted line. Mayo (1945 and July 1945) and Benscoter (1947) applied the two-dimensional theory to the solution of the case of the oblique impact of a Vee shaped surface. The fluid beneath the float is imagined as subdivided into slices of length  $ds$  by planes drawn normal to the keel of the float. As the float moves through these slices, the flow in each slice is assumed to be two-dimensional and identical with the flow in the case of the wedge dropped vertically into water as treated in the two-dimensional case. It is necessary to assume that the fluid in each slice is independent of the motions in adjacent slices and that the reaction on the float is due to combined action of all the slices which have a total width equal to the wetted keel length.

Before presenting the analytical solution for the three-dimensional case, two additional factors must be considered -- one concerns the definition of the virtual mass and the other the effect of end losses at the step. von Karman initially defined the added mass  $m$  on the basis of the half breadth  $c$  of the intersection of the wedge with the undisturbed water level. Herbert Wagner (1931, 1932), (see also Pierson, 1948 TR-336), took into account the rise of the water surface near the surface of the wedge and defined the diameter of the semi-cylinder of virtual mass on the basis of deadrise and depth of immersion. Thus, referring to Fig. 3b, the effective diameter  $2c$  is defined by Wagner as follows:

$$c = f(\beta)z$$

$$c = \left( \frac{\pi}{2\beta} - 1 \right) z \quad \beta \text{ in radians.}$$

A correction factor for approximating the three-dimensional condition on the basis of a two-dimensional calculation has been developed by Pabst

(1930), who showed that the correction was a function of the length/beam ration of the wetted area:

$$g(A) = 1 - \frac{\tan \tau}{2 \tan \beta}$$

As in the two-dimensional case the analysis proceeds with the equation for change of momentum. The fluid in each slice exerts an elemental force  $f$  on the bottom:

$$f = \frac{d}{dt} (m\dot{z}) = m\ddot{z} + \dot{m}\dot{z}$$

$$m = [f(\beta)]^2 \frac{\rho \pi}{2} z^2$$

$$f = [f(\beta)]^2 g(A) \frac{\rho \pi}{2} [z^2 \ddot{z} + 2z\dot{z}^2]$$

Integrating over the entire float length to obtain the total force  $F$  on the bottom:

$$F = [f(\beta)]^2 g(A) \frac{\rho \pi}{2} \int_0^{z_s/\tan \tau} (z^2 \ddot{z} + 2z\dot{z}^2) ds$$

substituting  $z = s \tan \tau$

$$F = [f(\beta)]^2 g(A) \frac{\rho \pi}{2} \int_0^{z_s/\tan \tau} (s^2 \tan^2 \tau \ddot{z} + 2s \tan \tau \dot{z}^2) ds$$

Integrating and letting  $F = -\frac{W}{g} \ddot{z}$

$$-\frac{W}{g} \ddot{z} = [f(\beta)]^2 g(A) \frac{\rho \pi}{2 \tan \tau} \left[ \frac{z_s^3}{3} \ddot{z} + z_s^2 \dot{z}^2 \right] \quad (\text{Eq. 7})$$

which expresses the general relationship that exists among the variables at any time during the impact process.

For convenience in application of the results, the above equation is transformed to a coordinate system relative to the water surface using the following relations (with Reference to Fig. 4):

$$\begin{aligned}\dot{z} &= \dot{x} \sin \tau + \dot{y} \cos \tau \\ V_p &= \dot{x} \cos \tau - \dot{y} \sin \tau \\ \text{or } \dot{z} &= \frac{\dot{y}}{\cos \tau} + k\end{aligned}$$

$$\text{where } k = V_p \tan \tau$$

$$\begin{aligned}\text{also: } z_s &= \frac{y}{\cos \tau} \\ \ddot{z} &= \frac{\ddot{y}}{\cos \tau}\end{aligned}$$

Substitution of these relations into general equation result in:

$$-\frac{W}{g} \ddot{y} = \frac{[f(\beta)]^2 g(A)}{6 \sin \tau \cos^2 \tau} \frac{\rho \pi}{3} \left[ y^3 \ddot{y} + 3y^2 (\dot{y} + k \cos \tau)^2 \right]$$

or

$$\left[ 1 + \left( \frac{\alpha g}{W} \right) y^3 \right] \ddot{y} + 3 \left( \frac{\alpha g}{W} \right) y^2 (\dot{y} + k \cos \tau)^2 = 0 \quad (\text{Eq. 8})$$

where,

$$\alpha = \frac{[f(\beta)]^2 g(A)}{6 \sin \tau \cos^2 \tau} \frac{\rho \pi}{3}$$

The solution of the above equation for acceleration, velocity and draft has not been carried out analytically but a numerical solution is given in Milwitzky (1948). The results presented are in coefficient form as follows:

$$\text{Draft coefficient} = C_d = yK$$

$$\text{Time coefficient} = C_t = \dot{y}_0 tK$$



## Impact

$$\text{Load factor coefficient} = C_\ell = \frac{n_w g}{\dot{y}_0^2 K}$$

Where,

$$K = \left( \frac{g Q}{W} \right)^{1/3}$$

$y$  = instantaneous value of draft at step

$\dot{y}_0$  = vertical component of the velocity at first contact with water

$\dot{y}$  = vertical component of the velocity at the instant under consideration, i.e. at the draft  $y$  and time  $t$

$t$  = time in seconds from the first contact with water to the instant under consideration

$n_w$  = load factor; i.e. ,  $\ddot{y}/g$

$W$  = weight of seaplane.

The above coefficients are shown in Milwitzky (1948) to be functions of the approach parameter  $\kappa$ , as defined on Figures 5 to 8. It is noted that approach parameter is a function of the trim angle  $\tau$  and the glide path angle  $\gamma_0$ . For each value of the approach parameter  $\kappa$  the values of coefficients are shown for the instant of maximum acceleration, the instant of the maximum immersion, and in some cases at rebound. All of the above data apply to the float of the uniform, straight Vee cross section throughout the wetted length. The method of using the data for the curved bottom sections is given in Milwitzky (1947).

Example: Consider the prismatic float of 22-1/2 degree angle of deadrise, loaded to 1100 pounds, landing with the flight path angle  $\gamma_0 = 8^\circ$ , the angle of trim  $\tau = 9^\circ$  and the velocity of 75 feet per second. Assume sea water with  $\rho = (64 \text{ lb/ft}^3) / (32.2 \text{ ft/s}^2) = 1.99 \text{ lb s}^2 / \text{ft}^4$

# Impact

$$y_o = V_o \sin \gamma_o = 75 \times .1392 = 10.45 \text{ ft./sec.}$$

$$f(\beta) = \frac{3.14 \times 57.3}{2 \times 22.5} - 1 = 3.0$$

$$g(A) = 1 - \frac{.1584}{2 \times .4112} = .908 \quad \leftarrow \text{should be } 0.808$$

$$K = \left( \frac{32.2 \times 3.0 \times .908 \times 1.99 \times 3.14}{1100 \times 6 \times .1564 \times .9877} \right)^{1/3} = 1.175$$

$$K = .1564 \times .956 / .1392 = 1.08 \quad \leftarrow \text{should be squared?}$$

At the instant of the maximum acceleration we have, from Fig. 7 and 8:

$$C_\ell = 1.6 \quad C_t = 0.5$$

whence:

$$\text{Load factor } n_w = 1.6 \times 1.175 \times 10.45^2 / 32.2 = 6.4$$

Time for the moment of the first contact to the instant of the max. acceleration:

$$t = \frac{0.5}{1.175 \times 10.45} = 0.04 \text{ sec}$$

# Impact

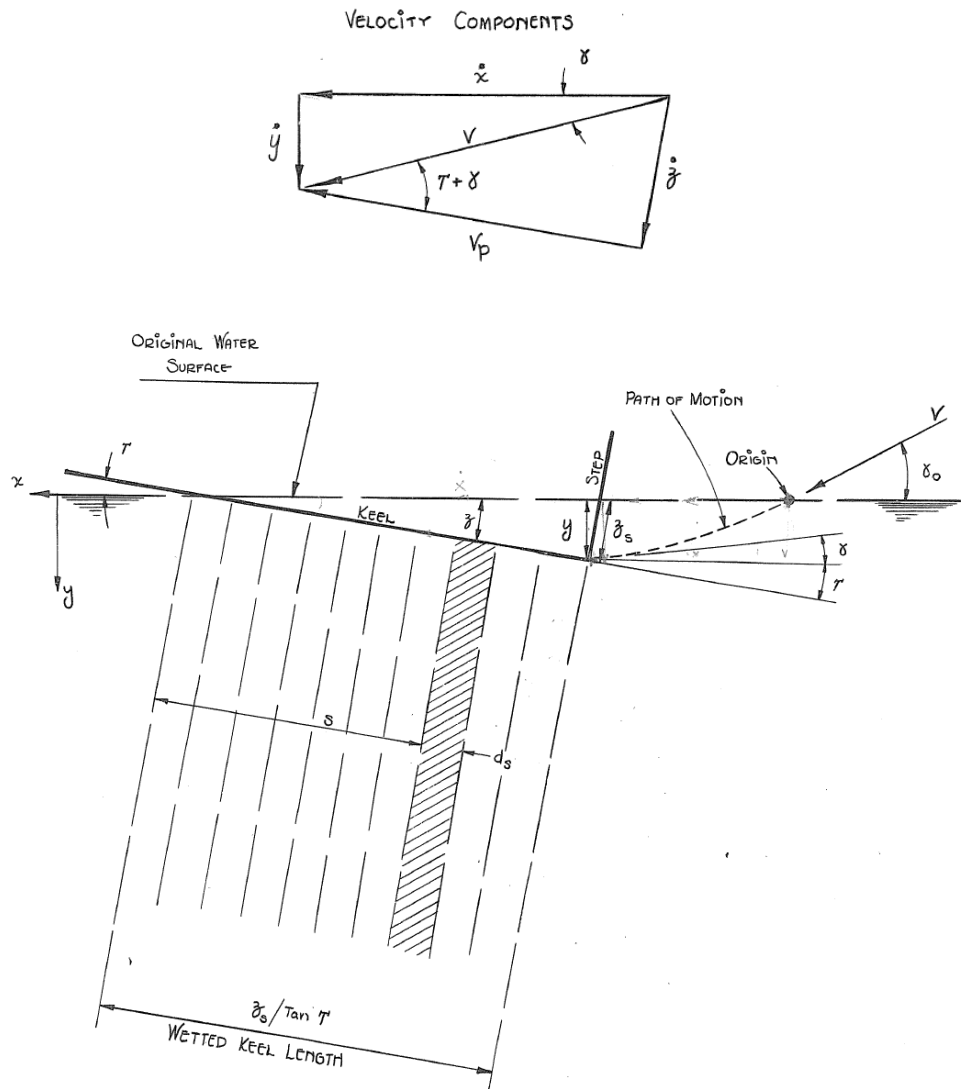


Figure 4: Instantaneous Position of the Float During Impact (taken from Benscoter, 1947)

# Impact

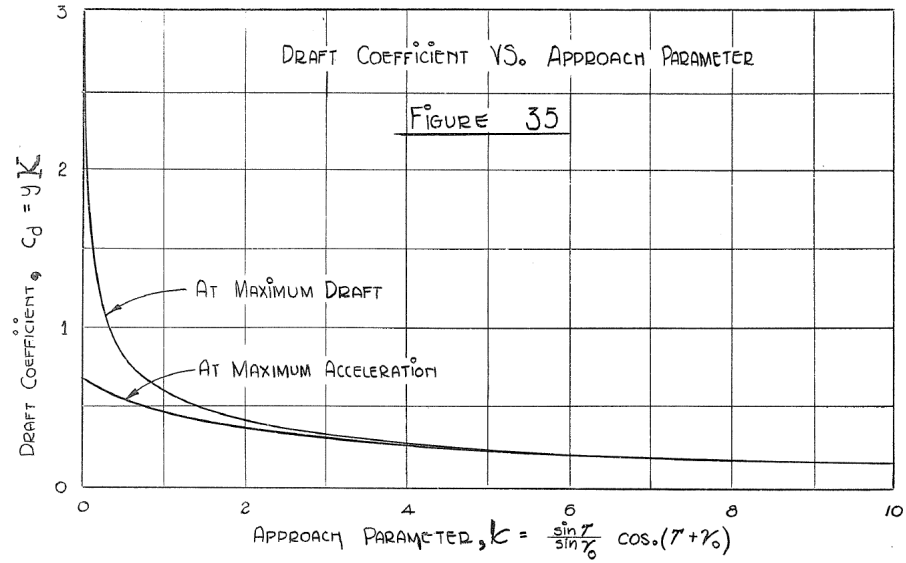


Figure 5: Draft Coefficient vs. Approach Parameter (taken from Milwitzky, 1948)

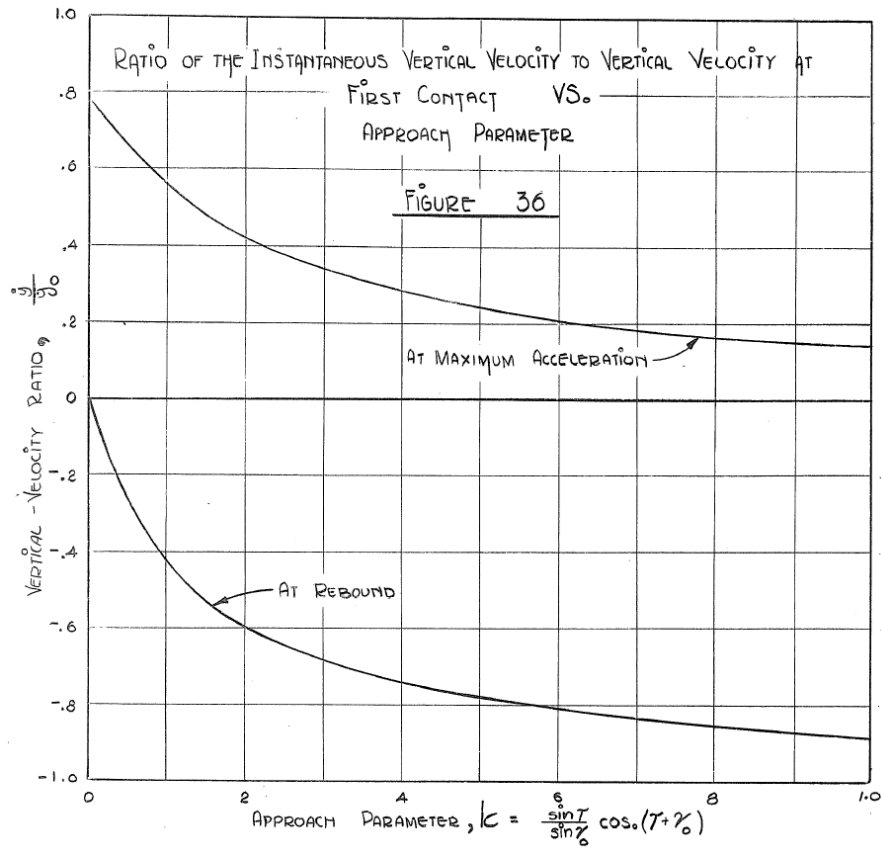


Figure 6: Ratio of the Instantaneous Vertical Velocity to the Vertical Velocity at First Contact vs. Approach Parameter (taken from Milwitzky, 1948)

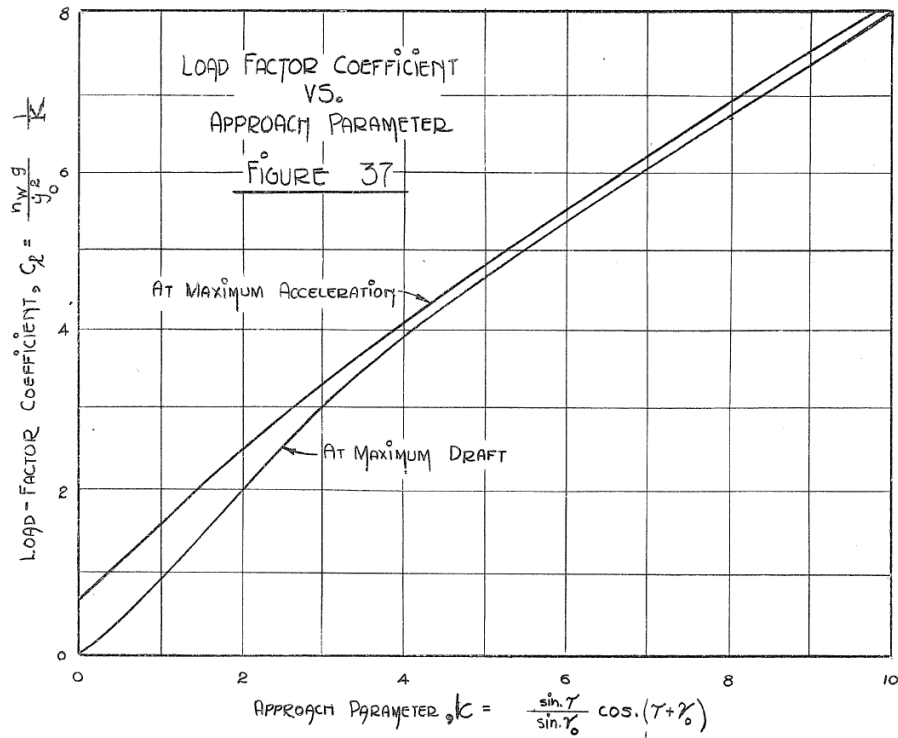


Figure 7: Load Factor Coefficient vs. Approach Parameter (taken from Milwitzky, 1948)

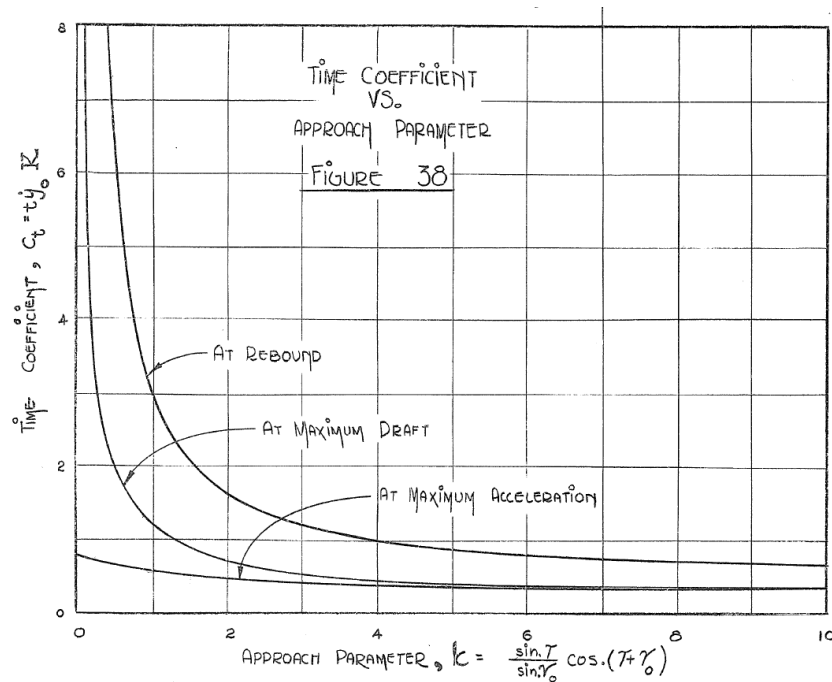


Figure 8: Time Coefficient vs. Approach Parameter (taken from Milwitzky, 1948)

#### 8.4 Impact Basin

Batterson (1944) describes experimental tank constructed at N.A.C.A laboratories specifically for the impact testing of large models - up to about 2400 pounds displacement (Figures 9 and 10). This float or model is attached to the carriage which is accelerated to the proper landing speed by means of a catapult. When the proper speed is reached the float with a certain part of the attaching structure is allowed to drop onto water, either smooth, or on waves as desired. The horizontal speed up to 110 feet per second and the height of drop up to 4 feet are available. The vertical travel of the float, and accelerations resulting from the impact are recorded. Batterson (1944, 1945a, 1945b, 1946, 1947) gives results of such impact tests in smooth water on the prismatic float of 22-1/2 deadrise at several angles of trim from -3 to 12 degrees. Milwitzky (1948) indicated excellent agreement between these test results and the theoretical data represented by Figures 5 to 8.



Figure 9: Impact Basin (NASA)

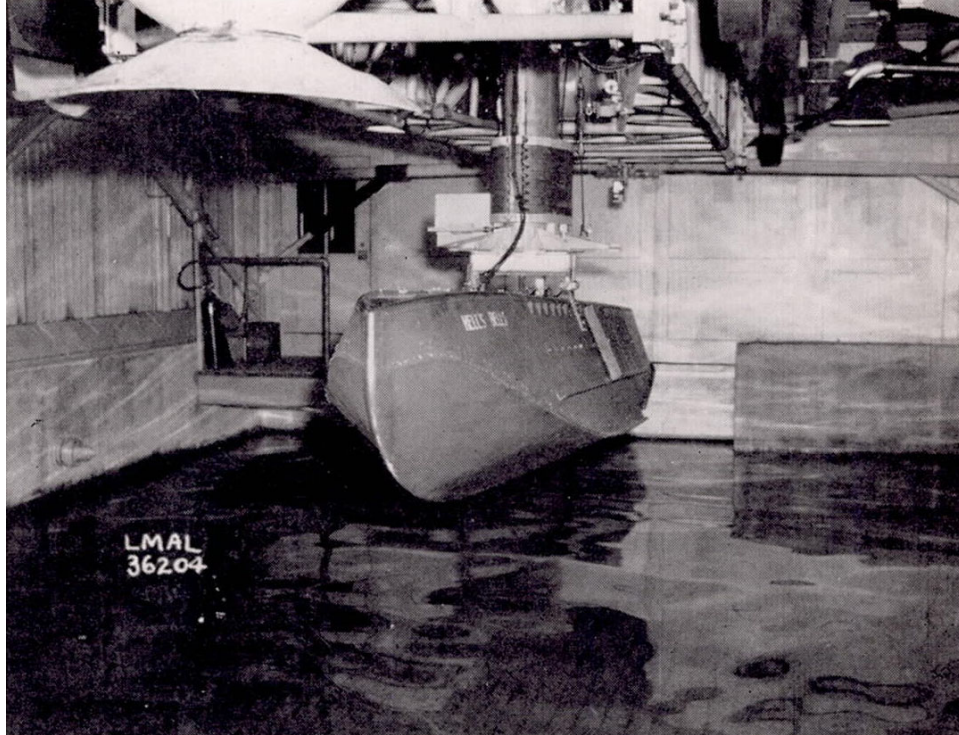


Figure 10: Front View of Model Attached to Boom (Batterson, 1944)

### 8.5 Landing on Waves

IN the previous paragraphs the impact of a Vee shape on smooth water was discussed. Figure 11 shows the seaplane landing on waves. All of the data of smooth water landing are applicable in this case, provided the angle of trim  $\tau$  is measured with respect to the part of the wave surface at which the hull makes contact with water, and  $\dot{y}_0$  used in the previous theory is replaced by  $v_n$ , which is the component of the velocity taken normal to the water surface, as shown on Figure 12. In a number of landings the contact will be made with a number of points on the wave profile; at certain points the combination of  $\tau$  and  $v_n$  produce the approach parameter  $k$  such that maximum acceleration at the impact will result. This will occur usually for the impacts at the steepest slope of the wave flank, which varies with the ratio of the wave length to height (for further information on waves see section 8.8). By making a large number of tests in a towing tank, in waves varying length, and with the model landing at random on any part of the wave profile, the curve can be drawn of the maximum impact acceleration vs. wave length. Such a curve is shown on Figure 13. As the wave length is decreased from about 750 feet to 250 feet, the maximum impact acceleration is increased, because the landing are made on progressively steeper slopes of shorter waves. As the wave length is decreased below 250 feet, the impacts become less severe, because the crest of the preceding wave begins to interfere, and the impacts can occur only on the higher points of the wave, where the slope is smaller.

Examination of the Figure 11 shows that in order to avoid a too small, or even negative angle of trim  $\tau$  the seaplane must be flown at a large angle of attack with respect to the flight path, and this in turn must be as flat as possible, i.e.  $\gamma_0$  must be as small as possible. Furthermore the acceleration of the impact is proportional to the square of the speed, and the speed therefore must be as small as possible. All three of these objectives, large angle of attack, small  $\gamma_0$  and the lowest possible speed, are obtained in a power landings. In these landings sufficient engine power is used to permit seaplane only a very slow rate of descent, while maintaining a very large angle of attack. The effect of the slipstream in this case gives added wing lift, and better elevator control, so that larger angle and lower speed can be obtained than would be possible in a power-off landing. Furthermore, should the seaplane bounce off severely, as it does all too



often, sufficient increase of engine power can be quickly obtained to permit a gentle letdown for the next contact.

The bounce often results in the partial loss of control and speed, and the seaplane comes to the second and the subsequent contacts with waves at a steeper and steeper "glide path" angles, and smaller and smaller angle of trim. The conditions cease to correspond to the "step landing" discussed in theory, the resultant force moves towards the bow, and in addition to the vertical force a large nose-up pitching moment is developed. Figure 12 gives the envelopes of the maximum translational acceleration and the maximum pitching acceleration for the various positions of the force along the hull length between the bow and the step. Excellent time history of the landing process obtained on two dynamic models in the towing tank will be found in Benson, Havens and Woodward (1947). Good data on the position of the resultant force will be found in Pabst (1931). These were obtained on the full-size tests of a Heinkel HE-9a twin-float seaplane.

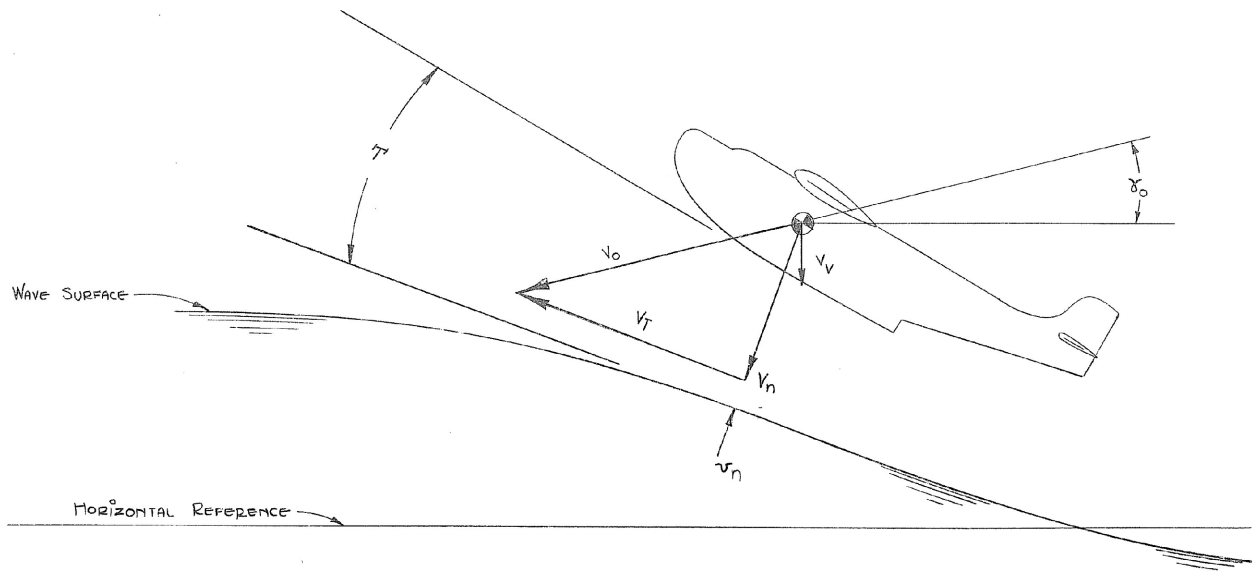


Figure 11: Landing on the Flank of the Wave (taken from Lyman, 1946)

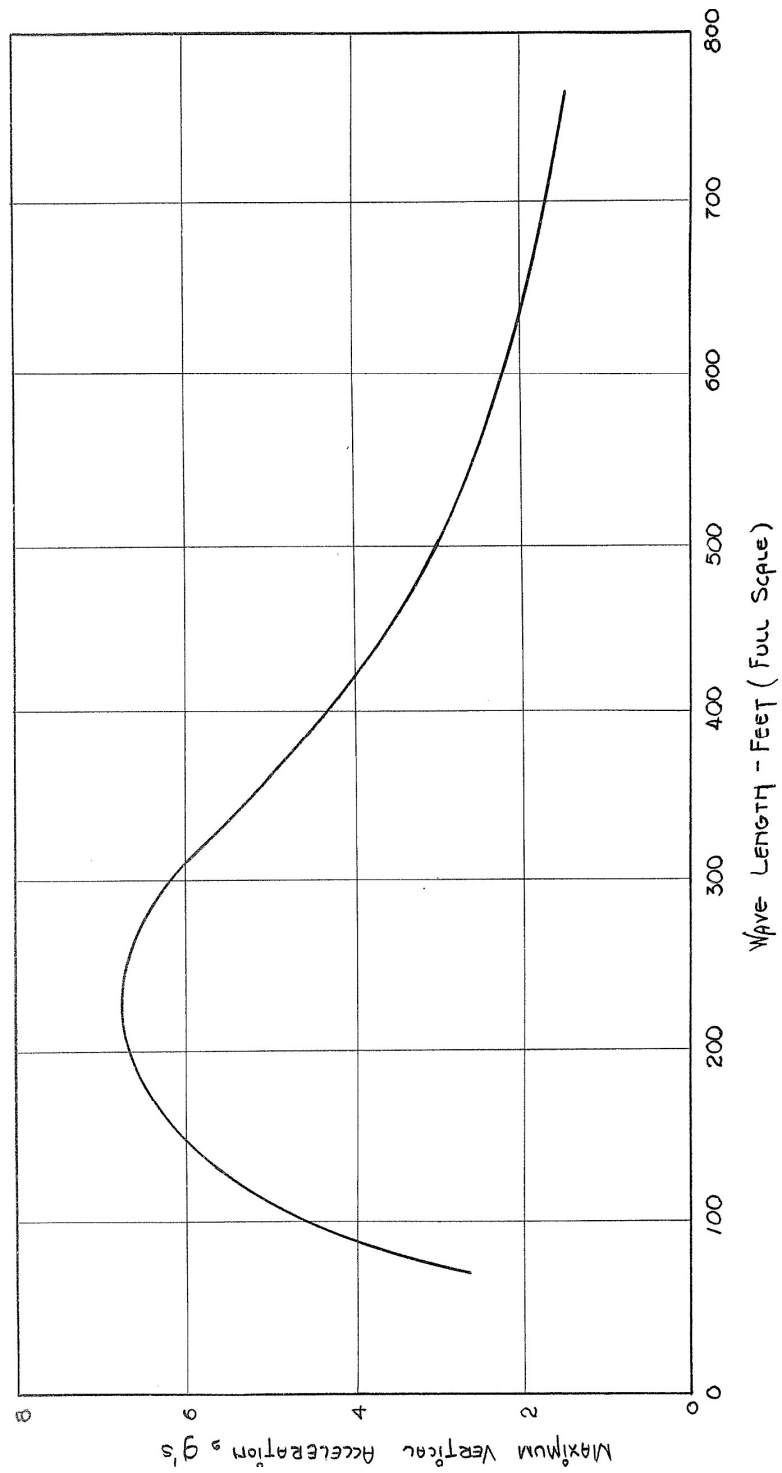


Figure 12: Acceleration plotted vs. wave Length in case of a seaplane landing in oncoming 4.4 foot waves. (Taken from Lyman, 1946)

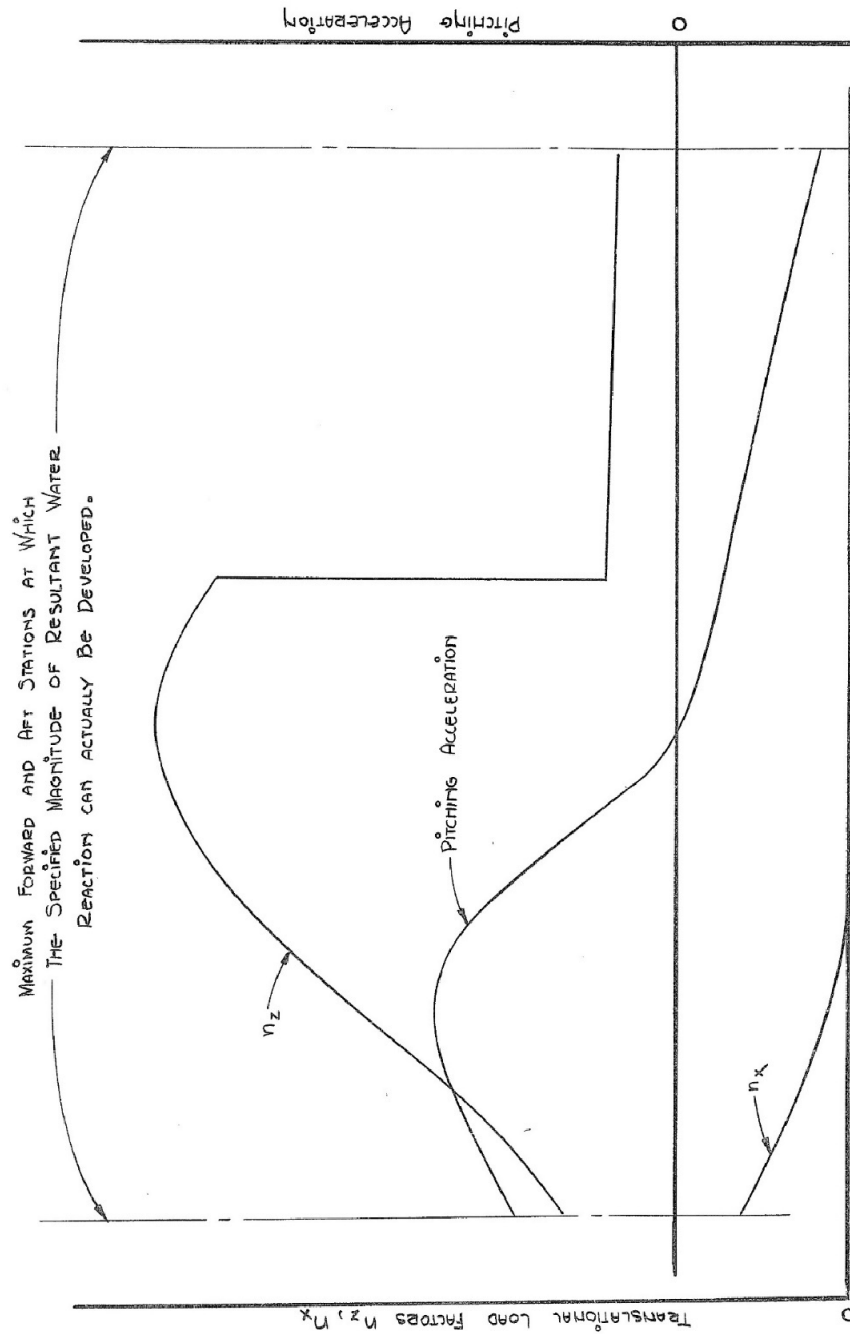


Figure 13: The Plot showing the magnitudes of the vertical, horizontal and pitching angular accelerations vs. position of the resultant force. (Taken from Lyman, 1946)

### 8.6 Pressures Acting on the Hull Bottom

In the section 8.2 it was explained how Th. von Karman represented the water force acting on the wedge entering water by assuming the wedge to be equivalent to the flat plate of the same wetted width, and using the concept of the "added mass" associated with such a plate. Herbert Wagner (1931, 1932) [and explained by Pierson 1948, TR-335, TR-336] also used the concept of the expanding plate, but in addition to the determination of the added mass he used the equation of the fluid flow about a plate. He has shown that immersion of the wedge is accompanied by the rise of water level in immediate proximity of the wedge so that wetted width  $C$  becomes  $\pi/2$  times the width defined by the intersection of the wedge with undisturbed water, as this is shown on Figure 3b. The velocity of the fluid at any point of the wedge is obtained from the flow equations, and is shown to vary from zero at the keel to the maximum at the chine. Since the velocity at any point is known, the pressures are readily obtained from this theory as shown by the dotted lines on Figure 14. The conspicuous part of this diagram is the sharp peak of pressure at the edge of the wetted area, with lower pressures towards keel. When the chines are submerged, and the flow corresponds to the plate of a fixed width, the maximum pressure is at the keel, and corresponds to the stagnation pressure due to the vertical velocity  $V$ , i.e. to  $\rho V^2/2$ . The penetration of the Vee shape is shown to be analogous to the expanding plate, and even at the keel the pressure is shown to be several times higher than above, while the peak pressure now occurs at the edge of the wetted area.

The "expanding plate" theory gave excellent insight into the general pattern of the flow, and into the pressures connected with it. It is evident, however, that conditions at the edge of the wetted area, point A on Figure 3b, requires further study, since the presence of the high pressure peak at the edge of the free surface must cause some form of an intensive local disturbance. H. Wagner applied the term "spray root" to the vicinity of the point A, and developed the mathematical theory representing the fluid flow in this region [see Pierson, 1948 TR-335 and TR-336 for complete derivation]. If the vertical velocity of the wedge be designated by  $V$ , the horizontal velocity  $v$  of the point A becomes:

$$v = dC/dt = \pi V/2 \tan \beta \quad (\text{Eq. 9})$$

Since the point A moves with velocity  $v$  with respect to the undisturbed water, the stagnation pressure at A is:

$$p_{\max.} = \rho v^2 / 2 \quad (\text{Eq.10})$$

This pressure accelerates the fluid particles along the bottom (forming the spray sheet) to the velocity  $v$  with respect to the point A, or approximately  $2v$  with respect to the undisturbed water. The existence of the spray, and of the high pressure peak are shown to be inseparably connected - one cannot exist without the other. It is demonstrated in Pierson (1948, TR-336) that the same value of the peak pressure is obtained from either the "expanding plate" or the "spray root" theories.

It has been shown in Par. 8.3 and on Fig. 4 that planing of a Vee-shaped surface can be compared to the penetration of the wedge in each of the imaginary vertical slices of water. At the leading edge of the wetted area of the planing surface the "spray root" is formed, with its characteristic pressure peak, and with pressures dropping towards keel. These phenomena cease to exist as the chines become wetted, and all pressures drop to lower values. Figure 16 shows the pressure distribution as measured by Dr. W. Sottorf on a prismatic planing surface of 15 degrees deadrise, planing at the angle of trim of 6 degrees. Figure 17 shows the results of the pressure distribution measurements on a full-size flying boat. Here the regions of the peak pressure and of the reduced pressure aft are approximated by rectangular step diagrams. Figure 18 shows similar pressure distribution for a longer wetted length, with a certain length of the chine forward of step wetted. Reader's attention is called to the fact that these diagrams represent the instantaneous distribution of pressure. They should not be confused with the diagrams often found in the literature on the subject, showing the maximum pressure occurring at any part of the bottom during a landing, which are the "envelopes" of the instantaneous pressure diagrams.

As the wetted length of the hull changes with the speed and load, the region of the peak pressure, always located at the leading edge of the wetted area, traverses the hull bottom area, so that almost any part of it is subjected to the high local pressure at some time. The bottom plating and stringers supporting a small bottom area must be designed therefore to withstand this high peak pressure. U.S. Navy, Bureau of Aeronautics calls for the yield strength of the plating and stringers of 25 pounds per square

inch. The supporting structure, however, will be affected by the average pressure over a certain larger area, and can be designed for somewhat lower pressure.

Equations 9 and 10 show that velocity of the stagnation point A, and therefore the pressure, increase with decrease of the deadrise. Figure 17 shows how the magnitude of the maximum pressure is affected by the transverse shape of the planing bottom. In case of the straight Vee the pressures gradually drop towards the chine, because of the decrease of the vertical velocity with increasing penetration into water. With a slight concavity of the bottom, pressures increase gently towards the chine, because of the decrease of the local deadrise angle. With the deep curvature of the bottom the pressures peak sharply towards the chine.

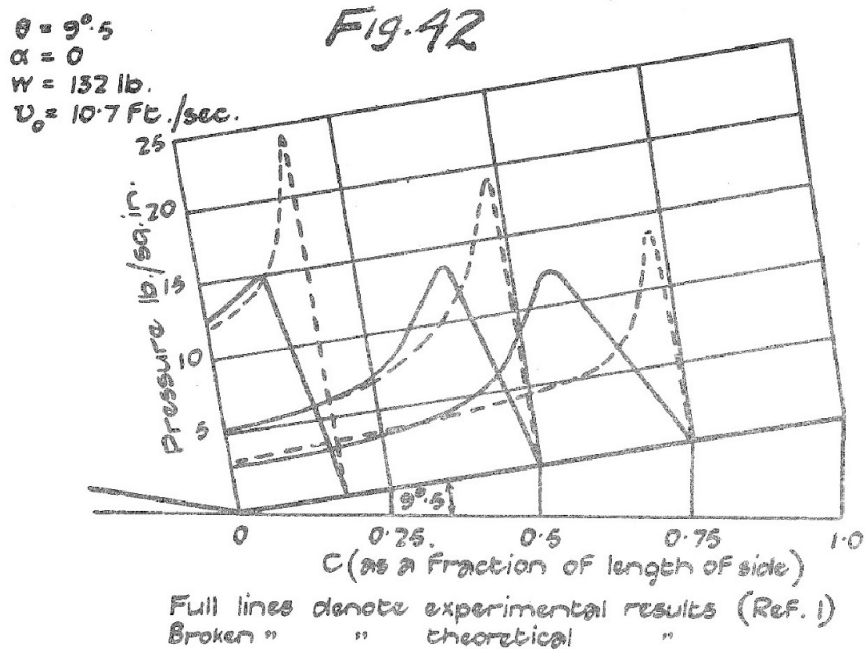


Figure 14: Theoretical Pressure Distribution over Straight Sided Vee Compared with Experimental Results when Pressure Surface Reaches  $C = 1/6$ ,  $1/2$  and  $3/4$  of the Distance between Keel and Chine (taken Jones and Blundell, 1932)

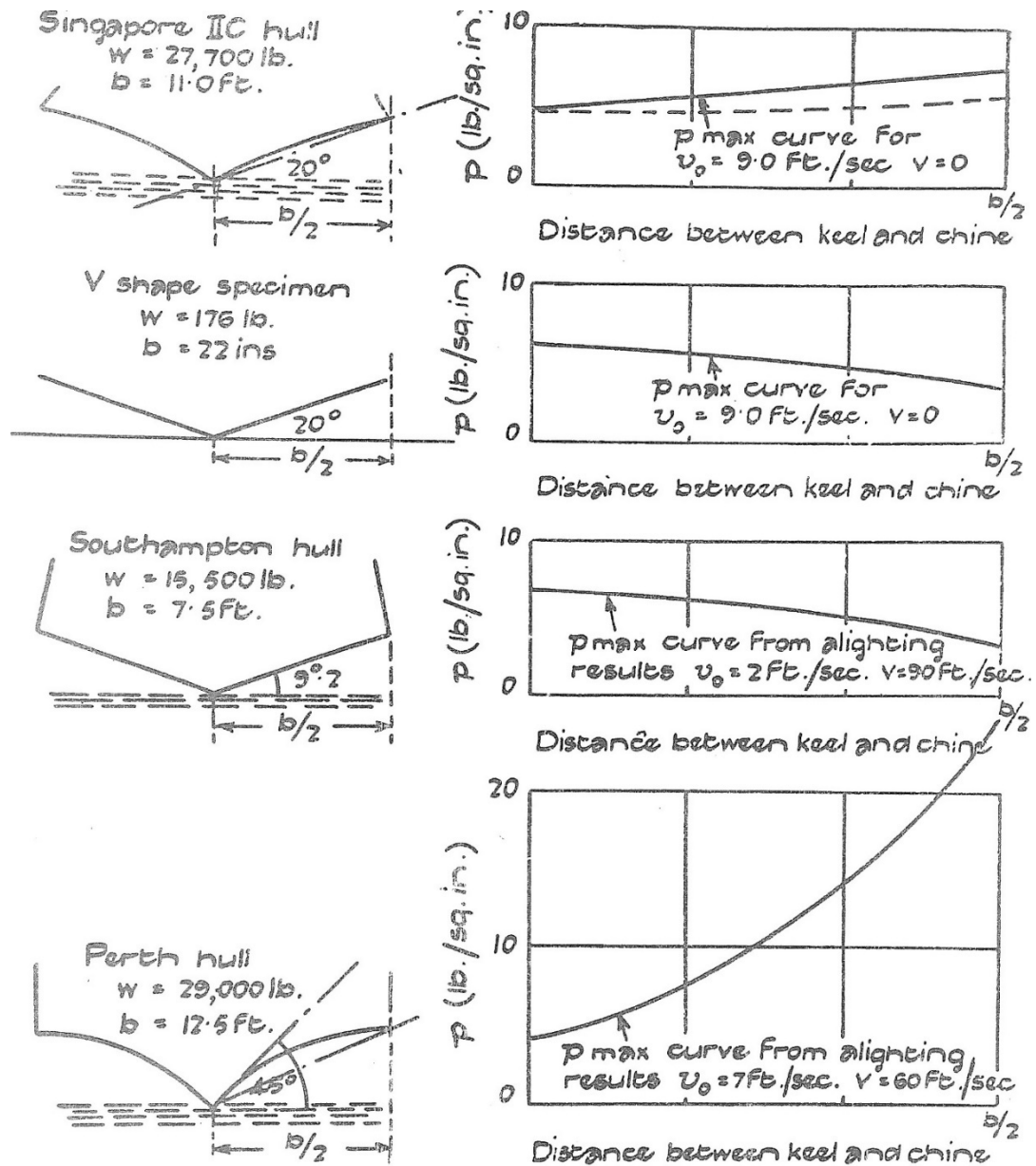


Figure 15: Peak Pressures across Several Typical Sections of Flying Boats  
 (taken from Jones and Blundell, 1932)

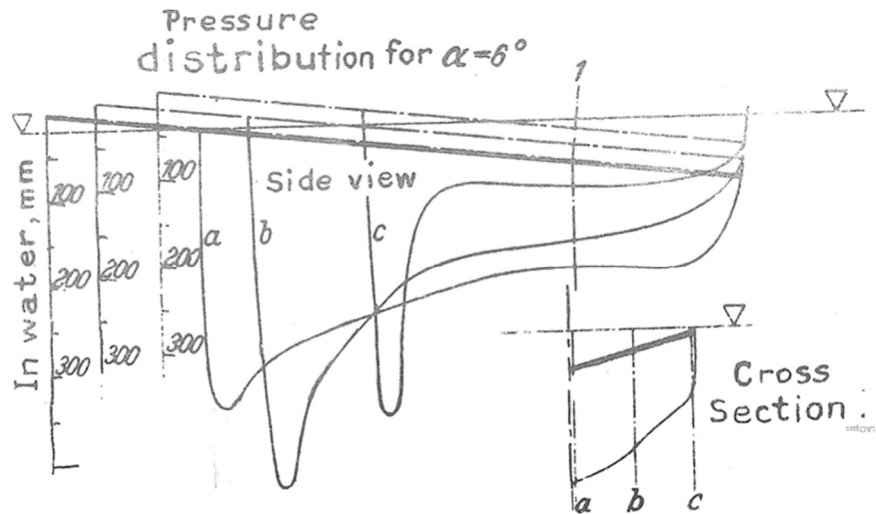


Figure 16: Pressure distribution in case of a 15-degree deadrise prismatic planing surface, planing at the angle of trim of 6-degrees and a speed of 6 m/sec. (taken from Sottorf, 1933)

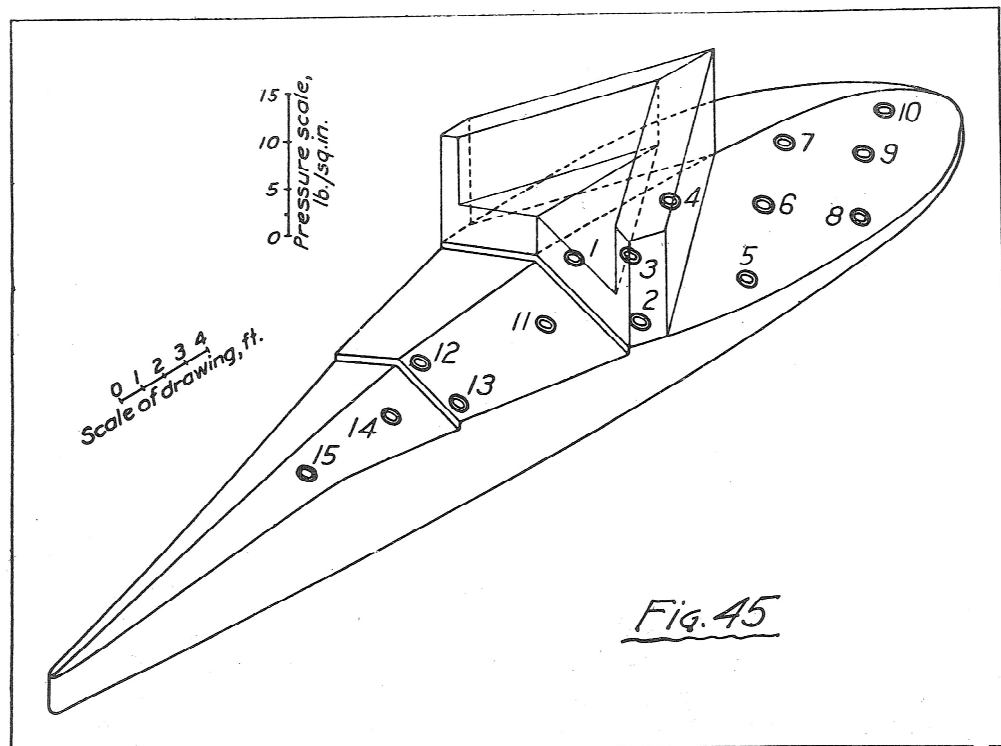


Figure 17: Approximate distribution of the maximum water pressure caused by impact with a wave in a take-off total load 4.7 times weight of seaplane (taken from Thompson, 1931)



## Impact

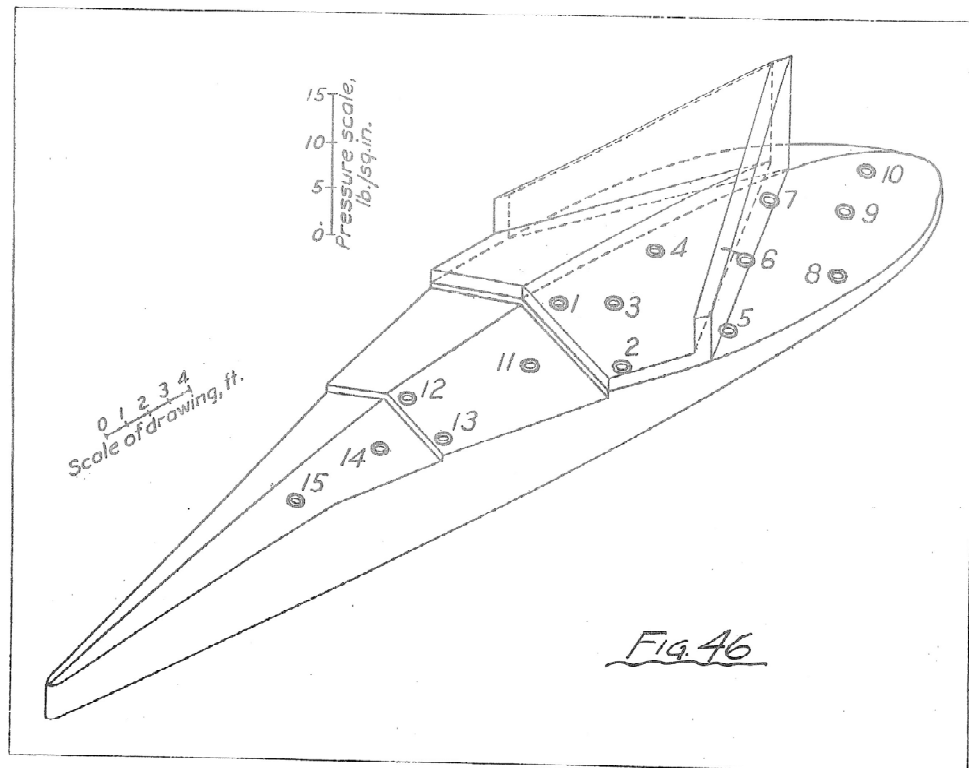


Figure 18: Approximate distribution of the maximum water pressure caused by impact with a wave in a take-off total load 3.0 times weight of seaplane (taken from Thompson, 1931)

### 8.7 Effect of the Elasticity of Supporting Structure

Figure 19 shows diagrammatically the main mass of the seaplane  $M$  attached to the mass of the planing bottom  $M'$ . Initially both masses have the same vertical velocity (SYMBOL), but during the impact the velocities become (SYMBOL) and (SYMBOL), using the notation shown on Figure 19. We have now two equations describing the motion: the conservation of momentum, expressed by Equation 1 for the rigid wedge, now becomes (according to Fagg, 1941):

$$(M + M') V_0 = M \dot{y} + (M' + m) \dot{z} \quad (\text{Eq.11})$$

and the force in the structure, or "spring", connection masses  $M$  and  $M'$ :

$$M \ddot{y} = -k(y - z)$$

where  $k$  is the spring constant.

Wilhelm Pabst (1930), neglecting the mass of the bottom structure  $M'$ , writes:

$$\left. \begin{aligned} M (d^2y/dt^2) &= kf - nW \\ m (d^2z/dt^2) &= -kf \\ y - z &= -f \end{aligned} \right\} \quad (\text{Eq.12})$$

In writing the above we modified the original notation of Pabst to correspond to the notation already used in Sec. 8.2 of this book. The additional symbols not used before are:

$n$  - the fraction of the weight remaining after deducting the lift of the wings. It is often permissible to take  $n = 0$ , i.e. to assume the entire weight to be supported by wings, as indeed it must be just before the impact.

$f$  - the deflection of the spring.

## Impact

Differentiating twice the last one of Eqs. 12:

$$\frac{d^2 y}{dt^2} - \frac{d^2 z}{dt^2} = - \frac{d^2 f}{dt^2}$$

and substituting from first two Eqs. 12:

$$\frac{d^2 f}{dt^2} + kf \left( \frac{1}{M} + \frac{1}{m} \right) - ng = 0 \quad (\text{Eq. 13})$$

the solution of this differential equation is:

$$\left. \begin{aligned} f &= A \sin \omega t + B \cos \omega t + ng/\omega^2 \\ \text{where} \quad \omega^2 &= k \frac{M+m}{Mm}; \quad A = \frac{V_o}{\omega}; \quad B = - \frac{ng}{\omega^2} \end{aligned} \right\} \quad (\text{Eq. 14})$$

Equation 14 can be written also in the alternate form:

$$\left. \begin{aligned} f &= Y \sin (\omega t - \beta) + ng/\omega^2 \\ \text{where} \quad Y &= \frac{1}{\omega} \left[ (ng/\omega)^2 + V_o^2 \right]^{1/2} = ng/\omega^2 \\ \beta &= \arctan \frac{ng}{\omega V_o} = \arctan \frac{B}{A} \end{aligned} \right\} \quad (\text{Eq. 15})$$

The important fact indicated by Eq. 15 is the oscillatory character of the deflection of the structure supporting the mass, and the resulting oscillatory variation of stresses in the structure. This may be very important in many types of trussed structures, such for instance, as the struts connecting the floats of a float seaplane to the fuselage. Such a structure may contain slender tension members, which will be subjected to compression, and may fail in buckling in the reversal of stress after the impact. The theory outlined above does not take account of the damping, and indicates the reversal of the stress of full magnitude. Actually all structures possess a certain amount of damping, reducing the intensity of stress in consecutive oscillations. A good rule of thumb, based on the above

## Impact

reasoning, is to check the slender tension members for the compressive stress equal to about half of the design tensile strength.

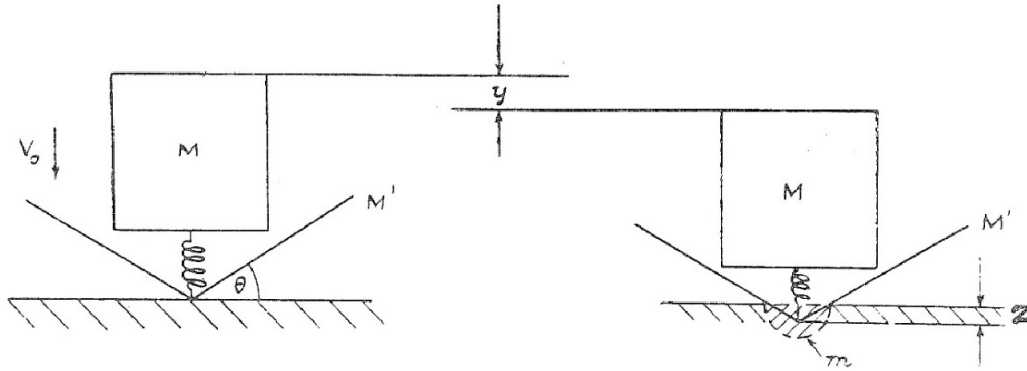


Figure 19: Sketch showing the effect of elastic connection between the mass of the seaplane and the planing bottom during impact (taken from Fagg, 1941)

### 8.8 Waves

A system of exact equations expressing a possible form of wave motion when the depth of the water is infinite was given as long ago as 1602 by Gerstner, and in 1862 independently by Rankine and by W. Froude (see Principles of Naval Architecture, 1939 and Lamb, 6<sup>th</sup> Edition). If the axis  $x$  be drawn horizontal, and that of  $y$  be drawn vertically upwards, the formulae in question may be written

$$\left. \begin{aligned} x &= a + r e^{kb} \sin k(a + ct) \\ y &= b - r e^{kb} \cos k(a + ct) \end{aligned} \right\} \quad (16=36)$$

where  $a$  and  $b$  are two coordinates defining the original position of a particle, and  $x$  and  $y$  are the coordinates of this particle at time  $t$ . The constant  $k = 2\pi/L$ , where  $L$  is the wave length, and  $c$  is the velocity of propagation (the celerity) of the wave. It is obvious from Eq. 16 that the path of any particle  $(a, b)$  is a circle of radius  $re^{kb}$ . Since  $b$  is negative, the radius of the circle diminishes rapidly with the increase of the depth of a particle. The surface particle moves through the height  $\pm r$ , i.e. the height  $H$  of the wave from trough to crest is  $2r$ . The velocities of the water particles resulting from the above circular motion are referred to as "orbital velocities".

The form of the wave resulting from the above motion of water particles is represented by the curve known as "curtate cycloid" or "trochoid", the construction of which is shown on Figure 20. The curve is traced by a certain point located at the radius  $r$  on a generating disk of radius  $R$  rolling along a straight track. The equations of the curve referred to the track are:

$$\begin{aligned} x &= R\theta + r \sin \theta \\ y &= R + r \cos \theta \end{aligned}$$

where  $R$ ,  $r$ , and the angle  $\theta$  are shown on Figure 20. The length of the wave is  $L = 2\pi R$ , and the height from the trough to the crest is  $H = 2r$ . The slope of the wave surface is:

$$\tan \bar{\phi} = \tan \beta = dy/dx = \frac{r \sin \theta}{R + r \cos \theta}$$

The celerity (the velocity of the wave propagation) is:

$$c = \sqrt{gL/2\pi}$$

and the period:

$$T = L/c = \sqrt{2\pi L/g}$$

The experimental verification of the wave theory is given in Beach Erosion Board, Report No.1 (1941), together with an excellent bibliography on the subject. A very close agreement between theoretical, and experimental wave shapes is indicated.

The waves are usually described by their height H, and the ration of length L/H. Harney, et. Al (1949) gives the statistical data on the wave height and the L/H ratio encountered at several stations in open sea. For the wave height over 15 feet, the predominating frequency of occurrence of L/H is in the range of 20 to 30. L/H of 20 is adopted in the Naval Architecture as the basis for the strength calculations of ship hulls. In the wave heights of 4 to 10 feet, in which seaplanes often have to operate, the frequently encountered waves are in the L/H range of 20 to 60.

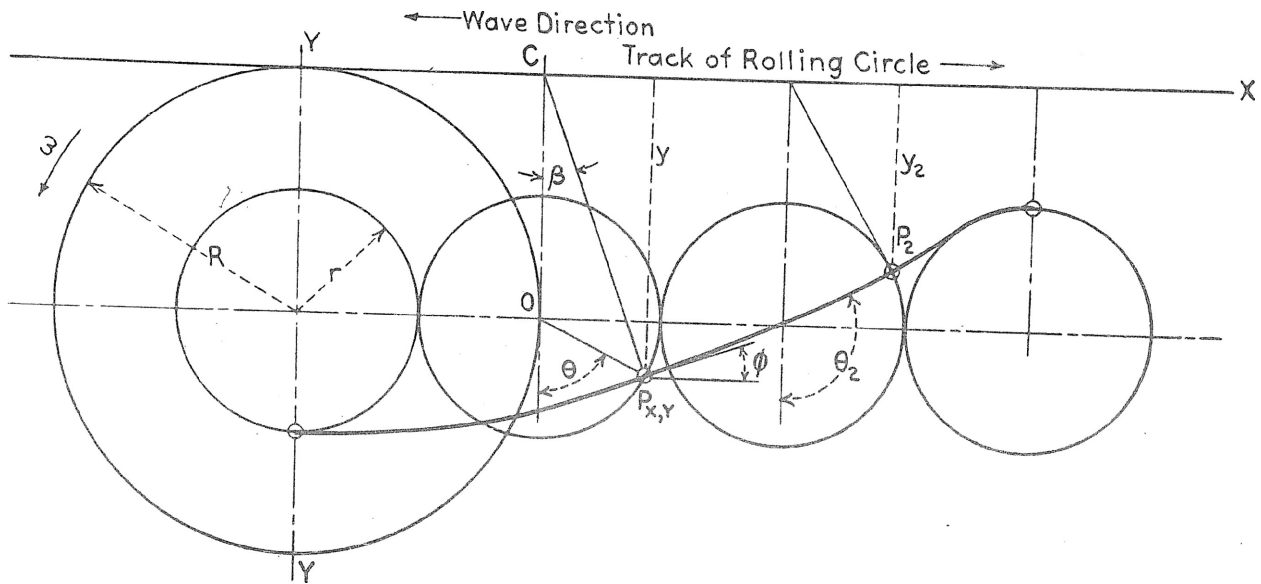


Figure 20: Diagram showing the generation of the trochoidal wave form (taken from Principles of Naval Architecture, Vol. 2 1939)

[U.S. Naval Academy Principles of Ship Performance Notes, 2024]

The true shape and configuration of the sea is far more complicated than the single wave due to the interaction of several different wave systems. Figure 21 shows a typical topological plot of the wave elevation for a portion of the North Atlantic.

The confused state of the sea at any point can be modeled as the destructive and constructive interference pattern created between several wave systems. This modeling of the sea is made possible by the Superposition Theorem that implies that the sea wave system is made up of many sinusoidal wave components superimposed upon each other. Each component sine wave has its own wavelength, speed and amplitude. This is shown diagrammatically in Figure 22. Figure 22 also shows that it is also possible to analyze the sea in the frequency domain. This is called the Sea Spectrum. Figure 23 shows a typical sea spectrum. Examination of sea spectra such as this allows the creation of tables of sea characteristics such as the NATO Seastate table reproduced below.

This table gives information regarding likely wave system characteristics at different sea states. The figure for "significant wave height" is often used to describe the height of the wave system. This

corresponds to the average of the 1/3 highest waves. It has been found over the years that this value corresponds to what a typical shipboard observer would give when asked to report the wave height. For each sea state there is a predominant modal frequency and wave height associated with that sea.

Design criteria are often given in terms of seastates for "fully operational" or "survivable," and tow tank tests may be run in irregular seastates to verify.

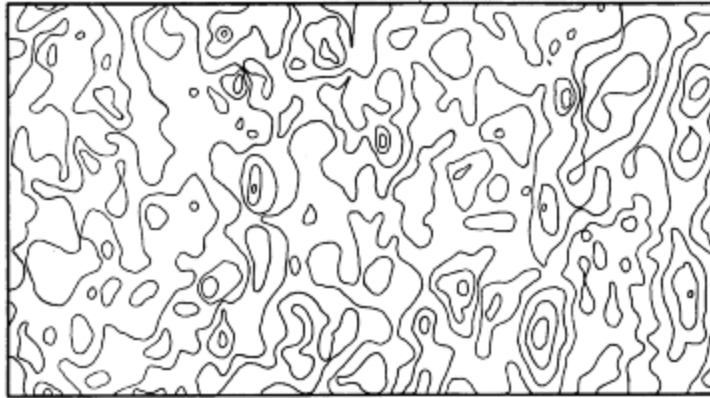


Figure 21: Topological Plot for the North Atlantic (Taken from PNA Vol. III, 1989)

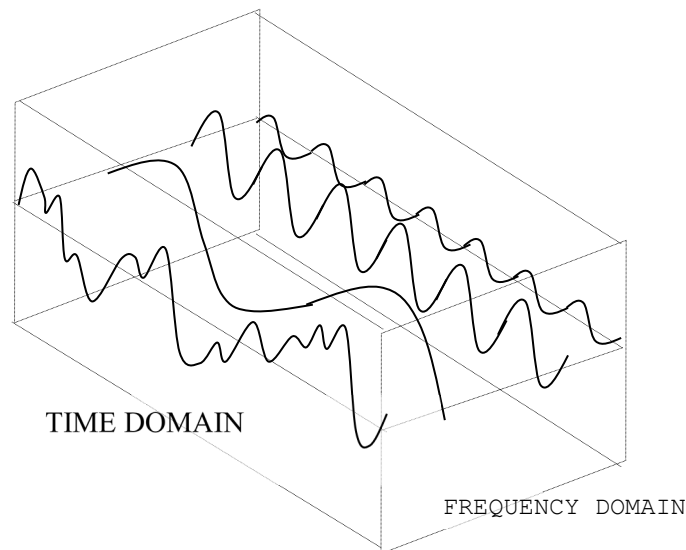


Figure 22 - Wave Creation from Superposition Theorem



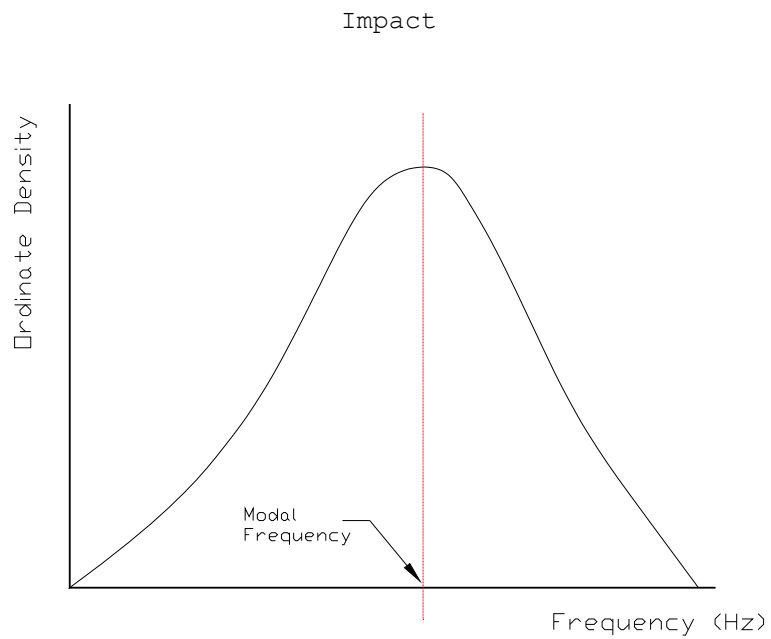


Figure 23 - Typical Sea Spectrum

Table 1 - NATO Sea State Numeral Table for the Open Ocean North Atlantic.

| Sea State Number | Significant Wave Height (ft) |      | Sustained Wind Speed (Kts) |      | Percentage Probability of Sea State | Modal Wave Period (s) |               |
|------------------|------------------------------|------|----------------------------|------|-------------------------------------|-----------------------|---------------|
|                  |                              |      |                            |      |                                     | Range                 | Most Probable |
|                  | Range                        | Mean | Range                      | Mean |                                     |                       |               |
| 0-1              | 0-0.3                        | 0.2  | 0-6                        | 3    | 0                                   | -                     | -             |
| 2                | 0.3-1.5                      | 1.0  | 7-10                       | 8.5  | 7.2                                 | 3.3-12.8              | 7.5           |
| 3                | 1.5-4                        | 2.9  | 11-16                      | 13.5 | 22.4                                | 5.0-14.8              | 7.5           |
| 4                | 4-8                          | 6.2  | 17-21                      | 19   | 28.7                                | 6.1-15.2              | 8.8           |
| 5                | 8-13                         | 10.7 | 22-27                      | 24.5 | 15.5                                | 8.3-15.5              | 9.7           |
| 6                | 13-20                        | 16.4 | 28-47                      | 37.5 | 18.7                                | 9.8-16.2              | 12.4          |
| 7                | 20-30                        | 24.6 | 48-55                      | 51.5 | 6.1                                 | 11.8-18.5             | 15.0          |
| 8                | 30-45                        | 37.7 | 56-63                      | 59.5 | 1.2                                 | 14.2-18.6             | 16.4          |
| >8               | >45                          | >45  | >63                        | >63  | <0.05                               | 15.7-23.7             | 20.0          |

References for Chapter 8

Batterson, Sydney A. "The N.A.C.A. Impact Basin and Water Landing Tests of a Float Model at Various Velocities and Weights" NACA Report No. 795. 1944.

(Originally ACR No. L4H15, 1944)

Batterson, Sydney A. "Variation of Hydrodynamic Impact Loads with Flight-Path Angle of a Prismatic Float at 3° Trim with a 22-1/2° Angle of Dead Rise." NACA RB No. L5824, 1945.

Batterson, Sydney A. and Stewar, Thelma, "Variation of Hydrodynamic Impact Loads with Flight Path Angle for a Prismatic Float at 6° and 9° Trim and a 22-1/2° Angle of Dead Rise," NACA RB NO L5K21, 1945.

Batterson, Sydney A. "Variation of Hydrodynamic Impact Loads with Flight-Path Angle for a Prismatic Float at 12° Trim and with 22-1/2° Angle of Dead Rise." NACA RB No. L5K21a. 1946.

Batterson, Sydney A. "Variation of Hydrodynamic Impact Loads with Flight Path Angle for a Prismatic Float at 0° and -3° Trim and with 22-1/2° Angle of Dead Rise." NACA TN-1166. April, 1947.

Benscoter, Stanley U. "Impact Theory for Seaplane Landing," NACA TN-1437. October, 1947.

Beach Erosion Board "A study of Progressive Oscillatory Waves in Water," Technical Report No. 1, Beach Erosion Board, Office of the Chief of Engineers, U.S. Government Printing Office. 1941.

Benson, J.M. Havens, R.F. and Woodward, D.R. "Landing Characteristics in Waves of Three Dynamic Models of Flying Boats." NACA RM L6L13, May 7, 1947.

Bottomly, G.G. "The Impact of a Model Seaplane Float on Water", A.C.A. (British) R&M No. 583. 1919.

Fagg, S.V. "A Theoretical Analysis of the Impact of an Elastic Body on Water" ARC (British) R&M No.1925. October, 1941.

Harney, L.A., Saur, J.F.T. and Robinson, A.R. "A statistical Study of Wave Conditions at Four Open-Sea Localities in the North Pacific Ocean" Scripps Institution of Oceanography. Wave Project Report No. 53. Contract No. Nobs2490 (Declassified). (Also NACA TN 1493, January, 1949)

## Impact

Jones, E.T. and Blundell, R.W. "Force and Pressure Measurements on V-Shapes on Impact with Water Compared with Theory and Seaplane Alighting Results," A.R.C. (British) R&M No.1932, January, 1938. (Formerly Marine Aircraft Experimental Establishment Report No. F/Res/107)

Kreps, H.G. "Experimental Investigation of Impact in Landing on Water" NACA TM-1046. 1943 (originally published as Report No. 438, Central Aero-Hydro Inst., Moscow 1939)

Lamb, Horace, "Hydrodynamics," Sixth revised edition, Dover Publications NY P. 421.

Lewis, E. "Principles of Naval Architecture Vol. III" Society of Naval Architects and Marine Engineers. 1989.

Lyman, C.S. "Water Load Criteria for the Design of Seaplanes," U.S. Navy Department, Bureau of Aeronautics, a Paper for presentation at the Sixth International Congress for Applied Mechanics, Paris 1946.

Mayo, Wilbur L. "Theoretical and Experimental Dynamic Loads for a Prismatic Float Having and Angle of Dead Rise of  $22\frac{1}{2}^{\circ}$ " NACA RB No. L5F15, July 1945.

Mayo, Wilbur L. "Analysis and Modification of Theory of Impact of Seaplanes on Water," NACA TN-1008, 1945.

Milwitzky, Benjamin "A Theoretical Investigation of Hydrodynamic Impact Loads on Scalloped-Bottom Seaplanes and Comparisons with Experiment." NACA TN-1363. 1947.

Miltitzky, Benjamin "A Generalized Theoretical and Experimental Investigation of the Motions and Hydrodynamic Loads Experienced by V-Bottom Seaplanes During Step-Landing Impacts. NACA TN-1516. February, 1948.

Pabst, Wilhelm "Theory of Landing Impact of Seaplanes." NACA TM-580. 1930.

Pabst, Wilhelm "Landing Impact of Seaplanes." NACA TM-634. 1931.

Pierson. John D. "On the Pressure Distrubition for a Wedge Penetrating a Fluid Surface." Stevens Institute of Technology, Experimental Towing Tank Report No. 336. October, 1948.

Pierson, John D. and Leshnover, Samuel, "An Analysis of the Fluid Flow in the Spray Root and Wake Regions of Flat Planing Surfaces," Stevens Institeu of Technology, Experimental Towing Tank Report No. 335. 1948?

## Impact

Rossell, H. and Chapman L., ed. "Principles of Naval Architecture" Vol II, Chapter I Section 1, Society of Naval Architects and Marine Engineers. New York. 1939.

Sottorf, W., "Experiments with Planing Surfaces" NACA TM No. 739. 1934  
(Originally Werft-Reederei-Hafen, Oct. 1, 1932, Feb. 15 and March 1, 1933)

Sydow (or Sedov) "The Effect of Spring Support and Keeling on Landing Impact," Jarbuch der Deurichen Lufthrtforschung, 1938. Vol. 1, (Available as British Air Ministry Translation No. 861)

Thompson, "Water Pressure Distribution on a Flying Boat Hull, N.A.C.A. Report No. 346. 1929.

Von Karman, Th. "The Impact on Seaplane Floats During Landing", NACA TN-321, 1929.

Wagner, H. "Landing of Seaplanes" NACA TM-622, 1931.

Wagner, H. "Uber Stoss- und Gleitvorgange an der Oberflache von Flussigkeiten", Z.f.a.M.M. Bd. 12, Heft 4, August 1932. pp 193-215



CHAPTER 9. FULL SCALE TRIALS

M.G. Morabito, 2024

Full-Scale trials frequently include observations of the following, usually in varying wind and wave conditions, resources permitting.

1. Low Speed Maneuvering
2. Low Speed Bow Spray
3. Take-off and Landing Time and Distance
4. Pre-Hump Directional Stability
5. Main Spray Characteristics
6. Longitudinal Stability during Take-off
7. Longitudinal stability during Landing
8. Directional Stability at Planing Speeds
9. Landing Impact

9.1 Low Speed Maneuvering

The low-speed maneuvering is characterized by the turning diameter and the time it takes to make the turn at different engine RPM and wind speeds. Figure 1 shows an example graph of the results. Figure 2 shows an extreme condition, where a wing has become completely submerged while making a turn.

## Full Scale Trials

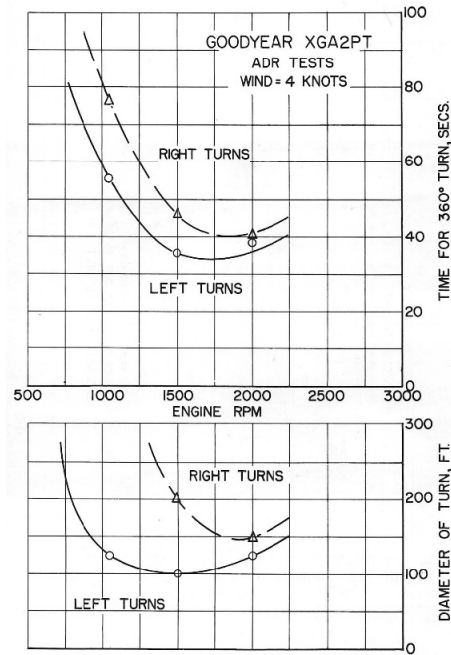


Figure 1: Low-Speed Maneuvering Characteristics (Locke, Nov 1949)



Figure 2: Submergence of Port wing and tip float while attempting left turn in 30-knot wind (Locke, April 1949)

### 9.2 Low Speed Bow Spray

Bow spray can severely affect visibility, as shown in Figure 3. These photos are taken in relatively calm water. The situation is worse in waves. Bow spray is the worst at pre-hump speeds, when the seaplane is moving fast enough to generate spray, but the trim is still low.

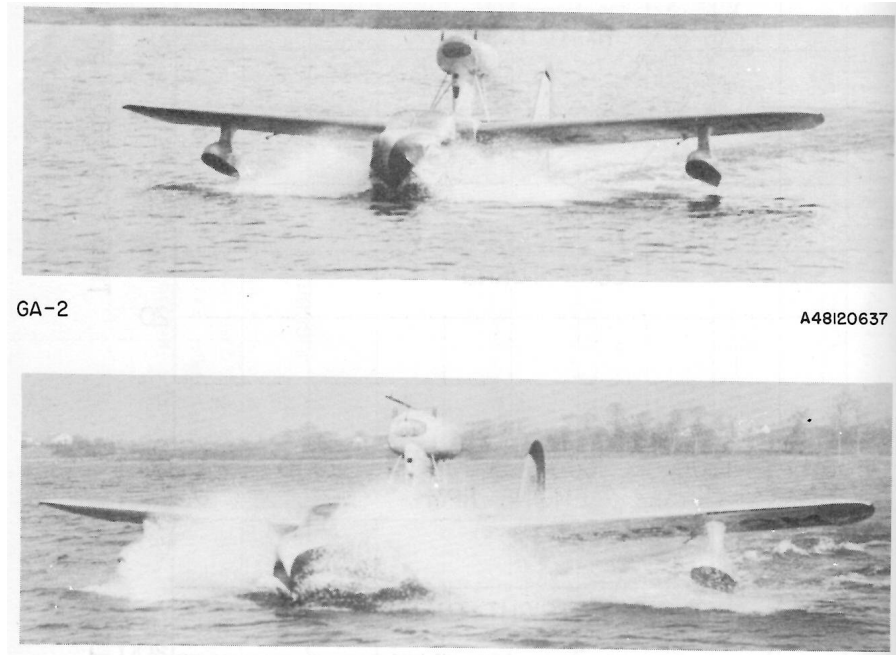


Figure 3: Comparison of Bow Spray Characteristics with Two Different Afterbody Configurations (Locke, November 1949)

### 9.3 Take-Off and Landing Time and Distance

Obviously, a critical parameter. This can be measured through a series of take-offs and landings at different load conditions. Typical measurements include: Weight, Water Speed, Wind Speed, Air Speed, Time, Distance.

### 9.4 Pre-Hump Directional Stability

The measure of Pre-hump directional stability is whether or not asymmetric power is required to maintain a straight course. If the air rudder is sufficient, the seaplane is considered stable. Figure 4 (left) shows a comparison of the directional stability of two seaplanes, one of which requires asymmetric power most of the time, whereas the other one is needed less. Figure 4 (right) shows the same graph, but including the effects of wind direction. This seaplane was stable in all conditions.



## Full Scale Trials

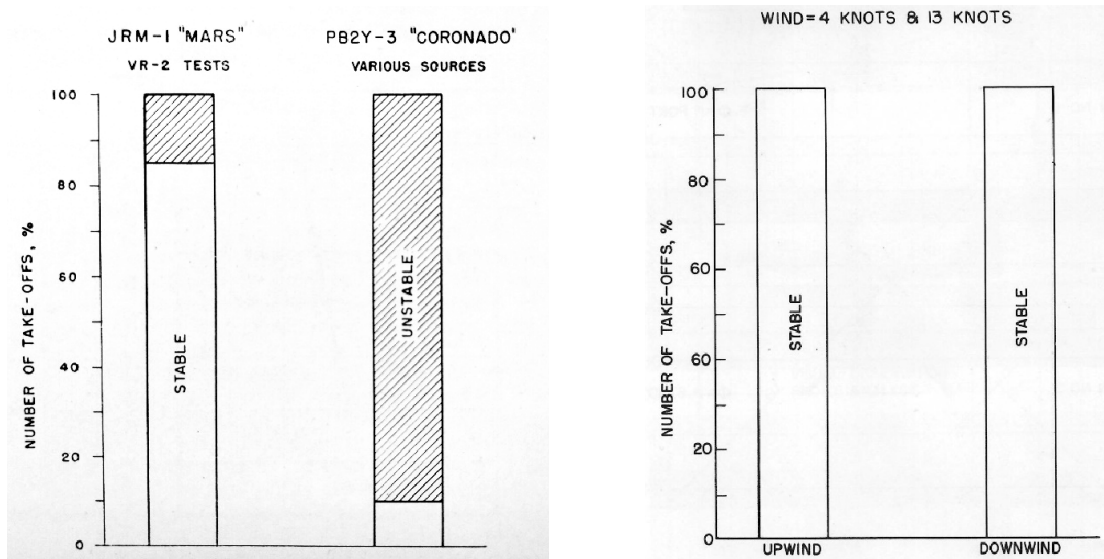


Figure 4: Prehump directional stability characteristics.

Figure Notes "Stable" means that asymmetric power was not required to maintain a straight course. The left chart shows a comparison between two different seaplanes. The right chart shows the effect of wind direction. (Taken from Locke, April 1949 and November 1949)

### 9.5 Main Spray Characteristics

The main spray may impact against the wings or the flaps, possibly causing damage. Large amounts of heavy spray into the propellers can cause a loss of RPM and propeller damage.

Figure 5 shows such photographs taken during some informal tests of a small experimental aircraft. Measurements from these photos enabled the test engineers to prepare a sketch of the spray envelope, showing spray height as a function of longitudinal position. They then normalized the spray using the spray coefficients,  $C_x$  and  $C_z$ . This allows comparison with other aircraft, as shown in the compilation plot in Figure 6.

Figure 7 shows two graphs, one of spray height and one of loss of propeller RPM as a function of gross weight. It can be seen that when the spray enters the propeller disc (at about 170,000 lb weight) the propeller RPM drops noticeably.

For more detailed spray measurements, the hull can be striped at regular increments, using a reference system as shown in Figure 8 and in Figure 9. After the photographs are analyzed, the spray results can be

## Full Scale Trials

presented as shown in Figure 10. This is a convenient format because it provides the viewer with a clear understanding of the effect of the spray.

The seaplane may be heeled during spray measurements, so a correction must be applied to the visual observations. This can be done if the heel angle is measured and the transverse distance of the spray apex is either observed or estimated. It has been found that this distance is fairly consistent for various seaplanes, and so a general correction can sometimes be applied. Figure 11 shows a diagram of the spray correction. Figure 12 shows a graph showing the effect of heel angle on measured spray height.

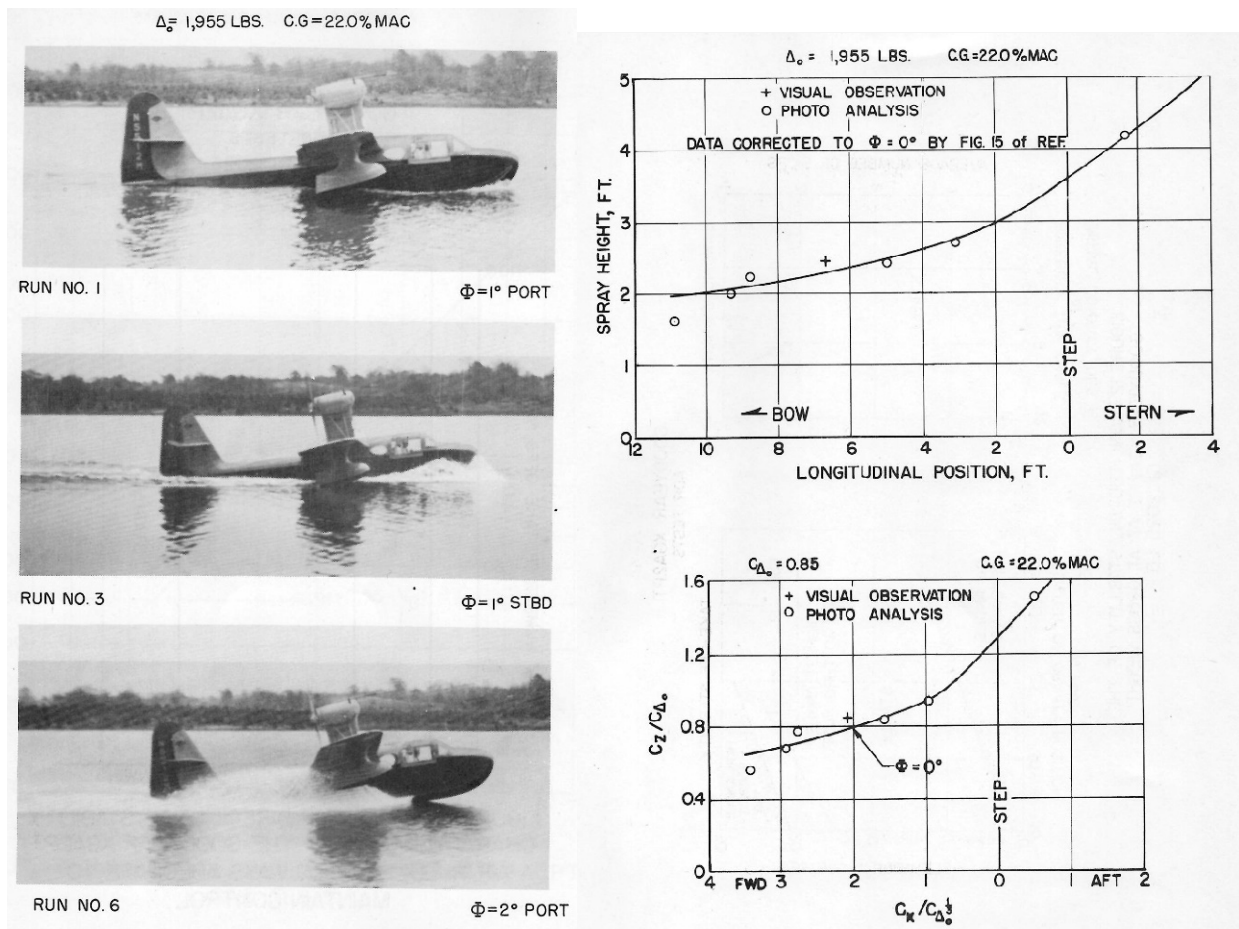


Figure 5: Spray photographs, measurements and analysis (Locke, November 1949)

# Full Scale Trials

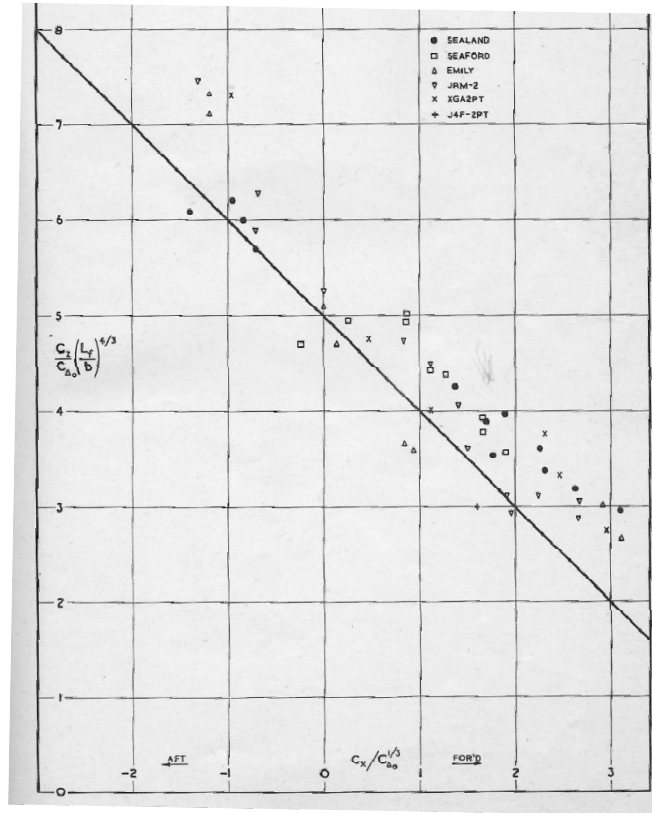


Figure 6: Compilation of Spray Data from Trials of Different Seaplanes  
(Brown. 1953)

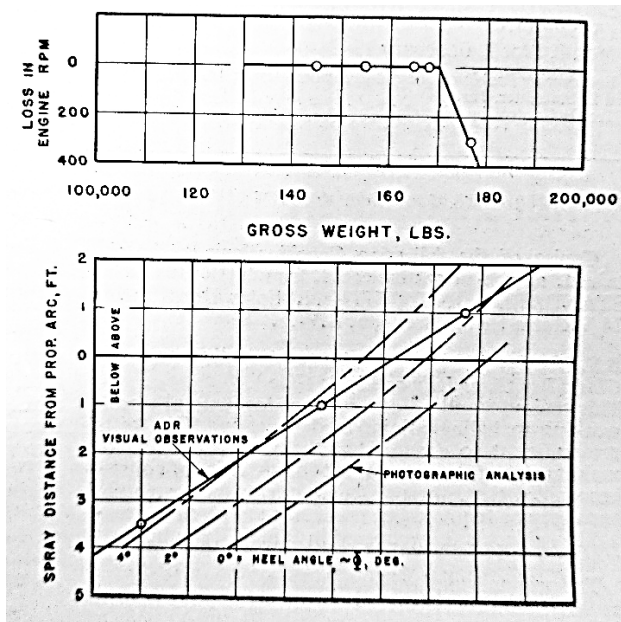


Figure 7: Effect of Gross Weight on Spray Height. Showing Relationship  
between Spray into Propellers and Loss of Engine RPM (Locke, April 1949)

## Full Scale Trials

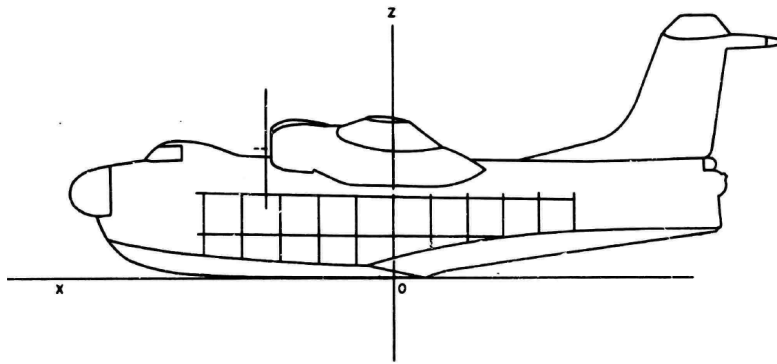


Figure 8: Striping Pattern for Full-Scale Spray Studies (Taken from deCallies, 1951)

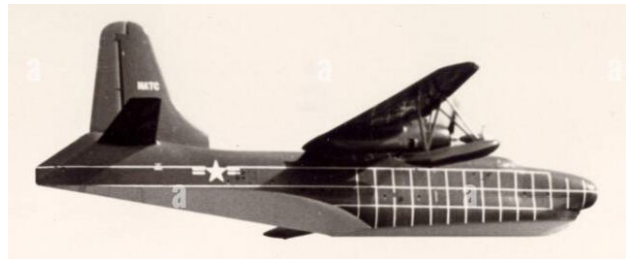


Figure 9: Martin M-270, showing spray striping

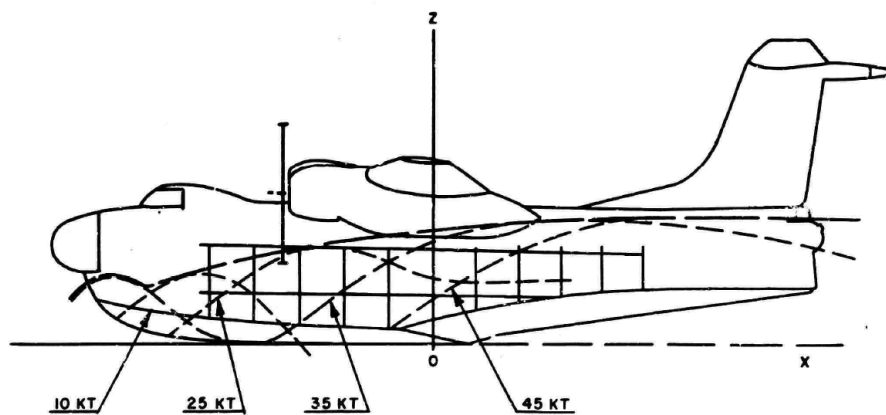


Figure 10: Presentation of Spray Results (Taken from deCallies, 1951)

## Full Scale Trials

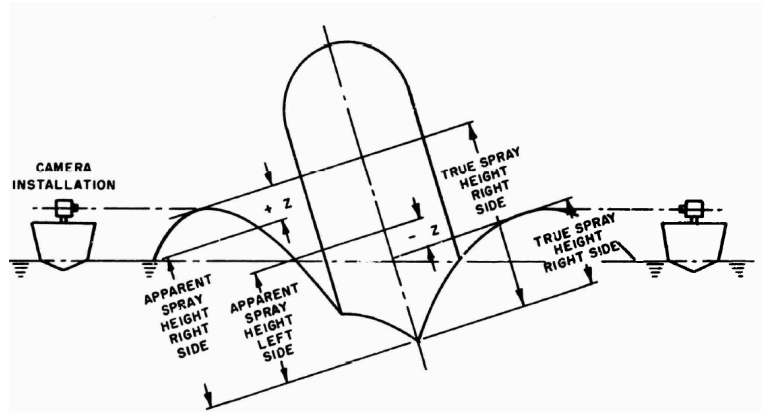


Figure 11: Correction for Heel Angle (Taken from deCallies, 1951)

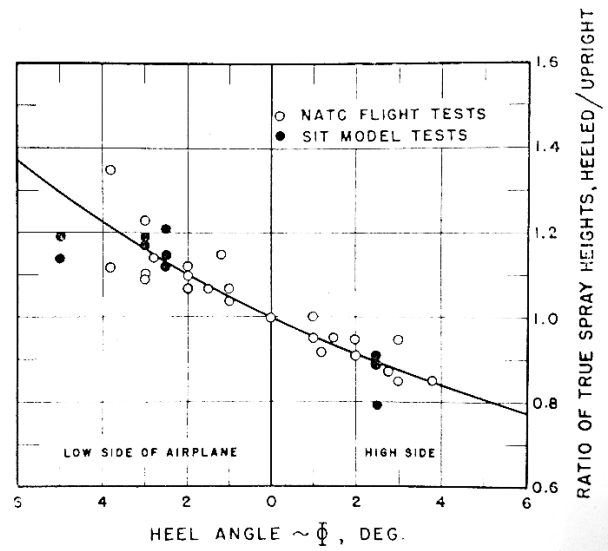


Figure 12: Correction of Spray for Heel Angle (Locke, April 1949)

### 9.6 Longitudinal Stability during Take-Off

Figure 13 shows a comparison of the stability limits for two different seaplanes. These are presented in terms of longitudinal center of gravity position, flap deflection, and elevator angle. The elevator angle is the main control that the pilot has to keep the seaplane between the porpoising limits. The JRF-5 "Grey Goose" has a much wider range of stability than the Japanese "Emily" shown in the figure.

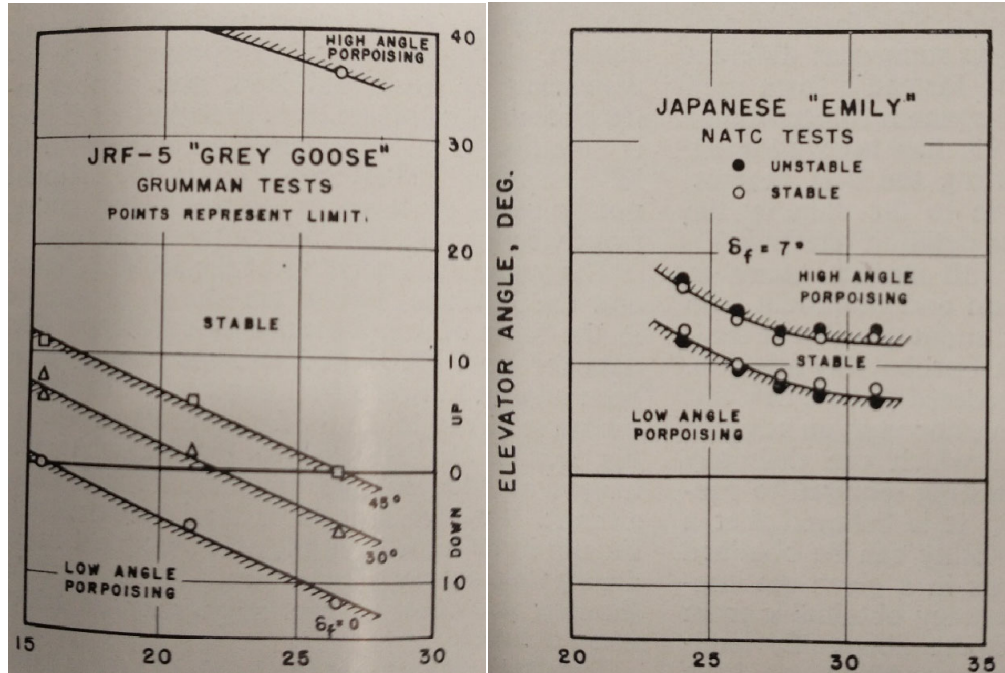


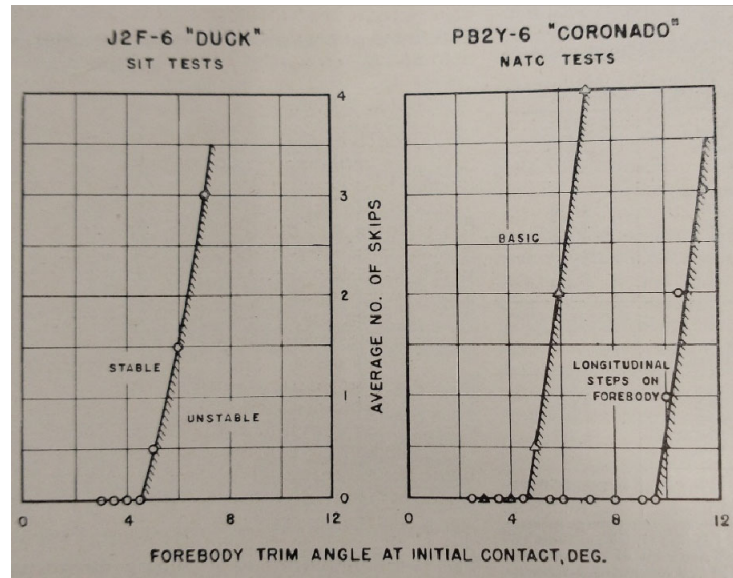
Figure 13: Effect of Center of Gravity Position (% of Mean Aerodynamic Chord) on Longitudinal Stability (Locke, April 1949)

### 9.7 Longitudinal Stability during Landing (Skipping)

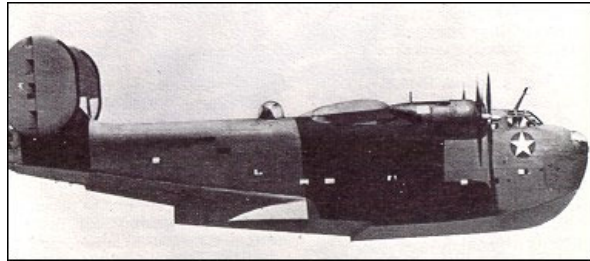
The primary instability on landing is "skipping," which is characterized by the average number of skips as a function of forebody trim on landing. Figure 14 shows comparisons of two different seaplanes, one from model tests and another from flight tests. Both seaplanes experience skipping at contact trim angles greater than 4-degrees, which is fairly unsatisfactory. Review of photos of both seaplanes show very low height of the main step. While a small main step height may reduce resistance at hump speed, it increases the propensity to skip.

In contrast, Figure 15, taken from a report on a "planing tail" seaplane shows it is stable at all contact trim angles.

# Full Scale Trials



J2F-6 "Duck"



PB2Y-6 "Coronado"

Figure 14: Effect of Forebody Trim at Contact on Skipping (Locke, April 1949)

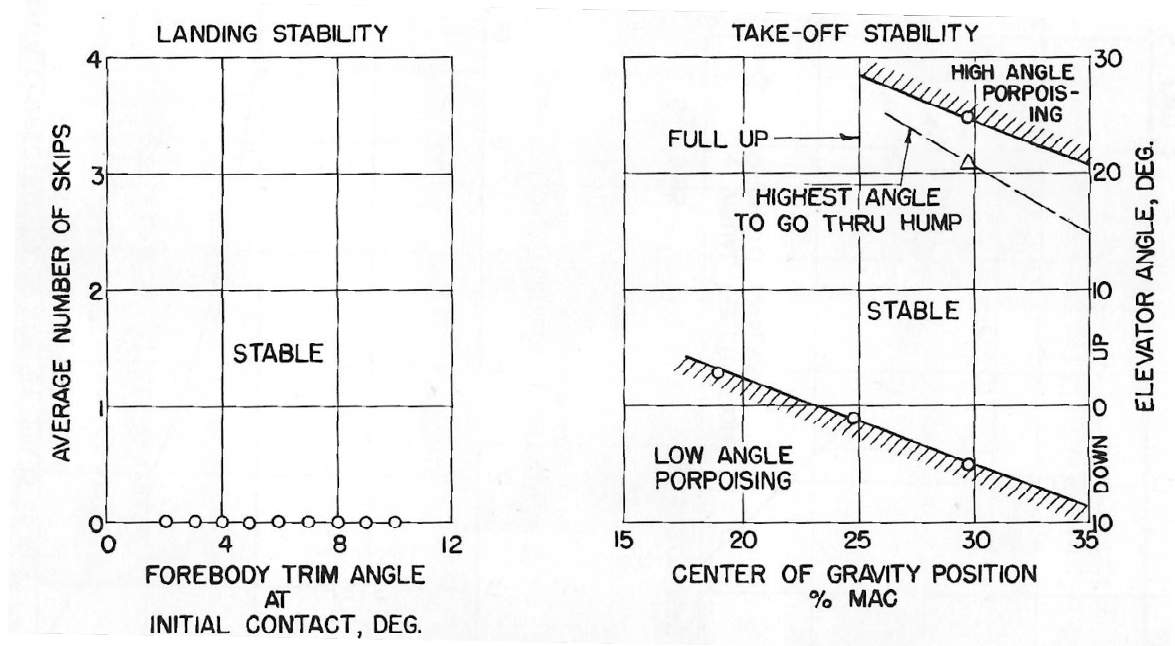


Figure 15: Landing Stability and Take-off Stability of a "Planing Tail" seaplane (Locke, November 1949)

### 9.8 Directional Stability and Control at Planing Speeds

Turns are made at mid-planing speeds at various combinations of trim angle and longitudinal center of gravity. The results of these tests are often qualitative, based on how comfortable the pilot is. Severe directional instability can result in a loss of control.

### 9.9 Landing Impact

Figure 16 shows a time history of the vertical acceleration during a landing. The figure shows that the initial contact is quite light (1 g is the static acceleration due to gravity). However, the uncontrolled bounces during the deceleration lead to a series of acceleration peaks. These peaks are sorted from smallest to largest, and a statistical distribution is used to predict extreme values for structural design estimates (Figure 17).



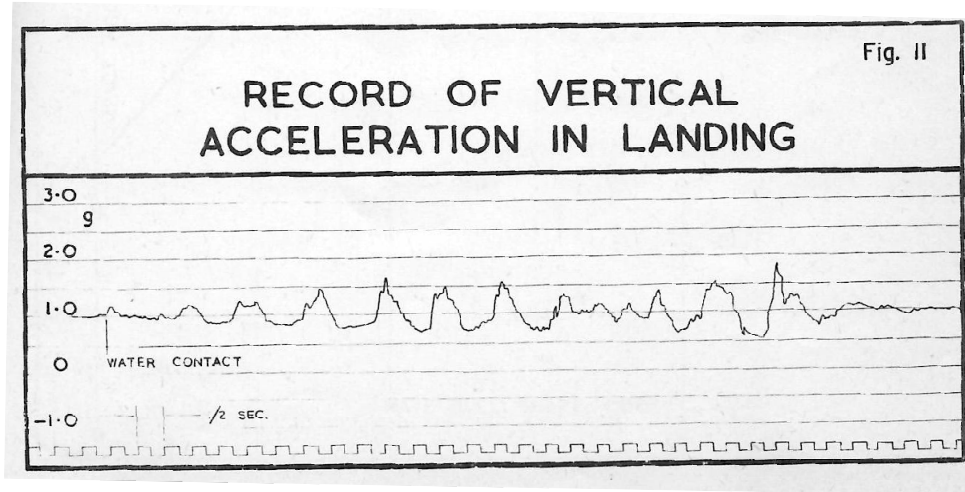


Figure 16: Record of Vertical Acceleration in Landing (Brown, 1953)

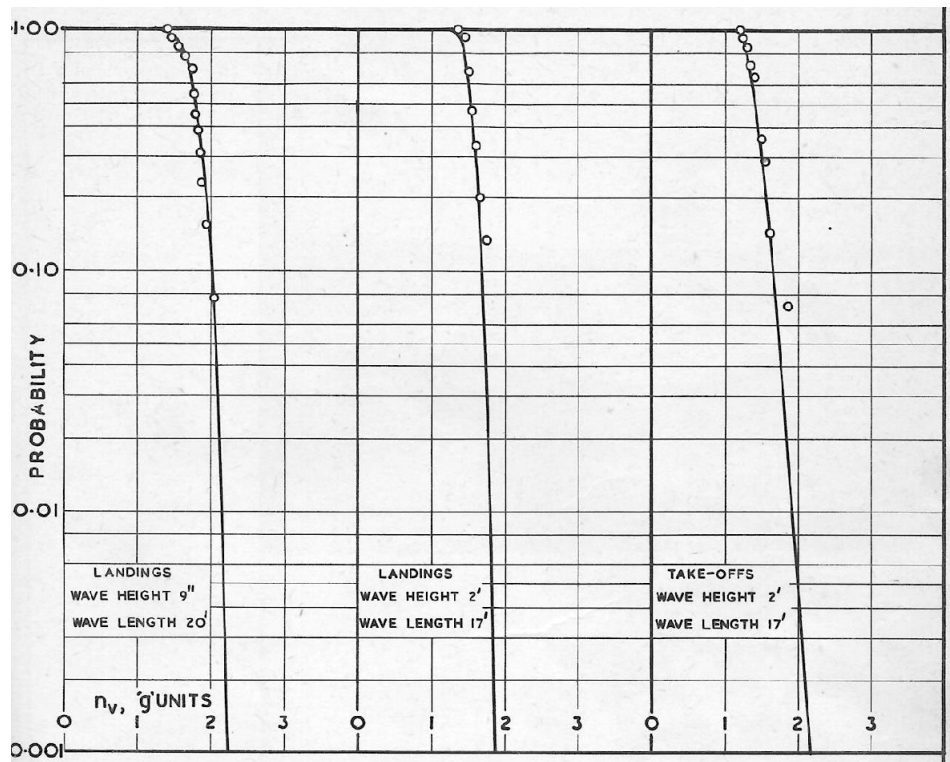


Figure 17: Load Factor (Vertical Acceleration) Probability (Taken from Brown, 1953)

References for Chapter 9

Brown, P. Ward. "Brief Water handling Trials of the Short SA6 Sealand Amphibian." Hydrodynamics Report No. 135. Short Brothers & Harland Limited. Shorts HR 135.

deCallias, R.N. "Hydrodynamics Manual". Naval Air Test Center Flight Test Division. 1958.

Locke, F.W.S. Determining the Hydrodynamic Characteristics of Flying Boats. Aircraft Engineering and Aerospace Technology, Vol. 21 No. 4, pp. 104-112. 1949.

Locke, F.W.S. Informal Tests of the Water Handling Characteristics of the Goodyear XGA2PT Planing Tail Flying Boat. Navy Department. Bureau of Aeronautics Research Division DR Report No. 1151. November, 1949.



CHAPTER 10. EARLY-STAGE SIZING

M.G. Morabito, 2021

10.1 Length and Beam of Planing Surfaces

10.2 Step Design

10.3 Deadrise Angle and Warp

10.4 Sternpost Angle

10.5 Design for Impact in Waves

This section discusses early-stage estimates of main hull parameters, such as length, beam, forebody length, sternpost angle and step height. Guidance is provided about how each of these characteristics affects performance.

10.1 Length and Beam of Planing Surfaces

The most important decision regarding overall performance of a seaplane is the size of the hull bottom to support a given load. Hulls with high bottom loadings (i.e. too heavy a load on too small a planing surface) will have large spray, increased trim, and high resistance at hump speed. The length-to-beam ratio of the hull is of primary importance for aerodynamic considerations, with higher length-to-beam ratio reducing parasitic drag of the aircraft. The length and beam of the planing surface is a driving factor for the volume of the fuselage on a flying boat, and therefore its cargo-carrying and mission capabilities.

Prior to World War II, most flying boats had a length-to-beam ratio of 5 to 6 (See Figure 1, Grumman Goose). Seaplane floats made during the last 80 years often have length-to-beam ratios of 6-7. During the 1940s, extensive model testing and analytics allowed for designs with much higher length-to-beam ratios (and improved aerodynamic performance), such as the Martin P6M (seen in Figure 2). High L/B seaplanes, such as the Beriev BE-200 (seen in Figure 3) and AG600 (Figure 2.3) are now in production.

### Bottom Loading

The Davidson load coefficient is often used to provide a guideline for the bottom loading of seaplanes with a wide variety of length-to-beam ratios, assuming that the length of the forebody is around the typical value of 55-60% of the overall length of the float.

$$K_2 = \frac{\Delta_o}{\rho g L^2 B}$$

Where,

$B$  is the hydrodynamic beam of the planing surface, measured at the chine.

$L$  is the length of the planing surface. As shown in Figure 3.1, "Length" of the bottom is not the overall length of the seaplane, but the length of the hydrodynamic hull (taken to the sternpost), which has some flexibility based on varying the tail overhang.

$\Delta_o$  is the load on the planing surface (half the weight of the seaplane for twin floats)

Davidson and Locke (1944) found that hulls with varying length-to-beam ratios had similar resistance and spray characteristics when the loading coefficient,  $K_2$  is kept constant. Stout (1950) provides the following recommendations for  $K_2$ , based on practical design experience with flying boats:

$K_2 = 0.018$  is optimum (light spray)

$K_2 = 0.022$  is maximum in design stages (heavy spray)

$K_2 = 0.025$  is maximum overload (excessive spray)

### Forebody-Afterbody Proportions and Effects

While the forebody is often 55-60% of the overall length of the float for typical flying boats and float planes (Stout, 1950), there is substantial room for flexibility on this value in design, Haar (1952) tested hulls with forebody lengths ranging from 33%-60% of the length of the float, showing that a wide

## Early-Stage Sizing

range is possible. Long afterbodies reduce the upper porpoising limit because they contact the surface at lower trim angles; however, this can be remedied by increasing the sternpost angle.

Spray characteristics are mainly related to forebody load and so shortening the forebody for the same Davidson load coefficient  $K_2$  will result in increased spray. For hulls with forebody lengths lower than the typical 55-60%, Parkinson's (1943) forebody load coefficient provides a useful guide.

$$k = \frac{\Delta_o}{\rho g L_f^2 B}$$

Where Parkinson recommends:

|                                    |            |
|------------------------------------|------------|
| Excessive Spray                    | $k=0.0975$ |
| Heavy, but acceptable for overload | $k=0.0825$ |
| Satisfactory for normal operation  | $k=0.0675$ |
| Extremely light spray              | $k=0.0525$ |

### Beam Loading

Beam-based coefficients are often used in seaplane references because while the wetted length varies with speed, the beam remains essentially constant. Most seaplane literature from NACA uses the load coefficient  $C_{\Delta_o}$ , which is based on beam. This coefficient can be related to  $K_2$  as follows:

$$C_{\Delta_o} = \frac{\Delta_o}{\rho g B^3} = K_2 \left( \frac{L}{B} \right)^2$$

Most of the guidance on seaplane loading,  $C_{\Delta_o}$ , during the pre-war period is based on the assumption that the length-to-beam ratio is somewhere around 6, and therefore it is important not to use these pre-war design guidelines for craft with very high length-to-beam ratio.

## Early-Stage Sizing



Figure 1: Typical Pre-War Flying Boat - Grumman G-21 Goose



Figure 2: 1950's Long-Rang Bomber - Martin P6M



Figure 3: Modern Production "Water Bomber" - Beriev Be-200

## 10.2 Step Design

The step allows flow to cleanly separate off the forebody at speeds above hump and permits the aircraft to rotate to a trim angle to allow take-off. The step is typically located 0.2 to 0.4 beams aft of the center of gravity. Placing the step too far forward will cause the seaplane to run at too high a trim angle, or balance on the afterbody at high speeds. Placing the step too far aft will prevent the seaplane from rotating to take off.

Larger step heights are typically better for hydrodynamic stability, but worse for aerodynamic resistance. It has been observed that hulls with too small a step tend to "skip." The airflow becomes blocked aft of the step creating a low-pressure region that causes the hull to be pulled downward. When the suction is broken, the hull jumps out of the water. This happens most often on landing, but sometimes during take-off and has been observed in full scale and in towing tanks. The effects of step height and afterbody angle also control the porpoising behavior of designs.

Locke (1946) investigated the skipping characteristics of full-scale seaplanes, based on pilot input, and found that increased step height, reduced beam loading  $C_{d0}$  and reduced sternpost angle  $\sigma$  all tend to improve performance. This study was limited to a length-to-beam ratio of six (based on existing designs) and can produce step heights that are too small for high L/B designs.

As work was going on to explore large variations in length-to-beam ratio, Olson and Land (1948) prepared systematic model tests of afterbody length, afterbody angle, and step depth to study the effects of these parameters on the take-off and landing stability of seaplanes (Figure 4). From these tests, they derived a formula relating these parameters and compared it with the results of model-scale landing tests of a variety of hulls previously tested by NACA. Their formula (in the notation used in this paper) is as follows,

$$h_{\%b} \geq 0.59 \frac{L_a}{b} AA$$

Where,

$h_{\%b}$  is step height in a percentage of beam

$L_a$  is the length of the afterbody (meters or ft)

$b$  is the beam of the planing surface (meters or ft)

$AA$  is the afterbody angle (degrees)



Step Height Example:

Estimate the minimum step height for the following seaplane using Olson and Land's (1948) criteria

$$L_a = 12.8m \quad b = 3m$$

$$AA = 5.5 \text{ degrees} \quad \sigma = 7.3 \text{ degrees} \quad \Delta_0 = 56,000 \text{ kg}$$

Ans:

$$h_{\%b} \geq 0.59 \frac{L_a}{b} AA \geq 0.59 \frac{12.8m}{3m} 5.5 \text{ deg} = 13.8\%$$

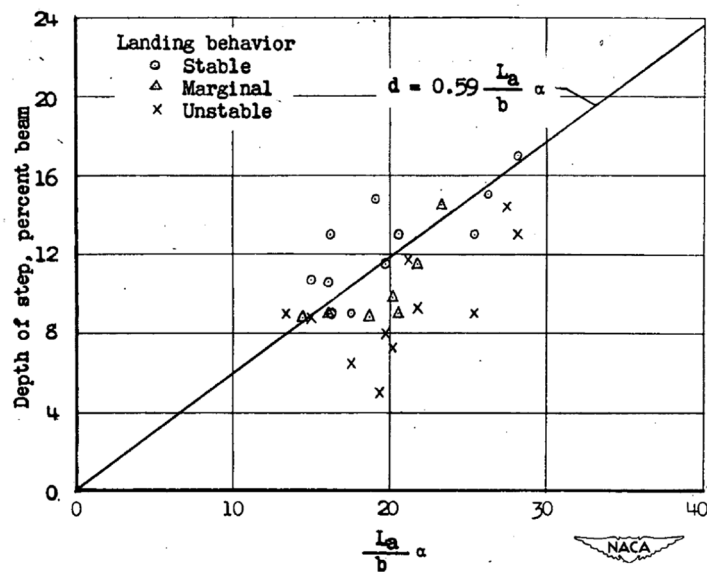


Figure 4: Guidance relating afterbody angle, afterbody length, step height and beam, based on take-off and landing tests of various models at NACA (Olson and Land, 1948)

Step Planform Shape

Many seaplane floats have transverse steps; however, it has been shown that adding a "Vee-Step," shown in Figure 5, can improve step ventilation and performance. Savitsky (1951) showed that for prismatic planing hulls, 30-degree and 45-degree vee step angles had a higher lift-to-drag ratio than a transverse step. Van Dyck (1954) confirmed that for seaplane hulls the 45-degree angle resulted in the minimum skipping tendency (evidence of good ventilation), did not affect directional stability, and had the least resistance of the configurations at hump speed.

The "Vee-Step" used on seaplanes differs from the re-entrant step advocated by Clement for use on stepped planing hulls (See Clement and Hoyt 2008 or Clement 1969). Re-entrant steps have the point facing forward and are designed to allow for the addition of longitudinal camber (hook) near the step, increasing the lift coefficient of the planing surface. Because of the poor ventilation characteristics of these steps, they must be fitted with vents aft of the step to prevent dynamic instabilities. Re-entrant steps have not, to the author's knowledge, been successfully used on seaplanes, and do not seem to be appropriate. The seaplane requires very low lift coefficients from the planing surface on take-off (light load on the water from aerodynamic lift, combined with high speeds), and so the addition of camber at the step is strongly discouraged.

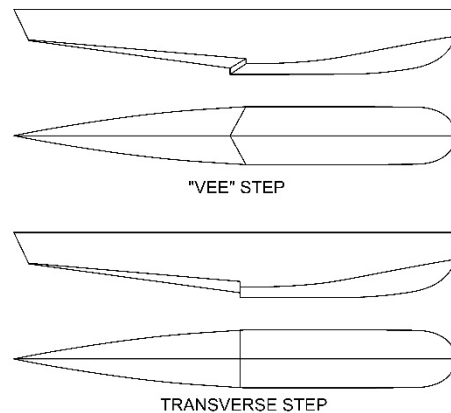


Figure 5: Transverse and Vee-Step Configurations

### Step Fairing

Fairing the step can reduce the aerodynamic resistance; however, care must be taken to ensure the water breaks cleanly from the step. If the flow does not cleanly separate there will be dynamic instabilities and increased resistance. Figure 6, taken from Smith and Allen (1954) shows a variety of step fairings that have been used, sorted with the most aerodynamic resistance at the top and least at bottom. The straight fairing has the least resistance; however, this is the most unlikely for the water to separate from, and least likely to naturally ventilate.

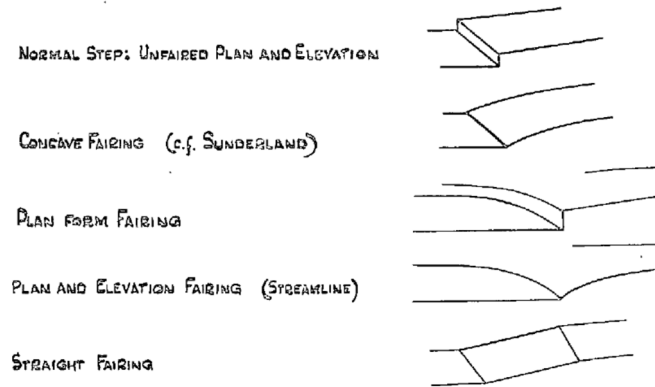


Figure 6: Step Fairing Options - Highest drag top, lowest drag bottom.  
(Adapted from Smith and Allen, 1954)

## 10.3 Deadrise Angle and Warp

Typical seaplanes have deadrise angles around 20-degrees at the step. Increasing deadrise makes the bottom a less effective lifting surface, resulting in reduced impact accelerations during landing and in waves. Increased deadrise also increases resistance of the hull, because more wetted area is required to generate a given lift. Reducing deadrise below 20-degrees increases the lower limit of porpoising and is usually not recommended.

It is essential to provide straight buttock lines on the forebody in the vicinity of the step. Convex curvature in this area results in dynamic instabilities. The hull naturally will have more curvature toward the bow, but convexity is still to be minimized.

The bottom often has a "forebody flat", which is a region ahead where the buttock lines are kept completely straight. The flat can be developed by either maintaining a constant deadrise, or by a linear warping (i.e. a linear increase in deadrise as a function of distance forward of the step). Warp has been shown to reduce the lower limit of porpoising at high speeds for high length-to-beam ratio hulls, increasing the region of safe operation. Figure 7, taken from Stout (1950) provides a recommendation on the amount of warp in the forebody flat. A high length-to-beam ratio hull, with a forebody length-to-beam ratio of 8 should have roughly 5-degrees per beam of warp. Thus, if it is a 20-degree deadrise at the step, it will have 25 degrees one beam forward of the step.

## Early-Stage Sizing

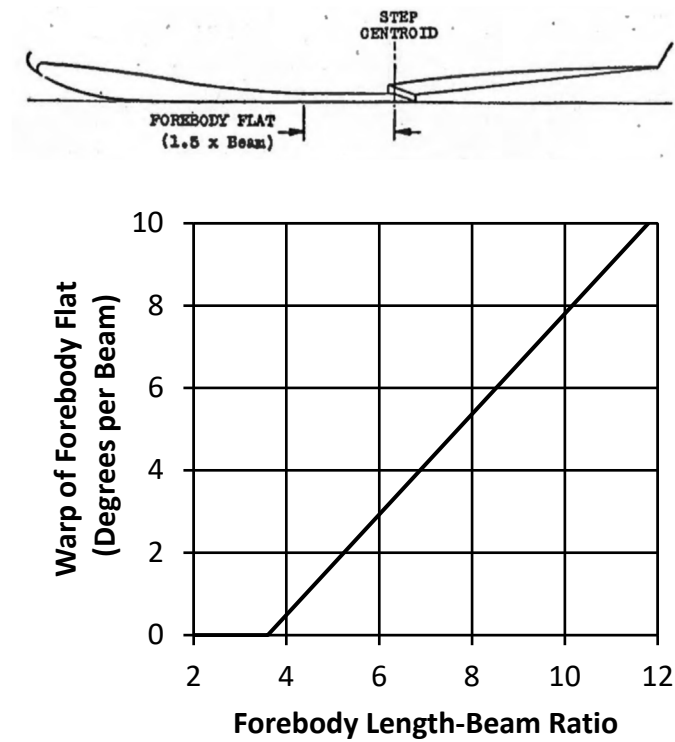


Figure 7: Recommended linear variation in deadrise forward of the step in degrees per beam of the forebody flat to maintain lower limit stability (Stout, 1950).

#### 10.4 Sternpost Angle

Sternpost angle (labeled  $\sigma$  in Figure 3.1) affects the resistance, porpoising stability limits and spray characteristics. Dathe (1989) lists the effects of changing sternpost angle. Increased Sternpost Angle:

1. Reduces afterbody interaction, raising the upper porpoising limit (good)
2. Reduces afterbody damping, raising lower porpoising limit at hump speed (bad)
3. Causes the seaplane to run at higher trim at lower speeds, increasing spray (bad)
4. May cause higher impact accelerations due to higher trim (bad)
5. May allow the seaplane to rotate to a more favorable take-off orientation (good)

It is not possible to provide a general guide to sternpost angle, other than to note that typical seaplanes that have been built have sternpost angles in the range of 7-9 degrees (Locke, 1946 and Hugli and Van Dyck, 1955). The previous guidance on step height may be of some aid in relating sternpost angle to step height.

#### 10.5 Alternative Hull Forms

The two most promising alternatives to the conventional seaplane hulls described above are the "planing tail" and "hydro-ski" seaplane concepts. The advantages and disadvantages are discussed below.

##### Planing Tail Seaplanes

Figure 8 shows a photograph of a planing tail seaplane. The primary difference between a conventional seaplane and a planing tail seaplane is the step height is substantially higher and the afterbody provides very little hydrostatic support. At high speeds the hull rides on two points - the forebody planing surface and the aft portion of the afterbody, located under the tail. Planing tail seaplanes have larger static trims and less internal volume than conventional seaplanes. However, they have better step ventilation, reduced aerodynamic resistance due to the long fairing of the step, and less hydrodynamic resistance (Suydam, 1953). Further, the planing tail seaplane

does not usually suffer from upper limit porpoising (which is a result of the afterbody) or skipping (which is a result of poor step ventillation). Suydam's study showed that the planing tail seaplane had a much lower lower-limit for porpoising stability, so a much wider range of trim angles were permissible.

For these reasons, planing tail designs are very popular today for light one or two passenger recreational aircraft, where cargo carrying capacity is not important. They are also an excellent choice for unmanned aerial vehicles.

Much of the same design guidance discussed above applies to planing tail seaplanes, except the use of the Davidson load coefficient,  $K_2 = \frac{\Delta_0}{\rho g l^2_B}$ , because of differences in the afterbody. Instead, we would recommend using Parkinson's (1943) forebody load coefficient  $k = \frac{\Delta_0}{\rho g l_f^2 B}$ , discussed earlier in the section on forebody-afterbody proportions.

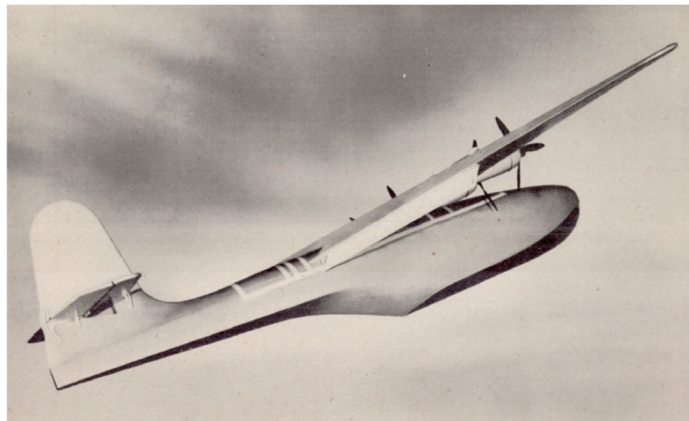


Figure 8: Planing Tail Seaplane (Suydam, 1953)

### Hydro-ski Seaplanes

High-speed aircraft, such as supersonic fighter jets, are designed to have a very small wing area to reduce parasitic drag at high speeds. As a result, they must take-off and land at higher speeds. Since hydrodynamic impact pressures typically vary with the square of speed, impact accelerations become problematic for high-speed seaplane designs. Figure 9 shows a photograph of Sea Dart, an experimental supersonic fighter jet seaplane. To reduce the landing impact loads, two narrow hydro-skis were deployed from the bottom. Reduction in beam of the planing surface reduced impact loads. Additionally, the hydro-skis could be mounted on shock absorbing struts.



Figure 9: Sea Dart - Hydroski Fighter Jet (Photo courtesy of Smithsonian National Air and Space Museum)

Hugli and Van Dyck (1955) prepared a limitations analysis, comparing the resistance of hydro-ski seaplanes and conventional seaplanes at similar values of impact accelerations. This study yielded a useful plot to estimate where each type of hull is appropriate (Figure 10). The figure shows the thrust-to-weight ratio required for take-off as a function of volumetric Froude number based on static load and getaway speed. The plot shows that at high Froude numbers the hydro-ski alighting gear has substantially lower thrust requirements. The reason for the increased thrust requirement for hulls at higher volumetric Froude numbers is the need for ever increasing deadrise to prevent impact accelerations. In contrast, hydro-skis can be made much narrower to limit impacts.

Since the 1950s there has been very little development in hydro-ski seaplanes. This is likely because few jet fighters require the ability to take-off and land from water. Thus, hydro-ski seaplanes are a feasible technical solution for which there is little need. A thorough summary on the hydrodynamic

design of hydro-ski planes is provided in a two-part technical report by Pepper and Kaplan (1966 and 1968). These reports (over 350 pages total) should provide the design data necessary for a very detailed analysis.

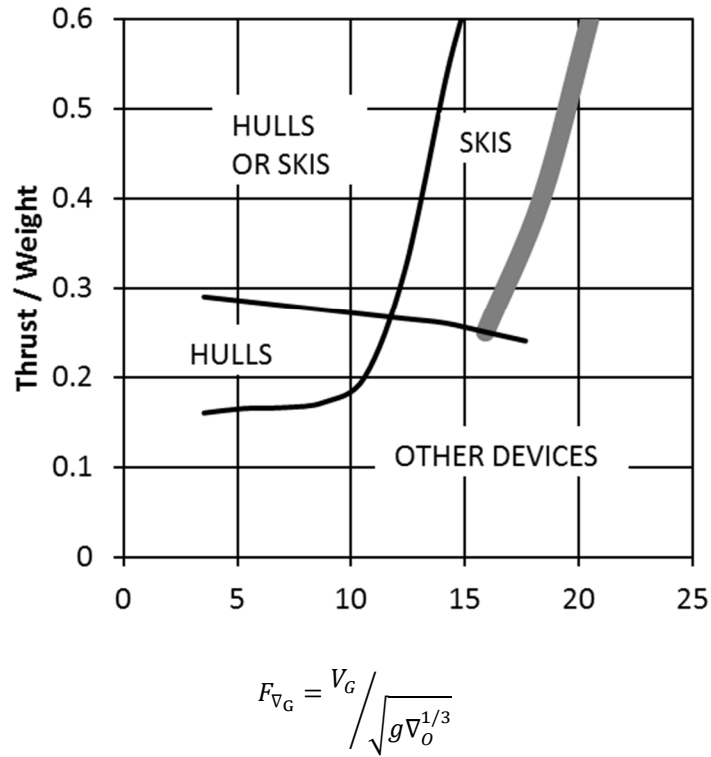


Figure 10: Regions for Alternative Hull Forms - Thrust-to-Weight ratio required for take-off for hulls and hydrofoils with equivalent impact accelerations  $L/B=15$  (Hugli and Van Dyck, 1955)



### 10.5 Design for Impact in Waves

Consideration of the impact accelerations early in the design enables rational decisions about the displacement, the deadrise and the getaway speed. It is possible to break any seaplane, depending on the conditions. And so, the forces it is designed to withstand are limited only by the allowable weight.

Van Dyck (1958) noted that,

"in a given rough water landing, maximum load factors are rarely obtained on the first impact - or even during the second or third... Usually the impact which produces the maximum load occurs when the seaplane still has a fairly large forward velocity (below stall) but has rebounded from a wave system so that the pilot has little control over the aircraft."

Van Dyck, seeing that the theoretical predictions of the first impact were of little value, and that full-scale or fully-dynamic model tests in an impact basin were quite costly, proposed testing seaplanes in irregular seas at approximately 80% of the landing speed, to determine the maximum impact. This is an effective and affordable test method in the towing tank. As the hull moves through the irregular seaway, its motions and forward speed are representative of what the craft would see during a decelerating landing on the 3<sup>rd</sup> or 4<sup>th</sup> wave impact, where the pilot lacks control of pitch.

### Empirical Equations

Empirical equations were developed by Hugli and Van Dyck (1955) to estimate the impact accelerations of a seaplane. These may be useful in the design stages for trade-off studies of hull parameters.

$$\eta = 0.00825 \gamma b V^2 \Delta_o^{-2/3} \left(1 - \beta/90\right)$$

Where,

$\eta$  is the impact acceleration at the center of gravity (g's)

$\gamma$  is the flight path angle, deg

## Early-Stage Sizing

$b$  is the beam of the planing surface (ft)

$V$  is the landing speed (ft/s)

$\Delta_o$  is the gross weight of the seaplane (lb)

$\beta$  is the deadrise angle (deg)

Savitsky and Roper (1990) note that this equation does not include trim; however, trim is limited by the sternpost angle of most seaplanes to 8-10 degrees. Savitsky and Roper estimate typical flight path angle  $\gamma = 5^\circ$  and also provided an empirical correction for impact accelerations in irregular waves based on unpublished data:

$$\gamma_e = 5^\circ + \tan^{-1} \left( \frac{h_{1/3} \pi}{3L} \right)$$

Where,

$\gamma_e$  is an effective flightpath angle in rough water

$h_{1/3}$  is the significant wave height

$L$  is the length of the seaplane

## Code of Federal Regulations

While the previous equations are useful qualitatively, CFR Title 14 part 23 and 25 include clear requirements for structural design of seaplanes. Equations are given to estimate the impact load factor (or acceleration), as well as the design bottom pressures to be used. The following equation is used to compute the load factors for the step landing case (other equations can include bow and stern impacts).

$$n_w = \frac{C_1 V_{SO}^2}{\left( \tan^{\frac{2}{3}} \beta \right) W^{\frac{1}{3}}}$$

## Early-Stage Sizing

Where,

$n_w$  is the water reaction load factor (that is, the water reaction divided by seaplane weight).

$C_1$  = empirical seaplane operations factor equal to 0.012 (except that this factor may not be less than that necessary to obtain the minimum value of step load factor of 2.33).

$V_{so}$  is the seaplane stalling speed in knots with flaps extended in the appropriate landing position and with no slipstream effect.

$\beta$  is the Angle of dead rise at the longitudinal station at which the load factor is being determined in accordance with figure 1 of appendix I of this part.

$W$  is the seaplane landing weight in pounds.

The CFR equation does not include trim, flight path angle and beam as parameters, and therefore assumes a fairly typical seaplane design.

### References for Chapter 10

Clement, E.P. The Design of Cambered Planing Surfaces for Small Motorboats. David Taylor Model Basin Report No. 3011. March, 1969.

Clement, E.P. and Hoyt, J.G. A Parametric Study of Dynaplane-Type Planing Motorboats. Proceedings 1<sup>st</sup> Chesapeake Power Boat Symposium. Annapolis, Maryland, 7-8 March, 2008.

Dathe, I., de Leo, M., Hydrodynamic Characteristics of Seaplanes as Affected by Hull Shape Parameters. Intersociety Advanced Marine Vehicles Conference. Arlington, VA. pp 275-284. June 1989.

Davidson, K.S.M. and Locke, F.W.S. General Tank Tests on the Hydrodynamic Characteristics of Four Flying Boat Hull Models of Differing Length-Beam Ratio, N.A.C.A. A.R.R. No. 4F15, 1944.

Haar, M. Effect of Forebody-Afterbody Proportions and Length-Beam Ratio on the Hydrodynamic Characteristics of a Series of Flying-Boat Hull Models. Experimental Towing Tank Report 465. Stevens Institute of Technology, Hoboken,

## Early-Stage Sizing

NJ. Prepared for the Bureau of Aeronautics, Department of the Navy. October 1952.

Hugli, W.C. and Van Dyck, R.L., A Limitations Analysis of Hulls and Hydro-Skis for Water-Based Aircraft. Experimental Towing Tank Technical Report No. 562. Stevens Institute of Technology. Prepared for U.S. Bureau of Aeronautics. April 1955.

Locke, F.W.S. An Analysis of the Skipping Characteristics of Some Full-Size Flying Boats. N.A.C.A. Wartime Report W-104. 1946.

Olson, R.E. and Land, N.S., Effect of Afterbody Length and Keel Angle on Minimum Depth of Step for Landing Stability and on Take-Off Stability of a Flying Boat. N.A.C.A. Technical Note No. 1571. September, 1948.

Parkinson, J.B. Design Criteria for the Dimensions of the Forebody of a Long-Range Flying Boat. N.A.C.A. A.R.R. No. 3K08. 1943

Pepper, P.A. and Kaplan, L., Survey on Seaplane Hydro-Ski Design Technology - Phase 1: Qualitative Study. Prepared by Edo Corporation for the Office of Naval Research and the Naval Air Systems Command. Department of the Navy Report 7489-1. 1966.

Pepper, P.A. and Kaplan, L., Survey on Seaplane Hydro-Ski Design Technology - Phase 2: Quantitative Study. Prepared by Edo Corporation for the Office of Naval Research and the Naval Air Systems Command. Department of the Navy Report 7489-2. 1968.

Savitsky, D. Wetted Length and Center of Pressure of Vee-Step Planing Surfaces. Experimental Towing Tank Report 378. Stevens Institute of Technology, Hoboken, NJ. Prepared for the Office of Naval Research. September, 1951.

Smith, A.G. and Allen, J.E. Water and Air Performance of Seaplane Hulls as affected by Fairing and Fineness Ratio. U.K. Aeronautical Research Council Reports and Memoranda No. 2896. 1954.

Stout, E. G. Development of High-Speed Water-Based Aircraft. Journal of the Aeronautical Sciences. Vol. 17, No. 8, pp. 457-480. August 1950.

Suydam, H.B. Hydrodynamic Characteristics of a Low-Drag Planing-Tail Flying-Boat Hull. N.A.C.A. Technical Note 2481. January 1952.

## Early-Stage Sizing

Van Dyck, R.L. An Investigation of the Effect of Vee-Step Angle on the Hydrodynamic Characteristics of Seaplanes. Experimental Towing Tank Report 532. Stevens Institute of Technology, Hoboken, NJ. Prepared for the Bureau of Aeronautics, Department of the Navy. April 1954

Van Dyck, R.L. A Constant-Speed Method for Obtaining Rough Water Landing Impact Characteristics of Water-Based Aircraft. Davidson Laboratory Report No 682. Stevens Institute of Technology. Prepared for Bureau of Aeronautics. April 1958.

## Standard Series

### CHAPTER 11. STANDARD SERIES

M.G. Morabito, 2024

1936 - NACA Deadrise Model 35 Series  
1938-1945 - DVL Series - Blohm and Voss Ha 139  
1943 - NACA Streamlined Body Model 84 Series  
1947 - Locke - Collapsed Results of Miscellaneous Flying-Boat Hulls  
1947 - PBV2-4 Consolidated Coronado Series  
1951 - Floatplane and Amphibian Series  
1952 - High L/B Forebody-Afterbody Proportions Series

#### Standard Series Overview

The Standard Series method is where a suitable "parent hull" is chosen, and then the effects of various geometric changes or difference in loading and speed are explored. Not all models in a standard series are good. Sometimes the series alerts the reader to unsatisfactory findings. This section reviews some of the available standard series and the goals set out in the development of each.

#### Hull Forms Tested

Prior to WWII, the majority of flying boats had a length-to-beam ratio about 6, and relatively shallow step heights. It was recognized that in order to develop into long-range high-speed transport, the aerodynamic resistance needed to be less, and hence the length-to-beam ratio of the hull must be increased.

The goal of some standard series investigations was to see how to increase L/B without having detrimental effects on hydrodynamic performance. The earlier coefficients were beam-based, and so increasing L/B with constant beam would change the bottom area significantly. Some series were tested on the basis of constant planform area (product of length times beam). It was observed in studies, with L/B from 6-10, that constant values of Davidson's "K2" or [Length x Length x Beam] would provide similar hydrodynamic performance, rather than constant  $K_{3/2}$  [Length x Beam]. The "3/2" comes from the exponent on length in the following equations for loading:

$$C_d = \frac{V}{b^3}$$

$$K_2 = \frac{V}{L^2 b}$$

$$K_{3/2} = \frac{V}{L^{1.5} b^{1.5}}$$

## Standard Series

The term "High Length-to-Beam Ratio" changed over the years. Mid 1940s it meant  $L/B = 10$ . Mid 1950's they were testing  $L/B$  up to 20. Thus, most standard series say that they are for "High  $L/B$ " hulls. Since the seaplane series had gradually evolved far from the typical small flying boat or amphibian, a standard series was done for these boats, having simple developable surfaces and more reasonable length-to-beam ratios.

The hulls with low step heights often encounter "skipping" instability, caused by intermittent ventilation of the step. This can be dangerous and so step heights needed to be increased. Other variations to the steps included longitudinal location as well as planform shape. Some series included landing tests for skipping, while for others, it is evident from the porpoising tests by a reduced upper limit at high speed.

### Method of Presentation:

Early series were tested in the mid-to-late 1930s and were reported in a variety of ways, including the NACA general tank test method, using the standard NACA coefficients. By World War II, F.W.S. Locke developed a means of collapsing the data from the many tests onto a one-page chart.

This method of presentation allowed tests to be rapidly conducted and presented on standard charts. It is immediately obvious after flipping through the charts which hulls are better than others. Four standard series were tested at Stevens Institute of Technology, in support of this effort. Each have advantages and disadvantage.

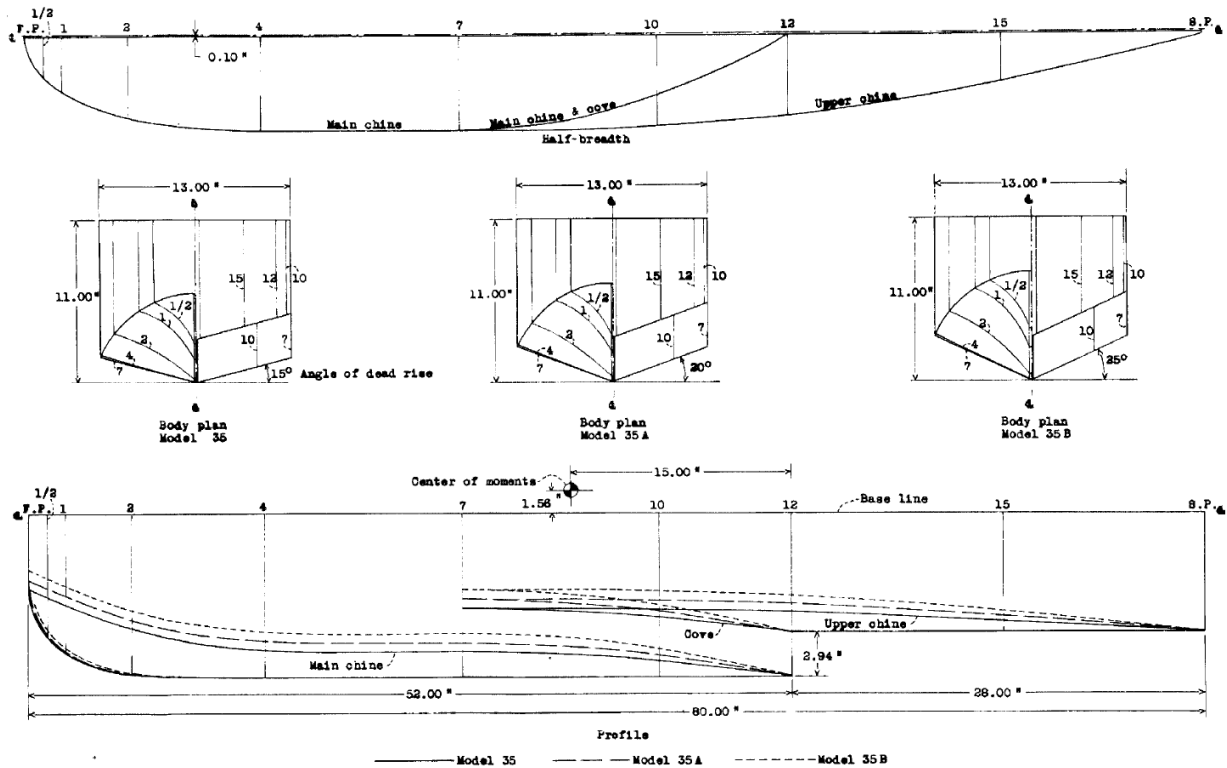
As of 2024, we haven't been able to develop a more convenient presentation of these results. Efforts have been made to computerize the charts, requiring complicated data tables and interpolation routines; however, it remains faster to flip through the charts, find one that looks good, and then type the values into a spreadsheet to do the expansion for you. It will be seen that the hulls with inadequate step height generally have lower resistance at hump speed, and therefore caution should be taken in the design trade-offs.

# Standard Series

## 1936 - NACA Deadrise Model 35 Series

Dawson, John R. "Tank Tests of Three Models of Flying-Boat Hulls for the Pointed-Step Type with Different Angles of Dead Rise - N.A.C.A. Model 35 Series" NACA Technical Note No. 551. January 1936.

The results of tank tests of three models of flying boat hulls of the pointed-step type with different angles of deadrise are given in charts and are compared with results from tests of more conventional hulls. Increasing the angle of deadrise from 15-degrees to 25-degrees: had little effect on the hump resistance; increased the resistance throughout the planing range; increased the best trim angle, reduced the maximum positive trimming moment required to obtain best trim angle; and had but a slight effect on the spray characteristics. For approximately the same angles of dead rise the resistance of the pointed-step hulls were considerably lower at high speeds than those of the more conventional hulls.



NACA Deadrise Model 35 Series



## Standard Series

### 1938-1945 - DVL Series - Blohm and Voss Ha 139

Sottorf, W, "The Design of Floats" NACA TM 860. April 1938. Also Luftfahrtforschung Vol. 14 No 4-5 April 20, 1937. Verlag von R. Oldenbourg Munchen und Berlin

Sottorf, W. "Systematic Model Researches on the Stability Limits of the DVL Series of Float Designs" NACA Technical Memorandum 1254. December, 1949. Also JArbuch 1942 der Deutschen Luftfahrtforschung pp I 451 - I 465.

Bidwell, J.M. and Goldenbaum, D.M. "Resistance Tests of Models of Three Flying-Boat Hulls with a Length-Beam Ratio of 10.5" NACA Wartime Report L-79. Also Advanced Restricted Report L5G19 September 1945.

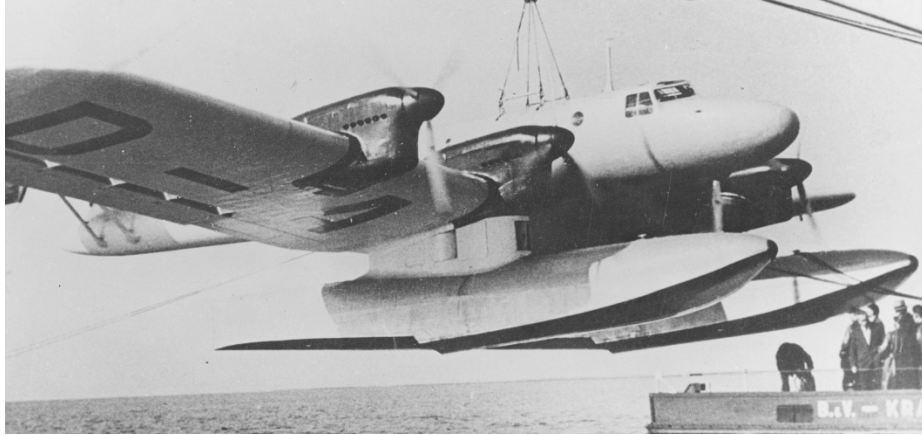
The DVL (Deutsche Versuchsanstalt für Luftfahrt) series was originally published in 1937 in Germany. The reports were subsequently translated into English. In 1942 the stability limits were published. In 1945, NACA extended the series to a higher length-to-beam ratio.

Sottorf (1937) Following a summary of the many floats worldwide, and a brief enumeration of the requirements of floats, the essential form parameters and their effect on the qualities of floats are detailed. On this basis a standard float design is developed which in model families with varying length/beam ratio and angles of dead rise is analyzed. The DVL standard float is used on the Ha 139 of the German Luft Hansa, among others.

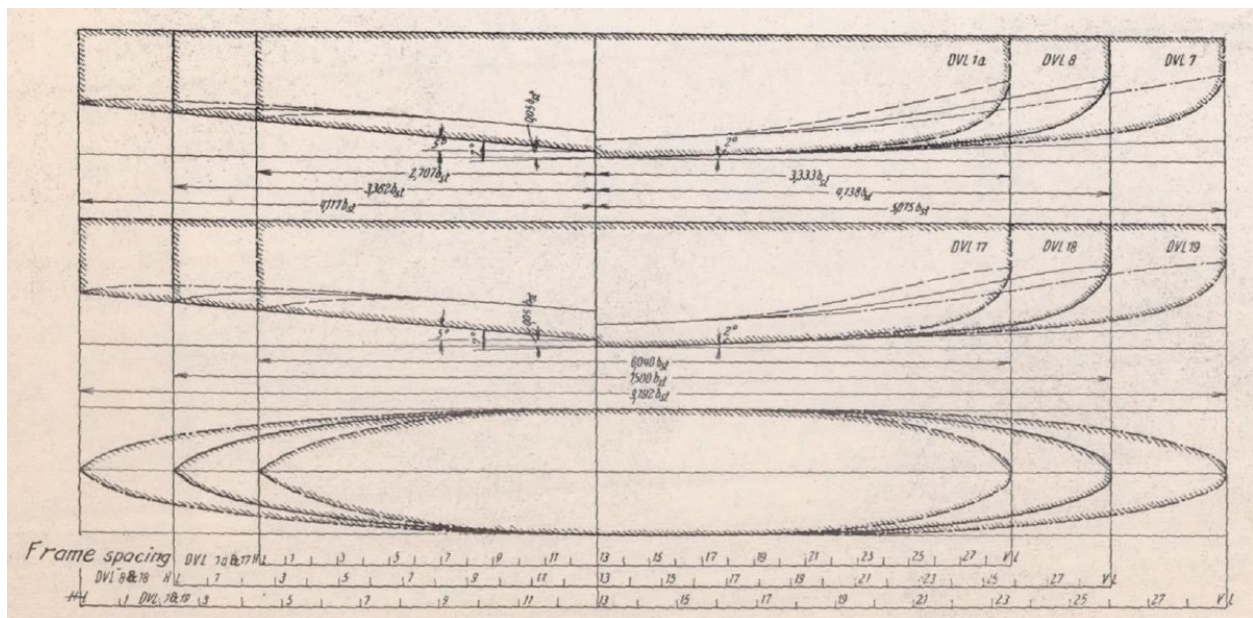
Sottorf (1942/1949) To determine the trim range in which a seaplane can take off without porpoising, stability tests were made of a plexiglass model, composed of float, wing, and tailplane, which corresponded to a full-size research airplane. The model and full-size stability limits are in good agreement. After all structural parts pertaining to the air frame were removed gradually, the aerodynamic forces replaced by weight forces, and the moment of inertia and position of the center of gravity changed, no marked change of limits of the stable zone was noticeable. The latter, therefore, is for practical purposes affected only by hydrodynamic phenomena. The stability limits of the DVL family of floats were determined by a systematic investigation independent of any particular seaplane design, thus a seaplane may be designed to give a run free from porpoising.

Bidwell and Goldenbaum (1945) N.A.C.A. extended the series to L/B around 10 and looked at the effect of step depth and deadrise on two models. of step and two angles of dead rise.

# Standard Series



Blohm and Voss Ha 139 - Based on DVL Series



DVL Series Model Comparison

1943 - NACA Streamlined Body Model 84 Series

Parkinson, J.B., Olson, R.E., Draley, E. Luoma, A. "Aerodynamic and Hydrodynamic Tests of a Family of Models of Flying-Boat Hulls Derived from a Streamline Body -NACA Model 84 Series" NACA Report No. 766. 1943

Bell, J.W., Garrison, C.C., and Zeck, H. Effect of Length-Beam Ratio on Resistance and Spray of Three Models of Flying-Boat Hulls," NACA Wartime Report L-358, Also Advance Restricted Report 3723. October, 1943.

Parkinson (1943) A series of related forms of flying-boat hulls representing various degrees of compromise between aerodynamic and hydrodynamic requirements was tested in the Langley Tank No. 1 and in the Langley 8-foot high-speed wind tunnel. The purpose of the investigation was to provide information regarding the penalties in water performance resulting from aerodynamic refinement and as a corollary to provide information regarding the aerodynamic penalties resulting from the retention of certain desirable hydrodynamic characteristics.

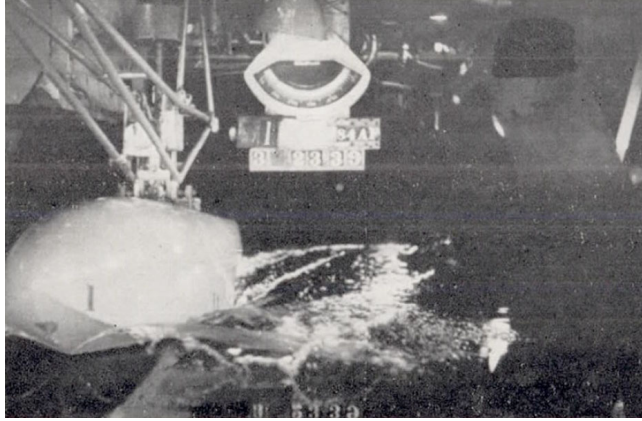
The related models were based on an arbitrary body of revolution and were developed to show clearly the effect of conventional departures from the ideal streamline body made in the design of flying-boat hulls. All models had the same overall length-to-diameter ratio of 7.21. The report provides excellent photographs of the spray patterns. Results are presented in the NACA General Test format.

Bell, Garrison and Zeck (1943) An investigation of the effect of changes in the length-beam ratio of flying boat hulls on the resistance and spray was conducted in NACA tank no. 1. A family of three models of hulls of different length-beam ratios was used and, in order to maintain comparable hull sizes, the plan-form areas of the hulls were made approximately equal by keeping equal products of length and beam.

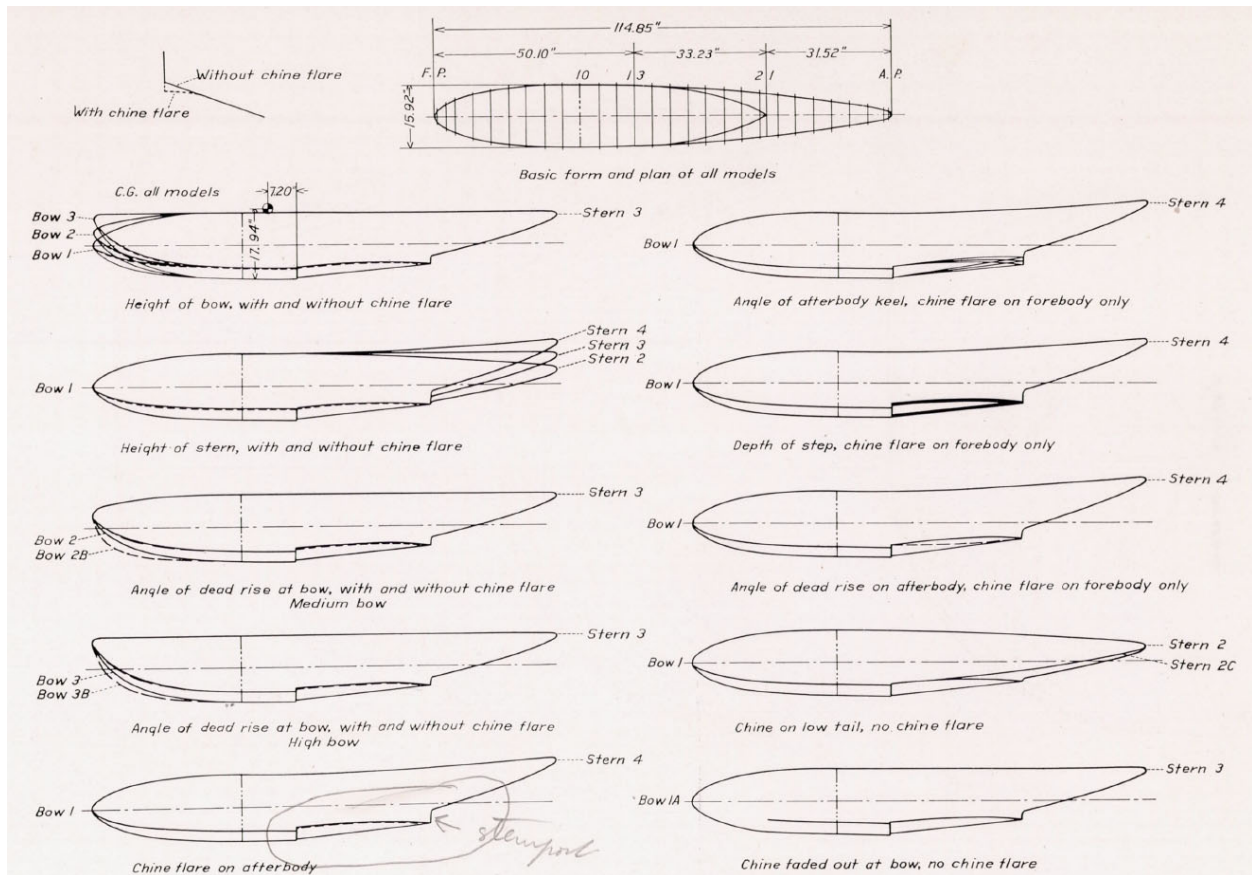
The tests were made by the general method for the fixed-trim condition as well as by the specific method for the free-to-trim condition. Photographs of the spray were taken during the free-to-trim tests. Resistance and trimming-moment data obtained from the tests were compared over a wide range of loads at best-trim and free-to-trim conditions. Further comparisons were made by means of take-off calculations for hypothetical flying boats that incorporated the lines of the models.

The spray photographs indicated that at very low speeds the height of the bow spray was reduced by increasing the length-beam ratio, but at high speeds the height of the spray was increased slightly by increasing the length-beam ratio. It was concluded from the results of the tests that by increasing the length-beam ratio the load coefficient may be increased and that, within the range of the tests, high length-beam ratios will give lower hump resistance and better take-off performance than low length-beam ratios.

# Standard Series



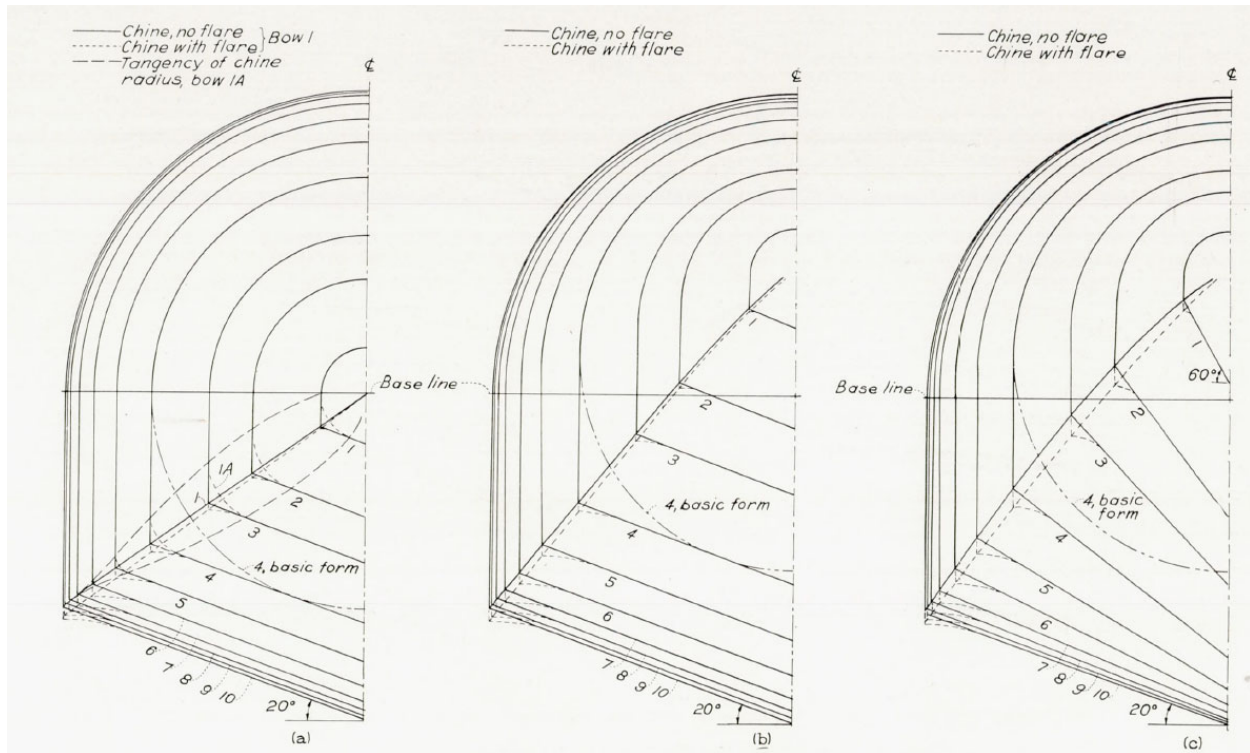
NACA Streamline Body Model 84 Series Photograph



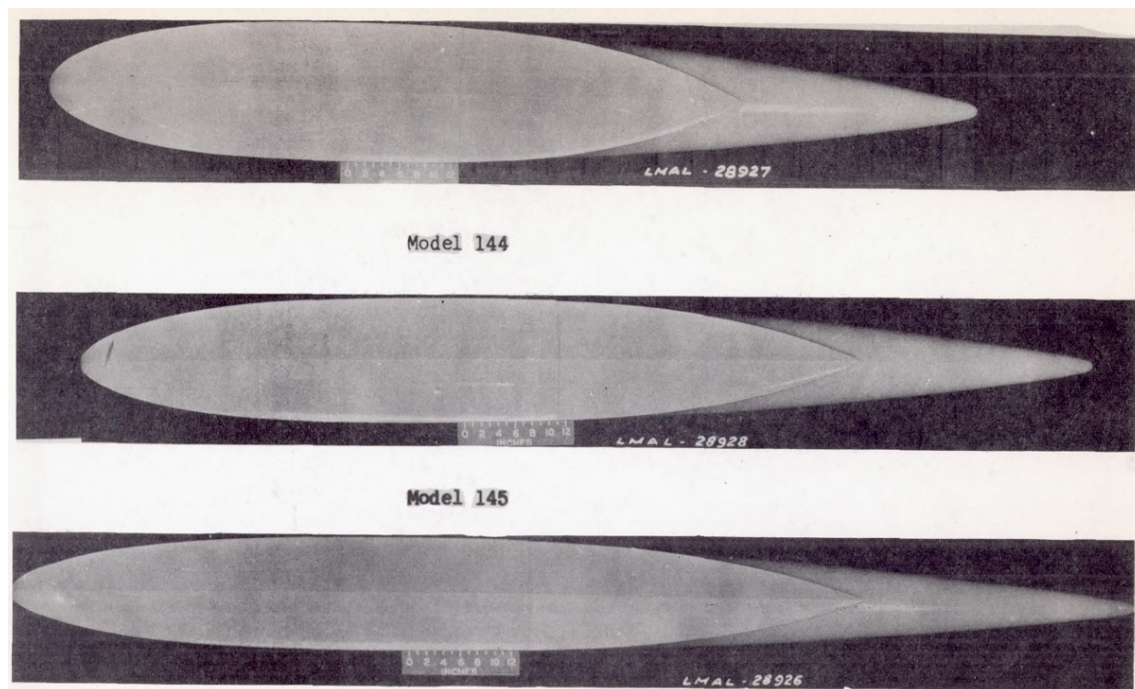
NACA Streamline Body Model 84 Series



# Standard Series



NACA Streamline Body Model 84 Series Body Plan



Models in NACA L/B Series

1947- Locke - Collapsed Results of Miscellaneous Flying-Boat Hulls

Locke, F.W.S. "A collection of the Collapsed Results of General Tank Tests of Miscellaneous Flying-Boat Hull Models." NACA Technical Note No. 1182. 1947.

This report presents summary charts of the collapsed results of general tank tests of about one hundred flying-boat-hull models, in the "Stevens Collapsed Data Set" format. These summary charts are intended to be used as an engineering tool to enable a flying boat designer to grasp more quickly the significance of various hull form parameters as they influence his particular airplane. The form in which the charts are prepared is discussed in some detail in order to make them clearer to the designer. This is a data report, but no attempt has been made to produce conclusions of the usual sort or correlations. However, some generalizations are put forward on the various methods in which the summary charts may be used.

## Standard Series

### 1947 - Martin Mars Series

Strumpf, Albert, "Model Tests on a Standard Series of Flying-Boat Hulls." Stevens Institute of Technology, Experimental Towing Tank Report No. 325. Prepared for Bureau of Aeronautics, Department of the Navy.

This report presents the results of a large standard series of flying-boat hulls tested at the Experimental Towing Tank at Stevens Institute of Technology, Hoboken, NJ. This report is one of a group of standard series investigations conducted during the 1940s and 1950s, during a time of rapid development for high-performance long-range transport seaplanes.

The parent hull is the XPB2M-1, which later entered production as the Martin JRM Mars. The series hulls have afterbody angles from 3 to 11 degrees, deadrise angles from 0 to 40 degrees and length-to-beam ratios of 5.07-8.45. The purpose of having such a wide range of variables was to explore the whole design space, identifying combinations that result in satisfactory or unsatisfactory performance. It is shown that increases in L/b can be accomplished without large degradation in performance. Later series explored higher L/b. Portions of this series were sequentially published in various NACA reports by Kenneth Davidson and/or Fred Locke, for topics such as resistance, longitudinal stability, and spray. This series shows all the results in one condensed report.

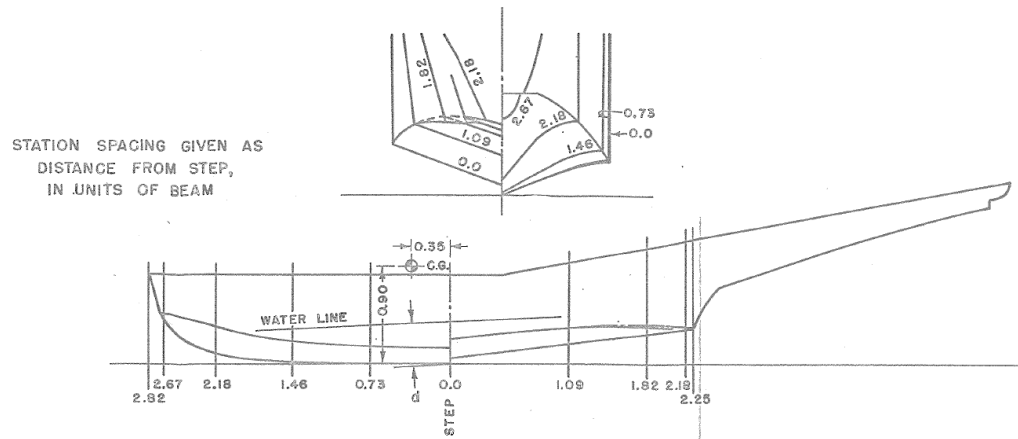
The presentation of the results in collapsed form permit the preliminary designer to rapidly flip through the datasheets to find hulls with acceptable longitudinal stability (porpoising), resistance, trim, and spray. Extensive efforts were made in 2023 and 2024 to digitize this standard series; however, it was found that the collapsed data sheets still provide the most simple and practical method of presenting seaplane test data. The best hulls are immediately visually apparent and the graphs present a multitude of information on one page. These charts can significantly shorten the time required to iterate to a functional design.

Many of these hulls have very good hump speed resistance. Care should be taken to observe the longitudinal stability limits though. Some of the combinations of low deadrise or low sternpost angle do not have a stable regime for takeoff. Further, the small step heights used here may result in porpoising or skipping instabilities. Later series used larger step heights for this reason. The goal of this series was not to have all good hulls - it was to explore the design space!

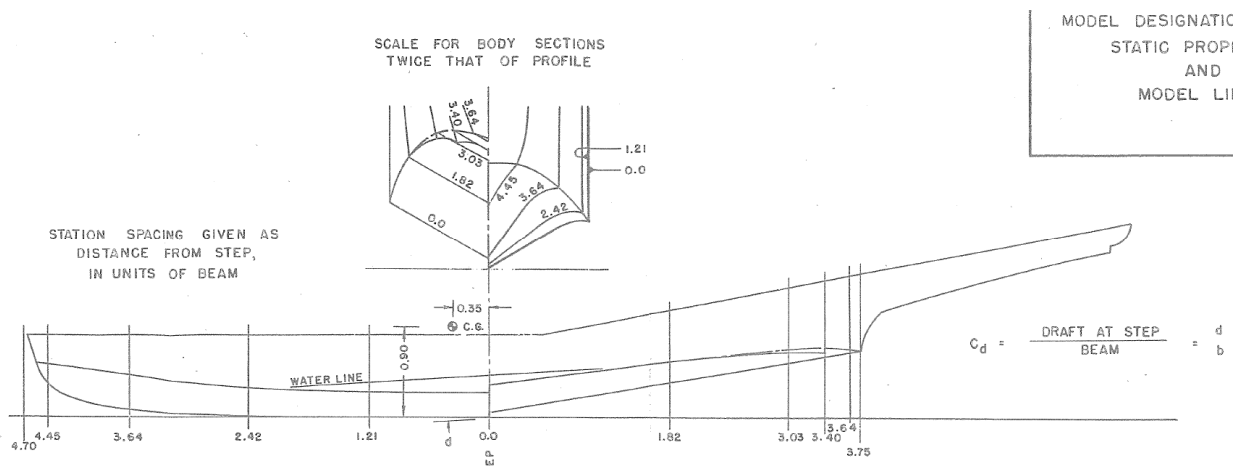
# Standard Series



Martin JRM Mars



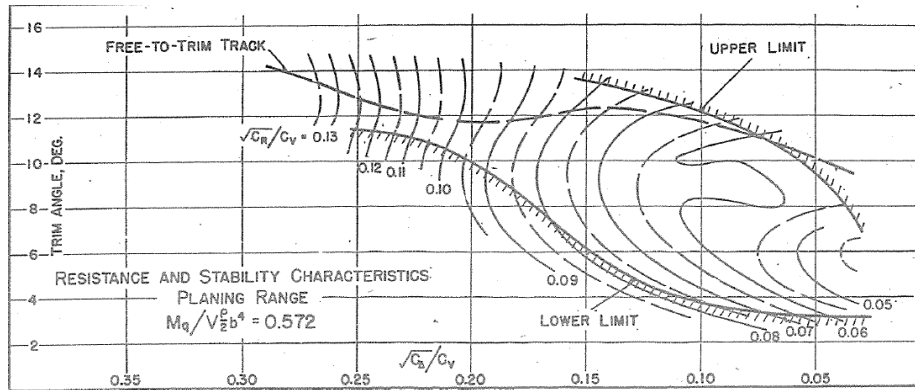
Parent Hull  $L/B = 6.19$



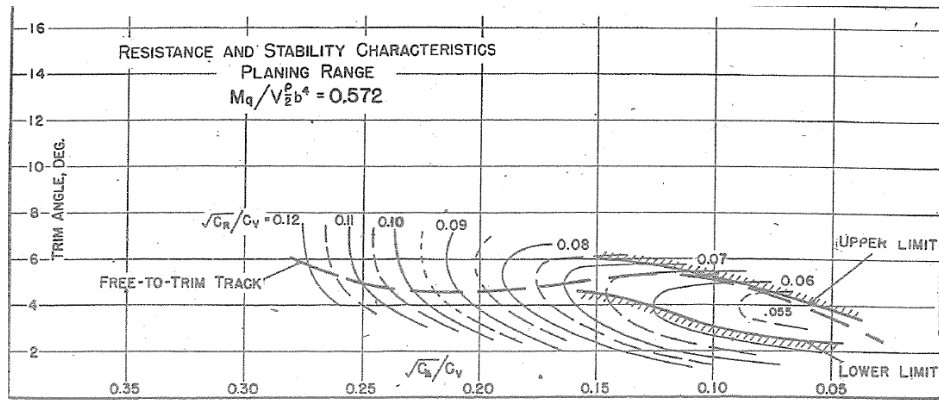
Extreme Model in Series



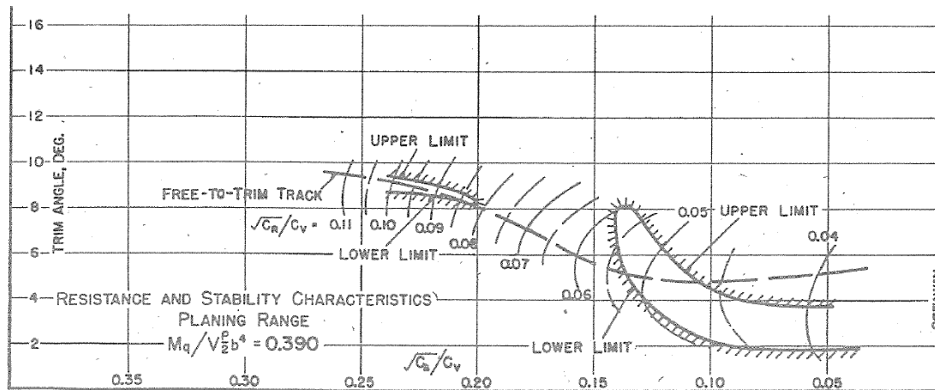
## Standard Series



Good Stability Limits - Good at hump, Getaway at 3 to 6.5 degrees



Low Stability Limits - Low Sternpost prevents take-off above 3.5 degrees



Speeds with No Stable Range

## Porpoising Charts from Martin Mars Series

Anyone Using this Series should First look at the Porpoising Graphs and Rule Out Bad Hulls

1947 - PBY2-4 Consolidated Coronado Series

Hugli, W.C., Jr. Strumpf, Albert, Axt, W.C. "An Investigation of the Effects of Hull Proportion and Step Depth on the Hydrodynamic Characteristics of Flying-Boat Hull Models with Varying Length-Beam Ratios" Experimental Towing Tank, Stevens Institute of Technology Report No. 312. Prepared for National Advisory Committee for Aeronautics. Contract No. Naw 3688. February 1947.

This report presents the results of "general" tests on the hydrodynamic characteristics of a family of flying-boat hull models. The purpose of these model tests was to explore higher length-beam ratio hulls than were previously investigated, and to explore the effects of forebody-afterbody proportion and step depth on the hydrodynamic characteristics of hulls with varying length-beam ratio. Previous Stevens Institute standard series tests (reported by Strumpf in May of 1947) utilized hull families that were arbitrarily expanded from a parent hull form, making every effort to isolate length-beam ratio as an independent parameter. The tests presented here explore the effects of changing the hull proportions that were fixed in the previous study.

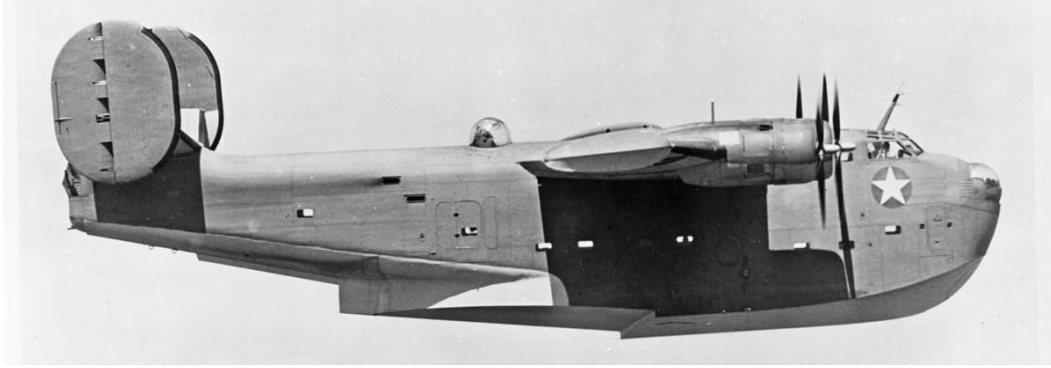
These tests show that increasing step depth (with a corresponding increase in sternpost angle) raises the upper limit trim, the spray height at the step, the resistance at hump, and the free-to-trim track in the vicinity of the hump. However, the effects attributed to changes in step-depth are mostly caused by sternpost angle variation. Step depth as an independent parameter (i.e., with constant sternpost angle) has its major effects on the skipping characteristics which were not investigated here. With the sternpost angle held constant, the shortest forebody length tested (55 percent of the length from forepoint to sternpost) is slightly better for each of the length-beam ratios considered ( $L/b = 6, 8, \text{ and } 10$ ). Later studies (conducted at Stevens and presented by Marvin Haar in October 1952) investigate the effects of further increases in afterbody length, while maintaining constant sternpost angles.

The test results are presented in the Stevens Collapsed Data format. Note, in this format the resistance is not ordinarily corrected for the difference in Reynolds number and friction coefficient (the typical Froude method expansion), instead maintaining the same resistance-to-weight ratio for model and full-size. Further, the aerodynamic resistance of the model is included. This will result in a conservative estimate of resistance.



Consolidated Coronado

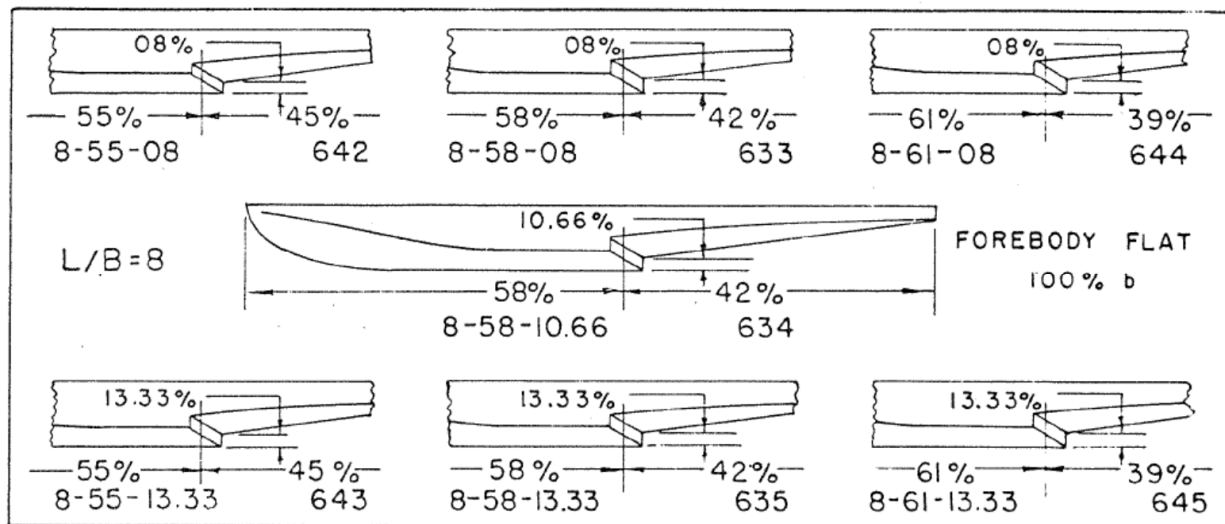
# Standard Series



Consolidated Coronado Profile



Photograph of Tests



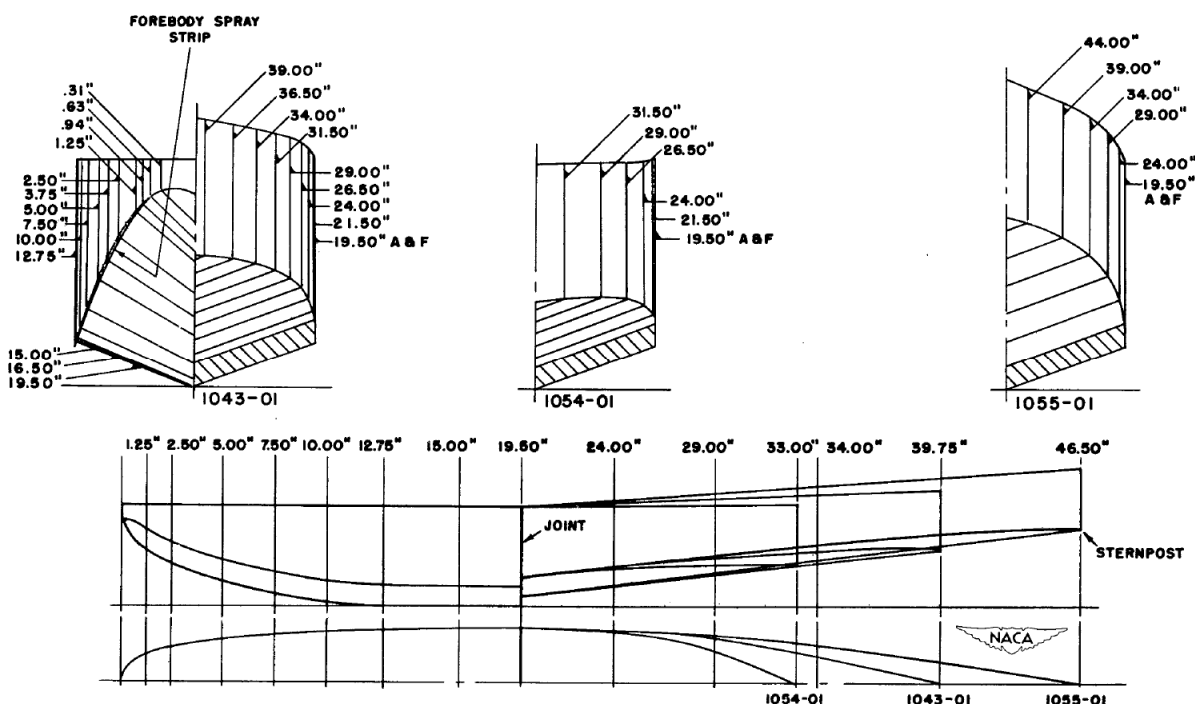
Example Geometric Variations (This was done for 3 L/B)

1951 - Small Flying Boat and Amphibian Series

Hugli, W.C. and Axt, W.C. Hydrodynamic Investigation of a Series of Hull Models Suitable for Small Flying Boats and Amphibians. NACA Technical Note 2503. November, 1951.

This report presents the results of an investigation made at the Experimental Towing Tank, Stevens Institute of Technology, to obtain hydrodynamic information on a series of hull models suitable for small flying boats or amphibians of from 2000 to 5000 pounds gross weight. The series of hulls consisted of a basic hull with simple lines, and of plus and minus variations to this design in which the beam, sternpost angle, and afterbody length were altered. Modifications were also investigated to determine the advantage of refining the hull lines.

The hulls were tested for hydrodynamic resistance and main spray. On the basis of these characteristics, the best beam and sternpost angle were selected for each of the three afterbody lengths investigated. The resulting three hulls were further tested for landing and porpoising characteristics. The results show that it is possible to design a hull with simple lines that will be suitable for small flying boats or amphibians. Refining the hull lines will improve the hydrodynamic characteristics slightly but will also increase the construction cost.



## Standard Series

### 1952 - High L/B Forebody-Afterbody Proportions Series

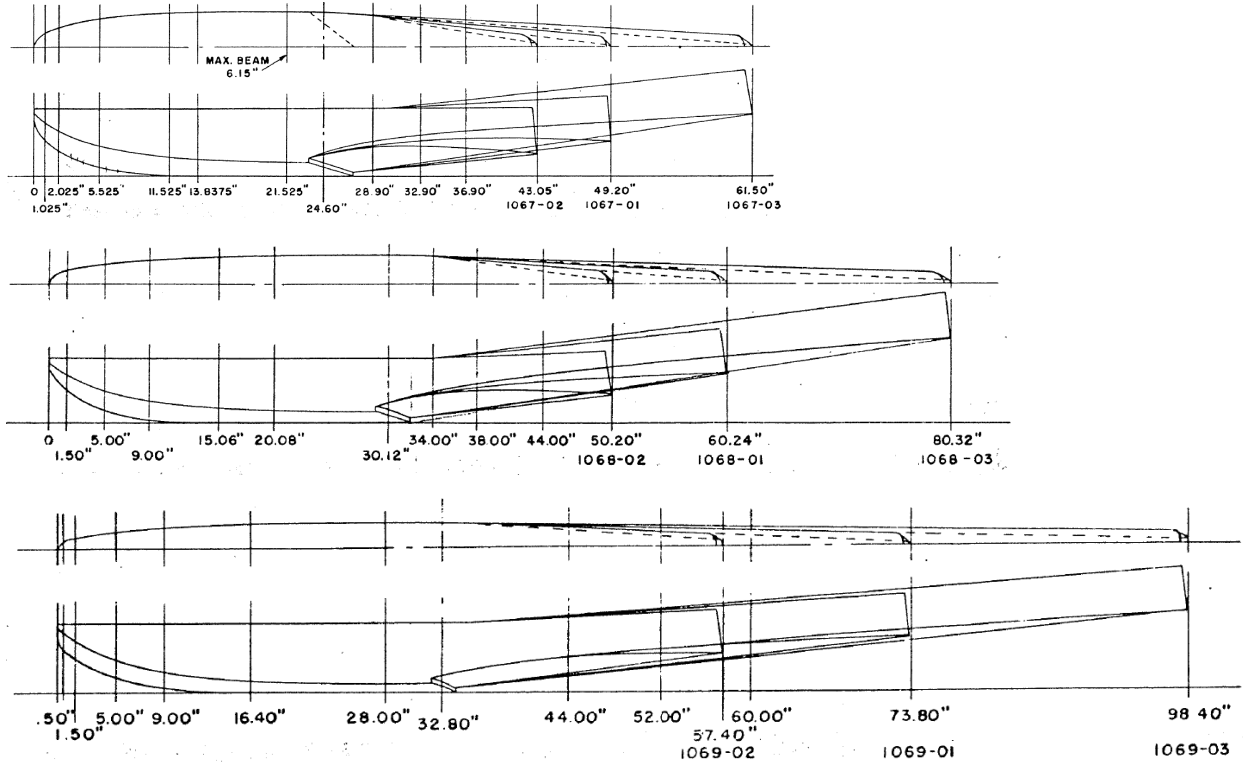
Haar, Marvin I. Effect of Forebody-Afterbody Proportions and Length-Beam Ratio on the Hydrodynamic Characteristics of a Series of Flying-Boat Models. Davidson Laboratory, Stevens Institute of Technology TR-465. October 1952. Prepared for Bureau of Aeronautics, Department of the Navy, Under the Sponsorship of the Office of Naval Research. Contract No. N6onr-247

This report presents the results of a standard series of flying-boat hulls tested at the high-speed towing basin at Stevens Institute of Technology, Hoboken, NJ. This report is one of a group of standard series investigations conducted during the 1940s and 1950s, during a time of rapid development for high-performance long-range transport seaplanes.

The purpose of this particular series is to investigate the effects of forebody-afterbody proportions on hulls with length-to-beam ratios from 7 to 24. A wide range of loadings are tested and the results are presented in collapsed form to be of aid in preliminary design. The parent hull includes some of the more advanced features of flying-boat development, including a pointed step, warped afterbody and substantial chine flare. The design process is presented, including mathematical equations to describe the keel and chine lines. The series makes unique use of forebody-only tests to measure the lift, pitching moment, spray and trim. This permits the determination of forebody-afterbody lift distribution.

When compared on the basis of load for a given planform area, there was an increase in resistance as length-to-beam ratio,  $L/b$  was increased. The height of the main spray was lowest at the intermediate value of  $L/b$ . The effect of forebody-afterbody proportions on hump resistance varied with the overall  $L/b$  of the hull. The shortest afterbody always yielded the lowest spray. The planing resistance and longitudinal stability characteristics of the models in the series were generally satisfactory, evidence that the choice of step height, sternpost angles, and loadings were good.

# Standard Series



Models in 1952 Haar High L/B Series



CHAPTER 12: HULL LINES DESIGN

(W.C. Hugli 1948-1951)

- 12.1 - Analytical Design Procedure
- 12.2 - Hull Design of Large Flying Boats
- 12.3 - Hull Design for Small Flying Boats or Amphibians
- 12.4 - Step Design
- 12.5 - Chine Configuration
- 12.6 - Forebody Intermediate Chine

12.1 - Analytical Design Procedure (W.C. Hugli, 1948)

Prior to the actual layout of the hull lines, values of hump speed, hump trim and waterborne load at hump speed can be assigned, based on prior experience or standard series data. From these data, an estimation of the forebody wetted length can be obtained using the Savitsky (1964) method, which, in turn, an estimation of the center of pressure and of the pitching moment due to resultant hydrodynamic force on the forebody to be made. This pitching moment has to be balanced by a moment produced by a force on the afterbody near the second step.

To determine the moment produced by the afterbody, the wave profile in the wake of the forebody may be plotted using the method of Korvin-Kroukovsky, Savitsky, and Lehman (1949). By trial and error, a location of the afterbody may be chosen such that the resulting position of the center of pressure, determined from the wetted length of the afterbody, produced the necessary moment to balance the moment due to the hydrodynamic force acting on the forebody. In this manner, the sternpost angle may be determined for a given afterbody length.

Attempts have been made to design hulls analytically on the basis of previous model tests on flying-boat hulls and on lift and wake equations for prismatic planing surfaces. Unfortunately, the data available are not sufficient to completely design hulls by analytic methods, making it necessary to resort to straight-forward comparisons with previous designs in many instances. Whether the design is based on previous experience or on analytical methods, there is a certain amount of flexibility in the choice of several design parameters. While these may be chosen as judiciously as possible, the merits of a proposed designs cannot be fully determined without model tests.

Figures 1 and 2, taken from Hugli (1951) show an example of the application of the analytical method to estimate the equilibrium forces and moments of a model.



## Hull Lines Design

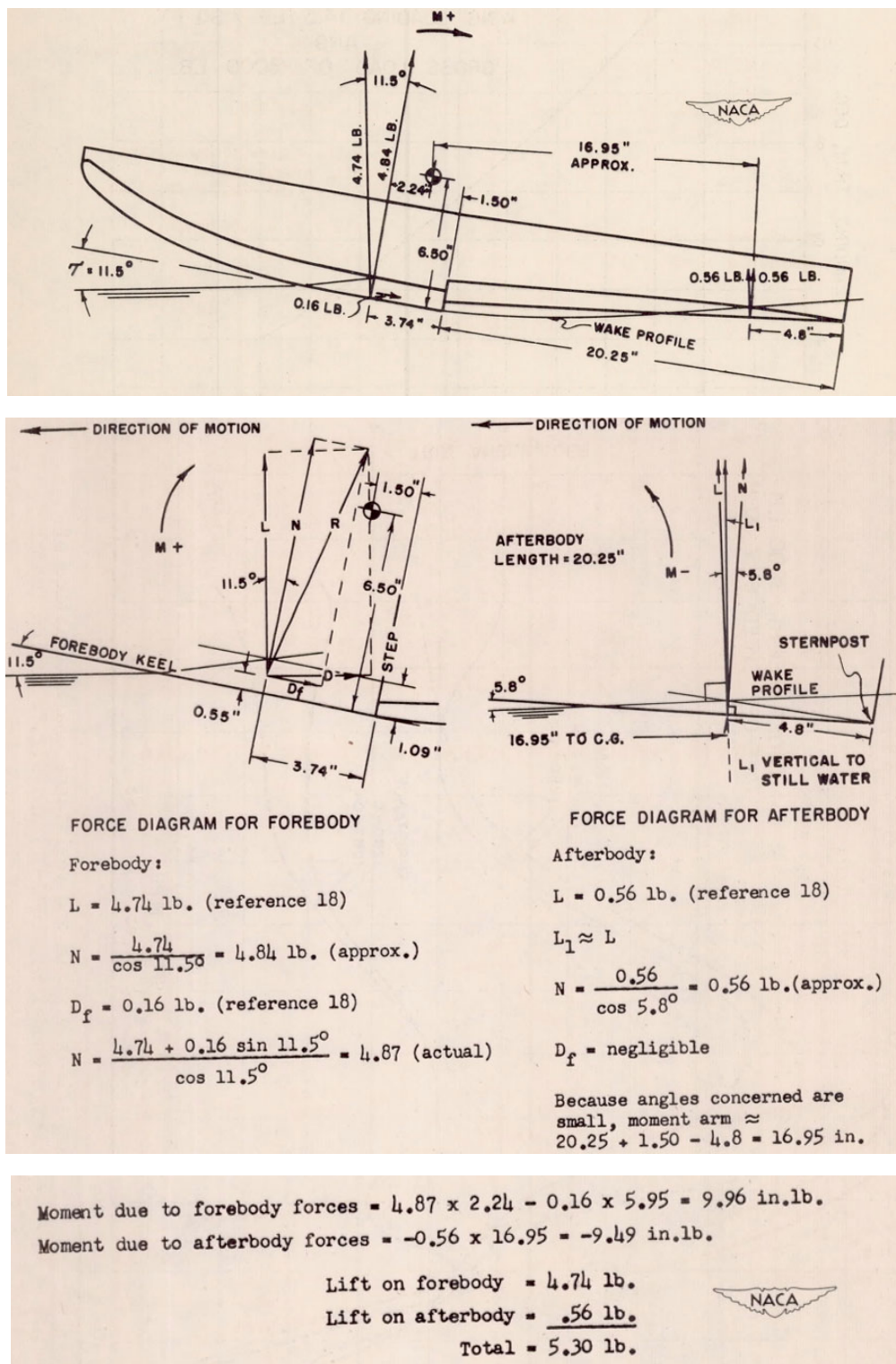


Figure 1: Example Calculations for flying-boat hull in two-step planing  
(Taken from Hugli, 1951) Note: Wake may be computed using Korvin-Kroukovsky,  
Savitsky and Lehman (1949) and forces estimated using the Savitsky (1964)  
method.

## Hull Lines Design

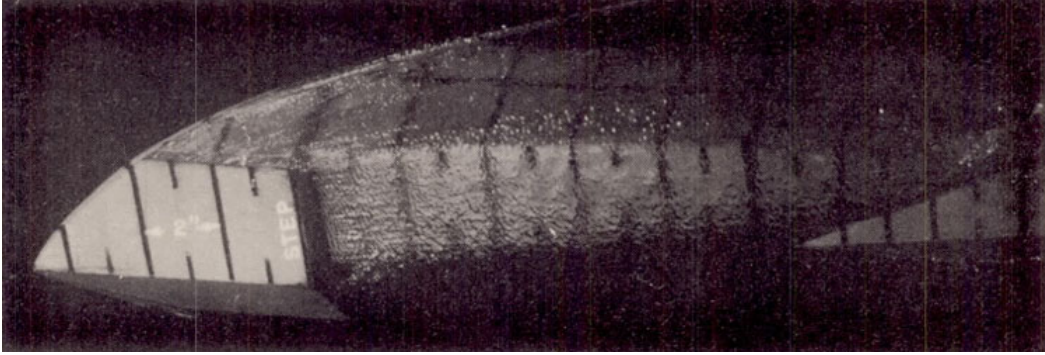


Figure 2: Underwater Photograph of Forebody and Afterbody Wetted Area (Taken from Hugli, 1951) Note: Photograph taken from the diagonal to show the side of the hull

## 12.2 - Hull Design of Large Flying Boats (W.C. Hugli, 1948)

Large flying boats and small amphibians have different levels of complexity; however, the development of the hull lines for both may be governed by the following principles:

- Wetted area of forebody flat sufficient to support the waterborne load at hump speed,
- Rearward portion of the afterbody supporting a small percentage of the waterborne load at hump speed,
- Details of forebody designed for definite control of spray
- Utilizing geometrical curves to the fullest extent possible

The following procedure was used to design the parent hull for the Haar (1952) Forebody-Afterbody Proportions standard series, shown below. This is a relatively late-stage, advanced hull form (Figure 3). There have been studies that indicate the chine could be somewhat lower at the bow (see subsection 12.5 for the "low-chine" bow); however, the design procedure is sound. Due to the complex curvature, it would not be suitable for a small flying boat, which could be fabricated at lower cost with developable surfaces.

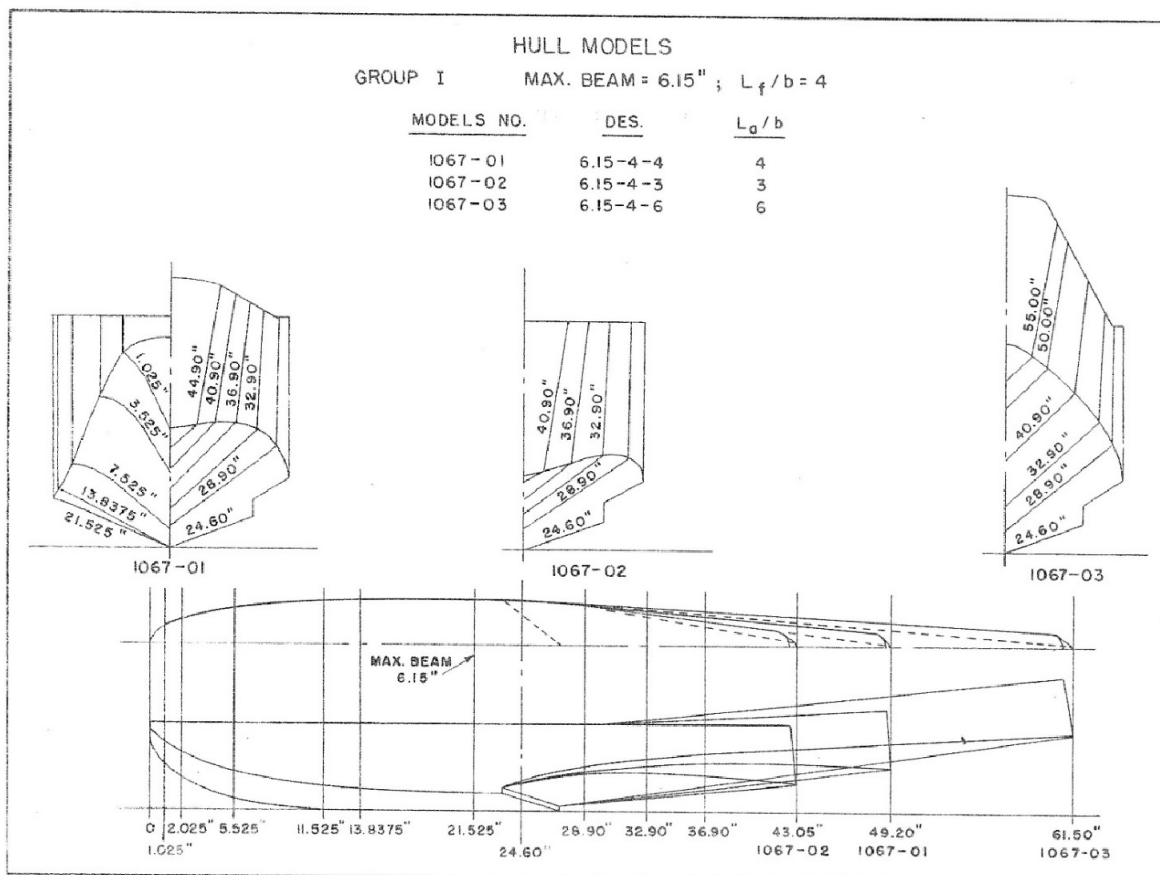


Figure 3: Linesplan for Hulls in Haar (1952) Standard Series

### Large Seaplanes - Forebody

Wherever practicable, the hull lines can be made of readily computable curves, a process which easily permits the scaling up or down of the lines.

The "forebody flat" - the region in which the deadrise increases linearly with the distance forward of the step centroid - is 37.5% of the forebody length. It is sufficiently long to satisfy the need of planing area at the humps and yet short enough to obtain easy buttock lines. A slight increase of the deadrise may be introduced in this portion of the forebody to ease the buttock lines further. Easy buttock lines are considered important since diving and spray characteristics are affected by curvature of the buttocks.

The keel curvatures starting at the forward end of the flat, is of essentially elliptical form with somewhat more fullness than a true ellipse as shown by the sketch below. The intersection of the keel and chine lines at the bow was placed approximately 90 percent of the beam above the baseline. This height is chosen to insure satisfactory operation in the expected wave condition (5-feet full scale)

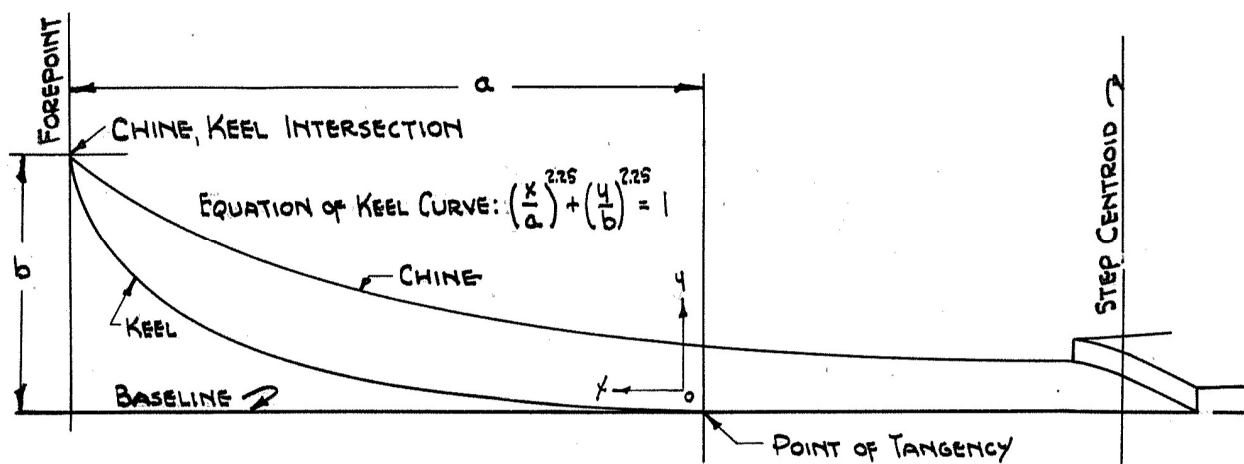


Figure 4: Forebody Keel and Chine Profiles

The variation in deadrise angle with forebody length is shown by the next figure. As can be seen on this chart, the variation in deadrise is linear over the region of the forebody flat and parabolic over region forward of the forebody flat. The deadrise at the step centroid is 22 degrees, while the deadrise at the bow is 70 degrees. It is believed that this combination of keel curvature and deadrise distribution is less likely to produce high speed diving than in the more conventional hull design which has a longer length of straight keel and more rapid curvature near the bow.

The plan of the forebody chine from bow to the maximum beam is of essentially elliptical form with somewhat more fullness than the true ellipse as shown in Figure 6.

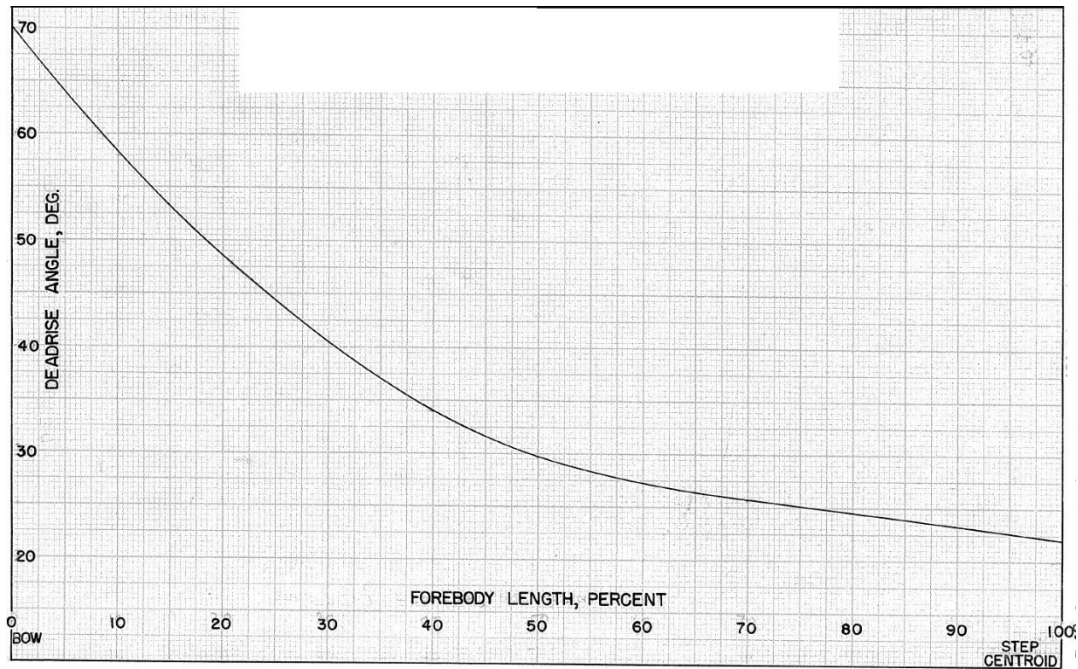


Figure 5: Forebody Deadrise Distribution

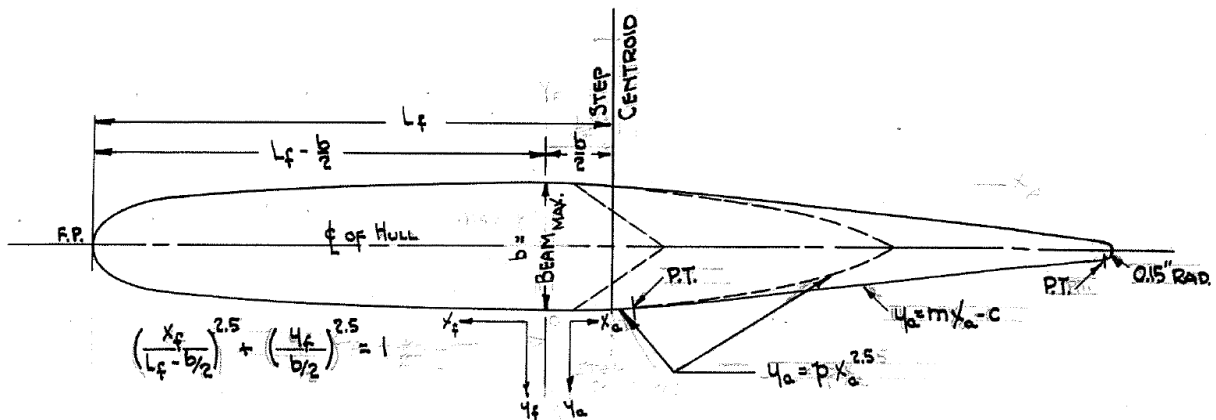


Figure 6: Forebody and Afterbody Chine Planforms

The profile of the forebody chine line was first obtained for the case of no chine flare from the keel line, the deadrise distribution, and the plan of the chine line. This chine line has been designated the "theoretical chine line".

The chine flare shown on the proposed forebody lines was obtained as follows: First, a trim track up to speed was estimated for the model. From this and the unloading curve, the forebody wetted lengths could be determined. These data enabled a determination of the local angles of attack

at the theoretical chine to be made. (The local angle of attack at the chine is defined as the angle -- measured in a plane parallel to the plane of symmetry -- between the still water surface and tangent to the chine at the point of intersection of the leading edge of the pressure area and the chine line.)

The theoretical chine heights were then adjusted where necessary to keep the local angles of attack at the chine below 16 degrees at every point (See Figure 7). A line was smoothed through the adjusted chine heights to make the actual profile of the forebody chine line. The chine-flare radius was then added.

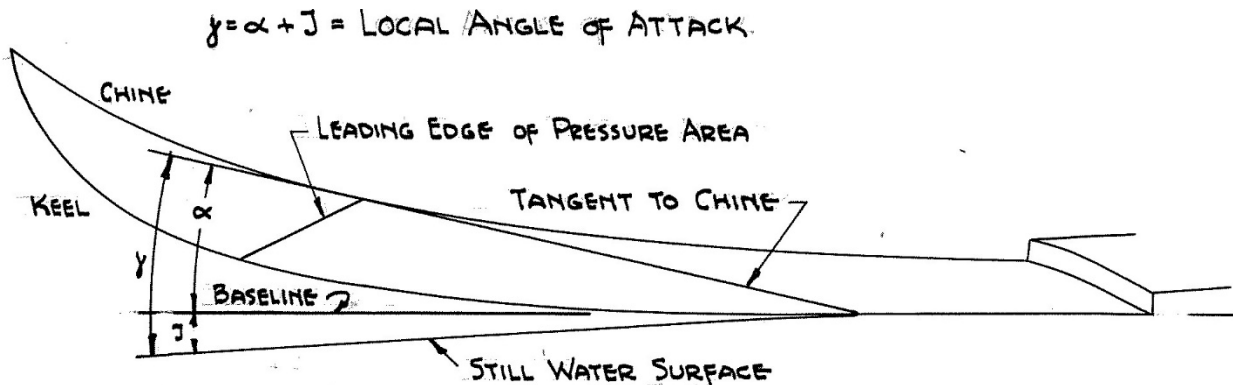


Figure 7: Sketch Defining Local Angle of Attack

#### Large Seaplanes - Beam

The maximum beam was placed 0.5 beams forward of the main step centroid. Placing the maximum beam forward of the step yields the maximum wetted area for a given wetted length -- a condition desired at hump speeds. As the speed increases and the wetted area diminishes, the wetted length becomes excessively short for a given beam and it is, therefore, of advantage to have a smaller beam at the step. In addition, this expedient provides for finer lines aft, thus reducing afterbody interference and also reduces the skin area of the hull which would reduce the weight.

### Large Seaplanes - Main Step

Essentially, a step of a flying-boat hull is a juncture between discontinuous surfaces. In the case of a "V"-planform step, the two discontinuous surfaces need not have the same deadrise angles in order to obtain a uniform depth of step. The proposed hull utilizes a 50 V-step to allow the joining of the forebody with lower deadrise angles with an afterbody of higher deadrise without obtaining an excessive depth of step at the chines. This is fortunate because the high afterbody deadrise angles, occurring at about 50 percent of the afterbody length, need not be fully reduced to those of the forebody at the main step.

The landing stability and the high-speed resistance characteristics for flying-boat hulls with moderate step depths are known to be improved by the use of V-steps. The increase in hump trim and planing resistance anticipated with a V-step has been shown to be small when the V-step is used in combination with a long afterbody.

The step depth at the centroid for the Haar standard series was 7 percent of the maximum beam.

### Large Seaplanes - Afterbody

The afterbody of a flying-boat hull is needed for static buoyancy and for trim control to speeds just beyond hump speed, while at high speeds the presence of the afterbody results in increased resistances. Furthermore, on landing the afterbody must also bear a portion of the impact loads. For trim control, only the rearward portion of the afterbody is necessary, but almost the entire bottom area of the afterbody may be subject to impact loads in rough water. Since an increase in the deadrise will reduce bottom pressures, and hence impact loads, all portions of the afterbody not utilized for trim control should have as high deadrise angle as possible.

Consequently, the deadrise angles may be increased behind the step to a maximum over the middle portion, and are then may be reduced to effective planing sections in the vicinity of the second step. The variation in deadrise angle with afterbody length for three models of differing afterbody lengths are shown in Figure 8.

In the vicinity of the main step, the afterbody deadrise angles are greater than those of the forebody thus providing greater clearance for spray thrown up by the step at high speeds.

# Hull Lines Design

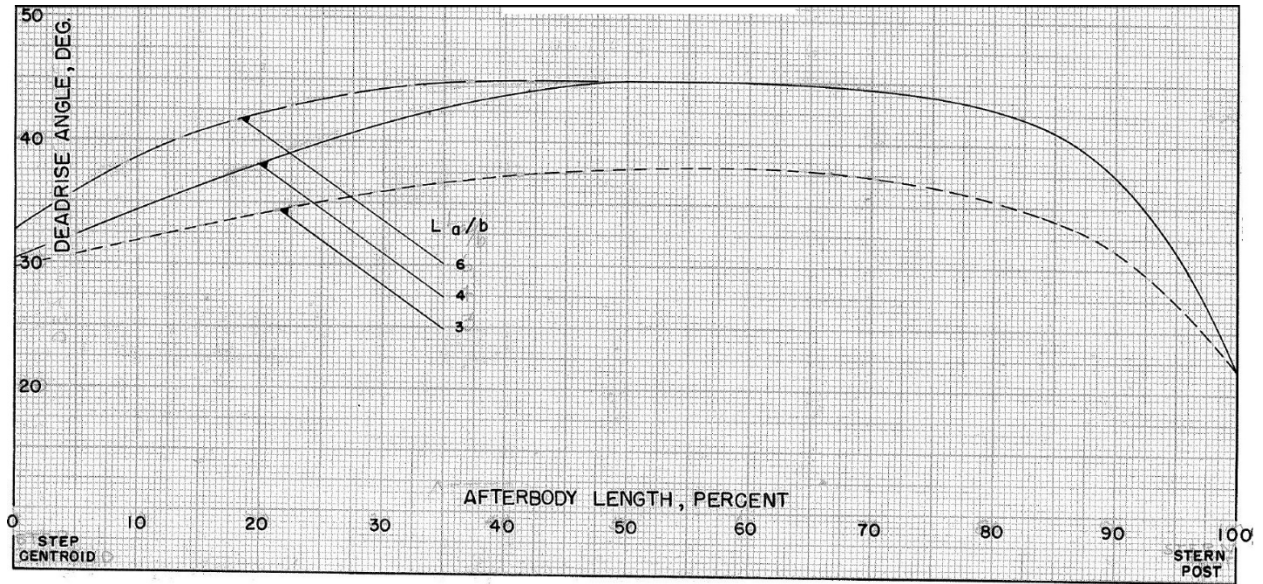


Figure 8: Afterbody Deadrise Distributions



### 12.3 - Hull Design for Small Flying Boats or Amphibians (W.C. Hugli, 1951)

It is possible to design an efficient hull with simplified lines suitable for small flying boats and amphibians. The hull design problems of large flying boats are different from those of small flying boats. The larger hulls, generally having lower power loadings and lower take-off-speed coefficients, are less sensitive to the hydrodynamic resistance characteristics than the smaller hulls. Furthermore, while it is feasible to incorporate into the lines of the larger hulls such refinements as chine flare and dead-rise warping, the lines of the smaller hulls must be as simple as possible in order to keep construction costs within reasonable limits.

While the standard series (Hugli, 1951) provides the details on the effects of major hull parameters, the following describes the development of the lines themselves. This description mirrors that of the larger flying boats.

#### Small Seaplanes - Forebody

As with the larger flying boat standard series, wherever practical, the hull lines may be developed from readily computable curves, to permit convenient scaling of the lines up or down. In addition, this procedure has construction advantages because it facilitates the accurate joining of component portions.

The "forebody flat" - the region in which the dead rise increases linearly with the distance forward of the step - was designed to 34.6 percent of the forebody length. This is about the same as used for the standard series of larger flying boats. It is sufficiently long to satisfy the need of planing area at the hump, and yet short enough to obtain easy buttock lines. The variation in dead-rise angle with forebody length is shown in figure 9. The dead rise at the bow of the amphibian is 45-degrees. It was not deemed necessary to make the bow dead rise as high as is customary on military flying boats since the whole forward portion of the basic forebody was lifted relatively higher above the base line. Because of the higher-placed bow sections, the basic design should be able to operate in waves of greater height.

The keel curvature, starting at the forward end of the flat, is of essentially elliptical form, as shown in figure 10.

## Hull Lines Design

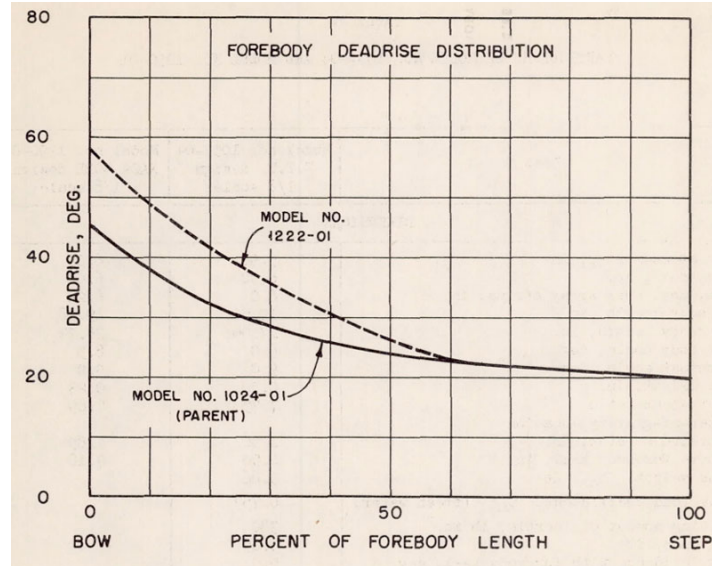


Figure 9: Forebody Deadrise Distribution (Taken from Hugli, 1951)

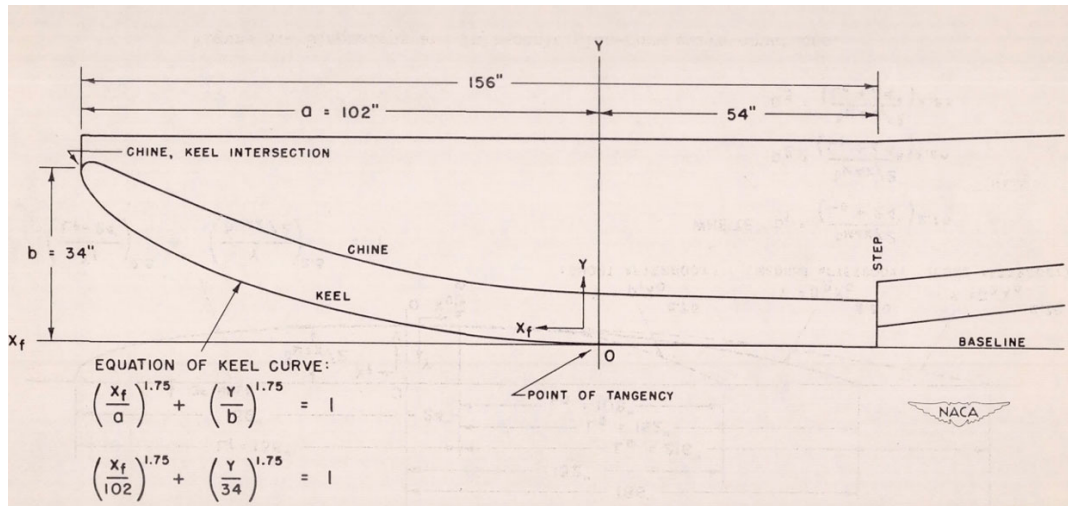


Figure 10: Forebody Keel Curve (Taken from Hugli, 1951)

### Small Seaplanes - Beam

The location of the maximum beam is the same as for the larger flying boats, and for the same reasons. The maximum beam was located 0.5 beams forward of the step. In addition to the reasons listed above, this expedient provides both a greater area forward and a greater space for the cockpit.

The plan of the forebody chine line from the bow to the maximum beam is, essentially, of elliptical form. From maximum beam to the sternpost of the afterbody, the plan form is a modified parabola, as indicated in figure 11.

## Hull Lines Design

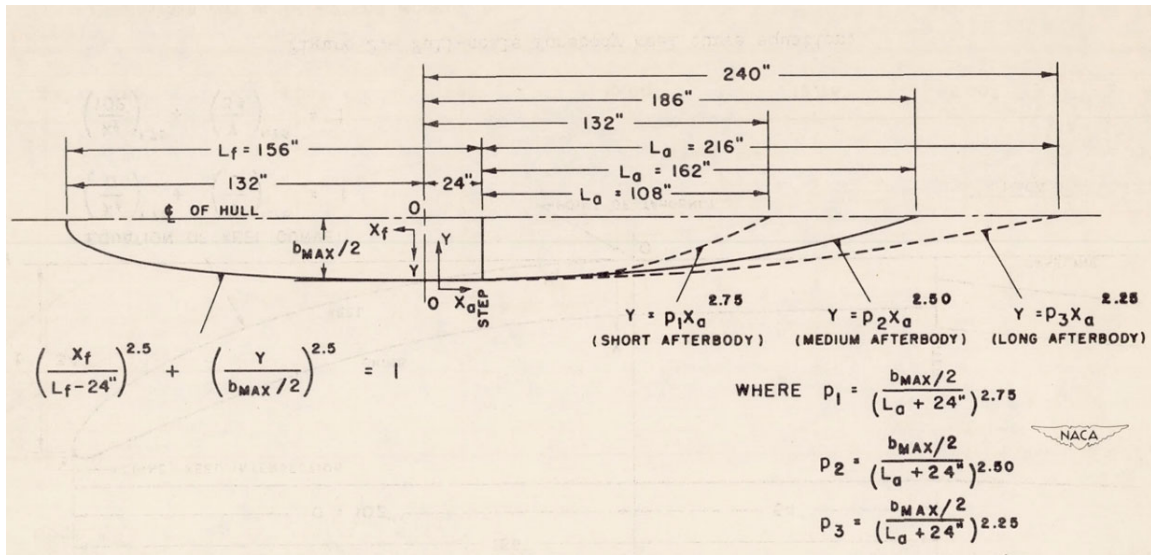


Figure 11: Plan View of Models (Taken from Hugli, 1951)

### Small Seaplanes - Main step

The depth of the step influences landing stability and resistance at high speeds. A step depth of around 8% of maximum beam was selected for the basic hull in the Amphibian series. The step height appears to be adequate when compared with the information on the influence of various hull parameters upon skipping (see Locke, 1946). A later report (Olson and Land, 1948) gives additional design information on step depth.

### Small Seaplanes - Afterbody

The dead-rise angle of the afterbody was maintained at 20-deg throughout the length of the afterbody. Tail cones were not included. Afterbody-roach profile measurements for the short afterbodies at prehump speeds were included in the test program to aid the designer. A model was tested with a warped afterbody.

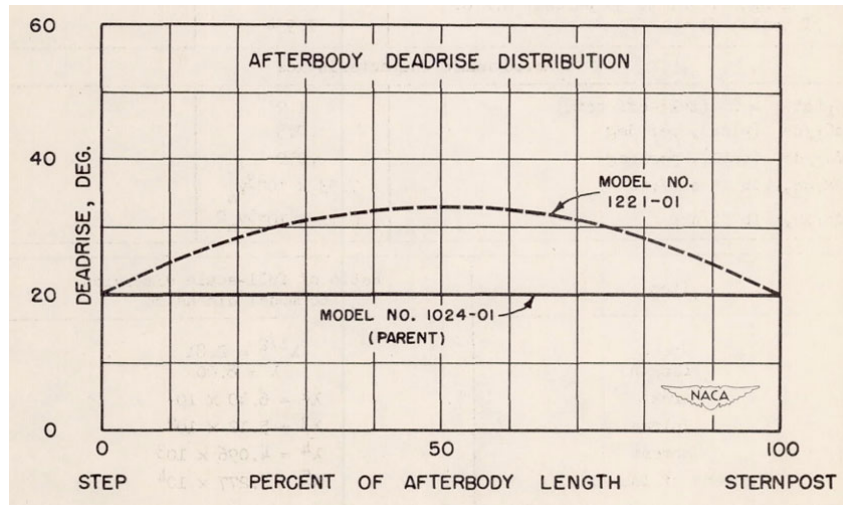


Figure 12: Afterbody Deadrise Distribution

#### Small Seaplanes - Add-Ons

As part of the standard series investigation, the effects of adding various complexities were tested.

- Vertical spray strips (Figure 13) were extremely effective at reducing the height of the main spray. These strips projected about 2% of the beam below the chine -- from the step forward -- tapering toward the bow.
- Concave forebody sections were effective in reducing spray height, but not as effective as the spray strips. There is a trade-off between the additional cost of concavity, and the aerodynamic penalty of the strips.
- Forebody warping had a fairly minimal effect.
- Warping the afterbody dead rise decreases the high-speed resistance appreciably. Warping the afterbody also enabled a reduction in step depth from 8.3% of beam to 4.2% of beam, without skipping.

The improvements from afterbody warp and concavity in the forebody were not large, and would probably not be justified since the complication of the hull lines would entail increased costs.

## Hull Lines Design

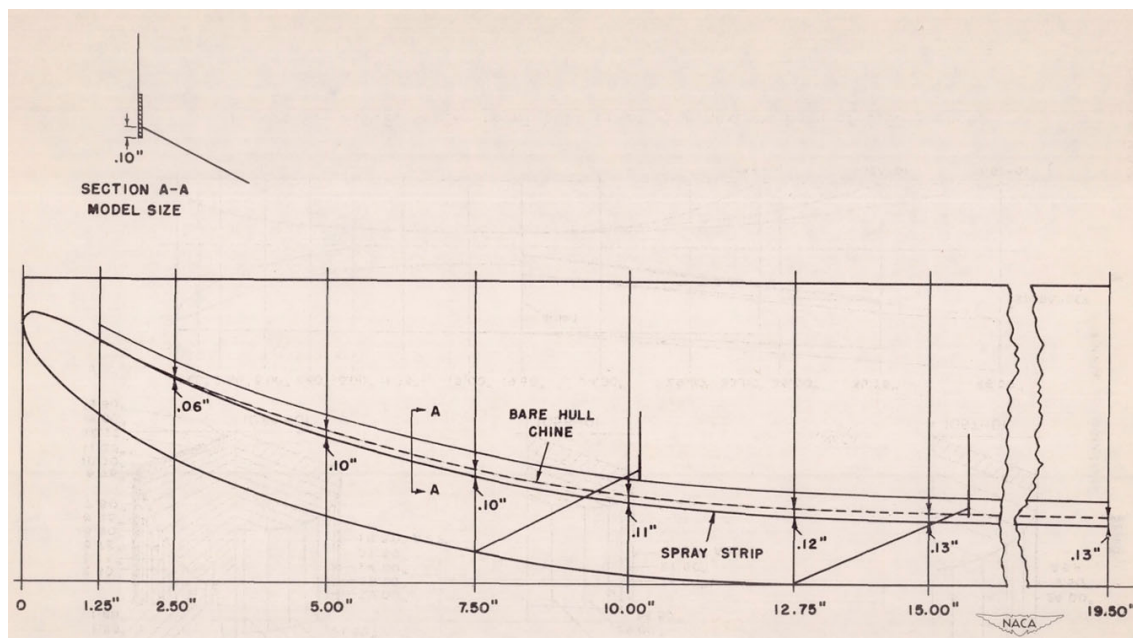


Figure 13: Vertical Chine Strips (Taken from Hugli, 1951) Note: Dimensions in Inches. Beam = 6 inches.

#### 12.4 Step Design (Daniel Savitsky, 1990)

The function of the step is to cause the flow to separate from the forebody and thus clear the afterbody to the extent possible. Thus, the resultant hydrodynamic force is located in the proximity of the center-of-gravity. The process of flow separation is associated with natural ventilation of the area above the forebody wake just aft of the step. The ventilation path is such that air flows from the chine region at the step down towards the keel and forms an air cavity between the afterbody and water surface. An average step depth of approximately 5% of the beam usually will provide sufficient natural ventilation to cause the forebody wake to separate.

The hydrodynamic consequence of the air cavity under the afterbody is to reduce afterbody wetting (and hence resistance) and to allow the forebody trim to increase in order to initiate planing action. The maximum trim angle is limited by the sternpost angle of the craft.

The traditional step design is a transverse step of constant depth. Unfortunately, the aerodynamic drag of this configuration is quite large. More recent designs employ a "faired" or vee step (Figure 14) which has a substantially smaller aerodynamic drag. In this design, the step depth is a maximum at the chine (through which natural ventilation is initiated) and can be zero at the keel. The afterbody buttock lines are faired into the forebody at the step in order to further reduce the aerodynamic drag.

An experimental study of the effect of vee-step angle on the hydrodynamic characteristics of seaplanes (Van Dyck, 1954) indicate that a 45-degree vee-step angle (measured in planform) results in optimum low-trim-angle landing stability and minimum hump resistance. These desirable characteristics are gained with no measurable sacrifices in directional and longitudinal stability.

If it is found that step depth is insufficient to cause natural ventilation of the step, so-called ventilation ducts can be built into the hull. The lower end of the duct is cut into the afterbody bottom just aft of the step and the upper end is inside the hull and open to the atmosphere. To be effective, the cross sectional area of the duct must be at least  $0.02 \times (\text{Beam Squared})$

Many times, the inclusion of ducts is a retrofit after it is found that the prototype has insufficient natural ventilation at the step. As previously described, insufficient ventilation at the step can also lead to skipping during high speed landings.

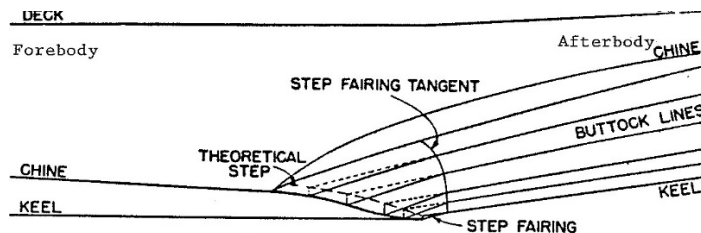


Figure 14: Faired Step

### 12.5 Chine Configuration (Daniel Savitsky, 1990)

The conventional vee-bottom planing surface, such as shown at the top of Figure 15 is not satisfactory for a seaplane hull since the spray is projected to large heights upon leaving the chine. Thus, most hulls have a chine configuration which is intended to suppress the spray and these are also illustrated in Figure 15.

The horizontal chine flare, in which the bottom is horizontal in the immediate vicinity of the chine, is the least effective in suppressing spray. This was demonstrated in the basic study of main spray presented by Savitsky and Breslin (1958) and confirmed by tests on a model of an existing seaplane hull (Locke, 1956). A chine configuration having slightly concave flare was effective in reducing the spray height. If an exaggerated reflexed chine flare is employed (Figure 15) the deflected spray will impact upon and be reflected from the level water surface to greater heights than experienced by the conventional vee-bottom. The most effective chine configuration consists of a vertical spray strip.

Unfortunately, due to structural design difficulties, the vertical chine strip may not be a practical configuration. Thus, the chine configuration with slightly concave flare is generally used in hull design.

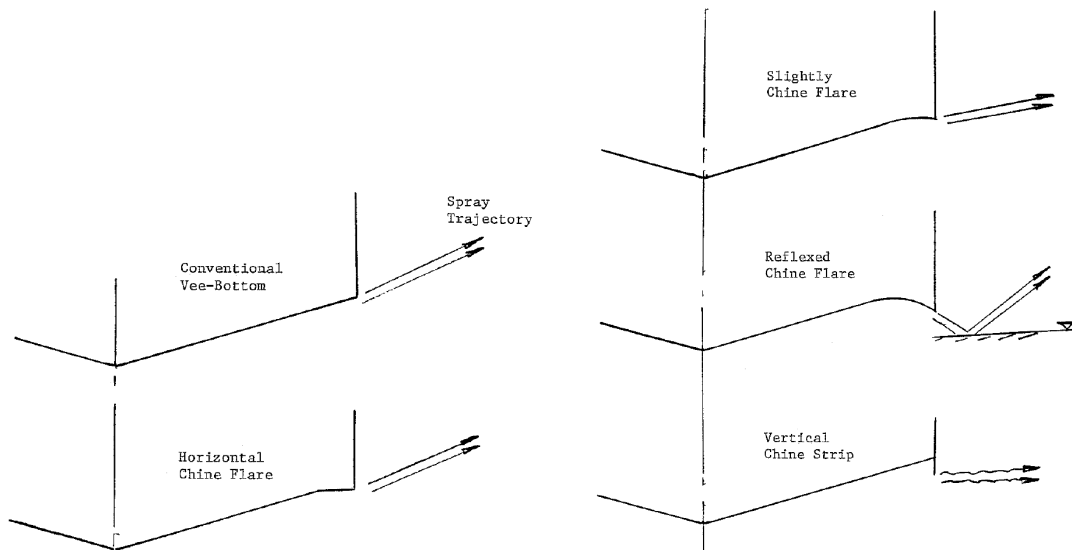


Figure 15: Influence of Various Chine Configurations

Chine Profile at Bow - "high-chine" vs "low-chine"

The more conventional chine profile used in early seaplane designs is the "high-chine" bow shown as the dashed line in Figure 16. It is seen that the chine line is pulled up sharply at the bow resulting in large, blunt, frontal areas which significantly increase the aerodynamic drag. In addition, the bow spray associated with this so-called "high chine" bow was most troublesome and required the addition of auxiliary spray strips to suppress the spray.

In the early 1950's a new 'low-chine" bow was developed which reduced the aerodynamic drag and effectively suppressed the spray. The solid line in Figure 16 shows the profile and body plan for a typical low chine bow which was incorporated into the designs of the P5M, P6M, etc. It is seen that the chine line in the bow is kept low and the chine flare is greater than for the conventional design. Flickinger (1950) demonstrated improvements in spray in the overload condition with this bow modification.

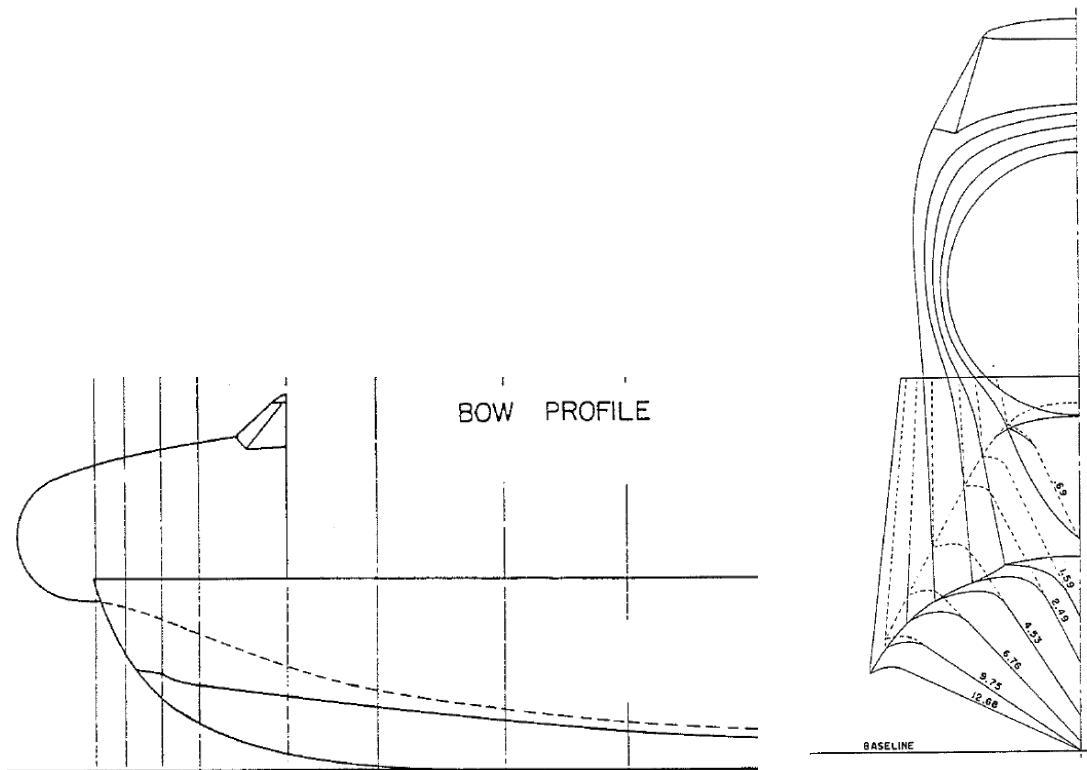


Figure 16: High-Chine Bow (dashed) vs. Low-Chine Bow (solid)



Figure 17 shows photographs of the experimental Martin XP5M-1 and the production P5M. Flickinger's (1950) low-chine bow appears to have been implemented on the production version. It's important to note that while the chine is lower, the radar enclosure or "radome" for both is in the same position, and so this low-chine bow does not mean less freeboard. It is very important that the bow be sufficiently high to prevent water from wetting the cockpit windows in a seaway.

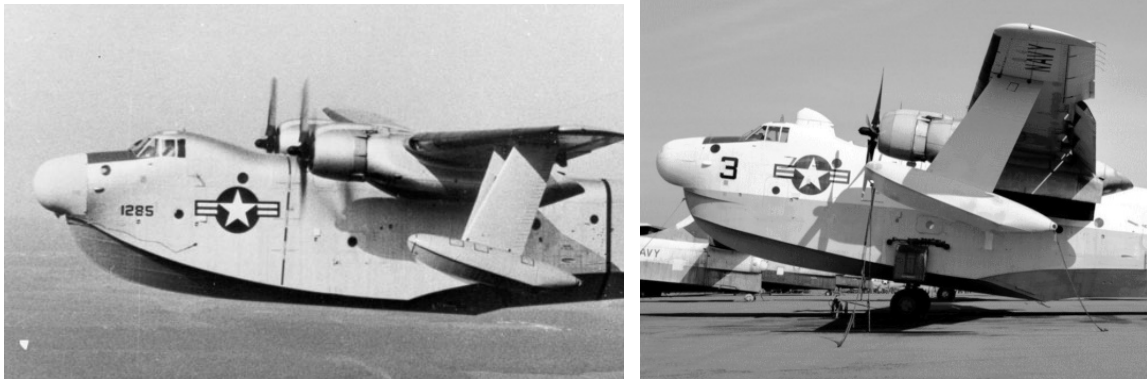


Figure 17: Experimental Martin XP5M-1 with high-chine bow (Left) and Production P5M with low-chine bow(right)

Figure 18 shows photographs of a variety of large flying boats. Many of the designs have auxiliary spray suppression.

- The Martin P5M and P6M low-chine bow is tucked under the radome
- The ShinMaywa US-2 has a radome, groove-type spray suppressors, and a horizontal brow to reduce bow spray into the windshield.
- Beriev BE-200 has large downward-angled spray suppression chine details at the bow.
- The AG600 has a large groove type spray suppressor.

## Hull Lines Design



Figure 18: Comparative Bow Geometries

### Groove-Type Spray Suppression

The "Groove-Type" or Kikuhara spray suppressor is a promising chine treatment. It has found its way onto the ShinMaywa US-2 seaplane, shown in Figure 17 and 18. This concept was developed by Kikuhara (1960) and is shown diagrammatically in Figure 19. Kikuhara describes the working principle as follows:

"The mechanism of spray generation ... suggests that there will be no blister spray if we can dispose of the high-speed water particles in the spray root before they are shot out high to form a spray sheet. If the chine is rounded (as in Figures 16) the water sticks on the surface and goes up a distance along the side wall and can easily be caught by a groove before being shot out in the air. The water will flow through the groove rearward without any spray or come out through a slit so low as to be harmless. The lid of the groove may be folded in the air to minimize the air resistance.

Figure 20 shows body plans of models tested by Van Dyck (1961) to evaluate this concept. Van Dyck's conclusions were that the groove-type suppressors reduced the spray to negligible proportions in calm water between 20 and 28 knots. However, the advantage did not extend to tests in regular and irregular waves. The modification resulted in more "dig-in" at the bow, and the development of large pitching motions. It is possible that increasing the beam forward would have alleviated this, as the lines show a significant reduction in bottom area by removing the width of the strips.

While these various contraptions may fix spray problems on designs that are too far along, it would be better to prevent them by keeping the bottom loading low enough to begin with, and recognizing that the hull will always end up overweight. Leaving a healthy margin on bottom loading protects the designer later.



Figure 18: Groove Type Spray Suppressors on ShinMaywa US2

# Hull Lines Design

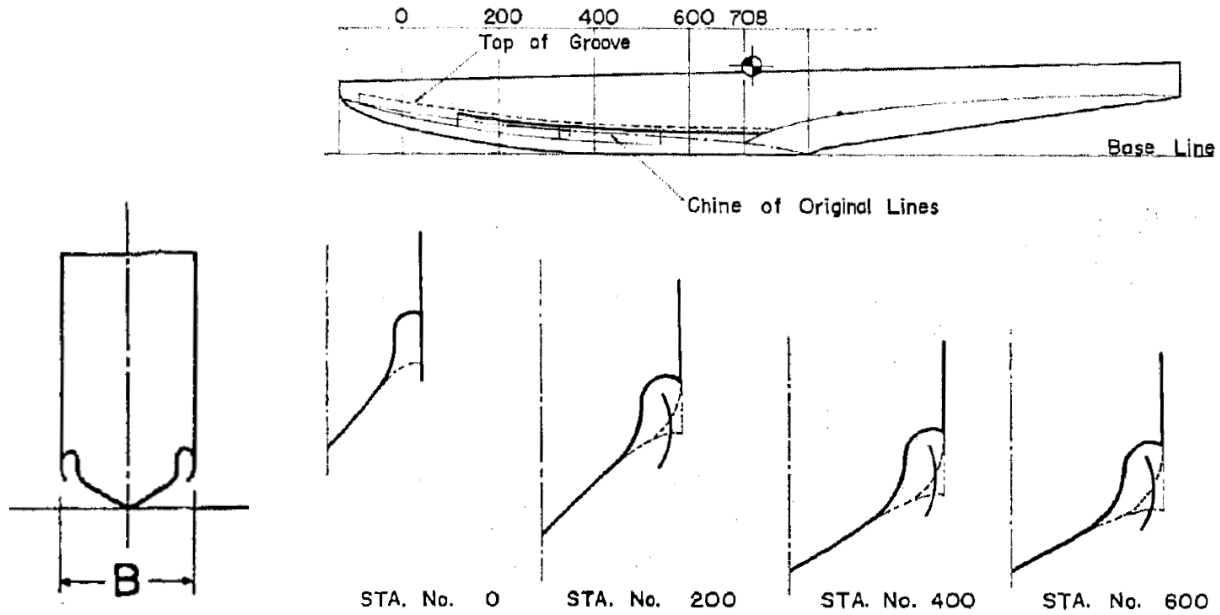


Figure 19 Diagrams of Groove Type Spray Suppressors (Taken from Kikuhara, 1960)

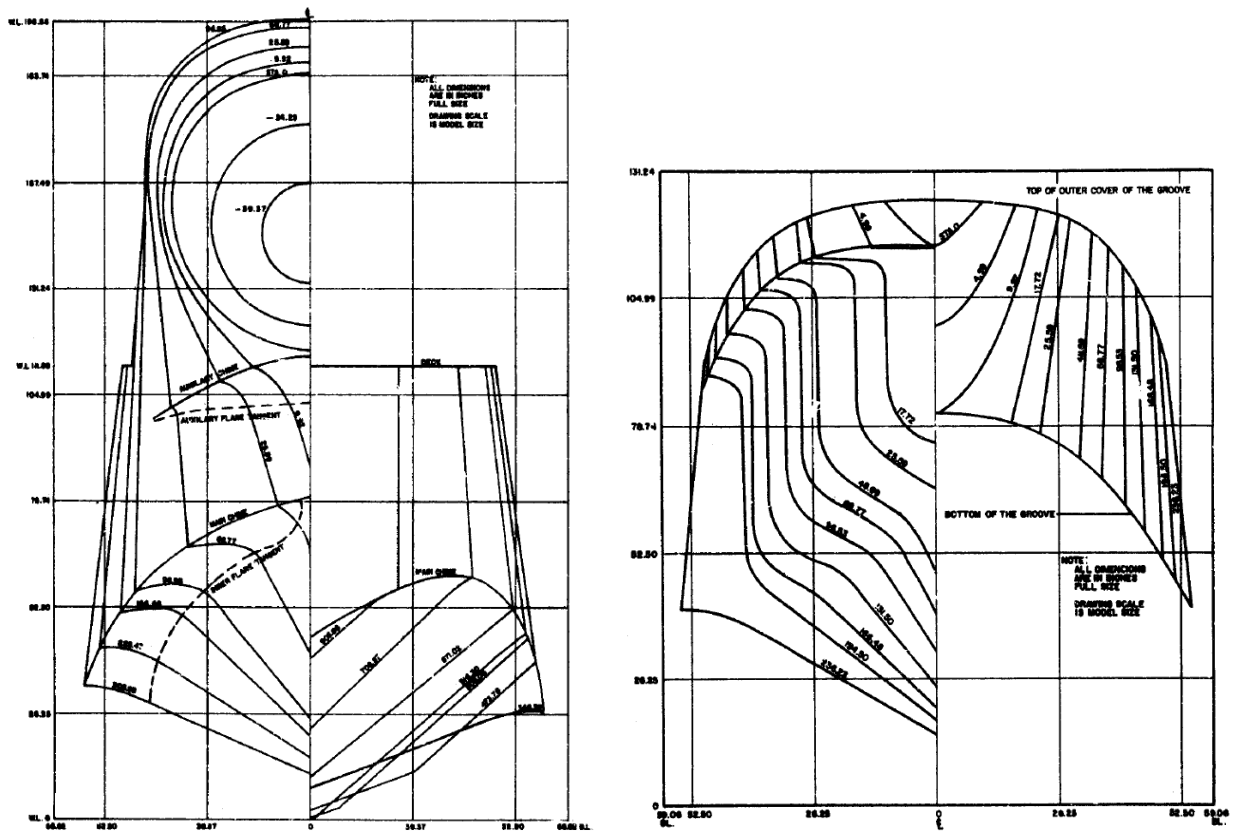


Figure 20: P5M-2 Model (Left) and Modifications for Groove-Type Spray Suppressors (Taken from Van Dyck, 1961)

## 12.6 Forebody Intermediate Chine (Daniel Savitsky, 1990)

Occasionally the transverse section through the forebody will be designed to incorporate an additional longitudinal chine located between the keel and the principal chine (Figure 21). This intermediate discontinuity in the hull bottom is sometimes referred to as the "sister-keel" and the total configuration is called a double chine hull. A majority of Edo Corporation floats incorporated a sister-keel during the 1930's and well into the 1950's.

There are several hydrodynamic advantages associated with the double chine hull. The first is, that at planing speeds, the transverse flow across the bottom separates along the sister-keel and unwets the bottom area between the sister-keel and the upper chine. This results in a reduction in hydrodynamic resistance. The second advantage follows from the fact that the effective beam decreases when the flow separates from the sister-keel. This in turn increases the effective beam loading  $C_{\Delta}$ . Landing impact accelerations decrease with increased beam loading (less bottom area per mass of hull). Hence the sister-keel hull configuration is expected to have improved seakeeping compared with the conventional vee-bottom hull.

There is also a structural advantage associated with the concave bottom curvature usually existing between the keel and sister-keel and between the upper chine and sister-keel. These curvatures enable some of the bottom load to be carried as tension forces in the bottom plating (Figure 19). Hence it is expected that the concave bottom structure will be lighter than the conventional straight bottom where the hydrodynamic loads are supported only by bending and shear forces in the plate.

A possible disadvantage with the concave hull section is that it may be more costly and time consuming to construct.

To maximize the benefit of such a configuration it is important that the upper chine location be within the cavity formed by the boundary of the flow separation from the sister-keel. As shown in Savitsky, Roper and Benen (1972), the trajectory of the free streamline representing the cavity of the separation boundary is a function of deadrise angle. Figure 20, taken from Savitsky, Roper and Benen (1972) plots the separation trajectory for various deadrise angles. It is seen that the width of the separation cavity increases with decreasing deadrise angle. If the upper chine is located outboard of this cavity boundary, the original separated flow from the sister-keel will reattach to the bottom and thus prevent complete flow separation from the sister-keel. This reattachment may preclude the attainment of some of the advantages of the sister keel. Figure 22 can thus be used as guidance in designing an effective double chine hull. This concept has been effectively applied on planing boats as well.

The trajectories shown on Figure 22 are associated with planing speeds greater than approximately 75% of the getaway speed. Thus, at lower speeds, where complete flow separation from the sister-keel is not expected, the resistance and spray characteristics are essentially the same as for a conventional vee-bottom hull. Model tests reported by Dawson (1935) have confirmed this conclusion.

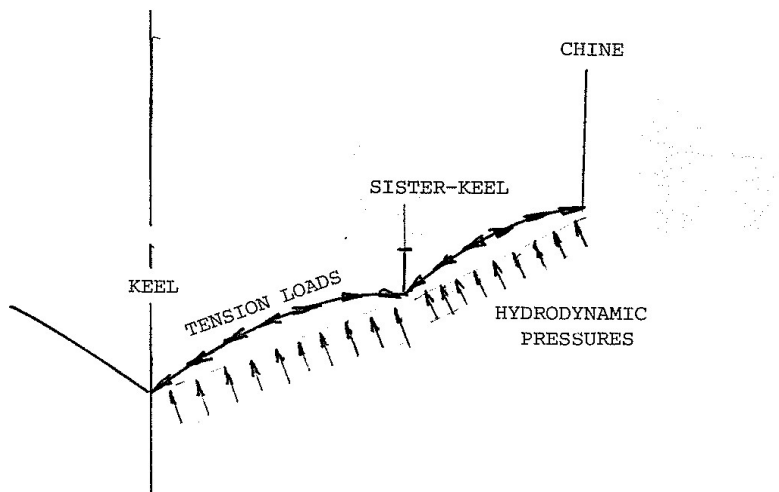


Figure 21: Double-Chine Hull with Sister-Keel

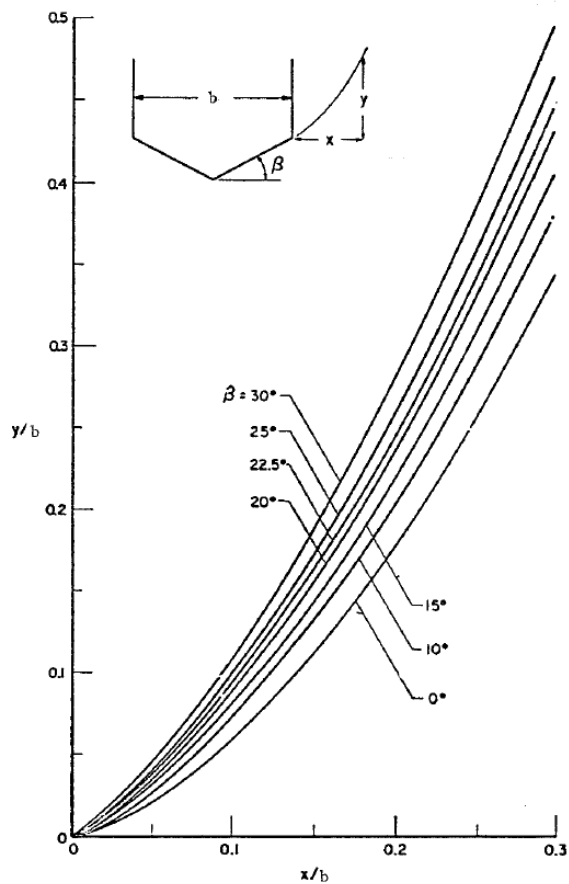


Figure 22: Shape of Free Streamline for Immersed V-Bottom

Reference for Chapter 12

Dawson, John R. "Tank Tests of a Model of a Flying Boat Hull with a Fluted Bottom", NACA TN No. 522, 1935.

Flickinger, Paul J. "Model Basin Tests of Bow Spray and Main Spray of Auxiliary Low Chine Bow Modification to XP5M-1 Hull", Davidson Laboratory, Stevens Institute of Technology, Report 403, October, 1950.

Haar, M. Effect of Forebody-Afterbody Proportions and Length-Beam Ratio on the Hydrodynamic Characteristics of a Series of Flying-Boat Hull Models. Experimental Towing Tank Report 465. Stevens Institute of Technology, Hoboken, NJ. Prepared for the Bureau of Aeronautics, Department of the Navy. October 1952.

Hugli, W.C. Jr "Data Report on the Preliminary Tank Tests of a Flying-Boat Model with a Planing-Tail Hull" Experimental Towing Tank Note No 609 September 1947

Hugli, W.C., Jr. Description of the Lines of the Proposed Flying-Boat Hull Models with Forebody Length-Beam Ratio of 4.0. Davidson Laboratory E.T.T. Technical Note No. 90. October 1948.

Hugli, W.C. and Axt, W.C. Hydrodynamic Investigation of a Series of Hull Models Suitable for Small Flying Boats and Amphibians. NACA Technical Note 2503. November, 1951.

Kikuhara, S. A Study of Spray Generated by Seaplane Hulls. Journal of the Aero/Space Sciences - June, 1960

Korvin-Kroukovsky, B.V., Savitsky, Daniel and Lehman, William F. "Wave Profile of a Vee-Planing Surface, Including Test Data on a 30-deg Deadrise Surface." Experimental Towing Tank Report No 339, April, 1949.  
Locke, F.W.S. An Analysis of the Skipping Characteristics of Some Full-Size Flying Boats. N.A.C.A. Wartime Report W-104. 1946.

Locke, F.W.S. Jr., "The Effect of Chine Flare on the Spray Characteristics of a Model of the JRF-5", Navy Department, BuAer, Research Division Report No. DR-1842. November 1956.

Olson, R.E. and Land, N.S., Effect of Afterbody Length and Keel Angle on Minimum Depth of Step for Landing Stability and on Take-Off Stability of a Flying Boat. N.A.C.A. Technical Note No. 1571. September, 1948.

Savitsky, D. and Breslin, J.P., "On the Main Spray Generated by Planing Surfaces", Davidson Laboratory, Stevens Institute of Technology Report 678, January 1958.

Savitsky, Daniel "Hydrodynamic Design of Planing Hulls" SNAME Marine Technology Vol. 1. 1964.

## Hull Lines Design

Savitsky, Daniel, Roper, John K; and Benen, Lawrence: "Hydrodynamic Development of a High Speed Planing Hull for Rough Water" , Ninth ONR Symposium on Naval Hydrodynamics. Paris, France, August 1972.

Van Dyck, R. L., "An Investigation of the Effect of Vee-Step Angle on the Hydrodynamic Characteristics of Seaplanes", Davidson Laboratory, Stevens Institute of Technology Report No. 532, April 1954.

Van Dyck, R. L. Resistance and Spray Characteristics of P5M-2 Seaplane Equipped with Groove-Type Spray Suppressors. Prepared for Bureau of Aeronautics. Davidson Laboratory Report R-815. June, 1961.





## Tip Floats

### CHAPTER 13. TIP FLOATS

#### 13.1 Float Design Criteria

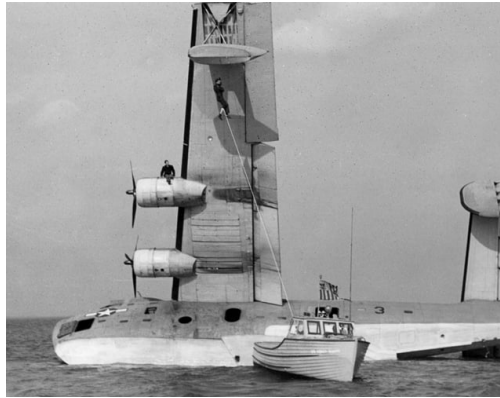
#### 13.2 Model Tests from Actual Designs

#### 13.3 Tip Float Design for Standard Series

#### 13.4 Steps for Floats

#### 13.5 Standard Series Findings

#### 13.6 Tip Float Position



Consolidated PBX Coronado After Losing Tip Float

The primary purpose of the tip float is to provide the required amount of static buoyancy at zero speed to maintain stability of the seaplane, meeting whatever stability criteria must be applied. From a hydrodynamic standpoint, it would appear that a float with a length-to-beam ratio of 5-7, high deadrise and heavy flare at the bow, a 25 to 35-degree deadrise farther aft, and including a small step, is the best compromise for operational requirements, aerodynamic resistance, and hydrodynamic lift at speed. Recommended float body plans are provided in Figures 5 and 6 of this chapter. The following discussion provides some evidence for the above recommendations.

### 13.1 Float Design Criteria (Van Dyck, 1952)

Some of the generally accepted criteria for wing-tip float design are: (1) a long, gradual bow or forebody surface for good spray characteristics, (2) a tapered stern for low air resistance, (3) chine lines high and wide near the bow and as nearly as possible in line with cruising air flow for low drag, and (4) a sufficiently low deadrise to provide good planing lift but not to exceed structural limitations.

Although wing-tip float design is based on buoyant lift, existing floats compared on a basis of equal displacement produce different dynamic lifts and show different stability characteristics under equivalent conditions of trim, load, and speed.

Length-beam ratios of 3 to 7 and deadrise angles of 15-degrees to 35-degrees near the stern cover the variations currently encountered or generally considered practical in tip float design.

### 13.2 Model Tests from Actual Designs (Morabito, 2024)

Marcinek (1951) tested models of 6 tip floats from actual seaplanes that were in service to identify those with the best dynamic lift. These were tested at various drafts, trim angles and speeds. Floats were all compared on the basis of total lift divided by the initial static displacement, and tested at various drafts. Table 1 shows a description of each float and Figure 1 shows a comparison of all the floats tested. The floats from PBM-3 and the XP5Y-1 had the best lift characteristics, as shown in Figure 2. There should be a linear increase in lift with draft. Large discontinuities represent a loss of dynamic lift.

Marcinek found that in the displacement regime, the lift was primarily a function of the submerged volume. He found that it was imperative that the bow be made to deflect the flow laterally from the float, otherwise the result is excess flow over the bow with consequent loss of lift, and in some cases vertical oscillations. For efficient deflection, the bow should have a small entrance angle in profile, steep deadrise, and an excessive chine flare. Stern taper may result in some loss of lift, but the advantage of lower aerodynamic drag might outweigh this loss.

# Tip Floats

Table 1: Float Characteristics (Taken from Marcinek, 1951)

| Model   | Hull Form                                       | After Section                                  | Type of Step      | Crown |
|---------|---|--|-------------------|-------|
| XP5Y-1  | Straight V-bottom with large chine flare at bow | Fine stern taper                               | None              | Round |
| PB2Y-3  | Straight V-bottom with slight chine flare       | Sharp stern taper                              | None              | Flat  |
| JRM-1   | Concave V-bottom                                | Fine-taper, straight warped V-bottom afterbody | Transverse        | Round |
| XJR2F-1 | Slightly convex V-bottom                        | Sharp stern taper                              | Faired Transverse | Round |
| PBM-3   | Straight V-bottom with chine flare              | Blunt stern-cone                               | Transverse        | Round |
| J4F-2   | Straight V-bottom                               | Sharp stern taper                              | None              | Round |

# Tip Floats

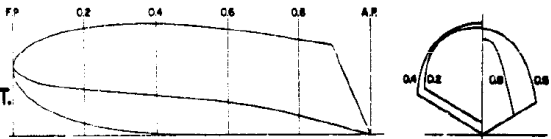

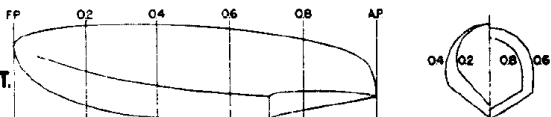

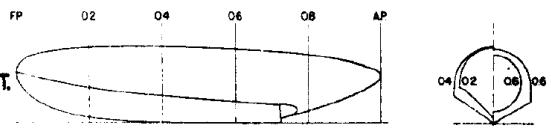

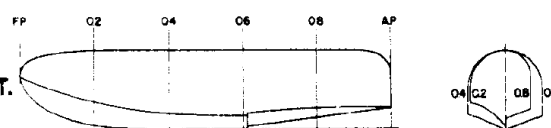

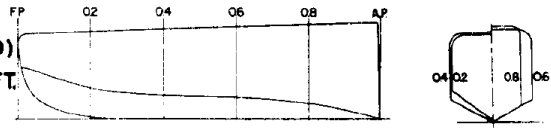

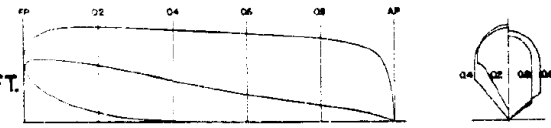

|   |  |
|---|--|
| <p>MODEL J4F-2<br/> BEAM 5.00 IN.<br/> LENGTH 14.48 IN.<br/> HEIGHT 4.31 IN.<br/> SUBMERGED VOL..077 CU.FT.<br/> TESTED AT E.T.T. TANK 1</p>                |  <p>Grumman Goose</p>           |
| <p>MODEL XJR2F-1<br/> BEAM 5.12 IN.<br/> LENGTH 21.17 IN.<br/> HEIGHT 5.39 IN.<br/> SUBMERGED VOL. .154 CU.FT.<br/> TESTED AT E.T.T. TANK 1</p>             |  <p>Grumman Albatross</p>       |
| <p>MODEL PBM-3<br/> BEAM 5.00 IN.<br/> LENGTH 23.41 IN.<br/> HEIGHT 4.73 IN.<br/> SUBMERGED VOL. .152 CU.FT.<br/> TESTED AT E.T.T. TANK 1</p>               |  <p>Martin Mariner</p>          |
| <p>MODEL JRM-1<br/> BEAM 4.68 IN.<br/> LENGTH 23.46 IN.<br/> HEIGHT 4.84 IN.<br/> SUBMERGED VOL. .172 CU.FT.<br/> TESTED AT E.T.T. TANK 1</p>             |  <p>Martin Mars</p>            |
| <p>MODEL PB2Y-3<br/> BEAM 5.10 IN.<br/> LENGTH 21.03 IN.<br/> HEIGHT 5.51 IN.(AFT END)<br/> SUBMERGED VOL. .216 CU. FT.<br/> TESTED AT E.T.T. TANK 1</p>  |  <p>Consolidated Coronado</p> |
| <p>MODEL XP5Y-1<br/> BEAM 5.00 IN.<br/> LENGTH 27.70 IN.<br/> HEIGHT 6.81 IN.<br/> SUBMERGED VOL..267 CU. FT.<br/> TESTED AT E.T.T. TANK 1</p>            |  <p>Convair Tradewind</p>     |

Figure 1: Comparison of Floats (Adapted from Marcinek, 1951)

# Tip Floats

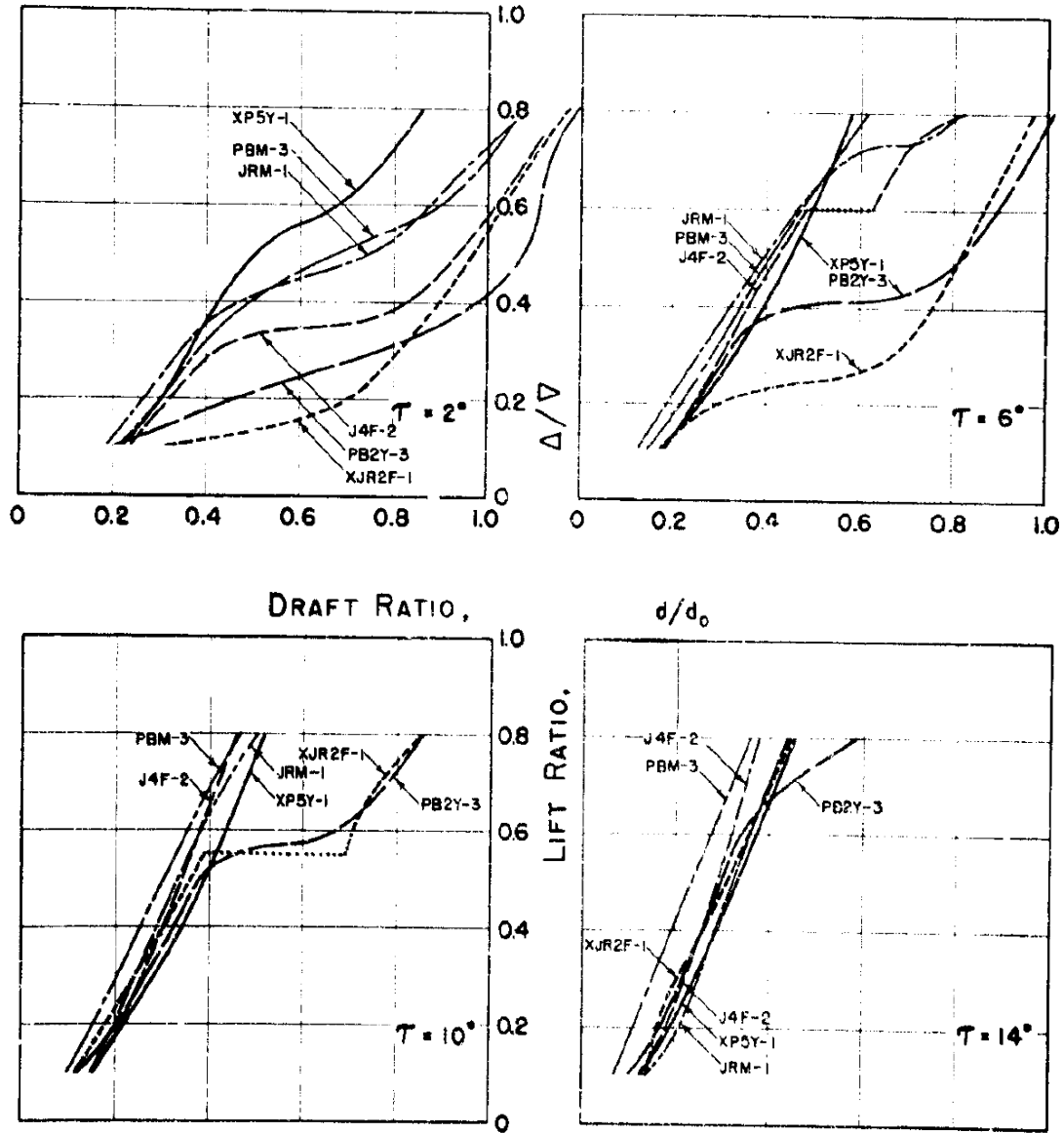


Figure 2: High-Speed Lift Characteristics of Six Tip Floats (Taken from Marcinek, 1951)

Figure Notes: The "Draft ratio" is draft divided by maximum submerged draft. Lift ratio is lift divided by the initial static buoyancy at full immersion. In the static condition Lift Ratio = 1.0 at Draft Ratio = 1.0. This graph applies to the highest speed tested, Volumetric Froude Number based on total enclosed volume of the float

$$K_V = \frac{V}{\sqrt{gV^{1/3}}} = 3.0$$

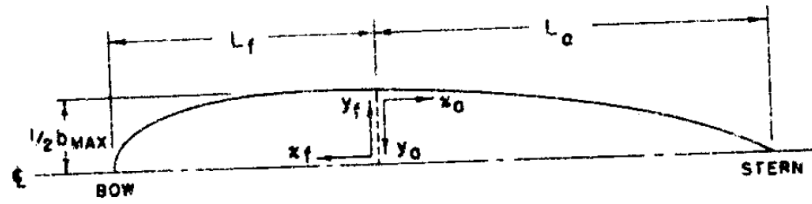
13.3 Tip Float Design for Standard Series (Van Dyck, 1952)

Based on the results of Marcinek's tests, and the list of desirable features for tip floats, a parent float was designed with a length-beam ratio of 5 and deadrise angle of 25-degrees near the stern. The rest of the family was comprised of four modifications to the parent float - two with the same cross sections but with the parent station distances reduced or increased, and two with a length-beam ratio of 5 but deadrise angles of 15 and 35 degrees.

The planform curve for the parent float (Figure 3) was derived using the equations from Hugli and Axt (1951), discussed in the chapter on hull lines design. The upper surface or deck of the float was generated by rotating the planform about its centerline.

To provide a bow with small entrance angle, steep deadrise, and extensive chine flare indicated desirable by Marcinek (1951), a deadrise distribution based on 90-degrees at the bow was plotted for the three variations of deadrise (See Figure 4). This distribution was arranged to provide the same bow lines for the first 10% of the length of all five floats in the family. The chines were designed as to provide approximately equal flare, with extensive flare at the bow diminishing to no flare near the stern. The keel profile was based on the lines of the Consolidated XP5Y-1 and Martin PBM-3 tip floats, which were shown by Marcinek to have good lift characteristics.

# Tip Floats



PARENT FLOAT:

$$L_o = 15.00 \text{ IN.}$$

$$L_f = 10.00 \text{ IN.}$$

$$1/2 b_{MAX} = 2.50 \text{ IN.}$$

$$\left(\frac{x_f}{L_f}\right)^{2.5} + \left(\frac{y_f}{1/2 b_{MAX}}\right)^{2.5} = 1 \quad y_o = \rho x_o^{2.75} \quad \text{WHERE: } \rho = \frac{2.50}{(10.00)^{2.75}}$$

$$\left(\frac{x_f}{10.00}\right)^{2.5} + \left(\frac{y_f}{2.50}\right)^{2.5} = 1 \quad y_o = (0.001458) x_o^{2.75}$$

Figure 3: Planform of L/B = 5 Float

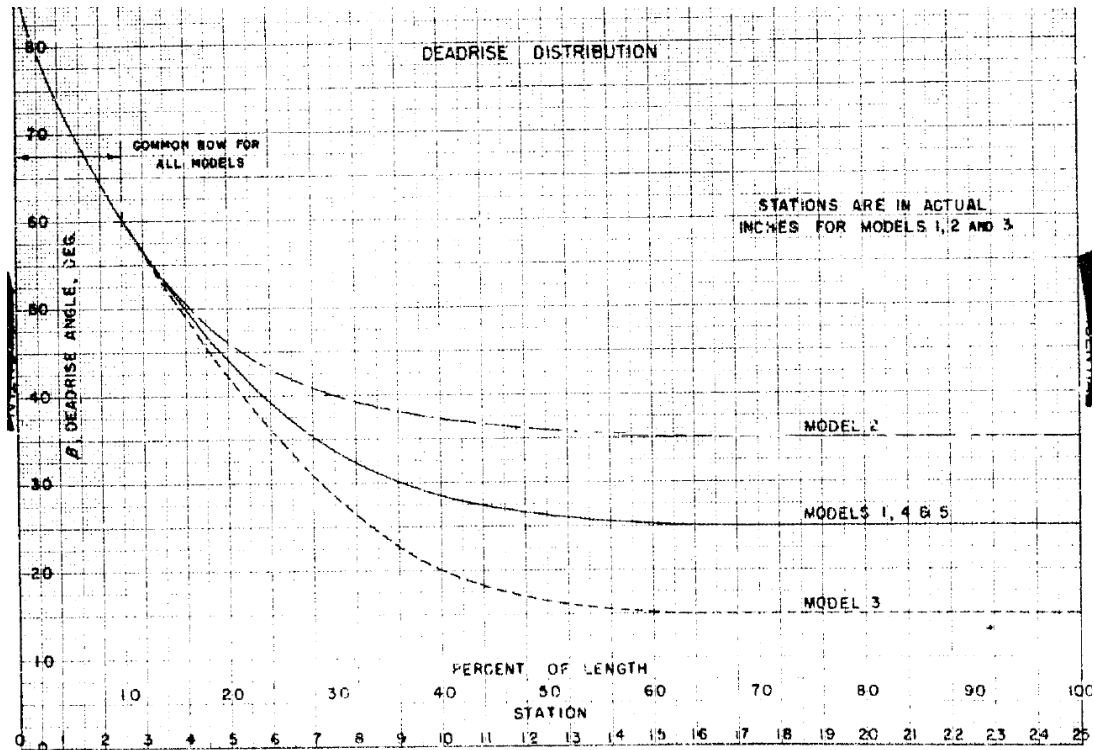


Figure 4: Deadrise Distribution of Tip Float Series



### 13.4 Steps for Floats

Unlike the hull, where the step is needed to allow the hull to rotate to an adequate take-off trim angle, the float does not need a step. Some do, while others don't.

Marcinek (1951) showed that the step was of minor importance, so no step was included in most of Van Dyck's (1952) float series. Some benefits of a step may be found in lower hydrodynamic resistance and burying tendency under rearward-drift conditions. Specifically, Richardson (1942) emphasized in letters to the NACA that the behavior of a tip float in drifting is of special importance in the event of a forced landing. His experience in "sailing" a disabled flying boat, the NC-3, for a distance of about 200 miles in the Atlantic Ocean led to the conclusion that satisfactory seaworthiness requires the tip float to be free of any tendency to "dig in" when making sternway. It appears that the inclusion of the step and the raised afterbody angle can improve rearward drift.

Van Dyck (1955) did a limited series of tests on a float with 45-degree Vee step, with its centroid located at 70% of the length, with a depth of 2% of beam and a sternpost angle of 10-degrees. The observed flow patterns indicated that a step may decrease the undesirable suction on a float under rearward drift conditions.

13.5 Standard Series Findings (Van Dyck, 1952)

The standard series floats were comparable to the XP5Y-1 float tested by Marcinek. Essentially three conditions of flow exist with respect to the bow: (1) bow clean - small blisters or spray sheets straight out to the sides; (2) bow wet - a smooth sheet of water over the bow and part or all of the float deck; (3) flow at the bow - sheets or spray breaking straight up and back from the bow. These three types of flow are evidenced to a greater or lesser degree at all speed coefficients depending on the critical trim-load combinations.

When the water is deflected upward at the bow instead of passing under or to the sides of the float, sudden changes of lift occur. As trim angle is increased, the critical draft also increases, which is a result of the bow entering the water.

Vertical oscillations occur when the flow is near the bow. The length-to-beam ratio appears to play an important part in the amplitude of vertical oscillations. Apparently, the higher length-beam ratio floats damp out the oscillations, whereas the lowest length-beam ratio float remains unstable even at low speeds.

In the planing range, the lower length-beam ratios produce greater lifts, provided the bow is clean. The varying rates of stern taper probably are the major factors causing this lift increase. Once the bow is wet, the lift variation with length-beam ratio is reversed, and the higher length-to-beam produces greater lift.

Within the range of configurations tested, a float with a length-beam ratio from 5 to 7 and deadrise angle of 35-degrees appears to possess the best resistance and aerodynamic drag characteristics. Body plans of the 25-degree, 35-degree and stepped float are shown in Figures 5 and 6.

# Tip Floats

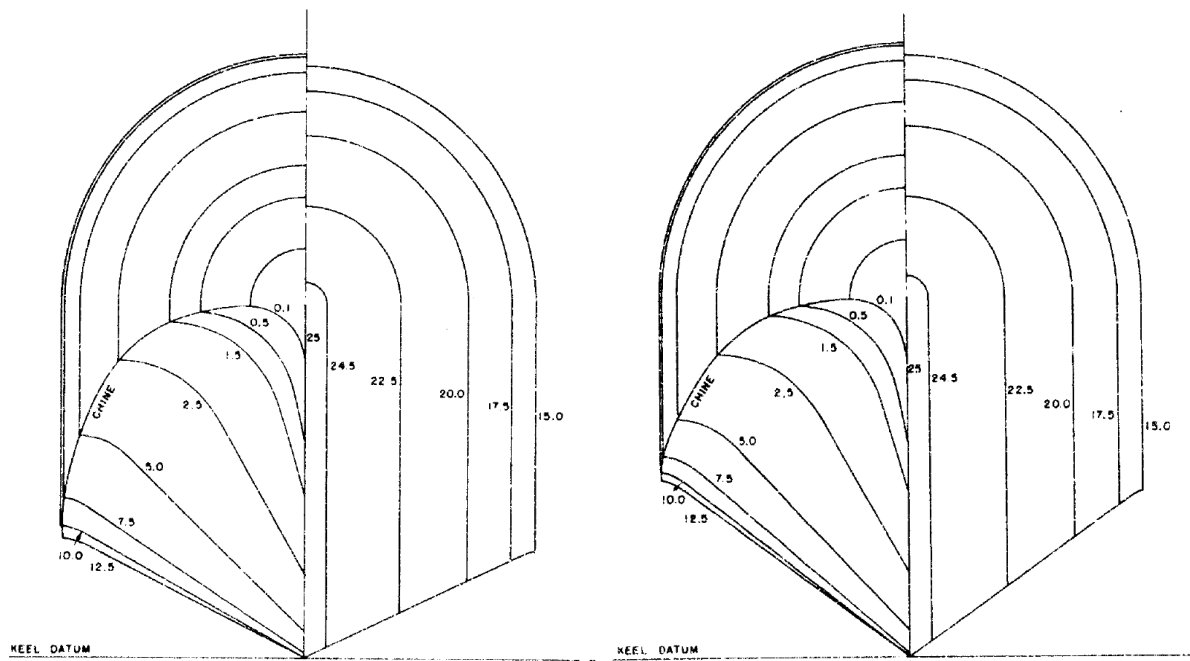


Figure 5: Recommended geometry for 25-degree and 35-degree Floats (Taken from Van Dyck, 1955)

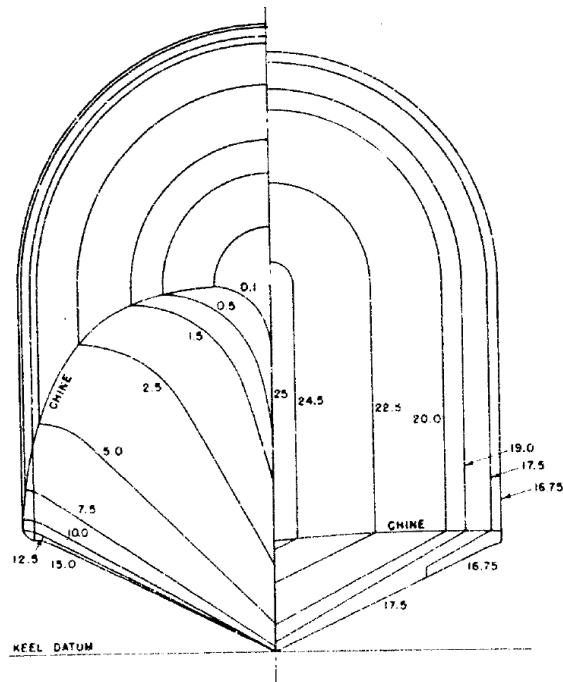


Figure 6: 25-Degree Float with 1 Step to Improve Rearward Drift (Taken from Van Dyck, 1955)

### 13.6 Tip Float Placement

The equations for required tip float volume (given in Chapter 2 - Buoyancy) show a decided advantage to floats that are more outboard. Generally, they are placed vertically very close to the water surface. The seaplane rises at planing speeds, and so they are out of the water at high speeds anyway. It would appear that the general guidelines are for floats to be positioned within a few inches of the water surface, above or below, or designed to touch the water at about 1-degree heel. This is based on Diehl's Engineering Aerodynamics (1936), Korvin-Kroukovsky's chapter on Buoyancy in these notes, and Nelson's (1934) book on seaplane design.

### References for Chapter 13

Dawson, J.R. and Hartman, S.P., "Hydrodynamic and Aerodynamic tests of Four Models of Outboard Floats," NACA TN 678, December 1938.

Diehl, W.S. Engineering Aerodynamics. Revised Edition. David W. Taylor Naval Ship Research and Development Center. Bethesda, Maryland. 2<sup>nd</sup> Edition 1936. Reprint 1986.

Hugli, W.C. Jr, and Axt, W.C. "Hydrodynamic Investigation of a Series of Hull Models Suitable for Small Flying Boats and Amphibians." NACA TN 2503. November 1951.

Marcinek, J. "Dynamic Lift Characteristics of Six Wing-Tip Floats." Experimental Towing Tank Report No. 371. September 1951.

Nelson, W. "Seaplane Design." First Edition. McGraw-Hill Book Company, inc. New York. 1934.

Richardson, Holden G., Beall, Wellwood E., and Manly, Charles W. "Flying Boats" National Aeronautics Council, Inc. New York. 1942.



## High L/B Prediction Summary

### CHAPTER 14. PREDICTION SUMMARY FOR HIGH L/B "MODERN" FLYING BOATS

(Daniel Savitsky and Jack Roper, 1990)

- 14.1 Trim Limits of Stability (Porpoising)
- 14.2 Spray Characteristics
- 14.3 Hydrodynamic Resistance (Post Hump Speeds):
- 14.4 Hydrodynamic Resistance (Hump Speed):
- 14.5 Aerodynamic Lift and Drag
- 14.6 Landing Impact Accelerations
- 14.7 Illustrative Example

The following is a straightforward and comprehensive prediction method for high L/B "modern" flying boats. (Figure 1) It is based on experimental test data on a proven hull, combined with scaling methods established by standard series tests. The summary graphs herein are applicable to hulls which are characterized by:

- high length-beam ratio
- high beam loading
- low chine bow
- extended afterbody
- faired step

The methodology could be repeated for other parent hulls to achieve similar effect.

## High L/B Prediction Summary



USA's Martin P6M Seamaster  
(Navy Photo)



Russia's Beriev Be-200  
(Dmitriy Pichugin)



China's AVIC AG600 (AVIC)

Figure 1 Examples of Modern High L/B Transport Aircraft

## High L/B Prediction Summary

The baseline design is the M-270 seaplane. This was an experimental aircraft that was near the high point of seaplane development in the United States. The results of this example are applicable to long-range transport aircraft; however, the methodology could be used for other parent hulls. The body plan is shown in Figure 2, photographs of the towing model at Stevens in Figure 3, and photographs of the flying prototype in Figure 4. It has a length-beam ratio of 15, a long afterbody, a low chine bow and a step fairing. The model test results are given by Flickinger (1951). These model test results have been verified by full scale flight tests of the M-270 seaplane (Glenn L. Martin, 1953).

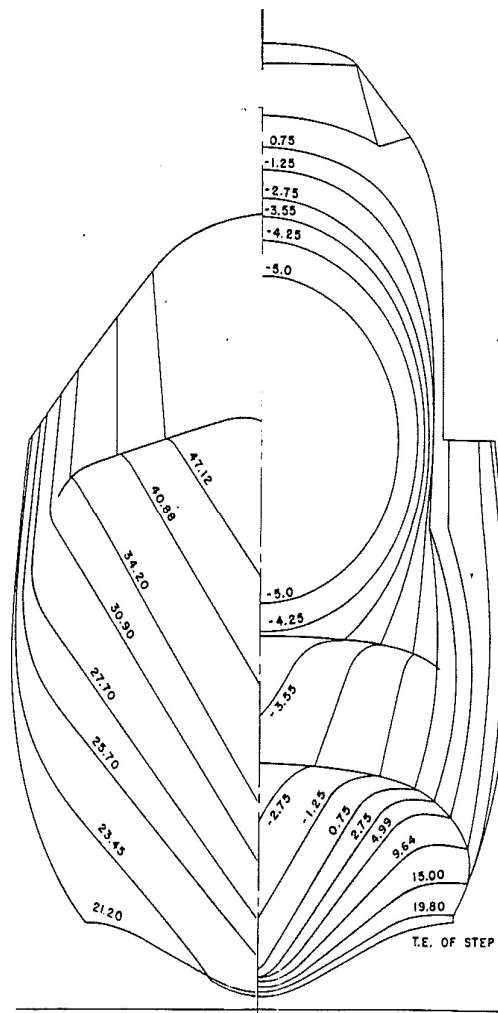


Figure 2: Martin M-270 L/B = 15 "Parent Hull" For this Chapter



# High L/B Prediction Summary

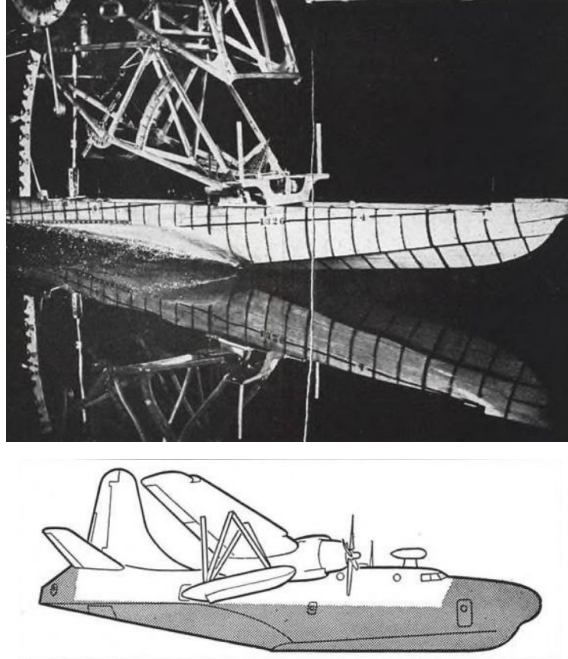


Figure 3: Martin M-270 Towing Model and Sketch of Areas Different from XP5M-1  
(Aviation Week, 1952)

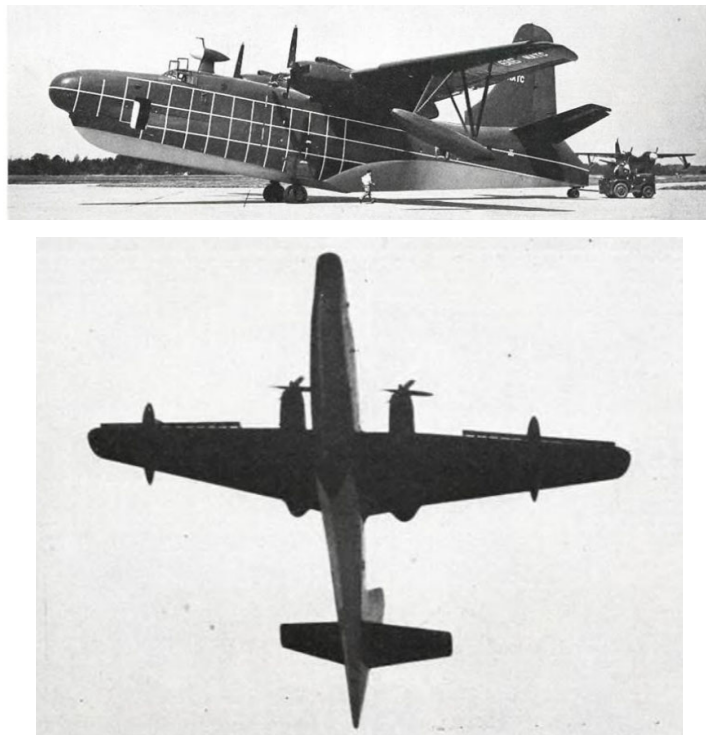


Figure 4: Photographs of Martin M-270 (Taken from Aviation Week, 1952)

14.1 Trim Limits of Stability (Porpoising)

The phenomenon of porpoising has been described earlier. It was stated that upper limit porpoising is mainly associated with afterbody Interaction with the forebody wake and that the lower limit depends mainly on forebody lines in the vicinity of the step. Both limits are dependent upon the load on the water and speed. These correlations are documented by the systematic model experiments described by Davidson and Locke (1943) which investigated factors that might influence porpoising and defined their relative importance. Studies were made for a wide range of values of each of a number of geometric and operational variables treated independently. The major conclusions of Davidson and Locke (1943) are summarized below:

1. The stability limits for a given hull under various loading and aerodynamic conditions are determined primarily by the load on the water at a given speed. This is expressed in terms of a lift coefficient:

$$\sqrt{2 C_L} = \sqrt{C_\Delta} / C_V$$

where:

$$C_\Delta = \Delta / w b^3$$

$$C_V = V / \sqrt{g b}$$

b = beam

w = water density

$\Delta$  = load on water at a given speed

$$C_L = \Delta / \frac{\rho}{2} V^2 b^2$$

This same coefficient has also been found to collapse, onto a single curve, the porpoising limits for prismatic planing hulls of constant deadrise.

2. Increasing the aerodynamic tail damping rate lowers the lower limit at high speed. The magnitude of the effect is greatest, however, at tail damping rates considerably below normal.

3. Forebody geometry effects primarily the lower limit particularly at post hump speed. The most powerful forebody variable is the amount of warping

of the bottom just ahead of the step. Increasing the warping lowers the lower limit at high speeds. Forebody length has negligible effect on the limits.

4. It was found that a forebody deadrise angle (at the step) of 20-deg appears to be optimum. Increasing deadrise angle raises the lower limit to the point where there may be only a small stable gap between upper and lower limit at take-off. Decreasing the deadrise angle causes the upper and lower limits to approach convergence just after hump speed. Thus it may be impossible for a low deadrise hull (approximately 10-deg or less) to take-off without passing through a region of instability.

5. Increasing the stern-post angle increases the upper limit significantly and vice-versa. As previously explained, upper limit porpoising is primarily a consequence of afterbody interaction with the forebody wake.

The effect of many other variables on the porpoising limits were also investigated by Davidson and Locke (1943). These included variations in moment of inertia; LCG position; wing lift rate; vertical velocity; aerodynamic damping; step height; etc. Nearly all had only a small effect on the porpoising limits. Thus, for the purpose of developing a simplified, first order, predictive technique, it may be assumed that the porpoising limits are primarily dependent upon the following three major parameters:

- 1)  $\sqrt{2 C_L} = \sqrt{\text{Lift Coefficient}}: \sqrt{C_\Delta}/C_V$
- 2)  $w^I$  = Forebody warp: degrees per beam forward of step.
- 3)  $\sigma$  = Sternpost angle

For the following example, the basic relations between stability limits and  $\sqrt{C_\Delta}/C_V$  were obtained from towing tank tests of model 1364-05 (Flickinger, 1951). This is the M-270 hull which has a step deadrise angle of 20-deg, a forebody warp of 6-deg/beam forward of the step; and a sternpost angle of 9-deg.

## High L/B Prediction Summary

The porpoising limits for this hull are shown on Figure 5, taken from Flickinger (1951). This is the baseline curve from which predictions will be made for hulls having different forebody warp and sternpost angles. The effect of warp and sternpost angle is obtained from the studies of Davidson and Locke (1943) and Locke (1942).

It is assumed that for the candidate design, the forebody deadrise angle at the step is approximately 20-deg since this appears to be the optimum value to attain the widest stability limits. It is further assumed that the aerodynamic pitch damping has a normal value consistent with flight requirements.

### Lower Limit at Low Speed ( $\tau_1$ ):

$$\tau_1 = \tau_{01} - (w^1 - w_o^1) \frac{dr}{dw^1}$$

where:

$\tau_1$  = Lower limit of candidate

$\tau_{01}$  = Lower limit of baseline configuration  
=  $f(C_{\Delta}^{1/2}/C_V)$  Figure 32

$w^1$  = Forebody warp of candidate = degrees/beam

$w_o^1$  = Forebody warp of baseline configuration

$\frac{dr}{dw^1}$  = Change in lower limit with respect to  
forebody warp = 0.25 deg/deg/beam

### Lower Limit at Low Speed ( $\tau_2$ ):

As shown in Davidson and Locke (1943), the lower limit at low speed (in the hump speed regime) is primarily dependent upon the sternpost angle and increases directly with increase in sternpost angle. Thus:

$$\tau_2 = \tau_{02} + (\sigma - \sigma_o) \frac{dr}{d\sigma}$$

where:

$\tau_2$  = Lower limit of candidate

$\tau_{02}$  = Lower limit of baseline hull = 8.5°  
(Figure 32)

## High L/B Prediction Summary

$$\begin{aligned}\sigma_o &= \text{Sternpost angle of baseline hull} = 9^\circ \\ \frac{d\tau}{d\sigma} &= \text{Change in low speed lower limit with} \\ &\quad \text{respect to change in sternpost angle} \\ &= 1.00 \text{ deg/deg (Reference 25)}\end{aligned}$$

### Upper Limit at High Speed ( $\tau_3$ ):

As shown in Davidson and Locke (1943), the upper limit at high speed increases directly with sternpost angle. Thus:

$$\tau_3 = \tau_{03} + (\sigma - \sigma_o) \frac{d\tau}{d\sigma}$$

where:

$$\begin{aligned}\tau_3 &= \text{Upper limit of candidate} \\ \tau_{03} &= \text{Upper limit of baseline hull} \\ &= f(C_\Delta^{1/2}/C_V) \text{ as shown in Figure 32} \\ \sigma &= \text{Sternpost angle of candidate} \\ \sigma_o &= \text{Sternpost angle of baseline hull} = 9^\circ \\ \frac{d\tau}{d\sigma} &= \text{Change in high speed upper limit with} \\ &\quad \text{respect to change in sternpost angle} \\ &= 1.00 \text{ deg/deg (Reference 25)}\end{aligned}$$

### Upper Limit Cutoff at High Speed:

There are values of  $\sqrt{C_\Delta}/C_V$  above which the upper limit no longer exists. For example, in Figure 5 there is no upper limit porpoising for values of  $\sqrt{C_\Delta}/C_V$  greater than 0.15. The results of Davidson and Locke (1943) can be used to show that the limiting values of  $\sqrt{C_\Delta}/C_V$  increases with increasing sternpost angle. Thus:

# High L/B Prediction Summary

$$m = m_o + (\sigma + \sigma_o) \frac{dm}{d\sigma}$$

where:

$$m = (C_{\Delta}^{1/2}/C_V) \text{ at upper limit cutoff of candidate}$$

$$m_o = (C_{\Delta}^{1/2}/C_V) \text{ at upper limit cutoff of baseline hull} = 0.15 \text{ (Figure 32)}$$

$$\sigma = \text{Sternpost angle of candidate}$$

$$\sigma_o = \text{Sternpost angle of baseline hull} = 9^\circ$$

$$\frac{dm}{d\sigma} = \text{change in cutoff with respect to change in sternpost angle} = .01/\text{deg (Reference 25)}$$

All the above equations have been plotted on Figure 6 using warp and sternpost angle as parameters. This simple chart can be used to estimate the porpoising limits of modern high length-beam ratio hulls. A subsequent section of this chapter will illustrate its use.

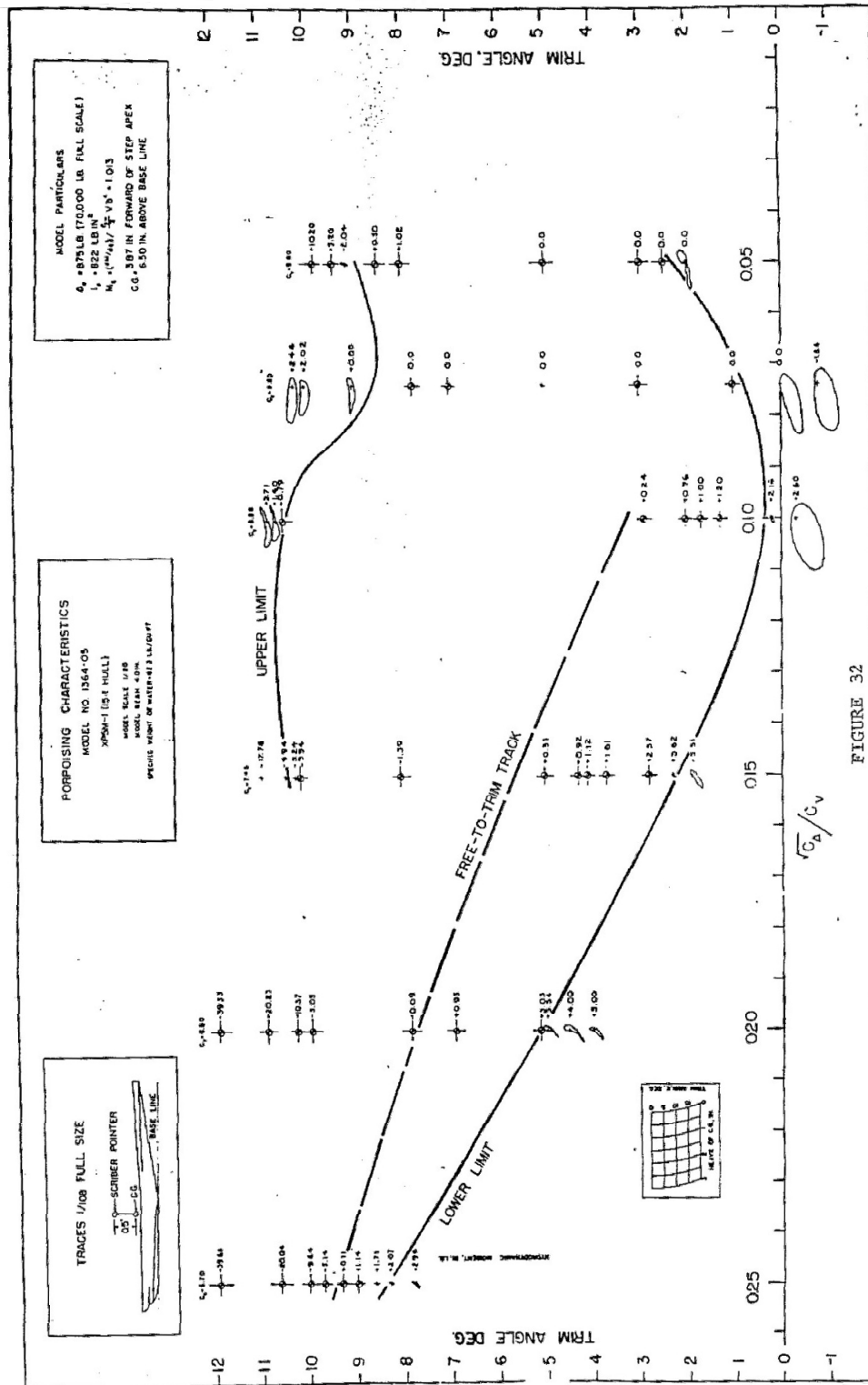


FIGURE 32

Figure 5: Porpoising Test Data for M-270 Seaplane (Taken from Flickinger, 1951)

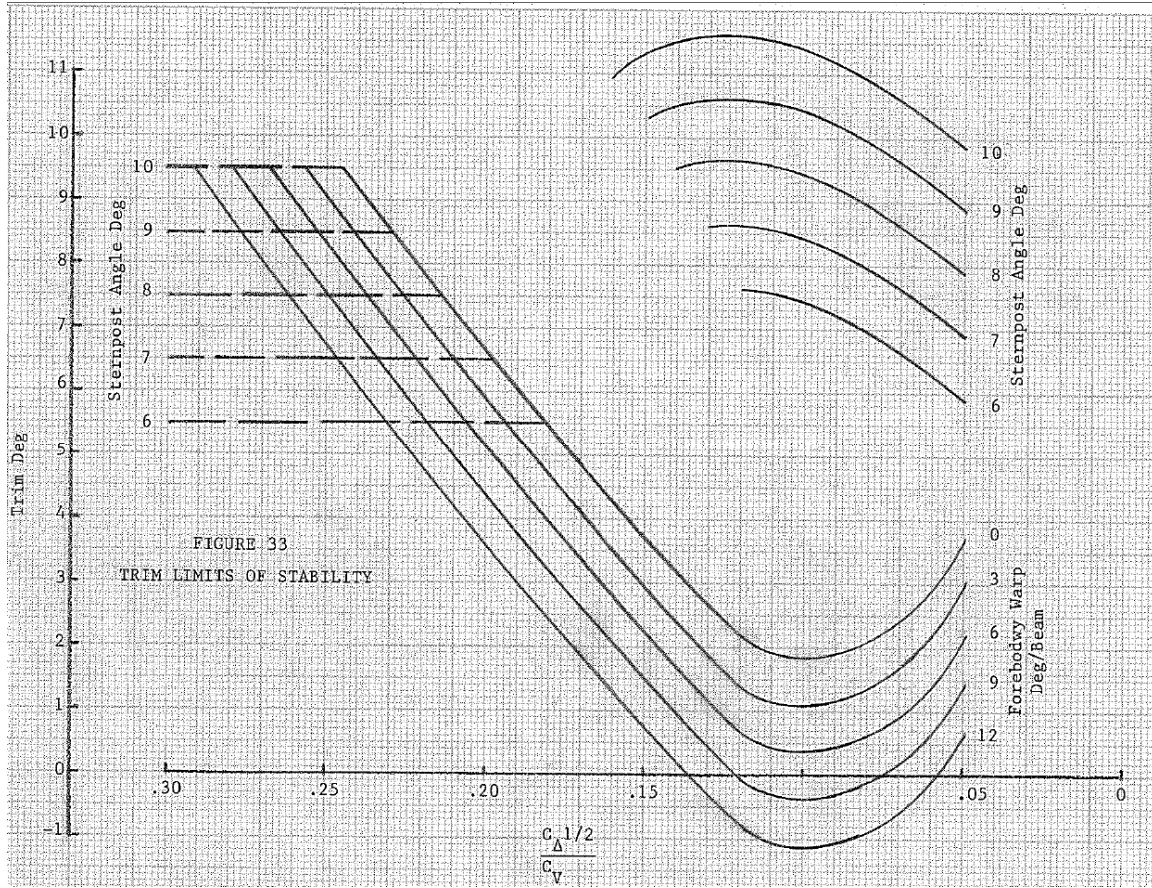


Figure 6: Generalized Trim Limits of Stability Derived from M-270 Test Data.

Note: The transition from the forebody lower limit to the cut-off at hump speed is usually a fair curve, but is simplified here.



## 14.2 Spray Characteristics

Typical spray patterns associated with seaplane hulls have already been described. A three-view schematic sketch of the main spray blister is shown on Figure 7. During model tests, measurements are made to define the X, Y, and Z components of the point of tangency to the envelope describing the main spray blister. These dimensions are normalized on the basis of beam b, so that

$$C_X = \frac{X}{b} = \text{Longitudinal spray coefficient}$$

$$C_Y = \frac{Y}{b} = \text{Lateral spray coefficient}$$

$$C_Z = \frac{Z}{b} = \text{Vertical spray coefficient}$$

where:

b = Beam at Step

X = Longitudinal position of main spray point of tangency to blister envelope, measured fore (+) or aft (-) of the step centroid

Y = Lateral position of main spray point of tangency to blister envelope, measured from hull centerline

Z = Vertical position of main spray point of tangency to blister envelope, measured from tangent to forebody keel at the step

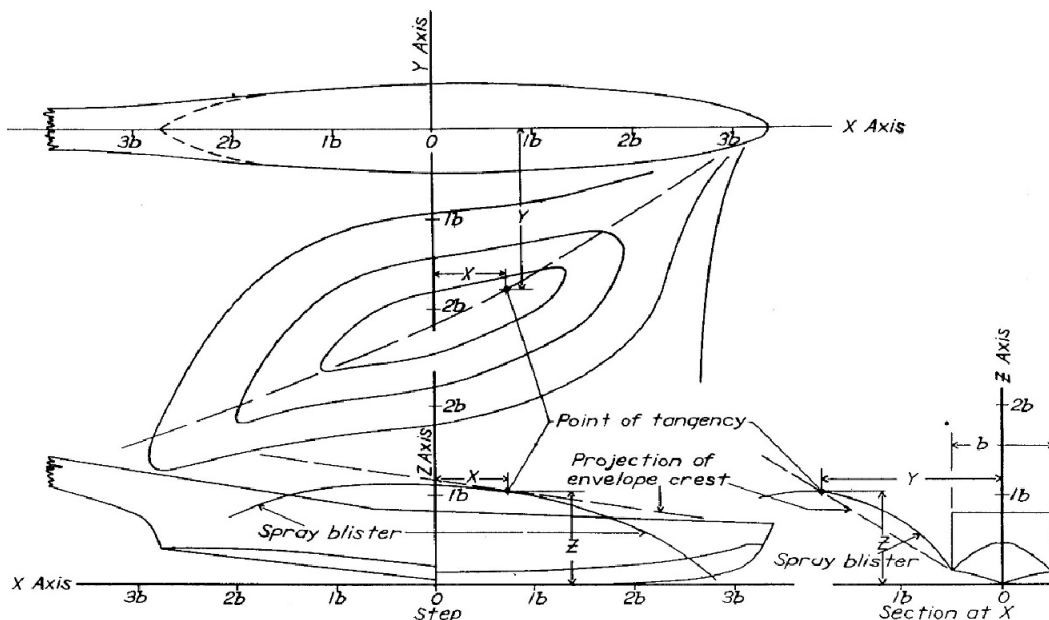


Figure 7: Typical Spray Geometry

Based on analysis of spray data obtained from "general" towing tank tests of various seaplane models in the displacement speed range a significant conclusion was developed by Locke (1945). It was shown that, for a given model, there is one curve each for the longitudinal position, the lateral position and the vertical position of the main-spray blister with the crest of the envelope. Further, each curve represents all the data taken at all combinations of load and speed in free- to- trim tests with a given position of the center-of- gravity. These curves are represented by the following relationship:

$$C_X/C_\Delta^{1/3} = \Phi_1 (C_V^2/C_\Delta^{1/3}) \quad \text{for longitudinal position}$$

$$C_Y/C_\Delta^{1/3} = \Phi_2 (C_V^2/C_\Delta^{1/3}) \quad \text{for lateral position}$$

$$C_Z/C_\Delta = \Phi_3 (C_V^2/C_\Delta^{1/3}) \quad \text{for vertical position}$$

The left-hand side represents the spray height position in terms of the size of the hull and the right hand side is a form of Froude number. Using this form of data presentation has the following advantages:

- a) Allows for extrapolating the limited data ordinarily obtained from specific tests.
- b) Reduces the number of tests required to obtain all adequate indications from general tests .
- c) Allows for comparisons between hull forms of the same general type.

This last advantage provides the means for estimating spray patterns for arbitrary hulls providing they can be related to a tested hull of the same general type and that the functions  $\Phi_1$ ,  $\Phi_2$ ,  $\Phi_3$  have been defined.

Figure 8 taken from Flickinger (1951), demonstrates the collapse of the 3 positions of the main spray when normalized and plotted as described above. These are data for a modern high-length beam ratio hull designed with a low chine bow. The actual data points represent test results for various combinations of beam loading coefficient  $C_\Delta$  and speed coefficient  $C_V$ . It is seen that the data collapse is quite good.

# High L/B Prediction Summary

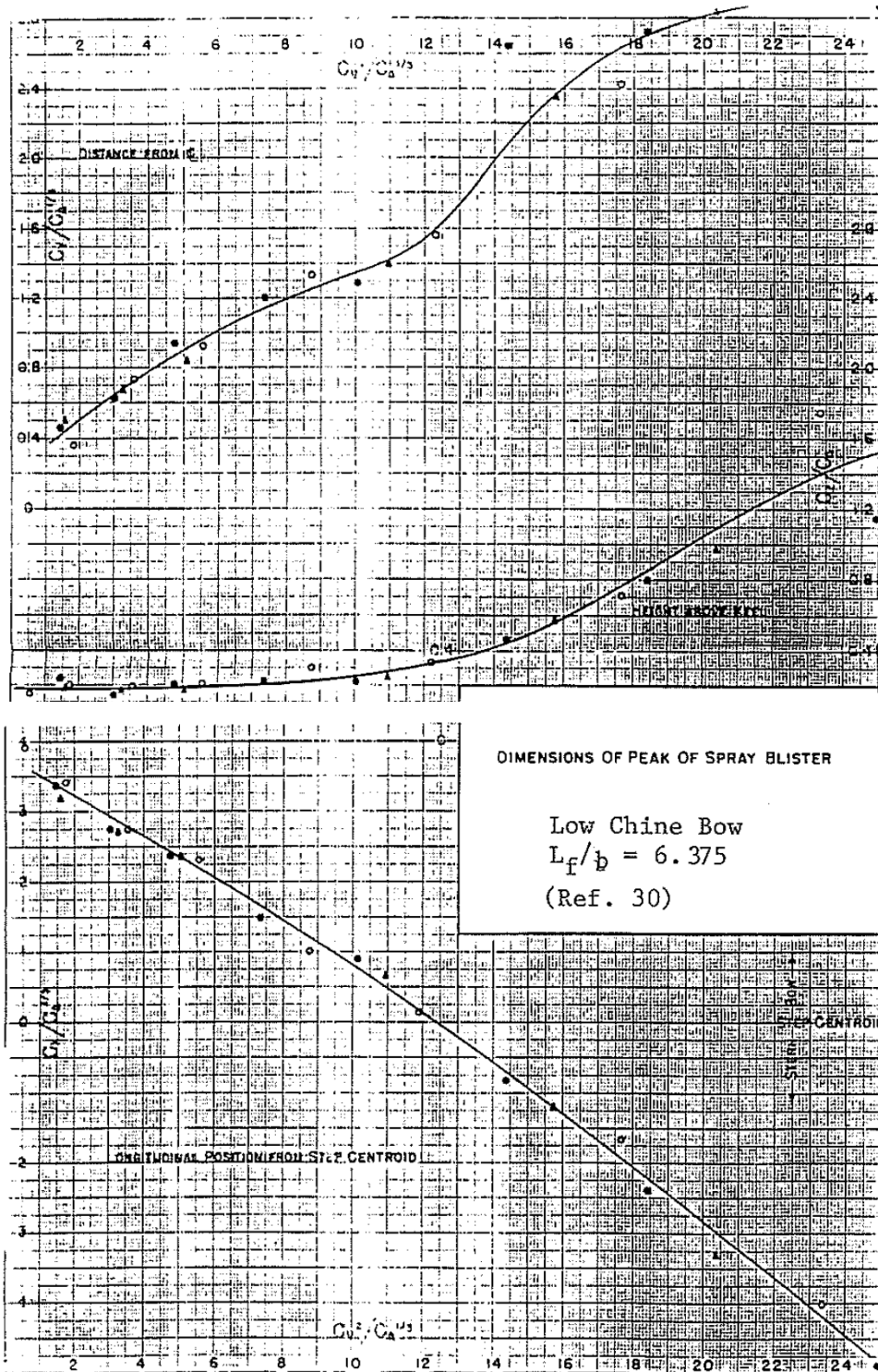


Figure 8: M-270 Normalized Spray Measurements (Flickinger, 1951)

The studies of Flickinger (1950, 1951) and Locke (1945, 1947) have shown that, for a given hull type, the longitudinal and vertical positions of

the point of tangency to the main spray blister are a function of forebody length-beam ratio and the coefficient  $C_V^2/C_\Delta^{1/3}$ . The lateral position is independent of forebody length-beam ratio. These relations are:

Longitudinal Position:

$$\frac{C_X}{C_\Delta^{1/3}} = \left( \frac{C_X}{C_\Delta^{1/3}} \right)_0 + \left( \frac{C_X}{C_\Delta^{1/3}} \right)_{00} \left[ \left( \frac{\lambda_F}{\lambda_{F0}} \right)^{1/2} - 1 \right]$$

where:

$$\frac{C_X}{C_\Delta^{1/3}} = \text{longitudinal coefficient for candidate hull}$$

$$\left( \frac{C_X}{C_\Delta^{1/3}} \right)_0 = \text{longitudinal coefficient for baseline hull} \\ = f(C_V^2/C_\Delta^{1/3})$$

$$\left( \frac{C_X}{C_\Delta^{1/3}} \right)_{00} = \left( \frac{C_X}{C_\Delta^{1/3}} \right)_0 \text{ at } \frac{C_V^2}{C_\Delta^{1/3}} = 0$$

$\lambda_F$  = forebody length-beam ratio of candidate

$\lambda_{F0}$  = forebody length-beam ratio of baseline hull

Vertical Position:

$$\frac{C_Z}{C_\Delta} = \left( \frac{C_Z}{C_\Delta} \right)_0 \left( \frac{\lambda_{F0}}{\lambda_F} \right)^{3/2}$$

where:

$$\frac{C_Z}{C_\Delta} = \text{vertical coefficient for candidate hull}$$

$$\left( \frac{C_Z}{C_\Delta} \right)_0 = \text{vertical coefficient for baseline hull} \\ = f(C_V^2/C_\Delta^{1/3})$$

Lateral Position:

$$\frac{C_Y}{C_{\Delta}^{1/3}} = \left( \frac{C_Y}{C_{\Delta}^{1/3}} \right)_0$$

where:

$$\frac{C_Y}{C_{\Delta}^{1/3}} = \text{lateral coefficient for candidate hull}$$

$$\left( \frac{C_Y}{C_{\Delta}^{1/3}} \right)_0 = \text{lateral coefficient for baseline hull} \\ = f(C_V^2/C_{\Delta}^{1/3})$$

Since the present study is directed at modern high length-beam ratio hulls with low chine bow, the M-270 model test results will be used as the baseline data. (Figure 8). For that hull:

$$\lambda_{F0} = L_F/b = 6.375$$

$$\left( \frac{C_X}{C_{\Delta}^{1/3}} \right)_{00} = 3.8$$

Thus:

$$\frac{C_X}{C_{\Delta}^{1/3}} = \left( \frac{C_X}{C_{\Delta}^{1/3}} \right)_0 + 3.80 \left[ \left( \frac{\lambda}{6.375} \right)^{1/2} - 1 \right]$$

$$\frac{C_Z}{C_{\Delta}} = \left( \frac{C_Z}{C_{\Delta}} \right)_0 \left( \frac{6.375}{\lambda_F} \right)^{3/2}$$

$$\frac{C_Y}{C_{\Delta}^{1/3}} = \left( \frac{C_Y}{C_{\Delta}^{1/3}} \right)_0$$

The values  $\left( \frac{C_X}{C_{\Delta}^{1/3}} \right)_0$ ,  $\left( \frac{C_Y}{C_{\Delta}^{1/3}} \right)_0$  and  $\left( \frac{C_Z}{C_{\Delta}} \right)_0$

are plotted in Figure 8 as a function of  $\left( \frac{C_V^2}{C_{\Delta}^{1/3}} \right)$

# High L/B Prediction Summary

These relationships are plotted in Figures 9, 10, and 11 with forebody length-beam ratio as a parameter. They are to be used for estimating the location of the maximum height of the main spray envelope for high- length beam ratio hulls with low chine bow.

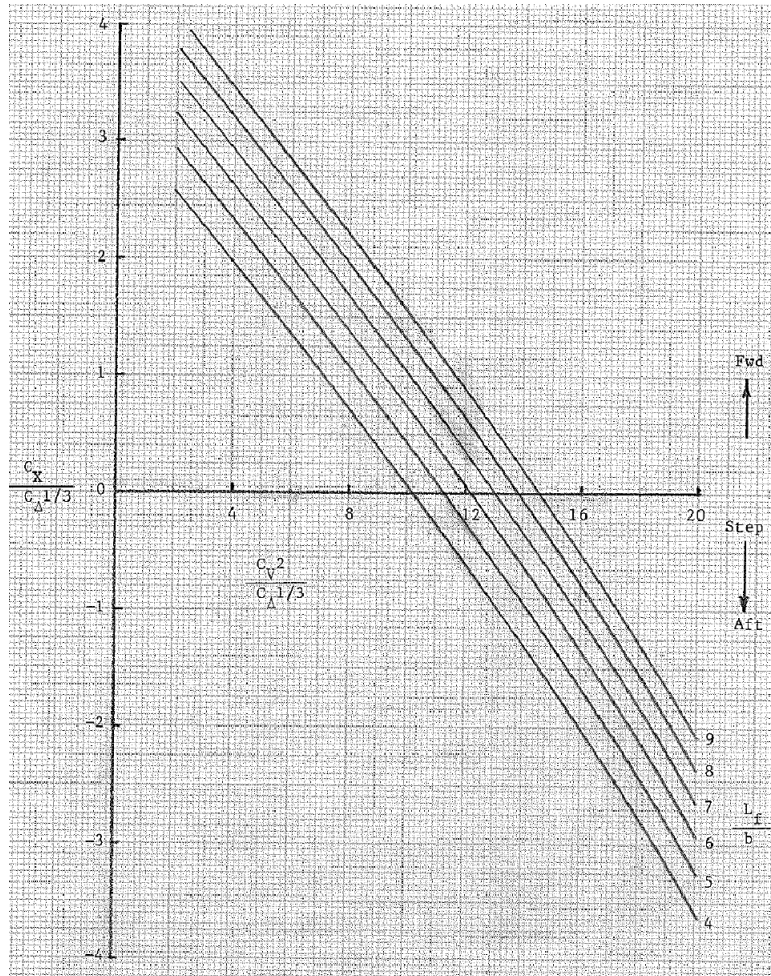


Figure 9 Generalized Longitudinal Spray Characteristics for High Length-Beam Ratio, Low Chine Hull

# High L/B Prediction Summary

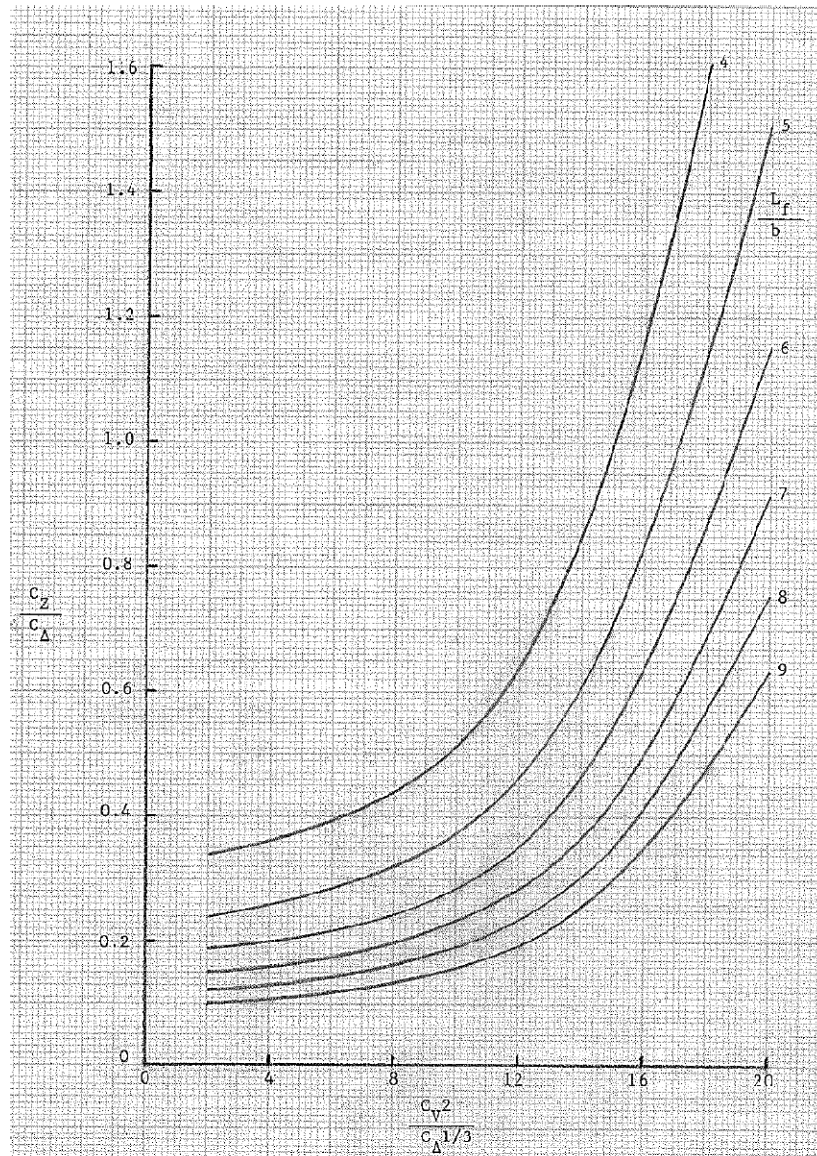


Figure 10: Generalized Vertical Spray Characteristics for High Length-Beam Ratio, Low Chine Hull

# High L/B Prediction Summary

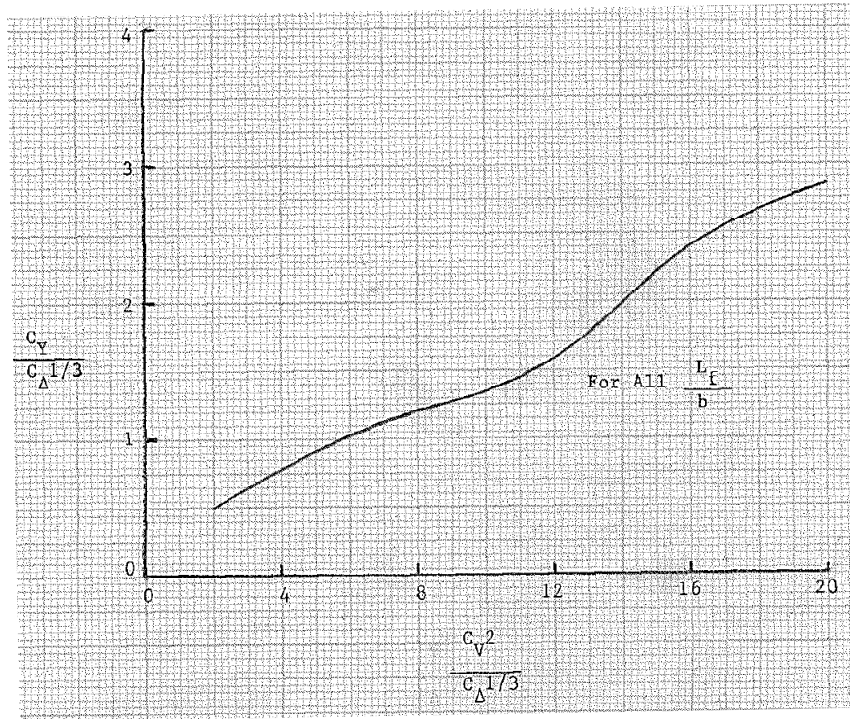


Figure 11: Generalized Transverse Spray Characteristics for High Length-Beam Ratio, Low Chine Hull



14.3 Hydrodynamic Resistance (Post Hump Speeds)

Hugli and Van Dyck (1955) presented an extensive review of hull resistance data obtained from the results of general tank tests made at the Davidson Laboratory and at the NACA. Data were collected for 10 flying boat hull configurations ranging in length-beam ratio from 6 to 16, with basic forebody deadrise angles ranging from 20-deg to 40-deg. and values of  $K_2 = C_{\Delta 0} / \left(\frac{L}{b}\right)^2$  equal to approximately 0.02 (a good value for spray and resistance). Analysis of the resistance was made throughout the take-off run at several combinations of gross weight and getaway speed. The basic equation representing the hull resistance,  $R_T$  is:

$$R_T = R_d + R_f$$

The first term is the dynamic resistance which is equal to  $\Delta \tan \tau$  where:

$$\Delta = \text{load on water} = \Delta_o \left[ 1 - \left( \frac{V}{V_G} \right)^2 \right]$$

$\Delta_o$  = gross weight of seaplane

$V$  = speed of interest

$V_G$  = get-away speed

$\tau$  = trim angle of hull at speed  $V$

The second term represents the frictional resistance. In the planing speed region:

$$R_f = C_f \frac{\rho}{2} S_H V^2$$

where:

$C_f$  = friction coefficient

$S_H$  = wetted area of hull,  $\text{ft}^2$

The wetted area is a function of deadrise angle,  $\beta$ ; trim angle  $\tau$ ; load on water  $\Delta$ , and speed.  $C_f$  is a function of Reynolds number. An empirical equation was developed by Hugli and Van Dyck, which collapsed the data and related the hull resistance to  $\beta$ ,  $\tau$ ,  $\Delta$ , and  $V$  as follows:

$$R_T = \Delta \tan \tau + .008 \left( \frac{\sec \beta \tan \beta}{\tau} \right) \Delta^{3/5} V^{9/5}$$

This equation can be used to make first order estimates of the hull drag even in the vicinity of the second hump where afterbody wetting and, consequently the frictional resistance become of major importance. In the post hump speed region, the trim angle to be used in the above equation should lie between the upper and lower porpoising limits.

NOTE (Morabito, 2024): Due to the utility of Hugli and Van Dyck's equation, and the complete obscurity of the original reference, it is worth including the full derivation as a side-bar. From Hugli and Van Dyck (1955):

It was found that, for hulls at both the first and second humps, the total resistance expressed as a fraction of the gross weight,  $R_T/\Delta_o$ , may be represented quite well by the following empirical formula

$$\frac{R_T}{\Delta_o} = \frac{\Delta}{\Delta_o} \tan \tau + 0.008 \frac{\sec \beta \tan \beta}{\tau} \frac{\Delta^{3/5} V^{9/5}}{\Delta_o} + 0.145 \left( \frac{V}{V_G} \right)^2$$

Which is an expression of the basic equation

$$\frac{R_T}{\Delta_o} = \frac{R_d}{\Delta_o} + \frac{R_f}{\Delta_o} + \frac{R_a}{\Delta_o}$$

The first term is the dynamic resistance, being nothing more than  $\Delta \tan \tau$  divided by  $\Delta_o$ .

The second, or frictional resistance, term is an empirical expression relating  $\beta, \tau, \Delta$ , and  $V$  in such a manner as to collapse the high-speed frictional resistance obtained from model data of various configurations. Although it is an empirical expression, the form of the frictional resistance term may be developed with the aid of a few logical assumptions, applicable in the planing speed region, as follows:

$$\frac{R_f}{\Delta_o} = \frac{C_f \frac{\rho}{2} S V^2}{\Delta_o}$$

The Prandtl-von Karman formula is less awkward than the Schoenherr curve or the ITTC 1957 line (though applicable over a smaller range of Reynolds numbers).

$$C_f = 0.074 (Re)^{-0.2}$$

# High L/B Prediction Summary

Where,  $Re = \frac{V\ell}{\nu}$ . This can be expressed as,

$$C_F = k_1 \left( \frac{\nu}{V\ell} \right)^{1/5}$$

Where  $k_1$  is a constant,  $\nu$  is kinematic viscosity,  $\ell$  is a characteristic length (usually wetted length). Assuming,

$$\ell = k_2 \Delta^{1/3}, \quad S = k_3 \Delta^{2/3}, \quad \text{and} \quad \frac{\rho_w}{2} = 1$$

where  $k_2$  and  $k_3$  are arbitrary constants, and substituting these relationships into the first equation gives

$$\frac{R_f}{\Delta_o} = k_1 \left( \frac{\nu}{k_2 V \Delta^{1/3}} \right)^{1/5} (k_3 \Delta^{2/3}) \frac{V^2}{\Delta_o}$$

Simplification of the above equation, and combining the constants  $k_1$ ,  $k_2$ ,  $k_3$ ,  $\nu$  to form a constant A

$$\frac{R_f}{\Delta_o} = A \frac{\Delta^{3/5} V^{9/5}}{\Delta_o}$$

This constant A was representable as  $A \approx 0.008 \left( \frac{\sec \beta \tan \beta}{\tau} \right)$ , in the vicinity of the second hump where afterbody wetting and, consequently, the frictional resistance becomes of major importance. The following table summarizes the hulls compared in the resistance study and the respective values of the constant represented as 0.008.

| Hull Designation | Reference | Deadrise Angle, $\beta$ , deg. | Length-Beam Ratio, L/b | Sternpost Angle, deg. | Gross Load Coeff., $C_{\Delta o}$ | Constant |
|------------------|-----------|--------------------------------|------------------------|-----------------------|-----------------------------------|----------|
| (1) XPB2M-1      | 8         | 20.0                           | 6.07                   | 8                     | 0.701                             | 0.010    |
| (2) PEM-3        | 8         | 20.0                           | 6.02                   | 8.5                   | 0.689                             | 0.008    |
| (3) XJR2F-1      | 9         | 22.5                           | 5.94                   | 8                     | 0.671                             | 0.007    |
| (4) P5M-1        | 10        | 20.0                           | 6.67                   | 8.5                   | 1.25                              | 0.008    |
| (5) IPSY-1       | 11        | 22.5                           | 10.00                  | 7.5                   | 1.80                              | 0.009    |
| (6) ETT No. 535  | 4         | 40.0                           | 6.19                   | 7                     | 0.729                             | 0.009    |
| (7) " 559        | 4         | 40.0                           | 6.19                   | 11                    | 0.729                             | 0.007    |
| (8) " 698        | 4         | 30.0                           | 8.45                   | 9                     | 1.357                             | 0.008    |
| (9) " 835        | 13        | 22.5                           | 16.00                  | 8.7                   | 4.86                              | 0.007    |
| (10) NACA No. 73 | 8         | 26.0                           | 6.70                   | 6                     | 0.854                             | 0.006    |

The third term, the aerodynamic resistance is:

$$\frac{R_a}{\Delta_o} = \frac{C_D \frac{\rho_a}{2} S V^2}{C_{L_{max}} \frac{\rho_a}{2} S V_G^2} = \frac{C_D}{C_{L_{max}}} \left( \frac{V}{V_G} \right)^2 ,$$

where

$$C_D = C_{D_p} + \frac{(C_{L_{max}})^2}{\pi(A)e} .$$

Assuming  $A = 6$ ,  $C_{L_{max}} = 2$ ,  $C_{D_p} = 0.025$ , and  $e = 0.8$  given

$$C_D = 0.025 + \frac{4}{\pi(6)0.8} = 0.290 ,$$

and therefore

$$\frac{R_a}{\Delta_o} = 0.145 \left( \frac{V}{V_G} \right)^2 .$$

It may be noted that use of a wing with aspect ratio of 3 and  $C_{L_{max}}$  of 0.9, which is similar to types used in high-speed aircraft, yields approximately the same variation of  $\frac{R_a}{\Delta_o} = 0.147 \left( \frac{V}{V_G} \right)^2$ . Therefore this equation may be considered as being fairly typical.

14.4 Hydrodynamic Resistance (Hump Speed)

The hull resistance equation previously defined also applies at the hump speed region providing reasonable estimates can be made of the hump trim and hump speed. Fortunately, Haar (1952) presents the results of a model test program, which among other objectives, examined the dependence of hump speed coefficient and trim angle on length-beam ratio, forebody length fraction, and sternpost angle. The data of Haar (1952) have been cross plotted on Figures 12 and 13. From these plots the hump speed coefficients and trim angle are readily obtained. The speed coefficient is defined as:

$$C_{V_H} = V_H / \sqrt{gb}$$

where:

$$V_H = \text{hump speed}$$

$$b = \text{beam of forebody at step}$$

It is seen in Figure 12 that the hump speed coefficient is mainly dependent on length-beam ratio, increasing with increasing L/b. In addition, the hump speed coefficient also increases as the forebody-afterbody length ratio decreases.

From Figure 13 it is seen that hump trim angle is mainly a function of forebody length fraction and sternpost angle, increasing with decreasing sternpost angle and increasing forebody length fraction.

For a given design, the values of  $C_{V_H}$  and  $\tau$  are obtained from Figures 12 and 13 and substituted into the resistance equation defined above to obtain the hull resistance at hump speed. This is usually the maximum hydrodynamic resistance encountered by the hull during the smooth water take-off process.

# High L/B Prediction Summary

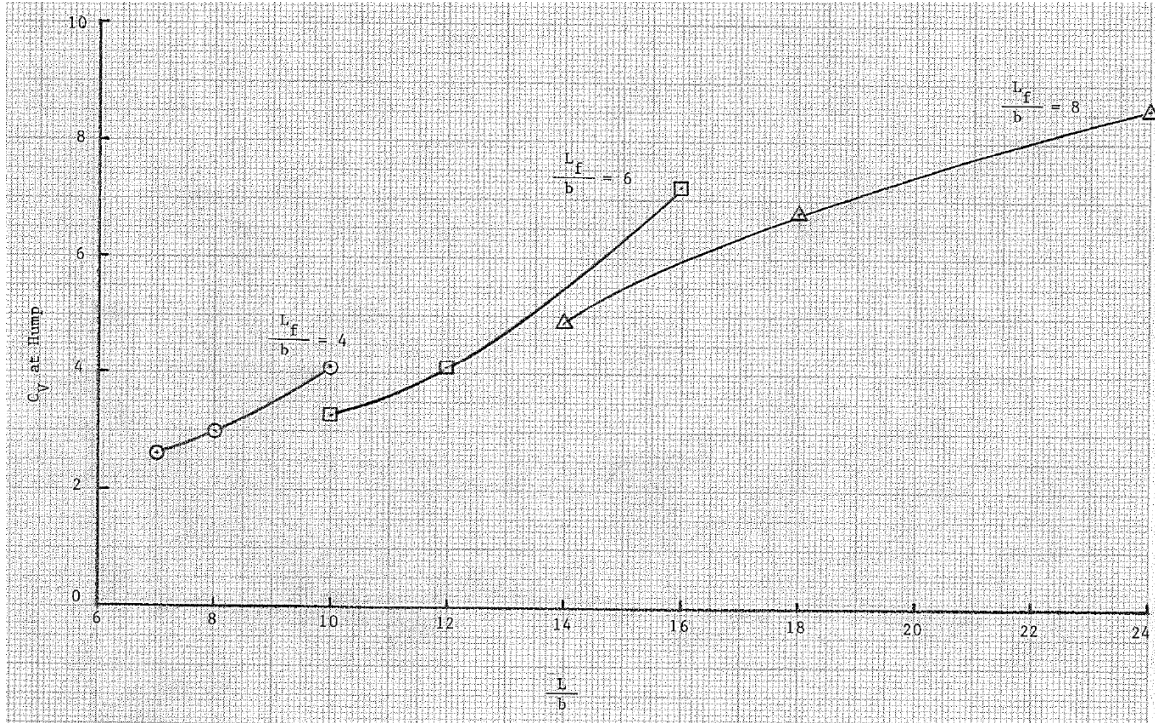


Figure 12: Speed Coefficient at Hump (Taken from Haar, 1952)

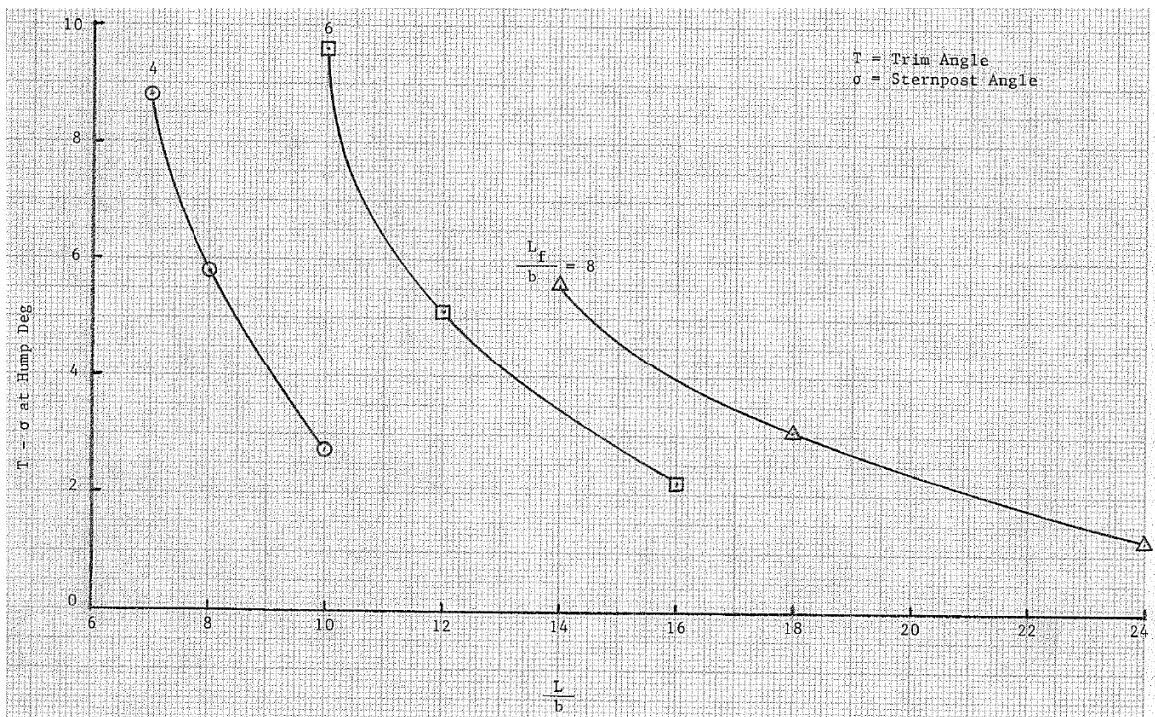


Figure 13: Difference between Trim Angle and Sternpost Angle at Hump (Taken from Haar, 1952)

#### 14.5 Aerodynamic Lift and Drag

For hydrodynamic take-off calculations, it is reasonable to assume that the seaplane aerodynamics are such that the craft can attain a stable running trim angle during take-off. In this case, only estimates of the aerodynamic lift and drag are needed. It is necessary to know the lift curve slope, taking into account the ground effect and the flap deflection, as well as the moments generated by the wing. These factors are discussed in any course on applied aerodynamics. The following simplified aerodynamics may be used in conjunction with the hydrodynamic predictions.

The lift is the standard parabolic unloading curve, which assumes a constant angle of attack of the wing.

$$\begin{aligned}\Delta &= \text{Weight on Water} \\ &= \Delta_o \left[ 1 - \left( \frac{V}{V_G} \right)^2 \right]\end{aligned}$$

During take-off, the wing is assumed to be operating at its maximum lift coefficient. The maximum lift coefficient occurs just prior to stall, and is often increased by (1) the use of flaps at the trailing edge, which increase the camber of the section and (2) leading edge slats, which control the boundary layer, increasing the angle of attack at stall. Figure 9.1 shows some typical high-lift configurations. It should be recognized that some of the most complex configurations will not be feasible for small aircraft. The following table of 2-D maximum lift coefficients is developed from data summarized by Kroo (2006).

## High L/B Prediction Summary

| <u>Configuration</u>                         | <u>CL<sub>max</sub></u> |
|--|-------------------------|
| Flaps Retracted                              | 1.3 - 1.6               |
| Single Slotted Flap                          | 2.0 - 2.5               |
| Single Slotted Flap Plus Leading Edge Device | 2.3 - 2.5               |
| Double Slotted Flap Plus Leading Edge Device | 2.2 - 3.0               |
| Triple Slotted Flap Plus Leading Edge Device | 2.5 - 3.0               |

Note: "Blown Wings" can have maximum lift coefficients in the 4-6 range.

The flaps (Figure 14, 15) are generally deflected during the take-off and landing, but are retracted during normal flight. The take-off distance can be reduced somewhat by keeping the flaps retracted at the low speeds.

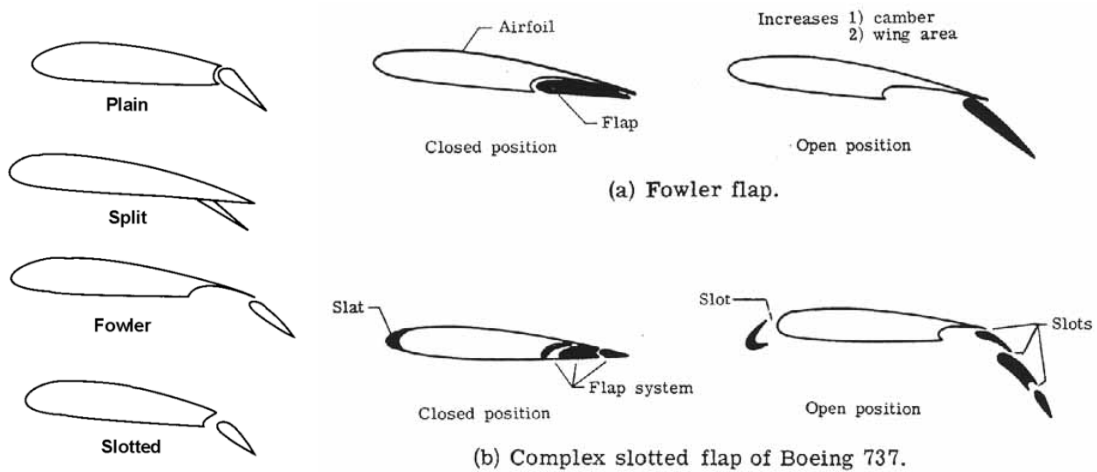


Figure 14: Typical High Lift Configurations (NASA)



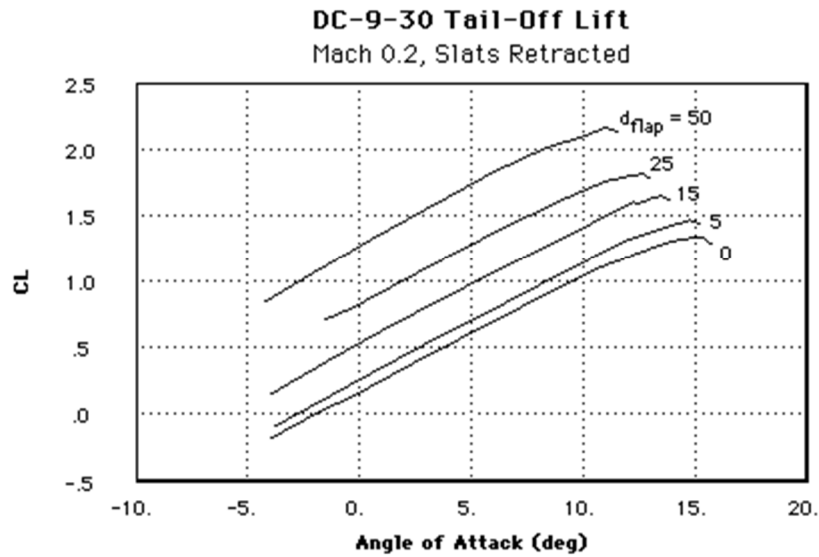


Figure 15: Effect of Flap Deflection on Lift Curve (Kroo, 2006)

Expressions for preliminary estimates of the aerodynamic drag are derived for conditions typical of those occurring during take-off and landing. These may be used when evaluating the total performance of a particular seaplane. In particular, the aerodynamic drag is added to the hydrodynamic resistance to determine the total drag during various phases of the take-off.

Using the conventional aerodynamic terminology and concepts:

and:

$C_{Dp}$  = parasitic drag coefficient of  
total aircraft. Typical value = 0.025  
(Reference 41)

$C_{Lmax}$  = maximum lift coefficient

AR = aspect ratio of wing

e = edge correction factor = 0.80

The effective aspect ratio in ground effect is higher, but for these simple calculations the difference may be neglected. The second term in the above equation represents the induced drag due to wing lift, Thus:

High L/B Prediction Summary

$$D = \left[ .025 + .40 \frac{C_{Lmax}^2}{AR} \right] .0012 V^2 S$$

Stall Speed: ( $V_{stall}$ ):

---

$$V_{stall} = \left[ \frac{\Delta_o}{C_{Lmax}} (\rho/2) S \right]^{1/2} = 29.01 \left[ \frac{\Delta_o}{C_{Lmax}} S \right]^{1/2}$$

Getaway Speed: ( $V_G$ ):

---

$$V_G = 1.10 V_{stall}$$

Minimum Landing Speed ( $V_{Lmin}$ ):

---

$$V_{Lmin} = V_{stall}$$

#### 14.6 Landing Impact Accelerations

A survey of existing formulae and computational methods for determining the maximum impact accelerations for seaplane hulls (Hugli and Van Dyck, 1955) revealed many good theoretical procedures for analyzing various hull geometries for a range of landing conditions (Schnitzer, 1952, Smiley, 1952, Miller, 1953). In general, two broad types of impact conditions are considered: (a) chines-dry impacts where the maximum impact acceleration occurs at drafts prior to chine immersion and which are usually associated with low beam loading and low flight path angle relative to the water surface and (b) chines immersed impact where the maximum acceleration occurs after chine immersion and which are usually associated with high beam loadings and/or high flight path angles.

The most useful method available for a general analysis of chines-dry impact are those given in a theoretical study (Milwitzky, 1948). [Sidebar: Ben Milwitzky spent about year meticulously drawing all of those figures] For the wetted chines case, the empirical study given by Hugli and Van Dyck has been shown to be quite useful for a wide range of practical beam loadings and flight path angles.

Since the chines-immersed impact is the type most likely to occur in rough water open sea landings particularly with the high beam loading associated with modern high length-beam ratio hulls the empirical formula presented by Hugli and Van Dyck will be used. For landings in smooth water the maximum impact acceleration is shown to be:

##### Smooth Water:

$$\eta = 0.00825 \gamma bV^2 \Delta_o^{-2/3} \left[ 1 - \frac{\beta}{90} \right]$$

This empirical formula was developed by taking a formula for impact of flat plates (by Locke, 1951 and modified somewhat by Scheider and King, 1953) and adding the deadrise correction (the bracketed term), commonly seen in impact theory.

substituting the beam loading coefficient  $C_{\Delta_o}$  into the above equation yields:

$$\frac{\eta}{\gamma} = 0.0021 \left[ \frac{V}{\Delta_o^{1/6}} \right]^2 \left[ 1 - \frac{\beta}{90} \right] / C_{\Delta_o}^{1/3}$$

where:

$\eta$  = impact acceleration at center-of-gravity, g's

$\gamma$  = flight path angle, deg

$\beta$  = forebody deadrise angle at step, degrees

$\Delta_o$  = gross weight of seaplane, lb

$V$  = landing speed, fps

It will be noted that the smooth water impact acceleration is linearly proportional to flight path angle; varies as the square of the landing speed; and is inversely proportional to the cube root of the beam loading. It will be further noted that trim angle does not appear in the empirical equation although it is known that, basically, impact accelerations decrease with decreasing trim angle (Locke, 1951 and Batterson, 1950). The omission of trim in the above equation may be attributed to the fact that, the experimental data upon which it is based had a limited trim range which was consistent with expected landing trim of typical seaplanes. The maximum trim is limited to the values of sternpost angle which, for most seaplanes, varies between 8 and 10-deg. In any event, Hugli and Van Dyck (1955) states that the empirical equation predicts maximum smooth water impact accelerations within  $\pm 10\%$  of those measured in model tests of some eight different seaplane hulls.

#### Rough Water:

When landing in regular waves, Hugli and Van Dyck (1955) state that the effective flight path angle,  $\gamma_e$ , should be measured relative to the maximum slope of the oncoming wave  $\theta_w$ . Thus:

$$\gamma_e = \gamma + \theta_w$$

where:

$\gamma$  = flight path angle relative to still water  
at time of wave contact, degree

$$\theta_w = \text{maximum wave slope} = \text{Tan}^{-1} \frac{h\pi}{L_w}$$

$h$  = wave height, ft

$L_w$  = wave length, ft

$\theta_w$  can be readily calculated for regular waves. For operation in irregular waves (which is the more common environment) after initial touchdown, the seaplane is generally in an uncontrolled condition as it bounces through the oncoming irregular wave train. The instantaneous values of  $\gamma$  and  $\theta_w$  at each subsequent wave impact are random and their statistical distribution and combinations are also unknown.

Based on observations of seaplane landings reported by Hugli and Van Dyck (1955), a typical value of  $\gamma$  in a landing approach is approximately 5-deg. The maximum value of wave slope will be assumed to be related to significant wave height and to a critical wave length which is taken to be 3 times the length of the seaplane. This is entirely an empirical assumption which is based on some unpublished model test data obtained at the Davidson Laboratory ["Recent" as of 1990]. The physical interpretation of this "effective" wave length is that it allows for forebody impact without afterbody contact with the wave train. It is emphasized, however, that much more research must be carried out before a documented procedure can be developed for predicting hull impact acceleration in irregular waves.

In summary then,

$$\gamma_e = 5^\circ + \text{Tan}^{-1} \left[ \frac{h_{1/3} \pi}{3 L} \right]$$

Substituting this value of  $\gamma_e$  into the previous equation provides the following estimate for the center-of-gravity acceleration in irregular head seas:

$$\eta = \left[ 5 + \text{Tan}^{-1} \left[ \frac{h_{1/3} \pi}{3 L} \right] \right] (.00825) \frac{bV^2}{\Delta_o^{2/3}} \left[ 1 - \frac{\beta}{90} \right]$$

Statistically, this appears to be the acceleration expected in one of 100 landings.

# High L/B Prediction Summary

Hugli and Van Dyck summarized the ratio of impact acceleration to flight path angle for 8 aircraft below. These aircraft were designed to withstand a 6-8 g vertical acceleration, yielding maximum flight path angles of 9-12 degrees. Assuming the 5-degree flare-out, this would give wave slopes of 4-7 degrees, or wavelength-to-height ratios of 45 to 26, which is not unreasonable.

VALUES OF IMPACT PARAMETER  $\eta_{max}/\gamma_{max}$   
FOR RECENT WATER-BASED AIRCRAFT DESIGNS

| Aircraft Designation | Reference | Beam, b, ft. | Gross Weight, $\Delta_c$ lb. | Getaway Speed (Approx), $V_1$ , ft./sec. | Deadrise Angle, $\beta$ , deg. | $\eta_{max}/\gamma_{max}$ , g/deg. |
|----------------------|-----------|--------------|------------------------------|--|--------------------------------|------------------------------------|
| (1) XPB2M-1          | 8,32      | 13.50        | 165,000                      | 145                                      | 20.0                           | 0.61                               |
| (2) PBM-3            | 8,32      | 10.00        | 47,000                       | 115                                      | 20.0                           | 0.65                               |
| (3) XJR2F-1          | 9         | 7.92         | 26,000                       | 120                                      | 22.5                           | 0.80                               |
| (4) XP5M-1           | 10,32     | 10.00        | 64,000                       | 125                                      | 20.0                           | 0.63                               |
| (5) XP5Y-1           | 11,32     | 10.00        | 123,500                      | 160                                      | 22.5                           | 0.64                               |
| (6) XP6M-1           | 12        | 9.17         | 160,000                      | 235                                      | ~35                            | 0.87                               |
| (7) "Princess"       | 33        | 16.66        | 310,000                      | 170                                      | 25.0                           | 0.65                               |
| (8) JR-77 (ski)      | 16        | 5.32         | 160,000                      | 250                                      | 30.0                           | 0.62                               |

#### 14.7 Illustrative Example

The previous discussion has enabled us, with mostly calculations, and reading from a minimal number of charts (Porpoising Limits, Spray Apex Coordinates, Hump Speed and Hump Speed Coefficient), to compute the following.

- Spray characteristics
- Trim limits of porpoising stability
- Landing impact accelerations in sea state 4 ( $H_{13} = 6.9$  ft)
- Resistance at hump
- Resistance approaching getaway

#### Description of Seaplane

|            |   |
|------------|---|
| $\Delta_o$ | = gross weight = 240,000 lb                 |
| L          | = load water line of hull = 128 ft          |
| b          | = beam at step = 7.7 ft                     |
| $\beta$    | = deadrise of forebody at step = $25^\circ$ |
| $L_f$      | = forebody length = 62 ft                   |
| $L_f/b$    | = 8   |
| $L_f/L$    | = .48                                       |
| $\sigma$   | = sternpost angle = $10^\circ$              |
| $w^I$      | = forebody warp = $0^\circ/\text{beam}$     |
| s          | = wing span = 137 ft                        |
| $C_s$      | = wing root chord = 25.6 ft                 |
| $C_t$      | = wing tip chord = 7.6 ft                   |
| S          | = wing planform area = 2274 ft <sup>2</sup> |
| AR         | = wing aspect ratio = $s^2/S = 8.25$        |
| $GM_T$     | = transverse metacentric height = 5.5 ft    |
| $C_{Lmax}$ | = maximum lift coefficient = 2.50           |

# High L/B Prediction Summary

From these, the simplified aerodynamic calculations can be made:

$$V_{\text{stall}} = \text{stall speed} = 29.01 \left[ \frac{\Delta_o}{C_{L\text{max}} S} \right]^{1/2} = 188 \text{ ft/sec} = 128 \text{ mph}$$

$$V_G = \text{getaway speed} = 1.10 V_{\text{stall}} = 207 \text{ ft/sec} = 141 \text{ mph}$$

$$V_L = \text{minimum landing speed} = V_{\text{stall}} = 188 \text{ ft/sec} = 128 \text{ mph}$$

$$\gamma_{\text{max}} = \text{maximum flight path angle} =$$

$$\tan^{-1} \left[ \frac{.025}{C_{L\text{max}}} + \frac{.40 C_{L\text{max}}}{AR} \right] = 7.48^\circ$$

## Calculations for Coefficients at Low Speeds

Once the getaway speed is known, calculations can be made of the load on water at each speed, as well as the coefficients for using graphs.

|  | $\frac{V}{V_G}$ |            |            |            |            |            |
|--|-----------------|------------|------------|------------|------------|------------|
|  | <u>.25</u>      | <u>.30</u> | <u>.35</u> | <u>.40</u> | <u>.45</u> | <u>.50</u> |
| $V_G = \text{Getaway Speed} =$                                   | 207.00          |            |            |            |            |            |
| $V = \text{Speed} = V_G \left( \frac{V}{V_G} \right) =$          | 51.75           | 62.10      | 72.45      | 82.80      | 93.15      | 103.50     |
| $b = \text{Beam at Step} =$                                      | 7.69            |            |            |            |            |            |
| $C_V = \text{Speed Coef.}$                                       |                 |            |            |            |            |            |
| $= \frac{V}{(gb)^{1/2}} =$                                       | 3.29            | 3.95       | 4.60       | 5.26       | 5.92       | 6.58       |
| $\Delta_o = \text{Gross Weight} =$                               | 240000          |            |            |            |            |            |
| $\Delta = \text{Weight on Water}$                                |                 |            |            |            |            |            |
| $= \Delta_o \left[ 1 - \left( \frac{V}{V_G} \right)^2 \right] =$ | 225000          | 218400     | 210600     | 201600     | 191400     | 180000     |
| $C_\Delta = \text{Beam Loading Coef.}$                           |                 |            |            |            |            |            |
| $= \frac{\Delta}{wb^3} =$  | 7.73            | 7.50       | 7.24       | 6.93       | 6.58       | 6.18       |
| $C_V^2 / C_\Delta^{1/3} =$                                       | 5.47            | 7.97       | 10.94      | 14.51      | 18.70      | 23.59      |



Spray Characteristics

The coordinates of the envelope of the main spray blister (very important for propellers and flaps) have to be read from the non-dimensional charts by hand, and then converted into dimensional units. Spray is more of an issue at the low speeds, as it usually dodges under the flaps and propellers at high speeds, since it originates near the step.

| V/VG  | <u>0.30</u> | <u>0.35</u> | <u>0.40</u> | <u>0.45</u> | <u>0.50</u> |
|---|-------------|-------------|-------------|-------------|-------------|
| $C_X/C_\Delta^{1/3} = f(C_V^2/C_\Delta^{1/3}, L_f/b)$ | 2.75        | 1.95        | 0.96        | -0.23       | -1.83       |
| = (Fig. 9)  |             |             |             |             |             |
| $C_Z/C_\Delta = f(C_V^2/C_\Delta^{1/3}, L_f/b)$       | 0.14        | 0.16        | 0.21        | 0.32        | 0.63        |
| = (Fig. 10)   |             |             |             |             |             |
| $C_Z/C_\Delta = f(C_V^2/C_\Delta^{1/3}, L_f/b)$       | 0.96        | 1.20        | 1.43        | 2.10        | 2.74        |
| = (Fig. 11)   |             |             |             |             |             |

These values (in feet) can then be calculated

X = Longitudinal Distance of Spray

Envelope Peak from Step

$$\text{Apex} = C_X/C_\Delta^{1/3} (C_\Delta)^{1/3} b \quad 41.81 \quad 29.35 \quad 14.28 \quad -3.37 \quad -26.37$$

Z = Vertical Height of Spray

Envelope Peak above Forebody

$$\text{keel} = (C_Z/C_\Delta) (C_\Delta) b \quad 8.32 \quad 9.23 \quad 11.69 \quad 17.05 \quad 31.88$$

Y = Lateral Distance of Spray

Envelope Peak from  $\phi_L =$

$$(C_Y/C_\Delta^{1/3}) (C_\Delta)^{1/3} b \quad 14.60 \quad 18.06 \quad 21.27 \quad 30.79 \quad 39.48$$

The spray envelope can be graphed, as shown in Figures 16. However, it may be useful when graphed on the 3-d model of the hull, especially if wings

## High L/B Prediction Summary

and flaps are there. Figure 17 was constructed by locating points at each of the spray envelope locations and then fairing an approximate envelope curve.

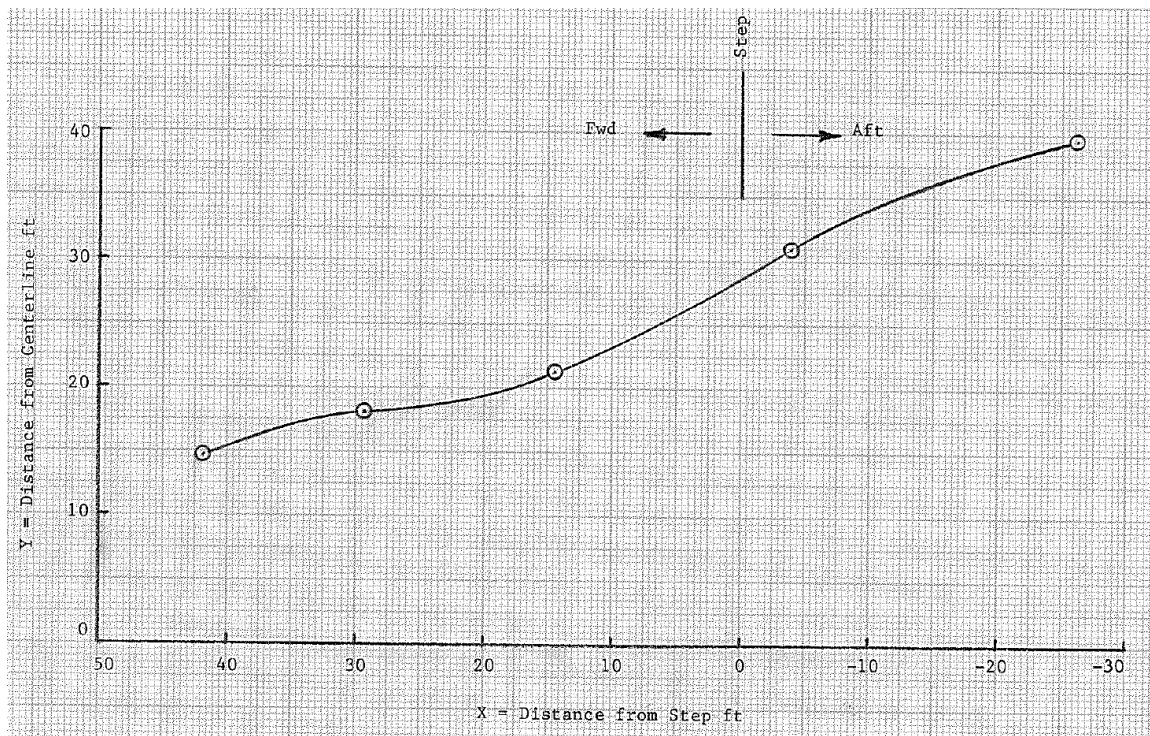
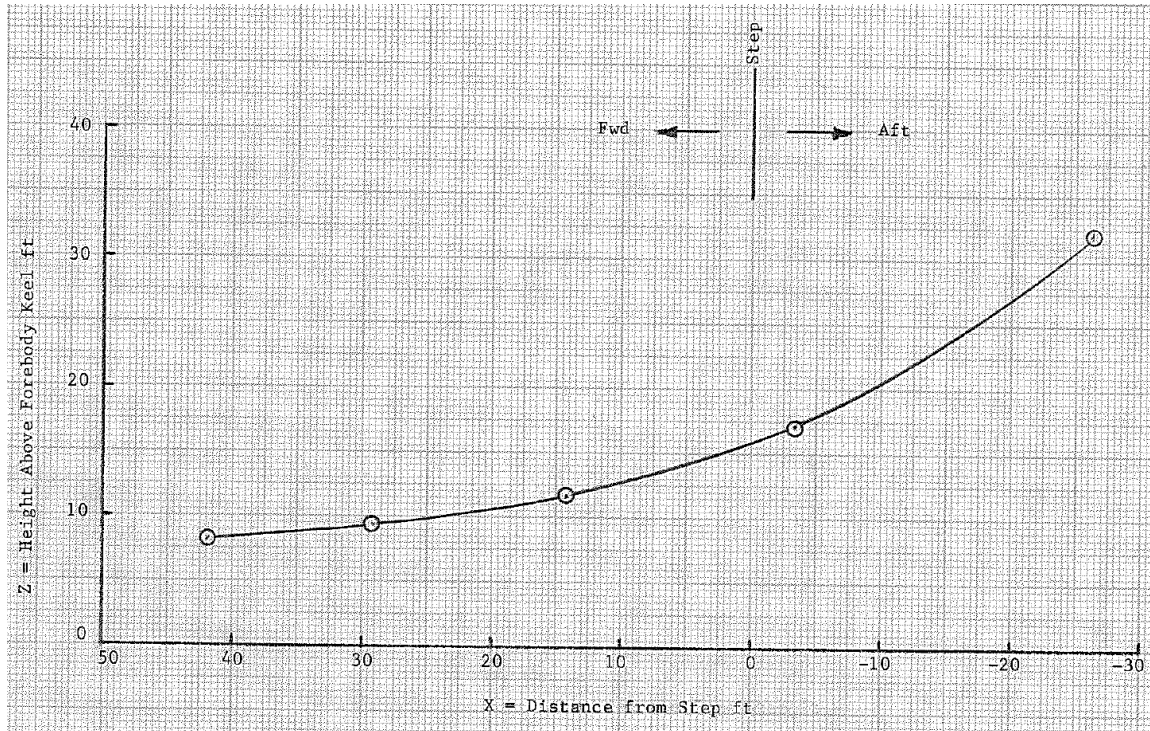


Figure 16: Example Design - Spray Envelope Coordinates

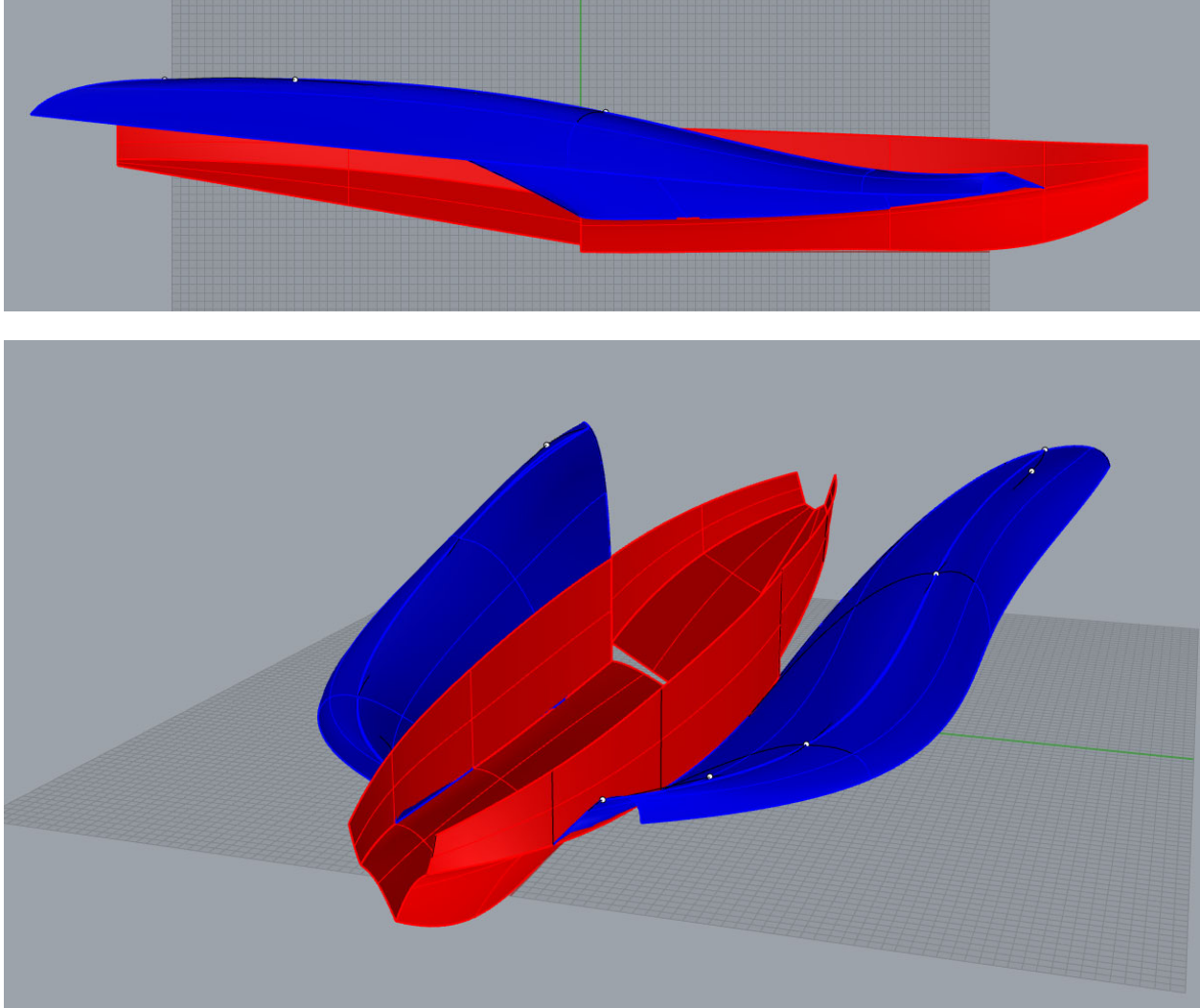


Figure 17: Profile and Perspective of 3-D Model with Spray Envelope Estimated.

Note: 3-d shape was estimated by sketching transverse curves starting at the chine, going through the apex. The surface was “lofted” through these approximate curves. This is a combination of all of the speeds.

# High L/B Prediction Summary

## Porpoising Limits

The porpoising limits for the given speeds, loadings and afterbody geometry can be estimated from the non-dimensional generalized curve shown in Figure 6, or from standard series charts, using the following calculation table.

|  | Trim Limits of Stability |        |        |        |        |        |        |        |        |
|--|--------------------------|--------|--------|--------|--------|--------|--------|--------|--------|
|  | $\frac{V}{V_G}$          |        |        |        |        |        |        |        |        |
| $V_G$ - Getaway Speed -                        | .60<br>207.00            | .65    | .70    | .75    | .80    | .85    | .90    | .95    | .975   |
| $V$ - Speed - $V_G (\frac{V}{V_G})$ -          | 124.20                   | 134.55 | 144.90 | 155.25 | 165.60 | 175.95 | 186.30 | 196.65 | 201.82 |
| $b$ - Beam at Step -                           | 7.69                     |        |        |        |        |        |        |        |        |
| $C_V$ - Speed Coef. - $\frac{V}{(gb)^{1/2}}$ - | 7.89                     | 8.55   | 9.21   | 9.87   | 10.52  | 11.18  | 11.84  | 12.50  | 12.82  |
| $\Delta_o$ - Gross Weight -                    | 240000                   |        |        |        |        |        |        |        |        |
| $\Delta$ - Weight on Water -                   |                          |        |        |        |        |        |        |        |        |
| $\Delta_o [1 - (\frac{V}{V_G})^2]$ -           | 153600                   | 138600 | 122400 | 105000 | 86400  | 66600  | 45600  | 23400  | 11850  |
| $C_\Delta$ - Beam Loading Coef. -              |                          |        |        |        |        |        |        |        |        |
| $\frac{\Delta}{wb^3}$ -                        | 5.28                     | 4.76   | 4.21   | 3.61   | 2.97   | 2.29   | 1.57   | .80    | .41    |
| $C_\Delta^{1/2}/C_V$ -                         | .291                     | .255   | .223   | .192   | .164   | .135   | .106   | .072   | .050   |

For the forebody warp,  $w=0$  and the sternpost angle,  $\sigma = 10$ -deg, the following are read by hand from the generalized trim limits in Figure 6, or from applicable series data.

|                                      |      |      |      |      |       |       |       |       |      |
|--------------------------------------|------|------|------|------|-------|-------|-------|-------|------|
| $w$ - Forebody Warp -                | 0°   |      |      |      |       |       |       |       |      |
| $\tau_1$ - Lower Limit at High       |      |      |      |      |       |       |       |       |      |
| Speed = $f(C_\Delta^{1/2}/C_V, w)$ - | -    | -    | 8.10 | 6.10 | 4.50  | 2.90  | 1.90  | 2.30  | 3.70 |
| $\sigma$ - Sternpost Angle - 10°     | 10°  |      |      |      |       |       |       |       |      |
| $\tau_2$ - Lower Limit at Low Speed  |      |      |      |      |       |       |       |       |      |
| - $f(\sigma)$                        | 9.50 | 9.50 | -    | -    | -     | -     | -     | -     | -    |
| $\tau_3$ - Upper Limit at High Speed |      |      |      |      |       |       |       |       |      |
| - $f(C_\Delta^{1/2}/C_V, \sigma)$ -  | -    | -    | -    | -    | 10.80 | 11.60 | 11.50 | 10.60 | 9.90 |

These porpoising limits are all in degrees, relative to forebody keel, so no more calculations are necessary. They are graphed below. Generally, the transition from  $\tau_1$  to  $\tau_2$  can be faired. It is important to note that these apply to the well-designed and properly ventilated step of the parent hull. The upper limit at high speeds will drop precipitously with inadequate step ventilation as skipping-type instabilities occur. This is why some of the porpoising limits in the standard series are so small, leaving very little room to take-off.

# High L/B Prediction Summary

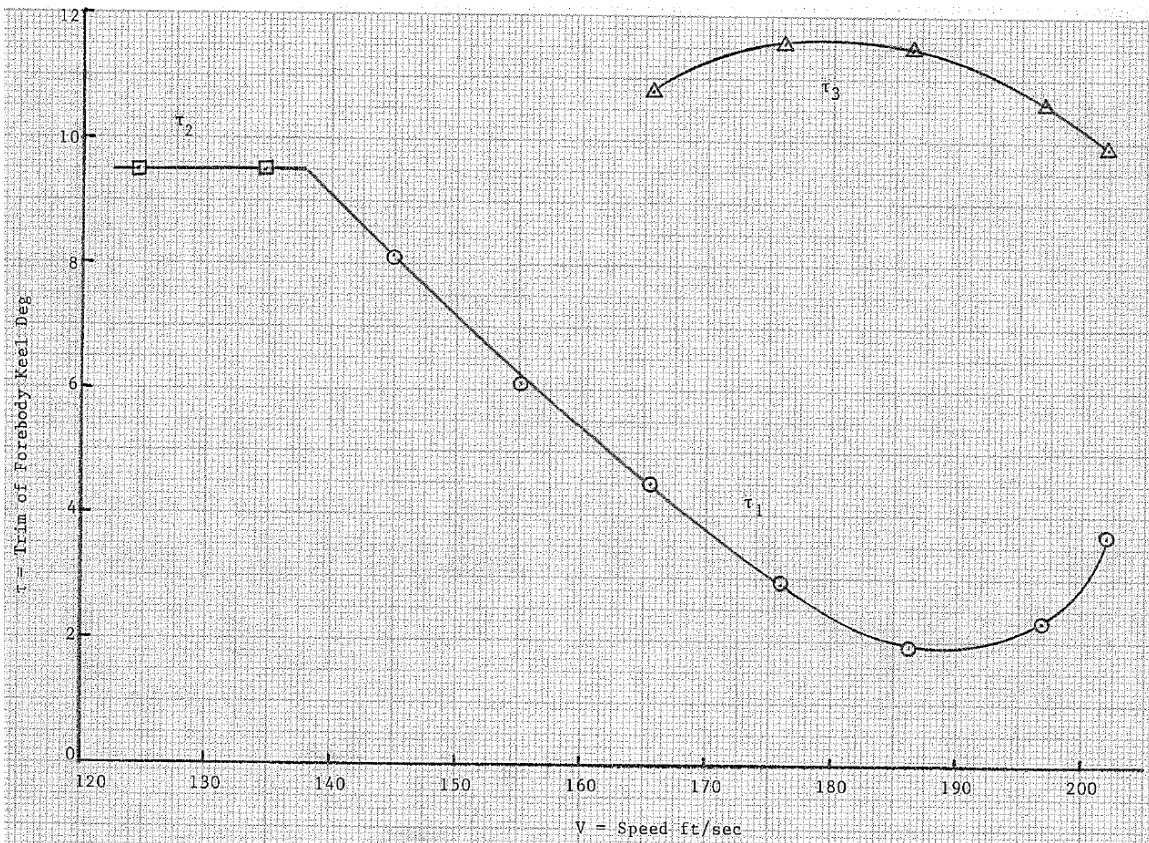


Figure 16: Porpoising Limits for Design Example, Estimated from Generalized Curve in Figure 6.

Hump Speed Resistance

The resistance can be estimated using Hugli and Van Dyck's (1955) equation. At high speeds, this can be computed for assumed values of trim (within the stability limits).

Hydrodynamic Resistance at Hump:

$$R = \Delta \tan \tau + \left( \frac{(.008 \sec \beta \tan \beta)}{\tau} \right) \Delta^{3/5} V^{9/5}$$

$$V_{\text{Hump}} = \text{Hump Speed} = C_{V\text{Hump}} (gb)^{1/2}$$

$$L_f/L = \text{Forebody Length Fraction} = .48$$

$$L/b = \text{Length-Beam Ratio} = 16.67$$

$$b = \text{Beam at Step} = 7.69 \text{ ft}$$

Speed coefficient at hump is a function of L/b and Lf/b and can be read from Figure 12.  $C_{v\text{hump}} = 6.28$

$$V_{\text{Hump}} = (6.28) (32.2 \times 7.69)^{1/2} = 97.56 \text{ ft/sec}$$

$$\Delta = \text{Weight on Water} = \Delta_o \left[ 1 - \left( \frac{V}{V_G} \right)^2 \right]$$

$$\Delta_o = \text{Gross Weight} = 240,000 \text{ lbs}$$

$$V = V_{\text{Hump}} = 97.56 \text{ ft/sec}$$

$$V_G = \text{Getaway Speed} = 207 \text{ ft/sec}$$

$$\Delta = 240,000 \left[ 1 - \left( \frac{97.56}{207} \right)^2 \right] = 186,687 \text{ lbs}$$

$$\tau_{\text{Hump}} = \text{Hump Trim} = \sigma + (\tau - \sigma)$$

$$\sigma = \text{Sternpost angle} = 10^\circ$$

The difference between hump trim and sternpost angle ( $\tau - \sigma$ ) can be read from Figure 13.  $(\tau - \sigma) = 2.65 \text{ deg}$

$$\tau_{\text{Hump}} = 10 + 2.65 = 12.65^\circ$$

$$\beta = \text{Deadrise} = 25^\circ$$

$$R = 186,687 (\tan 12.65) + \left( \frac{(.008 \sec 25 \tan 25)}{12.65} \right) (186,687)^{3/5} (97.56)^{9/5} = 43,703 \text{ lbs}$$

## High L/B Prediction Summary

The aerodynamic resistance at hump,

### Aerodynamic Drag at Hump:

$$D = \left[ .025 + .40 \frac{C_{Lmax}^2}{AR} \right] .0012 V^2 S$$

$$C_{Lmax} = \text{maximum Lift Coefficient} = 2.50$$

$$AR = \text{aspect Ratio} = 8.25$$

$$V_{Hump} = \text{hump Speed} = 97.56 \text{ ft/sec}$$

$$S = \text{wing Area} = 2274 \text{ ft}^2$$

$$D = \left[ .025 + .40 \frac{(2.50)^2}{8.25} \right] .0012 (97.56)^2 (2274) = 8520 \text{ lbs}$$

### Total Resistance at Hump:

$$R + D = 43703 + 8520 = 52223 \text{ lbs}$$

# High L/B Prediction Summary

## Resistance Approaching Getaway

The resistance approaching getaway can be estimated from Hugli and Van Dyck's (1955) equation. An assumption must be made on the trim angle approaching take-off. A good approximation is to assume the trim angle is the average of the upper and lower trim limits, providing the pilot the widest range of margin on take-off. However, there may be other reasons for the pilot to choose a higher or lower trim angle, within the range of stability.

### Hydrodynamic Resistance Approaching Getaway:

|   | $\frac{V}{V_G}$ |            |            |            |             |             |
|---|-----------------|------------|------------|------------|-------------|-------------|
|   | <u>.80</u>      | <u>.85</u> | <u>.90</u> | <u>.95</u> | <u>.975</u> | <u>1.00</u> |
| $V_G$ = Getaway Speed =   | 207.00          |            |            |            |             |             |
| $V$ = Speed = $V_G \left( \frac{V}{V_G} \right) =$  | 165.60          | 175.95     | 186.30     | 196.15     | 201.82      | 207.00      |
| $\Delta_o$ = Gross Weight =   | 240000          |            |            |            |             |             |
| $\Delta$ = Weight on Water<br>= $\Delta_o \left[ 1 - \left( \frac{V}{V_G} \right)^2 \right] =$                        | 86400           | 66600      | 45600      | 23400      | 11850       | 0           |
| $\beta$ = Deadrise =  | 25°             |            |            |            |             |             |
| $\tau_{UL}$ = Upper Limit Trim<br>)   | 10.80           | 11.60      | 11.50      | 10.60      | 9.90        |             |
| $\tau_{LL}$ = Lower Limit Trim<br>)   | 4.50            | 2.90       | 1.90       | 2.30       | 3.70        |             |
| $\tau_{Avg} = (\tau_{UL} + \tau_{LL})/2 =$  | 7.65            | 7.25       | 6.70       | 6.45       | 6.80        |             |
| $R = \Delta \tan \tau_{Avg}$<br>+ $\left[ \frac{.008 \sec \beta \tan \beta}{\tau_{Avg}} \right] \Delta^{3/5} V^{9/5}$ |                 |            |            |            |             |             |
| =   | 16470           | 13370      | 10036      | 6235       | 3785        | 0           |



# High L/B Prediction Summary

## Aerodynamic Drag Approaching Getaway:

|  |        | $\frac{V}{V_G}$ |            |            |            |             |             |
|--|--------|-----------------|------------|------------|------------|-------------|-------------|
|  |        | <u>.80</u>      | <u>.85</u> | <u>.90</u> | <u>.95</u> | <u>.975</u> | <u>1.00</u> |
| $V_G$ = Getaway Speed =  | 207.00 |                 |            |            |            |             |             |
| $V$ = Speed = $V_G \left(\frac{V}{V_G}\right)$ =                                   |        | 165.60          | 175.95     | 186.30     | 196.65     | 201.82      | 207.00      |
| $C_{Lmax}$ = Maximum Lift Coef. =  | 2.50   |                 |            |            |            |             |             |
| AR = Aspect Ratio =  | 8.25   |                 |            |            |            |             |             |
| S = Wing Planform Area =   | 2274   |                 |            |            |            |             |             |
| $D = \left[ .025 + .40 \frac{C_{Lmax}^2}{AR} \right] \left[ .0012 V^2 S \right] =$ |        | 24547           | 27712      | 31068      | 34616      | 36460       | 38356       |

## Total Resistance Approaching Getaway:

|                             |       | $\frac{V}{V_G}$ |            |            |            |             |             |
|-----------------------------|-------|-----------------|------------|------------|------------|-------------|-------------|
|                             |       | <u>.80</u>      | <u>.85</u> | <u>.90</u> | <u>.95</u> | <u>.975</u> | <u>1.00</u> |
| V = Speed                   |       | 165.60          | 175.95     | 186.30     | 196.65     | 201.82      | 207.00      |
| R = Hydrodynamic Resistance | 16470 | 13370           | 10036      | 6235       | 3785       |             | 0           |
| D = Aerodynamic Drag        | 24547 | 27712           | 31068      | 34616      | 36460      | 38356       |             |
| R+D = Total Resistance      | 41017 | 41082           | 41104      | 40851      | 40245      | 38356       |             |

# High L/B Prediction Summary

## Landing Impact Acceleration

$$\eta = (\gamma + \theta_w) (.0021) \left[ \frac{V}{\Delta_o^{1/6}} \right]^2 \left[ 1 - \frac{\beta}{90} \right] / C_{\Delta_o}^{1/3}$$

Assume seaplane is landing in state 4 head seas where

$$h_1/3 = 6.9 \text{ ft.}$$

$$b = 7.69 \text{ ft}$$

$$L = 128 \text{ ft}$$

$$V = \text{Landing Speed} = 188 \text{ ft/sec}$$

$$\Delta_o = 240,000 \text{ lb}$$

$$\beta = 25^\circ$$

$$C_{\Delta_o} = \frac{\Delta_o}{wb^3} = \frac{240,000}{(64) \times (7.69)^3} = 8.25$$

$$\gamma = 5^\circ \text{ (typical value)}$$

$$\begin{aligned} \theta_w &= \tan^{-1} \frac{h_1/3 \pi}{3 L} = \tan^{-1} \frac{(6.9) (\pi)}{(3) (128)} \\ &= \tan^{-1} .056 = 3.2^\circ \end{aligned}$$

Thus:

$$\eta = (5 + 3.2) (.0021) \left[ \frac{188}{240,000^{1/6}} \right]^2 \left[ 1 - \frac{25}{90} \right] / 8.25^{1/3}$$

$$\eta = 3.5g \text{ at center-of-gravity}$$

If the flight path angle is taken as,

$$\gamma_{\max} = \tan^{-1} \frac{C_D}{C_{L\max}} = \tan^{-1} \frac{.328}{2.50} = 7.5^\circ$$

$$\eta_{\max} = \left[ \frac{7.5 + 3.2}{5 + 3.2} \right] 3.5 = 4.3g \text{ at center-of-gravity}$$

This impact acceleration is expected to occur approximately 1 out of 100 landings. Note, in the case of a "sister-keel" designed for full separation of the flow, the effective beam for impact acceleration may be reduced to the beam measured at the sister keel.

References for Chapter

"Aviation Week" 23 June 1952. Page 32-37

Batterson, S.A. , and McArver, A. E. , "Water Landing Investigation of a Model Having a Heavy Beam Loading and a 30-deg Angle of Deadrise", NACA TN-2015, February 1950.

Flickinger, Paul J ."Model Basin Tests of Bow Spray and Main Spray of Auxiliary Low Chine Bow Modification to XP5M-1 Hull" , Davidson Laboratory, Stevens Institute of Technology, Report 403, October, 1950.

Davidson, k. S. M. , and Locke, F.W. S. Jr. , " Some Systematic Model Experiments on the Porpoising Characteristics of Flying-Boat Hulls" , NACA ARR No. 3F12, June 1943.

Froscher, C. T. and Greenwood, R. B., " Analytical Determination of Lower Limit Stability of Flying Boats" , Davidson Laboratory, Stevens Institute of Technology Note 195, May 1951.

Flickinger, Paul J."Hydrodynamic Investigation of a 1/20-Scale, 15:1 Length-Beam Ratio, Long Afterbody, Flying-Boat Hull Model" , Davidson Laboratory, Stevens Institute of Technology, Report 420, July 1951

Haar, M.I., "Effect of Forebody-Afterbody Proportions and Length- Beam Ratio on the Hydrodynamic Characteristics of a Series of Flying-Boat Hull Models", Davidson Laboratory, Stevens Institute of Technology Report 465 October 1952.

Hugli, W.C. Jr. and Axt, W.C. "Hydrodynamic Investigation of a Series of Hull Models Suitable for Small Flying Boats and Amphibians." NACA TN-2503, November 1951

Hugli, W.C., Jr. , and Van Dyck, R. L. , "A Limitations Analysis of Hulls and Hydro-Skis for Water Based Aircraft, Davidson Laboratory, Stevens Institute of Technology Report 562, April 1955.

## High L/B Prediction Summary

Korvin-kroukovsky, B. V. , Savitsky, D. and Lehman W.F. "Wake Profile of a Vee Planing Surface Including Test Data on a 30° Deadrise Surface" , Davidson Laboratory, Stevens Institute of Technology Report 339, April 1949.

Locke, F.W.S. Jr. " Systematic Model Experiments on the Hydrodynamic Characteristics of Flying Boat Hulls", Davidson Laboratory, Stevens Institute of Technology Report No. 217, December 1942.

Locke, F.W.S. Jr., "General Main Spray Tests of Flying Boat Models in the Displacement Range", NACA, ARR No. 5A02, April 1945.

Locke, F.W.S. Jr., "The Effect of Forebody Proportions on the Main Spray Characteristics of Flying Boats", BuAer A.D.R. Report No. 1027 December 1947.

Locke, F.W.S. Jr., "A Note on the Effect of Beam Loading on the Impact of Hydro -Skis", NAVAER DR Report No. 1356, October 1951, CONFIDENTIAL.

Martin, M., "Theoretical Determination of Porpoising Instability of High Speed Planing Boats", Journal of Ship Research, March 1978.

Miller, R.W., "Water-Landing Investigation of a Flat -Bottom V -Step Model and Comparison with a Theory Incorporating Planing Data", NACA TN-2932, May 1953.

Milwitzky, B. "A Generalized Theoretical and Experimental Investigation of the Motions and Hydrodynamic Loads Experienced by V -Bottom Seaplanes During Step-Landing Impacts" , NACA TN-1516, 1948.

Savitsky, D. "Hydrodynamic Design of Planing Hulls", SNAME, Marine Technology. Vol. 1, No. 1 October 1964.

Savitsky, Daniel and Roper, John. A Summary of Hydrodynamic Technology Related to Large Seaplanes and Methods for Estimating Their Performance. Davidson Laboratory Report SIT-DL-90-9-2647. JUNE 1990.

Schnitzer, E., "Theory and Procedure for Determining Loads and Motions in Chine- Immersed Hydrodynamic Impacts of Prismatic Bodies" , NACA TN-2813, 1952.

## High L/B Prediction Summary

Scheider, M.G. and King, D.A. "Phase II Report - High Speed Water-Basing Study," Glenn L. Martin Co. Engineering Report No. 5845, July 19, 1953.

Smiley, Robert F., "The Application of Planing Characteristics to the Calculation of the Water -Landing Loads and Motions of Seaplanes of Arbitrary Constant Cross Section", NACA TN-2814, 1952.

## Weights

### Chapter 15. Weights

M.G. Morabito, 2024

#### 15.1 Payload, Range and Gross Weight

#### 15.2 Weight Groups

#### 15.3 Froude Scaled Weight Equations

#### 15.4 Attempt to Extrapolate to High L/B

It is assumed that the designers have access to recent aircraft structural and equipment weights. This section focuses on the weights specific to seaplanes.

#### 15.1 Payload, Range and Gross Weight

Odedra, Hope and Kennell (2004) put together a database of seaplane information compiled from sources including US Navy interdepartmental libraries, professional societies, historical centers/museums, as well as Internet searches. The purpose was to guide the early-stage sizing of a seaplane conceptual design.

Figure 1 shows graphs of Length vs. Gross Weight, Wingspan vs. Gross Weight and (Gross Weight - Empty Weight) vs. Gross Weight. The (Gross Weight - Empty Weight) can be used for either fuel or useful payload. Figure 2 shows how this applies to operations. The graph includes range on the horizontal and payload on the vertical. As range increases, the required fuel increases, resulting in lower payload. Figure 3 shows the empty weight fraction,

$$\text{Empty Weight Fraction} = (\text{Empty Weight})/(\text{Gross Weight})$$

The figure shows that (with significant scatter), the seaplanes and landplanes built prior to 1950 had similar empty weight fractions. Since that time, the post 1950 landplanes have had a reduction in empty weight as a result of technological developments.

## Weights

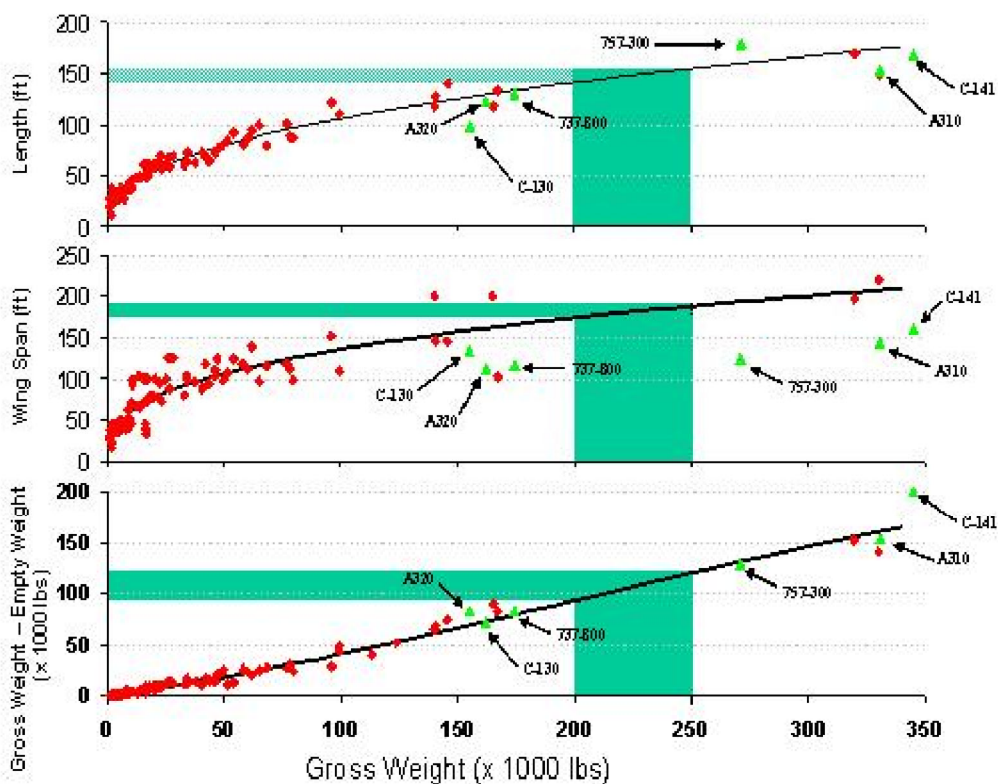


Figure 1: Aircraft length, weight, and wing span. Red=Seaplanes, Green = Select Landplanes. (Odedra, 2004)

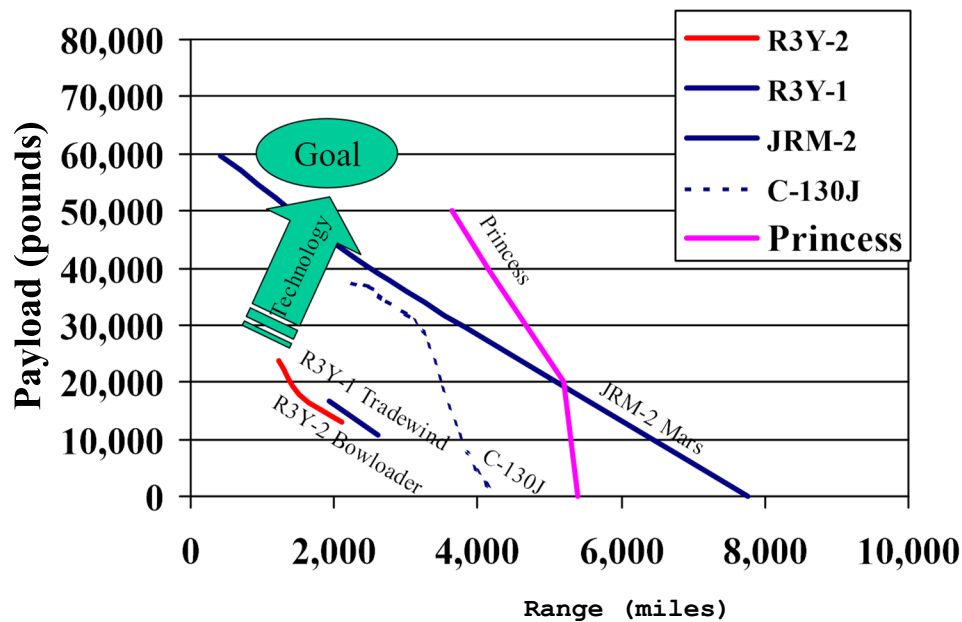


Figure 2: Payload-Range parametric data (Odedra, 2004)

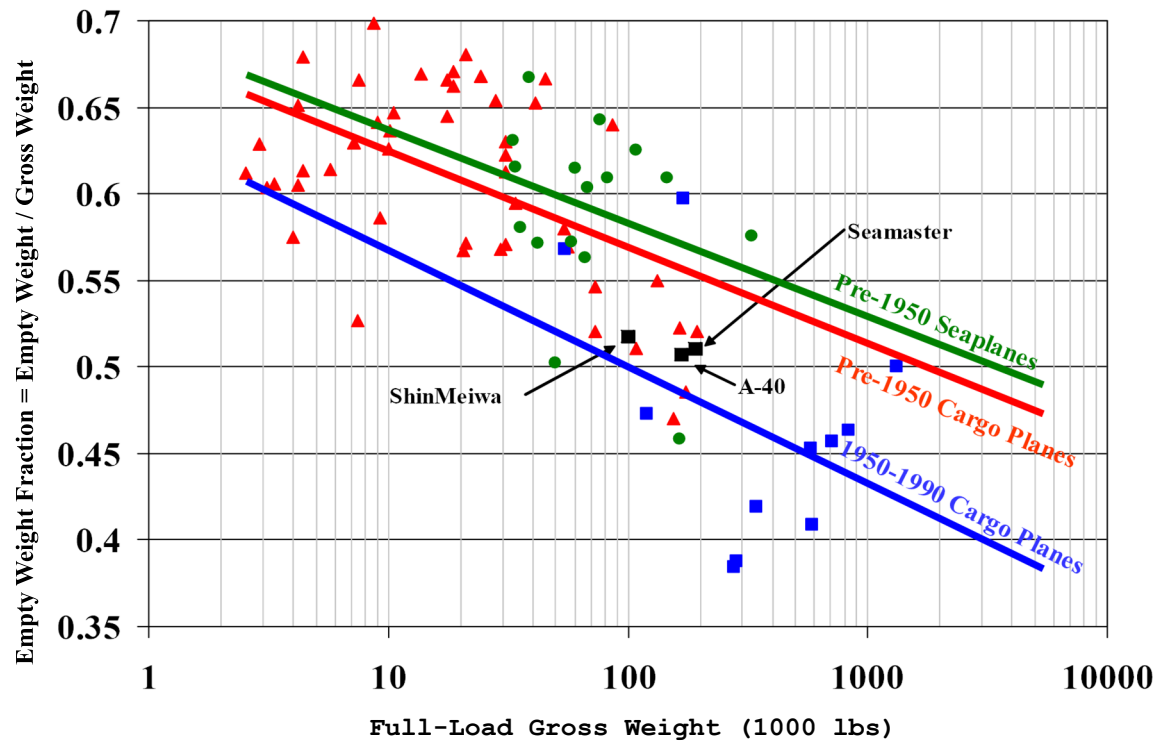


Figure 3: Empty weight fraction (Odedra, 2004)



15.2 Weight Groups

Locke (1945 and 1953) studied the weight groups of major components for Seaplanes and for Landplanes. The primary weight groups discussed below are those that would likely vary between landplanes and seaplanes. It is assumed that the other mechanical system weights can be found more accurately with modern references. Because of the rarity of the original publication, the relevant data tables are included in Tables 1 and 2. The equations for each weight group are included on Figures 4-11, with variables defined as follows;

$b$  = Wingspan (ft)

$d$  = Length of float bracing (ft)

$B$  = Body Width (ft)

$F_L$  = Landing Speed Froude Number (simplified) =  $V_L/\sqrt{B}$

$H$  = Body Height (ft)

$L$  = Body Length (ft)

$n$  = Load Factor (g's)

$S_T$  = Tail Area (ft<sup>2</sup>)

$V_L$  = Landing Speed (ft/s)

$W_B$  = Weight of float bracing (lb)

$W_F$  = Weight of auxiliary floats (lb)

$W_G$  = Gross Weight (lb)

$W_H$  = Hull Weight (lb)

$W_B$  = Fuselage Weight (lb)

$W_T$  = Tail Group Weight (lb)

$W_W$  = Wing Group Weight (lb)

Body Group - Hull or Fuselage

Figure 4 shows the hull weight of flying boats and the fuselage weight of landplanes as a function of the characteristic area, the product of Length\*(Beam + Height), as defined in Figure 5. This characteristic area represents the structure and plating. Locke (1945 and 1953) showed that either area or the volume Length\*Beam\*Height give about equal scatter, but the area measure was slightly better.

The comparison of the two charts shows that the flying boat falls between the weights of commercial and military landplanes. Locke (1943) suggests that the 40% difference between military and commercial landplanes is because of the cutout from the bomb bay. No such difference between commercial and military was seen for the seaplanes.

## Weights

### Wing Group

Figure 6 shows the Wing Group Weights as a function of the wingspan  $b$ . This weight includes wing structure only and does not include engines, nacelles, landing gear, or other mechanical systems within the wing. Locke (1945) showed that Flying Boats and Landplanes collapsed onto the same curve when compared on the basis of the product of Ultimate Flight Load Factor,  $n$  (This is the design acceleration value) and the gross weight. This product is the ultimate load that the wing carries. Load factors are shown in Figure 7, with both Landplanes and Seaplanes included.

### Tail Group

Figure 8 shows the Tail group weights for Seaplanes and Landplanes as a function of the tail area. The weight of the seaplane tail group is less than the landplane. Locke (1945) shows that this is because the landplanes are typically designed for higher speeds. When compared on the basis of the wing loading, both seaplanes and landplanes collapse onto the same curve.

### Landing Gear

Figure 9 shows the weight of landing gear and retracting mechanism for both amphibious seaplanes and for landplanes. Both are similar weights.

### Auxiliary Floatation

Figure 10 shows a comparison of the weights of Auxiliary Floatation, including Sponsons, Retractable Floats, and Fixed Floats. The fixed floats have the lowest weight, followed by the retractable floats. Sponsons are significantly heavier for the required righting moment due to their inboard placement.

Figure 11 shows the separate contributions of the tip floats themselves and tip float bracing. The weight of the floats themselves is proportional to the displaced volume when submerged. The bracing weight is a function of the length of the bracing and the displaced volume of the float.

### Seaplane Equipment

Figure 12 shows the additional marine equipment needed to be carried by a flying boat.

### 15.3 Froude Scaled Weight Equations

Locke (1953) revisited the seaplane weights, developing a scaling process based on Froude similarity. The goal was to unite the various weight scaling equations from many different structures into a common format. He shows that the equations are about as accurate as the ones presented in Figures 4-12; however, more data on disparate structures can be used to develop the equations, and they yield thought-provoking results. The following equations show the Froude weight scaling for Volume, Area, and Length.

$$\begin{aligned} W &= [(\lambda^3)]^n \\ W &= [(\lambda^2)^{3/2}]^n \\ W &= [(\lambda)^3]^n \end{aligned}$$

The exponent "n" would be 1.0 if everything were geometrically similar; however, it has been shown that larger structures can be built more efficiently. This is attributed to better use of available structural sizes and is known as the "minimum gauge law." Based on large amounts of data for aircraft structures, Locke arrives at the exponent  $n = 5/6$ . By using Froude scaling in this way, a common exponent is used for all of the weight scaling of various structures, including hull, wings and tails. Using  $n = 5/6$ , scaling relations become,

$$\begin{aligned} W &\equiv \text{volume}^{5/6} \\ W &\equiv \text{area}^{5/4} \\ W &\equiv \text{length}^{5/2} \end{aligned}$$

Based on the area scaling for hull and floats discussed above, this common format yields,

$$W_h = K_2 [L(B+H)]^{5/4} \quad (7)$$

$$K_2 = 0.506 \pm 8\% \text{ for hulls,}$$

$$K_2 = 0.674 \pm 4\% \text{ for main floats,}$$

$$K_2 = 0.707 \pm 12\% \text{ for auxiliary floats.}$$

Note, the term  $K_2$  is not the same as the Davidson bottom loading coefficient, but rather just another constant (they are numbered sequentially in the paper). Locke demonstrates that the weights of hulls, main floats, and auxiliary floats all collapse on the same basis with the addition of a Froude number based on landing speed. The definition of Froude number is,

$$F = v / \sqrt{g \lambda}$$

## Weights

Where,  $v$  is a characteristic speed and  $\lambda$  is a characteristic length. Using landing speed as the characteristic speed, beam as the characteristic length, and dropping the  $g$  for simplicity (it becomes part of the constant later),

$$F_L = V_L / B^{\frac{1}{2}}$$

Where  $V_L$  is the landing speed, in ft/s. Locke supposes that the structural weight constant is a function of this landing speed Froude number,

$$K_2 \equiv F_L^m$$

Locke suggests " $m$ " = 2/3, based on analysis of hull weight data, and arrives at a general equation for the weight of hulls, main floats, and auxiliary floats,

$$W_h = K_4 [L (B + H)]^{5/4} [F_L]^{2/3}$$
$$K_4 = 0.0667 \pm 11\%$$

This equation is graphed in Figure 13.

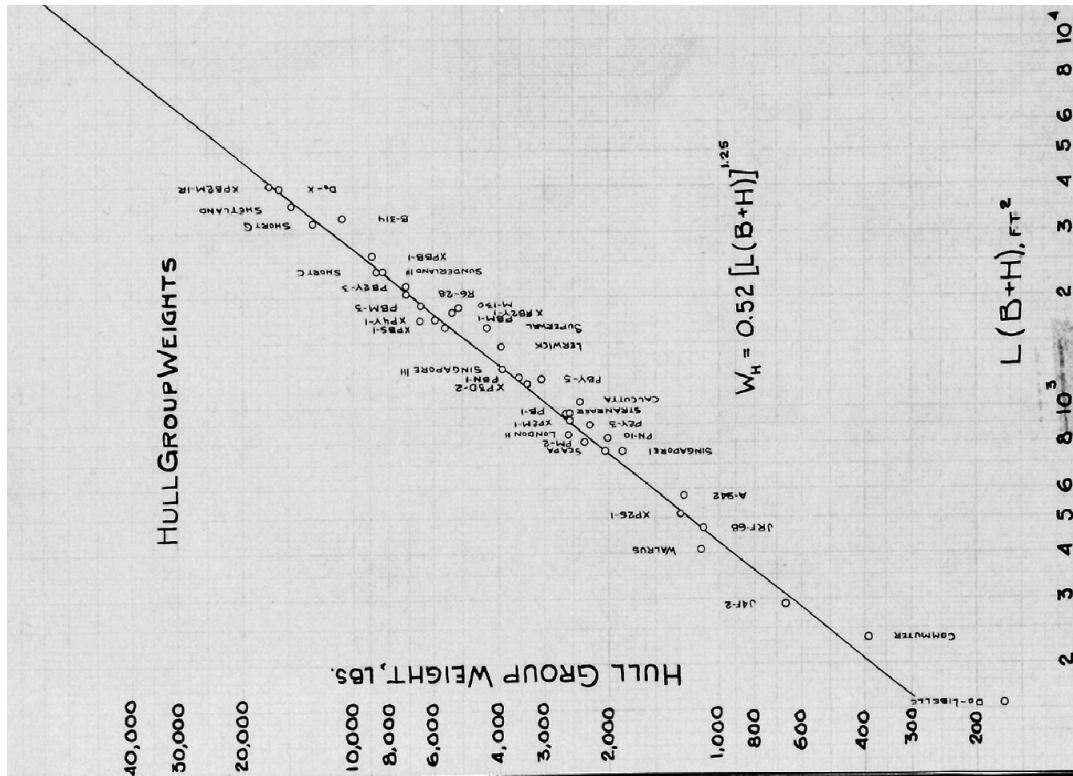
### 15.4 Attempt to Extrapolate to High L/B

Locke's weight scaling relationships are based on typical hulls as of the early 1950s (L/B around 6 or a little above). Extrapolation to very high L/B may invalidate the scaling, since the hulls are no longer geometrically similar. Benscoter (1947) discusses the scaling relations for high L/B hulls, showing results for 10 different categories of: Plating, Stringers, Keel, Frames, Bulkheads and Flooring. While holding the impact load factor, hull depth and the Davidson bottom loading coefficient constant, he computes the structural weight for a range of hulls from L/B = 6 to L/B = 15, and shows that the higher L/B seaplanes have reduced structural weight. He suggests that hulls with narrower beam may also be able to be designed with reduced impact load factors, further reducing structural weight.

For the purposes of testing Locke's (1945, 1953) weight scaling relationships, Benscoter's structural weights are normalized based on L(B+H) and LBH below. It shows below that when using Locke's area scaling  $[L (B + H)]$  and extrapolating to very high L/B, we may over-predict the structural weight of the hull. Interestingly, using volume scaling  $[L B H]$  under-predicts the weight. The difference between these two methods is the relative importance of length in both of the scaling methods. The main "takeaway" from this is that major changes in L/B and structural material require additional source data and careful analysis.

|             | L/B = 6 | L/B = 9 | L/B = 12 | L/B = 15 |
|-------------|---------|---------|----------|----------|
| Ws/[L(B+H)] | 1       | 0.87    | 0.81     | 0.78     |
| Ws/[LBH]    | 1       | 1.03    | 1.10     | 1.17     |

# Weights



## Weights

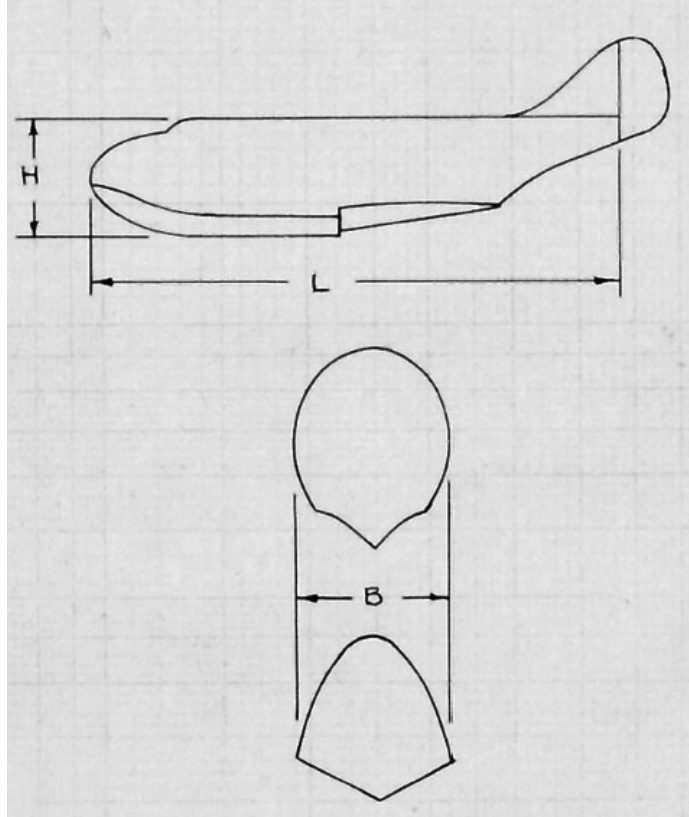
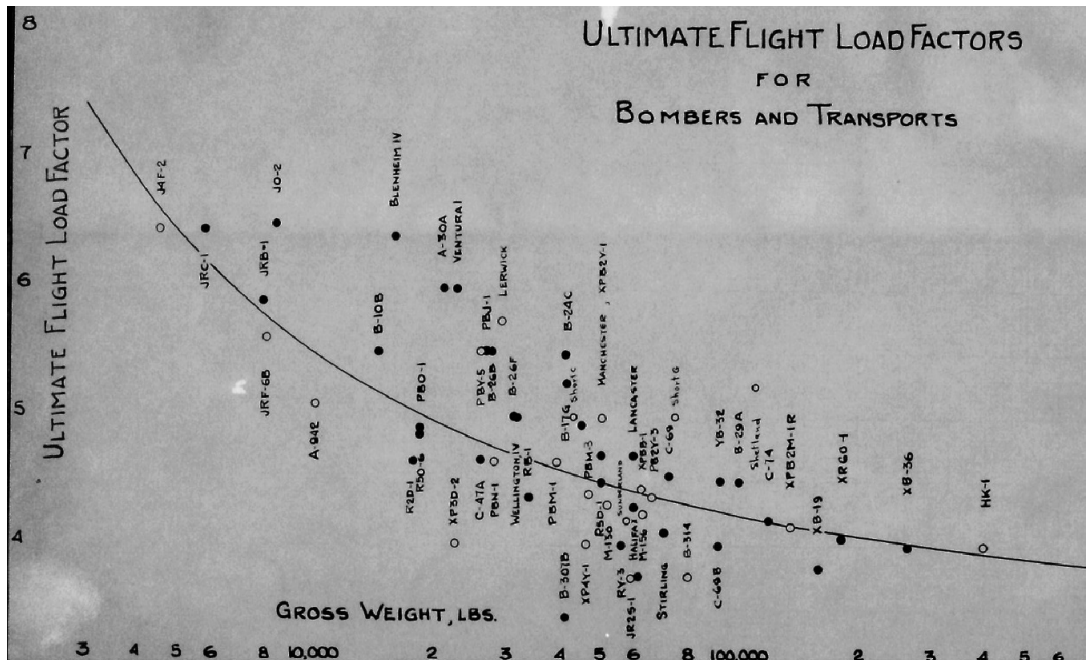
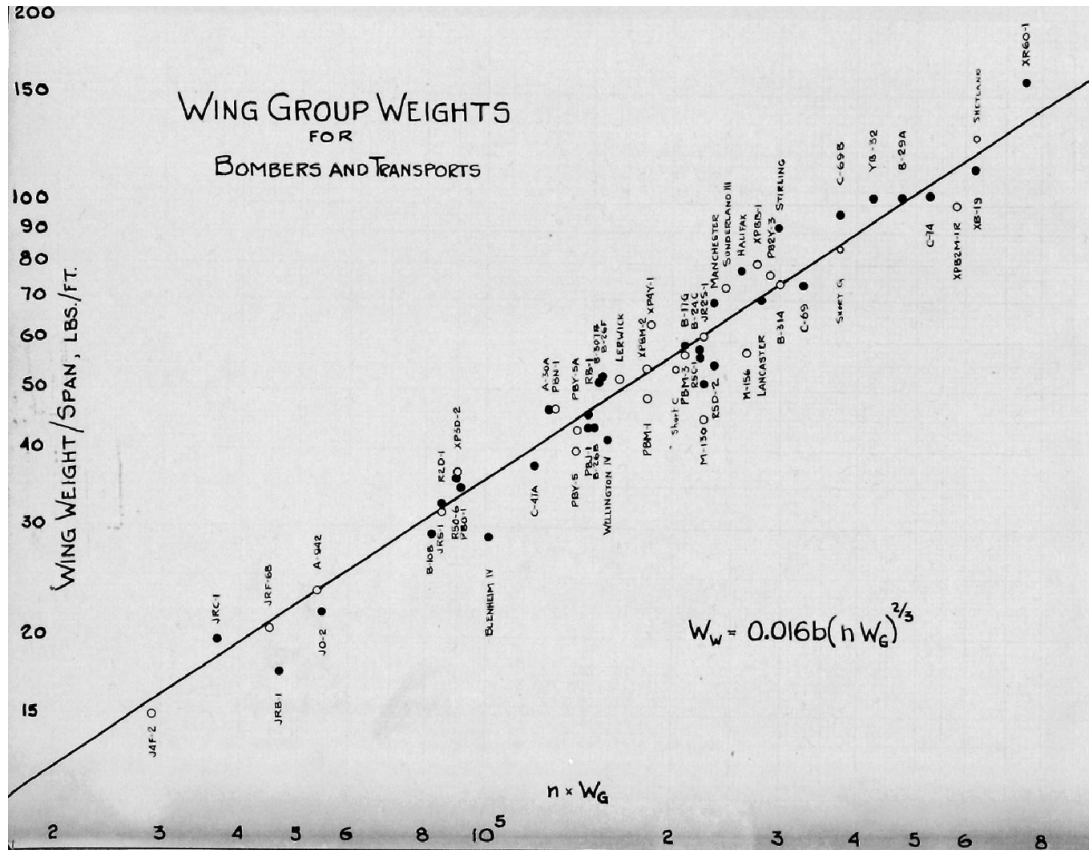


Figure 5: Definition of  $L, B, H$  (Taken from Locke, 1945)



# Weights

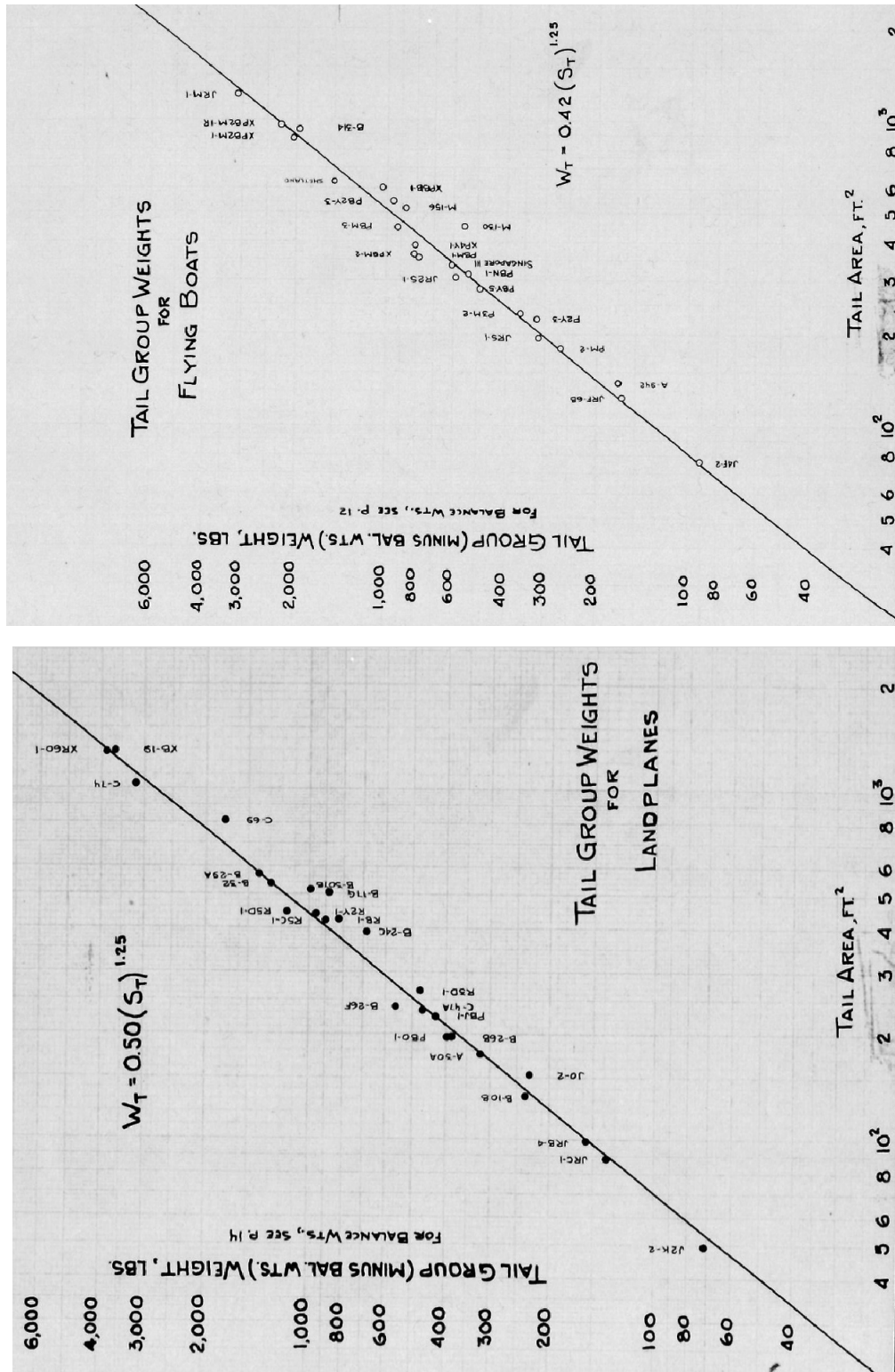


Figure 8: Tail Group Weights. Flying Boats (top), Landplanes (bottom). Taken from Locke, 1945. Note: Locke shows that when compared with wing loading as a parameter, landplanes and flying boats collapse onto one curve.



# Weights

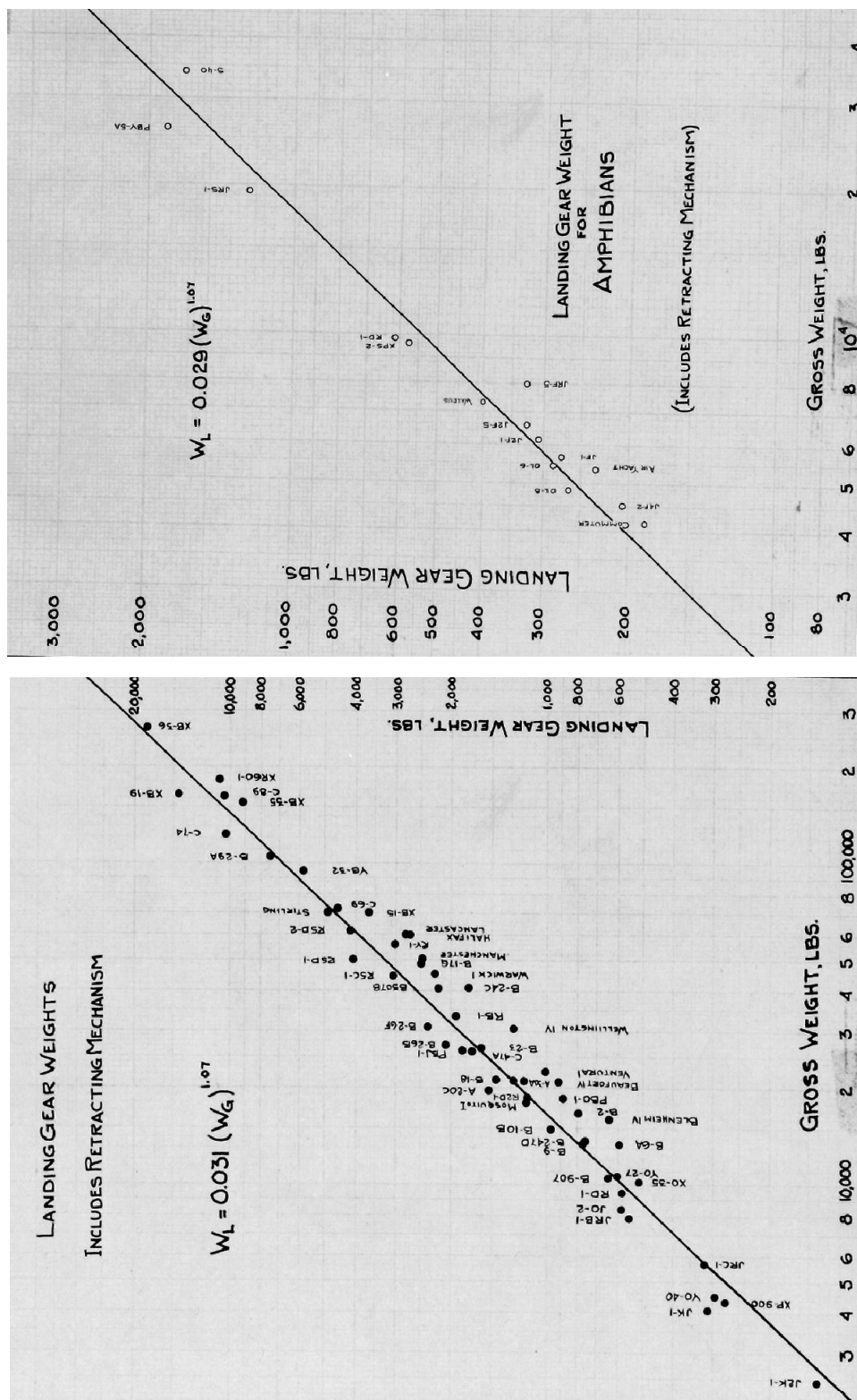


Figure 9: Landing Gear for Amphibians (top) and Landplanes (bottom). Taken from Locke, 1945

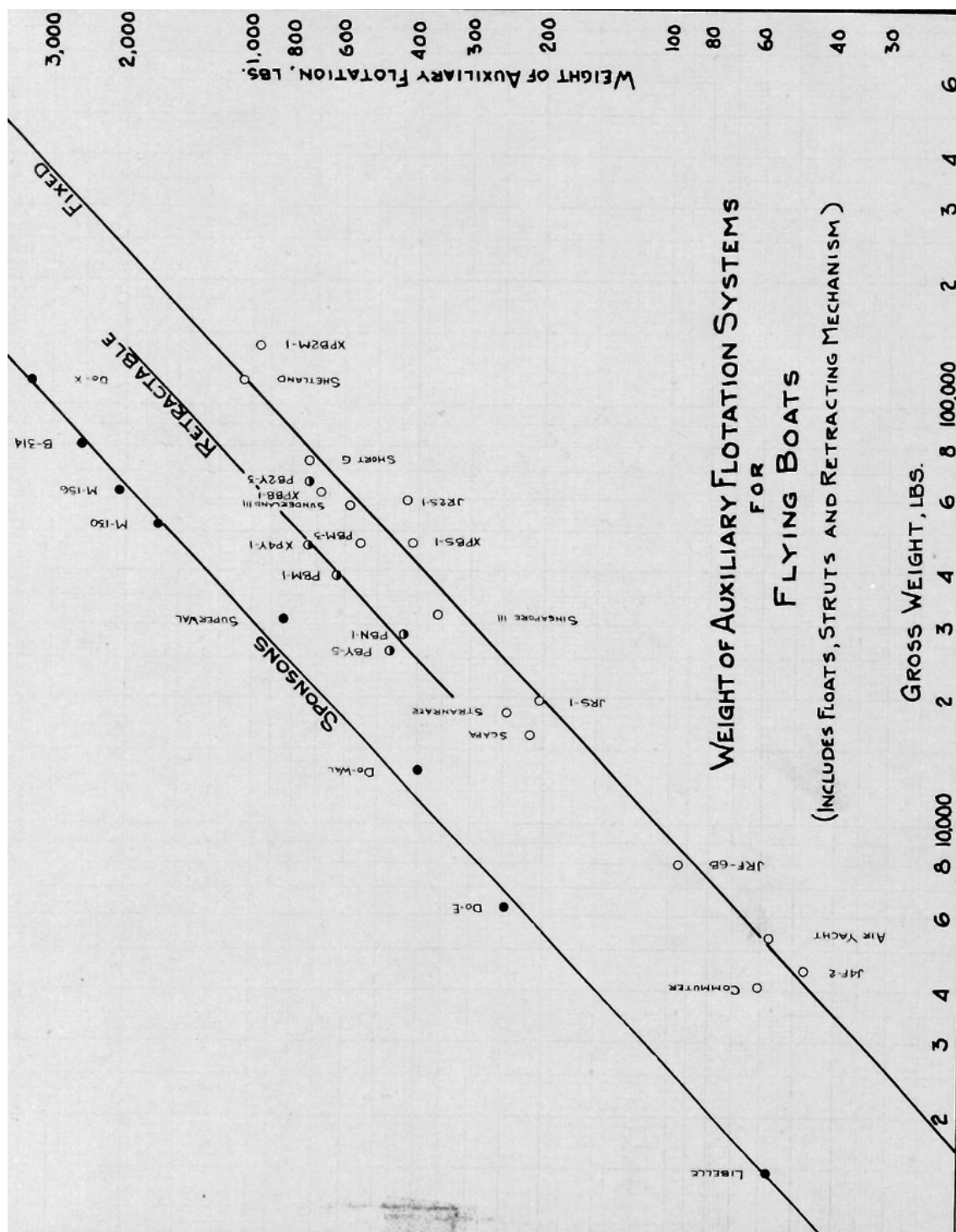


Figure 10: Comparison of Fixed Floats, Retractable Floats and Sponsons for Flying Boats. Taken from Locke, 1945.

## Weights

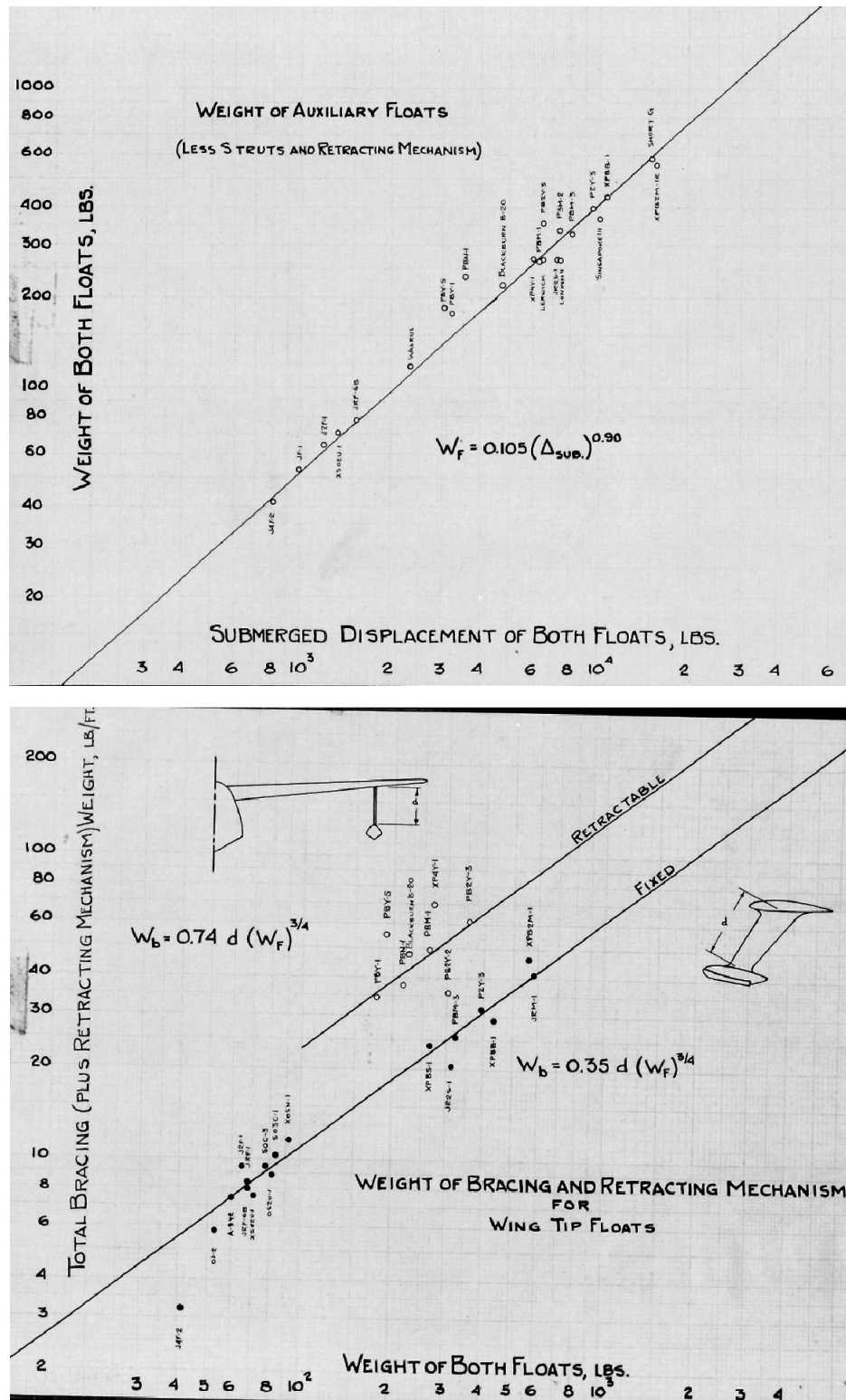


Figure 11: Separate Consideration of Weight of Floats (top) and Float Bracing (bottom). Taken from Locke, 1945.

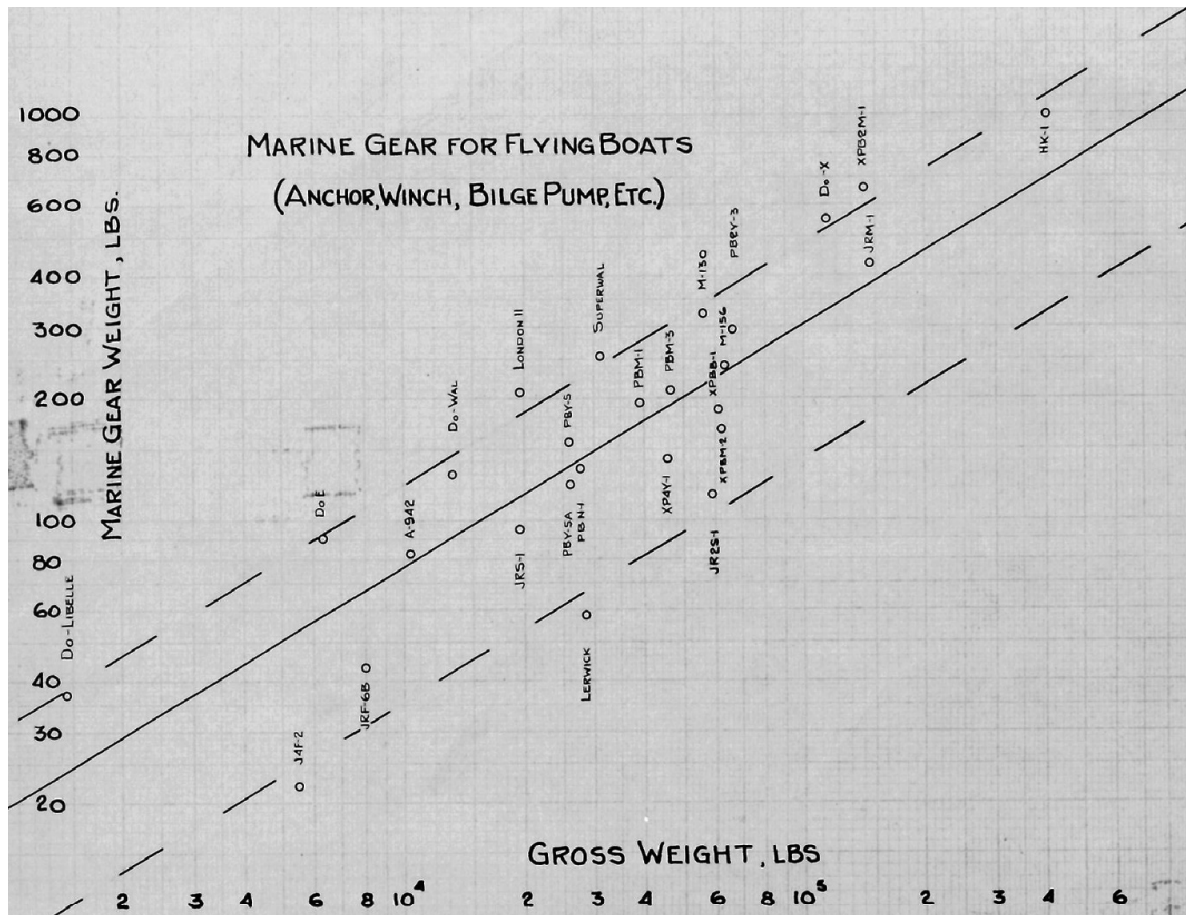


Figure 12: Weight of Marine Gear for Flying Boats. Taken from Locke, 1945.

# Weights

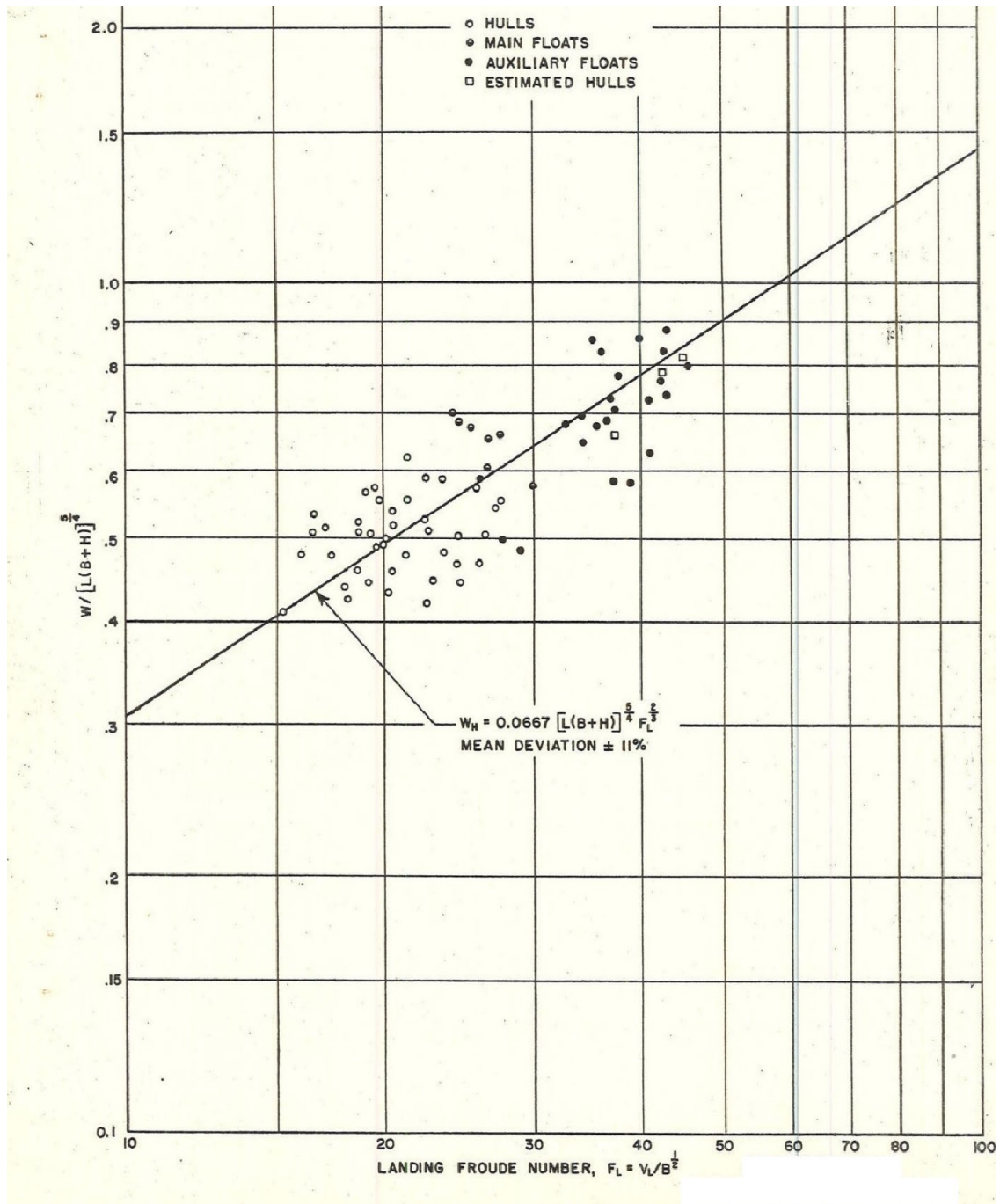


Figure 13: Generalized Equation for Hull, Main Floats and Auxiliary Floats (Locke, 1953)

# Weights

Table 1: Flying Boat Weight Groups, 1 of 4 (Taken from Locke, 1945)

| MANUFACTURER  | MODEL        | GROSS WEIGHT @ S.L. | V <sub>MAX</sub><br>m.p.h. | WING                 |                 |       |             |                |               |              | TAIL            |              |                |
|---------------|--------------|---------------------|----------------------------|----------------------|-----------------|-------|-------------|----------------|---------------|--------------|-----------------|--------------|----------------|
|               |              |                     |                            | ULTIMATE FLIGHT LOAD | AREA            | SPAN  | TAPER RATIO | ROOT THICKNESS | TIP THICKNESS | GROUP WEIGHT | TOTAL AREA      | BASIC WEIGHT | BALANCE WEIGHT |
|               |              |                     |                            | Factor               | ft <sup>2</sup> | ft    |             | ft             | ft            | lbs          | ft <sup>2</sup> | lbs          | lbs            |
|               |              | lbs                 |                            |                      |                 |       |             |                |               |              |                 |              |                |
| Grumman       | J4F-2        | 4,500               | 128                        | 6.45                 | 245             | 40.0  | 2.00        | 1.08           |               | 596          | 76.7            | 90           | 18             |
| KeyStone      | Commuter     | 4,150               |                            |                      |                 |       |             |                |               | 613          |                 | 123          |                |
| Supermarine   | Walrus       | 7,260               | 124                        |                      |                 |       |             |                |               | 1121         |                 |              |                |
| Grumman       | JRF-6B       | 8,000               | 156                        | 5.60                 | 315             | 49.0  | 2.00        | 1.50           | 0.46          | 1011         | 123.8           | 163          | 15             |
| Sikorsky      | XP2G-1       | 9,640               |                            |                      |                 |       |             |                |               |              |                 |              |                |
| Fairchild     | A-342        | 10,500              | 173                        | 5.10                 | 483             | 56    | 1.92        | 2.14           | 0.55          | 1300         | 139             | 170          |                |
| Short         | SINGAPORE II | 13,385              |                            |                      |                 |       |             |                |               |              |                 |              |                |
| Supermarine   | Scapa        | 16,700              |                            |                      |                 | 75    |             |                |               | 2452         |                 | 375          |                |
| NAF           | PN-10        | 17,000              |                            |                      |                 |       |             |                |               |              |                 |              |                |
| Martin        | PM-2         | 17,200              |                            |                      |                 |       |             |                |               |              | 180             | 267          | 0              |
| Supermarine   | Sirraway     | 18,710              | 150                        |                      | 1452            | 85    |             |                |               | 2907         |                 | 556          |                |
| Savo          | London II    | 19,230              | 142                        |                      | 1425            | 80    |             |                |               | 3428         | 270             | 617          |                |
| Sikorsky      | JRS-1        | 19,500              | 186                        | 4.35                 | 781             | 86    |             | 2.07           |               | 2705         | 194.1           | 314          |                |
| Short         | CALCUTTA     | 19,700              |                            |                      |                 |       |             |                |               |              |                 |              |                |
| Martin        | XP2M-1       | 20,170              |                            |                      |                 |       |             |                |               |              |                 |              |                |
| Consolidated  | P2Y-3        | 20,560              |                            |                      |                 |       |             |                |               |              | 225             | 320          | 0              |
| Douglas       | XP3D-2       | 22,500              |                            | 4.00                 | 1294            | 95    |             |                |               | 3470         |                 |              |                |
| Martin        | P3M-2        | 25,500              |                            |                      |                 |       |             |                |               |              | 232             | 359          | 0              |
| Consolidated  | PBY-5        | 26,000              | 175                        | 6.50                 | 1400            | 104   | 1.50        | 2.16           |               | 4134         | 280             | 492          | 24             |
| Consolidated  | PBY-SA       | 26,000              | 169                        | 8.10                 | 1400            | 104   | 1.50        | 2.16           |               | 4461         | 280             | 509          | 24             |
| Boeing        | PB-1         | 26,700              |                            |                      |                 |       |             |                |               |              |                 |              |                |
| NAF           | PBW-1        | 28,000              | 174                        | 4.65                 | 1400            | 104.3 | 1.50        | 2.15           |               | 4812         | 316             | 533          | 6              |
| Savo          | Lerwick      | 28,800              | 201                        | 5.73                 | 845             | 81    |             |                |               | 4190         | 217             | 613          |                |
| Dornier       | Super-Wal    | 31,100              |                            |                      |                 |       |             |                |               |              |                 |              |                |
| Short         | SINGAPORE II | 31,500              |                            |                      | 1760            |       |             |                |               | 4678         | 337             | 607          |                |
| Martin        | PBM-1        | 39,000              |                            | 4.65                 | 1406            | 118   | 3.00        | 3.61           | 0.54          | 5794         | 359             | 793          | 81             |
| Short         | C            | 42,600              | 200                        | 5.00                 | 1500            | 114   | 2.48        |                | 0.78          | 6192         | 307             | 628          |                |
| Consolidated  | XP4Y-1       | 46,000              |                            | 4.00                 | 1048            | 110   | 2.69        | 3.08           |               | 6959         | 390             | 814          |                |
| Martin        | PBM-3C       | 46,500              | 200                        | 4.40                 | 1408            | 118   | 3.00        | 3.61           | 0.60          | 6780         | 442             | 922          | 120            |
| Sikorsky      | XPBS-1       | 46,610              |                            |                      |                 |       |             |                |               |              |                 |              |                |
| Consolidated  | XPB2Y-1      | 50,000              |                            | 5.00                 | 1780            |       |             |                |               |              |                 |              |                |
| Martin        | M-130        | 52,000              |                            | 4.32                 | 2170            | 130   |             | 3.60           |               | 5991         | 454             | 558          |                |
| Short         | SINGAPORE II | 58,000              | 207                        | 4.20                 | 1687            | 112.8 | 2.60        | 4.42           | 0.78          | 8182         | 341             | 833          |                |
| Sikorsky      | JR2S-1       | 59,215              |                            | 3.75                 | 1670            | 124   | 4.03        | 3.61           |               | 7473         | 305             | 599          | 103            |
| Martin        | XPBM-2       | 62,000              |                            | 3.00                 | 1405            | 118   | 3.00        | 3.60           | 0.54          | 6372         | 368             | 810          | 80             |
| Boeing        | XPBB-1       | 62,000              | 214                        | 4.45                 | 1826            | 139.7 | 2.14        | 3.63           | 0.75          | 11,216       | 600             | 1040         | 35             |
| Martin        | M-156        | 63,000              |                            | 4.25                 | 2315            | 157   |             | 3.48           |               | 9,037        | 519             | 872          |                |
| Consolidated  | PB2Y-3       | 66,000              | 199                        | 4.39                 | 1780            | 115   | 1.75        | 3.42           | 0.86          | 8819         | 541             | 941          | 88             |
| Short         | R6-28        | 69,380              |                            |                      |                 |       |             |                |               |              |                 |              |                |
| Short         | G            | 74,500              | 213                        | 5.00                 | 2160            | 134.3 | 2.45        | 4.70           | 0.93          | 11427        | 440             | 1203         |                |
| Boeing        | 314          | 80,000              |                            | 3.75                 | 2867            | 152   |             | 5.24           |               | 11258        | 922.5           | 1961         | 320            |
| Dornier       | Do-X         | 114,640             |                            | 4.00                 | 5232            |       |             |                |               | 16,447       |                 | 1603         |                |
| Short         | Shetland     | 118,800             | 240                        | 5.25                 | 2636            | 150.3 | 3.06        | 4.95           | 0.78          | 19,340       | 638             | 1500         |                |
| Martin        | XPBM-1R      | 140,000             | 227                        | 4.15                 | 3683            | 200   | 3.94        | 5.92           | 0.90          | 20,146       | 961             | 2250         | 325            |
| Hughes Kaiser | HK-1         | 400,000             |                            | 4.00                 |                 | 320   |             |                |               |              |                 |              |                |



# Weights

Table 1 (cont'd): Flying Boat Weight Groups, 2 of 4 (Taken from Locke, 1945)

| MODEL        | HULL   |       |        |                 |        | AUX. FLOATS |      |        |              |            |            |         |            |  |  | LANDING GEAR |       |
|--------------|--------|-------|--------|-----------------|--------|-------------|------|--------|--------------|------------|------------|---------|------------|--|--|--------------|-------|
|              | LENGTH | BEAM  | HEIGHT | SUBMERGED       | WEIGHT | LENGTH      | BEAM | HEIGHT | SUBMERGED    | Wt. of Two | LENGTH     | Wt. of  | Wt. of     |  |  | MAIN         | AUX   |
|              |        |       |        | VOLUME          |        |             |      |        | DISPLACEMENT | FLOATS     | OF BEARING | BEARING | REFRACTING |  |  |              |       |
|              | ft     | ft    | ft     | ft <sup>3</sup> | lbs    | ft          | ft   | ft     | BOTH         | lbs        | lbs        | lbs     | lbs        |  |  | lbs          | lbs   |
| J4F-2        | 29.0   | 4.25  | 5.75   |                 | 664    | 6.2         | 1.72 | 1.75   | 810          | 40.4       | 2.1        | 6.6     |            |  |  | 173          | 31 T  |
| Commuter     | 28.0   | 5.7   | 4.7    |                 | 390    |             |      |        |              |            |            |         |            |  |  |              |       |
| Walrus       | 34.5   | 5.35  | 6.40   |                 | 1115   | 7.76        | 2.70 | 1.88   | 2320         | 118        | 1.4        | 6.4     |            |  |  | 360          | 40 T  |
| JRF-6B       | 38.0   | 5.00  | 8.50   |                 | 1106   | 6.5         | 1.91 | 2.34   | 1520         | 60         | 3.3        | 2.6     |            |  |  | 282          | 42 T  |
| XP25-1       | 41.17  | 6.33  | 6.21   |                 | 1283   |             |      |        |              |            |            |         |            |  |  |              |       |
| A-942        | 41.5   | 6.00  | 7.50   | 720             | 1250   | 5.4         | 1.25 | 1.20   |              | 60         | 5.4        | 40      |            |  |  |              |       |
| SINGAPORE I  | 43.0   | 8.00  | 7.50   |                 | 1850   |             |      |        |              |            |            |         |            |  |  |              |       |
| Scapa        | 51.5   | 7.75  | 6.94   |                 | 2016   | 12.2        | 3.15 | 2.25   |              | 220        | 2.1        | 178     |            |  |  |              |       |
| PN-10        | 51.0   | 9.17  | 6.88   |                 | 2000   |             |      |        |              |            |            |         |            |  |  |              |       |
| PM-2         | 46.25  | 10.21 | 7.00   | 985             | 2310   |             |      |        |              |            |            |         |            |  |  |              |       |
| Strauraer    | 55.7   | 8.35  | 8.75   |                 | 2547   |             |      |        | 5240         |            |            |         |            |  |  |              |       |
| London II    | 63.2   | 7.75  | 8.00   |                 | 2598   | 13.9        | 3.8  | 2.6    | 7580         | 264        | 2.2        | 240     |            |  |  |              |       |
| JR25-1       | 30.27  | 7.50  | 8.86   | 1,560           | 2871   | 8.0         | 2.2  | 2.2    | 2830         |            | 7.5        |         |            |  |  | 1075         | 148 T |
| Calcutta     | 58.7   | 10.00 | 7.67   |                 | 2400   |             |      |        |              |            |            |         |            |  |  |              |       |
| XP2M-1       | 58.0   | 8.67  | 7.25   | 1,640           | 2597   |             |      |        |              |            |            |         |            |  |  |              |       |
| P2Y-3        | 48.75  | 8.42  | 6.88   |                 | 2276   | 16.2        | 3.0  | 3.5    | 3510         | 394        | 1.0        | 31.4    |            |  |  |              |       |
| XP3D-2       | 44.75  | 8.33  | 10.83  | 2,600           | 3360   |             |      |        |              |            |            |         |            |  |  |              |       |
| P3M-2        | 48.75  | 8.42  | 6.88   | 1,528           | 2311   | 16.2        | 2.3  | 2.6    | 7410         | 334        | 0          | 0       |            |  |  |              |       |
| PBY-5        | 53.37  | 10.21 | 8.33   | 2,220           | 3065   | 10.4        | 2.06 | 2.00   | 3065         | 186        | 5.0        | 277     | R          |  |  |              |       |
| PBY-SA       | 53.37  | 10.21 | 8.33   |                 | 3931   | 10.4        | 2.06 | 2.00   | 3065         | 186        | 5.0        | 278     | R          |  |  | 1528         | 305N  |
| PB-1         | 37.0   | 9.33  | 7.51   |                 | 2581   |             |      |        |              |            |            |         |            |  |  |              |       |
| PBN-1        | 44.7   | 10.19 | 8.33   | 2,240           | 3585   | 11.8        | 2.08 | 2.15   | 3550         | 234        | 5.0        | 186     | R          |  |  |              |       |
| Larwick      | 53.46  | 8.60  | 14.58  |                 | 3989   | 10.5        | 3.25 | 3.17   | 6500         | 269        | 7.5        | 239     |            |  |  |              |       |
| Super-Wal    | 77.0   | 11.5  | 8.0    | 3,590           | 4284   |             |      |        | SPONSORS     |            | 842        |         |            |  |  |              |       |
| SINGAPORE II | 41.7   | 10.87 | 9.1    |                 | 3933   | 14.8        | 3.7  | 3.5    | 10,000       | 362        | 1.8        | 337     |            |  |  |              |       |
| PBM-1        | 77.16  | 8.52  | 14.00  | 4,550           | 5890   | 6.63        | 2.5  | 4.2    | 6340         | 263        | 7.5        | 289     | 131        |  |  |              |       |
| C            | 48.0   | 10.00 | 15.8   |                 | 8716   | 14.8        | 3.2  | 3.2    | 10,000       |            | 6.2        | 118     |            |  |  |              |       |
| XP4Y-1       | 70.0   | 9.17  | 15.42  | 5,000           | 6579   | 10.0        | 3.0  | 3.4    | 6150         | 270        | 6.6        | 467     | R          |  |  |              |       |
| PBM-3C       | 78.8   | 10.00 | 14.00  | 5,000           | 6,532  | 14.0        | 3.0  | 3.0    | 8200         | 324        | 8.0        | 206     |            |  |  |              |       |
| XPBS-1       | 76.1   | 10.0  | 11.92  | 4,200           | 5606   | 14.0        | 3.0  | 2.9    | 7350         | 264        | 6.3        | 151     |            |  |  |              |       |
| XPB2Y-1      | 71.28  | 10.5  | 12.92  | 5,190           | 6342   |             |      |        | 4196         |            |            |         |            |  |  |              |       |
| M-130        | 34.5   | 11.25 | 10.33  | 4,850           | 5114   |             |      |        | SPONSORS     |            | 1694       |         |            |  |  |              |       |
| Super-Wal    | 65.28  | 10.1  | 17.3   |                 | 8378   | 15.0        | 3.8  | 3.6    |              |            | 6.7        |         |            |  |  |              |       |
| JR25-1       | 30.3   | 10.00 | 11.92  | 4,210           | 5717   | 14.4        | 3.0  | 3.0    | 7340         | 315        | 7.2        | 107     |            |  |  |              |       |
| XPBM-2       |        |       |        |                 | 6780   | 6.63        | 2.5  | 4.2    | 6340         | 205        | 7.5        | 289     | 131        |  |  |              |       |
| XPBB-1       | 34.5   | 10.50 | 16.93  | 8780            | 8836   | 13.67       | 3.52 | 3.68   | 10,720       | 436        | 9.0        | 263     |            |  |  |              |       |
| M-156        | 34.5   | 11.25 | 10.33  | 5,220           | 5703   |             |      |        | SPONSORS     |            | 2089       |         |            |  |  |              |       |
| PB2Y-3       | 73.2   | 10.50 | 16.33  | 7,110           | 7192   | 11.45       | 2.67 | 2.75   | 6,500        | 355        | 5.8        |         |            |  |  |              |       |
| R6-28        | 33.0   | 13.75 | 10.75  |                 | 7200   |             |      |        |              |            |            |         |            |  |  |              |       |
| G            | 29.7   | 12.0  | 19.0   |                 | 12,964 |             |      |        | 15,000       | 586        | 9.0        | 148     |            |  |  |              |       |
| 314          | 40.5   | 12.50 | 18.92  |                 | 10,576 |             |      |        | SPONSORS     |            | 2583       |         |            |  |  |              |       |
| Do-X         | 51.35  | 15.33 | 15.5   | 13,940          | 15,413 |             |      |        | SPONSORS     |            | 3312       |         |            |  |  |              |       |
| Shetland     | 49.5   | 12.50 | 19.88  |                 | 14,630 | 13.5        | 5.8  | 4.0    | 16,600       |            | 7.8        |         |            |  |  |              |       |
| XPBM-1R      | 77.15  | 13.50 | 20.50  | 16,665          | 16,831 | 17.25       | 3.5  | 3.5    | 15,750       | 553        | 8.5        | 396     |            |  |  |              |       |
| HK-1         | 219    |       |        |                 |        |             |      |        |              |            |            |         |            |  |  |              |       |

# Weights

Table 1 (cont'd): Flying Boat Weight Groups, 3 of 4 (Taken from Locke, 1945)

| MANUFACTURER  | MODEL          | GROSS<br>WEIGHT<br>lbs | POWER PLANT GROUP |                             |                           |                      |                       |                              |           |                    |                |                              |                |                               |  |
|---------------|----------------|------------------------|-------------------|-----------------------------|---------------------------|----------------------|-----------------------|------------------------------|-----------|--------------------|----------------|------------------------------|----------------|-------------------------------|--|
|               |                |                        | BHP               | No. & Type<br>of<br>Engines | Engine<br>As<br>Installed | Wing Area<br>sq. ft. | Engine<br>Power<br>hp | Fuel<br>Consumption<br>lb/hr | Propeller | Starting<br>System | Lub.<br>System | Oil<br>Consumption<br>gal/hr | Fuel<br>System | Fuel<br>Consumption<br>gal/hr |  |
|               |                |                        | Take-Off          |                             | hp                        | sq. ft.              | lb/hr                 | lb/hr                        | lb/hr     | lb/hr              | lb/hr          | lb/hr                        | lb/hr          | lb/hr                         |  |
|               |                |                        |                   |                             |                           |                      |                       |                              |           |                    |                |                              |                |                               |  |
| Grumman       | JAF-2          | 4,500                  | 400               | 2<br>G-440C                 | 784                       | 132                  | 47                    | 15                           | 59        | 39                 | 10             | 7                            | 19             | 100                           |  |
| Keystone      | Commuter       | 4,150                  |                   |                             |                           |                      |                       |                              |           |                    |                |                              |                |                               |  |
| Supermarine   | Walrus         | 7,260                  | 840               |                             | 984                       | 78                   | 185                   |                              | 126       |                    | 24             |                              | 116            |                               |  |
| Grumman       | JRF-6B         | 8,000                  | 900               | 2<br>900-6                  | 1341                      | 246                  | 126                   | 26                           | 326       | 76                 | 41             | 15                           | 25             | 220                           |  |
| Sikorsky      | XP2S-1         | 9,640                  |                   |                             |                           |                      |                       |                              |           |                    |                |                              |                |                               |  |
| Fairchild     | A-942          | 10,500                 | 670               | R-1820                      | 1071                      |                      | 107                   | 11                           | 363       | 41                 | 27             | 15                           | 121            | 180                           |  |
| Short         | Singapore I    | 13,385                 |                   |                             |                           |                      |                       |                              |           |                    |                |                              |                |                               |  |
| Supermarine   | Scapa          | 16,700                 |                   |                             | 1812                      | 410                  |                       |                              | 192       |                    | 111            |                              | 282            |                               |  |
| NAF           | PN-10          | 17,000                 |                   |                             |                           |                      |                       |                              |           |                    |                |                              |                |                               |  |
| Martin        | PM-2           | 17,200                 |                   |                             |                           |                      |                       |                              |           |                    |                |                              |                |                               |  |
| Supermarine   | Stranraer      | 18,710                 | 1625              |                             | 2235                      | 456                  | 335                   |                              | 360       | 63                 | 134            | 37                           | 325            | 640                           |  |
| Saro          | Lantern II     | 19,290                 | 1580              |                             | 2095                      | 288                  |                       |                              | 466       |                    | 100            |                              | 464            |                               |  |
| Sikorsky      | JRS-1          | 19,500                 | 1600              | 2<br>1690-32                | 2038                      | 378                  | 270                   | 85                           | 717       | 97                 | 74             | 54                           | 361            | 600                           |  |
| Short         | Calcutta       | 19,700                 |                   |                             |                           |                      |                       |                              |           |                    |                |                              |                |                               |  |
| Martin        | XP2M-1         | 20,170                 |                   |                             |                           |                      |                       |                              |           |                    |                |                              |                |                               |  |
| Consolidated  | P2Y-3          | 20,500                 |                   |                             |                           |                      |                       |                              |           |                    |                |                              |                |                               |  |
| Douglas       | XP3D-2         | 22,500                 |                   |                             |                           |                      |                       |                              |           |                    |                |                              |                |                               |  |
| Martin        | P3M-2          | 25,500                 | 1720              |                             |                           |                      |                       |                              |           |                    |                |                              |                |                               |  |
| Consolidated  | PBY-5          | 26,000                 | 2400              |                             | 2930                      | 565                  | 200                   | 110                          | 801       | 127                | 118            | 110                          | 831            | 1478                          |  |
| Consolidated  | PBY-5A         | 26,000                 | 2400              |                             | 2936                      | 569                  | 220                   | 48                           | 848       | 106                | 129            | 110                          | 860            | 1478                          |  |
| Boeing        | PB-1           | 26,700                 | 1600              |                             |                           |                      |                       |                              |           |                    |                |                              |                |                               |  |
| NAF           | PBN-1          | 28,000                 | 2400              |                             | 2935                      | 320                  | 194                   | 49                           | 861       | 127                | 302            | 110                          | 724            | 2085                          |  |
| Saro          | Lerwick        | 28,800                 | 3200              |                             | 3340                      | 926                  | 443                   | 111                          | 1100      | 103                | 212            | 100                          | 956            | 1440                          |  |
| Dornier       | Super Wal      | 31,100                 | 2000              |                             |                           |                      |                       |                              |           |                    |                |                              |                |                               |  |
| Short         | Singapore III  | 31,500                 |                   |                             |                           |                      |                       |                              |           |                    |                |                              |                |                               |  |
| Martin        | PBM-1          | 39,000                 | 3200              | 2<br>XR-2600                | 3871                      | 496                  | 406                   | 77                           | 1039      | 127                | 171            | 86                           | 520            | 1275                          |  |
| Short         | C              | 42,600                 | 3180              |                             | 4430                      | 826                  |                       |                              | 1511      |                    | 266            | 63                           | 595            | 1330                          |  |
| Consolidated  | XP4Y-1         | 46,000                 | 4600              | 2<br>R-3350                 | 5380                      | 888                  | 494                   | 138                          | 1231      | 112                | 228            | 260                          | 249            | 3000                          |  |
| Martin        | PBM-3c         | 46,500                 | 3400              | 2<br>R-2600                 | 4026                      | 1474                 | 190                   | 134                          | 1329      | 112                | 316            | 150                          | 1021           | 1902                          |  |
| Sikorsky      | XPBS-1         | 46,610                 |                   |                             |                           |                      |                       |                              |           |                    |                |                              |                |                               |  |
| Consolidated  | XPBZY-1        | 50,000                 |                   |                             |                           |                      |                       |                              |           |                    |                |                              |                |                               |  |
| Martin        | M-130          | 52,000                 | 3600              | 2<br>R-1850                 | 5140                      | 903                  | 413                   | 123                          | 1540      | 152                | 220            | 216                          | 415            | 4154                          |  |
| Short         | Sunderland III | 58,000                 | 4640              |                             | 4673                      | 1085                 |                       |                              | 1564      |                    | 377            | 154                          | 1260           | 3060                          |  |
| Sikorsky      | JR2S-1         | 59,225                 | 4800              | 2<br>R-1820                 | 5920                      | 1076                 | 352                   | 100                          | 1604      | 169                | 418            | 208                          | 223            | 3770                          |  |
| Martin        | XPBM-2         | 62,000                 | 1600              | 2<br>XR-2600                | 3820                      | 503                  | 401                   | 85                           | 1035      | 146                | 220            | 292                          | 921            | 3881                          |  |
| Boeing        | XPBB-1         | 62,000                 | 4600              | 2<br>R-3350                 | 5205                      | 1163                 | 229                   | 134                          | 1331      | 110                | 391            | 503                          | 353            | 9080                          |  |
| Martin        | M-156          | 63,000                 | 3800              | 2<br>R-1820                 | 4660                      | 1404                 | 371                   | 161                          | 1600      | 136                | 232            | 216                          | 465            | 4497                          |  |
| Consolidated  | PBZY-3         | 66,000                 | 4800              | 2<br>R-1820                 | 6432                      | 1869                 | 825                   | 161                          | 1996      | 223                | 374            | 240                          | 1818           | 3880                          |  |
| Short         | R6-18          | 69,380                 |                   |                             |                           |                      |                       |                              |           |                    |                |                              |                |                               |  |
| Short         | G              | 74,500                 | 5500              |                             | 6863                      | 1476                 |                       |                              | 2286      |                    | 511            | 90                           | 1387           | 3430                          |  |
| Boeing        | 314            | 80,000                 | 6400              | 2<br>R-2600                 | 7714                      | 2075                 | 558                   | 63                           | 2046      | 143                | 588            | 206                          | 914            | 5448                          |  |
| Dornier       | Do-X           | 114,640                | 7200              |                             |                           |                      |                       |                              |           |                    |                |                              |                |                               |  |
| Short         | Shetland       | 118,800                | 9320              |                             | 10760                     | 3070                 | 1745                  |                              | 3000      |                    | 620            | 336                          | 2156           | 7000                          |  |
| Martin        | XPBM-1R        | 140,000                | 8800              | 2<br>R-3350                 | 10562                     | 2565                 | 798                   | 651                          | 2722      | 292                | 932            | 664                          | 1267           | 10710                         |  |
| Hughes-Kaiser | HK-1           | 240,000                | 24000             | 2<br>R-4360                 | 26360                     | 9913                 | 2491                  | 670                          | 7486      | 240                | 3003           |                              | 4492           |                               |  |



# Weights

Table 1 (cont'd): Flying Boat Weight Groups, 4 of 4 (Taken from Locke, 1945)

| MODEL        | FIXED EQUIPMENT GROUP |                     |                     |                      |                |                  |                       |                |                     |                | PROTECTION |                    |                     |         | USEFUL<br>LOAD<br>EQUIP. |
|--------------|-----------------------|---------------------|---------------------|----------------------|----------------|------------------|-----------------------|----------------|---------------------|----------------|------------|--------------------|---------------------|---------|--------------------------|
|              | Instru-<br>MENTS      | SURFACE<br>CONTROLS | Hydraulic<br>SYSTEM | Electrical<br>SYSTEM | Communications | Armored<br>Power | Armored<br>Furnishing | Anti-<br>icing | AUX.<br>Power Plant | Marine<br>GEAR | ARMOR      | SELF-SEAL<br>CELLS | Guns<br>AND<br>AMMO | Torpedo |                          |
|              | lbs                   | lbs                 | lbs                 | lbs                  | lbs            | lbs              | lbs                   | lbs            | lbs                 | lbs            | lbs        | lbs                | lbs                 | lbs     |                          |
| J4F-2        | 27                    | 103                 | 0                   | 102                  | 37             |                  | 197                   |                |                     | 22             |            |                    |                     |         | 14                       |
| Commuter     |                       |                     |                     |                      |                |                  |                       |                |                     |                |            |                    |                     |         |                          |
| Walrus       |                       |                     |                     |                      |                |                  |                       |                |                     |                |            |                    |                     |         |                          |
| JRF-6B       | 49                    | 173                 | 0                   | 205                  | 274            |                  | 290                   |                |                     | 43             |            |                    |                     |         | 69                       |
| XP25-1       |                       |                     |                     |                      |                |                  |                       |                |                     |                |            |                    |                     |         |                          |
| A-942        | 82                    | 171                 |                     | 163                  |                |                  | 688                   |                |                     | 83             |            |                    |                     |         |                          |
| SINGAPORE I  |                       |                     |                     |                      |                |                  |                       |                |                     |                |            |                    |                     |         |                          |
| Scapa        |                       | 289                 |                     |                      |                |                  |                       |                |                     |                |            |                    |                     |         |                          |
| PN-10        |                       |                     |                     |                      |                |                  |                       |                |                     |                |            |                    |                     |         |                          |
| PM-2         |                       |                     |                     |                      |                |                  |                       |                |                     |                |            |                    |                     |         |                          |
| Straubner    | 173                   | 333                 |                     | 308                  | 172            |                  | 335                   |                | 160                 | 210            |            |                    | 341                 |         |                          |
| London II    |                       | 203                 |                     |                      |                |                  |                       |                |                     |                |            |                    |                     |         |                          |
| JRS-1        | 87                    | 373                 | 349                 | 515                  |                |                  |                       |                |                     | 95             |            |                    |                     |         |                          |
| Calcutta     |                       |                     |                     |                      |                |                  |                       |                |                     |                |            |                    |                     |         |                          |
| XP2M-1       |                       |                     |                     |                      |                |                  |                       |                |                     |                |            |                    |                     |         |                          |
| P2Y-3        |                       |                     |                     |                      |                |                  |                       |                |                     |                |            |                    |                     |         |                          |
| XP3D-2       |                       |                     |                     |                      |                |                  |                       |                |                     |                |            |                    |                     |         |                          |
| P3M-2        |                       |                     |                     |                      |                |                  |                       |                |                     |                |            |                    |                     |         |                          |
| PBY-5        | 188                   | 425                 |                     | 766                  | 701            | 110              | 866                   | 400            | 261                 | 156            | 503        |                    | 634                 | 374     | 1195                     |
| PBY-SA       | 118                   | 392                 | 204                 | 719                  | 575            | 80               | 704                   | 347            | 136                 | 123            | 611        | 465                | 786                 | 331     | 685                      |
| PB-1         |                       |                     |                     |                      |                |                  |                       |                |                     |                |            |                    |                     |         |                          |
| PBN-1        | 165                   | 425                 |                     | 641                  | 873            | 108              | 727                   | 31             | 268                 | 132            | 459        |                    | 1083                | 414     |                          |
| Larwick      |                       | 500                 | 204                 |                      |                |                  | 215                   | 196            | 191                 | 58             |            |                    |                     |         |                          |
| Super-Wal    |                       |                     |                     |                      |                |                  |                       | 0              |                     | 251            |            |                    |                     |         |                          |
| SINGAPORE II |                       |                     |                     |                      |                |                  |                       |                |                     |                |            |                    |                     |         |                          |
| PBM-1        | 166                   | 522                 | 133                 | 919                  | 358            | 277              | 888                   | 205            | 732                 | 195            | 0          |                    | 1045                | 494     | 1369                     |
| C            |                       | 319                 |                     |                      |                |                  |                       | 391            |                     |                | 455        |                    | 502                 | 750     |                          |
| XP4Y-1       | 147                   | 528                 | 297                 | 728                  | 937            | 252              | 1086                  | 256            | 238                 | 141            | 744        |                    | 1745                | 872     | 522                      |
| PBM-3C       | 191                   | 677                 |                     | 1400                 | 792            | 545              | 898                   | 898            | 374                 | 210            | 1053       | 1031               | 2052                | 1693    | 1585                     |
| XPBS-1       |                       |                     |                     |                      |                |                  |                       |                |                     |                |            |                    |                     |         |                          |
| XPBSY-1      |                       |                     |                     |                      |                |                  |                       |                |                     |                |            |                    |                     |         |                          |
| M-130        | 157                   | 309                 | 250                 | 584                  | 202            |                  | 4109                  |                |                     | 321            |            |                    |                     |         |                          |
| Super-Wal    |                       | 425                 |                     |                      |                |                  | 683                   |                |                     |                | 156        | 946                | 778                 | 897     |                          |
| JR2S-1       | 175                   | 438                 |                     | 978                  |                |                  | 2759                  | 185            | 232                 | 115            |            |                    |                     |         | 870                      |
| XPBM-2       | 166                   | 522                 | 133                 | 723                  | 358            | 598              | 1104                  | 205            | 732                 | 168            |            |                    |                     |         |                          |
| XPBS-1       | 198                   | 632                 |                     | 853                  | 480            | 204              | 1826                  | 234            | 384                 | 184            | 985        | 0                  | 1623                | 1995    | 1694                     |
| M-156        | 154                   | 720                 | 230                 | 687                  | 305            |                  | 3981                  | 208            |                     | 243            |            |                    |                     |         |                          |
| PBY-3        | 233                   | 606                 |                     | 1212                 | 981            | 635              | 2130                  | 143            | 375                 | 299            | 1263       | 654                | 2264                | 1477    | 1060                     |
| R6-28        |                       |                     |                     |                      |                |                  |                       |                |                     |                |            |                    |                     |         |                          |
| G            |                       | 483                 |                     |                      |                |                  |                       | 1067           |                     |                | 593        | 666                |                     |         |                          |
| 314          | 149                   | 732                 |                     | 1061                 | 451            |                  | 5000                  | 306            |                     | 101            |            |                    |                     |         |                          |
| Do-X         |                       |                     |                     |                      |                |                  |                       |                |                     | 551            |            |                    |                     |         |                          |
| Shetland     | 800                   | 580                 | 75                  | 2395                 | 830            |                  | 1510                  | 280            |                     |                | 665        | 1699               | 2200                |         |                          |
| XPBM-HR      | 864                   | 1074                | 194                 | 2793                 | 910            | 1632             | 5251                  | 437            | 669                 | 653            |            |                    |                     |         | 1567                     |
| HK-1         | 800                   | 4377                | 1840                | 1800                 |                |                  | 2907                  | 1800           | 1000                | 1005           |            |                    |                     |         |                          |

# Weights

Table 2: Landplane Weight Groups, 1 of 4 (Taken from Locke, 1945)

| MANUFACTURER   | MODEL         | GROSS WEIGHT<br>lbs | V <sub>MAX</sub><br>@ S.L.<br>m.p.h. | WING                        |                         |            |             |                      |                     |                        |
|----------------|---------------|---------------------|--------------------------------------|-----------------------------|-------------------------|------------|-------------|----------------------|---------------------|------------------------|
|                |               |                     |                                      | ULTIMATE FLIGHT LOAD FACTOR | AREA<br>ft <sup>2</sup> | SPAN<br>ft | TAPER RATIO | ROOT THICKNESS<br>ft | TIP THICKNESS<br>ft | GROUP<br>WEIGHT<br>lbs |
|                |               |                     |                                      |                             |                         |            |             |                      |                     |                        |
|                |               |                     |                                      |                             |                         |            |             |                      |                     |                        |
| Fairchild      | J2K-2         | 2,460               |                                      |                             | 173                     |            |             |                      |                     | 314                    |
| Cessna         | JRC-1         | 5,700               |                                      | 6.45                        | 295                     | 41.9       |             |                      |                     | 824                    |
| Beech          | JRB-4         | 7,850               | 216                                  | 5.90                        | 349                     | 47.7       | 3.21        |                      |                     | 830                    |
| Lockheed       | JO-2          | 8,400               |                                      | 6.50                        | 352                     | 49.5       |             | 1.73                 |                     | 1071                   |
| Martin         | B-10B         | 14,890              |                                      | 5.50                        | 678                     | 70.5       |             |                      |                     | 2022                   |
| Bristol        | Blenheim      | 16,000              |                                      | 6.40                        | 469                     | 56.3       | 2.70        |                      |                     | 1615                   |
| DeHavilland    | Mosquito I    | 18,000              |                                      | 7.70                        | 440                     | 40.8       | 3.20        |                      |                     | 2273                   |
| Lockheed       | PBO-1         | 18,500              |                                      | 4.90                        | 551                     | 65.5       | 4.28        | 2.43                 | 0.36                | 2267                   |
| Lockheed       | R5D-6         | 18,500              | 231                                  | 4.87                        | 551                     | 65.5       | 4.28        | 2.48                 | 0.36                | 2352                   |
| Douglas        | R2D-1         | 18,500              |                                      | 4.65                        | 939                     | 85         |             | 2.12                 |                     | 2790                   |
| Douglas        | A-20C         | 19,750              | 300                                  |                             | 465                     | 61.3       |             | 2.08                 |                     | 2282                   |
| Martin         | A-30A         | 21,000              |                                      | 6.00                        | 539                     | 61.3       | 3.00        | 1.81                 | 0.36                | 2816                   |
| Douglas        | R3D-1         | 21,000              | 208                                  |                             | 824                     | 78.0       | 2.36        | 2.34                 | 0.66                |                        |
| Bristol        | Beaufort IV   | 21,500              |                                      | 7.40                        | 503                     | 57.8       | 1.90        |                      |                     | 1890                   |
| Vega           | Venture I     | 22,500              |                                      | 6.00                        | 551                     | 65.5       | 3.42        | 2.48                 | 0.52                | 2701                   |
| Douglas        | C-47A         | 26,000              | 212                                  | 4.65                        | 987                     | 95.0       | 3.20        | 2.49                 | 0.27                | 3540                   |
| North American | PBJ-1         | 26,122              | 249                                  | 5.50                        | 610                     | 67.7       | 2.41        |                      |                     | 2938                   |
| Martin         | B-26B         | 27,200              |                                      | 5.50                        | 602                     | 65         |             | 2.38                 |                     | 2885                   |
| Martin         | B-26F         | 31,000              |                                      | 5.00                        | 658                     | 71         | 2.86        | 2.18                 | 0.59                | 3728                   |
| Vickers        | Wellington IV | 31,500              |                                      | 5.00                        | 840                     | 86.2       | 3.00        |                      |                     | 3590                   |
| Budd           | RB-1          | 33,850              | 183                                  | 4.38                        | 1399                    | 100        | 2.48        | 3.00                 | 0.96                | 4653                   |
| Boeing         | B-307B        | 41,000              |                                      | 3.41                        | 1486                    | 107.3      |             | 3.42                 |                     | 5549                   |
| Consolidated   | B-24C         | 41,000              | 0                                    | 5.50                        | 1048                    | 110        | 2.69        | 3.08                 | 0.48                | 6484                   |
| Curtiss        | R5C-1         | 45,000              | 221                                  | 4.96                        | 1360                    | 108        | 3.00        |                      |                     | 6108                   |
| Vickers        | Warwick I     | 45,000              |                                      | 5.00                        | 1020                    | 96.8       | 4.00        | 3.04                 |                     | 5530                   |
| Boeing         | B-17G         | 48,700              | 233                                  | 5.28                        | 1420                    | 103.8      |             | 3.38                 |                     | 6006                   |
| Avro           | Manchester    | 50,000              |                                      | 4.70                        | 1131                    | 90.1       | 1.50        |                      |                     | 6250                   |
| Douglas        | R5D-1         | 50,000              | 260                                  | 4.50                        | 1461                    | 117.5      | 3.26        | 3.05                 | 0.71                | 5995                   |
| Consolidated   | RY-3          | 56,000              | 245                                  | 4.00                        | 1048                    | 110        | 2.69        | 3.08                 | 0.48                | 6418                   |
| Consolidated   | R2Y-1         | 56,000              |                                      |                             | 1048                    | 110        | 2.70        |                      |                     | 6110                   |
| Consolidated   | PB4Y-2        | 56,000              |                                      | 4.00                        | 1048                    | 110        | 2.69        | 3.08                 | 0.47                | 6134                   |
| Handley-Page   | Halifax II    | 60,000              |                                      | 4.30                        | 1250                    | 99         | 1.80        |                      |                     | 7750                   |
| Avro           | Lancaster     | 60,000              |                                      | 4.70                        | 1297                    | 102        | 1.70        |                      |                     | 7200                   |
| Douglas        | R5D-2         | 62,000              | 251                                  | 3.75                        | 1462                    | 117.5      | 3.26        | 3.05                 | 0.71                | 6422                   |
| Short          | Stirling      | 70,000              |                                      | 4.10                        | 1458                    | 99.0       | 2.60        |                      |                     | 9100                   |
| Boeing         | XB-15         | 70,700              |                                      |                             |                         |            |             |                      |                     |                        |
| Lockheed       | C-69          | 72,000              |                                      | 4.55                        | 1650                    | 123        | 2.16        | 3.30                 | 1.01                | 9085                   |
| Consolidated   | YB-32         | 95,000              | 292                                  | 4.50                        | 1422                    | 135        |             | 3.66                 |                     | 13820                  |
| Boeing         | XB-29         | 105,000             |                                      | 4.50                        | 1739                    | 141.2      | 2.29        | 3.74                 | 0.80                | 13755                  |
| Boeing         | B-29A         | 105,000             | 285                                  | 4.50                        | 1739                    | 141.2      | 2.28        | 2.48                 | 0.36                | 14569                  |
| Lockheed       | C-69B         | 94,000              | 314                                  | 4.00                        | 1650                    | 123        | 2.16        | 3.30                 | 1.01                | 11776                  |
| Douglas        | C-74          | 125,000             |                                      | 4.20                        | 2510                    | 173.2      | 4.25        | 4.46                 | 0.77                | 18379                  |
| Douglas        | XB-19         | 162,800             |                                      | 3.82                        | 4285                    | 212        | 4.30        | 6.26                 | 0.59                | 23994                  |
| Lockheed       | XR60-1        | 184,000             |                                      | 4.06                        | 3610                    | 189.1      | 3.04        | 5.66                 | 1.12                | 30275                  |
| Consolidated   | XB-36         | 265,000             | 260                                  | 4.00                        | 4772                    | 230        | 4.00        | 7.33                 | 1.42                | 34494                  |
| Consolidated   | XC-99         | 265,000             |                                      |                             |                         |            |             |                      |                     |                        |

## Weights

Table 2 (cont'd): Landplane Weight Groups, 2 of 4 (Taken from Locke, 1945)

| Model         | TAIL            |        |         | FUSELAGE |       |        |                 |        | LANDING GEAR |         |        |      |          |        |        |  |
|---------------|-----------------|--------|---------|----------|-------|--------|-----------------|--------|--------------|---------|--------|------|----------|--------|--------|--|
|               | Total           | Basic  | Balance | Length   | Width | Height | Submerged       | Weight | Main         | Retract | Length | Aux. | Retract. | Length | Total  |  |
|               | Area            | Weight | Weight  |          |       |        | Volume          |        | Gear         | Mech    |        | Gear | Mech     |        | Weight |  |
|               | ft <sup>2</sup> | lbs    | lbs     | ft       | ft    | ft     | ft <sup>3</sup> | lb.    | lbs          | lbs     | ft     | lbs  | lbs      | ft     | lbs    |  |
| J2K-2         | 49.1            | 71     |         |          |       |        |                 | 312    | 130          |         |        | 11   |          |        | 141    |  |
| JRC-1         | 88.5            | 139.1  | 13.5    | 31.1     | 4.50  | 4.58   |                 | 463    | 289          |         |        | 27   | —        |        | 316    |  |
| JRB-4         | 29              | 154.3  | 12.13   | 33.5     | 4.62  | 5.80   |                 | 676    | 431          | 69      |        | 35   | 6        |        | 555    |  |
| JO-2          | 154             | 228    | 19.0    | 36.3     | 5.0   | 5.9    |                 | 755    | 439          | 87      |        | 53   |          |        | 579    |  |
| B-10B         | 134             | 232    | 2.0     | 40.2     | 3.60  | 7.30   |                 | 912    | 923          | 0       |        | 53   | 0        |        | 976    |  |
| Blanchard     |                 | 224    |         | 40.9     | 4.35  | 5.60   |                 | 1615   |              |         |        |      |          |        | 640    |  |
| Monaco I      |                 | 288    | 40      | 40.8     | 4.42  | 5.46   |                 | 897    | 1001         | 48      |        | 99   | 6        |        | 1154   |  |
| PB0-1         | 191             | 394    | 55      | 44.8     | 5.75  | 8.75   |                 | 1826   | 775          | 37      |        | 71.2 | 0        |        | 885    |  |
| R50-6         | 198             | 398    | 55      | 44.8     | 5.75  | 8.75   |                 | 1533   | 800          | 37      |        | 71   | 0        |        | 908    |  |
| R20-1         | 239             | 467    | 0       | 61.9     | 5.75  | 8.2    |                 | 1609   | 1036         |         |        | 128  |          |        | 1164   |  |
| A-20c         | 163.5           | 396    |         | 48.0     | 4.09  | 6.83   |                 | 1383   | 1252         | 63      |        | 168  | 23       |        | 1506   |  |
| A-30A         | 177             | 320    | 69      | 44.0     | 3.67  | 7.92   | 150             | 1274   | 1020         | 54      | 3.25   | 90   | —        | 2.06   | 1163   |  |
| R3D-1         | 268             | 471    |         | 62.16    | 8.50  | 8.50   |                 | 2395   | 1032         | 40      |        | 161  | 22       |        | 1273   |  |
| Beaufort IV   |                 | 301    |         | 41.0     | 4.95  | 7.25   |                 | 2,280  |              |         |        |      |          |        | 904    |  |
| Ventura I     | 198             | 390    | 48      | 52.8     | 7.00  | 8.89   |                 | 1893   | 897          |         | 4.5    | 118  |          |        | 1016   |  |
| C-47A         | 232             | 464    | 37      | 62.8     | 7.5   | 8.50   |                 | 1916   | 1524         |         |        | 204  |          |        | 1728   |  |
| PBJ-1         | 223             | 424    | 84      | 52.9     | 4.7   | 7.5    |                 | 1945   | 1414         | 148     |        | 236  | 27       |        | 1837   |  |
| B-26B         | 195             | 393    | 50.5    |          |       |        |                 |        | 1645         | 125     |        | 277  | 37       |        | 2084   |  |
| B-26F         | 237             | 559    | 68.5    | 58.2     | 7.65  | 7.65   |                 | 3,050  | 1966         |         |        | 378  |          |        | 2344   |  |
| Wellington IV |                 | 545    |         | 64.0     | 6.0   | 9.70   |                 | 3,215  |              |         |        |      |          |        | 1260   |  |
| RB-1          | 421             | 824    | 23      | 67.25    | 10.80 | 12.00  |                 | 4863   | 1466         | 92      |        | 326  | 25       |        | 1911   |  |
| B-307B        | 516             | 993    | 126     | 74.3     | 11.67 | 11.67  |                 | 5075   | 845          | 32      |        | 156  | 42       |        | 2194   |  |
| B-24C         | 390             | 679    | 49      | 66.0     | 7.42  | 10.42  |                 | 2502   | 2438         |         |        | 349  |          |        | 2187   |  |
| R5C-1         | 425             | 894    | 88      | 76.3     | 9.83  | 12.50  |                 | 4854   | 2565         | 53      |        | 451  | 18       |        | 3087   |  |
| Warwick I     | 224             | 585    |         | 70.5     | 5.6   | 9.30   |                 | 4100   |              |         |        |      |          |        | 2205   |  |
| B-17G         | 502             | 884    | 38.4    | 74.7     | 7.50  | 8.58   |                 | 3635   | 2419         | 180     |        | 220  | 36       |        | 2479   |  |
| Manchester    |                 | 900    |         | 69.3     | 5.8   | 8.20   |                 | 4750   |              |         |        |      |          |        | 2450   |  |
| R5D-1         | 447             | 1171   |         | 93.9     | 10.40 | 11.50  |                 | 5558   | 3173         | 208     |        | 659  | 40       |        | 4080   |  |
| RY-3          | 437             | 1157   |         | 75.45    | 7.17  | 10.3   |                 | 4544   | 2590         | 96.4    |        | 352  | 12.5     |        | 3074   |  |
| R2Y-1         | 441             | 955    | 45      |          |       |        |                 | 5768   | 2516         | 68      |        | 335  | 11       |        | 3004   |  |
| PB4Y-2        | 437             | 1182   |         | 74.69    | 7.42  | 10.42  |                 | 3907   | 2626         | 74.1    |        | 347  | 15.1     |        | 3093   |  |
| Halifax II    |                 | 900    |         | 70.2     | 5.6   | 9.50   |                 | 4,080  |              |         |        |      |          |        | 2700   |  |
| Lancaster     |                 | 1080   |         | 70.0     | 5.9   | 9.35   |                 | 4,980  |              |         |        |      |          |        | 2760   |  |
| R5D-2         | 447             | 1133   |         | 93.9     | 10.40 | 11.50  |                 | 5496   | 3436         |         |        | 698  |          |        | 4162   |  |
| Stirling      |                 | 910    |         | 83.5     | 6.40  | 8.25   |                 | 5740   |              |         |        |      |          |        | 4900   |  |
| XB-15         |                 |        |         |          |       |        |                 |        | 2979         | 324     |        | 286  | 50       |        | 3639   |  |
| C-69          | 706             | 1767   | 305     | 95.1     | 11.00 | 11.00  | 6020            | 6876   | 3410         | 31.8    | 7.21   | 926  | 87       |        | 4483   |  |
| YB-32         | 535             | 1295   |         | 82.9     | 9.50  | 9.50   |                 | 6798   |              |         |        |      |          |        | 5822   |  |
| XB-29         |                 |        |         |          |       |        |                 |        |              |         |        |      |          |        |        |  |
| B-29A         | 571             | 1398   | 44      | 99.0     | 9.50  | 9.50   |                 | 7246   | 5880         | 528     |        | 815  | 113      |        | 7447   |  |
| C-69B         |                 |        |         |          |       |        |                 |        |              |         |        |      |          |        |        |  |
| C-74          | 1037            | 3167   |         | 124.2    | 13.2  | 13.16  |                 | 10763  | 8498         |         |        | 1774 |          |        | 10272  |  |
| XB-19         | 1289            | 3617   |         | 132      | 10.8  | 13.5   |                 | 10073  | 12656        |         |        | 1769 |          |        | 14425  |  |
| XR60-1        | 1290            | 3850   | 408     | 156.1    | 12.0  | 19.6   |                 | 16375  | 9109         |         |        | 1594 |          |        | 10822  |  |
| XB-36         | 1524            | 3437   |         | 163      | 12.5  | 12.5   |                 | 14458  | 16605        | 260     |        | 1217 | 29       |        | 18,101 |  |
| XC-99         | 1532            | 3500   |         | 182.5    | 14.5  | 20.42  |                 | 25735  |              |         |        |      |          |        |        |  |

# Weights

Table 2 (cont'd): Landplane Weight Groups, 3 of 4 (Taken from Locke, 1945)

| MANUFACTURER   | MODEL      | Gross<br>Weight<br>lbs | POWER PLANT GROUP |                             |                           |                  |                |                         |           |                    |                |              |                |               |       |
|----------------|------------|------------------------|-------------------|-----------------------------|---------------------------|------------------|----------------|-------------------------|-----------|--------------------|----------------|--------------|----------------|---------------|-------|
|                |            |                        | BHP               | No. & Type<br>of<br>Engines | ENGINE<br>AS<br>INSTALLED | NACELLE<br>GROUP | ENGINE<br>Acc. | POWER PLANT<br>CONTROLS | PROPELLER | STARTING<br>SYSTEM | LUB.<br>SYSTEM | Oil<br>Gals. | FUEL<br>SYSTEM | FUEL<br>Gals. |       |
|                |            |                        | @                 |                             | lbs                       | lbs              | lbs            | lbs                     | lbs       | lbs                | lbs            | lbs          | lbs            | lbs           |       |
|                |            |                        | Take-Off          |                             |                           |                  |                |                         |           |                    |                |              |                |               |       |
| Fairchild      | J2K-2      | 2,460                  | 165               | 1                           | 6-3900                    | 379              |                | 28                      | 3.1       | 31                 | 22             | 6.8          | 3              | 37.6          | 40    |
| Cessna         | JRC-1      | 5,700                  | 490               | 2                           | L4M0                      | 1035             | 258            | 85                      | 23.1      | 221                | 42             | 41           | 10             | 115           | 120   |
| Boech          | JRB-4      | 7,850                  | 900               | 2                           | R985                      | 1336             | 294            | 165                     | 23.2      | 353                | 457            | 91           | 16             | 146           | 206   |
| Lockheed       | JO-2       | 8,400                  |                   |                             |                           |                  |                |                         |           |                    |                |              |                |               |       |
| Martin         | B-10B      | 14,890                 |                   |                             |                           |                  |                |                         |           |                    |                |              |                |               |       |
| Bristol        | Blenheim   | 16,000                 |                   |                             |                           | 544              |                |                         |           |                    |                |              |                |               |       |
| DeHavilland    | Mosquitaf  | 18,000                 |                   |                             | 2943                      | 637              | 1107           | 40                      | 919       | 97                 | 187            | 39           | 767            | 647           |       |
| Lockheed       | PBO-1      | 18,500                 | 2400              | 2                           | E-1820                    | 2640             | 515            | 334                     | 43        | 735                | 72             | 178          |                | 194           |       |
| Lockheed       | R50-6      | 18,500                 | 2400              | 2                           | E-1820                    | 2645             | 533            | 404                     | 43        | 784                | 72             | 236          | 40             | 111           | 644   |
| Douglas        | R2D-1      | 18,500                 |                   |                             |                           |                  |                |                         |           |                    |                |              |                |               |       |
| Douglas        | A-20C      | 19,750                 |                   | 2                           | E-2600                    | 3876             | 896            | 241                     | 138       | 766                | 145            | 337          | 46             | 618           | 400   |
| Martin         | A-30A      | 21,000                 | 3400              | 2                           | E-2600                    | 4000             | 960            | 213                     | 96        | 860                | 115            | 197          | 45             | 599           | 499   |
| Douglas        | R3D-1      | 21,000                 | 1900              | 2                           | E-1820                    | 2412             | 564            | 163                     | 67        | 864                | 76             | 62           | 42             | 313           | 640   |
| Bristol        | Beaufort   | 21,500                 |                   |                             |                           | 688              |                |                         |           |                    |                |              |                |               |       |
| Vega           | Ventura I  | 22,500                 | 4000              | 2                           | E-2800                    | 4610             | 1288           | 175                     | 73.5      | 926                | 127            | 292          | 30             | 777           | 568   |
| Douglas        | C-47A      | 26,000                 | 2400              | 2                           | E-1830                    | 2958             | 802            | 255                     | 80        | 913                | 108            | 203          | 58             | 567           | 804   |
| North American | PBJ-1      | 26,122                 | 3400              | 2                           | E-2600                    | 3941             | 914            | 217                     | 120       | 971                | 103            | 436          | 75             | 1330          | 971   |
| Martin         | B-26B      | 27,200                 |                   |                             |                           |                  |                |                         |           |                    |                |              |                |               |       |
| Martin         | B-26F      | 31,000                 | 4000              | 2                           | E-2800                    | 4536             | 1522           | 210                     | 85        | 1389               | 119            | 268          | 85             | 1062          | 1071  |
| Vickers        | Wellington | 31,500                 |                   |                             |                           | 1700             |                |                         |           |                    |                |              |                |               |       |
| Budd           | RB-1       | 33,850                 | 3400              | 2                           | E-1830                    | 2929             | 1180           | 143                     | 102       | 960                | 118            | 265          | 60             | 557           | 940   |
| Boeing         | B-307B     | 41,000                 | 3800              | 2                           | E-1820                    | 5100             | 1753           | 428                     | 119       | 1652               | 140            | 430          |                | 859           |       |
| Consolidated   | B-24C      | 41,000                 | 4800              | 4                           | E-1830                    | 6020             | 1593           | 1653                    | 401       | 1804               | 197            | 728          | 128            | 2457          | 2814  |
| Curtiss        | R5C-1      | 45,000                 | 4000              | 2                           | E-2800                    | 4560             | 1509           | 428                     | 70        | 1277               | 104            | 301          | 80             | 909           | 1480  |
| Vickers        | Warwick I  | 45,000                 |                   |                             |                           | 1670             |                |                         |           |                    |                |              |                |               |       |
| Boeing         | B-17G      | 48,700                 | 3800              | 4                           | E-1820                    | 5289             | 2259           | 1712                    | 57        | 1911               | 204            | 817          | 148            | 3602          | 2810  |
| AVRO           | Manchester | 50,000                 |                   |                             |                           | 1700             |                |                         |           |                    |                |              |                |               |       |
| Douglas        | R5D-1      | 50,000                 | 5400              | 4                           | E-2000                    | 6296             | 2113           | 772                     | 397       | 2064               | 229            | 696          | 163            | 1529          | 3715  |
| Consolidated   | RY-3       | 50,000                 | 6800              | 4                           | E-1830                    | 6292             | 1462           | 663                     | 320       | 1635               | 181            | 485          | 180            | 238           | 3000  |
| Consolidated   | R2Y-1      | 56,000                 | 6800              | 4                           | E-1830                    | 6300             | 1692           | 463                     | 444       | 1424               | 177            | 385          | 155            | 591           | 3000  |
| Consolidated   | PB4Y-2     | 56,000                 | 6800              | 4                           | E-1830                    | 6292             | 1470           | 698                     | 322       | 1634               | 184            | 336          |                | 759           |       |
| Handley-Page   | Halifax II | 60,000                 |                   |                             |                           | 1920             |                |                         |           |                    |                |              |                |               |       |
| AVRO           | Lancaster  | 60,000                 |                   |                             |                           | 1980             |                |                         |           |                    |                |              |                |               |       |
| Douglas        | R5D-2      | 62,000                 | 5400              | 4                           | E-2000                    | 6232             | 2096           | 831                     | 345       | 2060               | 255            | 706          | 163            | 1680          | 3800  |
| Short          | Stirling   | 70,000                 |                   |                             |                           | 1820             |                |                         |           |                    |                |              |                |               |       |
| Boeing         | XB-15      | 70,700                 |                   |                             |                           |                  |                |                         |           |                    |                |              |                |               |       |
| Lockheed       | C-69       | 72,000                 | 9200              | 4                           | E-3350                    | 10568            | 2666           | 1016                    | 464       | 2406               | 221            | 622          | 184            | 669           | 4800  |
| Consolidated   | YB-32      | 95,000                 | 9200              | 4                           | E-3350                    | 10672            | 2400           | 3266                    | 532       | 2712               | 154            | 485          | 288            | 2844          | 5200  |
| Boeing         | XB-29      | 105,000                |                   |                             |                           |                  |                |                         |           |                    |                |              |                |               |       |
| Boeing         | B-29A      | 105,000                | 9200              | 4                           | E-3350                    | 10525            | 4370           | 3677                    | 265       | 3613               | 209            | 1581         | 340            | 4421          | 5600  |
| Lockheed       | C-69B      | 94,000                 |                   |                             |                           |                  |                |                         |           |                    |                |              |                |               |       |
| Douglas        | C-74       | 125,000                | 12000             | 4                           | E-4360                    | 13324            | 5104           | 1208                    | 363       | 3373               | 230            | 921          | 330            | 2105          | 11000 |
| Douglas        | XB-19      | 162,800                | 6800              | 4                           | E-4360                    | 9956             | 2434           | 2129                    | 442       | 3019               | 334            | 474          |                | 2562          |       |
| Lockheed       | XR60-1     | 184,000                | 12000             | 4                           | E-4360                    | 14140            | 5394           | 5714                    | 435       | 4758               | 191            | 1385         | 402            | 464           | 9700  |
| Consolidated   | XB-36      | 265,000                | 18000             | 6                           | E-4860                    | 21984            | 3121           | 7306                    | 798       | 6481               | 97             | 1022         | 1176           | 2493          | 21116 |
| Consolidated   | XC-99      | 265,000                |                   |                             |                           |                  |                |                         |           |                    |                |              |                |               |       |

# Weights

Table 2 (cont'd): Landplane Weight Groups, 4 of 4 (Taken from Locke, 1945)

| MODEL      | FIXED EQUIPMENT GROUP |                  |                  |                   |               |          |       |            |            |           | PROTECTION |                 |               |         |            | USEFUL |
|------------|-----------------------|------------------|------------------|-------------------|---------------|----------|-------|------------|------------|-----------|------------|-----------------|---------------|---------|------------|--------|
|            | INSTRUMENTS           | SURFACE CONTROLS | HYDRAULIC SYSTEM | ELECTRICAL SYSTEM | COMMUNICATING | ARMAMENT | FUEL  | ANTI-ICING | AUX. POWER | MUX. GEAR | ARMOR      | SELF SEAL CELLS | GUNS AND AMMO | TURRETS | LOAD EQUIP |        |
|            | lbs                   | lbs              | lbs              | lbs               | lbs           | lbs      | lbs   | lbs        | lbs        | lbs       | lbs        | lbs             | lbs           | lbs     | lbs        |        |
|            |                       |                  |                  |                   |               |          |       |            |            |           |            |                 |               |         |            |        |
| J2K-2      | 17.0                  | 50.3             |                  | 70.8              | 24.5          |          | 89.3  |            |            |           |            |                 |               |         |            |        |
| JRC-1      | 42.1                  | 73.7             | 9.6              | 238               | 87            |          | 144   |            |            |           |            |                 |               |         | -          |        |
| JRB-4      | 68.9                  | 197.8            |                  | 255               | 244           |          | 326   | 82.0       |            |           |            |                 |               |         | -          |        |
| JO-2       |                       |                  |                  |                   |               |          |       |            |            |           |            |                 |               |         |            |        |
| B-10B      |                       |                  |                  |                   |               |          |       |            |            |           |            |                 |               |         |            |        |
| Blenheim   |                       | 128              |                  |                   |               |          |       |            |            |           |            |                 |               |         |            |        |
| Mosquito   | 100                   | 141              | 144              | 310               | 67            |          | 158   | 27         |            |           | 221        |                 |               |         |            |        |
| PBO-1      | 100                   | 253              | 133              | 444               | 356           | 124      | 571   | 149        |            |           | 51         | 265             | 402           | 321     |            |        |
| R50-6      | 98                    | 233              | 124              | 415               | 749           |          | 820   | 176        |            |           |            |                 |               |         | 57         |        |
| R2D-1      |                       |                  |                  |                   |               |          |       |            |            |           |            |                 |               |         |            |        |
| A-20C      | 100                   | 284              | 143              | 440               | 222           | 232      | 349   | 33         |            |           | 444        | 334             | 335           |         |            |        |
| A-30A      | 75                    | 223              | 186              | 603               | 395           | 389      | 474   | 154        |            |           | 394        |                 | 635           | 175     | 496        |        |
| R3D-1      | 100                   | 313              | 236              | 524               | 384           |          | 1272  | 107        |            |           |            |                 |               |         | 49         |        |
| Beaufort   |                       | 172              |                  |                   |               |          |       |            |            |           |            |                 |               |         |            |        |
| Ventura I  | 101                   | 310              | 133              | 500               | 415           | 299      | 697   | 182        |            |           | 349        |                 | 2057          | 404     | 236        |        |
| C-47A      | 100                   | 349              | 140              | 470               | 780           |          | 1749  | 237        |            | 307       |            |                 |               |         | -          |        |
| PBJ-1      | 102                   | 423              | 186              | 514               | 263           | 429      | 567   | 75         |            |           | 891        |                 | 1046          | 478     |            |        |
| B-26B      |                       |                  |                  |                   |               |          |       |            |            |           |            |                 |               |         |            |        |
| B-26F      |                       |                  |                  |                   |               |          |       |            |            |           |            |                 |               |         |            |        |
| Wellington | 109                   | 394              | 305              | 864               | 630           | 696      | 583   | 112        |            |           | 994        |                 | 1673          | 553     |            |        |
| RB-1       |                       | 189              |                  |                   |               |          |       |            |            |           |            |                 |               |         |            |        |
| B-30TB     | 100                   | 381              |                  | 563               | 28            |          | 479   | 172        |            | 233       |            |                 |               |         | 150        |        |
| B-24C      | 109                   | 556              | 160              | 929               | 304           |          | 3250  | 375        |            |           |            |                 |               |         |            |        |
| R5C-1      | 106                   | 635              | 479              | 1036              | 578           | 315      | 602   | 213        | 123        |           | 774        | 2135            | 2180          | 1670    |            |        |
| Warwick I  | 100                   | 375              | 852              | 896               | 658           | 0        | 4341  | 432        |            |           |            |                 |               |         |            |        |
| B-17G      |                       | 225              |                  |                   |               |          |       |            |            |           |            |                 |               |         |            |        |
| Manchester | 208                   | 572              |                  | 1244              | 631           | 534      | 998   | 299        |            |           | 534        |                 | 2248          | 1861    |            |        |
| R5D-1      |                       | 300              |                  |                   |               |          |       |            |            |           |            |                 |               |         |            |        |
| EY-3       | 103                   | 867              | 293              | 689               | 718           |          | 2786  | 657        |            |           |            |                 |               |         | -          |        |
| R2Y-1      | 176                   | 504              | 416              | 948               | 625           |          | 873   | 405        |            |           |            |                 |               |         | -          |        |
| PB4Y-2     | 103                   | 652              | 492              | 724               | 696           |          | 487   | 504        |            |           |            |                 |               |         | 455        |        |
| Halifax II | 102                   | 538              | 513              | 1207              | 1454          | 1440     | 568   | 442        |            |           | 885        | 2077            | 2735          | 3289    |            |        |
| Lancaster  |                       | 300              |                  |                   |               |          |       |            |            |           |            |                 |               |         |            |        |
| R5D-2      |                       | 300              |                  |                   |               |          |       |            |            |           |            |                 |               |         |            |        |
| Stirling   | 103                   | 879              | 328              | 712               | 655           |          | 2742  | 427        |            |           |            |                 |               |         |            |        |
| XB-15      |                       | 280              |                  |                   |               |          |       |            |            |           |            |                 |               |         |            |        |
| C-69       |                       |                  |                  |                   |               |          |       |            |            |           |            |                 |               |         |            |        |
| YB-32      | 656                   | 1253             | 457              | 691               | 540           |          | 3462  | 319        |            |           |            |                 |               |         | 1441       |        |
| XB-29      | 319                   | 909              |                  | 932               | 596           |          |       |            |            |           | 1221       |                 | 3738          | 2035    |            |        |
| B-29A      |                       |                  |                  |                   |               |          |       |            |            |           |            |                 |               |         |            |        |
| C-69B      | 103                   | 728              |                  | 1988              | 563           | 1110     | 2327  | 276        | 167        |           | 1260       |                 | 5850          | 2318    |            |        |
| C-74       |                       |                  |                  |                   |               |          |       |            |            |           |            |                 |               |         |            |        |
| XB-19      | 696                   | 1863             | 534              | 1544              | 646           |          | 6520  | 1294       | 198        |           |            |                 |               |         |            |        |
| XR60-1     | 836                   | 1045             |                  | 2132              | 725           | 1913     | 2193  | 1069       |            |           |            |                 |               |         |            |        |
| XB-36      | 583                   | 1156             | 1324             | 1522              | 1498          |          | 14301 | 1023       |            |           |            |                 |               |         | 1802       |        |
| XC-99      | 493                   | 1374             | 101              | 1341              | 986           | 382      | 1733  | 830        | 302        |           | 1320       |                 | 6162          | 7227    |            |        |

References for Chapter 15

Benscoter, Stanley, U. "Estimate of Hull-Weight Change with Varying Length-Beam Ratio for Flying Boats". NACA Research Memorandum RM No. L7F24. August 14, 1947.

Locke, F.W.S. "A Correlation of the Group Weights and Dimensions of Multi-Engine Flying Boats". BuAer Navy Department 1 March 1945. NAVAER A.D.R. Report M-34.

Locke, F.W.S. "The Effect of Size and Speed on Flying Boat Structural Weights". NAVAER Report No. DR-1389. April, 1953.

Odedra, Jessaji. Hope, Geoff. and Kennell, Colen "Use of Seaplanes and Integration within a Sea Base" Naval Surface Warfare Center Carderock Division, Total Ship Systems Directorate Technical Report NSWCCD-20-TR-2004/08 September 2004.



# Stability Theory

## CHAPTER 16: THEORETICAL DETERMINATION OF LONGITUDINAL STABILITY

Kenneth E. Ward, 1942

Introduction

Limits of Stability

Equations of Motion

Non-Dimensional Derivative Coefficients

The Stability Equation

Hydrodynamic Derivatives

Aerodynamic Derivatives

Thrust Derivatives

Example Problem

This chapter was originally Lecture 9 of a 15-lecture course on "Hydrodynamics and Hull Design," taught by Ernest G. Stout, of Consolidated Aircraft Corporation, in San Diego. The University of California organized this as one of several courses specifically developed to give specialized training in the fields essential to National Defense. The notes are part of Course 426.1, taught Wednesdays 7:00 PM - 9:00 PM, starting January 6<sup>th</sup> 1943, Classroom #9, Don Lee building, 1<sup>st</sup> Avenue and A street. For this chapter, Stout enlisted the help of Kenneth E. Ward, formerly of the Langley Memorial Aeronautical Laboratory, who had taken a job with Consolidated Aircraft.

The application of these methods, even with today's computing power, remains a major challenge. However, this lecture is one of the most complete and approachable expositions of the topic.



### Introduction

The subject of the longitudinal stability of a seaplane has been thoroughly covered by a great number of authors. Until recent years, however, the subject has been confined to the stability of the airplane in the air. With the advent of the large flying boat, the stability of the seaplane on the water has become of increasing importance. Perhaps the most important theoretical work that has been published on this subject is that by Ferring and Clauert (reference 1). Later contributions, notably that presented by Klemm, Pierson, and Storer (reference 2) have further analyzed the problem of studying the dynamic stability of the seaplane by analytical methods. Coombes, Ferring, and Johnston (reference 3), Stout (reference 4) and Olson and Land (reference 5), have published interesting papers on experimental methods of studying dynamic stability but there has been no direct correlation between experimental and analytical results other than those presented in reference 2.

The present paper reviews the theoretical developments in a non-dimensional form for direct substitution of tank and wind tunnel data. No attempt is made to analyze the resulting motion of the seaplane.

The reference system which is used is that designated by the NACA which is given on the cover of any NACA technical report.

### Limits of stability

The limits of stability (see figure 1) are defined as the curves of trim plotted against speed which join the points of neutral stability and enclose the trim-speed area within which the flying boat will be stable.

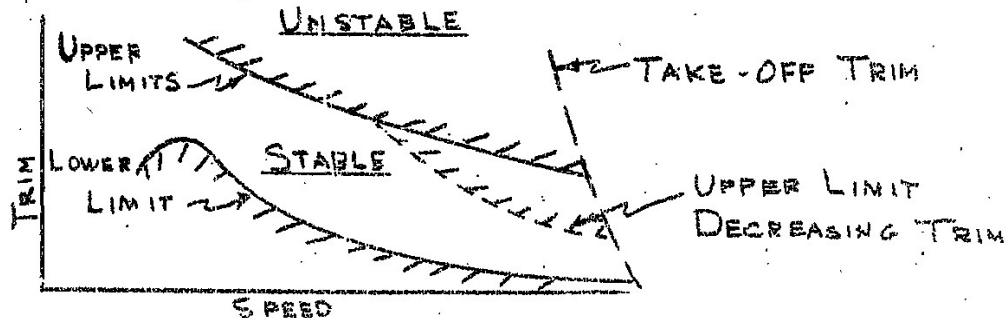


FIG. 1 - LIMITS OF STABILITY

The lower limit of stability is due mainly to the forces acting on the forebody and is affected most by changes in gross weight. An increase in the gross weight tends to raise the lower limit of stability.

The upper limit of stability is due mainly to afterbody interference and may be raised or lowered depending on the resulting interference effects of the flow of water from the forebody as it strikes the afterbody. Changes in gross weight and changes in the effective depth of the step have the largest effect on the upper limit of stability. It will be noticed that two curves are drawn for the upper limit. The solid curve is the principal limit and is obtained analytically, or experimentally with increasing trim. The dashed curve represents a "hysteresis" effect with decreasing trim, which is obtained experimentally, and is caused by interference on the afterbody due to the unstable oscillations (porpoising or skipping) of the seaplane once unstable motion has begun.

The problem of the designer is to estimate the limits of stability for the seaplane from the data available and then so arrange the relative positions of the wing, center of gravity, and steps in order that the airplane will have a reasonable range of centers of gravity and yet remain within the stable limits for take-off and landing with the available aerodynamic control. The equations and derivatives that are required for this estimate form the subject of this paper.

#### Equations of Motion

When a rigid body moves in a plane, three independent variables are, in general, necessary to specify its position; two such as  $x, z$ , to determine the position of some point fixed in the body, and one, such as  $\theta$ , to determine the angle through which the body has turned. This fixed point,  $G$  (figure 2), is ordinarily taken as the center of gravity of the body. It can be shown by simple dynamics that the motion of the body is fully defined by the motion of its center of gravity.

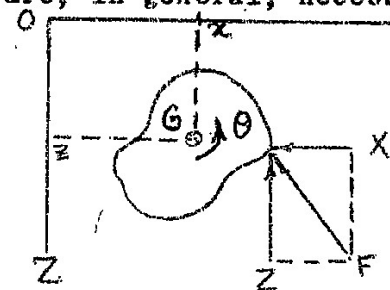


Figure 2 - Forces Acting on a Body

The general expressions for the equations of motion of the body are,

$$m \frac{d^2 x}{dt^2} = X, \quad m \frac{d^2 z}{dt^2} = Z, \quad mk^2 \frac{d^2 \theta}{dt^2} = M$$

where  $m$  = total mass of the body

$x, z$  = coordinates of the center of gravity

$X, Z$  = components of the total resultant external force

$M$  = moment of the resultant force

$mk^2$  = moment of inertia about the center of gravity

$\theta$  = angle of rotation about the center of gravity

In defining the motion of the seaplane let us consider the system of axes to be moving parallel with the surface of the water and with the forward velocity of the seaplane. The equations of motion will then refer to small motions and rotation of the center of gravity in the X-Z plane.

The system of external forces acting on the seaplane are shown in figure 3. This system of forces is conveniently established as the usual components, parallel to the system of axes, of the forces acting on the hull, wing and tail plane. The moments, weight force, parasite drag, and thrust complete the condition of equilibrium. Then for the seaplane in steady motion

$$\left. \begin{aligned} Z &= W - L_h - L_w - L_t - T \sin \beta = 0 \\ X &= T \cos \beta - D_h - D_w - D_t - D_p = 0 \\ M &= l_h L_h + l_w L_w + l_t L_t + l_T T \sin \beta \\ &\quad - h_h D_h - h_w D_w - h_t D_t - h_T T \cos \beta \\ &\quad + M_h + M_w + M_t = 0 \end{aligned} \right\} \quad (1)$$

where  $\beta = i_T + \tau$

$\tau = \text{trim}$

$i_T = \text{angle of thrust line with base line of seaplane}$

$l = \text{moment arm of vertical force}$

$h = \text{moment arm of horizontal force}$

and the subscripts refer to the particular force systems. The base line of the seaplane, to which angles and dimensions are referred, is defined as the tangent to the forebody keel at the step.

Now let a small disturbance take place which causes a small motion of the seaplane from the steady condition. It has been shown earlier that the resulting motion can be regarded as the motion of the c.g. The effect of small changes in accelerations will be considered negligible. The effect of the small disturbance is to change the forces acting on the seaplane by a small amount from those acting for the steady condition. The equations for the resulting motion are

$$\left. \begin{aligned} m \frac{d^2 x}{dt^2} &= m \frac{du}{dt} = (X + dX) - X \\ m \frac{d^2 z}{dt^2} &= m \frac{dw}{dt} = (Z + dZ) - Z \\ mk^2 \frac{d^2 \theta}{dt^2} &= mk^2 \frac{dq}{dt} = (M + dM) - M \end{aligned} \right\} \quad (2)$$

where  $m = W/g$ , the total mass of the seaplane

$du/dt = \text{horizontal acceleration}$

$dw/dt = \text{vertical acceleration}$

$dq/dt = \text{angular acceleration}$

$mk^2 = \text{moment of inertia about the c.g.}$

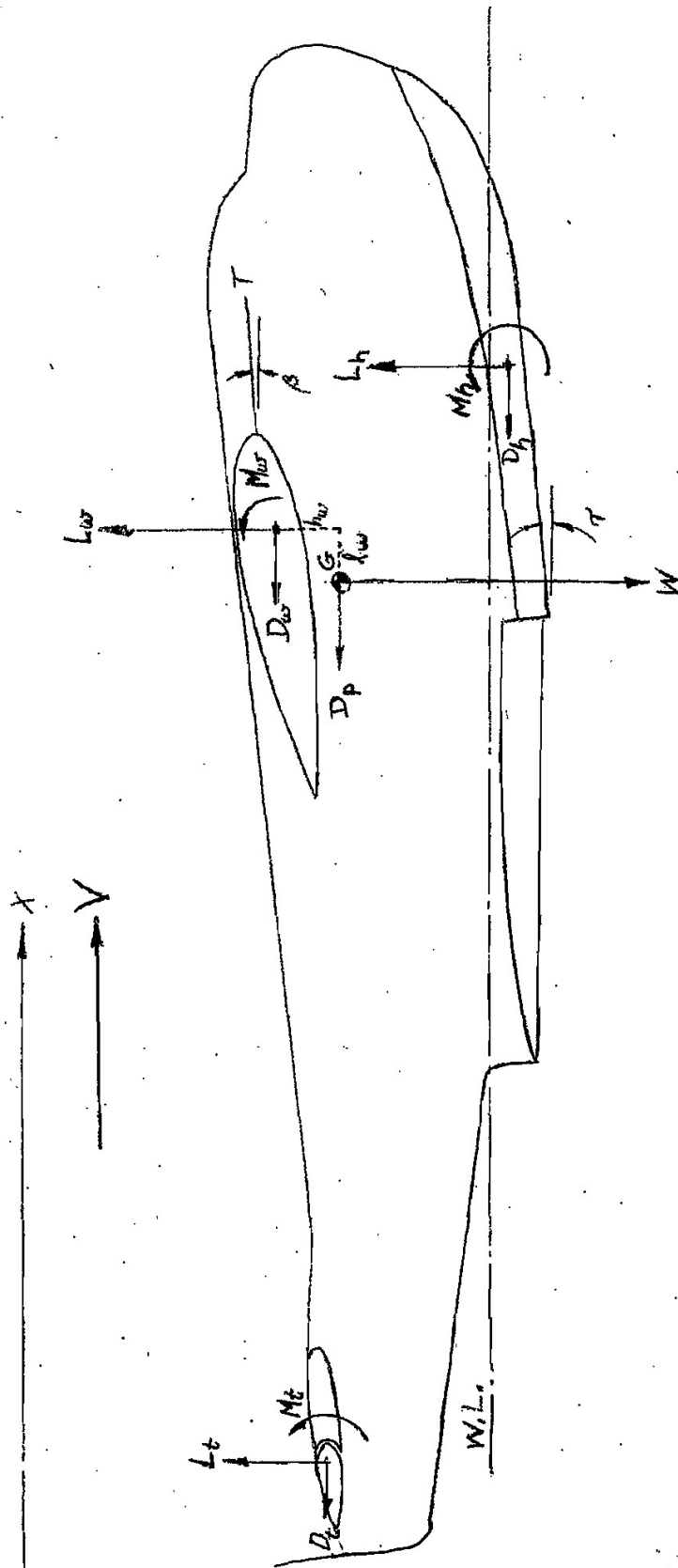


FIG 3  
FORCES ACTING ON A SEAPLANE

Collecting terms, the equations become

$$\begin{aligned} m \frac{du}{dt} &= dX \\ m \frac{dw}{dt} &= dZ \\ mk^2 \frac{dq}{dt} &= dM \end{aligned} \quad (3)$$

The incremental forces  $dX$ ,  $dZ$ , and  $dM$  depend on the velocities,  $u$ ,  $w$  of the center of gravity of the seaplane, the vertical position  $z$ , the angular velocity  $q$  about the c.g., and the angle  $\theta$  through which the seaplane has changed trim. It is assumed that these quantities are all small. The force derivatives may be expanded, neglecting derivatives of a higher order, into the series

$$\left. \begin{aligned} m \frac{du}{dt} &= \frac{\partial X}{\partial u} du + \frac{\partial X}{\partial w} dw + \frac{\partial X}{\partial z} dz + \frac{\partial X}{\partial q} dq + \frac{\partial X}{\partial \theta} d\theta \\ m \frac{dw}{dt} &= \frac{\partial Z}{\partial u} du + \frac{\partial Z}{\partial w} dw + \frac{\partial Z}{\partial z} dz + \frac{\partial Z}{\partial q} dq + \frac{\partial Z}{\partial \theta} d\theta \\ mk^2 \frac{dq}{dt} &= \frac{\partial M}{\partial u} du + \frac{\partial M}{\partial w} dw + \frac{\partial M}{\partial z} dz + \frac{\partial M}{\partial q} dq + \frac{\partial M}{\partial \theta} d\theta \end{aligned} \right\} \quad (4)$$

Because the quantities involved are all small, the increment changes in these quantities may be replaced by the quantities themselves. Then

$$\left. \begin{aligned} m \frac{du}{dt} - \frac{\partial X}{\partial u} u - \frac{\partial X}{\partial w} w - \frac{\partial X}{\partial z} z - \frac{\partial X}{\partial q} q - \frac{\partial X}{\partial \theta} \theta &= 0 \\ m \frac{dw}{dt} - \frac{\partial Z}{\partial u} u - \frac{\partial Z}{\partial w} w - \frac{\partial Z}{\partial z} z - \frac{\partial Z}{\partial q} q - \frac{\partial Z}{\partial \theta} \theta &= 0 \\ mk^2 \frac{dq}{dt} - \frac{\partial M}{\partial u} u - \frac{\partial M}{\partial w} w - \frac{\partial M}{\partial z} z - \frac{\partial M}{\partial q} q - \frac{\partial M}{\partial \theta} \theta &= 0 \end{aligned} \right\} \quad (5)$$

Equations (5) are simultaneous linear equations in  $u$ ,  $z$  and  $\theta$  with constant coefficients and the solutions of these equations are series of terms of the form  $C e^{\lambda t}$

The stability of the seaplane depends on whether it will return to the steady conditions after having been displaced by a small disturbance. If the damping coefficient  $\lambda$  is negative, the motion will be damped with respect to time  $t$  and will be stable. If  $\lambda$  is positive, the amplitude increases with time and the motion is unstable. The three variables  $u$ ,  $z$  and  $\theta$  change according to the function of the damped vibration; that is

$$\left. \begin{aligned} u &= C_1 e^{\lambda t} \\ \frac{du}{dt} &= \lambda C_1 e^{\lambda t} \\ z &= C_2 e^{\lambda t} \\ w = \frac{dz}{dt} &= \lambda C_2 e^{\lambda t} \\ \frac{dw}{dt} &= \lambda^2 C_2 e^{\lambda t} \\ \theta &= C_3 e^{\lambda t} \\ q = \frac{d\theta}{dt} &= \lambda C_3 e^{\lambda t} \\ \frac{dq}{dt} &= \lambda^2 C_3 e^{\lambda t} \end{aligned} \right\} \quad (5A)$$

Substituting these values in equations (5) and cancelling the common factor  $e^{\lambda t}$

$$\left. \begin{aligned} m\lambda c_1 - \frac{\partial X}{\partial u} c_1 - \frac{\partial X}{\partial z} c_2 - \lambda \frac{\partial X}{\partial w} c_2 - \frac{\partial X}{\partial \theta} c_3 - \lambda \frac{\partial X}{\partial q} c_3 &= 0 \\ m\lambda^2 c_2 - \frac{\partial Z}{\partial u} c_1 - \frac{\partial Z}{\partial z} c_2 - \lambda \frac{\partial Z}{\partial w} c_2 - \frac{\partial Z}{\partial \theta} c_3 - \lambda \frac{\partial Z}{\partial q} c_3 &= 0 \\ mk^2\lambda^2 c_3 - \frac{\partial M}{\partial u} c_1 - \frac{\partial M}{\partial z} c_2 - \lambda \frac{\partial M}{\partial w} c_2 - \frac{\partial M}{\partial \theta} c_3 - \lambda \frac{\partial M}{\partial q} c_3 &= 0 \end{aligned} \right\} (6)$$

Collecting terms

$$\left. \begin{aligned} (m\lambda - \frac{\partial X}{\partial u}) c_1 - (\lambda \frac{\partial X}{\partial w} + \frac{\partial X}{\partial z}) c_2 - (\lambda \frac{\partial X}{\partial q} + \frac{\partial X}{\partial \theta}) c_3 &= 0 \\ -\frac{\partial Z}{\partial u} c_1 + (m\lambda^2 - \lambda \frac{\partial Z}{\partial w} - \frac{\partial Z}{\partial z}) c_2 - (\lambda \frac{\partial Z}{\partial q} + \frac{\partial Z}{\partial \theta}) c_3 &= 0 \\ -\frac{\partial M}{\partial u} c_1 - (\lambda \frac{\partial M}{\partial w} + \frac{\partial M}{\partial z}) c_2 + (mk^2\lambda^2 - \lambda \frac{\partial M}{\partial q} - \frac{\partial M}{\partial \theta}) c_3 &= 0 \end{aligned} \right\} (7)$$

which are three simultaneous linear algebraic equations in the three unknowns  $c_1$ ,  $c_2$ , and  $c_3$ . The stability equation is obtained by solving equations (7) simultaneously.

The labor of solving these equations is greatly simplified by putting them in determinant form. A sufficient condition for the solution is that the equation of the coefficients of  $c_1$ ,  $c_2$  and  $c_3$  shall equal zero. That is, in determinant form and using the usual symbols for the derivative coefficients ( $X_u = \partial X / \partial u$ , etc.)

$$\begin{vmatrix} m\lambda - X_u & -\lambda X_w - X_z & -\lambda X_q - X_\theta \\ -Z_u & m\lambda^2 - \lambda Z_w - Z_z & -\lambda Z_q - Z_\theta \\ -M_u & -\lambda M_w - M_z & mk^2\lambda^2 - \lambda M_q - M_\theta \end{vmatrix} = 0 \quad (8)$$

Non-Dimensional Derivative Coefficients

It is now convenient to put equations (8) in non-dimensional form. One of the properties of determinants is: If all elements in any column or row are multiplied by any factor, the determinant is multiplied by that factor; that is,

$$D = \begin{vmatrix} fa_1 & b_1 & c_1 \\ fa_2 & b_2 & c_2 \\ fa_3 & b_3 & c_3 \end{vmatrix} = \begin{vmatrix} a_1 & b_1 & c_1 \\ fa_2 & fb_2 & fc_2 \\ a_3 & b_3 & c_3 \end{vmatrix} = f \begin{vmatrix} a_1 & b_1 & c_1 \\ a_2 & b_2 & c_2 \\ a_3 & b_3 & c_3 \end{vmatrix}$$

Making use of this property we can reduce equations (8), after substituting for the dimensional terms, by eliminating all factors common to any column or row because the determinant is equal to zero. We will therefore define non-dimensional derivative coefficients and certain ratios so that all of the dimensional factors may be cancelled out of the determinant

The general equations of motion were developed by considering all of the external forces acting on the seaplane. Therefore, in order to use the non-dimensional coefficients we must express the forces in consistent units

Theory states that the force on a body moving in a fluid can be expressed (neglecting all but the effects of fluid friction and mass forces) as the Newtonian relation

$$F = \rho V^2 L^2 \left[ f_1 \left( \frac{VL}{\nu} \right) + f_2 \left( \frac{Lg}{V^2} \right) \right] \quad (9)$$

where  $\rho$  = mass density of the fluid  
 $V$  = velocity  
 $L$  = a linear dimension  
 $\nu$  = kinematic viscosity  
 $g$  = acceleration of gravity

The first non-dimensional ratio ( $VL/\nu$ ), which depends on the fluid friction, is Reynold's number and the second ( $Lg/V^2$ ), which depends on the mass forces, is Froude's number. In testing models of seaplanes it is assumed that the wave-making, or mass effects, predominate for the hydrodynamic forces and that the viscous effects predominate for the aerodynamic forces. Non-dimensional coefficients may then be used in place of the two functions; that is,

$$F_h = \frac{1}{2} \rho V^2 L^2 C_{F_h} \quad \text{for the hydrodynamic forces} \quad (10)$$

$$\text{and } F_a = \frac{1}{2} \rho V^2 L^2 C_{F_a} \quad \text{for the aerodynamic forces} \quad (11)$$

where  $C_{F_h} = f_2 (Lg/V^2)$  and  $C_{F_a} = f_1 (VL/\nu)$

and each coefficient is considered independent of the other function. The factor  $1/2$  is introduced because of the significance of the fluid dynamic pressure,  $1/2 \rho V^2$ . The usual NACA coefficients will be used to define the forces and moments except that the hydrodynamic coefficients

will not include the Froude number for the main part of the analysis.

By introducing the non-dimensional ratio

$$\sigma = \frac{1}{2} \frac{S}{b^2} \frac{\rho}{\rho'} \quad (12)$$

the aerodynamic coefficients may be expressed in the same terms as the hydrodynamic coefficients; that is,

$$F_a = \frac{1}{2} \rho v^2 S C_{F_a} = \frac{1}{2} \rho' v^2 b^2 (2\sigma C_{F_a}) \quad (13)$$

The non-dimensional derivative coefficients are defined by forms similar to the derivatives of the basic force and moment equations as follows:

|   | Force                               | Moment                              |
|---|-------------------------------------|-------------------------------------|
| Basic equation                              | $F = \frac{1}{2} \rho' v^2 b^2 C_F$ | $M = \frac{1}{2} \rho' v^2 b^3 C_M$ |
| Derivative with respect to linear velocity  | $F_u, w = \rho' v b^2 C_{F1}$       | $M_u, w = \rho' v b^3 C_{M1}$       |
| Derivative with respect to linear position  | $F_x = \rho' v^2 b C_{F2}$          | $M_x = \rho' v^2 b^2 C_{M2}$        |
| Derivative with respect to angular position | $F_\theta = \rho' v^2 b^2 C_{F3}$   | $M_\theta = \rho' v^2 b^3 C_{M3}$   |
| Derivative with respect to angular velocity | $F_q = \rho' v b^3 C_{F4}$          | $M_q = \rho' v b^4 C_{M4}$          |

Letting the coefficients  $C_{F1}$ ,  $C_{F2}$ , ...  $C_{M1}$ ,  $C_{M2}$ --- etc., equal  $x_u$ ,  $x_x$ , ...  $m_u$ ,  $m_x$ ...etc., where the subscript as before represents the derivative ( $x_u = \frac{\partial x}{\partial u}$ , etc.), the derivative coefficients are as follows:

$$\left. \begin{aligned} x_u &= X_u / \rho' v b^2 & z_u &= Z_u / \rho' v b^2 & m_u &= \eta M_u / \rho' v b^3 \\ x_x &= C_{\Delta_0} X_x / \rho' v^2 b & z_x &= C_{\Delta_0} Z_x / \rho' v^2 b & m_x &= C_{\Delta_0} \eta M_x / \rho' v^2 b^2 \\ x_w &= X_w / \rho' v b^2 & z_w &= Z_w / \rho' v b^2 & m_w &= \eta M_w / \rho' v b^3 \\ x_\theta &= C_{\Delta_0} X_\theta / \rho' v^2 b^2 & z_\theta &= C_{\Delta_0} Z_\theta / \rho' v^2 b^2 & m_\theta &= C_{\Delta_0} \eta M_\theta / \rho' v^2 b^3 \\ x_q &= X_q / \rho' v b^3 & z_q &= Z_q / \rho' v b^3 & m_q &= \eta M_q / \rho' v b^4 \end{aligned} \right\} \quad (14)$$

where the factor  $C_{\Delta_0}$  represents the ratio of relative densities. (Note: This factor is the familiar hydrodynamic coefficient for the gross load),



$$C_{\Delta 0} = m / e' b^3 \quad (15)$$

The damping factor  $\lambda$  and the moment of inertia  $mk^2$  are put in non-dimensional form by defining a damping coefficient.

$$\mu = \frac{m}{e' \sqrt{b^2} \lambda} \quad (16)$$

and a moment of inertia coefficient

$$1/\eta = mk^2 / mb^2 \quad (17)$$

Substituting these coefficients, equations (14) to (17), in the determinant equation (8) and cancelling all factors common to any column or row, the equation in non-dimensional form becomes

$$\begin{vmatrix} \mu - \chi_0 & -\mu \chi_w - \chi_z & -\mu \chi_q - \chi_\theta \\ -z_0 & \mu^2 - \mu z_w - z_z & -\mu z_q - z_\theta \\ -m_0 & -\mu m_w - m_z & \mu^2 - \mu m_q - m_\theta \end{vmatrix} = 0 \quad (18)$$

which is an equation in the fifth degree of the damping coefficient  $\mu$ .

#### The Stability Equation

Glauert and Perring concluded in their theoretical analysis that small longitudinal velocity changes will not affect the stability of the seaplane. Recent tests at the NACA (reference 5) have verified this conclusion. The stability equation may, therefore, be greatly simplified by eliminating all of the  $u$  derivatives. Equation (18), by eliminating the first column and first row, becomes

$$\begin{vmatrix} \mu^2 - \mu z_w - z_z & -\mu z_q - z_\theta \\ -\mu m_w - m_z & \mu^2 - \mu m_q - m_\theta \end{vmatrix} = 0 \quad (19)$$

This is the stability equation in the fourth degree which, on expansion, becomes

$$\left. \begin{aligned} &\mu^4 \\ &+ \mu^3 (-z_w - m_q) \\ &+ \mu^2 (-z_z - z_q m_w + z_w m_q - m_\theta) \\ &+ \mu (z_q m_q - z_q m_z - z_w m_\theta - z_\theta m_w) \\ &+ (z_z m_\theta - z_\theta m_z) \\ &= 0 \end{aligned} \right\} \quad (20)$$

Equation (20) can be written in the form

$$A\mu^4 + B\mu^3 + C\mu^2 + D\mu + E = 0 \quad (21)$$

where

$$A = 1$$

$$B = (-Z_w - m_z)$$

$$C = (-Z_z - Z_z m_w + Z_w m_z - m_\theta)$$

$$D = (Z_z m_z - Z_z m_z + Z_w m_\theta - Z_\theta m_w)$$

$$E = (Z_z m_\theta - Z_\theta m_z)$$

Equation (21) is the general equation of motion for any body acted on by a system of forces which differ slightly from those which maintain equilibrium of the body in the steady condition. The equation describes the resulting motion of the body and the signs of its roots determine whether the motion will increase in amplitude with time so that the motion is unstable, or will decrease with time so that the motion is stable.

Fortunately, it is not necessary to solve the equation in order to determine the stability characteristics. Routh (reference 6) has shown that the motion will be stable if each one of the coefficients A, B, C, D, and E and the discriminant

$$R = (CD - BE) B - AD^2 \quad (22)$$

are positive and not zero as the roots of the equation will then all be negative.

#### Hydrodynamic Derivatives

The forces acting on the hull are measured in a general tank test of a model. These forces are defined in terms of their non-dimensional coefficients as discussed previously (equation 10).

$$\Delta = L_n = \frac{1}{2} \rho' v^2 b^2 C_{\Delta}' = w b^3 C_{\Delta} \quad (23)$$

$$R = D_n = \frac{1}{2} \rho' v^2 b^2 C_R' = w b^3 C_R \quad (24)$$

and the moment, taken about the c.g., is

$$M = \frac{1}{2} \rho' v^2 b^3 C_M' = w b^4 C_M \quad (25)$$

where the fundamental length L is taken as the beam b. The primed coefficients are used to differentiate them from the usual coefficients (unprimed) given in publications of hydrodynamic tests. The coefficients are related by the simple factor  $1/2 \rho' v^2$  as, for example, the load coefficient

$$C_{\Delta} = C_{\Delta}' \frac{1}{2} C_v^2$$

In the following analysis, all of the derivatives involved in the general stability, equation (18), will be evaluated in order that a more complete understanding of the derivatives may be obtained.

u - derivatives - The small variation in forward velocity  $u$  is the equivalent of a variation in the total velocity  $V$ . That part of the X-force due to the hydrodynamic resistance  $R$  is expressed as

$$X = -R = -\frac{1}{2} \rho' V^2 b^2 C_R$$

Differentiating with respect to the velocity,

$$X_u = \frac{\partial X}{\partial V} = \frac{\partial X}{\partial V} = -\frac{1}{2} \rho' V b^2 \cdot 2 C_R' \quad (26)$$

and the non-dimensional derivative coefficient is

$$x_u = X_u / \rho' V b^2 = -C_R' = -2 C_R / C_V^2 \quad (27)$$

The lift and moment derivatives are found in a similar manner as

$$Z_u = -C_\Delta' = -2 C_\Delta / C_V^2 \quad (28)$$

$$m_u = C_M' / \eta = 2 \eta C_M / C_V^2 \quad (29)$$

z - Derivatives - The small change in vertical position may be obtained directly as the change in rise of the center of gravity, or the change in draft at constant trim. The non-dimensional coefficient for the rise is

$$C_r = \frac{I}{b} = \frac{z}{b} \quad (30)$$

Then

$$\partial z = -b \partial C_r$$

and

$$X_z = \frac{-\partial R}{-\partial z} = \frac{1}{2} \rho' V^2 b \frac{\partial C_R'}{\partial C_r} \quad (31)$$

where the rise is measured positively with increase in rise. The non-dimensional derivative coefficient is

$$X_z = C_{\Delta_0} X_z / \rho' V^2 b = \frac{1}{2} C_{\Delta_0} \frac{\partial C_R'}{\partial C_r} = C_{\Delta_0} (\partial C_R / \partial C_r) / C_V^2 \quad (32)$$

The lift and moment derivatives are found in a similar manner as

$$Z_z = \frac{1}{2} C_{\Delta_0} (\partial C_\Delta' / \partial C_r) = C_{\Delta_0} (\partial C_\Delta / \partial C_r) / C_V^2 \quad (33)$$

$$m_z = -\frac{1}{2} \eta C_{\Delta_0} (\partial C_M' / \partial C_r) = -\eta C_{\Delta_0} (\partial C_M / \partial C_r) / C_V^2 \quad (34)$$

w - derivatives - A small vertical velocity  $w$  combined with the forward velocity  $V$  is the equivalent of a small positive change in angle  $w/V$  radians. Because the forces are measured parallel to the axes, the change in forces accompanying the change in direction of

the resultant velocity must be taken into account. (See figure 4). Let the change in angle be designated  $\partial\tau$ , the change in trim. Then

$$\partial\tau = w/V \text{ RADIANS}$$

The new values of the forces will be

$$X + \partial X = -(R + \partial R) \cos \partial\tau - (\Delta + \partial\Delta) \sin \partial\tau$$

$$= -R - \partial R + \Delta \partial\tau$$

$$Z + \partial Z = -(\Delta + \partial\Delta) \cos \partial\tau - (R + \partial R) \sin \partial\tau$$

$$= -\Delta - \partial\Delta - R \partial\tau$$

neglecting second order terms

as  $X = -R$ ,  $Z = -\Delta$ , and  $\partial\tau = w/V$  then

$$\partial X = -\partial R + \Delta (w/V) = -\left(\frac{1}{V} \frac{\partial R}{\partial \tau} - \frac{\Delta}{V}\right) w$$

$$\text{AND } X_w = -\frac{1}{V} \left(\frac{\partial R}{\partial \tau} - \Delta\right) = \frac{1}{2} \rho' V b^2 \left(\frac{\partial C_R}{\partial \tau} - C_{\Delta}\right) \quad (35)$$

$$\text{THEN } x_w = X_w / \rho' V b^2 = -\left(\frac{\partial C_R}{\partial \tau} - C_{\Delta}\right) / C_v^2 \quad (36)$$

and the lift derivative is

$$z_w = -(\partial C_{\Delta} / \partial \tau + C_R) / C_v^2 \quad (37)$$

The moment derivative is not affected by the rotation of the force vectors so that

$$M_w = \frac{1}{2} \rho' V^2 b^3 \frac{\partial C_M}{\partial w} = \frac{1}{2} \rho' V b^3 \frac{\partial C_M}{\partial \tau} \quad (38)$$

$$m_w = \frac{1}{2} \eta \frac{\partial C_M}{\partial \tau} = \eta \frac{\partial C_M}{\partial \tau} / C_v^2 \quad (39)$$

$\theta$  - derivatives - A change in the angle  $\theta$  is the same as a change in the trim  $\tau$  so that

$$X_{\theta} = -\frac{\partial R}{\partial \tau} = -\frac{1}{2} \rho' V^2 b^2 \frac{\partial C_R}{\partial \tau} \quad (40)$$

$$x_{\theta} = C_{\Delta_0} X_{\theta} / \rho' V^2 b^2 = -\frac{1}{2} C_{\Delta_0} \frac{\partial C_R}{\partial \tau} = -C_{\Delta_0} \frac{\partial C_R}{\partial \tau} / C_v^2 \quad (41)$$

$$z_{\theta} = -\frac{1}{2} C_{\Delta_0} \frac{\partial C_{\Delta}}{\partial \tau} = -C_{\Delta_0} \frac{\partial C_{\Delta}}{\partial \tau} / C_v^2 \quad (42)$$

$$m_{\theta} = \frac{1}{2} \eta C_{\Delta_0} \frac{\partial C_M}{\partial \tau} = \eta C_{\Delta_0} \frac{\partial C_M}{\partial \tau} / C_v^2 \quad (43)$$

$q$  - derivatives - The change in angular velocity may be considered as a change in the two components of the linear velocity at the center of pressure (figure 5). Although this assumption is not strictly true because of the distribution of forces all along the bottom of the seaplane, the approximation is probably of sufficient accuracy for the study of stability. The linear velocity at the center of pressure is  $u$ ,  $q$  and the two components are

$$\partial u = h \partial q, \quad -\partial w = l \partial q$$

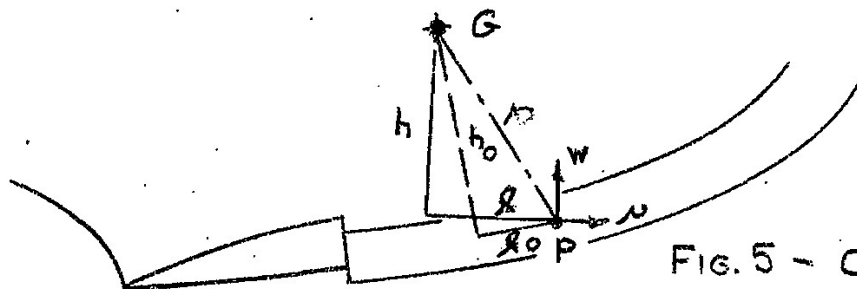


FIG. 5 - CENTER OF PRESSURE ON HULL BOTTOM

Then

$$X_q = \frac{\partial X}{\partial v} \cdot \frac{\partial v}{\partial q} + \frac{\partial X}{\partial w} \cdot \frac{\partial w}{\partial q} \quad (44)$$

$$\text{or } X_q = hX_u - lX_w \quad (45)$$

$$\text{and } x_q = \frac{h}{b} x_u - \frac{l}{b} x_w \quad (46)$$

where  $h$  = vertical distance from the c.g. to the c.p.  
 $l$  = horizontal distance from the c.g. to the c.p.  
 $b$  = beam

The other two derivatives are evaluated in a similar manner as,

$$z_q = \frac{h}{b} z_u - \frac{l}{b} z_w \quad (47)$$

$$m_q = \frac{h}{b} m_u - \frac{l}{b} m_w \quad (48)$$

The position of the center of pressure may be located with sufficient accuracy by assuming the least-important vertical dimension and computing the horizontal dimension from the known force and moment coefficients. Let us therefore assume that the center of pressure lies in a plane half way between the keel and the chines. The dimension normal to the base line is designated  $h_0$ . The dimension parallel with the base line is designated  $l_0$  and is computed from the moment equation as

$$\frac{l_0}{b} = \frac{C_M + \frac{h_0}{b} (C_R \cos \gamma - C_\Delta \sin \gamma)}{C_\Delta \cos \gamma + C_R \sin \gamma} \quad (49)$$

where  $C_M$ ,  $C_\Delta$ , and  $C_R$  are the usual hydrodynamic coefficients ( $C_{Mh}$  is included in the measured value of  $C_M$ ). Then

$$\left. \begin{aligned} l &= l_0 \cos \gamma + h_0 \sin \gamma \\ h &= h_0 \cos \gamma - l_0 \sin \gamma \end{aligned} \right\} \quad (50)$$

Aerodynamic Derivatives

The aerodynamic derivatives are evaluated in exactly the same manner as were the hydrodynamic derivatives. The forces and moments are defined in terms of their usual non-dimensional coefficients (See equation 11) as

$$C_D = D / \frac{1}{2} \rho v^2 S \quad ; \quad C_L = L / \frac{1}{2} \rho v^2 S$$

$$C_M = M / \frac{1}{2} \rho v^2 S c = C_{M_{ac}} + \left( \frac{2}{b} C_L - \frac{h}{b} C_D \right) \frac{c}{b}$$

where the fundamental length  $l$  squared is taken as the area  $S$  of the aerodynamic surface, the chord  $c$  is the mean aerodynamic chord of the surface,  $b$  is the beam, and the moment  $M$  is taken about the c.g.

u - derivatives

$$X = -D = -\frac{1}{2} \rho v^2 S C_D \quad (51)$$

$$X_u = -\frac{1}{2} \rho v S (2 C_D) = -\rho' v b^2 \sigma C_D \quad (52)$$

$$x_u = X_u / \rho' v b^2 = -2 \sigma C_D \quad (53)$$

where  $\sigma = \frac{1}{2} \frac{S}{b^2} \frac{\rho}{\rho'}$  as defined previously.

$$\text{Likewise, } z_u = -2 \sigma C_L \quad (54)$$

$$M = \frac{1}{2} \rho v^2 S c C_M \quad (55)$$

$$M_u = \frac{1}{2} \rho v S c (2 C_M) = \rho' v b^3 \sigma \left( 2 \frac{c}{b} C_M \right) \quad (56)$$

$$m_u = M_u / \rho' v b^3 = \eta \sigma \left( 2 \frac{c}{b} C_M \right) \quad (57)$$

z = derivatives - The derivatives for the change in vertical position are generally neglected as the change in forces due to the change in ground effect is very small.

w - derivatives - The small vertical velocity  $w$ , as for the hydrodynamic derivative, is equivalent to a small change in trim, or angle of attack,  $\partial \alpha = w/v$ .

$$\partial X = -\partial D + L (w/v) = -\left( \frac{1}{v} \frac{\partial D}{\partial \alpha} - \frac{L}{v} \right) w \quad (58)$$

$$X_w = -\frac{1}{2} \rho v S \left( \frac{\partial C_D}{\partial \alpha} - C_L \right) = -\frac{1}{2} \rho' v b^2 \sigma \left( \frac{\partial C_D}{\partial \alpha} - C_L \right) \quad (59)$$

$$x_w = x_w / \rho' v b^2 = -\sigma \left( \frac{\partial c_D}{\partial \alpha} - c_L \right) \quad (60)$$

$$x_w = -\sigma \left( \frac{\partial c_L}{\partial \alpha} + c_D \right) \quad (61)$$

$$m_w = \frac{1}{2} \rho v^2 s \cdot \frac{\partial c_M}{\partial w} = \rho' v b^3 \sigma \frac{c}{b} \frac{\partial c_M}{\partial \alpha} \quad (62)$$

$$m_w = \eta \sigma \frac{c}{b} \frac{\partial c_M}{\partial \alpha} \quad (63)$$

$\theta$  - derivatives

$$x_\theta = -\frac{\partial D}{\partial \alpha} = -\frac{1}{2} \rho v^2 s \frac{\partial c_D}{\partial \alpha} = -\frac{1}{2} \rho' v^2 b^2 \sigma \frac{\partial c_D}{\partial \alpha} \quad (64)$$

$$x_\theta = -C_{D_0} \sigma \frac{\partial C_0}{\partial \alpha} \quad (65)$$

$$z_\theta = -C_{A_0} \sigma \frac{\partial c_L}{\partial \alpha} \quad (66)$$

$$m_\theta = \eta \sigma C_{D_0} \frac{c}{b} \frac{\partial c_M}{\partial \alpha} \quad (67)$$

q - derivatives - By analogy with the hydrodynamic derivatives

$$x_q = \frac{h}{b} x_u - \frac{1}{b} x_w \quad (68)$$

$$z_q = \frac{h}{b} z_u - \frac{1}{b} z_w \quad (69)$$

$$m_q = \frac{h}{b} m_u - \frac{1}{b} m_w \quad (70)$$

### Thrust Derivatives

The thrust is usually considered as applying only a constant moment and therefore all of the derivatives are zero. In the case of high-powered airplanes, the variation in thrust should probably be considered. This subject, however, will not be discussed at this time.

The various derivative coefficients are summarized below:

| Derivative | Hydrodynamic  | Aerodynamic   |
|------------|---|---|
| $x_u$      | $-2 C_R / C_v^2$  | $-2 \sigma C_D$   |
| $x_z$      | $C_{D_0} \frac{\partial C_R}{\partial C_L} / C_v^2$         | 0   |
| $x_w$      | $-(\frac{\partial C_R}{\partial \alpha} - C_D) / C_v^2$     | $-\sigma (\frac{\partial C_D}{\partial \alpha} - C_L)$      |
| $x_\theta$ | $-C_{D_0} \frac{\partial C_R}{\partial \alpha} / C_v^2$     | $-\sigma C_{D_0} \frac{\partial C_D}{\partial \alpha}$      |
| $x_q$      | $\frac{h}{b} x_u - \frac{e}{b} x_w$                         | $\frac{h}{b} x_u - \frac{e}{b} x_w$                         |
| $z_u$      | $-2 C_D / C_v^2$  | $-2 \sigma C_L$   |
| $z_z$      | $C_{D_0} \frac{\partial C_D}{\partial C_L} / C_v^2$         | 0   |
| $z_w$      | $-(\frac{\partial C_D}{\partial \alpha} + C_R) / C_v^2$     | $-\sigma (\frac{\partial C_L}{\partial \alpha} + C_D)$      |
| $z_\theta$ | $-C_{D_0} \frac{\partial C_D}{\partial \alpha} / C_v^2$     | $-\sigma C_{D_0} \frac{\partial C_L}{\partial \alpha}$      |
| $z_q$      | $\frac{h}{b} z_u - \frac{e}{b} z_w$                         | $\frac{h}{b} z_u - \frac{e}{b} z_w$                         |
| $m_u$      | $2 \eta C_M / C_v^2$  | $2 \eta \sigma \frac{C}{b} C_M$                             |
| $m_z$      | $-\eta C_{D_0} \frac{\partial C_M}{\partial C_L} / C_v^2$   | 0   |
| $m_w$      | $-\eta \frac{\partial C_M}{\partial \alpha} / C_v^2$        | $2 \sigma \frac{C}{b} \frac{\partial C_M}{\partial \alpha}$ |
| $m_\theta$ | $\eta C_{D_0} \frac{\partial C_M}{\partial \alpha} / C_v^2$ | $C_{D_0} m_w$   |
| $m_q$      | $\frac{h}{b} m_u - \frac{e}{b} m_w$                         | $\frac{h}{b} m_u - \frac{e}{b} m_w$                         |

WHERE:  $\eta = mb^2 / mk^2 = mb^2 / I$   
 AND  $\sigma = \frac{1}{2} \frac{\rho S}{b^2 \rho^1}$



References

1. Perring, W.G.A., and Glaupert, H. - Stability on the water of a Seaplane in the Planing Condition. British R & M No.1493, September, 1932.
2. Klemm, A., Pierson, J.D., and Storer, E.M. - An Introduction to Seaplane Porpoising - Jour.Aero.Sc., Vol. 6, No.8, June 1939.
3. Coombes, L.P., Perring, W.G.A., and Johnston, L. - The Use of Dynamically Similar Models for Determining the Porpoising Characteristics of Seaplanes. British R & M No.1718, Nov. 1935.
4. Stout, E.G. - Experimental Determination of Hydrodynamic Stability - Jour.Aero. Sc., Vol.8, No.2, Dec.1940.
5. Olson, E.R., and Land, N.L. - The Longitudinal Stability of Flying Boats as determined by Tests of Models in the N.A.C.A. Tank. Part I - N.A.C.A. Confidential Report.
6. Routh, E.J. - Advanced Rigid Dynamics, Vol. II - The MacMillan Company, 1905.

SAMPLE COMPUTATION

A sample computation will be worked out for a 46,000 lb. flying boat at a speed of 41 knots ( $C_v = 4.0$ ) and a trim of 7 degrees. The sign of the roots of the stability equation will determine whether the airplane is stable at this speed and trim.

It is assumed that a general tank test of the hull has been made and that these data have been reduced to give the required slopes of hydrodynamic forces and moments versus trim at constant draft and versus draft at constant trim. Either wind tunnel data, if available, or estimated data may be used for the aerodynamic forces and moments. Basic data for the airplane are as follows:

# Stability Theory

## GENERAL

|  |                |                      |                       |
|--|----------------|----------------------|-----------------------|
| Gross weight   | W              | 46000                | lb.                   |
| Gross-load coefficient ( $W/\rho'gb^3$ )                 | $C_{\Delta_0}$ | 0.932                |                       |
| Beam   | b              | 9.17                 | ft.                   |
| Center of gravity (Percent MAC ahead of step above keel) | cg             | 28.85<br>32.5<br>154 | in.<br>in.            |
| Longitudinal moment of inertia about c.g. I              |                | 166000               | slug-ft. <sup>2</sup> |
| Moment-of-inertia ratio ( $mb^2/I$ )                     | $\eta$         | 0.725                |                       |
| Mass of airplane   | m              | 1430                 | slugs                 |
| Mass density of seawater                                 | $\rho'$        | 1.99                 | slugs/cu.ft.          |
| Effective deadrise of forebody at step                   | $\delta$       | 18                   | deg.                  |
| Aerodynamic conversion ratio                             | $\sigma$       | 0.00745              |                       |

## WING

|  |                        |                 |          |
|--|------------------------|-----------------|----------|
| Area                                       | S                      | 1048            | sq.ft.   |
| Span                                       | s                      | 110             | ft.      |
| Mean aerodynamic chord                     | c                      | 10.3            | ft.      |
| Effective aspect ratio (incl.gnd.effect) A |                        | 20              |          |
| Lift curve slope for inf.A.R.(flaps down)  | $\alpha_0$             | 6.9             | per rad. |
| Aerodynamic center from c.g.               | $(h_0/b)$<br>$(l_0/b)$ | -0.218<br>0.077 |          |
| Incidence                                  | i                      | 3               | deg.     |
| Flap deflection                            | $\delta_f$             | 40              | deg.     |

## HORIZONTAL TAILPLANE

|                                |                        |                 |          |
|--------------------------------|------------------------|-----------------|----------|
| Area                           | S                      | 192             | sq.ft.   |
| Span                           | s                      | 26              | ft.      |
| Aspect ratio                   | A                      | 3.52            |          |
| Lift curve slope for inf. A.R. | $\alpha_0$             | 5.7             | per rad. |
| Elevator hinge from c.g.       | $(h_0/b)$<br>$(l_0/b)$ | -0.582<br>-4.94 |          |

Wing Coefficients

The moment arms of the aerodynamic center of the wing are found from equation (50) as,

$$\begin{aligned} l/b &= (l_0/b) \cos \tau + (h_0/b) \sin \tau \\ &= .077 \times .99255 - .218 \times .12187 \\ &= .050 \end{aligned}$$

$$\begin{aligned} h/b &= (h_0/b) \cos \tau - (l_0/b) \sin \tau \\ &= -.218 \times .99255 - .077 \times .12187 \\ &= -.225 \end{aligned}$$

The slope of the lift curve and the lift coefficient are determined as follows:

$$\frac{\partial C_L}{\partial \alpha} = \frac{a_0}{1 + a_0/\pi A} = \frac{6.9}{1 + 6.9/20\pi} = 6.20$$

$$C_L = \frac{\partial C_L}{\partial \alpha} (\tau + i - \alpha_{10}) = 6.20 (.122 + .052 + .128) = 1.87$$

where the angle of zero lift,  $\alpha_{10} = -7.3$  deg.

The drag coefficient and the slope of the drag curve are determined as follows:

$$C_D = C_{D_0} + k C_L^2 = .0345 + .0050 \times 1.87^2 = .0520$$

$$\frac{\partial C_D}{\partial \alpha} = \frac{\partial C_D}{\partial C_L} \times \frac{\partial C_L}{\partial \alpha} = (.010 \times 1.87) \times 6.20 = .116$$

The moment coefficient and the slope of the moment curve are determined as follows:

$$\begin{aligned} C_M &= C_{M_{ac}} + (l/b) C_L - (h/b) C_D \\ &= -.310 + .050 \times 1.87 - .225 \times .0520 \\ &= -.205 \end{aligned}$$

$$\begin{aligned} \frac{\partial C_M}{\partial \alpha} &= \left( \frac{\partial C_L}{\partial \alpha} + C_D \right) \left( \frac{l_0}{b} + \frac{h_0}{b} \tau \right) - \left( \frac{\partial C_D}{\partial \alpha} - C_L \right) \left( \frac{h_0}{b} - \frac{l_0}{b} \tau \right) \\ &= (6.20 + .052)(.077 - .218 \times .122) - (.116 - 1.87)(-.218 - .077 \times .122) \\ &= -.086 \end{aligned}$$

where it is assumed, for simplicity, that  $\cos \tau = 1$  and  $\sin \tau = \tau$

Hull Coefficients

The load on the water is found from the difference between the gross weight and the lift provided by the wing and tail plane:

$$\begin{aligned} C_{\Delta} &= C_{\Delta 0} = \frac{1}{2} C_v^2 (C_{L_w} + C_{L_t}) \\ &= .932 - .00745 \times 4.0^2 (1.87 + 0.27) \\ &= .677 \end{aligned}$$

where the subscripts (w) and (t) are used to denote wing and tail. (It is necessary to assume a lift coefficient for the tail which is later checked and the computations repeated if necessary.)

The remaining coefficients are obtained from prepared charts of the measured characteristics.

$$\begin{array}{lll} C_{\Delta} = .677 & C_R = .115 & C_M = .23 \\ \frac{\partial C_{\Delta}}{\partial C_R} = -5.8 & \frac{\partial C_R}{\partial C_T} = -1.0 & \frac{\partial C_M}{\partial C_R} = -5.5 \\ \frac{\partial C_{\Delta}}{\partial T} = 4.6 & \frac{\partial C_R}{\partial T} = 1.2 & \frac{\partial C_M}{\partial T} = -2.1 \end{array}$$

The position of the center of pressure on the hull is determined from equation (49) and the assumed vertical position as described on the same page.

$$\begin{aligned} \frac{h_0}{b} &= \frac{\text{keel to c.g.}}{\text{beam}} - 1/4 \tan \delta \\ &= \frac{154}{110} - 1/4 \tan \text{deg.} \\ &= 1.32 \\ \frac{l_0}{b} &= \frac{C_M + (h_0/b) (C_R - C_{\Delta} T)}{C_{\Delta} + C_R T} \\ &= \frac{.23 + 1.32 (.115 - .677 \times .122)}{.677 + .115 \times .122} \\ &= .396 \end{aligned}$$

$$\frac{l}{b} = \frac{l_0}{b} + \frac{h_0}{b} T = .396 + 1.32 \times .122 = .557$$

$$\frac{h}{b} = \frac{h_0}{b} - \frac{l_0}{b} T = 1.32 - .396 \times .122 = 1.27$$

Thrust Moment

The thrust is assumed to vary with the speed according to the following relation:

$$T = 11000 - 70 CV^2 \text{ lb.}$$

and has a moment arm about the c.g. normal to the thrust line (in terms of the MAC),

$$h_T/c = -.178$$

The thrust moment is defined in non-dimensional form with terms similar to those used to define the aerodynamic moment coefficients,

$$\begin{aligned} C_{MT} &= \frac{T(h_T/c)}{\frac{1}{2} \rho V^2 S_w} \\ &= \frac{(11000 - 70 \times 4.02) (-.178)}{.00256 \times 47^2 \times 1048} \\ &= -.297 \end{aligned}$$

Tailplane Coefficients

(Note: All aerodynamic coefficients are based on the wing area and mean aerodynamic chord. Subscripts (w), (t), (h), and (T) are used where required to designate wing, tail, hull, and thrust.)

Because of the varying conditions under which the tailplane must operate, and the abnormal values of the tail lift that are required to obtain the trim limits of stability, the moment and lift are computed from the moment required to maintain the trim under consideration. The moment is obtained from the expression for the moment balance as,

$$\begin{aligned} C_{Mt} &= -C_{Mw} - C_{MT} - \frac{C_{Mh}}{\sigma C_v^2 (c/b)} \\ &= .205 + .297 - .23 / (.00745 \times 4.0^2 \times 1.12) \\ &= -1.223 \end{aligned}$$

The moment arms of the tailplane are found in the usual manner:

$$\begin{aligned} l/b &= -4.94 \times .99255 - .582 \times .12187 = -4.97 \\ h/b &= -.582 \times .99255 + 4.94 \times .12187 = .01 \end{aligned}$$

The drag of the tail, including the vertical surfaces, is assumed constant for the range of trims under consideration:

$$C_D = .0040 \quad \partial C_D / \partial \alpha = 0$$

The lift of the tail is obtained from the moment which was computed above:

$$\begin{aligned} C_{Mt} &= b/c (C_L l/b - C_D h/b)_t \\ C_{Lt} &= \frac{1}{(l/b)_t} [C_{Mt} (c/b) + C_{Dt} (h/b)_t] \\ &= \frac{1}{-4.97} (-1.223 \times 1.12 + .0040 \times .01) \\ &= .275 \end{aligned}$$

The slope of the lift curve for the tail is obtained from the usual equation for the tail lift:

$$\begin{aligned} \frac{\partial C_{Lt}}{\partial \alpha} &= \frac{\partial C_{Lw}}{\partial \alpha} \left( \frac{1 - \alpha_{ow}/\pi A_w}{1 + \alpha_{ot}/\pi A_t} \right) \frac{S_t}{S_w} \eta_t \\ &= 6.20 \left( \frac{1 - 6.9/20 \pi}{1 + 5.7/3.52 \pi} \right) \frac{192}{1048} \times .70 \\ &= .46 \quad (\text{assuming a tail efficiency } \eta_t = .70) \end{aligned}$$

The slope of the moment curve is given approximately by:

$$\frac{\partial C_{Mt}}{\partial \alpha} = \frac{\partial C_{Lt}}{\partial \alpha} \frac{(l/b)_t}{c/b} = .46 \times \frac{-4.94}{1.12} = -2.03$$

Stability Derivative Coefficients

$$\begin{aligned} X_u &= -2C_R \frac{1}{CV^2} - 2\sigma_{CD_w} - 2\sigma_{CD_t} \\ &= -2 \times .115 \times \frac{1}{4^2} - 2 \times .00745 \times .0520 - 2 \times .00745 \times .0040 \\ &= -.0144 -.00075 -.00006 \\ &= -.0152 \end{aligned}$$

$$\begin{aligned} X_{\dot{u}} &= C_{\Delta_0} \frac{\partial C_R}{\partial Cr} \frac{1}{CV^2} \\ &= .932 \times (-1.0) \times \frac{1}{4^2} \\ &= -.0582 \end{aligned}$$

$$\begin{aligned} X_w &= -\left(\frac{\partial C_R}{\partial T} - C_{\Delta}\right) \frac{1}{CV^2} - \sigma\left(\frac{\partial C_D}{\partial \alpha} - CL\right)_w - \sigma\left(\frac{\partial C_D}{\partial \alpha} - CL\right)_t \\ &= -(1.2 - .677) \frac{1}{4^2} - .00745 (.116 - 1.87) - .00745 (0 - .275) \\ &= -.523 \times 1/16 + .00745 \times 1.754 + .00745 \times .275 \\ &= -.0327 + .0131 + .0020 \\ &= -.0176 \end{aligned}$$

$$\begin{aligned} X_{\dot{w}} &= -C_{\Delta_0} \frac{\partial C_R}{\partial T} \frac{1}{CV^2} - \sigma C_{\Delta_0} \left(\frac{\partial C_D}{\partial \alpha}\right)_w - \sigma C_{\Delta_0} \left(\frac{\partial C_D}{\partial \alpha}\right)_t \\ &= -.932 \times 1.2 \times \frac{1}{4^2} - .00745 \times .932 \times .116 - 0 \\ &= -.0698 - .0008 - 0 \\ &= -.0706 \end{aligned}$$

$$\begin{aligned} X_{\ddot{u}} &= \Sigma(h/b X_u - 1/b X_{\dot{w}}) \\ &= [1227 \times (-.0144) - .557 (-.0327)] + [-.225 (-.00075) - .050 (.0131) \\ &\quad + \{.01 (-.00006) - (-4.97)(.0020)\}] \\ &= (-.0183 + .0182) + (.0002 - .0007) - (0 - .0100) \\ &= 0 - .0005 + .0100 \\ &= .0095 \end{aligned}$$



Stability Derivative Coefficients (Contd.)

$$Z_u = -2 C_{\Delta} \cdot \frac{1}{CV^2} - 2 \sigma C_{LW} - 2 \sigma C_{Lt}$$

$$= -2 \times .677 \times \frac{1}{4^2} - 2 \times .00745 \times 1.87 - 2 \times .00745 \times .275$$

$$= -.0846 - .0279 - .0041$$

$$= -.1166$$

$$Z_z = C_{\Delta_0} \cdot \frac{\partial C_{\Delta}}{\partial C_r} \cdot \frac{1}{CV^2} = .932 \times (-5.8) \times \frac{1}{4^2} = -.338$$

$$Z_w = -\left(\frac{\partial C_{\Delta}}{\partial r} + C_R\right) \frac{1}{CV^2} - \sigma \left(\frac{\partial C_L}{\partial \alpha} + C_D\right)_w - \sigma \left(\frac{\partial C_L}{\partial \alpha} + C_D\right)_t$$

$$= -\left[4.6 + .115\right] \frac{1}{4^2} - .00745 [6.20 + .052] - .00745 [.46 + .004]$$

$$= -4.715 \cdot 1/16 - .00745 \times 6.252 - .00745 \times .464$$

$$= -.2950 - .0466 - .0035$$

$$= -.3451$$

$$Z_0 = -C_{\Delta_0} \frac{\partial C_{\Delta}}{\partial r} \cdot \frac{1}{CV^2} - \sigma C_{\Delta_0} \left(\frac{\partial C_L}{\partial \alpha}\right)_w - \sigma C_{\Delta_0} \left(\frac{\partial C_L}{\partial \alpha}\right)_t$$

$$= -.932 \times 4.6 \times \frac{1}{4^2} - .00745 \times .932 \times 6.20 - .00745 \times .932 \times .46$$

$$= -.2680 - .0430 - .0032$$

$$= -.3142$$

$$Z_2 = \sum (h/b \cdot F_u - 1/b \cdot Z_w)$$

$$= [1.27 (-.0846) - .557 (-.2950)] + [-.225 (-.0279) - .050 (-.0466)]$$

$$+ [0.01 (-.0041) - (-4.97) (-.0035)]$$

$$= [-.1075 + .1645] + [.0063 + .0023] + [0 - .0174]$$

$$= .0570 + .0086 - .0174$$

$$= .0482$$

$$M_u = 2\eta C_M \frac{1}{CV^2} + 2\eta \sigma c/b C_{Mw} + 2\eta \sigma c/b C_{Mt}$$

$$= 2 \times .725 \times .23 \times \frac{1}{4^2} + 2 \times .725 \times .00745 \times 1.12 \times (-.205) + 2 \times .725 \times .00745 \times 1.12 \times (-1.223)$$

$$= .0208 - .0025 - .0145$$

$$= .0038$$

Stability Derivative Coefficients (Contd.)

$$M_z = -\eta C_{\Delta_0} \frac{\partial C_M}{\partial C_r} \frac{1}{C_V^2} = -.725 \times .932 \times (-5.5) \times \frac{1}{42} = .232$$

$$\begin{aligned} M_w &= \eta \frac{\partial C_M}{\partial \gamma} \frac{1}{C_V^2} + \eta \sigma_{c/b} \left( \frac{\partial C_M}{\partial \alpha} \right)_w + \eta \sigma_{c/b} \left( \frac{\partial C_M}{\partial \alpha} \right)_t \\ &= .725 \times (-2.1) \times \frac{1}{42} + .725 \times .00745 \times 1.12 \times \frac{(-.086)}{1.12} + .725 \times .00745 \\ &= -.0950 - .0005 - .0123 \\ &= -.1078 \end{aligned}$$

$$\begin{aligned} M_Q &= \sum C_{\Delta_0} M_w \\ &= .932 (-.0950) - .932 (-.0005) + .932 (-.0123) \\ &= -.0885 - .0005 - .0115 \\ &= -.1005 \end{aligned}$$

$$\begin{aligned} M_2 &= \sum (h/b M_u - l/b M_w) \\ &= [1.27 (.0208) - .557 (-.0950)] + [-.225 (-.0025) - .050 (-.0005)] \\ &\quad + [.01 (-.0145) - (-4.97)(-.0123)] \\ &= [.0264 + .0530] + [.0006 + 0] + [-.0001 - .0611] \\ &= .0794 + .0006 - .0612 \\ &= .0188 \end{aligned}$$

Summarized Values for  $C_v = 4.0$ ,  $\tau = 7$  deg.

|          | <u>Hull</u> | <u>Wing</u> | <u>Tail</u> | <u>Total</u> |
|----------|-------------|-------------|-------------|--------------|
| $X_u$    | -.0144      | -.0007      | -.0001      | -.0152       |
| $X_z$    | -.0582      | 0           | 0           | -.0582       |
| $X_w$    | -.0327      | +.0131      | +.0020      | -.0176       |
| $X_\phi$ | -.0698      | -.0008      | 0           | -.0706       |
| $X_\psi$ | 0           | -.0005      | +.0100      | +.0095       |
|          |             |             |             |              |
| $Z_u$    | -.0846      | -.0279      | -.0041      | -.1166       |
| $Z_z$    | -.3380      | 0           | 0           | -.3380       |
| $Z_w$    | -.2950      | -.0466      | -.0035      | -.3451       |
| $Z_\phi$ | -.2680      | -.0430      | -.0032      | -.3142       |
| $Z_\psi$ | +.0570      | +.0086      | -.0174      | +.0482       |
|          |             |             |             |              |
| $M_u$    | +.0208      | -.0025      | -.0145      | +.0038       |
| $M_z$    | +.2320      | 0           | 0           | +.2320       |
| $M_w$    | -.0950      | -.0005      | -.0123      | -.1078       |
| $M_\phi$ | -.0885      | -.0005      | -.0115      | -.1005       |
| $M_\psi$ | +.0794      | +.0006      | -.0612      | +.0188       |

Coefficients of Stability Equation

$$A = 1$$

$$B = (-Z_w - M_z) = .3451 - .0188 = +.3263$$

$$\begin{aligned} C &= (-Z_z - Z_z M_w + Z_w M_z - M_\theta) \\ &= (.3380 + .0482 \times .1078 - .3451 \times .0188 + .1005) \\ &= (.3380 + .0052 - .0065 + .1005) \\ &= +.4372 \end{aligned}$$

$$\begin{aligned} D &= (Z_z M_z - Z_z M_z - Z_w M_\theta - Z_\theta M_w) \\ &= (-.3380 \times .0188 - .0482 \times .2320 + .3451 \times .1005 - .3142 \times .1078) \\ &= (-.0064 - .0112 + .0347 - .0339) \\ &= -.0168 \end{aligned}$$

$$\begin{aligned} E &= (Z_z M_\theta - Z_\theta M_z) \\ &= (.3380 \times .1005 + .3142 \times .2320) \\ &= .0340 + .0730 \\ &= +.1070 \end{aligned}$$

$$\begin{aligned} R &= (CD - BE) B - AD^2 \\ &= (-.4372 \times .0168 - .3263 \times .1070) .3263 - .0168^2 \\ &= (-.0073 - .0349) .3263 - .0003 \\ &= -.0422 \times .3263 - .0003 \\ &= -.0138 - .0003 \\ &= -.0141 \end{aligned}$$

As the coefficient (D) and the discriminant (R) are negative, the motion is divergent and the airplane is unstable for the speed and trim investigated.



APPENDIX I. FAA SEAPLANE OPERATIONS HANDBOOK

Selected Text and Figures Extracted From:

Seaplane, Skiplane and Float/Ski Equipped Helicopter Operations Handbook, U.S. Department of Transportation, Federal Aviation Administration, Flight Standards Service, 2004.

## Chapter 2 – Principles of Seaplanes

### SEAPLANE CHARACTERISTICS

There are two main types of seaplane: flying boats (often called hull seaplanes) and floatplanes (Figure 2-1). The bottom of a flying boat's fuselage is its main landing gear. This is usually supplemented with smaller floats near the wingtips, called wing or tip floats. Some flying boats have sponsons, which are short, wing-like projections from the sides of the hull near the waterline. Their purpose is to stabilize the hull from rolling motion when the flying boat is on the water, and they may also provide some aerodynamic lift in flight. Tip floats are sometimes known as sponsons. The hull of a flying boat holds the crew, passengers, and cargo; it has many features in common with the hull of a ship or boat. On the other hand, floatplanes typically are conventional landplanes that have been fitted with separate floats (sometimes called pontoons) in place of their wheels. The fuselage of a floatplane is supported well above the water's surface.



Figure 2-1. Flying boats, floatplanes, and amphibians.

Some flying boats and floatplanes are equipped with retractable wheels for landing on dry land. These aircraft are called amphibians. On amphibious flying boats, the main wheels generally retract into the sides of the hull above the waterline. The main wheels for amphibious floats retract upward into the floats themselves, just behind the step.

There are considerable differences between handling a floatplane and a flying boat on the water, but similar principles govern the procedures and techniques for both.

A number of amphibious hull seaplanes have their engines mounted above the fuselage. Because the thrust line is well above the center of drag, these airplanes tend to nose down when power is applied and nose up as power is reduced. This response is the opposite of what pilots have come to expect in most other airplanes, and can lead to unexpected pitch changes and dangerous situations if the pilot is not thoroughly familiar with these characteristics.

Figures 2-2 and 2-3 describe some of the basic terms used to describe seaplane floats. Other nautical terms are commonly used when operating seaplanes, such as port and starboard for left and right, windward and leeward for the upwind and downwind sides of objects, and bow and stern for the front and rear ends of objects.

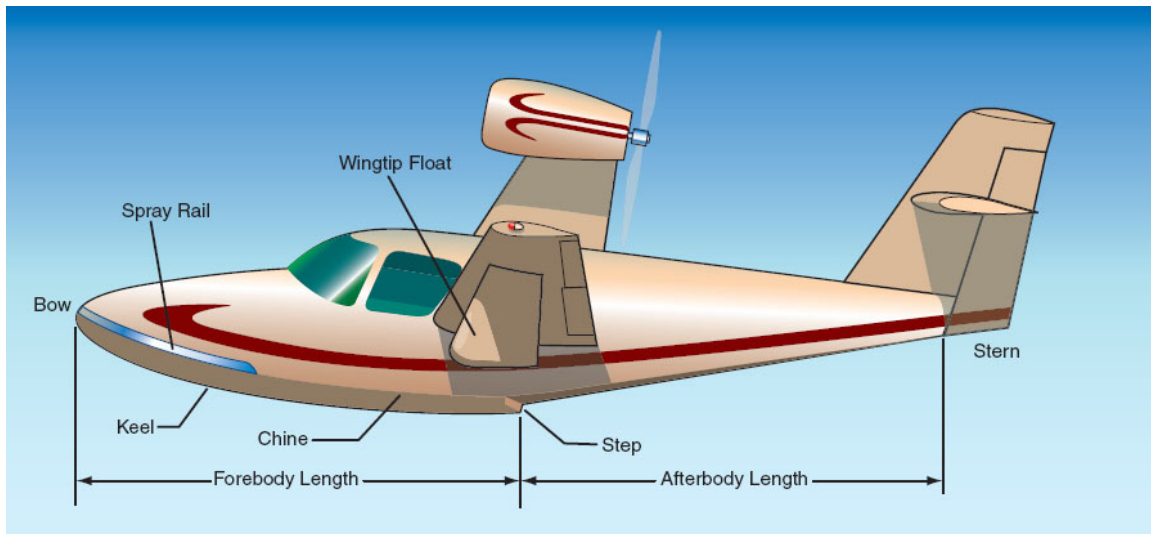
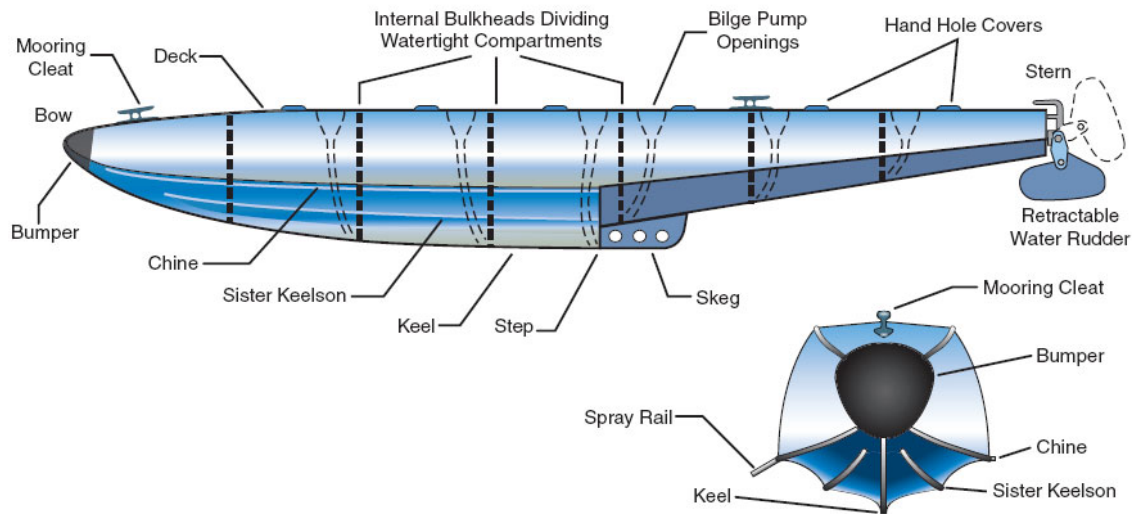


Figure 2-2. Hull components.



**Figure 2-3. Float components.**

Floats usually have bottoms, sides, and tops. A strong keel runs the length of the float along the center of the bottom. Besides supporting the seaplane on land, the keel serves the same purpose as the keel of a boat when the seaplane is in the water. It guides the float in a straight line through the water and resists sideways motion. A short, strong extension of the keel directly behind the step is called the skeg. The chine is the seam where the sides of the float are joined to the bottom. The chine helps guide water out and away from the float, reducing spray and helping with hydrodynamic lift.

On the front portion of the float, midway between the keel and chine, are the two sister keelsons. These longitudinal members add strength to the structure and function as additional keels. The top of the float forms a deck that provides access for entering and leaving the cabin. Bilge pump openings, hand hole covers, and cleats for mooring the seaplane are typically located along the deck. The front of each float has a rubber bumper to cushion minor impacts with docks, etc. Many floats also have spray rails along the inboard forward portions of the chines. Since water spray is surprisingly destructive to propellers, especially at high r.p.m., these metal flanges are designed to reduce the amount of spray hitting the propeller.

Floats are rated according to the amount of weight they can support, which is based on the weight of the actual volume of fresh water they displace. Fresh water is the standard because sea water is about 3 percent denser than fresh water and can therefore support more weight. If a particular float design displaces 2,500 pounds of fresh water when the float is pushed under the surface, the float can nominally support 2,500 pounds. A seaplane equipped with two such floats would seemingly be able to support an airplane weighing 5,000 pounds, but the floats would both be completely submerged at that weight. Obviously, such a situation would be impractical, so seaplanes are required to have a buoyancy of 80 percent in excess of that required to support the maximum weight of the seaplane in fresh water. To determine the maximum weight allowed for a seaplane equipped with two floats, divide the total displacement by 180 percent, or 1.8. Using the example of two floats that each displace 2,500 pounds, the total displacement of 5,000 pounds divided by 1.8 gives a maximum weight for the seaplane of 2,778 pounds. Many other considerations determine the suitability of a particular set of floats for a specific type of airplane, and float installations are carefully evaluated by the Federal Aviation Administration (FAA) prior to certification.



## Appendix I. Seaplane Operations

All floats are required to have at least four watertight compartments. These prevent the entire float from filling with water if it is ruptured at any point. The floats can support the seaplane with any two compartments flooded, which makes the seaplane difficult to sink.

Most floats have openings with watertight covers along the deck to provide access to the inside of each compartment for inspection and maintenance. There are also smaller holes connected by tubes to the lowest point in each compartment, called the bilge. These bilge pump openings are used for pumping out the bilge water that leaks into the float. The openings are typically closed with small rubber balls that push snugly into place.

Both the lateral and longitudinal lines of a float or hull are designed to achieve a maximum lifting force by diverting the water and the air downward. The forward bottom portion of a float or hull is designed very much like the bottom of a speedboat. While speedboats are intended to travel at a fairly constant pitch angle, seaplanes need to be able to rotate in pitch to vary the wings' angle of attack and increase lift for takeoffs and landings. The underside of a seaplane float has a sudden break in the longitudinal lines called the step. The step provides a means of reducing water drag during takeoff and during high-speed taxi. At very low speeds, the entire length of the floats supports the weight of the seaplane through buoyancy, that is, the floats displace a weight of water equal to the weight of the seaplane. As speed increases, aerodynamic lift begins to support a certain amount of the weight, and the rest is supported by hydrodynamic lift, the upward force produced by the motion of the floats through the water. Speed increases this hydrodynamic lift, but water drag increases more quickly. To minimize water drag while allowing hydrodynamic lift to do the work of supporting the seaplane on the water, the pilot relaxes elevator back pressure, allowing the seaplane to assume a pitch attitude that brings the aft portions of the floats out of the water. The step makes this possible. When running on the step, a relatively small portion of the float ahead of the step supports the seaplane. Without a step, the flow of water aft along the float would tend to remain attached all the way to the rear of the float, creating unnecessary drag.

The steps are located slightly behind the airplane's center of gravity (CG), approximately at the point where the main wheels are located on a landplane with tricycle gear. If the steps were located too far aft or forward of this point, it would be difficult, if not impossible, to rotate the airplane into a nose-up attitude prior to lifting off. Although steps are necessary, the sharp break along the underside of the float or hull concentrates structural stress into this area, and the disruption in airflow produces considerable drag in flight. The keel under the front portion of each float is intended to bear the weight of the seaplane when it is on dry land. The location of the step near the CG would make it very easy to tip the seaplane back onto the rear of the floats, which are not designed for such loads. The skeg is located behind the step and acts as a sort of chock when the seaplane is on land, making it more difficult to tip the seaplane backward. Most floatplanes are equipped with retractable water rudders at the rear tip of each float. The water rudders are connected by cables and springs to the rudder

pedals in the cockpit. While they are very useful in maneuvering on the water surface, they are quite susceptible to damage. The water rudders should be retracted whenever the seaplane is in shallow water or where they might hit objects under the water surface. They are also retracted during takeoff and landing, when dynamic water forces could cause damage.

## Chapter 4 – Seaplane Operations – Preflight and Takeoffs



### TAXIING AND SAILING

There are three basic positions or attitudes used in moving a seaplane on the water, differentiated by the position of the floats and the speed of the seaplane through the water. They are the idling or displacement position, the plowing position, and the planing or step position.

#### IDLING POSITION

In the idling position or displacement position, the buoyancy of the floats supports the entire weight of the seaplane and it remains in an attitude similar to being at rest on the water. Engine r.p.m. is kept as low as possible to control speed, to keep the engine from overheating, and to minimize spray. In almost all circumstances, the elevator control should be held all the way back to keep the nose as high as possible and minimize spray damage to the propeller. This also improves maneuverability by keeping more of the water rudder underwater. The exception is when a strong tailwind component or heavy swells could allow the wind to lift the tail and possibly flip the seaplane over. In such conditions, hold the elevator control forward enough to keep the tail down.[Figure 4-5 on next page]

Use the idling or displacement position for most taxiing operations, and keep speeds below 6-7 knots to minimize spray getting to the propeller. It is especially important to taxi at low speed in congested or confined areas because inertia forces at higher speeds allow the seaplane to coast farther and serious damage can result from even minor collisions. Cross boat wakes or swells at a 45° angle, if possible, to minimize pitching or rolling and the possibility of an upset.

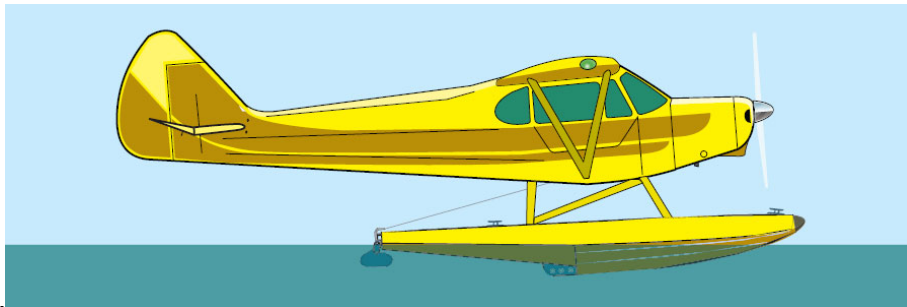


Figure 4-5. Idling position. The engine is at idle r.p.m., the seaplane moves slowly, the attitude is nearly level, and buoyancy supports the seaplane.

#### PLOWING POSITION

Applying power causes the center of buoyancy to shift back, due to increased hydrodynamic pressure on the bottoms of the floats. This places more of the seaplane's weight behind the step, and because the floats are

narrower toward the rear, the sterns sink farther into the water. Holding the elevator full up also helps push the tail down due to the increased airflow from the propeller. The plowing position creates high drag, requiring a relatively large amount of power for a modest gain in speed. Because of the higher r.p.m., the propeller may pick up spray even though the nose is high. The higher engine power combined with low cooling airflow creates a danger of heat buildup in the engine. Monitor engine temperature carefully to avoid overheating. Taxiing in the plowing position is not recommended. It is usually just the transitional phase between idle taxi and planing. [Figure 4-6]

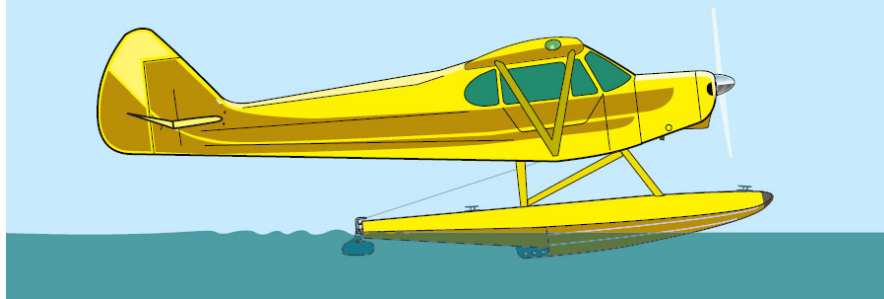


Figure 4-6. Plowing position.

### PLANING OR STEP POSITION

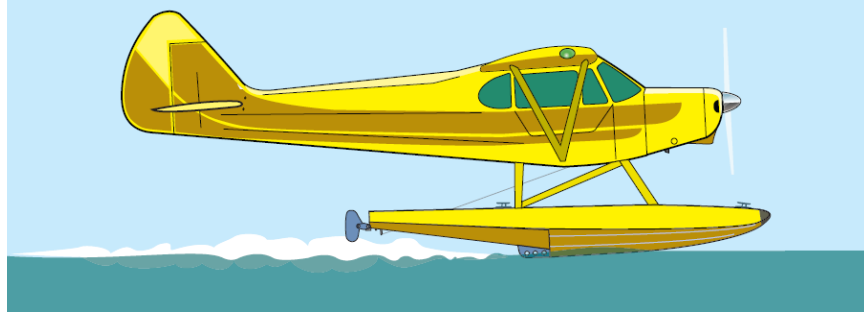
In the planing position, most of the seaplane's weight is supported by hydrodynamic lift rather than the buoyancy of the floats. (Because of the wing's speed through the air, aerodynamic lift may also be supporting some of the weight of the seaplane.) As the float moves faster through the water, it becomes possible to change the pitch attitude to raise the rear portions of the floats clear of the water. This greatly reduces water drag, allowing the seaplane to accelerate to lift-off speed. This position is most often called on the step. [Figure 4-7]

There is one pitch attitude that produces the minimum amount of drag when the seaplane is on the step. An experienced seaplane pilot can easily find this "sweet spot" or "slick spot" by the feel of the floats on the water. If the nose is considerably high, the rear portions of the floats contact the water, drag increases, and the seaplane tends to start settling back into more of a plowing position. If the nose is held only slightly higher than the ideal planing attitude, the seaplane may remain on the step but take much longer to accelerate to rotation speed. On the other hand, if the nose is too low, more of the front portion of the float contacts the water, creating more drag. This condition is called dragging, and as the nose pulls down and the seaplane begins to slow.

Taxiing on the step is a useful technique for covering long distances on the water. Carefully reducing power as the seaplane comes onto the step stops acceleration so that the seaplane maintains a high speed across the water, but remains well below flying speed. At these speeds, the water rudders must be retracted to prevent damage, but there is plenty of airflow for the air rudder.

With the seaplane on the step, gentle turns can be made by using the air rudder and the ailerons, always maintaining a precise planing attitude with elevator. The ailerons are positioned into the turn, except when aileron into the wind is needed to keep the upwind wing from lifting.

Besides the obvious danger of collision, other water traffic creates dangerous wakes, which are a much more frequent cause of damage. If you see that you are going to cross a wake, reduce power to idle and idle taxi across it, preferably at an angle.



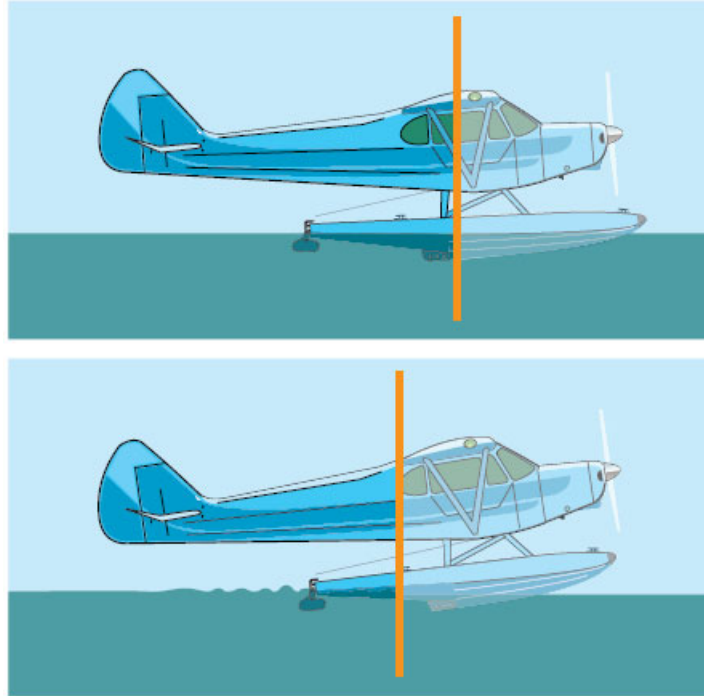
**Figure 4-7. On the step. The attitude is nearly level, and the weight of the seaplane is supported mostly by hydrodynamic lift. Behind the step, the floats are essentially clear of the water.**

## **TURNS**

At low speeds and in light winds, make turns using the water rudders, which move in conjunction with the air rudder. As with a landplane, the ailerons should be positioned to minimize the possibility of the wind lifting a wing. In most airplanes, left turns are somewhat easier and can be made tighter than right turns because of torque. If water rudders have the proper amount of movement, most seaplanes can be turned within a radius less than the span of the wing in calm conditions or a light breeze. Water rudders are usually more effective at slow speeds because they are acting in comparatively undisturbed water. At higher speeds, the stern of the float churns the adjacent water, causing the water rudder to become less effective. The dynamic pressure of the water at high speeds may tend to force the water rudders to swing up or retract, and the pounding can cause damage. For these reasons, water rudders should be retracted whenever the seaplane is moving at high speed.

The weathervaning tendency is more evident in seaplanes, and the taxiing seaplane pilot must be constantly aware of the wind's effect on the ability to maneuver. In stronger winds, weathervaning forces may make it difficult to turn downwind. Often a short burst of power provides sufficient air over the rudder to overcome weathervaning. Since the elevator is held all the way up, the airflow also forces the tail down, making the water rudders more effective. Short bursts of power are preferable to a longer, continuous power application. With continuous power, the seaplane accelerates, increasing the turn radius. The churning of the water in the wake of the floats also makes the water rudders less effective. At the same time, low cooling airflow may cause the engine to heat up.

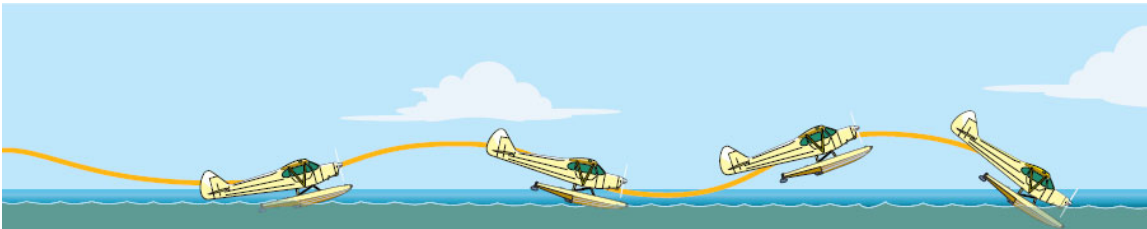
During a high speed taxiing turn, centrifugal force tends to tip the seaplane toward the outside of the turn. When turning from an upwind heading to a downwind heading, the wind force acts in opposition to centrifugal force, helping stabilize the seaplane. On the other hand, when turning from downwind to upwind, the wind force against the fuselage and the underside of the wing increases the tendency for the seaplane to lean to the outside of the turn, forcing the downwind float deeper into the water. In a tight turn or in strong winds, the combination of these two forces may be sufficient to tip the seaplane to the extent that the downwind float submerges or the outside wing drags in the water, and may even flip the seaplane onto its back. The further the seaplane tips, the greater the effect of the crosswind, as the wing presents more vertical area to the wind force. [Figure 4-8]



**Figure 4-9.** In the plowing position, the exposed area at the front of the floats, combined with the rearward shift of the center of buoyancy, can help to counteract the weathervaning

## PORPOISING

Porpoising is a rhythmic pitching motion caused by dynamic instability in forces along the float bottoms while on the step. An incorrect planing attitude sets off a cyclic oscillation that steadily increases in amplitude unless the proper pitch attitude is reestablished. [Figure 4-13]



**Figure 4-13.** Porpoising increases in amplitude if not corrected promptly.

A seaplane travels smoothly across the water on the step only if the floats or hull remain within a moderately tolerant range of pitch angles. If the nose is held too low during planing, water pressure in the form of a small crest or wall builds up under the bows of the floats. Eventually, the crest becomes large enough that the fronts of the floats ride up over the crest, pitching the bows upward. As the step passes over the crest, the floats tip forward abruptly, digging the bows a little deeper into the water. This builds a new crest in front of the floats, resulting in another oscillation. Each oscillation becomes increasingly severe, and if not corrected, will cause the seaplane to nose into the water, resulting in extensive damage or possible capsizing.

A second type of porpoising can occur if the nose is held too high while on the step. Porpoising can also cause a premature lift-off with an extremely high angle of attack, which can result in a stall and a subsequent nose-down drop into the water. Porpoising occurs during the takeoff run if the planing angle is not properly controlled with elevator pressure just after passing through the “hump” speed. The pitching created when the seaplane encounters a swell system while on the step can also initiate porpoising. Usually, porpoising does not

start until the seaplane has passed a degree or two beyond the acceptable planing angle range, and does not cease until after the seaplane has passed out of the critical range by a degree or two.

If porpoising occurs due to a nose-low planing attitude, stop it by applying timely back pressure on the elevator control to prevent the bows of the floats from digging into the water. The back pressure must be applied and maintained until porpoising stops. If porpoising does not stop by the time the second oscillation occurs, reduce the power to idle and hold the elevator control back firmly so the seaplane settles onto the water with no further instability. Never try to “chase” the oscillations, as this usually makes them worse and results in an accident.

Pilots must learn and practice the correct pitch attitudes for takeoff, planing, and landing for each type of seaplane until there is no doubt as to the proper angles for the various maneuvers. The upper and lower limits of these pitch angles are established by the design of the seaplane; however, changing the seaplane’s gross weight, wing flap position, or center of gravity location also changes these limits. Increased weight increases the displacement of the floats or hull and raises the lower limit considerably. Extending the wing flaps frequently trims the seaplane to the lower limit at lower speeds, and may lower the upper limit at high speeds. A forward center of gravity increases the possibility of high angle porpoising, especially during landing.

## **SKIPPING**

Skipping is a form of instability that may occur when landing at excessive speed with the nose at too high a pitch angle. This nose-up attitude places the seaplane at the upper trim limit of stability and causes the seaplane to enter a cyclic oscillation when touching the water, which results in the seaplane skipping across the surface. This action is similar to skipping flat stones across the water. Skipping can also occur by crossing a boat wake while taxiing on the step or during a takeoff. Sometimes the new seaplane pilot confuses a skip with a porpoise, but the pilot’s body sensations can quickly distinguish between the two. A skip gives the body vertical “G” forces, similar to bouncing a landplane. Porpoising is a rocking chair type forward and aft motion feeling.

To correct for skipping, first increase back pressure on the elevator control and add sufficient power to prevent the floats from contacting the water. Then establish the proper pitch attitude and reduce the power gradually to allow the seaplane to settle gently onto the water. Skipping oscillations do not tend to increase in amplitude, as in porpoising, but they do subject the floats and airframe to unnecessary pounding and can lead to porpoising.

## **TAKEOFFS**

A seaplane takeoff may be divided into four distinct phases: (1) The displacement phase, (2) the hump or plowing phase, (3) the planing or on the step phase, and (4) the lift-off. The displacement phase should be familiar from the taxiing discussion. During idle taxi, the displacement of water supports nearly all of the seaplane’s weight. The weight of the seaplane forces the floats down into the water until a volume that weighs exactly as much as the seaplane has been displaced. The surface area of the float below the waterline is called the wetted area, and it varies depending on the seaplane’s weight. An empty seaplane has less wetted area than when it is fully loaded. Wetted area is a major factor in the creation of drag as the seaplane moves through the water.

As power is applied, the floats move faster through the water. The water resists this motion, creating drag. The forward portion of the float is shaped to transform the horizontal movement through the water into an upward lifting force by diverting the water downward. Newton’s Third Law of Motion states that for every action, there is an equal and opposite reaction, and in this case, pushing water downward results in an upward force known as hydrodynamic lift.

In the plowing phase, hydrodynamic lift begins pushing up the front of the floats, raising the seaplane’s nose and moving the center of buoyancy aft. This, combined with the downward pressure on the tail generated by holding the elevator control all the way back, forces the rear part of the floats deeper into the water. This

creates more wetted area and consequently more drag, and explains why the seaplane accelerates so slowly during this part of the takeoff.

This resistance typically reaches its peak just before the floats are placed into a planing attitude. Figure 4-14 shows a graph of the drag forces at work during a seaplane takeoff run. The area of greatest resistance is referred to as the hump because of the shape of the water drag curve. During the plowing phase, the increasing water speed generates more and more hydrodynamic lift. With more of the weight supported by hydrodynamic lift, proportionately less is supported by displacement and the floats are able to rise in the water. As they do, there is less wetted area to cause drag, which allows more acceleration, which in turn increases hydrodynamic lift. There is a limit to how far this cycle can go, however, because as speed builds, so does the amount of drag on the remaining wetted area.

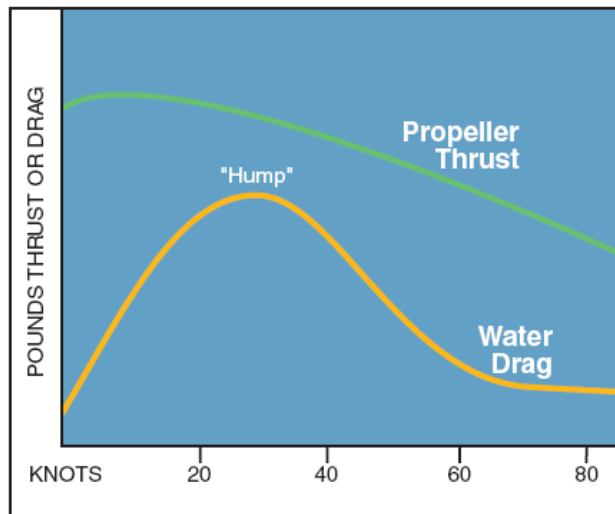


Figure 4-14. This graph shows water drag and propeller thrust during a takeoff run.

Drag increases as the square of speed, and eventually drag forces would balance the power output of the engine and the seaplane would continue along the surface without further acceleration.

Seaplanes have been built with sufficient power to accelerate to takeoff speed this way, but fortunately the step was invented, and it makes further acceleration possible without additional power. After passing over the hump, the seaplane is traveling fast enough that its weight can be supported entirely by hydrodynamic lift. Relaxing the back pressure on the elevator control allows the float to rock up onto the step, and lifts the rear portions of the floats clear of the water. This eliminates all of the wetted area aft of the step, along with the associated drag.

As further acceleration takes place, the flight controls become more responsive, just as in a landplane. Elevator deflection is gradually reduced to hold the required planing attitude. As the seaplane continues to accelerate, more and more weight is being supported by the aerodynamic lift of the wings and water resistance continues to decrease. When all of the weight is transferred to the wings, the seaplane becomes airborne.

Several factors greatly increase the water drag or resistance, such as heavy loading of the seaplane or glassy water conditions. In extreme cases, the drag may exceed the available thrust and prevent the seaplane from becoming airborne. This is particularly true when operating in areas with high density altitudes (high elevations/ high temperatures) where the engine cannot develop full rated power. For this reason the pilot should practice takeoffs using only partial power to simulate the longer takeoff runs needed when operating where the density altitude is high and/or the seaplane is heavily loaded. This practice should be conducted under the supervision of an experienced seaplane instructor, and in accordance with any cautions or limitations



in the AFM/POH. Plan for the additional takeoff area required, as well as the flatter angle of climb after takeoff, and allow plenty of room for error.

### **ROUGH WATER TAKEOFFS**

The objective in a rough water takeoff is similar to that of a rough or soft field takeoff in a landplane: to transfer the weight of the airplane to the wings as soon as possible, get airborne at a minimum airspeed, accelerate in ground effect to a safe climb speed, and climb out. In most cases an experienced seaplane pilot can safely take off in rough water, but a beginner should not attempt to take off if the waves are too high. Using the proper procedure during rough water operation lessens the abuse of the floats, as well as the entire seaplane.

During rough water takeoffs, open the throttle to takeoff power just as the floats begin rising on a wave. This prevents the float bows from digging into the water and helps keep the spray away from the propeller. Apply a little more back elevator pressure than on a smooth water takeoff. This raises the nose to a higher angle and helps keep the float bows clear of the water.

Once on the step, the seaplane can begin to bounce from one wave crest to the next, raising its nose higher with each bounce, so each successive wave is struck with increasing severity. To correct this situation and to prevent a stall, smooth elevator pressures should be used to set up a fairly constant pitch attitude that allows the seaplane to skim across each successive wave as speed increases. Maintain control pressure to prevent the float bows from being pushed under the water surface, and to keep the seaplane from being thrown into the air at a high pitch angle and low airspeed.

Fortunately, a takeoff in rough water is generally accomplished within a short time because if there is sufficient wind to make water rough, the wind is also strong enough to produce aerodynamic lift earlier and enable the seaplane to become airborne quickly.

The relationship of the spacing of the waves to the length of the floats is very important. If the wavelength is less than half the length of the floats, the seaplane is always supported by at least two waves at a time. If the wavelength is longer than the floats, only one wave at a time supports the seaplane. This creates dangerous pitching motions, and takeoff should not be attempted in this situation.

## **Chapter 5 - Performance**

### **FLIGHT CHARACTERISTICS OF SEAPLANES WITH HIGH THRUST LINES**

Many of the most common flying boat designs have the engine and propeller mounted well above the airframe's CG. This results in some unique handling characteristics. The piloting techniques necessary to fly these airplanes safely are not intuitive and must be learned.

Pilots who fly typical light twins are familiar with what happens when one engine is producing power and the other is not. The airplane tends to yaw toward the dead engine. This happens because the thrust line is located some distance from the airplane's CG. In some respects, this situation is similar to the single-engine seaplane with a high thrust line, except that the seaplane flies on one engine all the time. When power is applied, the thrust tends to pitch the nose down, and as power is reduced, the nose tends to rise. [Figure 5-4] This is exactly the opposite of what most pilots are accustomed to. In typical airplanes, including most floatplanes, applying power raises the nose and initiates a climb.

Depending on how far the engine is from the airplane's CG, the mass of the engine can have detrimental effects on roll stability. Some seaplanes have the engine mounted within the upper fuselage, while others have engines mounted on a pylon well above the main fuselage. If it is far from the CG, the engine can act like a weight at the end of a lever, and once started in motion it tends to continue in motion. Imagine balancing a hammer upright with the handle on the palm of the hand. [Figure 5-5]



## Appendix I. Seaplane Operations

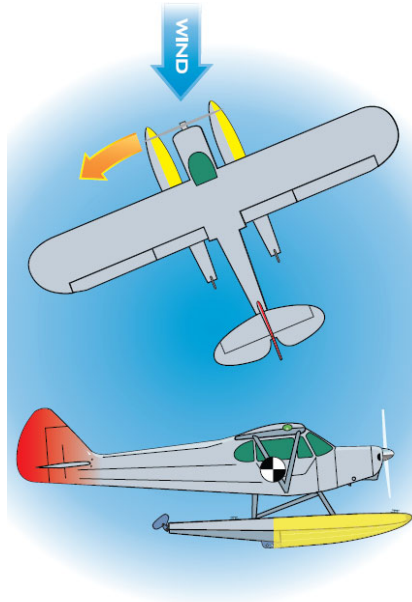


Figure 5-2. The side area of the floats can decrease directional stability.



Figure 5-3. Vertical surfaces added to the tail help restore directional stability.

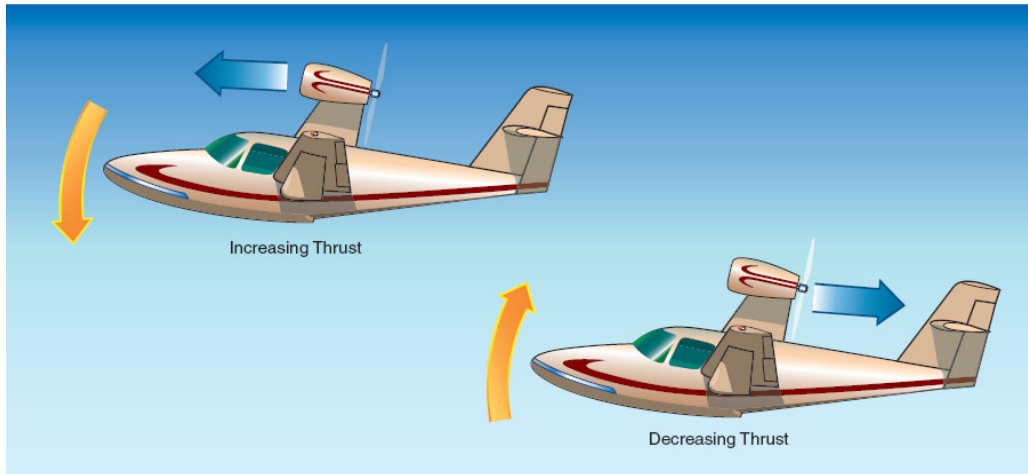


Figure 5-4. Pitching forces in seaplanes with a high thrust line.

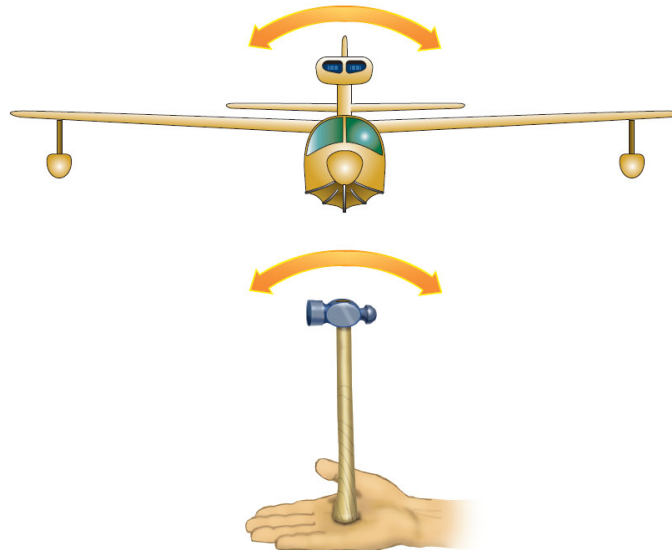


Figure 5-5. Roll instability with a high-mounted engine.

## Chapter 6 – Seaplane Operations - Landings

### LANDING

In water landings, the major objectives are to touch down at the lowest speed possible, in the correct pitch attitude, without side drift, and with full control throughout the approach, landing, and transition to taxiing.

The correct pitch attitude at touchdown in a landplane varies between wide limits. For example, wheel landings in an airplane with conventional-gear, require a nearly flat pitch attitude, with virtually zero angle of attack, while a full-stall landing on a short field might call for a nose-high attitude. The touchdown attitude for a seaplane typically is very close to the attitude for taxiing on the step. The nose may be a few degrees higher. The objective is to touch down on the steps, with the sterns of the floats near or touching the water at the same time. [Figure 6-2] If the nose is much higher or lower, the excessive water drag puts unnecessary stress on the floats and struts, and can cause the nose to pitch down, allowing the bows of the floats to dig into the water. Touching down on the step keeps water drag forces to a minimum and allows energy to dissipate more gradually.

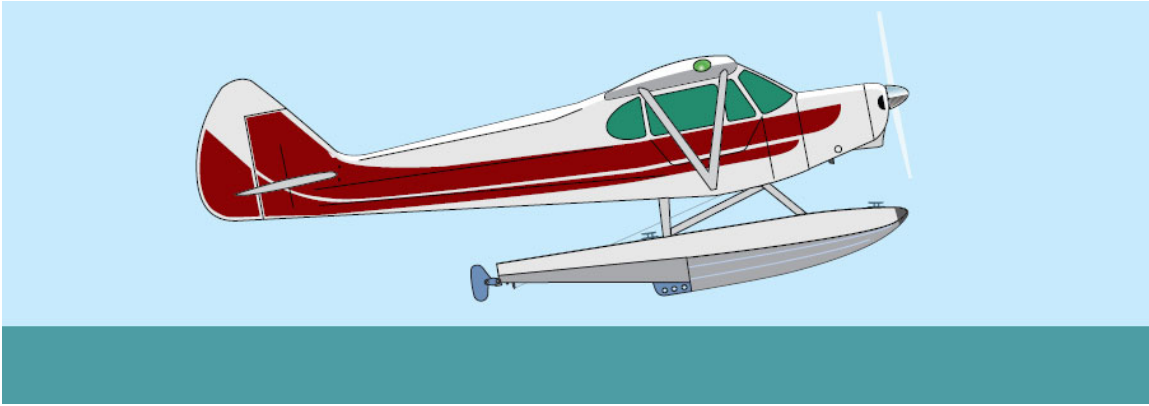


Figure 6-2. The touchdown attitude for most seaplanes is almost the same as for taxiing on the step.

### CROSSWIND LANDING

Landing directly into the wind might not be practical due to water traffic in the area, obstructions on or under the water, or a confined landing area, such as a river or canal. In landing a seaplane with any degree of crosswind component, the objectives are the same as when landing a landplane: to minimize sideways drift during touchdown and maintain directional control afterward. Because floats have so much more side area than wheels, even a small amount of drift at touchdown can create large sideways forces. This is important because enough side force can lead to capsizing. Also, the float hardware is primarily designed to take vertical and fore-and-aft loads rather than side loads.

If the seaplane touches down while drifting sideways, the sudden resistance as the floats contact the water creates a skidding force that tends to push the downwind float deeper into the water. The combination of the skidding force, wind, and weathervaning as the seaplane slows down can lead to a loss of directional control and a waterloop. If the downwind float submerges and the wingtip contacts the water when the seaplane is moving at a significant speed, the seaplane could flip over. [Figure 6-3]

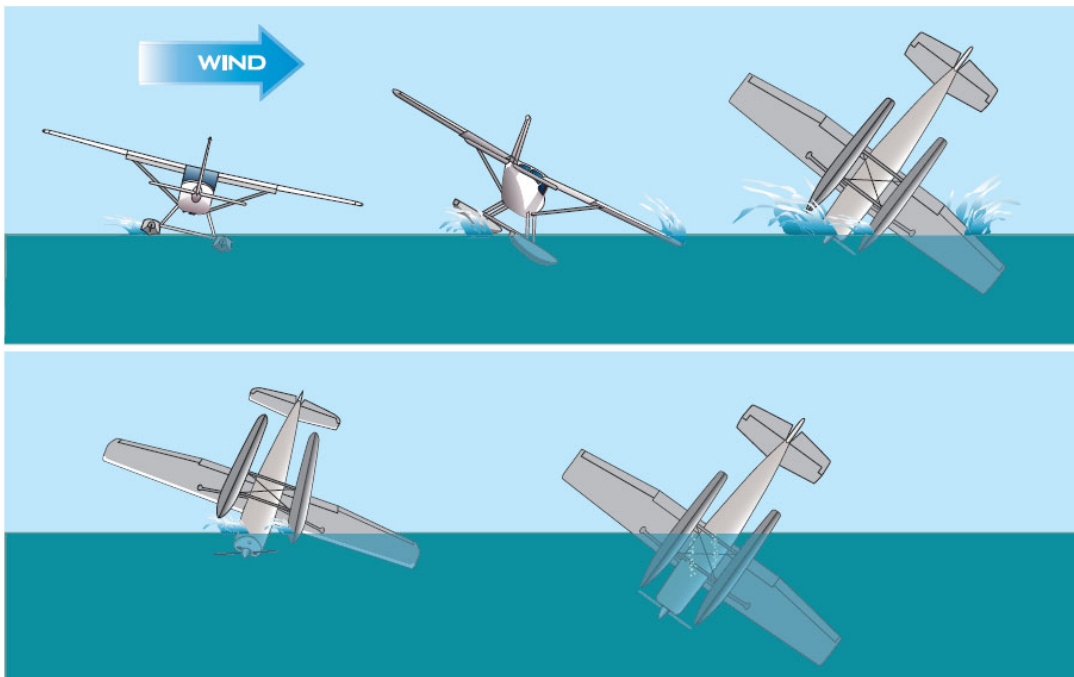


Figure 6-3. Improper technique or excessive crosswind forces can result in an accident

## GLASSY WATER LANDING

Flat, calm, glassy water certainly looks inviting and may give the pilot a false sense of safety. By its nature, glassy water indicates no wind, so there are no concerns about which direction to land, no crosswind to consider, no weathervaning, and obviously no rough water. Unfortunately, both the visual and the physical characteristics of glassy water hold potential hazards for complacent pilots. Consequently, this surface condition is frequently more dangerous than it appears for a landing seaplane.

The visual aspects of glassy water make it difficult to judge the seaplane's height above the water. The lack of surface features can make accurate depth perception very difficult, even for experienced seaplane pilots. Without adequate knowledge of the seaplane's height above the surface, the pilot may flare too high or too low. Either case can lead to an upset. If the seaplane flares too high and stalls, it will pitch down, very likely hitting the water with the bows of the floats and flipping over. If the pilot flares too late or not at all, the seaplane may fly into the water at relatively high speed, landing on the float bows, driving them underwater and flipping the seaplane. [Figure 6-6]

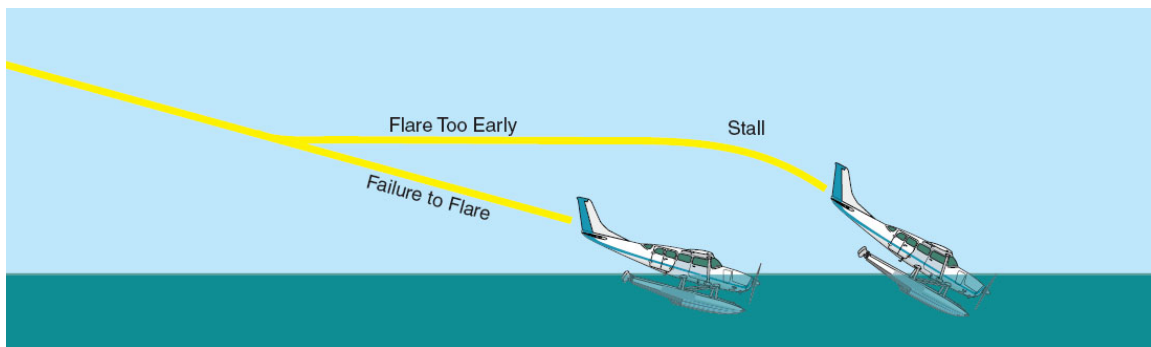


Figure 6-6. The consequences of misjudging altitude over glassy water can be catastrophic.

## ROUGH WATER LANDING

Rough is a very subjective and relative term. Water conditions that cause no difficulty for small boats can be too rough for a seaplane. Likewise, water that poses no challenge to a large seaplane or an experienced pilot may be very dangerous for a smaller seaplane or a less experienced pilot.

Describing a typical or ideal rough water landing procedure is impractical because of the many variables that affect the water's surface. Wind direction and speed must be weighed along with the surface conditions of the water. In most instances, though, make the approach the same as for any other water landing. It may be better, however, to level off just above the water surface and increase the power sufficiently to maintain a rather flat attitude until conditions appear more acceptable, and then reduce the power to touch down. If severe bounces occur, add power and lift off to search for a smoother landing spot.

In general, make the touchdown at a somewhat flatter pitch attitude than usual. This prevents the seaplane from being tossed back into the air at a dangerously low airspeed, and helps the floats to slice through the tops of the waves rather than slamming hard against them. Reduce power as the seaplane settles into the water, and apply back pressure as it comes off the step to keep the float bows from digging into a wave face.

If a particularly large wave throws the seaplane into the air before coming off the step, be ready to apply full power to go around.

Avoid downwind landings on rough water or in strong winds. Rough water is usually an indication of strong winds, and vice versa. Although the airspeed for landing is the same, wind velocity added to the seaplane's normal landing speed can result in a much higher groundspeed, imposing excessive stress on the floats,

## Appendix I. Seaplane Operations

increasing the nose-down tendency at touchdown, and prolonging the water run, since more kinetic energy must be dissipated. As the seaplane slows, the tendency to weathervane may combine with the motion created by the rough surface to create an unstable situation. In strong winds, an upwind landing means a much lower touchdown speed, a shorter water run, and subsequently much less pounding of the floats and airframe.

Likewise, crosswind landings on rough water or in strong winds can leave the seaplane vulnerable to capsizing. The pitching and rolling produced by the water motion increases the likelihood of the wind lifting a wing and flipping the seaplane. There is additional information on rough water landings in Chapter 8, Emergency Open Sea Operations.

## Chapter 8 – Emergency Open Sea Operations

### OPERATIONS IN OPEN SEAS

Open sea operations are very risky and should be avoided if possible. If an open sea landing cannot be avoided, a thorough reconnaissance and evaluation of the conditions must be performed to ensure safety. The sea usually heaves in a complicated crisscross pattern of swells of various magnitudes, overlaid by whatever chop the wind is producing. A relatively smooth spot may be found where the cross swells are less turbulent.

### DEFINITIONS

When performing open sea operations, it is important to know and understand some basic ocean terms. A thorough knowledge of these definitions allows the pilot to receive and understand sea condition reports from other aircraft, surface vessels, and weather services.

**Fetch**—An area where wind is generating waves on the water surface. Also the distance the waves have been driven by the wind blowing in a constant direction without obstruction.

**Sea**—Waves generated by the existing winds in the area. These wind waves are typically a chaotic mix of heights, periods, and wavelengths. Sometimes the term refers to the condition of the surface resulting from both wind waves and swells.

**Swell**—Waves that persist outside the fetch or in the absence of the force that generated them. The waves have a uniform and orderly appearance characterized by smooth, regularly spaced wave crests.

**Primary Swell**—The swell system having the greatest height from trough to crest.

**Secondary Swells**—Swell systems of less height than the primary swell.

**Swell Direction**—The direction from which a swell is moving. This direction is not necessarily the result of the wind present at the scene. The swell encountered may be moving into or across the local wind. A swell tends to maintain its original direction for as long as it continues in deep water, regardless of changes in wind direction.

**Swell Face**—The side of the swell toward the observer.  
The back is the side away from the observer.

**Swell Length**—The horizontal distance between successive crests.

**Swell Period**—The time interval between the passage of two successive crests at the same spot in the water, measured in seconds.

**Swell Velocity**—The velocity with which the swell advances in relation to a fixed reference point, measured in knots. (There is little movement of water in the horizontal direction. Each water particle transmits energy to its neighbor, resulting primarily in a vertical motion, similar to the motion observed when shaking out a carpet.)

**Chop**—A roughened condition of the water surface caused by local winds. It is characterized by its irregularity, short distance between crests, and whitecaps.

**Downswell**—Motion in the same direction the swell is moving.

**Upswell**—Motion opposite the direction the swell is moving. If the swell is moving from north to south, a seaplane going from south to north is moving upswell.

## SEA STATE EVALUATION

Wind is the primary cause of ocean waves and there is a direct relationship between speed of the wind and the state of the sea in the immediate vicinity. Windspeed forecasts can help the pilot anticipate sea conditions. Conversely, the condition of the sea can be useful in determining the speed of the wind. Figure 8-1 on the next page illustrates the Beaufort wind scale with the corresponding sea state condition number.

| BEAUFORT WIND SCALE WITH CORRESPONDING SEA STATE CODES |                       |                  |  |                                 |                  |
|--|-----------------------|------------------|--|---------------------------------|------------------|
| Beaufort Number  | Wind Velocity (Knots) | Wind Description | Sea State Description  | Sea State                       |                  |
|  |                       |                  |  | Term and Height of Waves (Feet) | Condition Number |
| 0  | Less than 1           | Calm             | Sea surface smooth and mirror-like   | Calm, glassy<br>0               | 0                |
| 1  | 1-3                   | Light Air        | Scaly ripples, no foam crests  |                                 |                  |
| 2  | 4-6                   | Light Breeze     | Small wavelets, crests glassy, no breaking   | Calm, rippled<br>0 – 0.3        | 1                |
| 3  | 7-10                  | Gentle Breeze    | Large wavelets, crests begin to break, scattered whitecaps   | Smooth, wavelets<br>0.3-1       | 2                |
| 4  | 11-16                 | Moderate Breeze  | Small waves, becoming longer, numerous whitecaps   | Slight<br>1-4                   | 3                |
| 5  | 17-21                 | Fresh Breeze     | Moderate waves, taking longer form, many whitecaps, some spray   | Moderate<br>4-8                 | 4                |
| 6  | 22-27                 | Strong Breeze    | Larger waves, whitecaps common, more spray   | Rough<br>8-13                   | 5                |
| 7  | 28-33                 | Near Gale        | Sea heaps up, white foam streaks off breakers  | Very rough<br>13-20             | 6                |
| 8  | 34-40                 | Gale             | Moderately high, waves of greater length, edges of crests begin to break into spindrift, foam blown in streaks |                                 |                  |
| 9  | 41-47                 | Strong Gale      | High waves, sea begins to roll, dense streaks of foam, spray may reduce visibility                             |                                 |                  |
| 10   | 48-55                 | Storm            | Very high waves, with overhanging crests, sea white with densely blown foam, heavy rolling, lowered visibility | High<br>20-30                   | 7                |
| 11   | 56-63                 | Violent Storm    | Exceptionally high waves, foam patches cover sea, visibility more reduced                                      | Very high<br>30-45              | 8                |
| 12   | 64 and over           | Hurricane        | Air filled with foam, sea completely white with driving spray, visibility greatly reduced                      | Phenomenal<br>45 and over       | 9                |

Figure 8-1. Beaufort wind scale.

While the height of the waves is important, it is often less of a consideration than the wavelength, or the distance between swells. Closely spaced swells can be very violent, and can destroy a seaplane even though the wave height is relatively small. On the other hand, the same seaplane might be able to handle much higher waves if the swells are several thousand feet apart. The relationship between the swell length and the height of the waves is the height-to-length ratio [Figure 8-2].

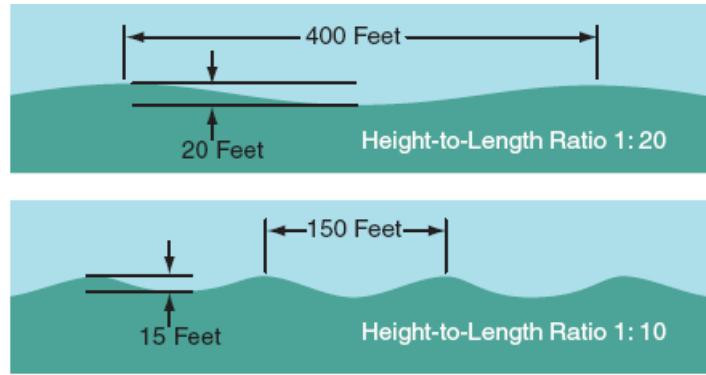


Figure 8-2. Height-to-length ratio.

This ratio is an indication of the amount of motion a seaplane experiences on the water and the threat to capsizing. For example, a body of water with 20-foot waves and a swell length of 400 feet has a height-to-length ratio of 1:20, which may not put the seaplane at risk of capsizing, depending on the crosswinds.

However, 15-foot waves with a length of 150 feet produce a height-to-length ratio of 1:10, which greatly increases the risk of capsizing, especially if the wave is breaking abeam of the seaplane. As the swell length decreases, swell height becomes increasingly critical to capsizing. Thus, when a high swell height-to-length ratio exists, a crosswind takeoff or landing should not be attempted. Downwind takeoff and landing may be made downswell in light and moderate wind; however, a downwind landing should never be attempted when wind velocities are high regardless of swell direction.

When two swell systems are in phase, the swells act together and result in higher swells. However, when two swell systems are in opposition, the swells tend to cancel each other or “fill in the troughs.” This provides a relatively flat area that appears as a lesser concentration of whitecaps and shadows. This flat area is a good touchdown spot for landing. [Figure 8-3]

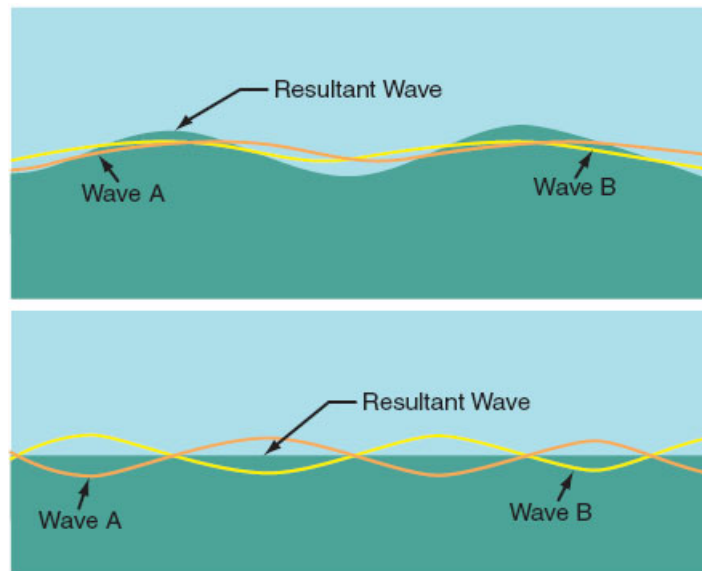


Figure 8-3. Wave interference.

## LANDING PARALLEL TO THE SWELL



When landing on a swell system with large, widely spaced crests more than four times the length of the floats, the best landing heading parallels the crests and has the most favorable headwind component. In this situation, it makes little difference whether touchdown is on top of the crest or in the trough.

### LANDING PERPENDICULAR TO THE SWELL

If crosswind limits would be exceeded by landing parallel to the swell, landing perpendicular to the swell might be the only option. Landing in closely spaced swells less than four times the length of the floats should be considered an emergency procedure only, since damage or loss of the seaplane can be expected.

If the distance between crests is less than half the length of the floats, the touchdown may be smooth, since the floats will always be supported by at least two waves, but expect severe motion and forces as the seaplane slows.

A downswell landing on the back of the swell is preferred. However, strong winds may dictate landing into the swell. To compare landing downswell with landing into the swell, consider the following example.

Assuming a 10-second swell period, the length of the swell is 500 feet, and it has a velocity of 30 knots or 50 feet per second. Assume the seaplane takes 890 feet and 5 seconds for its runout.

**Downswell Landing**—The swell is moving with the seaplane during the landing runout, thereby increasing the effective swell length by about 250 feet and resulting in an effective swell length of 750 feet. If the seaplane touches down just beyond the crest, it finishes its runout about 140 feet beyond the next crest. [Figure 8-5]

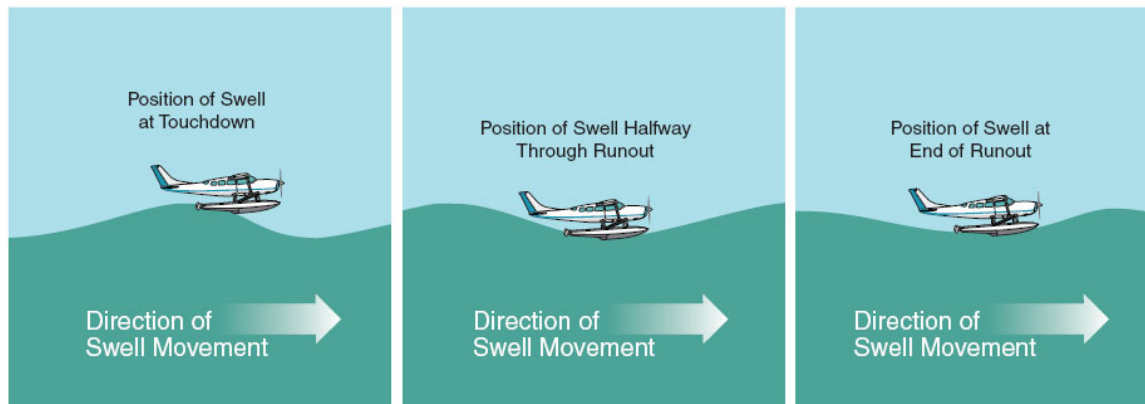
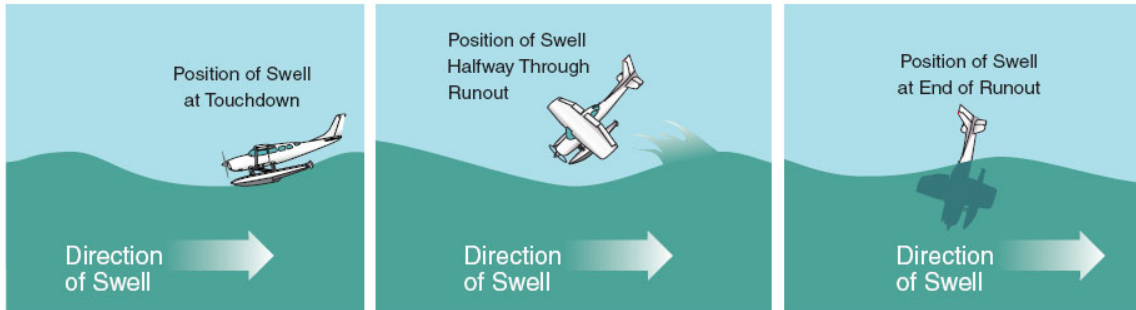


Figure 8-5. Landing in the same direction as the movement of the swell increases the apparent length between swell crests.

**Landing into the Swell**—During the 5 seconds of runout, the oncoming swell moves toward the seaplane a distance of about 250 feet, thereby shortening the effective swell length to about 250 feet. Since the seaplane takes 890 feet to come to rest, it would meet the oncoming swell less than halfway through its runout and it would probably be thrown into the air, out of control. Avoid this landing heading if at all possible. [Figure 8-6]



**Figure 8-6. Landing against the swell shortens the apparent distance between crests, and could lead to trouble**

If low ceilings prevent complete sea evaluation from the altitudes prescribed above, any open sea landing should be considered a calculated risk, as a dangerous but unobserved swell system may be present in the proposed landing area. Complete the descent and before-landing checklists prior to descending below 1,000 feet if the ceiling is low.

### **LANDING WITH MORE THAN ONE SWELL SYSTEM**

Open water often has two or more swell systems running in different directions, which can present a confusing appearance to the pilot. When the secondary swell system is from the same direction as the wind, the preferred direction of landing is parallel to the primary swell with the secondary swell at some angle. When landing parallel to the primary swell, the two choices of heading are either upwind and into the secondary swell, or downwind and downswell. The heading with the greatest headwind is preferred; however, if a pronounced secondary swell system is present, it may be desirable to land downswell to the secondary swell system and accept some tailwind component. The risks associated with landing downwind versus downswell must be carefully considered. The choice of heading depends on the velocity of the wind versus the velocity and the height of the secondary swell.



APPENDIX II. CFR AIRWORTHINESS STANDARDS

SELECTED PORTIONS, 2010

**Code of Federal Regulations**

**Title 14: Aeronautics and Space**

**Part 23 – Airworthiness Standards: Normal, Utility, Acrobatic and Commuter Category Airplanes**

**Subpart B – Flight**

**Ground and Water Handling Characteristics**

**§ 23.231 Longitudinal stability and control.**

(b) A seaplane or amphibian may not have dangerous or uncontrollable porpoising characteristics at any normal operating speed on the water.

**§ 23.239 Spray characteristics.**

Spray may not dangerously obscure the vision of the pilots or damage the propellers or other parts of a seaplane or amphibian at any time during taxiing, takeoff, and landing.

**Subpart C – Structure**

**Water Loads**

**§ 23.521 Water load conditions.**

(a) The structure of seaplanes and amphibians must be designed for water loads developed during takeoff and landing with the seaplane in any attitude likely to occur in normal operation at appropriate forward and sinking velocities under the most severe sea conditions likely to be encountered.

(b) Unless the applicant makes a rational analysis of the water loads, §§23.523 through 23.537 apply.

[Doc. No. 4080, 29 FR 17955, Dec. 18, 1964, as amended by Amdt. 23–45, 58 FR 42160, Aug. 6, 1993; Amdt. 23–48, 61 FR 5147, Feb. 9, 1996]

**§ 23.523 Design weights and center of gravity positions.**

(a) *Design weights.* The water load requirements must be met at each operating weight up to the design landing weight except that, for the takeoff condition prescribed in §23.531, the design water takeoff weight (the maximum weight for water taxi and takeoff run) must be used.

(b) *Center of gravity positions.* The critical centers of gravity within the limits for which certification is requested must be considered to reach maximum design loads for each part of the seaplane structure.

[Doc. No. 26269, 58 FR 42160, Aug. 6, 1993]

**§ 23.525 Application of loads.**

(a) Unless otherwise prescribed, the seaplane as a whole is assumed to be subjected to the loads corresponding to the load factors specified in §23.527.

(b) In applying the loads resulting from the load factors prescribed in §23.527, the loads may be distributed over the hull or main float bottom (in order to avoid excessive local shear loads and bending moments at the location of water load application) using pressures not less than those prescribed in §23.533(c).

(c) For twin float seaplanes, each float must be treated as an equivalent hull on a fictitious seaplane with a weight equal to one-half the weight of the twin float seaplane.

(d) Except in the takeoff condition of §23.531, the aerodynamic lift on the seaplane during the impact is assumed to be 2/3 of the weight of the seaplane.

[Doc. No. 26269, 58 FR 42161, Aug. 6, 1993; 58 FR 51970, Oct. 5, 1993]

#### § 23.527 Hull and main float load factors.

(a) Water reaction load factors  $n_w$  must be computed in the following manner:

(1) For the step landing case

$$n_w = \frac{C_1 V_{so}^2}{\left( \tan^{\frac{2}{3}} \beta \right) W^{\frac{1}{3}}}$$

(2) For the bow and stern landing cases

$$n_w = \frac{C_1 V_{so}^2}{\left( \tan^{\frac{2}{3}} \beta \right) W^{\frac{1}{3}}} \times \frac{K_1}{\left( 1 + r_x^2 \right)^{\frac{1}{2}}}$$

(b) The following values are used:

(1)  $n_w$ =water reaction load factor (that is, the water reaction divided by seaplane weight).

(2)  $C_1$ =empirical seaplane operations factor equal to 0.012 (except that this factor may not be less than that necessary to obtain the minimum value of step load factor of 2.33).

(3)  $V_{so}$ =seaplane stalling speed in knots with flaps extended in the appropriate landing position and with no slipstream effect.

(4)  $\beta$ =Angle of dead rise at the longitudinal station at which the load factor is being determined in accordance with figure 1 of appendix I of this part.

(5)  $W$ =seaplane landing weight in pounds.

(6)  $K_1$ =empirical hull station weighing factor, in accordance with figure 2 of appendix I of this part.

(7)  $r_x$ =ratio of distance, measured parallel to hull reference axis, from the center of gravity of the seaplane to the hull longitudinal station at which the load factor is being computed to the radius of gyration in pitch of the seaplane, the hull reference axis being a straight line, in the plane of symmetry, tangential to the keel at the main step.

(c) For a twin float seaplane, because of the effect of flexibility of the attachment of the floats to the seaplane, the factor  $K_1$  may be reduced at the bow and stern to 0.8 of the value shown in figure 2 of appendix I of this part. This reduction applies only to the design of the carrythrough and seaplane structure.

[Doc. No. 26269, 58 FR 42161, Aug. 6, 1993; 58 FR 51970, Oct. 5, 1993]

#### § 23.529 Hull and main float landing conditions.

(a) *Symmetrical step, bow, and stern landing.* For symmetrical step, bow, and stern landings, the limit water reaction load factors are those computed under §23.527. In addition—

(1) For symmetrical step landings, the resultant water load must be applied at the keel, through the center of gravity, and must be directed perpendicularly to the keel line;

(2) For symmetrical bow landings, the resultant water load must be applied at the keel, one-fifth of the longitudinal distance from the bow to the step, and must be directed perpendicularly to the keel line; and

(3) For symmetrical stern landings, the resultant water load must be applied at the keel, at a point 85 percent of the longitudinal distance from the step to the stern post, and must be directed perpendicularly to the keel line.

(b) *Unsymmetrical landing for hull and single float seaplanes.* Unsymmetrical step, bow, and stern landing conditions must be investigated. In addition—

(1) The loading for each condition consists of an upward component and a side component equal, respectively, to 0.75 and 0.25  $\tan \beta$  times the resultant load in the corresponding symmetrical landing condition; and

(2) The point of application and direction of the upward component of the load is the same as that in the symmetrical condition, and the point of application of the side component is at the same longitudinal station as the upward component but is directed inward perpendicularly to the plane of symmetry at a point midway between the keel and chine lines.

(c) *Unsymmetrical landing; twin float seaplanes.* The unsymmetrical loading consists of an upward load at the step of each float of 0.75 and a side load of 0.25  $\tan \beta$  at one float times the step landing load reached under §23.527. The side load is directed inboard, perpendicularly to the plane of symmetry midway between the keel and chine lines of the float, at the same longitudinal station as the upward load.

[Doc. No. 26269, 58 FR 42161, Aug. 6, 1993]

#### **§ 23.531 Hull and main float takeoff condition.**

For the wing and its attachment to the hull or main float—

(a) The aerodynamic wing lift is assumed to be zero; and

(b) A downward inertia load, corresponding to a load factor computed from the following formula, must be applied:

$$n = \frac{C_{TO} V_{S1}^2}{\left( \tan^{\frac{2}{3}} \beta \right) W^{\frac{1}{3}}}$$

Where—

n=inertia load factor;

$C_{TO}$ =empirical seaplane operations factor equal to 0.004;

$V_{S1}$ =seaplane stalling speed (knots) at the design takeoff weight with the flaps extended in the appropriate takeoff position;

$\beta$ =angle of dead rise at the main step (degrees); and

W=design water takeoff weight in pounds.

[Doc. No. 26269, 58 FR 42161, Aug. 6, 1993]

#### **§ 23.533 Hull and main float bottom pressures.**

(a) *General.* The hull and main float structure, including frames and bulkheads, stringers, and bottom plating, must be designed under this section.

(b) *Local pressures.* For the design of the bottom plating and stringers and their attachments to the supporting structure, the following pressure distributions must be applied:

(1) For an unflared bottom, the pressure at the chine is 0.75 times the pressure at the keel, and the pressures between the keel and chine vary linearly, in accordance with figure 3 of appendix I of this part. The pressure at the keel (p.s.i.) is computed as follows:

$$P_K = \frac{C_2 K_2 V_{S1}^2}{\tan \beta_K}$$

where—

$P_K$ =pressure (p.s.i.) at the keel;

$C_2$ =0.00213;

$K_2$ =hull station weighing factor, in accordance with figure 2 of appendix I of this part;

$V_{S1}$ =seaplane stalling speed (knots) at the design water takeoff weight with flaps extended in the appropriate takeoff position; and

$\beta_K$ =angle of dead rise at keel, in accordance with figure 1 of appendix I of this part.

(2) For a flared bottom, the pressure at the beginning of the flare is the same as that for an unflared bottom, and the pressure between the chine and the beginning of the flare varies linearly, in accordance with figure 3 of appendix I of this part. The pressure distribution is the same as that prescribed in paragraph (b)(1) of this section for an unflared bottom except that the pressure at the chine is computed as follows:

$$P_{ch} = \frac{C_3 K_2 V_{s1}^2}{\tan \beta}$$

where—

$P_{ch}$ =pressure (p.s.i.) at the chine;

$C_3$ =0.0016;

$K_2$ =hull station weighing factor, in accordance with figure 2 of appendix I of this part;

$V_{s1}$ =seaplane stalling speed (knots) at the design water takeoff weight with flaps extended in the appropriate takeoff position; and

$\beta$ =angle of dead rise at appropriate station.

The area over which these pressures are applied must simulate pressures occurring during high localized impacts on the hull or float, but need not extend over an area that would induce critical stresses in the frames or in the overall structure.

(c) *Distributed pressures.* For the design of the frames, keel, and chine structure, the following pressure distributions apply:

(1) Symmetrical pressures are computed as follows:

$$P = \frac{C_4 K_2 V_{s0}^2}{\tan \beta}$$

where—

$P$ =pressure (p.s.i.);

$C_4$ =0.078  $C_1$ (with  $C_1$  computed under §23.527);

$K_2$ =hull station weighing factor, determined in accordance with figure 2 of appendix I of this part;

$V_{s0}$ =seaplane stalling speed (knots) with landing flaps extended in the appropriate position and with no slipstream effect; and

$\beta$ =angle of dead rise at appropriate station.

(2) The unsymmetrical pressure distribution consists of the pressures prescribed in paragraph (c)(1) of this section on one side of the hull or main float centerline and one-half of that pressure on the other side of the hull or main float centerline, in accordance with figure 3 of appendix I of this part.

(3) These pressures are uniform and must be applied simultaneously over the entire hull or main float bottom. The loads obtained must be carried into the sidewall structure of the hull proper, but need not be transmitted in a fore and aft direction as shear and bending loads.

[Doc. No. 26269, 58 FR 42161, Aug. 6, 1993; 58 FR 51970, Oct. 5, 1993]

### § 23.535 Auxiliary float loads.

(a) *General.* Auxiliary floats and their attachments and supporting structures must be designed for the conditions prescribed in this section. In the cases specified in paragraphs (b) through (e) of this section, the prescribed water loads may be distributed over the float bottom to avoid excessive local loads, using bottom pressures not less than those prescribed in paragraph (g) of this section.

(b) *Step loading.* The resultant water load must be applied in the plane of symmetry of the float at a point three-fourths of the distance from the bow to the step and must be perpendicular to the keel. The resultant limit load is computed as follows, except that the value of  $L$  need not exceed three times the weight of the displaced water when the float is completely submerged:

$$L = \frac{C_s V_{so}^2 W^{\frac{1}{2}}}{\tan^{\frac{1}{2}} \beta_s (1 + r_y^2)^{\frac{1}{2}}}$$

where—

L=limit load (lbs.);

$C_s=0.0053$ ;

$V_{so}$ =seaplane stalling speed (knots) with landing flaps extended in the appropriate position and with no slipstream effect;

W=seaplane design landing weight in pounds;

$\beta_s$ =angle of dead rise at a station 3/4 of the distance from the bow to the step, but need not be less than 15 degrees; and

$r_y$ =ratio of the lateral distance between the center of gravity and the plane of symmetry of the float to the radius of gyration in roll.

(c) *Bow loading.* The resultant limit load must be applied in the plane of symmetry of the float at a point one-fourth of the distance from the bow to the step and must be perpendicular to the tangent to the keel line at that point. The magnitude of the resultant load is that specified in paragraph (b) of this section.

(d) *Unsymmetrical step loading.* The resultant water load consists of a component equal to 0.75 times the load specified in paragraph (a) of this section and a side component equal to  $0.025 \tan \beta$  times the load specified in paragraph (b) of this section. The side load must be applied perpendicularly to the plane of symmetry of the float at a point midway between the keel and the chine.

(e) *Unsymmetrical bow loading.* The resultant water load consists of a component equal to 0.75 times the load specified in paragraph (b) of this section and a side component equal to 0.25  $\tan \beta$  times the load specified in paragraph (c) of this section. The side load must be applied perpendicularly to the plane of symmetry at a point midway between the keel and the chine.

(f) *Immersed float condition.* The resultant load must be applied at the centroid of the cross section of the float at a point one-third of the distance from the bow to the step. The limit load components are as follows:

vertical =  $P_g V$

$$\text{aft} = \frac{C_x P V^{\frac{1}{2}} (K V_{so})^2}{2}$$

$$\text{side} = \frac{C_y P V^{\frac{1}{2}} (K V_{so})^2}{2}$$

where—

P=mass density of water (slugs/ft.<sup>3</sup>)

V=volume of float (ft.<sup>3</sup>);

$C_x$ =coefficient of drag force, equal to 0.133;

$C_y$ =coefficient of side force, equal to 0.106;

K=0.8, except that lower values may be used if it is shown that the floats are incapable of submerging at a speed of 0.8  $V_{so}$  in normal operations;

$V_{so}$ =seaplane stalling speed (knots) with landing flaps extended in the appropriate position and with no slipstream effect; and

g=acceleration due to gravity (ft/sec<sup>2</sup>).

(g) *Float bottom pressures.* The float bottom pressures must be established under §23.533, except that the value of  $K_2$  in the formulae may be taken as 1.0. The angle of dead rise to be used in determining the float bottom pressures is set forth in paragraph (b) of this section.

[Doc. No. 26269, 58 FR 42162, Aug. 6, 1993; 58 FR 51970, Oct. 5, 1993]

### § 23.537 Seawing loads.

Seawing design loads must be based on applicable test data.

[Doc. No. 26269, 58 FR 42163, Aug. 6, 1993]



**Subpart D – Design and Construction**

**Floats and Hulls**

**§ 23.751 Main float buoyancy.**

(a) Each main float must have—

(1) A buoyancy of 80 percent in excess of the buoyancy required by that float to support its portion of the maximum weight of the seaplane or amphibian in fresh water; and

(2) Enough watertight compartments to provide reasonable assurance that the seaplane or amphibian will stay afloat without capsizing if any two compartments of any main float are flooded.

(b) Each main float must contain at least four watertight compartments approximately equal in volume.

[Doc. No. 4080, 29 FR 17955, Dec. 18, 1964, as amended by Amdt. 23–45, 58 FR 42165, Aug. 6, 1993]

**§ 23.753 Main float design.**

Each seaplane main float must meet the requirements of §23.521.

[Doc. No. 26269, 58 FR 42165, Aug. 6, 1993]

**§ 23.755 Hulls.**

(a) The hull of a hull seaplane or amphibian of 1,500 pounds or more maximum weight must have watertight compartments designed and arranged so that the hull auxiliary floats, and tires (if used), will keep the airplane afloat without capsizing in fresh water when—

(1) For airplanes of 5,000 pounds or more maximum weight, any two adjacent compartments are flooded; and

(2) For airplanes of 1,500 pounds up to, but not including, 5,000 pounds maximum weight, any single compartment is flooded.

(b) Watertight doors in bulkheads may be used for communication between compartments.

[Doc. No. 4080, 29 FR 17955, Dec. 18, 1964, as amended by Amdt. 23–45, 58 FR 42165, Aug. 6, 1993; Amdt. 23–48, 61 FR 5148, Feb. 9, 1996]

**§ 23.757 Auxiliary floats.**

Auxiliary floats must be arranged so that, when completely submerged in fresh water, they provide a righting moment of at least 1.5 times the upsetting moment caused by the seaplane or amphibian being tilted.

**APPENDIX I – SAME AS PART 25**

**Code of Federal Regulations**

**Title 14: Aeronautics and Space**

**Part 25 – Airworthiness Standards: Transport Category Airplanes**

**Subpart B – Flight**

**Ground and Water Handling  
Characteristics**

**§ 25.231 Longitudinal stability and  
control.**

(b) For seaplanes and amphibians, the most adverse water conditions safe for takeoff, taxiing, and landing, must be established.

**§ 25.237 Wind velocities.**

(b) For seaplanes and amphibians, the following applies:

(1) A 90-degree cross component of wind velocity, up to which takeoff and landing is safe under all water conditions that may reasonably be expected in normal operation, must be established and must be at least 20 knots or 0.2 VSR<sub>0</sub>, whichever is greater, except that it need not exceed 25 knots.

(2) A wind velocity, for which taxiing is safe in any direction under all water conditions that may reasonably be expected in normal operation, must be established and must be at least 20 knots or 0.2 VSR<sub>0</sub>, whichever is greater, except that it need not exceed 25 knots.

[Amdt. 25–42, 43 FR 2322, Jan. 16, 1978, as amended by Amdt. 25–108, 67 FR 70827, Nov. 26, 2002; Amdt. 25–121, 72 FR 44668, Aug. 8, 2007]

**§ 25.239 Spray characteristics, control,  
and stability on water.**

(a) For seaplanes and amphibians, during takeoff, taxiing, and landing, and in the

conditions set forth in paragraph (b) of this section, there may be no—

(1) Spray characteristics that would impair the pilot's view, cause damage, or result in the taking in of an undue quantity of water;

(2) Dangerously uncontrollable porpoising, bounding, or swinging tendency; or

(3) Immersion of auxiliary floats or sponsons, wing tips, propeller blades, or other parts not designed to withstand the resulting water loads.

(b) Compliance with the requirements of paragraph (a) of this section must be shown—

(1) In water conditions, from smooth to the most adverse condition established in accordance with §25.231;

(2) In wind and cross-wind velocities, water currents, and associated waves and swells that may reasonably be expected in operation on water;

(3) At speeds that may reasonably be expected in operation on water;

(4) With sudden failure of the critical engine at any time while on water; and

(5) At each weight and center of gravity position, relevant to each operating condition, within the range of loading conditions for which certification is requested.

(c) In the water conditions of paragraph (b) of this section, and in the corresponding wind conditions, the seaplane or amphibian must be able to drift for five minutes with engines inoperative, aided, if necessary, by a sea anchor.

## Subpart C – Structure

### Water Loads

#### § 25.521 General.

(a) Seaplanes must be designed for the water loads developed during takeoff and landing, with the seaplane in any attitude likely to occur in normal operation, and at the appropriate forward and sinking velocities under the most severe sea conditions likely to be encountered.

(b) Unless a more rational analysis of the water loads is made, or the standards in ANC-3 are used, §§25.523 through 25.537 apply.

(c) The requirements of this section and §§25.523 through 25.537 apply also to amphibians.

#### § 25.523 Design weights and center of gravity positions.

(a) *Design weights.* The water load requirements must be met at each operating weight up to the design landing weight except that, for the takeoff condition prescribed in §25.531, the design water takeoff weight (the maximum weight for water taxi and takeoff run) must be used.

(b) *Center of gravity positions.* The critical centers of gravity within the limits for which certification is requested must be considered to reach maximum design loads for each part of the seaplane structure.

[Doc. No. 5066, 29 FR 18291, Dec. 24, 1964, as amended by Amdt. 25-23, 35 FR 5673, Apr. 8, 1970]

#### § 25.525 Application of loads.

(a) Unless otherwise prescribed, the seaplane as a whole is assumed to be subjected to the loads corresponding to the load factors specified in §25.527.

(b) In applying the loads resulting from the load factors prescribed in §25.527, the loads

may be distributed over the hull or main float bottom (in order to avoid excessive local shear loads and bending moments at the location of water load application) using pressures not less than those prescribed in §25.533(b).

(c) For twin float seaplanes, each float must be treated as an equivalent hull on a fictitious seaplane with a weight equal to one-half the weight of the twin float seaplane.

(d) Except in the takeoff condition of §25.531, the aerodynamic lift on the seaplane during the impact is assumed to be 2/3 of the weight of the seaplane.

#### § 25.527 Hull and main float load factors.

(a) Water reaction load factors  $n_w$  must be computed in the following manner:

(1) For the step landing case

$$n_w = \frac{C_1 V_{S0}^2}{\left( \tan^{\frac{2}{3}} \beta \right) W^{\frac{1}{3}}}$$

(2) For the bow and stern landing cases

$$n_w = \frac{C_1 V_{S0}^2}{\left( \tan^{\frac{2}{3}} \beta \right) W^{\frac{1}{3}}} \times \frac{K_1}{\left( 1 + r_x^2 \right)^{\frac{2}{3}}}$$

(b) The following values are used:

(1)  $n_w$  = water reaction load factor (that is, the water reaction divided by seaplane weight).

(2)  $C_1$  = empirical seaplane operations factor equal to 0.012 (except that this factor may not be less than that necessary to obtain the minimum value of step load factor of 2.33).

(3)  $V_{S0}$  = seaplane stalling speed in knots with flaps extended in the appropriate landing position and with no slipstream effect.

(4)  $\beta$  = angle of dead rise at the longitudinal station at which the load factor is being determined in accordance with figure 1 of appendix B.

(5)  $W$ = seaplane design landing weight in pounds.

(6)  $K_1$ =empirical hull station weighing factor, in accordance with figure 2 of appendix B.

(7)  $r_x$ =ratio of distance, measured parallel to hull reference axis, from the center of gravity of the seaplane to the hull longitudinal station at which the load factor is being computed to the radius of gyration in pitch of the seaplane, the hull reference axis being a straight line, in the plane of symmetry, tangential to the keel at the main step.

(c) For a twin float seaplane, because of the effect of flexibility of the attachment of the floats to the seaplane, the factor  $K_1$  may be reduced at the bow and stern to 0.8 of the value shown in figure 2 of appendix B. This reduction applies only to the design of the carrythrough and seaplane structure.

[Doc. No. 5066, 29 FR 18291, Dec. 24, 1964, as amended by Amdt. 25-23, 35 FR 5673, Apr. 8, 1970]

#### **§ 25.529 Hull and main float landing conditions.**

(a) *Symmetrical step, bow, and stern landing.* For symmetrical step, bow, and stern landings, the limit water reaction load factors are those computed under §25.527. In addition—

(1) For symmetrical step landings, the resultant water load must be applied at the keel, through the center of gravity, and must be directed perpendicularly to the keel line;

(2) For symmetrical bow landings, the resultant water load must be applied at the keel, one-fifth of the longitudinal distance from the bow to the step, and must be directed perpendicularly to the keel line; and

(3) For symmetrical stern landings, the resultant water load must be applied at the keel, at a point 85 percent of the longitudinal distance from the step to the stern post, and must be directed perpendicularly to the keel line.

(b) *Unsymmetrical landing for hull and single float seaplanes.* Unsymmetrical step, bow, and

stern landing conditions must be investigated. In addition—

(1) The loading for each condition consists of an upward component and a side component equal, respectively, to 0.75 and 0.25  $\tan \beta$  times the resultant load in the corresponding symmetrical landing condition; and

(2) The point of application and direction of the upward component of the load is the same as that in the symmetrical condition, and the point of application of the side component is at the same longitudinal station as the upward component but is directed inward perpendicularly to the plane of symmetry at a point midway between the keel and chine lines.

(c) *Unsymmetrical landing; twin float seaplanes.* The unsymmetrical loading consists of an upward load at the step of each float of 0.75 and a side load of 0.25  $\tan \beta$  at one float times the step landing load reached under §25.527. The side load is directed inboard, perpendicularly to the plane of symmetry midway between the keel and chine lines of the float, at the same longitudinal station as the upward load.

#### **§ 25.531 Hull and main float takeoff condition.**

For the wing and its attachment to the hull or main float—

(a) The aerodynamic wing lift is assumed to be zero; and

(b) A downward inertia load, corresponding to a load factor computed from the following formula, must be applied:

$$n = \frac{C_{ro} V_{sl}^2}{\left( \tan^{\frac{2}{3}} \beta \right) W^{\frac{1}{3}}}$$

where—

$n$  =inertia load factor;

$C_{TO}$ =empirical seaplane operations factor equal to 0.004;

$V_{S1}$ =seaplane stalling speed (knots) at the design takeoff weight with the flaps extended in the appropriate takeoff position;

$\beta$ =angle of dead rise at the main step (degrees); and

$W$ =design water takeoff weight in pounds.

[Doc. No. 5066, 29 FR 18291, Dec. 24, 1964, as amended by Amdt. 25-23, 35 FR 5673, Apr. 8, 1970]

**§ 25.533 Hull and main float bottom pressures.**

(a) *General.* The hull and main float structure, including frames and bulkheads, stringers, and bottom plating, must be designed under this section.

(b) *Local pressures.* For the design of the bottom plating and stringers and their attachments to the supporting structure, the following pressure distributions must be applied:

(1) For an unflared bottom, the pressure at the chine is 0.75 times the pressure at the keel, and the pressures between the keel and chine vary linearly, in accordance with figure 3 of appendix B. The pressure at the keel (psi) is computed as follows:

$$P_k = C_2 \times \frac{K_2 V_{S1}^2}{\tan \beta_k}$$

where—

$P_k$ =pressure (p.s.i.) at the keel;

$C_2$ =0.00213;

$K_2$ =hull station weighing factor, in accordance with figure 2 of appendix B;

$V_{S1}$ =seaplane stalling speed (Knots) at the design water takeoff weight with flaps extended in the appropriate takeoff position; and

$\beta_k$ =angle of dead rise at keel, in accordance with figure 1 of appendix B.

(2) For a flared bottom, the pressure at the beginning of the flare is the same as that for an unflared bottom, and the pressure between the chine and the beginning of the flare varies linearly, in accordance with figure 3 of appendix B. The pressure distribution is the same as that prescribed in paragraph (b)(1) of this section for an unflared bottom except that the pressure at the chine is computed as follows:

$$P_{ch} = C_3 \times \frac{K_2 V_{S1}^2}{\tan \beta}$$

where—

$P_{ch}$ =pressure (p.s.i.) at the chine;

$C_3$ =0.0016;

$K_2$ =hull station weighing factor, in accordance with figure 2 of appendix B;

$V_{S1}$ =seaplane stalling speed at the design water takeoff weight with flaps extended in the appropriate takeoff position; and

$\beta$ =angle of dead rise at appropriate station.

The area over which these pressures are applied must simulate pressures occurring during high localized impacts on the hull or float, but need not extend over an area that would induce critical stresses in the frames or in the overall structure.

(c) *Distributed pressures.* For the design of the frames, keel, and chine structure, the following pressure distributions apply:

(1) Symmetrical pressures are computed as follows:

$$P = C_4 \times \frac{K_2 V_{S0}^2}{\tan \beta}$$

where—

$P$ =pressure (p.s.i.);

$C_4$ =0.078  $C_1$  (with  $C_1$  computed under §25.527);

$K_2$ =hull station weighing factor, determined in accordance with figure 2 of appendix B;

$V_{S_0}$ =seaplane stalling speed (Knots) with landing flaps extended in the appropriate position and with no slipstream effect; and

$V_{S_0}$ =seaplane stalling speed with landing flaps extended in the appropriate position and with no slipstream effect; and  $\beta$ =angle of dead rise at appropriate station.

(2) The unsymmetrical pressure distribution consists of the pressures prescribed in paragraph (c)(1) of this section on one side of the hull or main float centerline and one-half of that pressure on the other side of the hull or main float centerline, in accordance with figure 3 of appendix B.

These pressures are uniform and must be applied simultaneously over the entire hull or main float bottom. The loads obtained must be carried into the sidewall structure of the hull proper, but need not be transmitted in a fore and aft direction as shear and bending loads.

[Doc. No. 5066, 29 FR 18291, Dec. 24, 1964, as amended by Amdt. 25-23, 35 FR 5673, Apr. 8, 1970]

#### § 25.535 Auxiliary float loads.

(a) *General.* Auxiliary floats and their attachments and supporting structures must be designed for the conditions prescribed in this section. In the cases specified in paragraphs (b) through (e) of this section, the prescribed water loads may be distributed over the float bottom to avoid excessive local loads, using bottom pressures not less than those prescribed in paragraph (g) of this section.

(b) *Step loading.* The resultant water load must be applied in the plane of symmetry of the float at a point three-fourths of the distance from the bow to the step and must be perpendicular to the keel. The resultant limit load is computed as follows, except that the value of  $L$  need not exceed three times the weight of the displaced water when the float is completely submerged:

$$L = \frac{C_5 V_{S_0}^2 W^{\frac{2}{3}}}{\tan^{\frac{2}{3}} \beta (1 + r_y^2)^{\frac{2}{3}}}$$

where—

$L$  =limit load (lbs.);

$C_5$ =0.0053;

$V_{S_0}$ =seaplane stalling speed (knots) with landing flaps extended in the appropriate position and with no slipstream effect;

$W$ =seaplane design landing weight in pounds;

$\beta$ =angle of dead rise at a station  $\frac{3}{4}$  of the distance from the bow to the step, but need not be less than 15 degrees; and

$r_y$ =ratio of the lateral distance between the center of gravity and the plane of symmetry of the float to the radius of gyration in roll.

(c) *Bow loading.* The resultant limit load must be applied in the plane of symmetry of the float at a point one-fourth of the distance from the bow to the step and must be perpendicular to the tangent to the keel line at that point. The magnitude of the resultant load is that specified in paragraph (b) of this section.

(d) *Unsymmetrical step loading.* The resultant water load consists of a component equal to 0.75 times the load specified in paragraph (a) of this section and a side component equal to  $3.25 \tan \beta$  times the load specified in paragraph (b) of this section. The side load must be applied perpendicularly to the plane of symmetry of the float at a point midway between the keel and the chine.

(e) *Unsymmetrical bow loading.* The resultant water load consists of a component equal to 0.75 times the load specified in paragraph (b) of this section and a side component equal to  $0.25 \tan \beta$  times the load specified in paragraph (c) of this section. The side load must be applied perpendicularly to the plane of symmetry at a point midway between the keel and the chine.

(f) *Immersed float condition.* The resultant load must be applied at the centroid of the cross section of the float at a point one-third of the distance from the bow to the step. The limit load components are as follows:

$$\text{vertical} = \rho g V$$

$$\text{aft} = C_{x2} \rho V^{\frac{3}{2}} \left( K V_{s_0} \right)^2$$

$$\text{side} = C_{y2} \rho V^{\frac{3}{2}} \left( K V_{s_0} \right)^2$$

where—

$\rho$ =mass density of water (slugs/ft.<sup>2</sup>);

$V$ =volume of float (ft.<sup>2</sup>);

$C_x$ =coefficient of drag force, equal to 0.133;

$C_y$ =coefficient of side force, equal to 0.106;

$K=0.8$ , except that lower values may be used if it is shown that the floats are incapable of submerging at a speed of  $0.8 V_{S_0}$  in normal operations;

$V_{S_0}$ =seaplane stalling speed (knots) with landing flaps extended in the appropriate position and with no slipstream effect; and

$g$ =acceleration due to gravity (ft./sec.<sup>2</sup>).

(g) *Float bottom pressures.* The float bottom pressures must be established under §25.533, except that the value of  $K_2$  in the formulae may be taken as 1.0. The angle of dead rise to be used in determining the float bottom pressures is set forth in paragraph (b) of this section.

[Doc. No. 5066, 29 FR 18291, Dec. 24, 1964, as amended by Amdt. 25-23, 35 FR 5673, Apr. 8, 1970]

#### § 25.537 Seawing loads.

Seawing design loads must be based on applicable test data.

### Subpart D – Design and Construction

#### Floats and Hulls

##### § 25.751 Main float buoyancy.

Each main float must have—

(a) A buoyancy of 80 percent in excess of that required to support the maximum weight of the seaplane or amphibian in fresh water; and

(b) Not less than five watertight compartments approximately equal in volume.

##### § 25.753 Main float design.

Each main float must be approved and must meet the requirements of §25.521.

##### § 25.755 Hulls.

(a) Each hull must have enough watertight compartments so that, with any two adjacent compartments flooded, the buoyancy of the hull and auxiliary floats (and wheel tires, if used) provides a margin of positive stability great enough to minimize the probability of capsizing in rough, fresh water.

(b) Bulkheads with watertight doors may be used for communication between compartments.

#### APPENDIX B – SAME AS PART 23

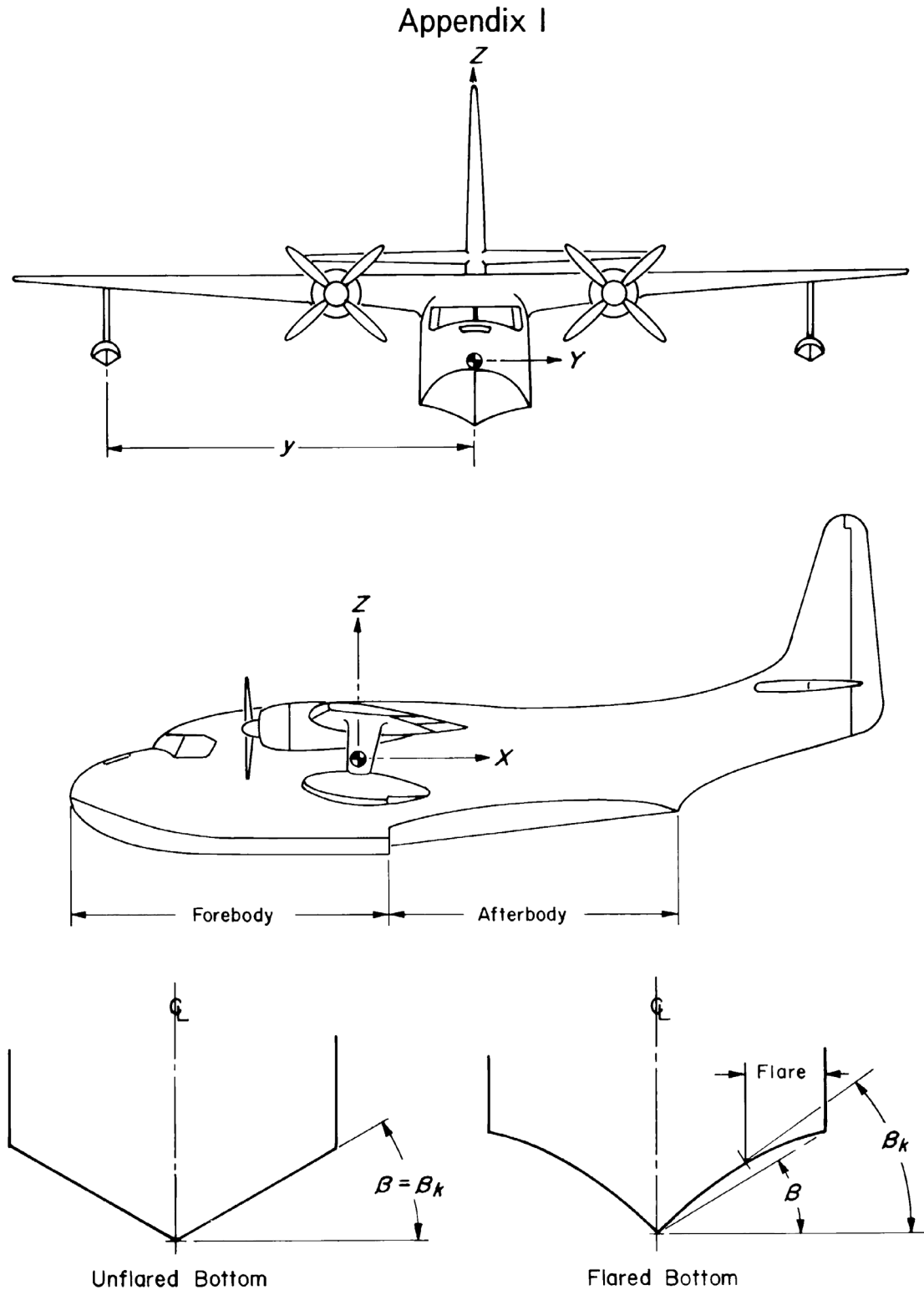


FIGURE 1. Pictorial definition of angles, dimensions, and directions on a seaplane.



Appendix I (continued)

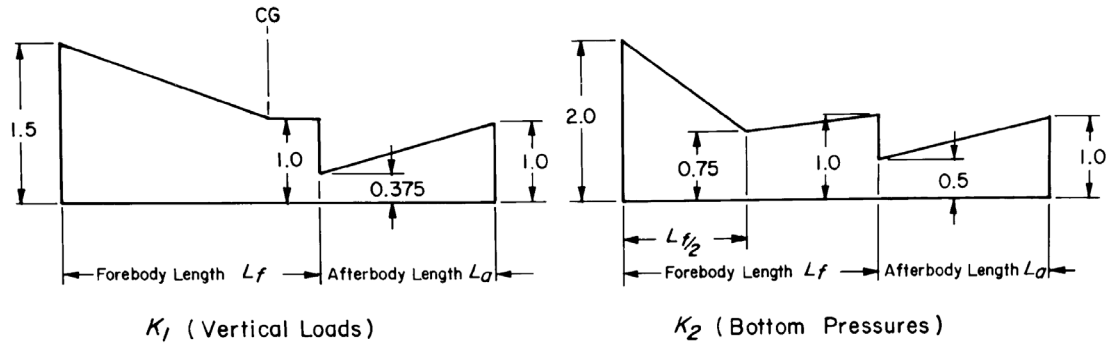


FIGURE 2. Hull station weighing factor.

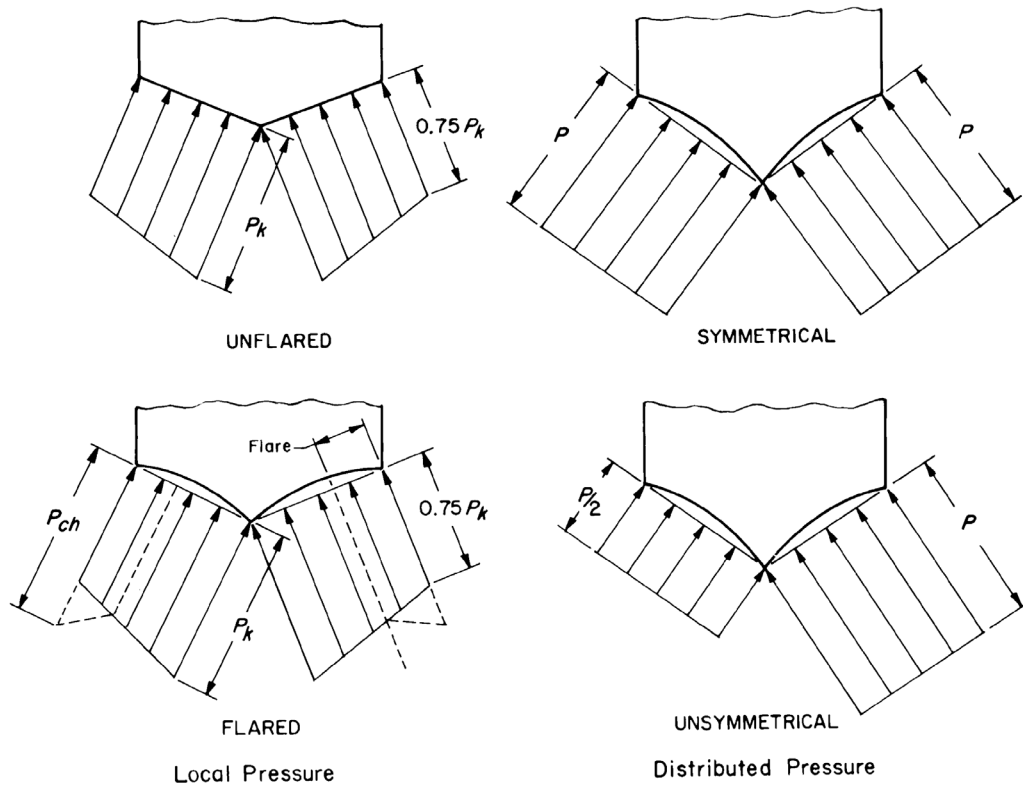


FIGURE 3. Transverse pressure distributions.

EXPERIMENTAL TOWING TANK  
STEVENS INSTITUTE OF TECHNOLOGY

REPORT NO. 325

PART I

MODEL TESTS ON A STANDARD SERIES  
OF  
FLYING-BOAT HULLS

by

Albert Strumpf

HOBOKEN, NEW JERSEY

MAY, 1947

GRID OF THE MODELS TESTED

| Deadrise<br>Angle,<br>deg. | L/b                          | Afterbody Angle, deg.    |                          |                                   |                          |                          |
|----------------------------|------------------------------|--------------------------|--------------------------|-----------------------------------|--------------------------|--------------------------|
|                            |                              | 3                        | 5                        | 7                                 | 9                        | 11                       |
| 0                          | 5.07<br>6.19<br>7.32<br>8.45 | 556                      |                          | 532                               |                          | 557                      |
| 10                         | 5.07<br>6.19<br>7.32<br>8.45 |                          | 610<br>604<br>624<br>695 | 533                               | 611<br>605<br>625<br>696 |                          |
| 20                         | 5.07<br>6.19<br>7.32<br>8.45 | 573<br>536<br>626<br>693 | 537                      | 339-22<br>[591]*<br>339-23<br>651 | 538                      | 574<br>539<br>627<br>694 |
| 30                         | 5.07<br>6.19<br>7.32<br>8.45 |                          | 612<br>606<br>628<br>697 | 534                               | 613<br>607<br>629<br>698 |                          |
| 40                         | 5.07<br>6.19<br>7.32<br>8.45 | 558                      |                          | 535                               |                          | 559                      |

\* [591] is a model of the XPB2M-1 and is the parent of the Series.

Note: The hulls in the Series are designated on the grid by their Stevens model numbers.

R268  
-15-

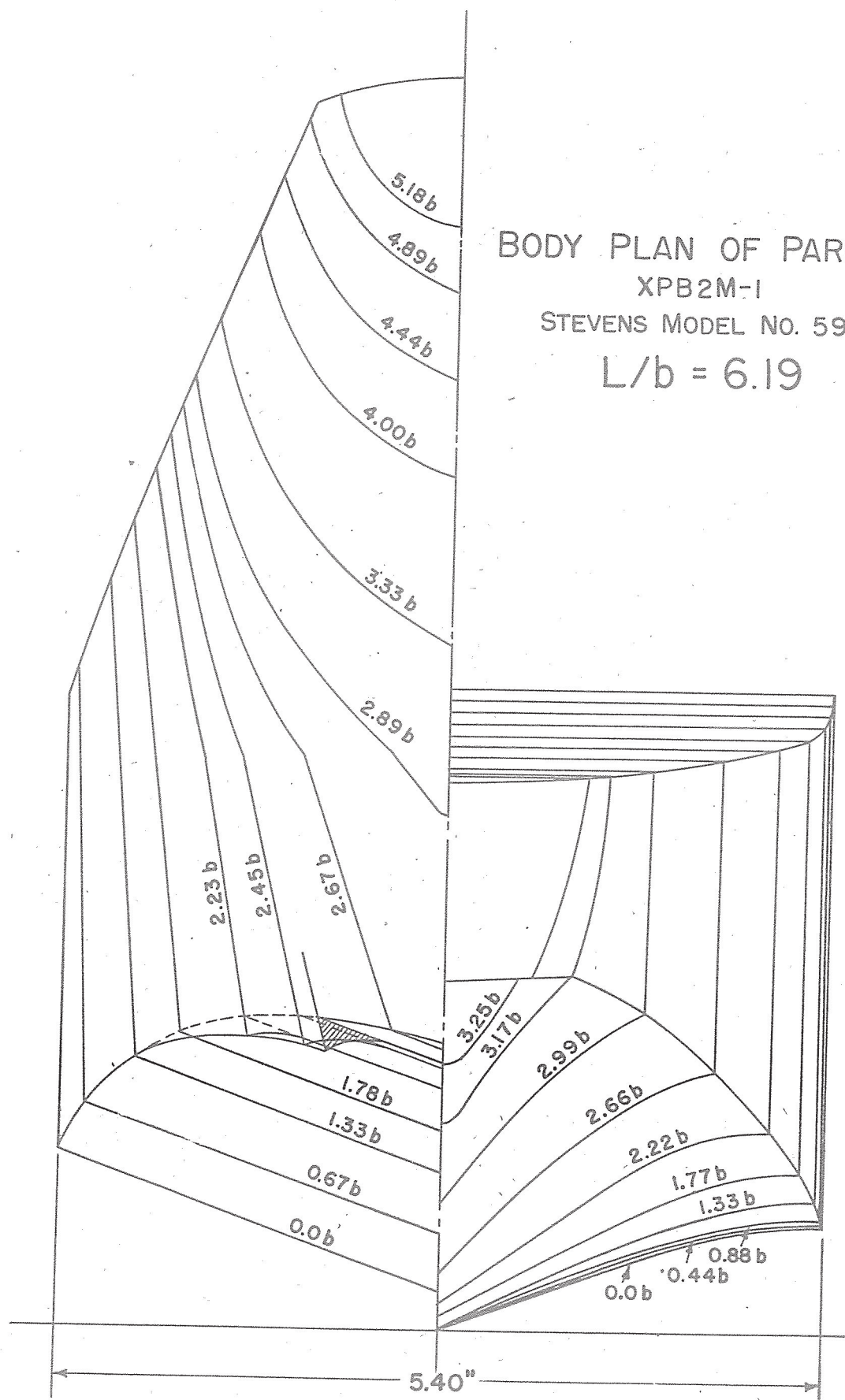
R-325  
-31-

BODY PLAN OF PARENT

XPB2M-I

STEVENS MODEL NO. 591

$$L/b = 6.19$$



SCALE: FULL SIZE FOR MODEL

TABULATION OF STERNPOST ANGLE VALUES  
FOR THE MODELS USED IN THE COMPARISONS

| <u>Model<br/>No.</u> | <u>Designation</u> | <u>Sternpost<br/>Height<br/>in.</u> | <u>Afterbody<br/>Length Along<br/>Afterbody Keel<br/>in.</u> | <u>Afterbody<br/>Length<br/>Along Baseline<br/>in.</u> | <u>Sternpost<br/>Angle<br/>deg.</u> |
|----------------------|--------------------|-------------------------------------|--|--|-------------------------------------|
| 573                  | 5.07-3-20          | 0.91                                | 12.24  | 12.20  | 4.25                                |
| 339-22               | 5.07-7-20          | 1.76                                | 12.24  | 12.15  | 8.25                                |
| 574                  | 5.07-11-20         | 2.61                                | 12.24  | 12.00  | 12.3                                |
| 532                  | 6.19-7-0           | 2.09                                | 14.96  | 14.85  | 8.0                                 |
| 533                  | 6.19-7-10          | 2.09                                | 14.96  | 14.85  | 8.0                                 |
| 591                  | 6.19-7-20          | 2.09                                | 14.96  | 14.85  | 8.0                                 |
| 534                  | 6.19-7-30          | 2.09                                | 14.96  | 14.85  | 8.0                                 |
| 535                  | 6.19-7-40          | 2.09                                | 14.96  | 14.85  | 8.0                                 |
| 536                  | 6.19-3-20          | 1.05                                | 14.96  | 14.94  | 4.0                                 |
| 537                  | 6.19-5-20          | 1.57                                | 14.96  | 14.90  | 6.0                                 |
| 538                  | 6.19-9-20          | 2.61                                | 14.96  | 14.88  | 10.1                                |
| 539                  | 6.19-11-20         | 3.13                                | 14.96  | 14.70  | 12.0                                |
| 605                  | 6.19-9-10          | 2.61                                | 14.96  | 14.88  | 10.1                                |
| 606                  | 6.19-5-30          | 1.57                                | 14.96  | 14.90  | 6.0                                 |
| 607                  | 6.19-9-30          | 2.61                                | 14.96  | 14.88  | 10.1                                |
| 626                  | 7.32-3-20          | 1.19                                | 17.67  | 17.65  | 3.9                                 |
| 339-23               | 7.32-7-20          | 2.43                                | 17.67  | 17.55  | 7.9                                 |
| 627                  | 7.32-11-20         | 3.64                                | 17.67  | 17.35  | 11.65                               |
| 693                  | 8.45-3-20          | 1.34                                | 20.40  | 20.35  | 3.75                                |
| 651                  | 8.45-7-20          | 2.76                                | 20.40  | 20.25  | 7.8                                 |
| 694                  | 8.45-11-20         | 4.15                                | 20.40  | 20.05  | 11.7                                |

DIMENSIONS AND PARTICULARS OF MODELS ON A  $L^2b$  (or  $K_2$ ) CONSTANT BASIS

| $L/b$                      | 5.07   | 6.19   | 7.32   | 8.45   |   |
|----------------------------|--------|--------|--------|--------|---|
| $L^2b$                     | 6040   | 6040   | 6040   | 6040   |   |
| $K_2$                      | 0.0279 | 0.0279 | 0.0279 | 0.0279 |   |
| $\Delta_o$                 | 6.07   | 6.07   | 6.07   | 6.07   | $\Delta_o = wL^2b K_2$  |
| $L$                        | 31.29  | 33.44  | 35.36  | 37.09  | $L = \sqrt[3]{L^2b(L/b)}$   |
| $b$                        | 6.17   | 5.40   | 4.83   | 4.39   | $b = \sqrt[3]{\frac{L^2b}{(L/b)^2}}$  |
| $C_{\Delta_o}$             | 0.72   | 1.07   | 1.49   | 1.99   | $C_{\Delta_o} = K_2(L/b)^2$ or $\Delta_o/wb^3$  |
| $L_B$                      | 15.23  | 16.70  | 17.97  | 19.09  | $L_B = \left[ \left( \frac{L_{fo}}{L_o} \right) \frac{L}{b} - 0.35 \right] b = \left[ 0.556 \frac{L}{b} - 0.35 \right] b$       |
| $L_{OA}$                   | 45.42  | 46.89  | 48.16  | 49.28  | $L_{OA} = L_B + 30.19$  |
| $K$                        | 7.28   | 7.52   | 7.72   | 7.90   | $K = K_o \frac{L_{OA}}{L_{OA_o}} = 7.52 \frac{L_{OA}}{46.90} = \frac{L_{OA}}{6.24}$   |
| $K/L$                      | 0.233  | 0.225  | 0.218  | 0.213  |   |
| $M_q/v$                    | 9.94   | 9.94   | 9.94   | 9.94   |   |
| $M_q/v \frac{\rho}{2} b^4$ | 0.147  | 0.250  | 0.391  | 0.572  | $M_q/v \frac{\rho}{2} b^4 = (M_q/v \frac{\rho}{2} b_o^4) \left( \frac{b_o}{b} \right)^4 = 0.250 \left( \frac{b_o}{b} \right)^4$ |

FOR MODELS OF CONSTANT 5.40" BEAM THESE VALUES BECOME FOR TEST MODELS

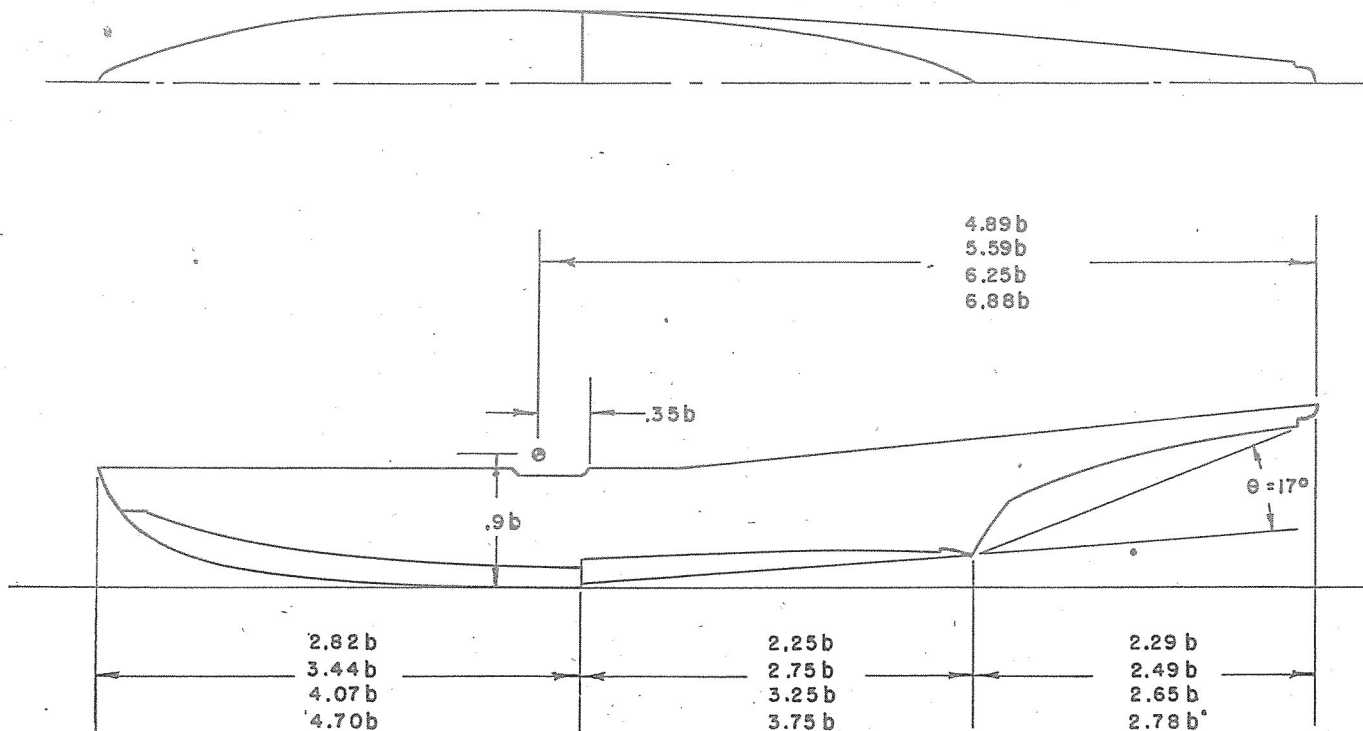
| $L/b$         | 5.07  | 6.19  | 7.32  | 8.45  |   |
|---------------|-------|-------|-------|-------|---|
| $\Delta_{om}$ | 4.07  | 6.07  | 8.50  | 11.29 | $\Delta_{om} = 6.07 \left( \frac{5.40}{b} \right)^3$                        |
| $L_m$         | 27.38 | 33.44 | 39.53 | 45.62 | $L_m = L \left( \frac{5.40}{b} \right)$                                     |
| $K_m$         | 6.37  | 7.52  | 8.63  | 9.72  | $K_m = \left( \frac{K}{L} \right) L_m$ or $K \left( \frac{5.40}{b} \right)$ |
| $I_m$         | 166   | 343   | 633   | 1067  | $I_m = \Delta_{om} K_m^2$   |
| $(M_q/v)_m$   | 5.83  | 9.94  | 15.54 | 22.75 | $(M_q/v)_m = (M_q/v) \left( \frac{5.40}{b} \right)^4$                       |



EXPERIMENTAL TOWING TANK  
STEVENS INSTITUTE OF TECHNOLOGY  
HOBOKEN, NEW JERSEY

R-325  
-34-

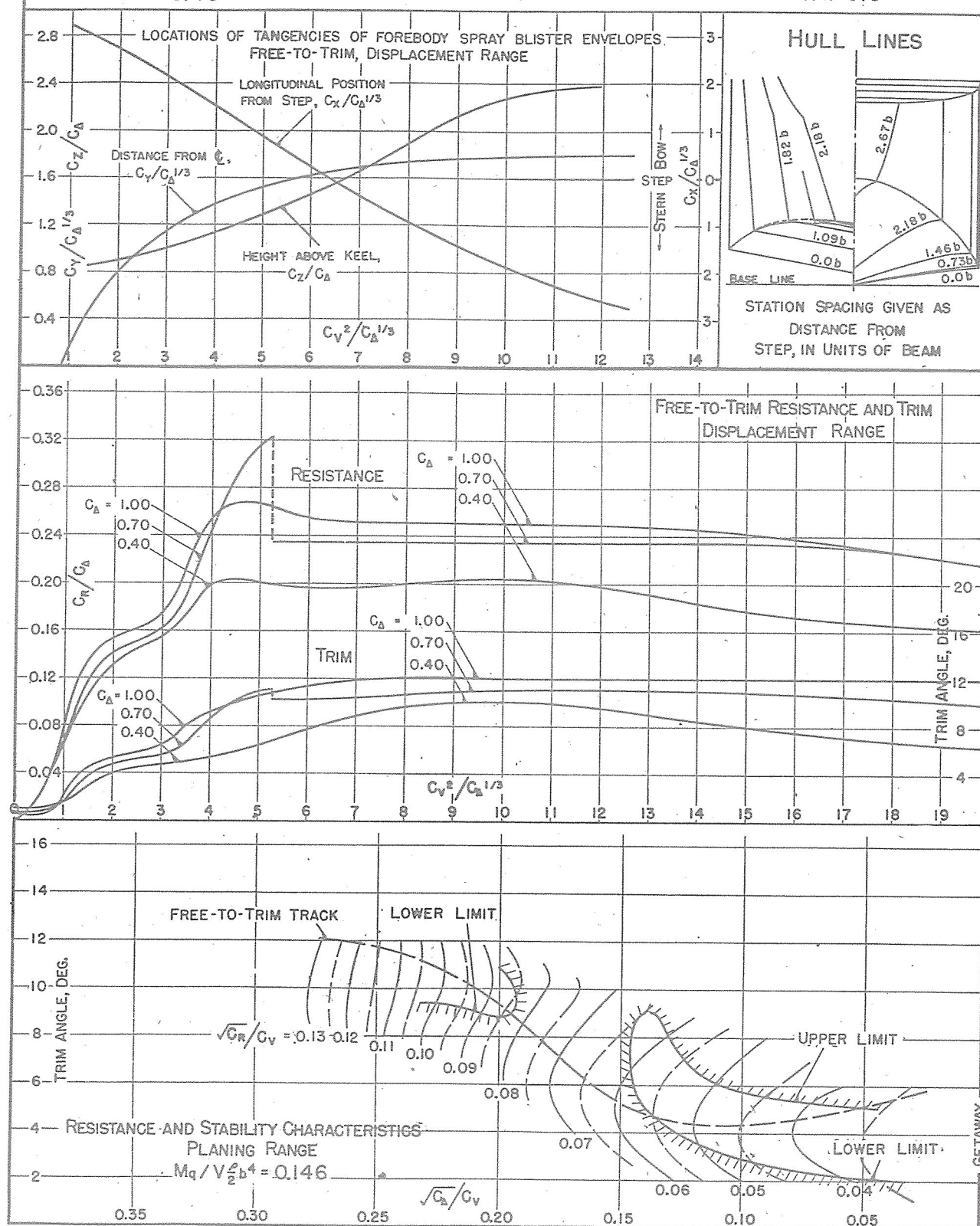
DIMENSIONS OF THE VARIOUS LENGTH-BEAM RATIO HULLS  
IN TERMS OF THEIR BEAMS DETERMINED ON A  
 $K_2$  CONSTANT BASIS



EXPERIMENTAL TOWING TANK  
STEVENS INSTITUTE OF TECHNOLOGY  
HOBOKEN, NEW JERSEY

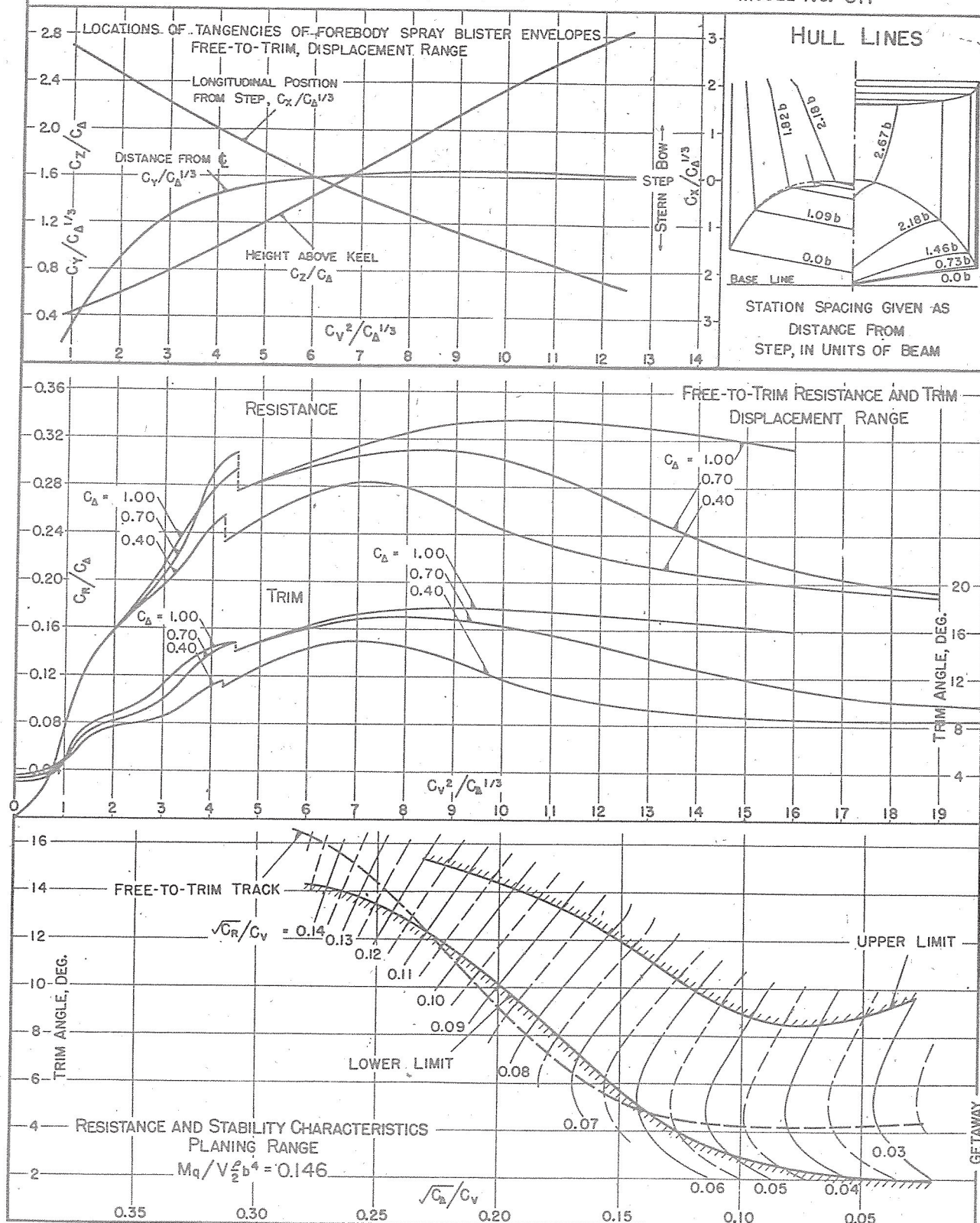
## SUMMARY CHART OF PRINCIPAL HYDRODYNAMIC CHARACTERISTICS

DATE: 3-27-45

C.G. = 0.35 b FWD. OF STEP  
0.90 b ABOVE KEEL $C_{da} = 0.72$  (NOMINAL)  
 $k/L = 0.234$ DESIGNATION: 5.07-5-10  
MODEL NO. 610

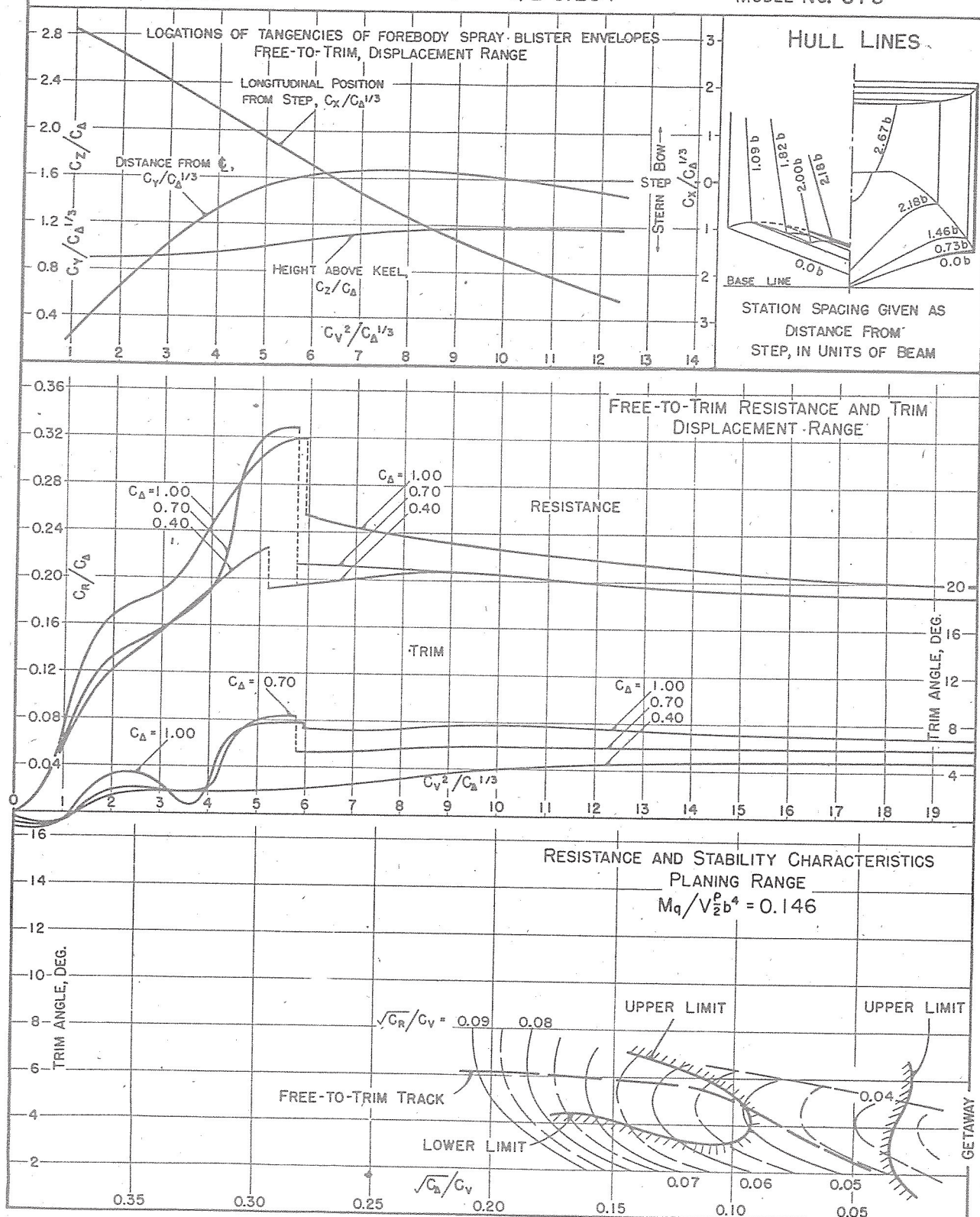


## SUMMARY CHART OF PRINCIPAL HYDRODYNAMIC CHARACTERISTICS

DATE: 3-27-45  
MODEL BEAM: 5.40"C.G. = 0.35 b FWD. OF STEP  
0.90 b ABOVE KEEL $C_{da} = 0.72$  (NOMINAL)  
 $k/L = 0.234$ DESIGNATION: 5.07-9-10  
MODEL NO. 611

EXPERIMENTAL TOWING TANK  
STEVENS INSTITUTE OF TECHNOLOGY  
HOBOKEN, NEW JERSEY

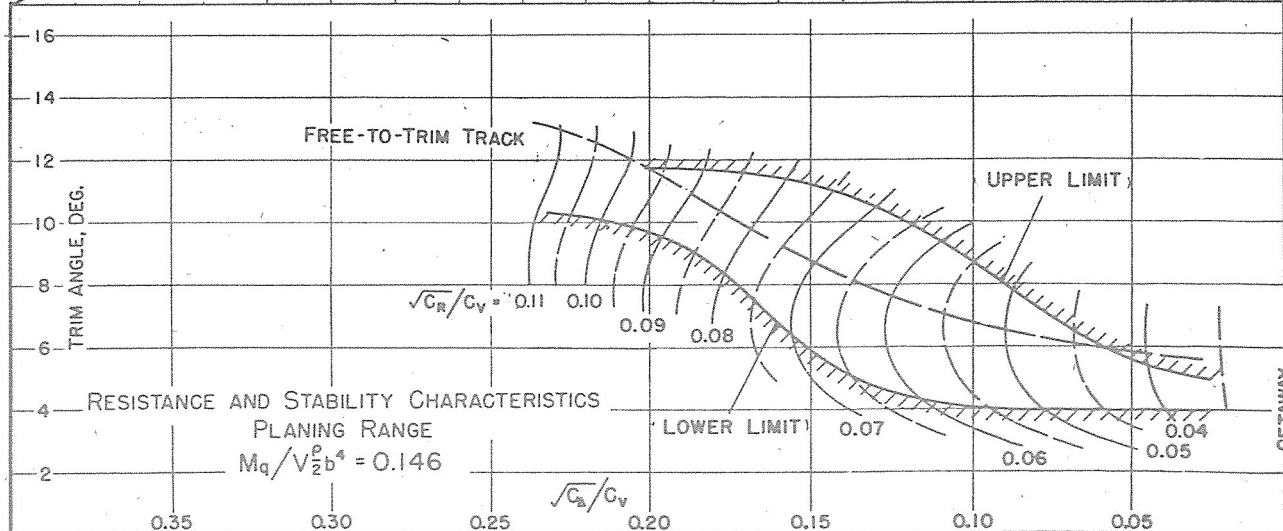
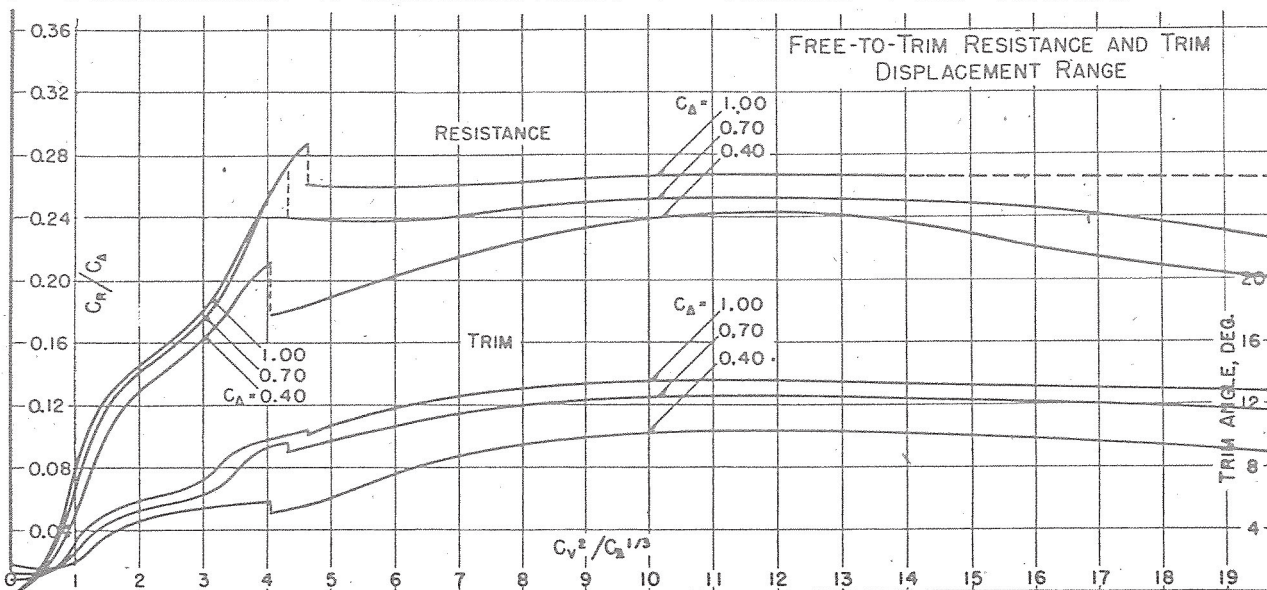
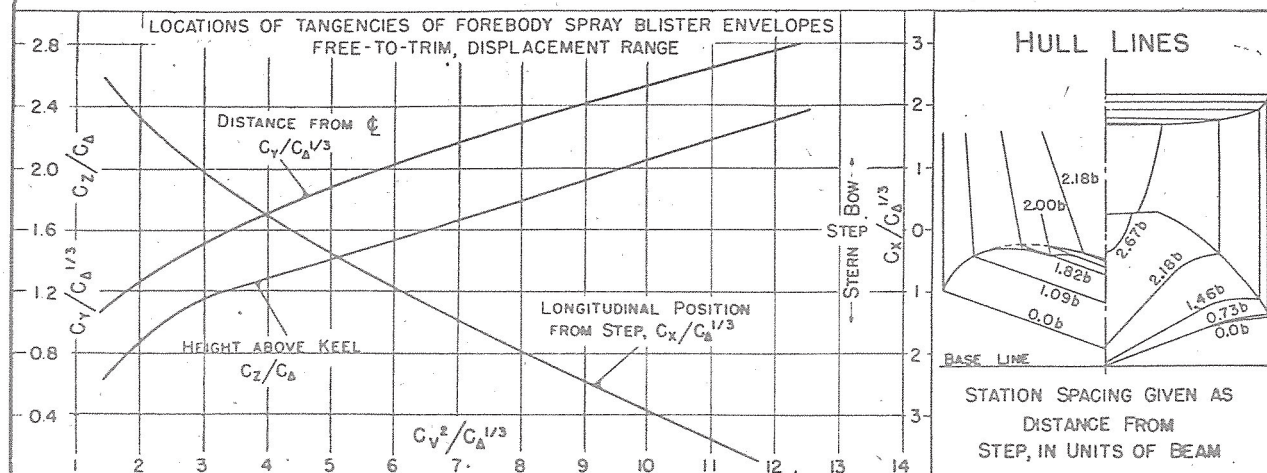
## SUMMARY CHART OF PRINCIPAL HYDRODYNAMIC CHARACTERISTICS

DATE: 5-9-45  
MODEL BEAM: 5.40"C.G. = 0.35 b FWD. OF STEP  
0.90 b ABOVE KEEL $C_{A0} = 0.72$  (NOMINAL)  
 $k/L = 0.234$ DESIGNATION: 5.07-3-20  
MODEL NO. 573



EXPERIMENTAL TOWING TANK  
STEVENS INSTITUTE OF TECHNOLOGY  
HOBOKEN, NEW JERSEY

## SUMMARY CHART OF PRINCIPAL HYDRODYNAMIC CHARACTERISTICS

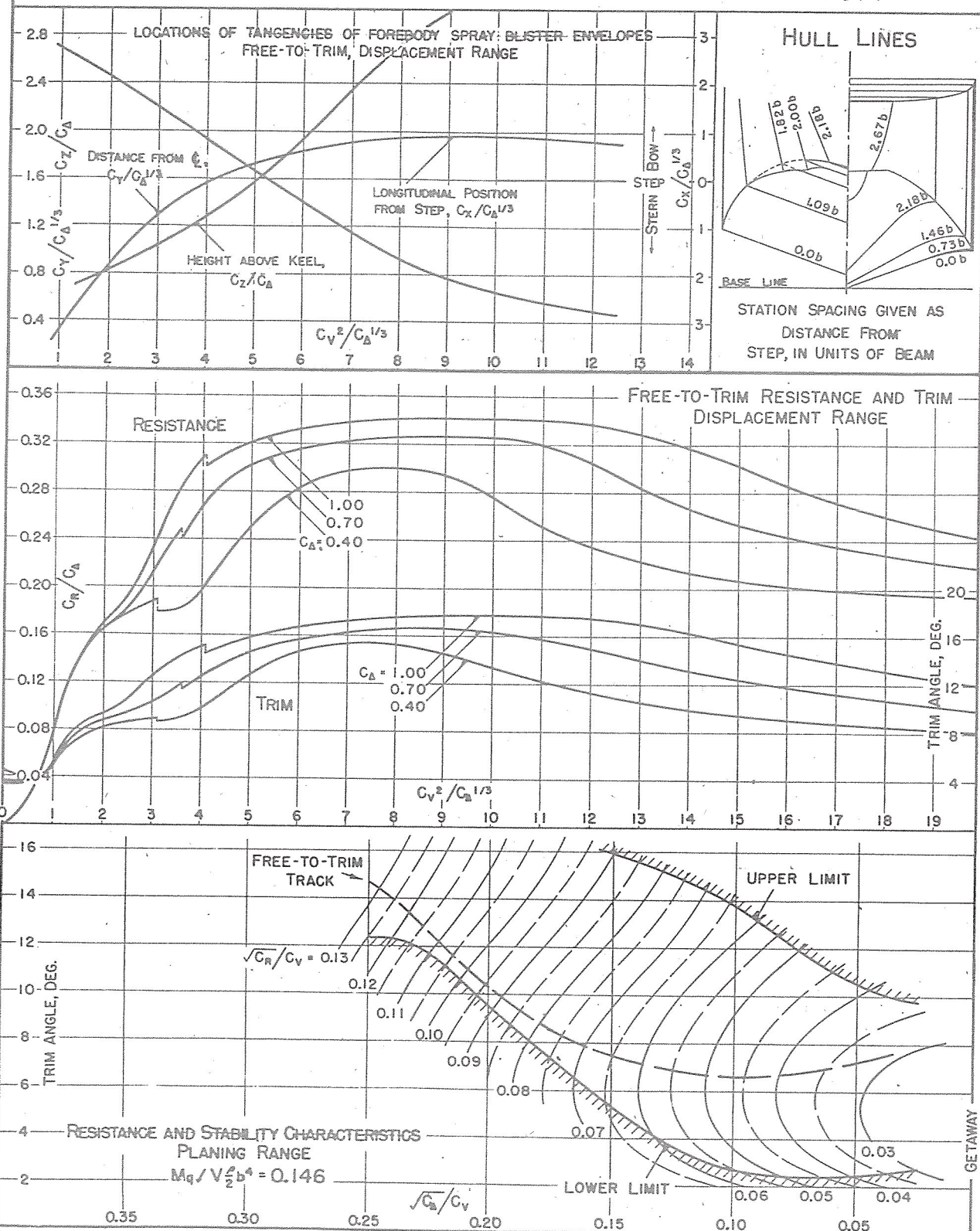
DATE: 5-9-45  
MODEL BEAM: 5.40"C.G. = 0.35 b FWD. OF STEP  
0.90 b ABOVE KEEL $C_{D0} = 0.72$  (NOMINAL)  
 $k/L = 0.234$ DESIGNATION: 5.07-7-20  
MODEL NO. 339-22

EXPERIMENTAL TOWING TANK  
STEVENS INSTITUTE OF TECHNOLOGY  
HOBOKEN, NEW JERSEY

## SUMMARY CHART OF PRINCIPAL HYDRODYNAMIC CHARACTERISTICS

DATE: 5-8-45

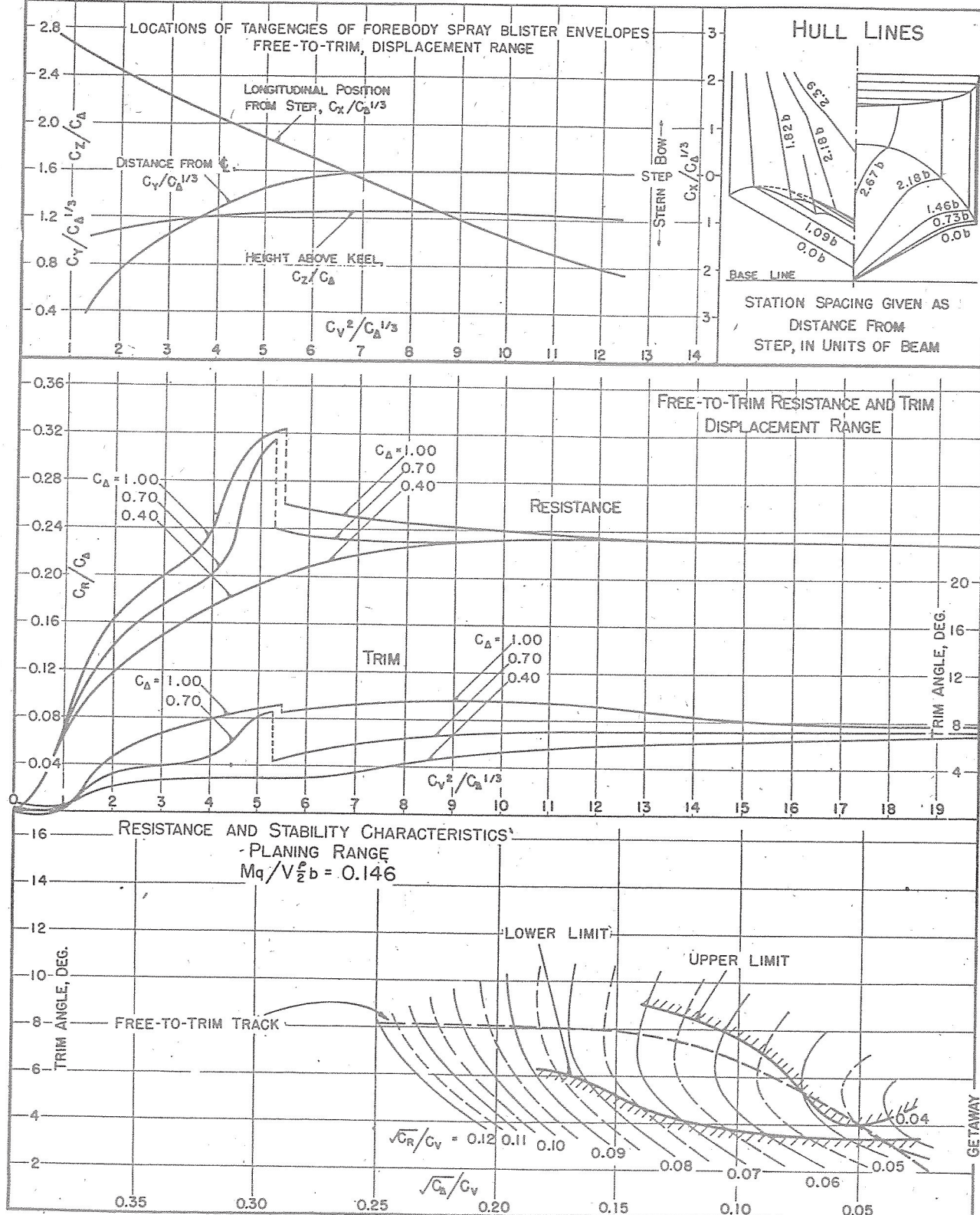
MODEL BEAM: 5.40"

C.G. = 0.35 b FWD. OF STEP  
0.90 b ABOVE KEEL $C_{A0} = 0.72$  (NOMINAL)  
 $k/L = 0.234$ DESIGNATION: 5.07-11-20  
MODEL NO. 574



EXPERIMENTAL TOWING TANK  
STEVENS INSTITUTE OF TECHNOLOGY  
HOBOKEN, NEW JERSEY

## SUMMARY CHART OF PRINCIPAL HYDRODYNAMIC CHARACTERISTICS

DATE: 3-27-45  
MODEL BEAM: 5.40"C.G. = 0.35 b FWD. OF STEP  
0.90 b ABOVE KEEL $C_{D_0} = 0.72$  (NOMINAL)  
 $K/L = 0.234$ DESIGNATION: 5.07-5-30  
MODEL NO. 612

EXPERIMENTAL TOWING TANK  
STEVENS INSTITUTE OF TECHNOLOGY  
HOBOKEN, NEW JERSEY

## SUMMARY CHART OF PRINCIPAL HYDRODYNAMIC CHARACTERISTICS

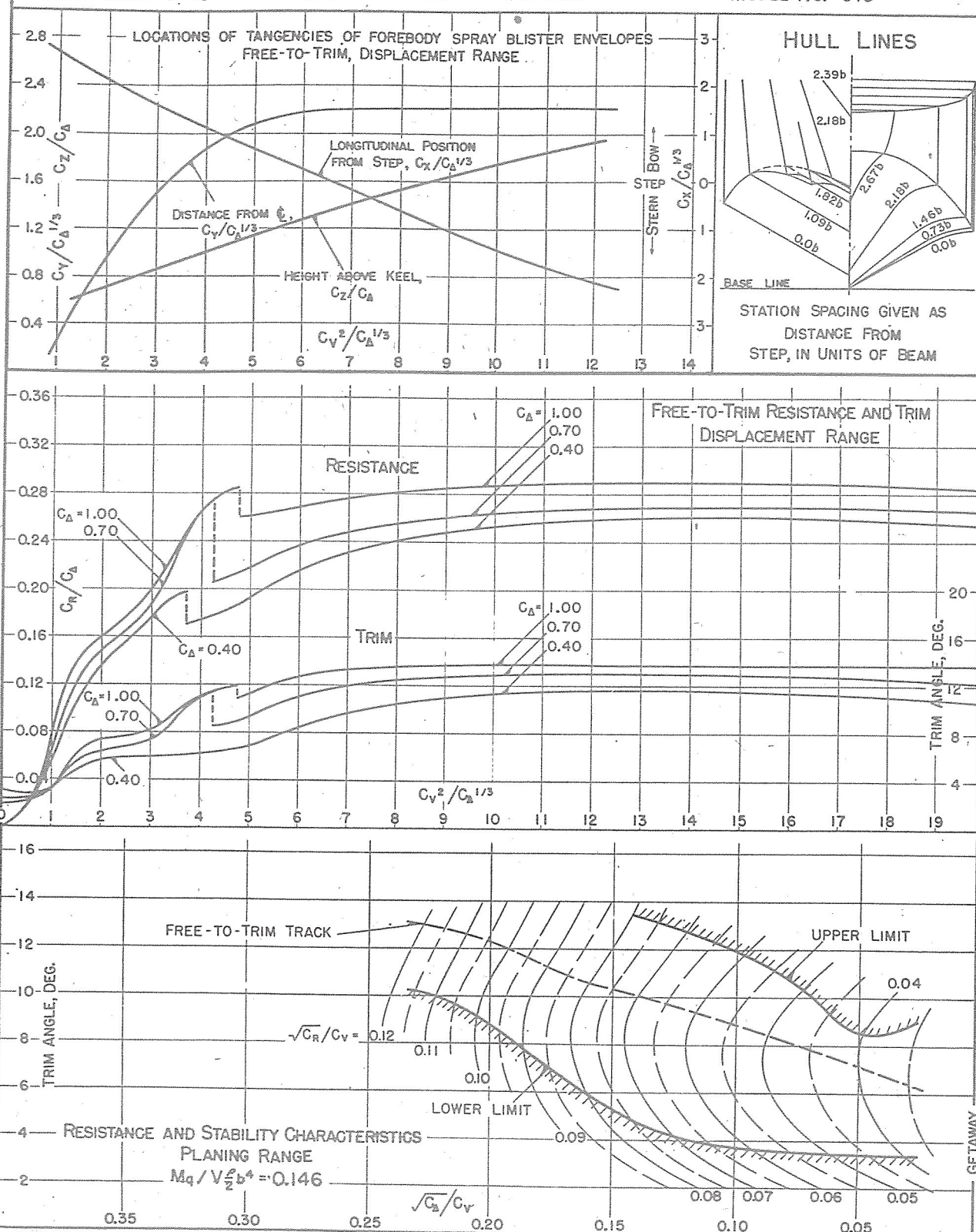
DATE: 3-27-45

MODEL BEAM: 5.40"

C.G. = 0.35 b FWD. OF STEP  
0.90 b ABOVE KEEL $C_{D0} = 0.72$  (NOMINAL) $k/L = 0.234$ 

DESIGNATION: 5.07-9-30

MODEL NO. 613

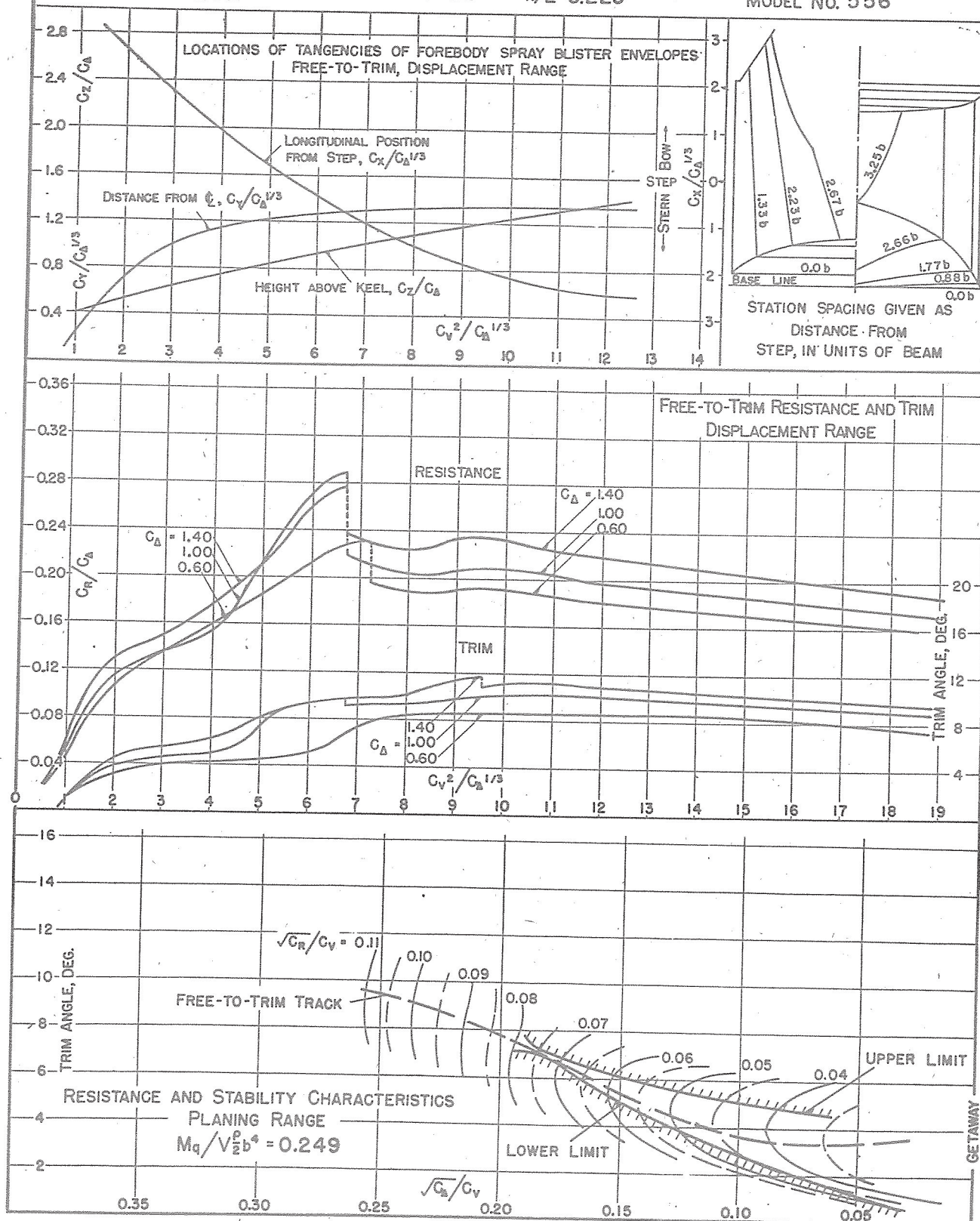




EXPERIMENTAL TOWING TANK  
STEVENS INSTITUTE OF TECHNOLOGY  
HOBOKEN, NEW JERSEY

## SUMMARY CHART OF PRINCIPAL HYDRODYNAMIC CHARACTERISTICS

8-8-44

DATE: 12-26-45 (REVISED)  $C_G = 0.35b$  FWD. OF STEP  
MODEL BEAM: 5.40" 0.90b ABOVE KEEL $C_{A_0} = 1.07$  (NOMINAL)  
 $k/L = 0.225$ DESIGNATION: 6.19-3-0  
MODEL NO. 556

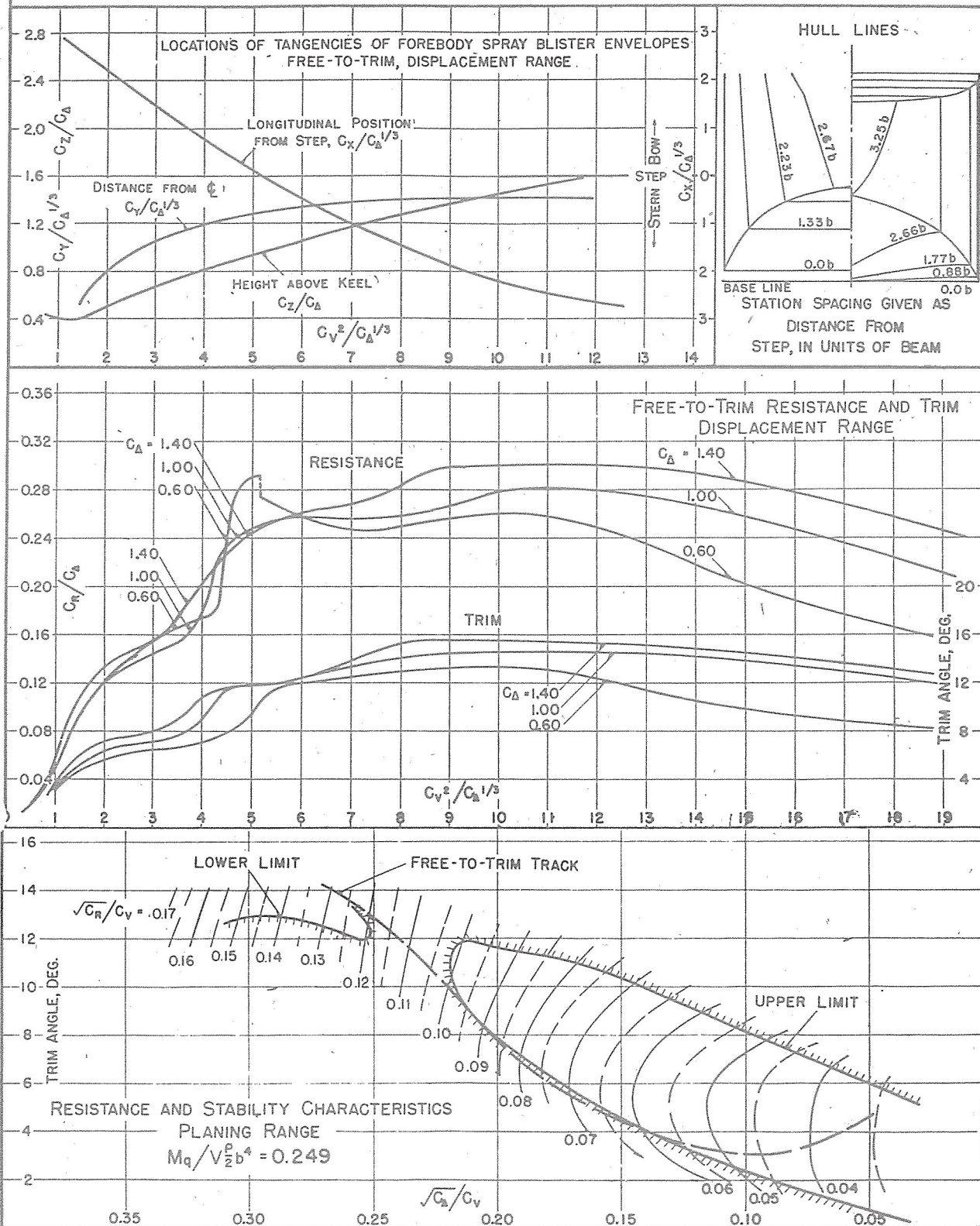
EXPERIMENTAL TOWING TANK  
STEVENS INSTITUTE OF TECHNOLOGY  
HOBOKEN, NEW JERSEY

## SUMMARY CHART OF PRINCIPAL HYDRODYNAMIC CHARACTERISTICS

8-8-44  
DATE: 7-20-45 (REVISED) C.G. = 0.35b FWD. OF STEP  
MODEL BEAM: 5.40" 0.90b ABOVE KEEL

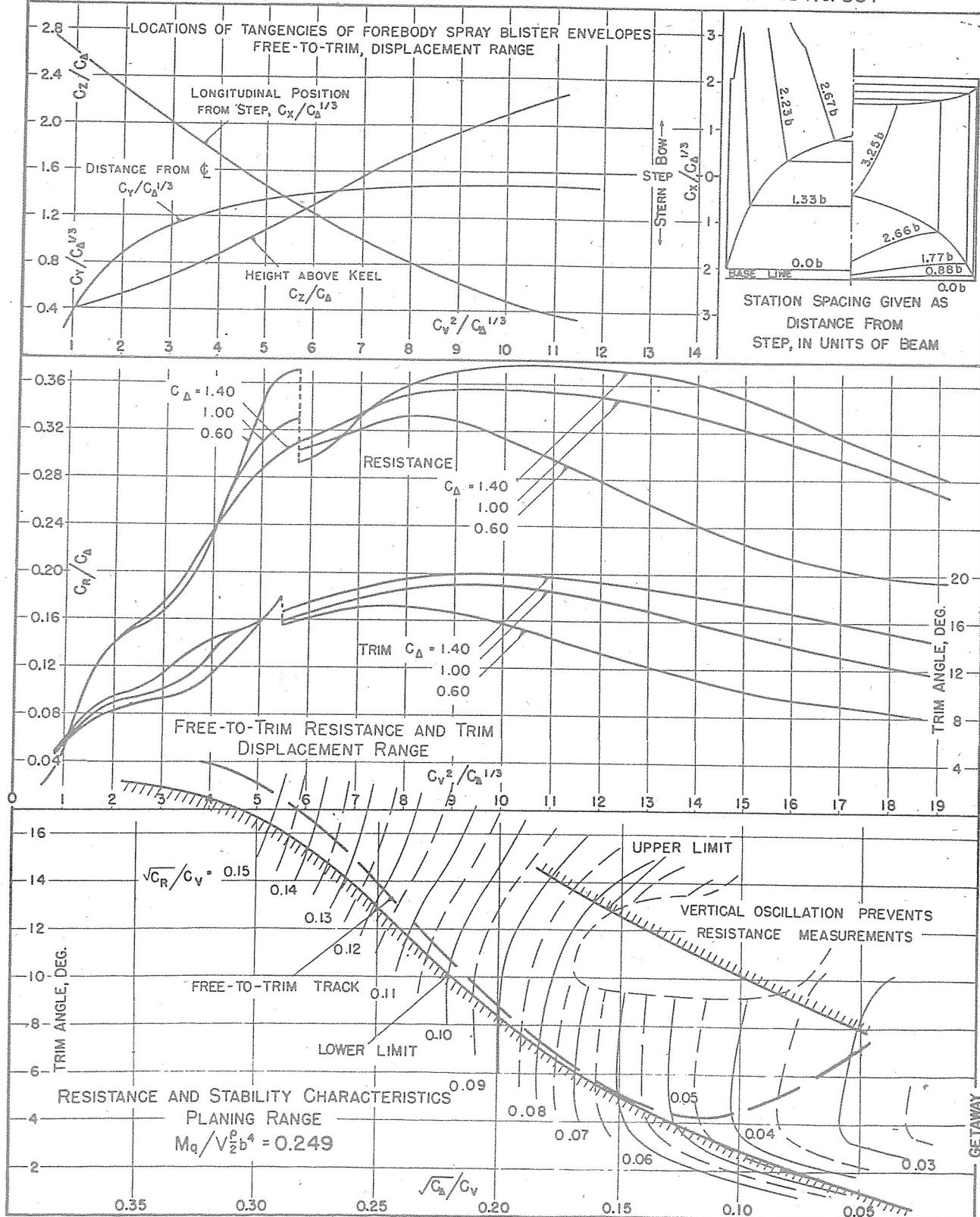
$C_{d0} = 1.07$  (NOMINAL)  
 $k/L = 0.225$

DESIGNATION: 6.19-7-0  
MODEL NO. 532





## SUMMARY CHART OF PRINCIPAL HYDRODYNAMIC CHARACTERISTICS

DATE: 8-8-44  
12-4-45 (REVISED)  
MODEL BEAM: 5.40"C.G. = 0.35b FWD. OF STEP  
0.90b ABOVE KEEL $C_{D0} = 1.07$  (NOMINAL)  
 $k/L = 0.225$ DESIGNATION: 6.19-II-O  
MODEL NO. 557

EXPERIMENTAL TOWING TANK  
STEVENS INSTITUTE OF TECHNOLOGY  
HOBOKEN, NEW JERSEY

## SUMMARY CHART OF PRINCIPAL HYDRODYNAMIC CHARACTERISTICS

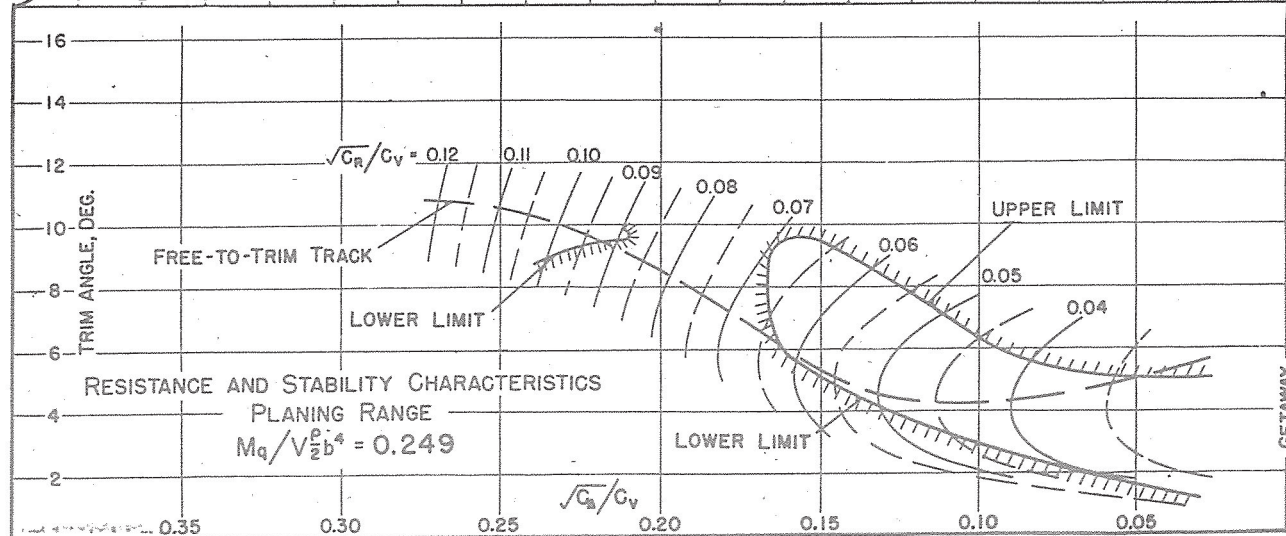
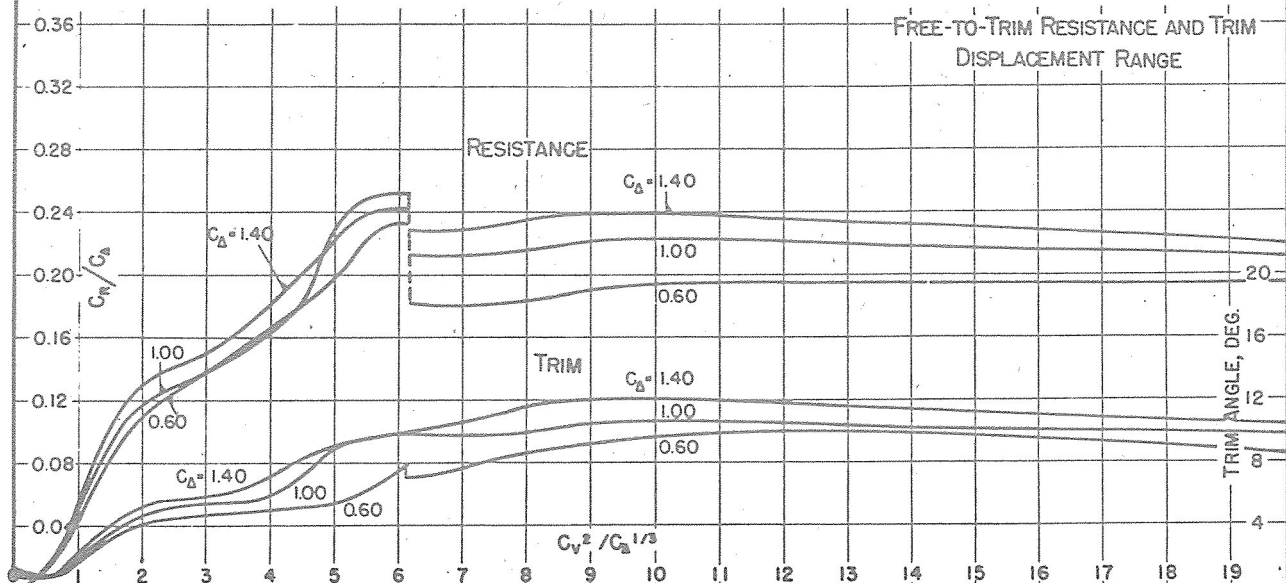
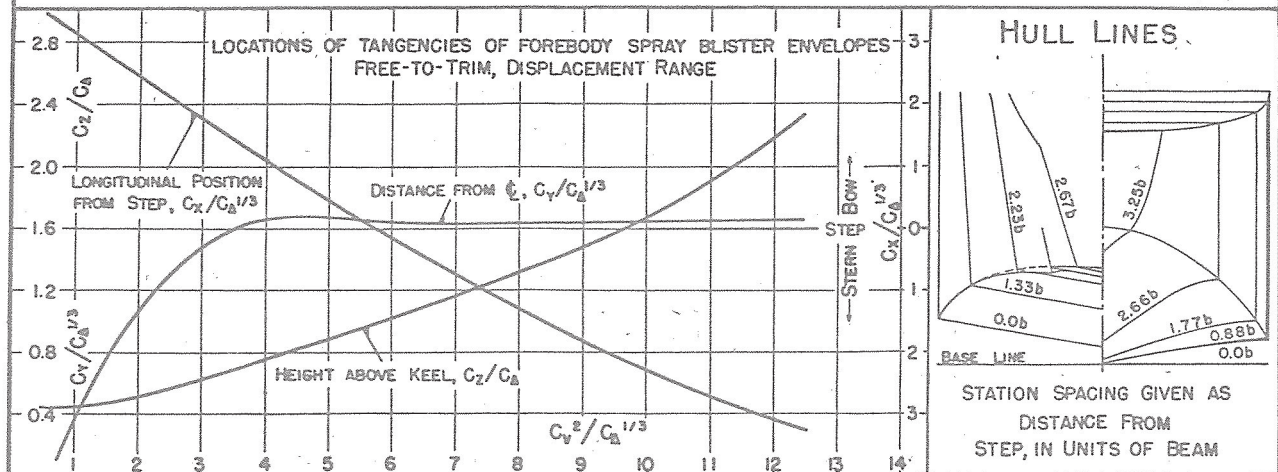
DATE: 12-4-44

MODEL BEAM: 5.40"

C.G. = 0.35 b FWD. OF STEP  
0.90 b ABOVE KEEL $C_{D_0} = 1.07$  (NOMINAL) $k/L = 0.225$ 

DESIGNATION: 6.19-5-10

MODEL NO. 604





EXPERIMENTAL TOWING TANK  
STEVENS INSTITUTE OF TECHNOLOGY  
HOBOKEN, NEW JERSEY

## SUMMARY CHART OF PRINCIPAL HYDRODYNAMIC CHARACTERISTICS

8-8-44

DATE: 7-13-45 (REVISED) C.G. = 0.35b FWD. OF STEP

 $C_{da} = 1.07$  (NOMINAL)

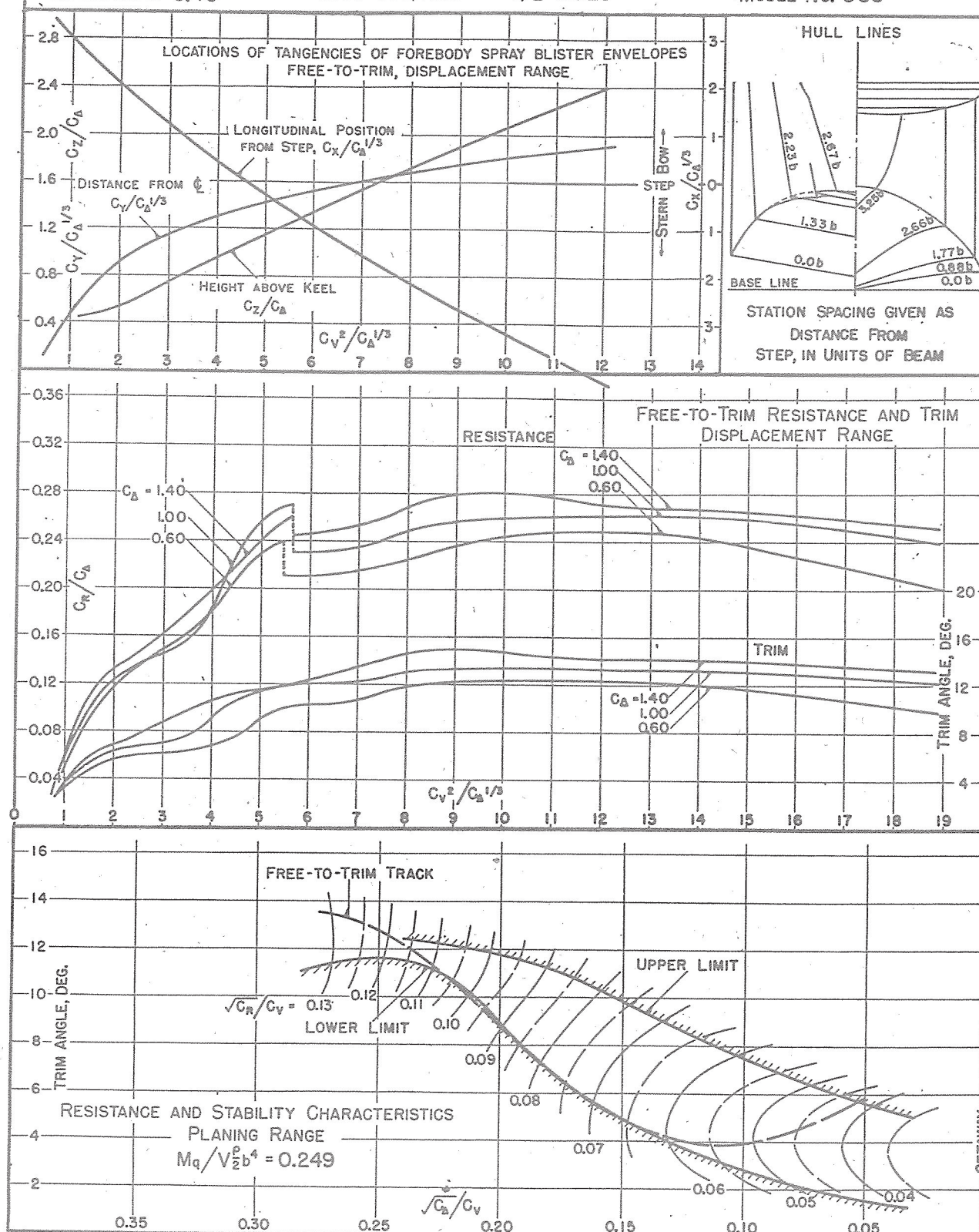
DESIGNATION: 6.19-7-10

MODEL BEAM: 5.40"

0.90b ABOVE KEEL

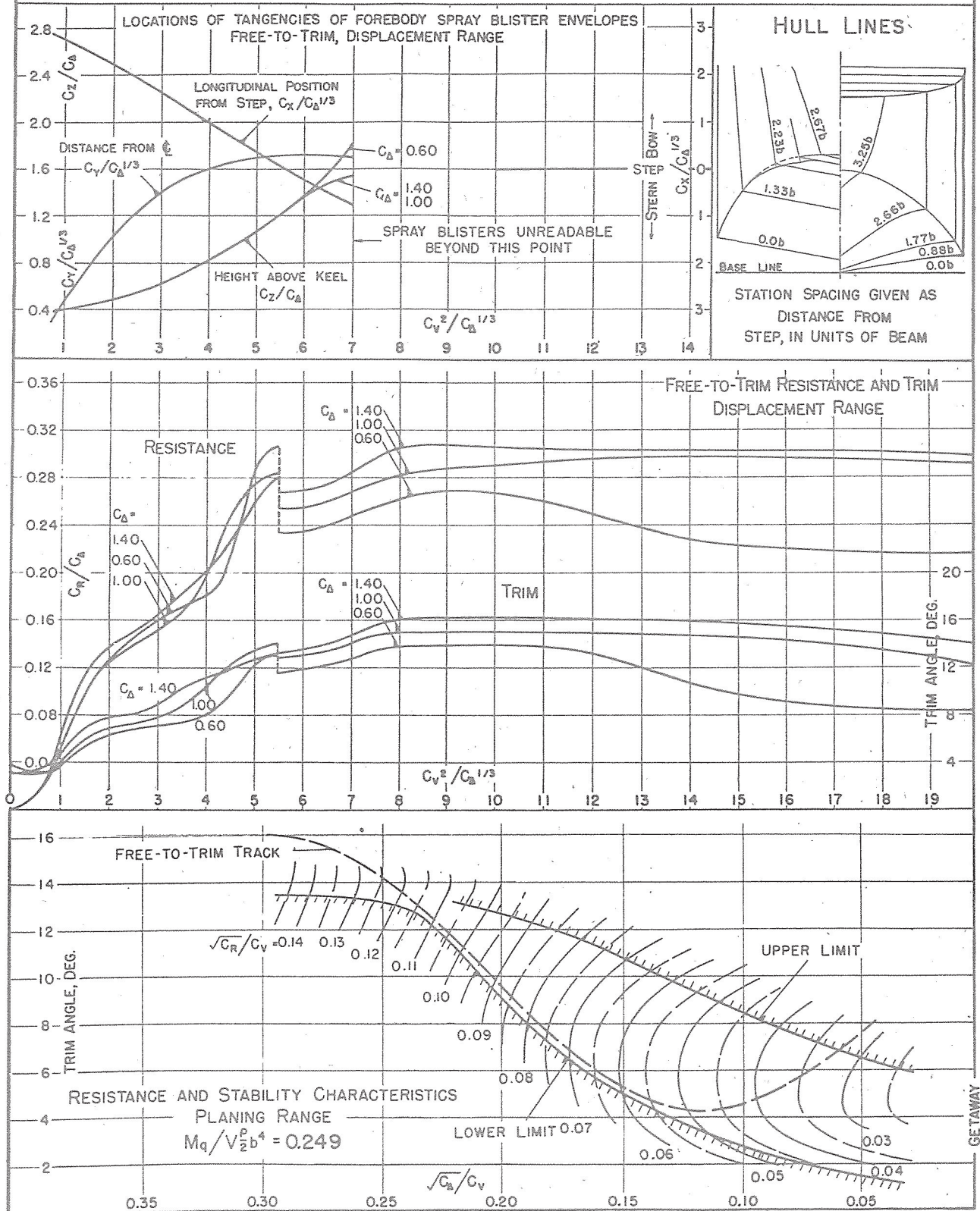
 $k/L = 0.225$ 

MODEL NO. 533



EXPERIMENTAL TOWING TANK  
STEVENS INSTITUTE OF TECHNOLOGY  
HOBOKEN, NEW JERSEY

## SUMMARY CHART OF PRINCIPAL HYDRODYNAMIC CHARACTERISTICS

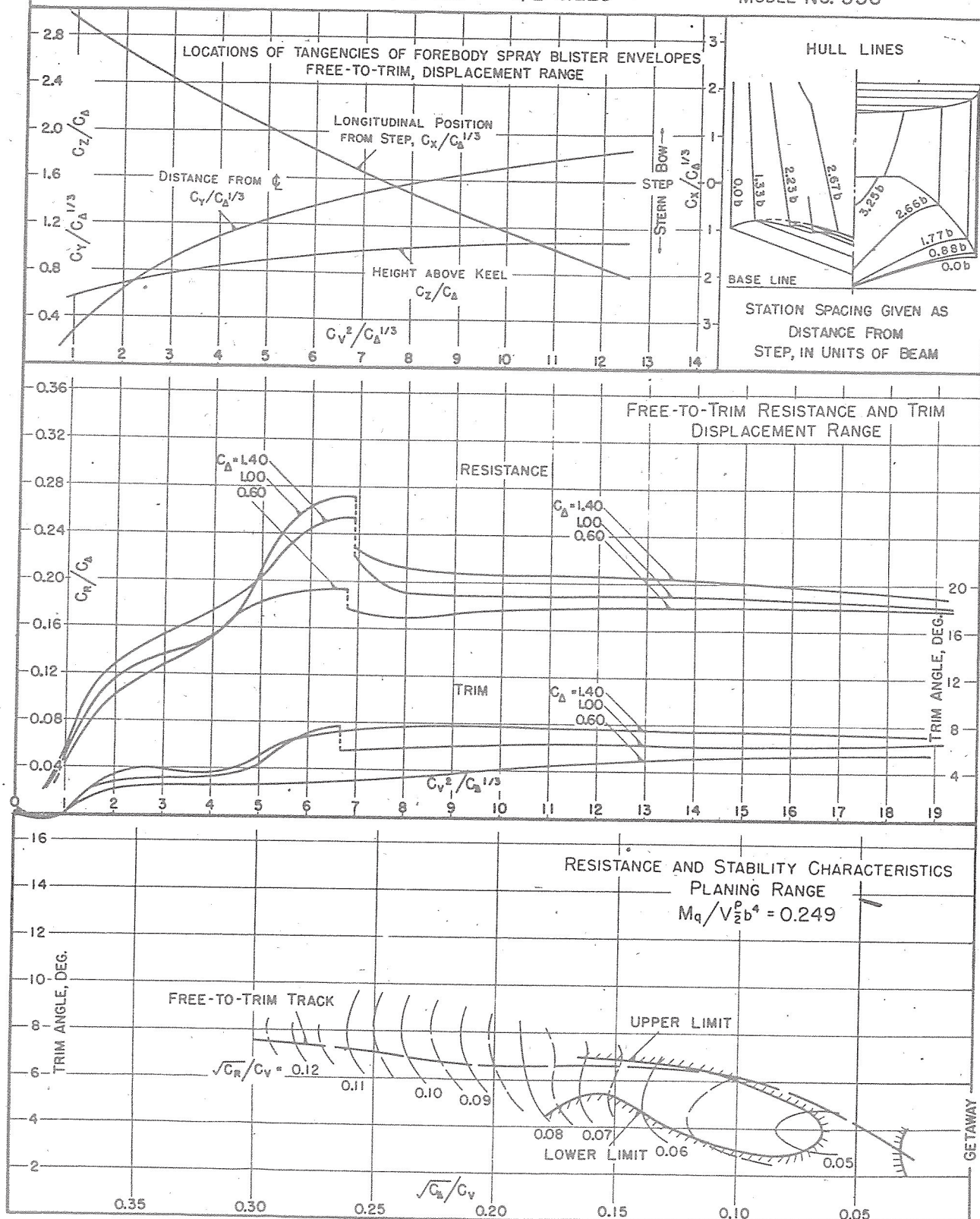
DATE: 12-23-44  
10-23-45 (REVISED)  
MODEL BEAM: 5.40" $C_G = 0.35b$  FWD. OF STEP  
 $0.90b$  ABOVE KEEL $C_{da} = 1.07$  (NOMINAL)  
 $k/L = 0.225$ DESIGNATION: 6.19-9-10  
MODEL NO. 605



EXPERIMENTAL TOWING TANK  
STEVENS INSTITUTE OF TECHNOLOGY  
HOBOKEN, NEW JERSEY

## SUMMARY CHART OF PRINCIPAL HYDRODYNAMIC CHARACTERISTICS

8-8-44

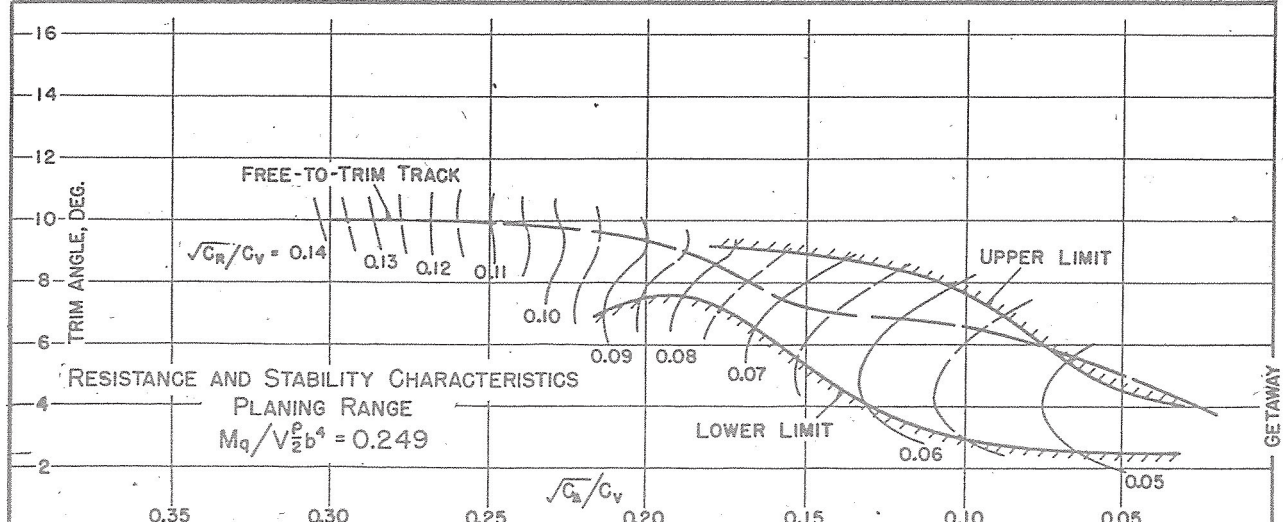
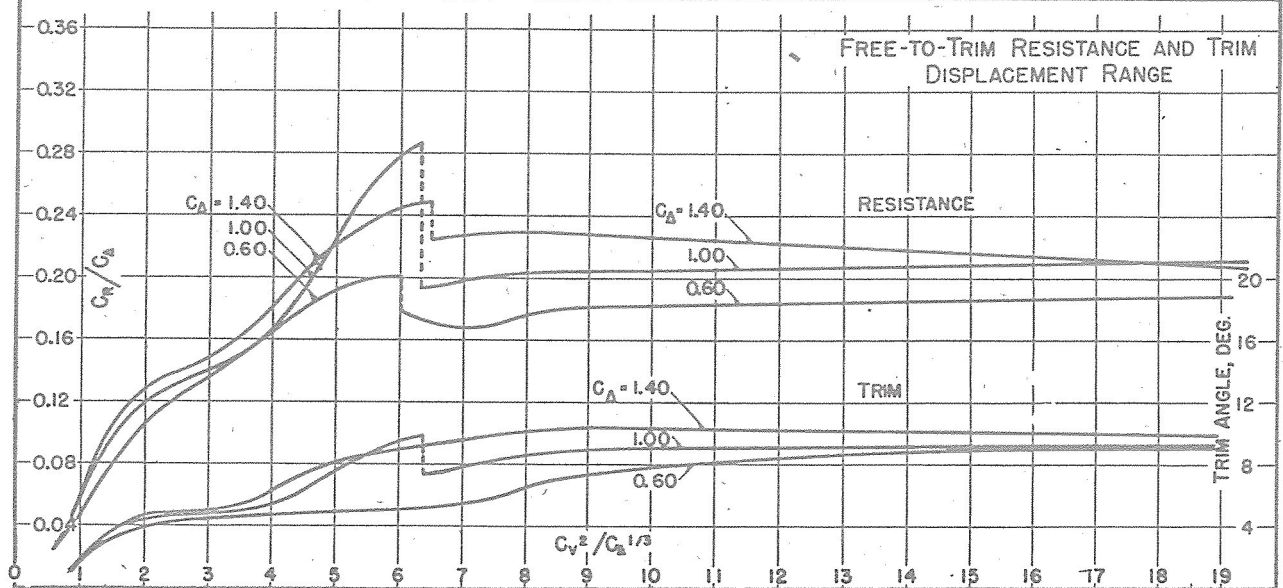
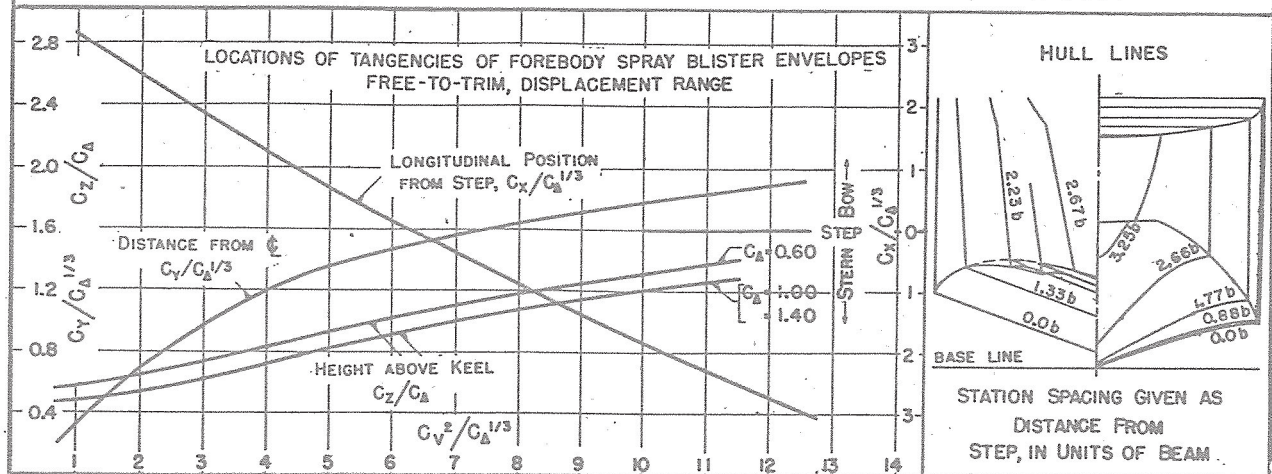
DATE: 10-23-45 (REVISED) C.G. = 0.35b FWD. OF STEP  
MODEL BEAM: 5.40" 0.90b ABOVE KEEL $C_{D0} = 1.07$  (NOMINAL)  
 $k/L = 0.225$ DESIGNATION: 6.19-3-20  
MODEL NO. 536

EXPERIMENTAL TOWING TANK  
STEVENS INSTITUTE OF TECHNOLOGY  
HOBOKEN, NEW JERSEY

## SUMMARY CHART OF PRINCIPAL HYDRODYNAMIC CHARACTERISTICS

DATE: 8-8-44

MODEL BEAM: 5.40"

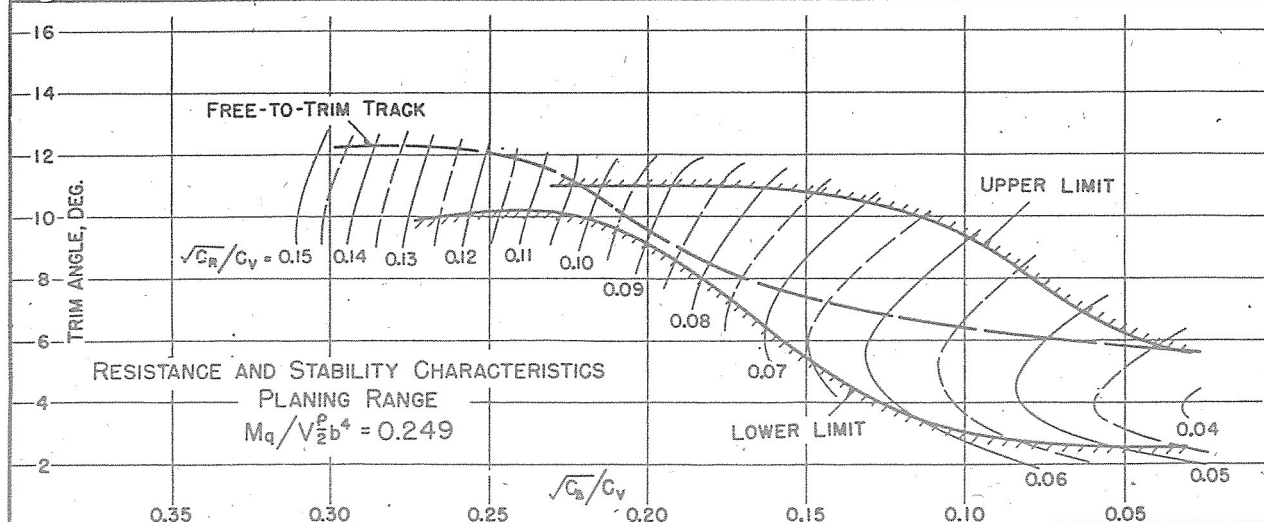
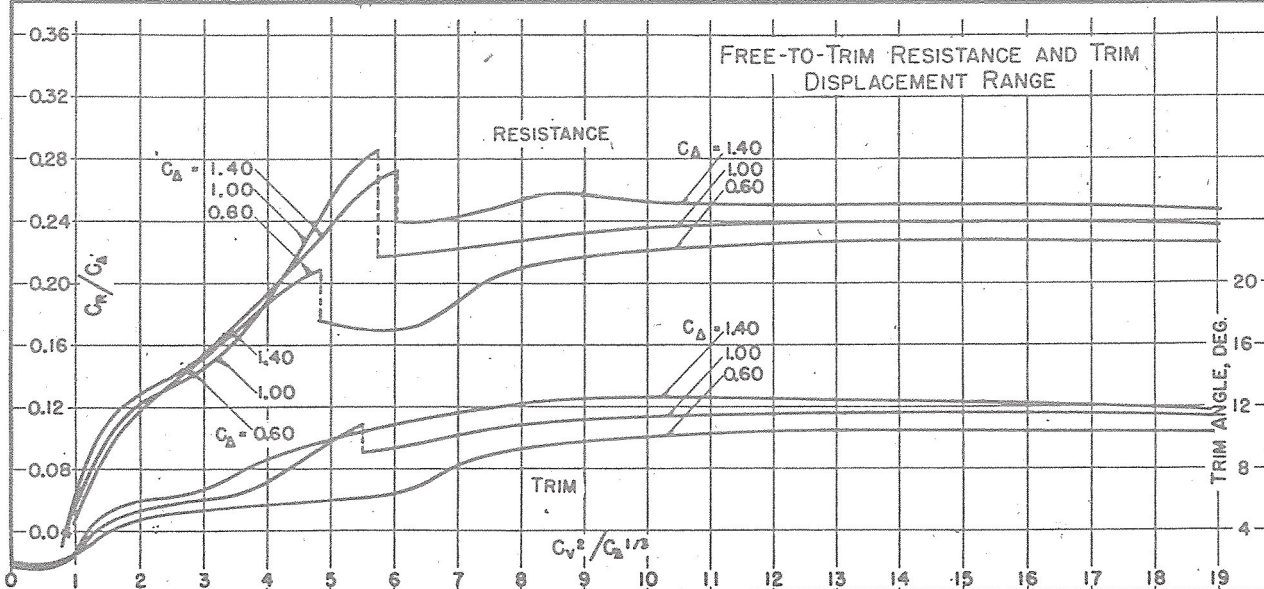
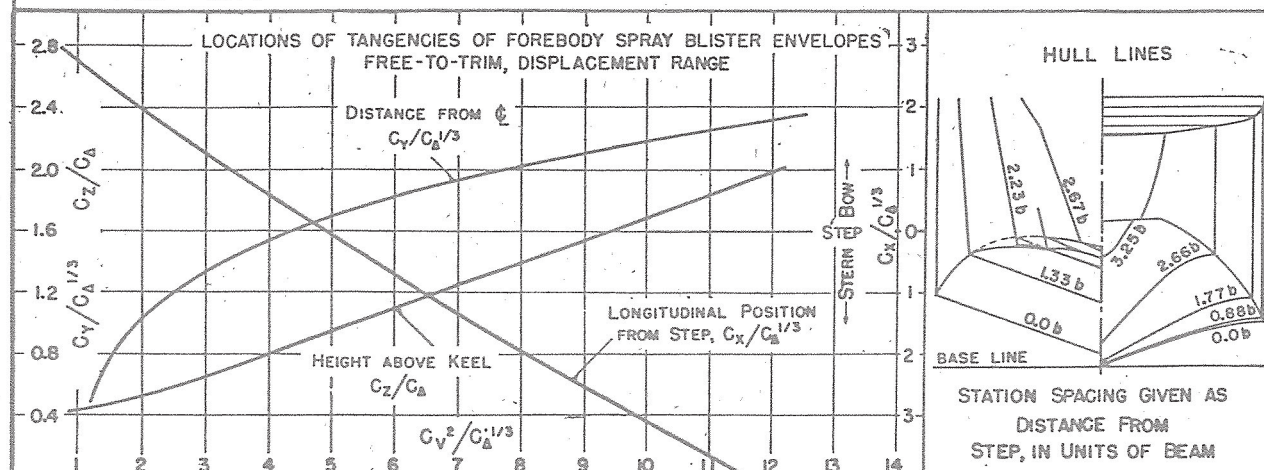
C.G. = 0.35b FWD. OF STEP  
0.90b ABOVE KEEL $C_{Ao} = 1.07$  (NOMINAL)  
 $k/L = 0.225$ DESIGNATION: 6.19-5-20  
MODEL No. 537



EXPERIMENTAL TOWING TANK  
STEVENS INSTITUTE OF TECHNOLOGY  
HOBOKEN, NEW JERSEY

## SUMMARY CHART OF PRINCIPAL HYDRODYNAMIC CHARACTERISTICS

11-4-43

DATE: 8-15-45 (REVISED) C.G. = 0.35b FWD. OF STEP  
MODEL BEAM: 5.40" 0.90b ABOVE KEEL $C_{D0} = 1.07$  (NOMINAL)  
 $k/L = 0.225$ DESIGNATION: 6.19-7-20  
MODEL NO. 591

EXPERIMENTAL TOWING TANK  
STEVENS INSTITUTE OF TECHNOLOGY  
HOBOKEN, NEW JERSEY

## SUMMARY CHART OF PRINCIPAL HYDRODYNAMIC CHARACTERISTICS

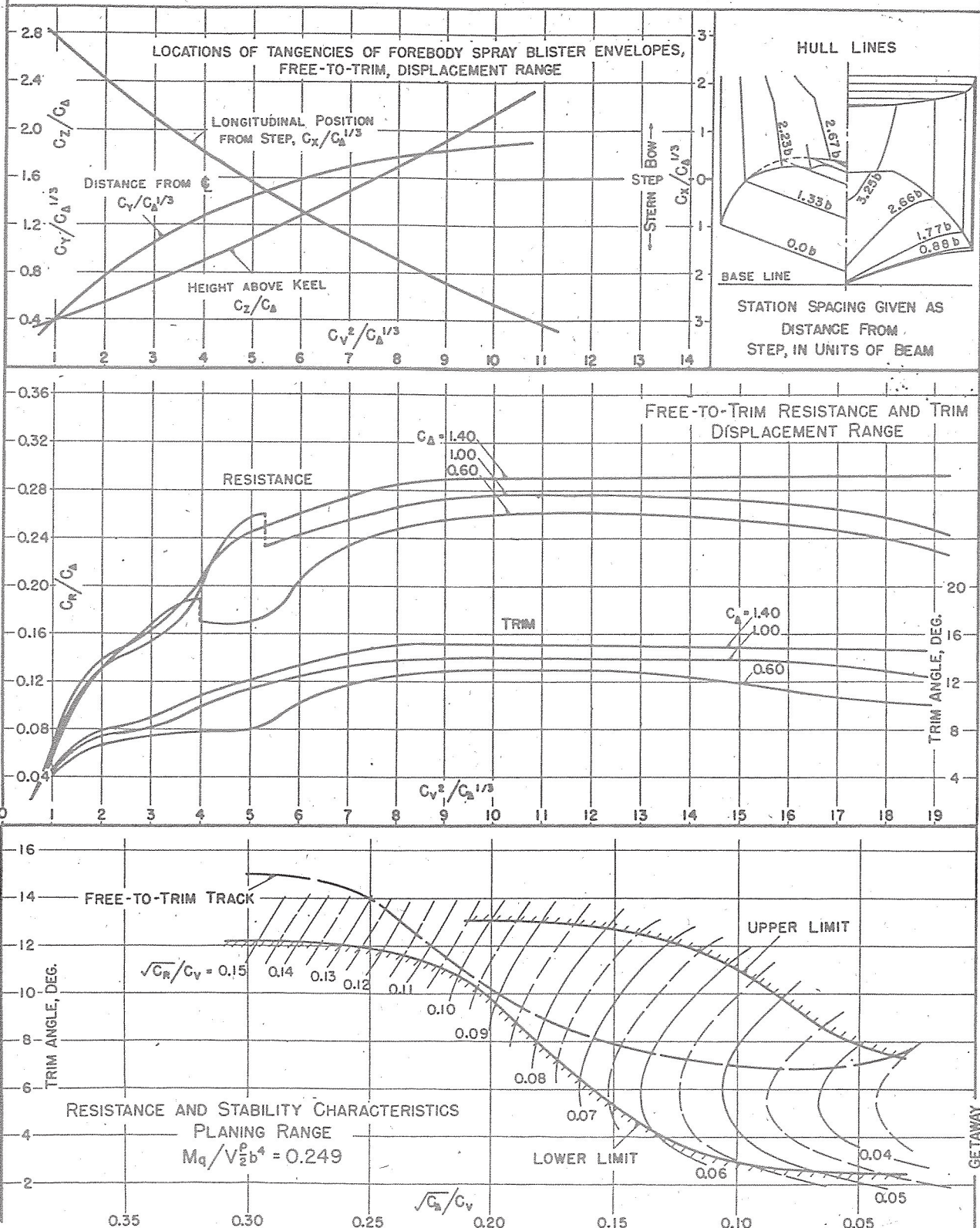
DATE: 8-8-44

MODEL BEAM: 5.40"

C.G. = 0.35b FWD. OF STEP  
0.90b ABOVE KEEL $C_{d0} = 1.07$  (NOMINAL) $k/L = 0.225$ 

DESIGNATION: 6.19-9-20

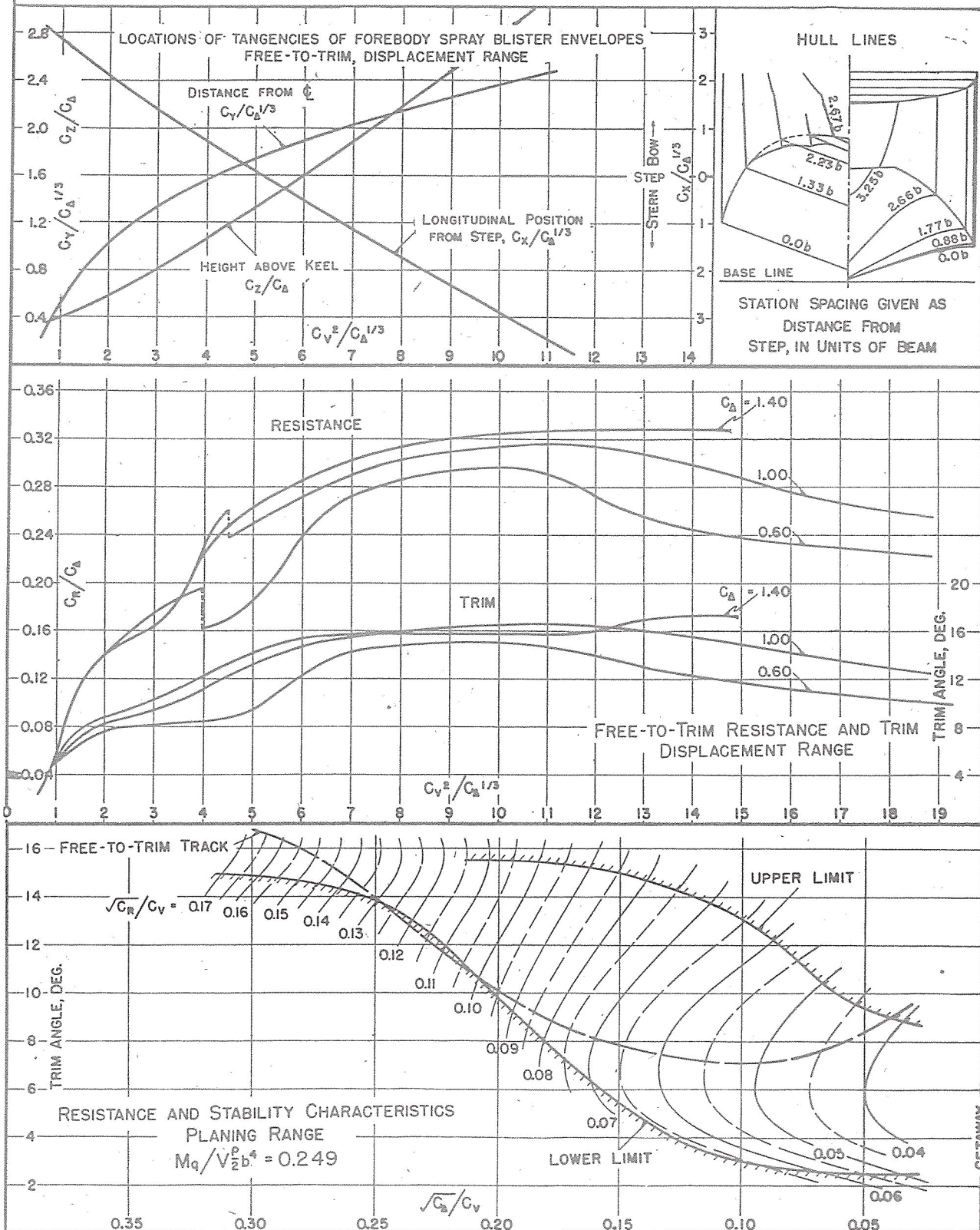
MODEL NO. 538





## SUMMARY CHART OF PRINCIPAL HYDRODYNAMIC CHARACTERISTICS

DATE: 8-8-44  
 10-12-45 (REVISED) C.G. = 0.35b FWD. OF STEP  $C_{d0} = 1.07$  (NOMINAL) DESIGNATION: 6.19-11-20  
 MODEL BEAM: 5.40" 0.90b ABOVE KEEL  $k/L = 0.225$  MODEL No. 539



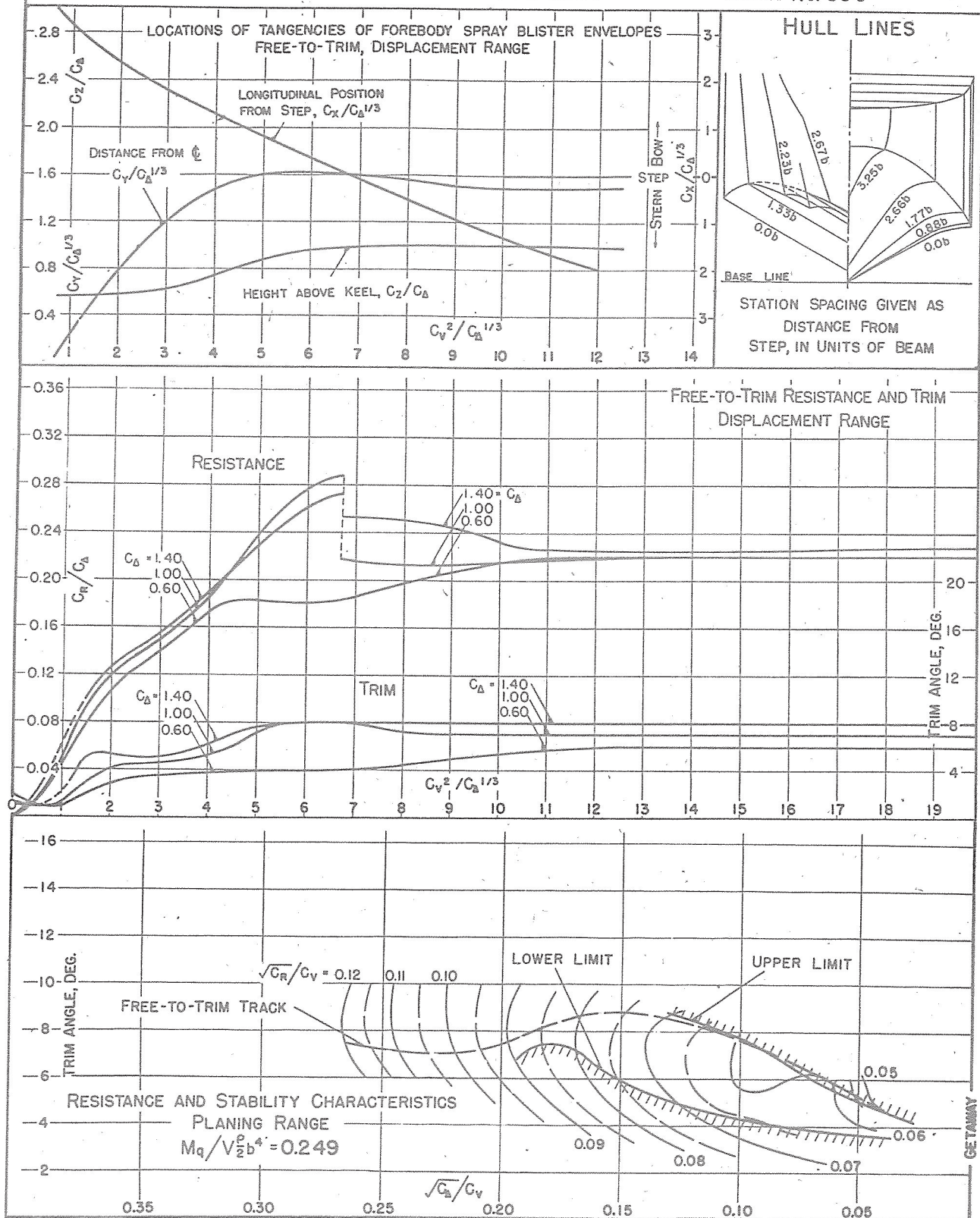
## SUMMARY CHART OF PRINCIPAL HYDRODYNAMIC CHARACTERISTICS

DATE: 12-6-44

DATE: 9-17-45 (REVISED) C.G. = 0.35b FWD. OF STEP  
MODEL BEAM: 5.40" 0.90b ABOVE KEEL

$C_{\Delta_0} = 1.07$  (NOMINAL)  
 $k/L = 0.225$

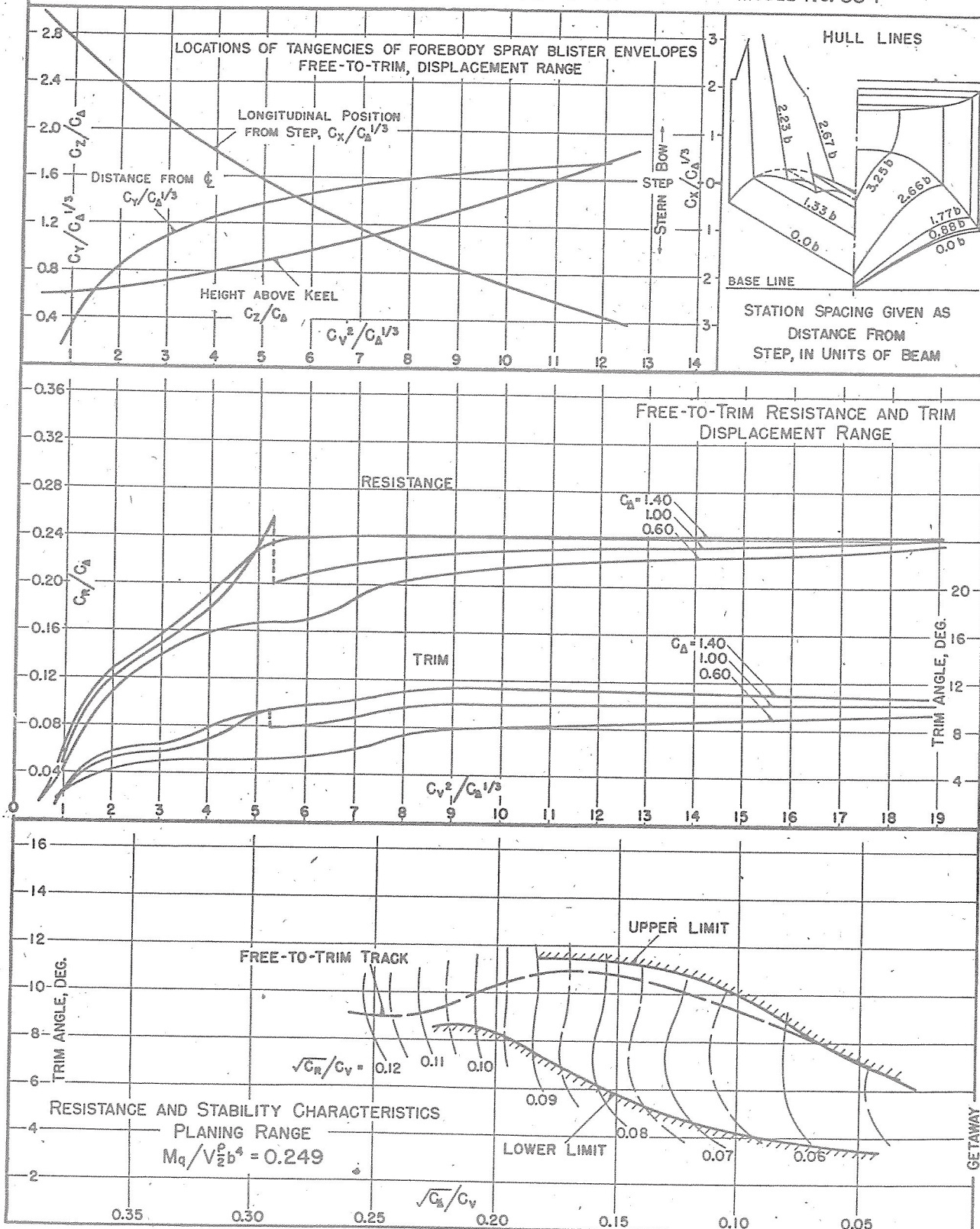
DESIGNATION: 6.19 - 5-30  
MODEL NO. 606





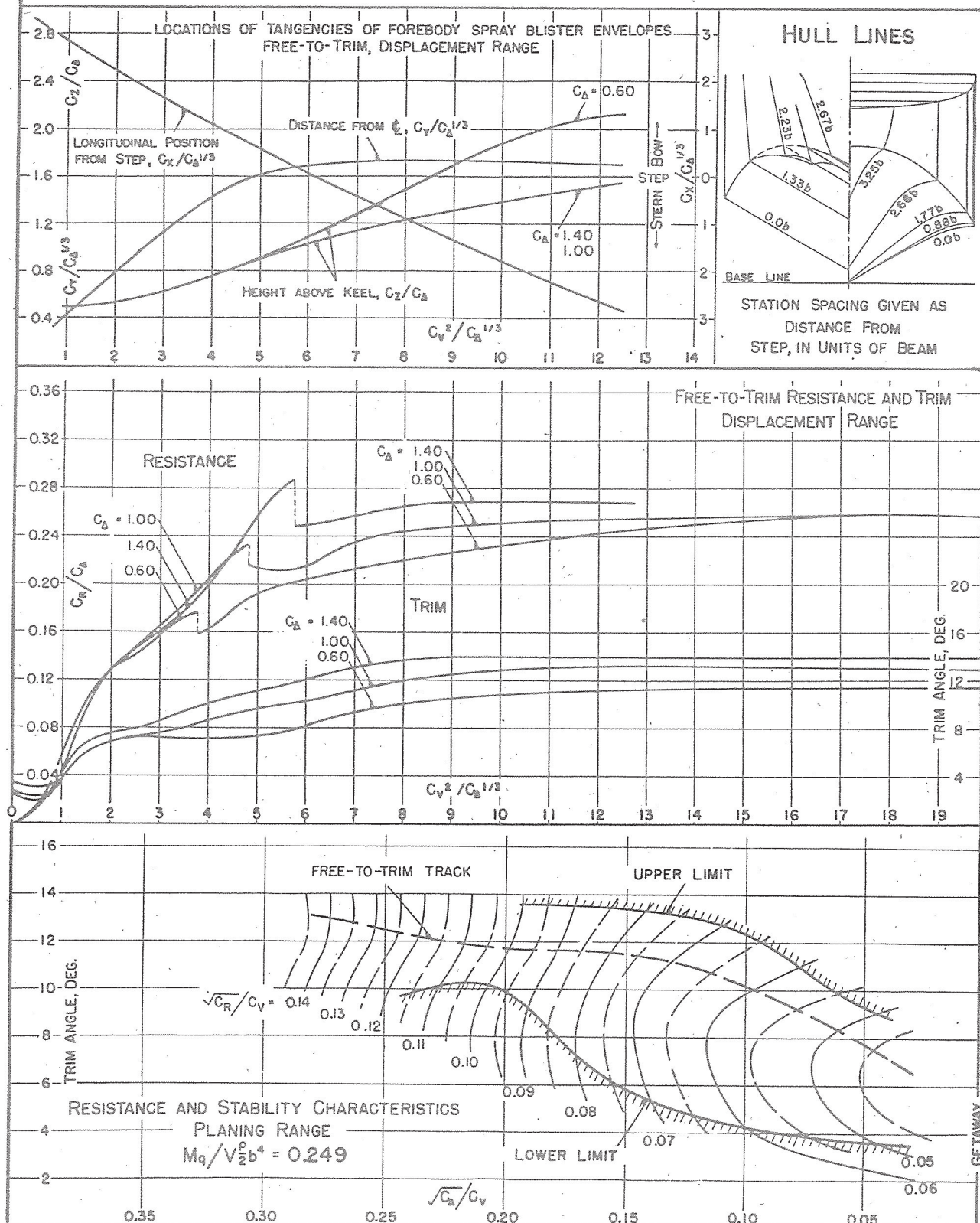
EXPERIMENTAL TOWING TANK  
STEVENS INSTITUTE OF TECHNOLOGY  
HOBOKEN, NEW JERSEY

## SUMMARY CHART OF PRINCIPAL HYDRODYNAMIC CHARACTERISTICS

DATE: 8-8-44  
7-25-45 (REVISED)  
MODEL BEAM: 5.40"C.G. = 0.35b FWD. OF STEP  
0.90b ABOVE KEEL $C_{D_0} = 1.07$  (NOMINAL)  
 $k/L = 0.225$ DESIGNATION: 6.19-7-30  
MODEL NO. 534

EXPERIMENTAL TOWING TANK  
STEVENS INSTITUTE OF TECHNOLOGY  
HOBOKEN, NEW JERSEY

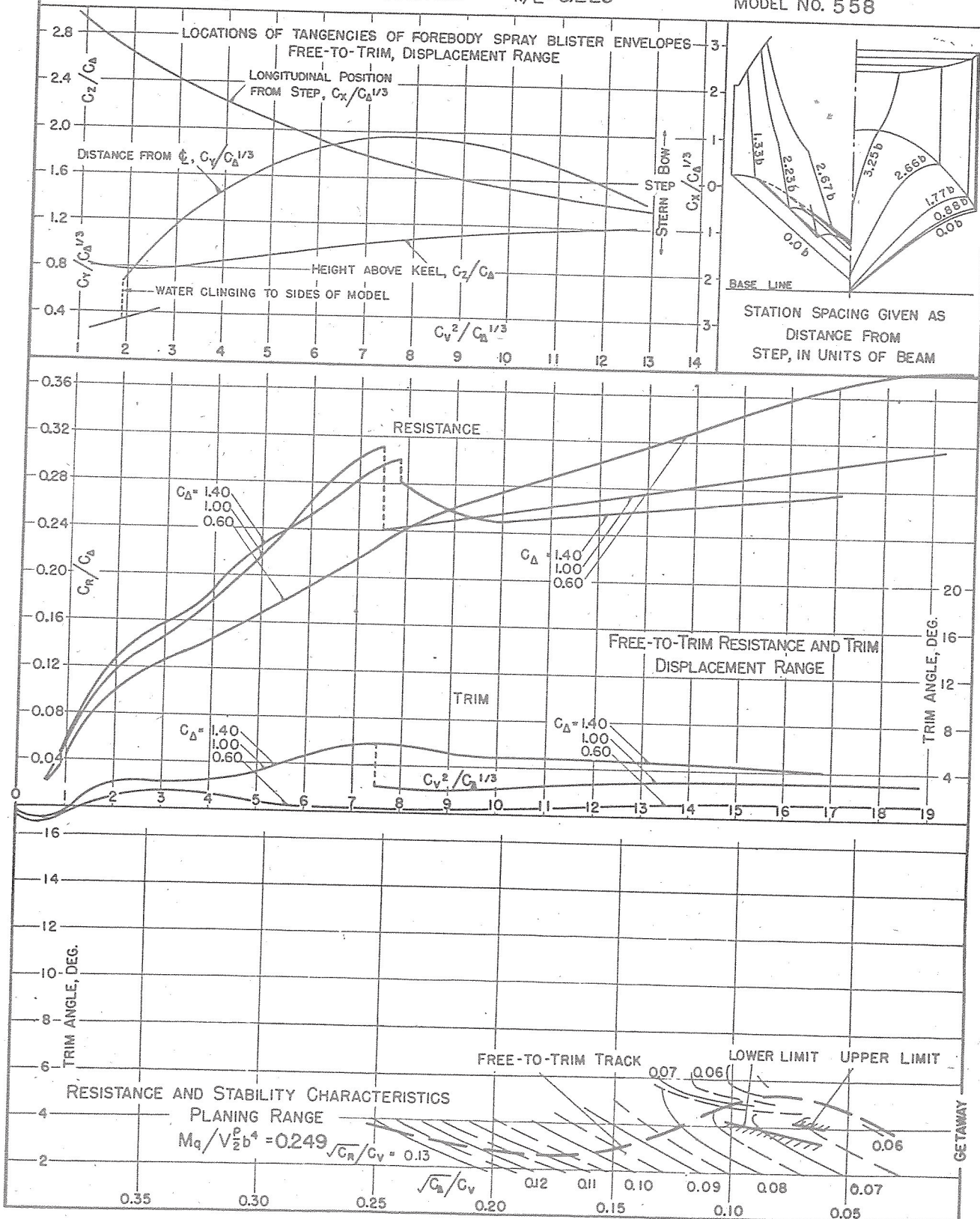
## SUMMARY CHART OF PRINCIPAL HYDRODYNAMIC CHARACTERISTICS

DATE: 12-23-44  
9-14-45 (REVISED) C.G. = 0.35 b FWD. OF STEP  
MODEL BEAM: 5.40' 0.90 b ABOVE KEEL $C_{D0} = 1.07$  (NOMINAL)  
 $k/L = 0.225$ DESIGNATION: 6.19-9-30  
MODEL No. 607



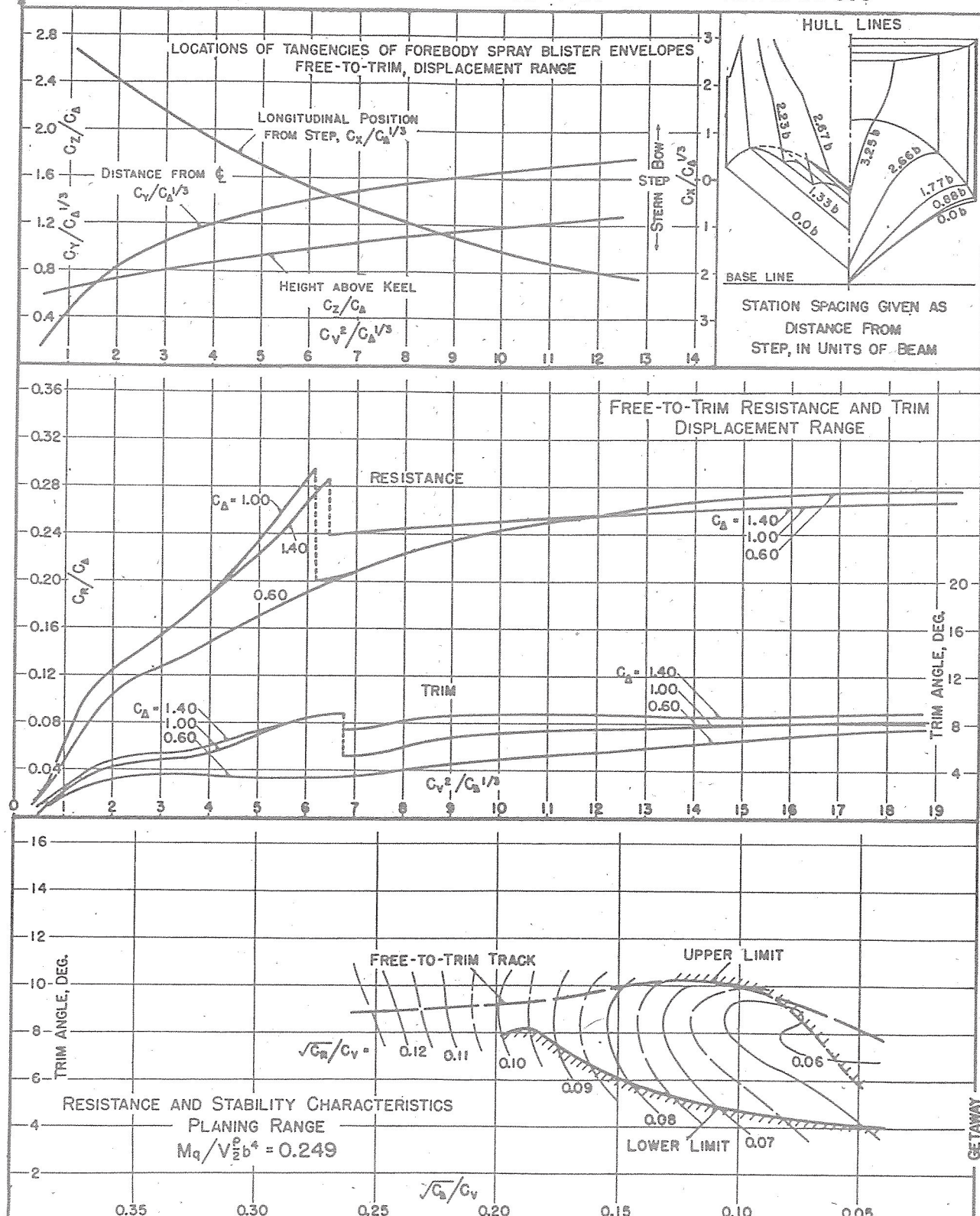
## SUMMARY CHART OF PRINCIPAL HYDRODYNAMIC CHARACTERISTICS

DATE: 8-8-44

12-28-45 (REVISED) C.G. = 0.35 b FWD. OF STEP  
MODEL BEAM: 5.40" 0.90 b ABOVE KEEL $C_{De} = 1.07$  (NOMINAL)  
 $k/L = 0.225$ DESIGNATION: 6.19 -3-40  
MODEL NO. 558

## SUMMARY CHART OF PRINCIPAL HYDRODYNAMIC CHARACTERISTICS

DESIGNATION: 6.19-7-40  
MODEL NO. 535





## SUMMARY CHART OF PRINCIPAL HYDRODYNAMIC CHARACTERISTICS

8-8-44

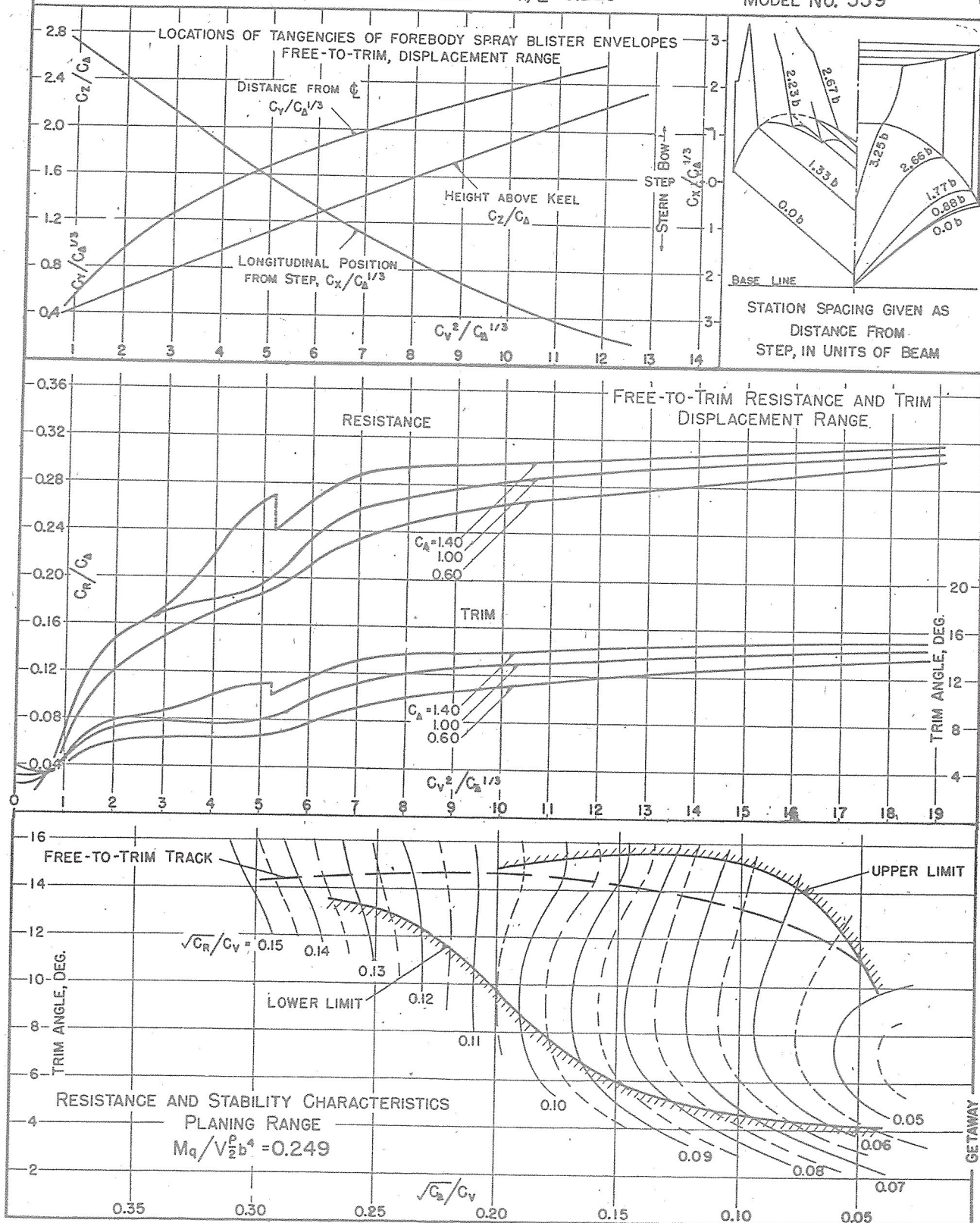
DATE: 1-15-46 (REVISED)

MODEL BEAM: 5.40"

 $C_G = 0.35$  b FWD. OF STEP  
0.90 b ABOVE KEEL $C_{D_0} = 1.07$  (NOMINAL) $k/L = 0.225$ 

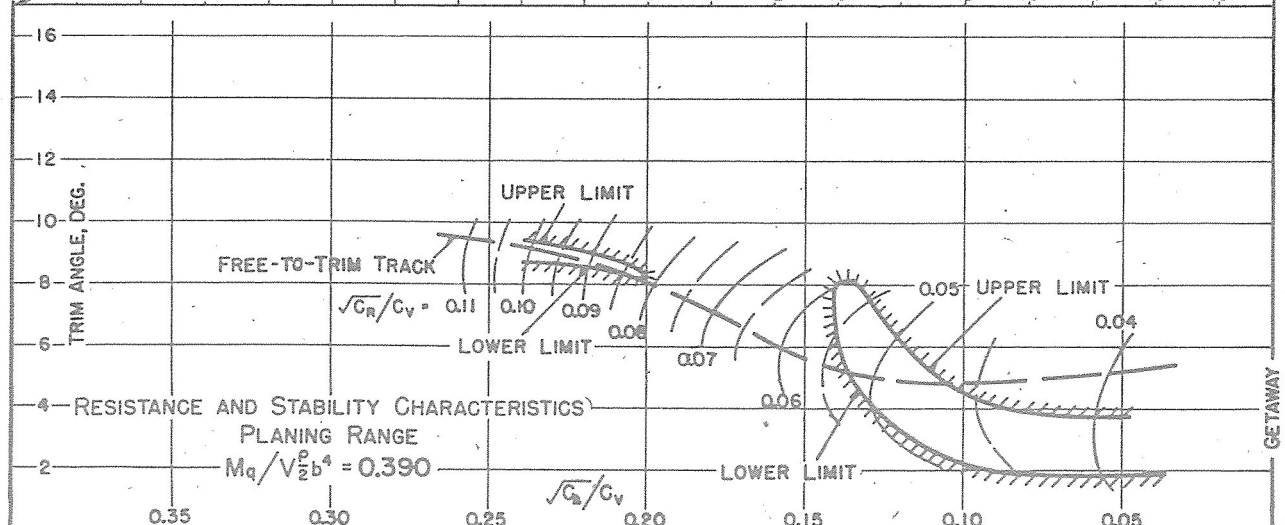
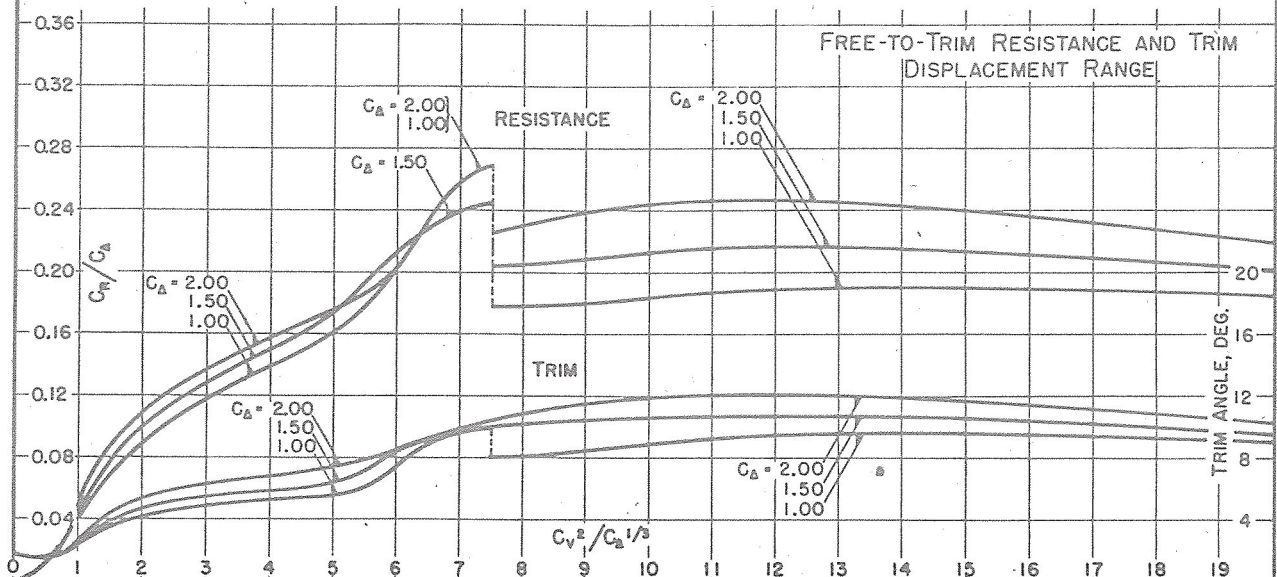
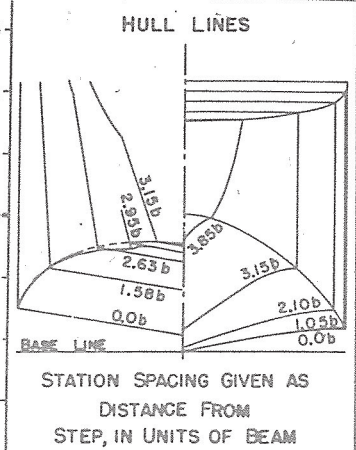
DESIGNATION: 6.19-II-40

MODEL NO. 559



## SUMMARY CHART OF PRINCIPAL HYDRODYNAMIC CHARACTERISTICS

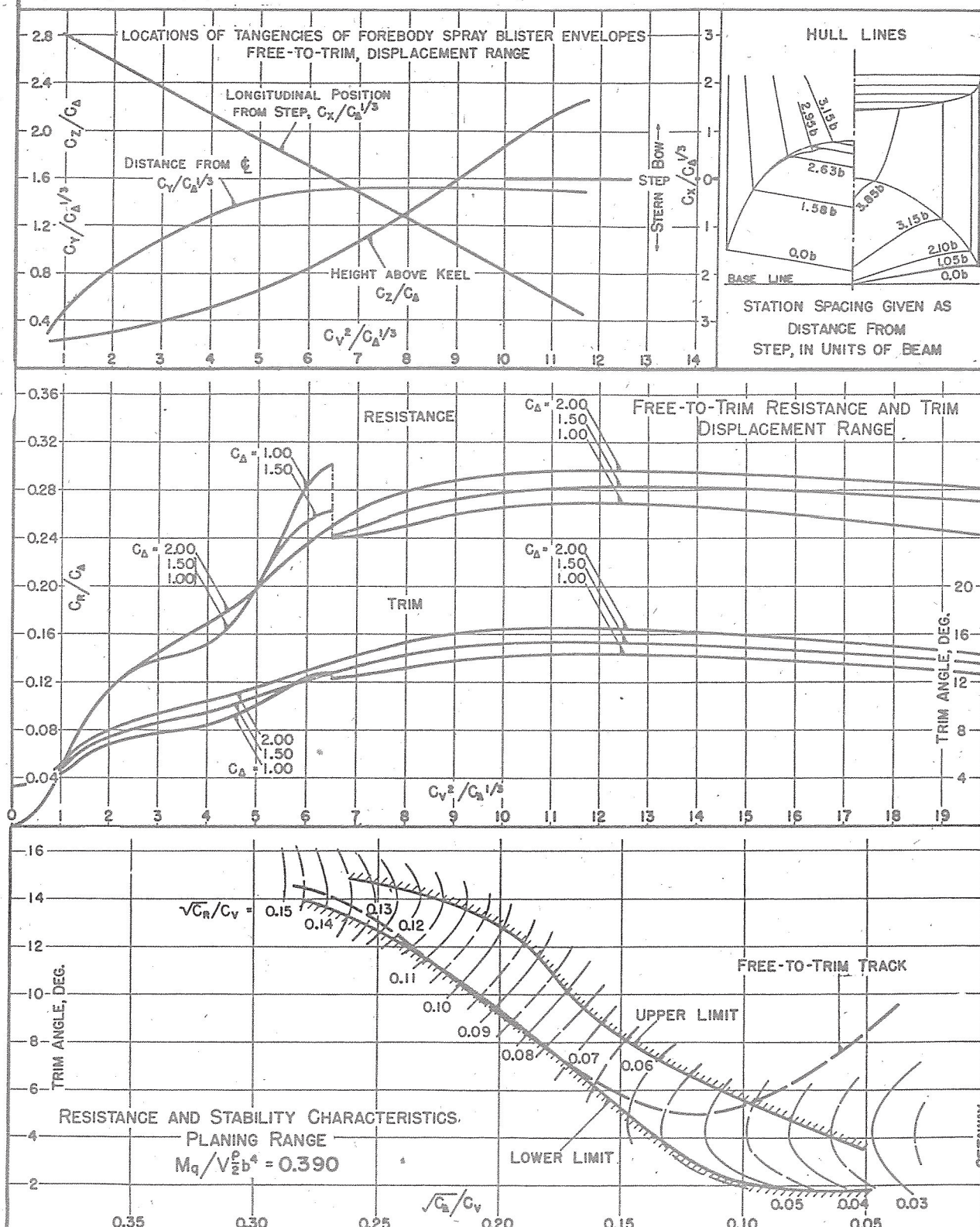
DESIGNATION: 7.32-5-10  
MODEL NO. 624





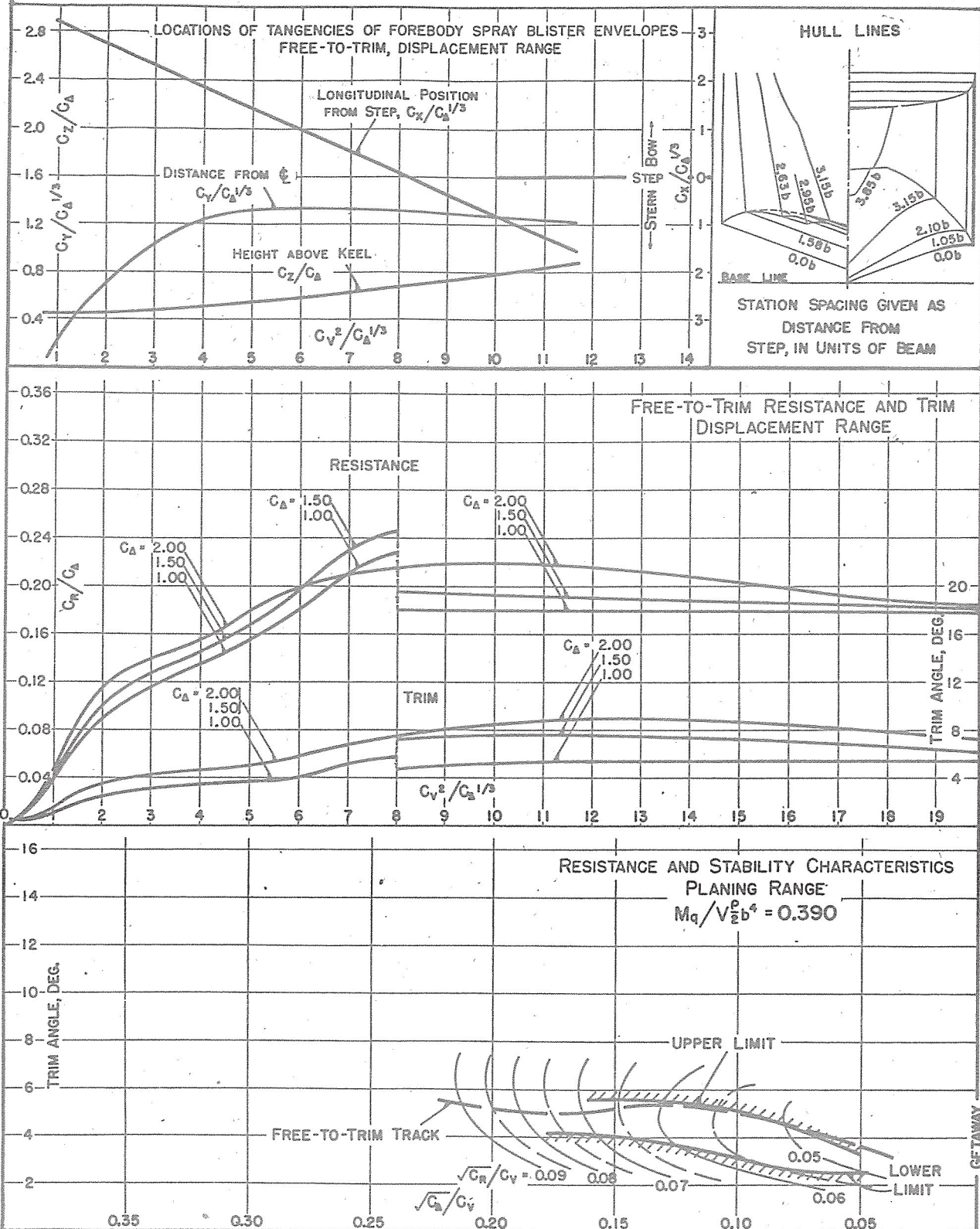
EXPERIMENTAL TOWING TANK  
STEVENS INSTITUTE OF TECHNOLOGY  
HOBOKEN, NEW JERSEY

## SUMMARY CHART OF PRINCIPAL HYDRODYNAMIC CHARACTERISTICS

DATE: 7-5-45  
MODEL BEAM: 5.40"C.G. = 0.35 b FWD. OF STEP  
0.90 b ABOVE KEEL $C_{d_0} = 1.49$  (NOMINAL)  
 $k/L = 0.217$ DESIGNATION: 7.32-9-10  
MODEL NO. 625

EXPERIMENTAL TOWING TANK  
STEVENS INSTITUTE OF TECHNOLOGY  
HOBOKEN, NEW JERSEY

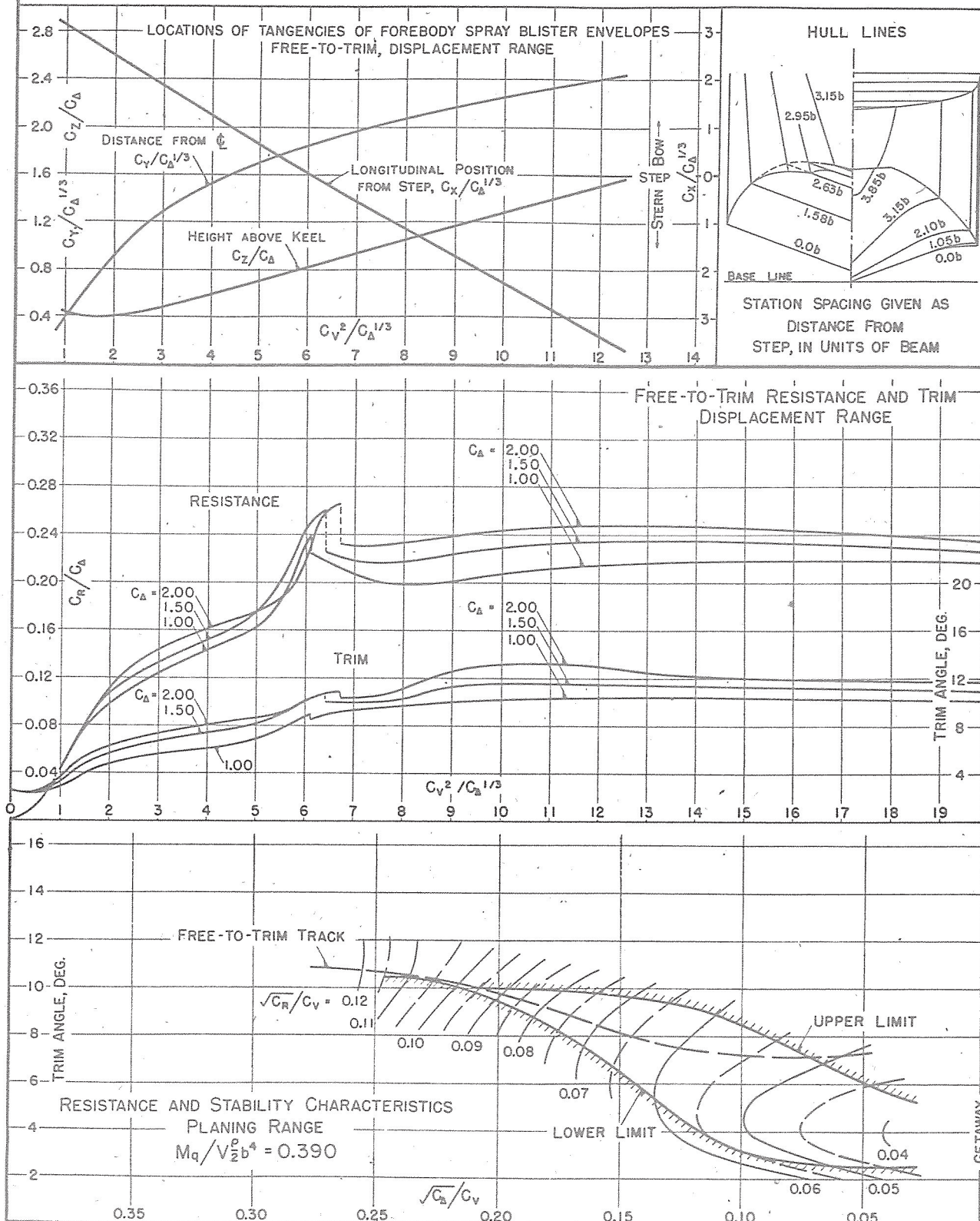
## SUMMARY CHART OF PRINCIPAL HYDRODYNAMIC CHARACTERISTICS

DATE: 6-20-45  
MODEL BEAM: 5.40"C.G. = 0.35 b FWD. OF STEP  
0.90 b ABOVE KEEL $C_{A0} = 1.49$  (NOMINAL)  
 $k/L = 0.217$ DESIGNATION: 7.32-3-20  
MODEL NO. 626



EXPERIMENTAL TOWING TANK  
STEVENS INSTITUTE OF TECHNOLOGY  
HOBOKEN, NEW JERSEY

## SUMMARY CHART OF PRINCIPAL HYDRODYNAMIC CHARACTERISTICS

DATE: 7-31-45  
MODEL BEAM: 5.40"C.G. = 0.35 b FWD. OF STEP  
0.90 b ABOVE KEEL $C_{d0} = 1.49$  (NOMINAL)  
 $k/L = 0.217$ DESIGNATION: 7.32-7-20  
MODEL NO. 339-23

## SUMMARY CHART OF PRINCIPAL HYDRODYNAMIC CHARACTERISTICS

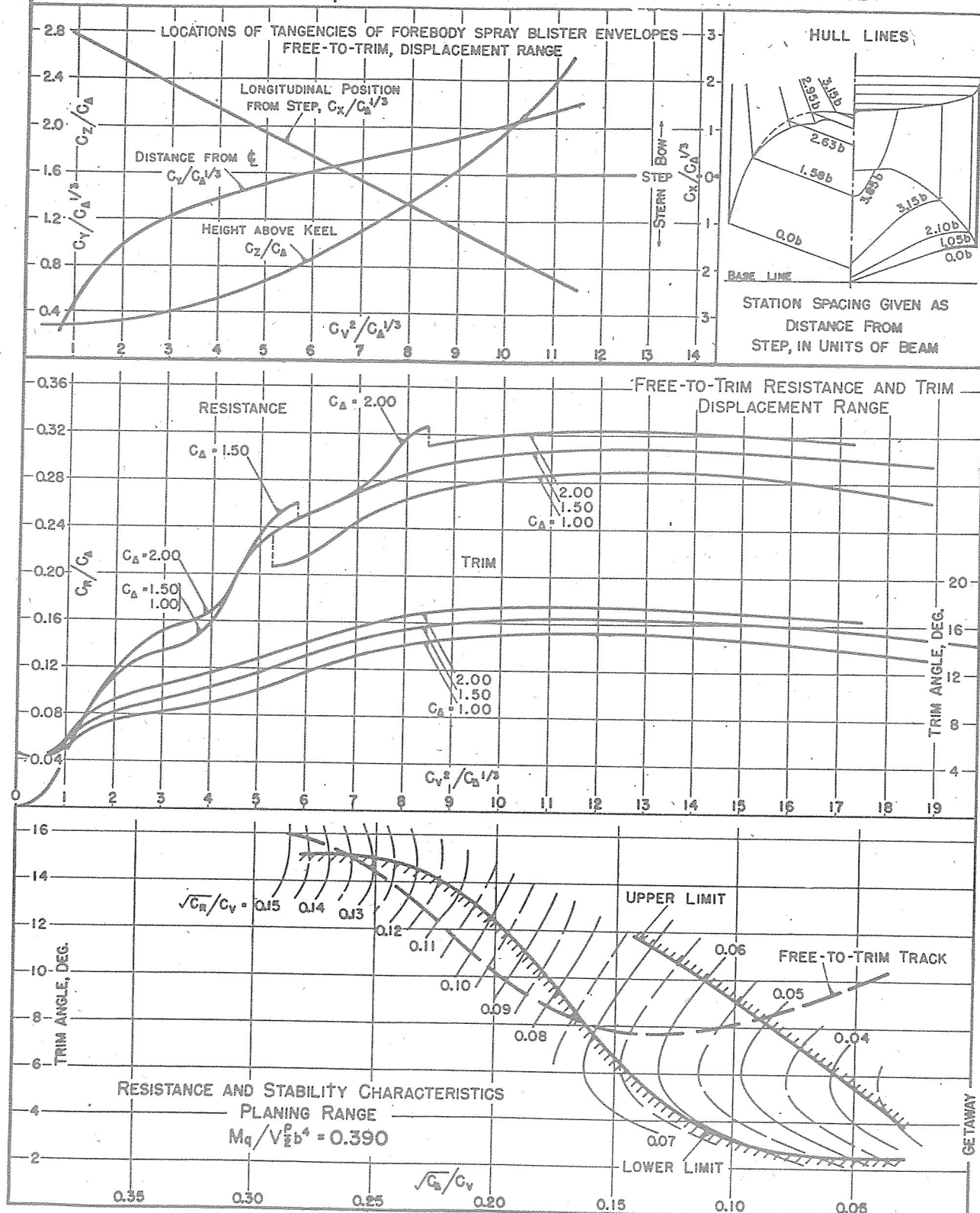
DATE: 4-25-45

MODEL BEAM: 5.40"

C.G. = 0.35 b FWD. OF STEP  
0.90 b ABOVE KEEL $C_{A_0} = 1.49$  (NOMINAL) $k/L = 0.217$ 

DESIGNATION: 7.32-11-20

MODEL NO. 627



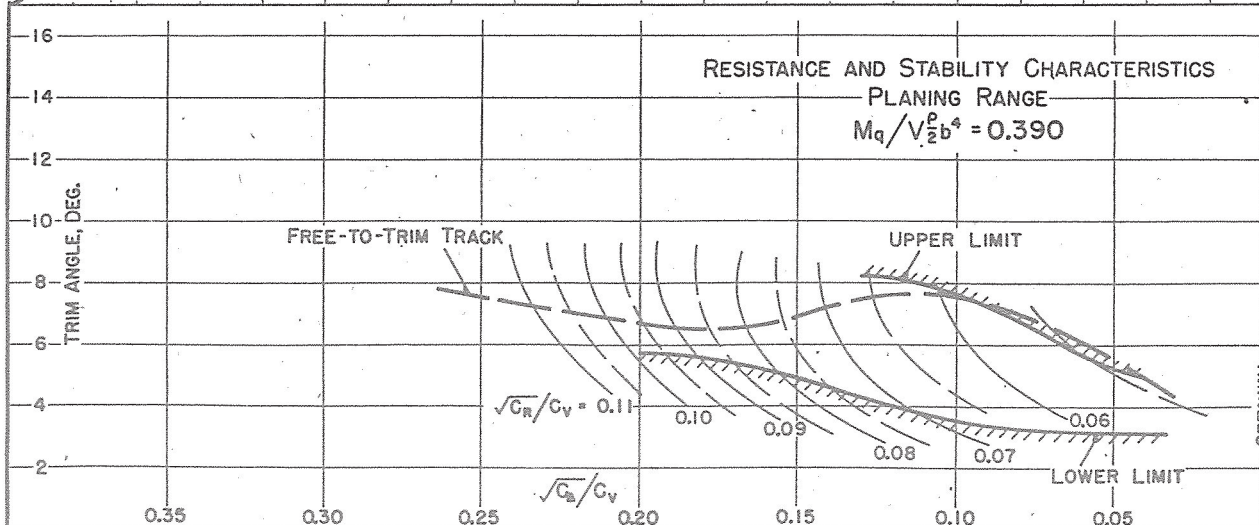
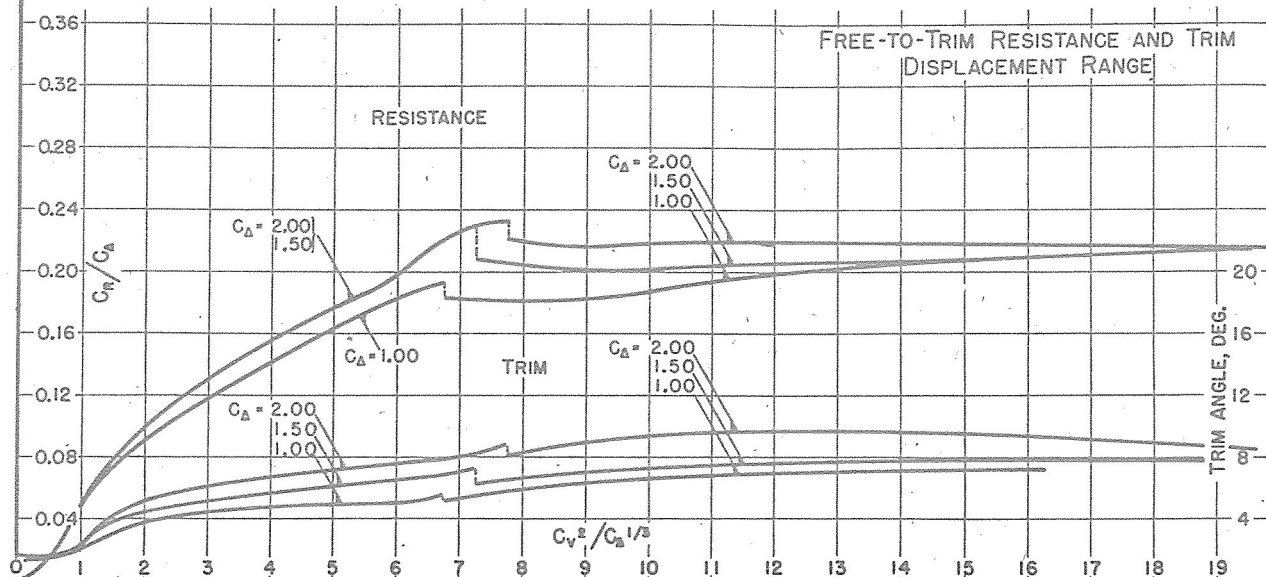
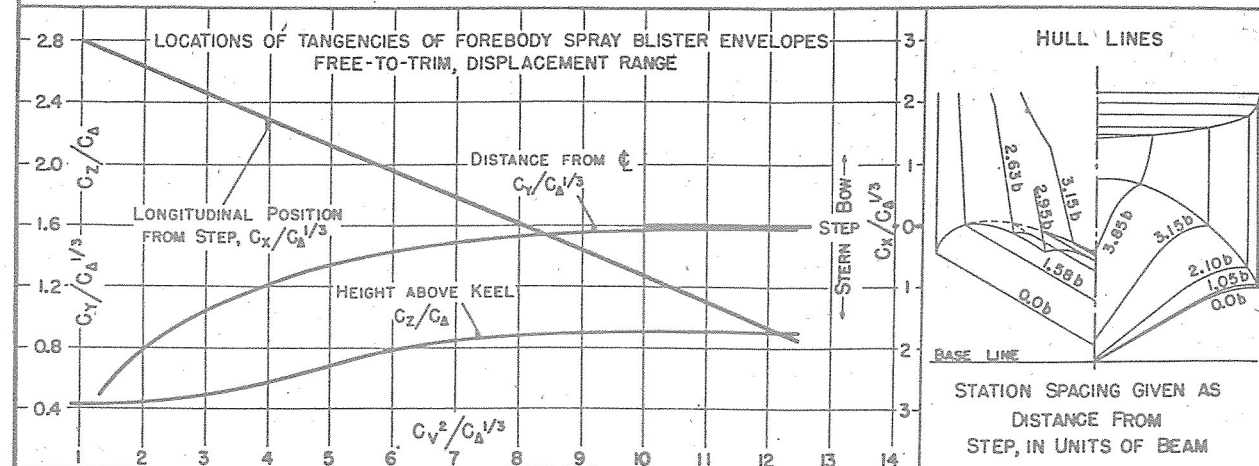


EXPERIMENTAL TOWING TANK  
STEVENS INSTITUTE OF TECHNOLOGY  
HOBOKEN, NEW JERSEY

## SUMMARY CHART OF PRINCIPAL HYDRODYNAMIC CHARACTERISTICS

DATE: 7-18-45

MODEL BEAM: 5.40"

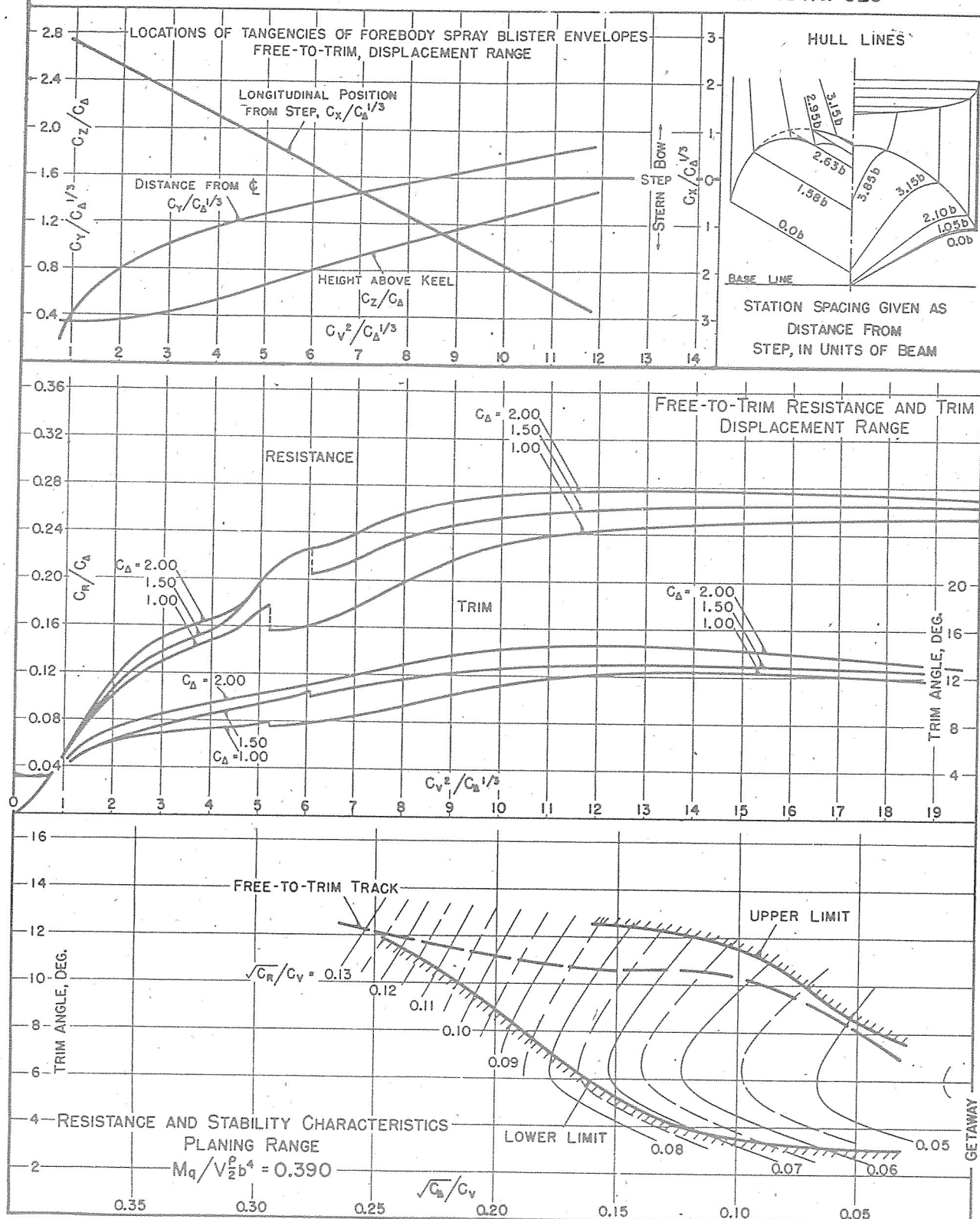
 $C.G. = 0.35$  b FWD. OF STEP  
 $0.90$  b ABOVE KEEL $C_{D0} = 1.49$  (NOMINAL)  
 $k/L = 0.217$ DESIGNATION: 7.32-5-30  
MODEL NO. 628

EXPERIMENTAL TOWING TANK  
STEVENS INSTITUTE OF TECHNOLOGY  
HOBOKEN, NEW JERSEY

## SUMMARY CHART OF PRINCIPAL HYDRODYNAMIC CHARACTERISTICS

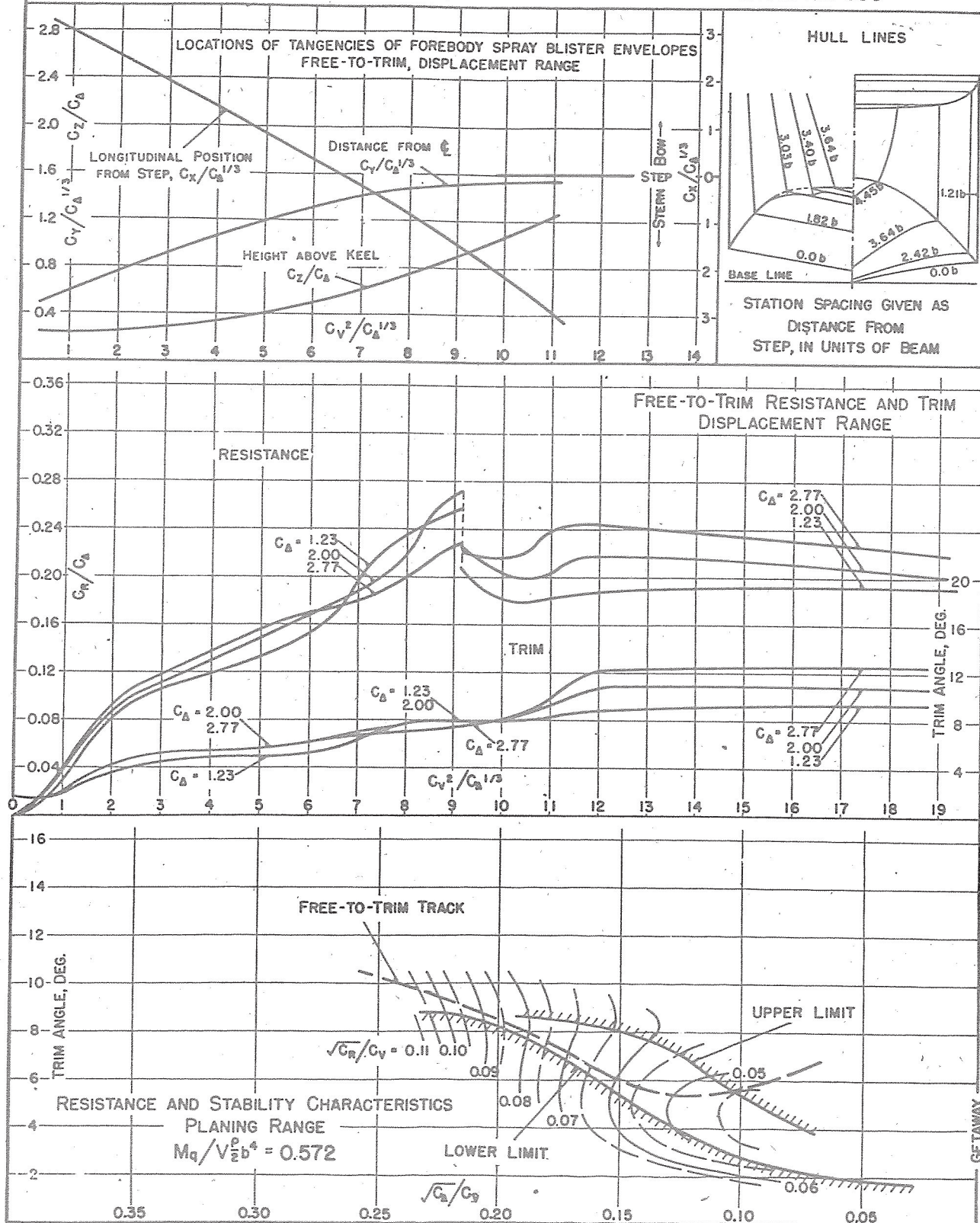
DATE: 7-19-45

MODEL BEAM: 5.40"

C.G. = 0.35 b FWD. OF STEP  
0.90 b ABOVE KEEL $C_{\Delta} = 1.49$  (NOMINAL)  
 $k/L = 0.217$ DESIGNATION: 7.32-9-30  
MODEL NO. 629



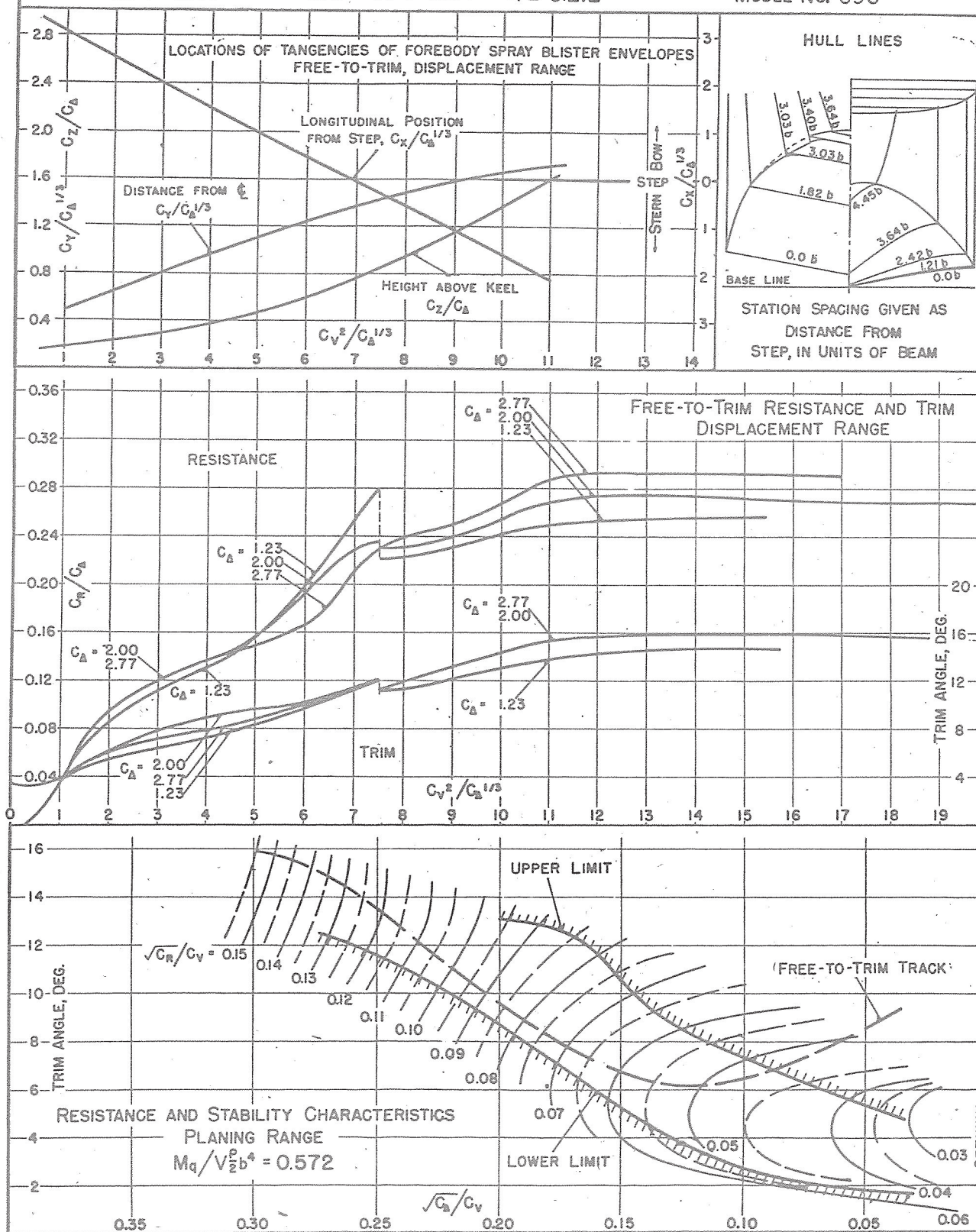
## SUMMARY CHART OF PRINCIPAL HYDRODYNAMIC CHARACTERISTICS

DATE: 12-10-45  
MODEL BEAM: 5.40 $C.G. = 0.35$  b FWD. OF STEP  
 $0.90$  b ABOVE KEEL $C_{A0} = 2.00$  (NOMINAL)  
 $k/L = 0.212$ DESIGNATION: 8.45-5-10  
MODEL NO. 695

## SUMMARY CHART OF PRINCIPAL HYDRODYNAMIC CHARACTERISTICS

DATE: 12-13-45

MODEL BEAM: 5.40

 $C.G. = 0.35$  b FWD. OF STEP  
 $0.90$  b ABOVE KEEL $C_{A_0} = 2.00$  (NOMINAL)  
 $k/L = 0.212$ DESIGNATION: 8.45-9-10  
MODEL NO. 696



EXPERIMENTAL TOWING TANK  
STEVENS INSTITUTE OF TECHNOLOGY  
HOBOKEN, NEW JERSEY

## SUMMARY CHART OF PRINCIPAL HYDRODYNAMIC CHARACTERISTICS

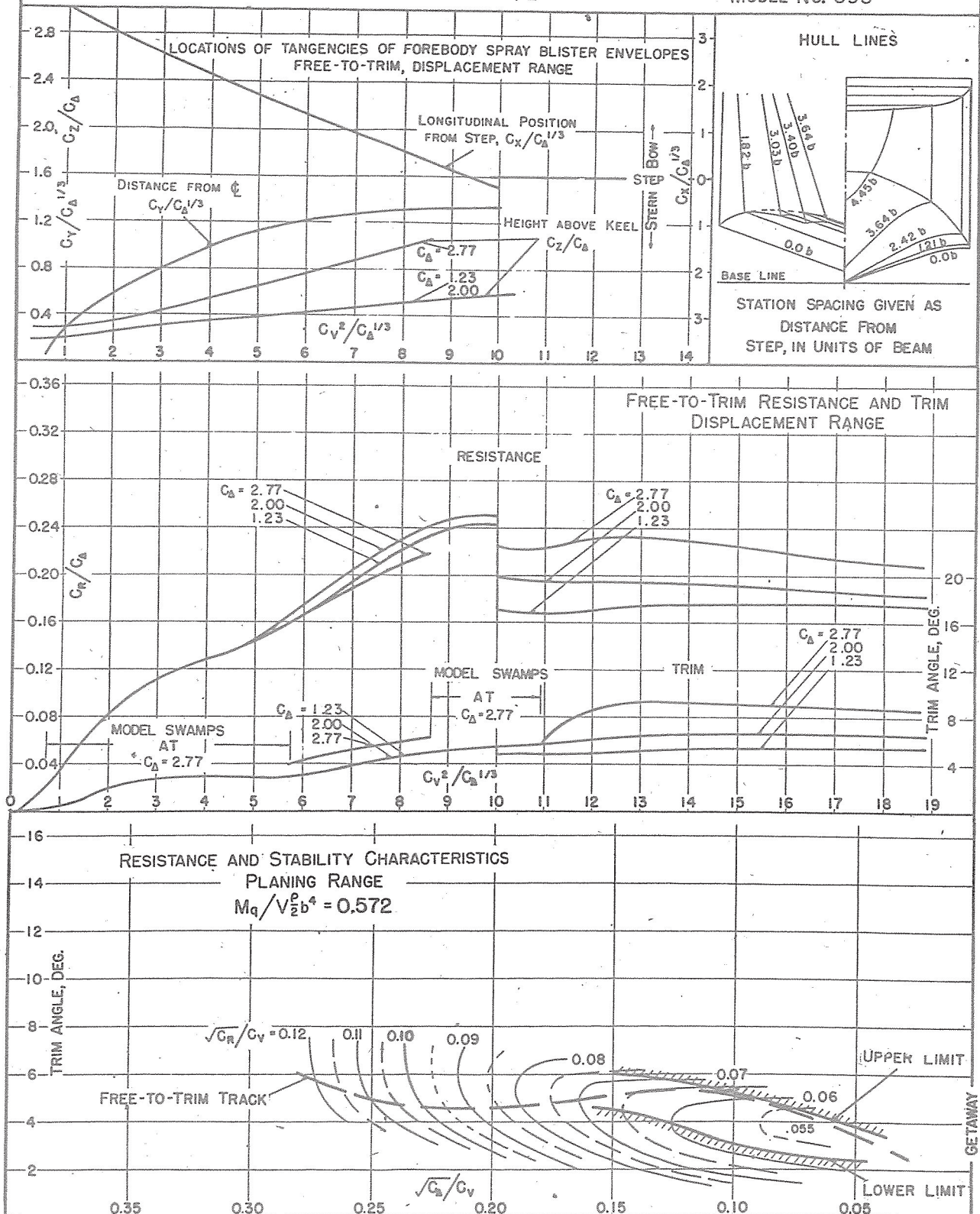
DATE: 10-16-45

MODEL BEAM: 5.40"

 $C.G. = 0.35 b$  FWD. OF STEP  
 $0.90 b$  ABOVE KEEL $C_{Ae} = 2.00$  (NOMINAL) $k/L = 0.212$ 

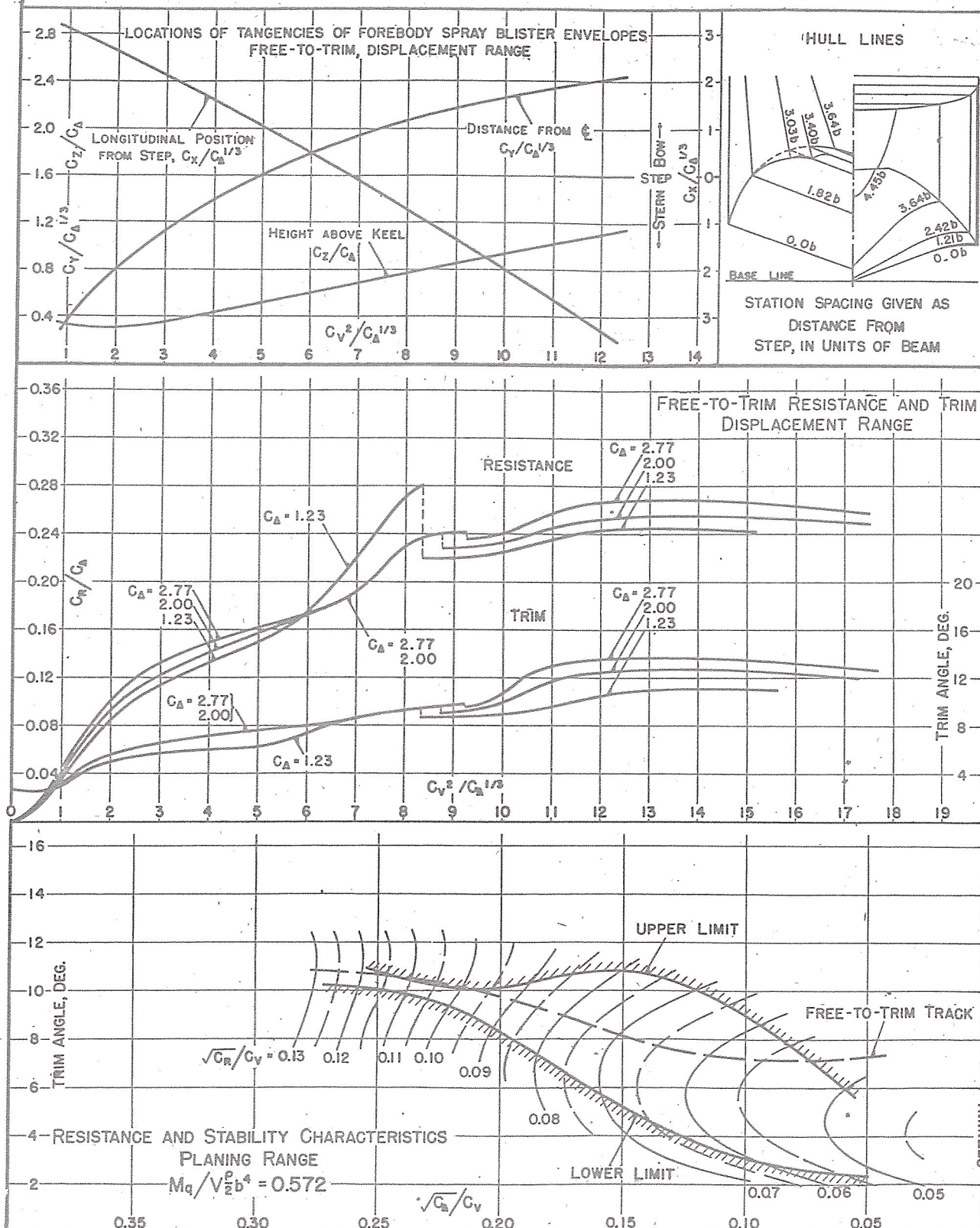
DESIGNATION: 8.45-3-20

MODEL NO. 693



EXPERIMENTAL TOWING TANK  
STEVENS INSTITUTE OF TECHNOLOGY  
HOBOKEN, NEW JERSEY

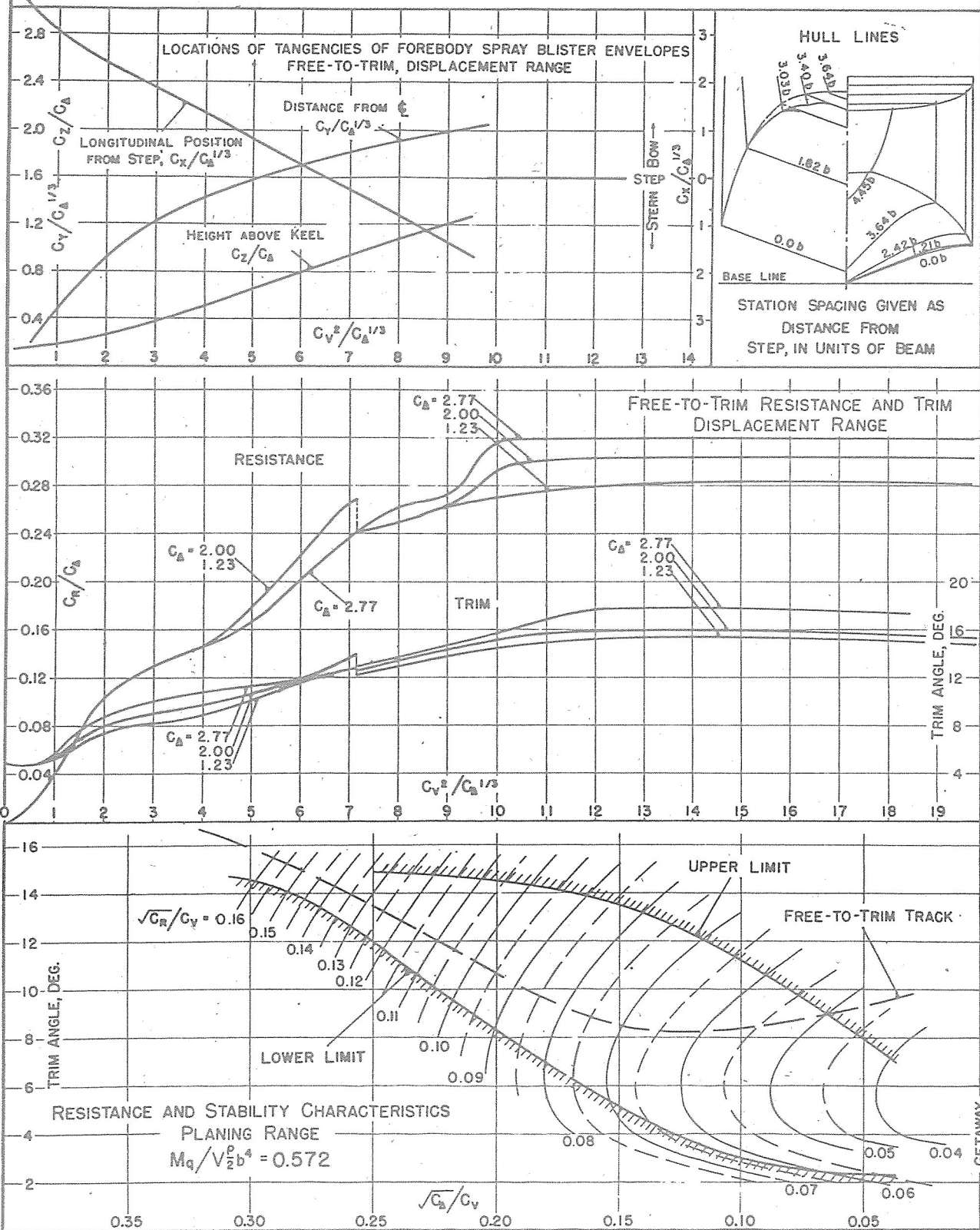
## SUMMARY CHART OF PRINCIPAL HYDRODYNAMIC CHARACTERISTICS

DATE: 7-31-45  
MODEL BEAM: 5.40"C.G. = 0.35 b FWD. OF STEP  
0.90 b ABOVE KEEL $C_{D_0} = 2.00$  (NOMINAL)  
 $k/L = 0.212$ DESIGNATION: 8.45-7-20  
MODEL NO. 651



EXPERIMENTAL TOWING TANK  
STEVENS INSTITUTE OF TECHNOLOGY  
HOBOKEN, NEW JERSEY

## SUMMARY CHART OF PRINCIPAL HYDRODYNAMIC CHARACTERISTICS

DATE: 10-16-45  
MODEL BEAM: 5.40C.G. = 0.35 b FWD. OF STEP  
0.90 b ABOVE KEEL $C_{D0} = 2.00$  (NOMINAL)  
 $k/L = 0.212$ DESIGNATION: 8.45-11-20  
MODEL NO. 694

## SUMMARY CHART OF PRINCIPAL HYDRODYNAMIC CHARACTERISTICS

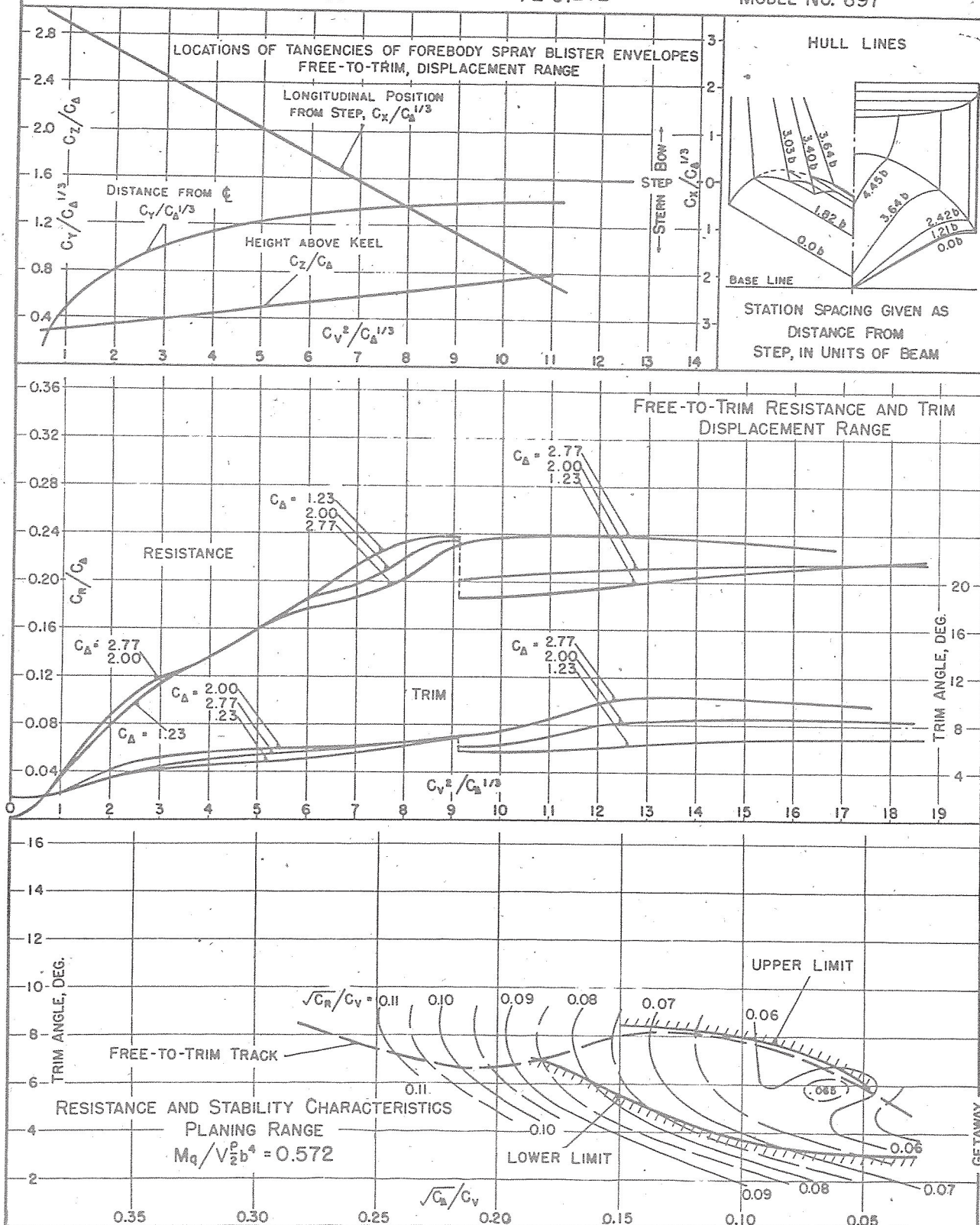
DATE: 11-8-45

MODEL BEAM: 5.40"

C.G. = 0.35 b FWD. OF STEP  
0.90 b ABOVE KEEL $C_{d0} = 2.00$  (NOMINAL) $k/L = 0.212$ 

DESIGNATION: 8.45-5-30

MODEL NO. 697





## EXPERIMENTAL TOWING TANK

STEVENS INSTITUTE OF TECHNOLOGY  
HOBOKEN, NEW JERSEY

## SUMMARY CHART OF PRINCIPAL HYDRODYNAMIC CHARACTERISTICS

DATE: 11-5-45

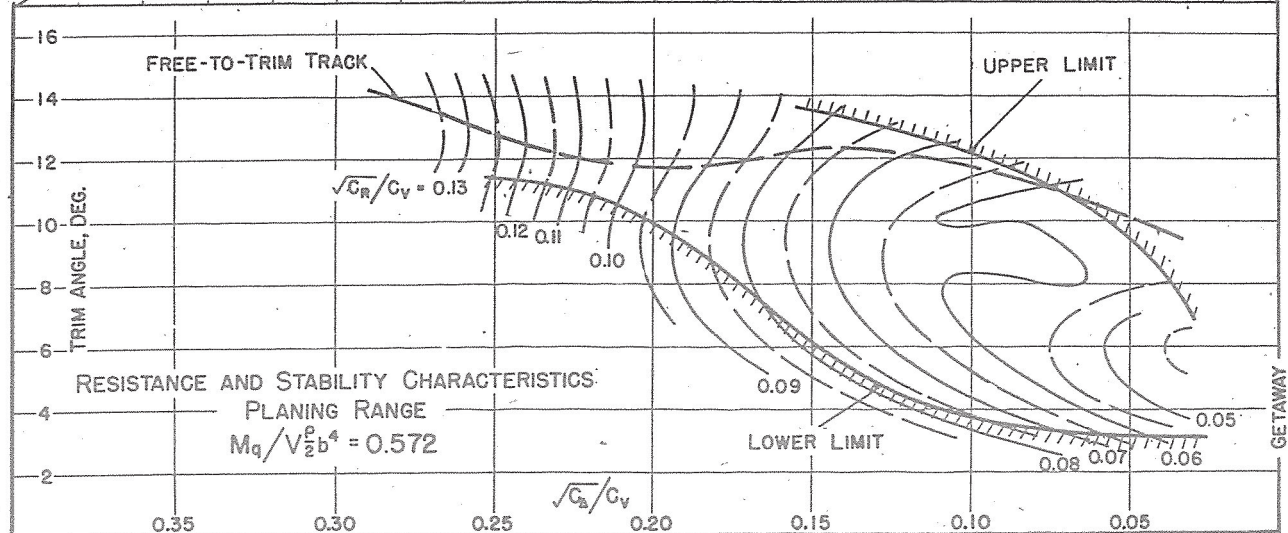
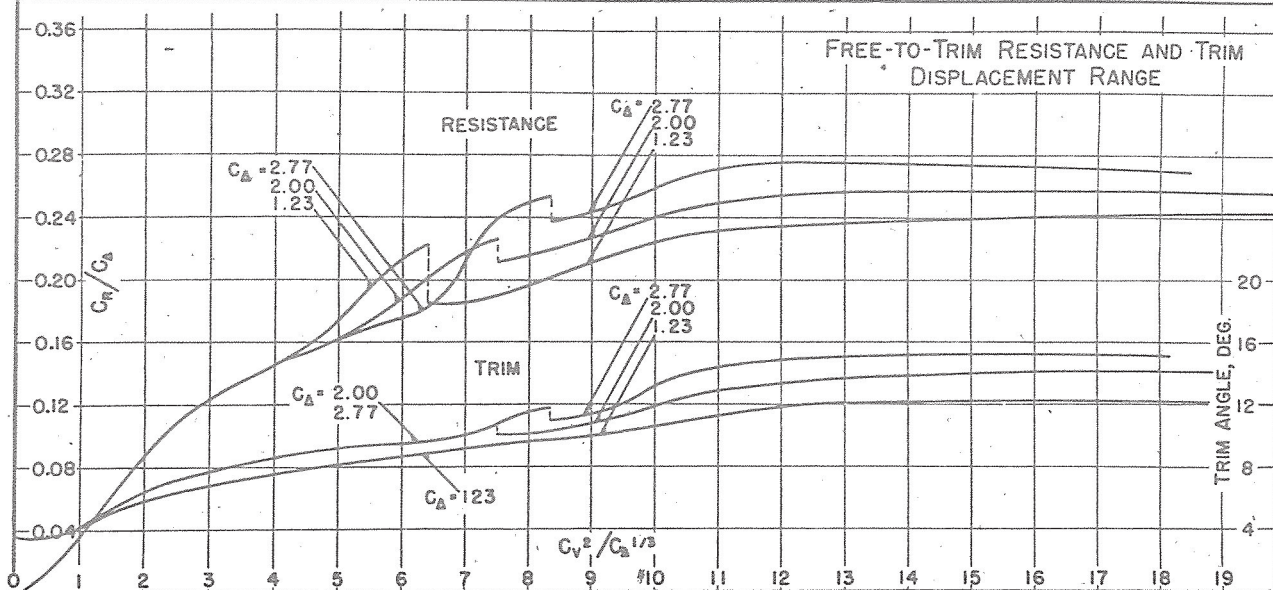
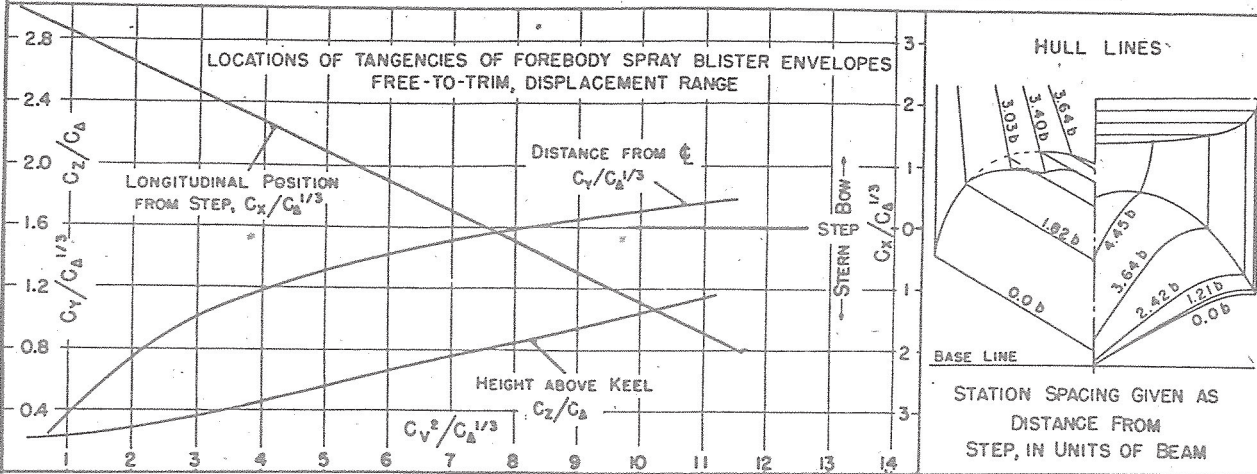
C.G. = 0.35 b FWD. OF STEP  
0.90 b ABOVE KEEL $C_{d0} = 2.00$  (NOMINAL)

DESIGNATION: 8.45-9-30

MODEL BEAM: 5.40

 $k/L = 0.212$ 

MODEL No. 698



AN INVESTIGATION OF THE EFFECTS OF  
HULL PROPORTION AND STEP DEPTH ON  
THE HYDRODYNAMIC CHARACTERISTICS OF  
FLYING-BOAT HULL MODELS WITH  
VARYING LENGTH-BEAM RATIOS

for

National Advisory Committee for Aeronautics

REPORT NO. 312

by

W. C. Hugli, Jr.

Albert Strumpf

W. C. Axt

February 1947

Experimental Towing Tank  
Stevens Institute of Technology  
Hoboken, New Jersey

MODEL PARTICULARS

| Model | Designation | Hull<br>Lgth.<br>in. | F.B.<br>Lgth.<br>in. | A.B.<br>Lgth.<br>in. | Tail<br>Cone<br>Lgth.<br>in. | F.B.<br>Flat<br>Lgth.<br>in. | Step<br>Height<br>at<br>Keel      at<br>Centroid<br>in.      in. |     | Stern<br>Post<br>Height<br>in. | Stern<br>Post<br>Angle<br>Deg. |
|-------|-------------|----------------------|----------------------|----------------------|------------------------------|------------------------------|--|-----|--------------------------------|--------------------------------|
| 656   | 6-55-6      | 32.4                 | 17.82                | 14.58                | 14.48                        | 7.20                         | .32  | .20 | 1.99                           | 8.4                            |
| 657   | 6-55-10     |                      | 17.82                | 14.58                |                              |                              | .54  | .41 | 2.20                           | 9.2                            |
| 653   | 6-58-6      |                      | 18.79                | 13.61                |                              |                              | .32  | .20 | 1.87                           | 8.5                            |
| 654   | 6-58-8      |                      | 18.79                | 13.61                |                              |                              | .43  | .30 | 1.98                           | 9.0                            |
| 655   | 6-58-10     |                      | 18.79                | 13.61                |                              |                              | .54  | .41 | 2.08                           | 9.4                            |
| 658   | 6-61-6      |                      | 19.76                | 12.64                |                              |                              | .32  | .20 | 1.75                           | 8.6                            |
| 659   | 6-61-10     |                      | 19.76                | 12.64                |                              |                              | .54  | .41 | 1.96                           | 9.6                            |
|       |             |                      |                      |                      |                              |                              |  |     |                                |                                |
| 642   | 8-55-8      | 43.2                 | 23.76                | 19.34                | 15.89                        | 5.40                         | .43  | .30 | 2.68                           | 8.3                            |
| 643   | 8-55-13.33  |                      | 23.76                | 19.34                |                              |                              | .72  | .59 | 2.97                           | 9.2                            |
| 633   | 8-58-8      |                      | 25.06                | 18.14                |                              |                              | .43  | .30 | 2.53                           | 8.4                            |
| 634   | 8-58-10.66  |                      | 25.06                | 18.14                |                              |                              | .58  | .45 | 2.68                           | 8.9                            |
| 635   | 8-58-13.33  |                      | 25.06                | 18.14                |                              |                              | .72  | .59 | 2.82                           | 9.4                            |
| 644   | 8-61-8      |                      | 26.35                | 16.85                |                              |                              | .43  | .30 | 2.37                           | 8.5                            |
| 645   | 8-61-13.33  |                      | 26.35                | 16.85                |                              |                              | .72  | .59 | 2.66                           | 9.6                            |
|       |             |                      |                      |                      |                              |                              |  |     |                                |                                |
| 674   | 10-55-10    | 54.0                 | 29.70                | 24.30                | 17.00                        | 3.60                         | .54  | .41 | 3.40                           | 8.3                            |
| 675   | 10-55-16.67 |                      | 29.70                | 24.30                |                              |                              | .90  | .77 | 3.76                           | 9.2                            |
| 689   | 10-58-10    |                      | 31.32                | 22.68                |                              |                              | .54  | .37 | 3.20                           | 8.4                            |
| 685   | 10-58-13.33 |                      | 31.32                | 22.68                |                              |                              | .72  | .54 | 3.38                           | 8.9                            |
| 686   | 10-58-16.67 |                      | 31.32                | 22.68                |                              |                              | .90  | .72 | 3.56                           | 9.3                            |
| 687   | 10-61-10    |                      | 32.94                | 21.06                |                              |                              | .54  | .37 | 3.00                           | 8.5                            |
| 688   | 10-61-16.67 |                      | 32.94                | 21.06                |                              |                              | .90  | .72 | 3.36                           | 9.5                            |

Beam at Step: 5.40 in.

Deadrise of Forebody Flat and Afterbody: 22.5 deg.

Afterbody Angle: 7 deg.

Length of Step V: 1.56 in.

Step Centroid 1.04 in. forward of apex

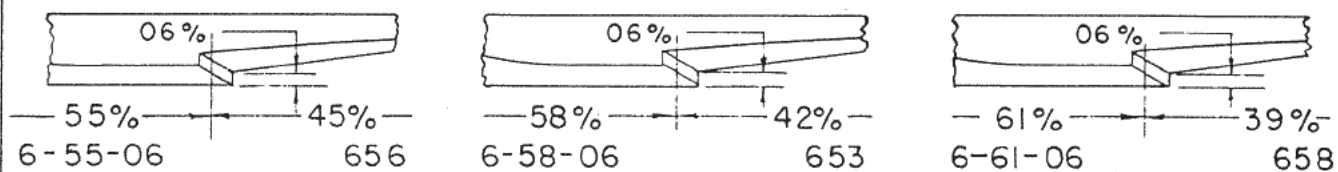
CG Location

Forward of Step Centroid: 1.89 in.

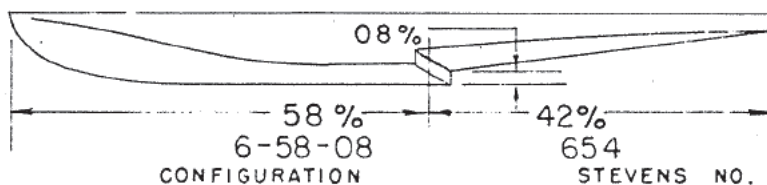
Above Baseline: 4.86 in.

The sternpost angle is the angle between a line through the sternpost and step apex, and the tangent to the forebody keel at the step.

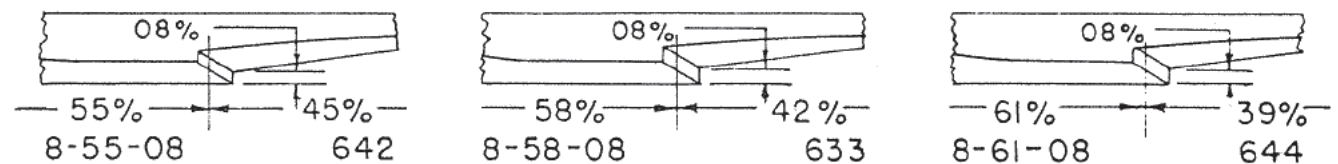
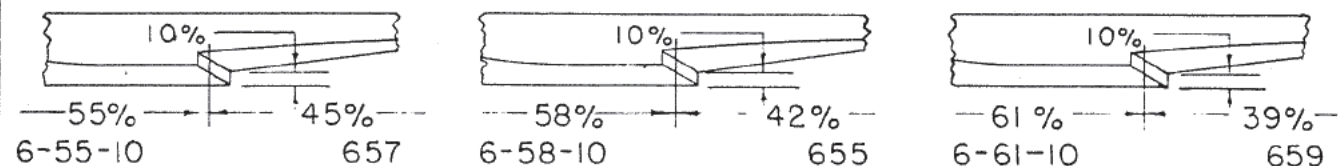
# SCHEMATIC DIAGRAMS OF HULLS



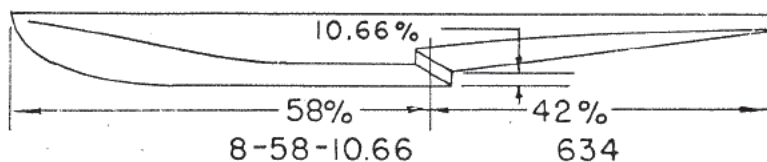
L/B = 6



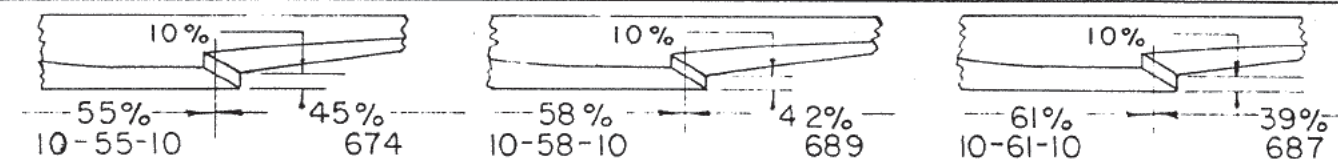
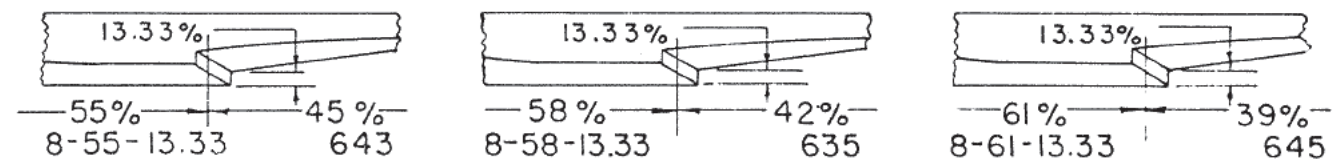
FOREBODY FLAT  
 133 % b



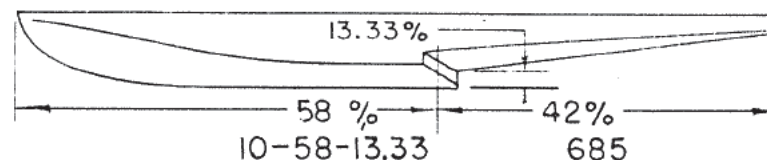
L/B = 8



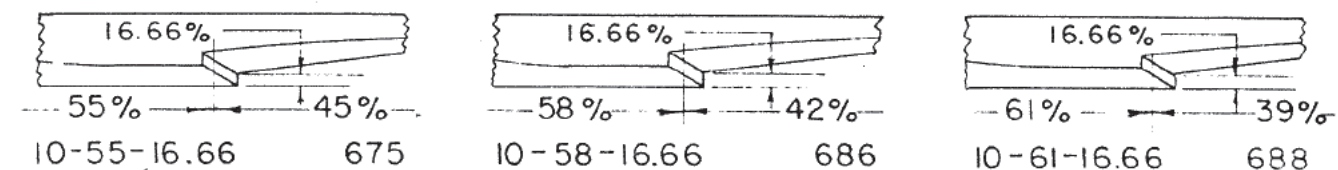
FOREBODY FLAT  
 100 % b



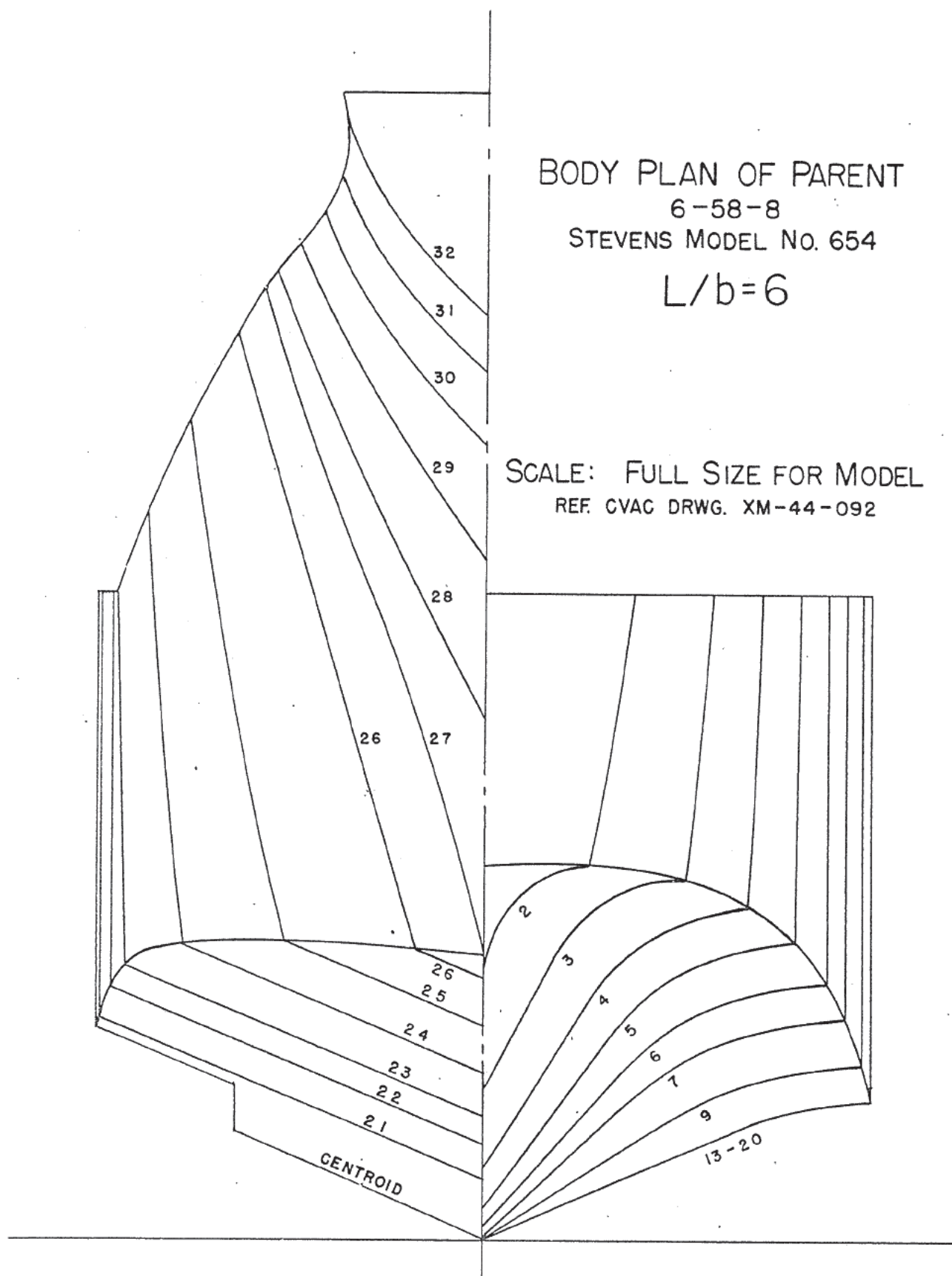
L/B = 10

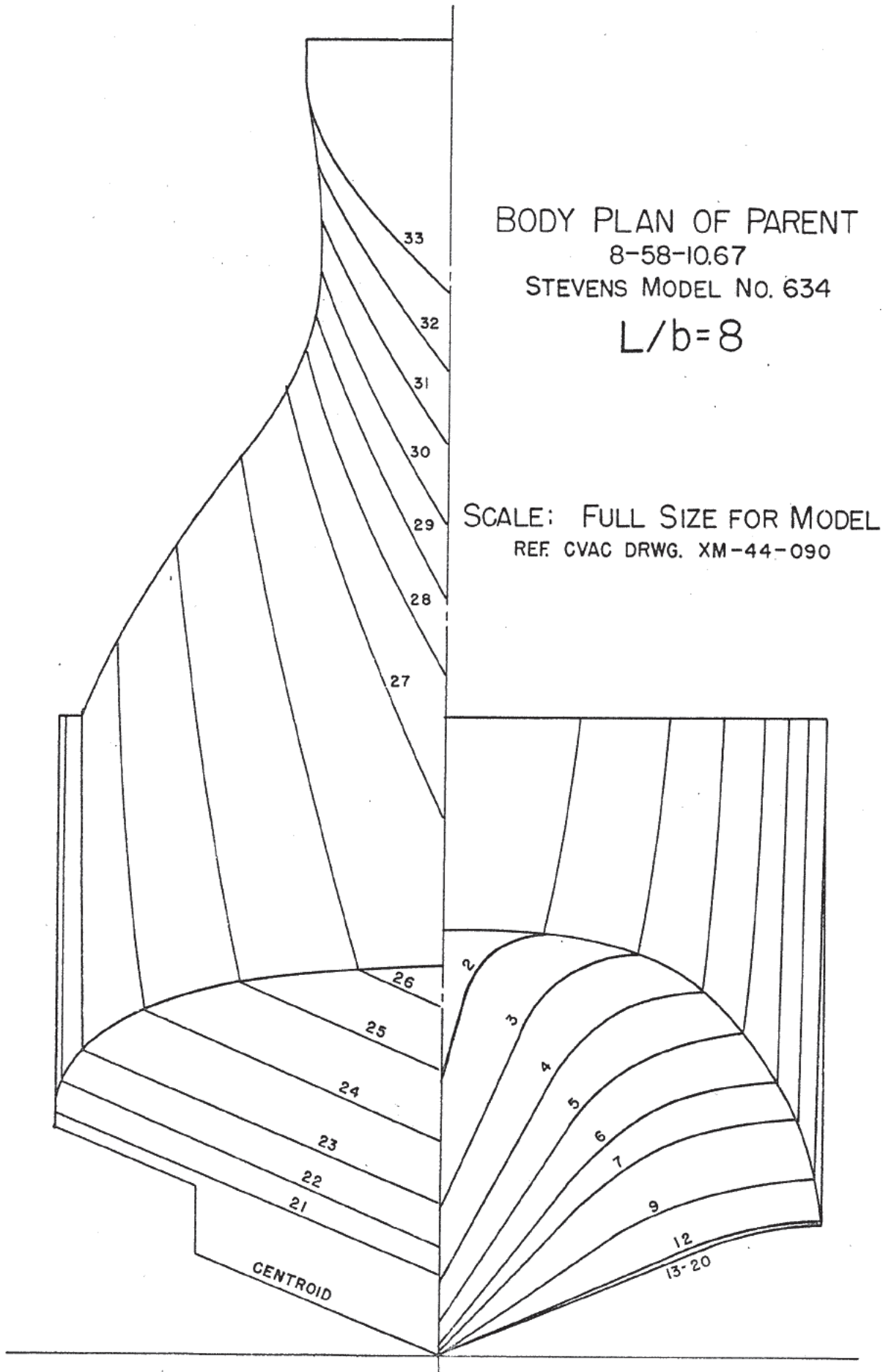


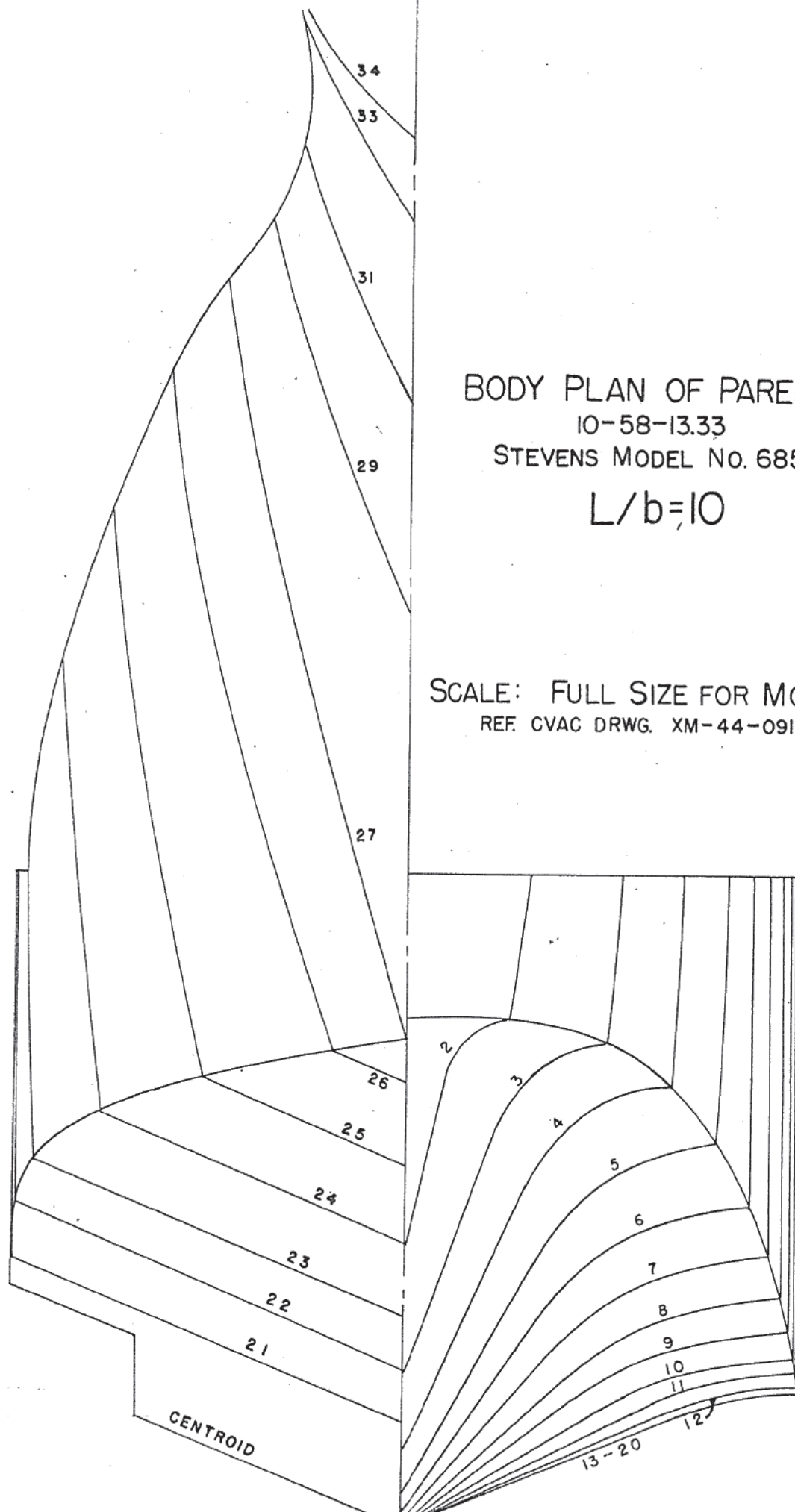
FOREBODY FLAT  
 66.67 % b











BODY PLAN OF PARENT  
10-58-13.33  
STEVENS MODEL NO. 685  
 $L/b=10$

SCALE: FULL SIZE FOR MODEL  
REF. CVAC DRWG. XM-44-091

NATIONAL ADVISORY COMMITTEE FOR AERONAUTICS  
INVESTIGATION CONDUCTED BY  
EXPERIMENTAL TOWING TANK-STEVENS INSTITUTE OF TECHNOLOGY  
HOBOKEN, NEW JERSEY

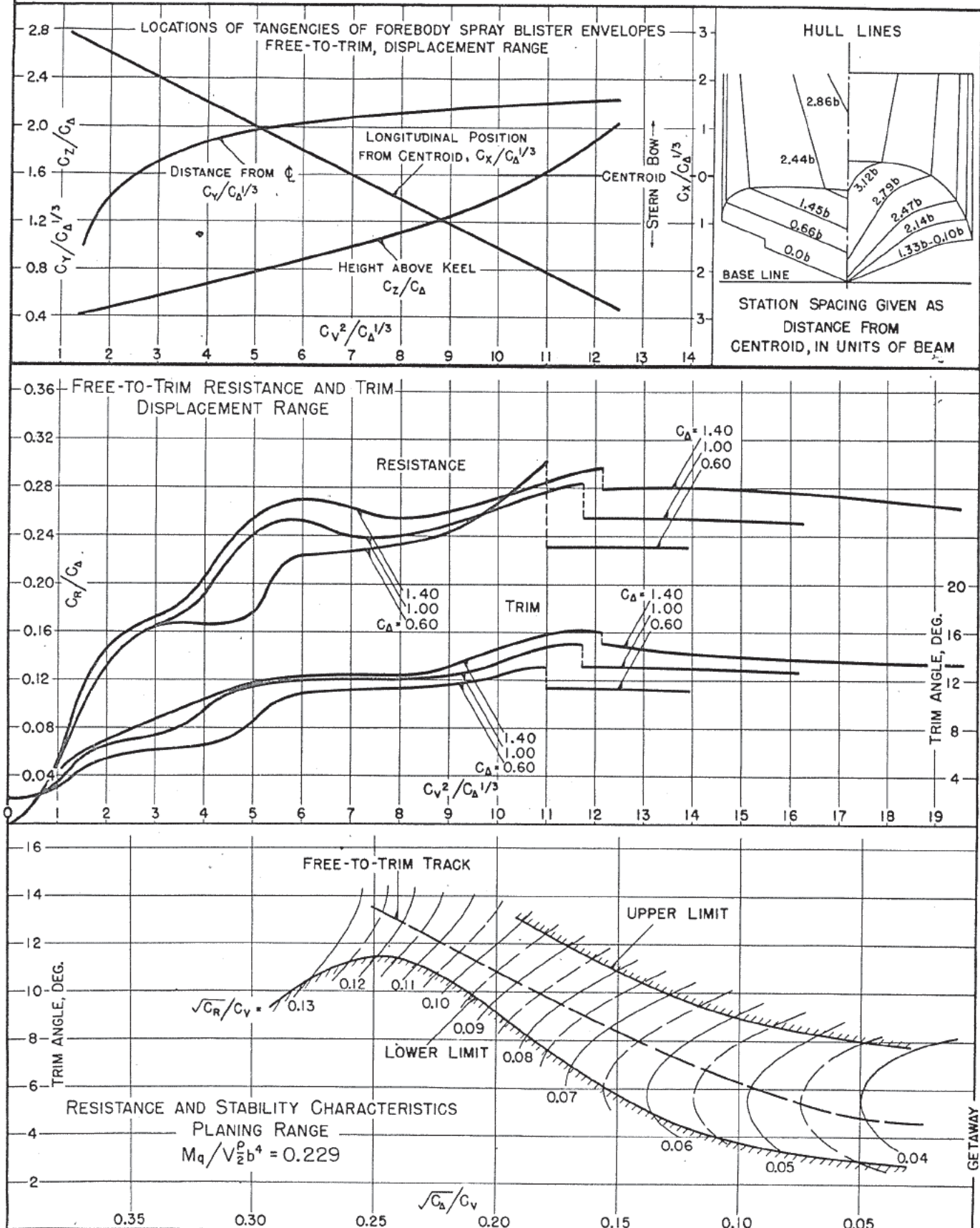
### SUMMARY CHART OF PRINCIPAL HYDRODYNAMIC CHARACTERISTICS

DATE: JUNE 13, 1945

C.G. = 0.35 b FWD. OF CENTROID  $C_{D_0} = 1.00$  (NOMINAL)  
MODEL BEAM: 5.40" 0.90 b ABOVE KEEL  $k/L = 0.234$

DESIGNATION: 6-55-6

MODEL No. 656



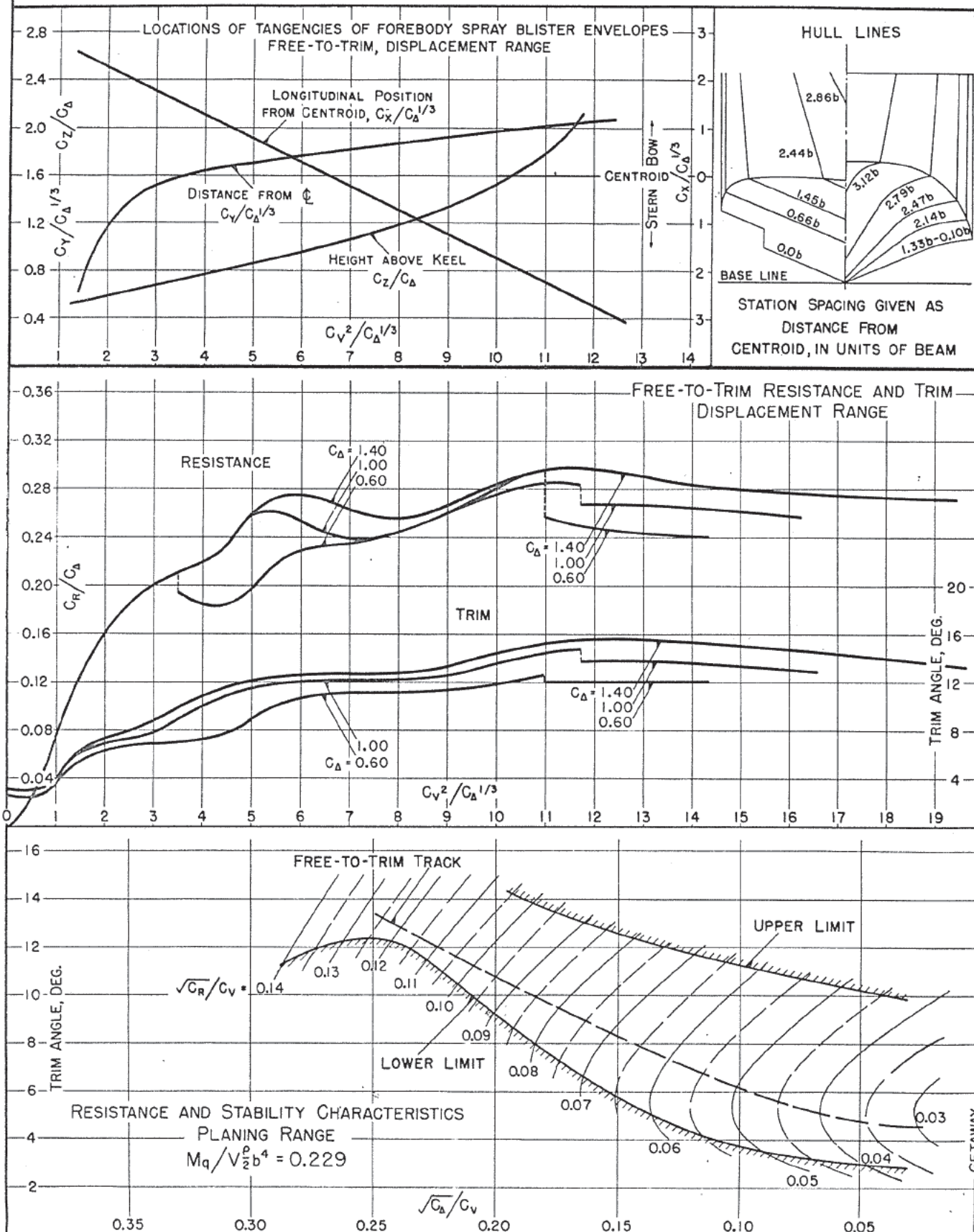
NATIONAL ADVISORY COMMITTEE FOR AERONAUTICS  
INVESTIGATION CONDUCTED BY  
EXPERIMENTAL TOWING TANK-STEVENS INSTITUTE OF TECHNOLOGY  
HOBOKEN, NEW JERSEY

### SUMMARY CHART OF PRINCIPAL HYDRODYNAMIC CHARACTERISTICS

DATE: MAY 9, 1945  
MODEL BEAM: 5.40"

C.G. = 0.35 b FWD. OF CENTROID  $C_{D_0} = 1.00$  (NOMINAL)  
0.90 b ABOVE KEEL  $k/L = 0.234$

DESIGNATION: 6-55-10  
MODEL NO. 657





NATIONAL ADVISORY COMMITTEE FOR AERONAUTICS  
INVESTIGATION CONDUCTED BY  
EXPERIMENTAL TOWING TANK-STEVENS INSTITUTE OF TECHNOLOGY  
HOBOKEN, NEW JERSEY

### SUMMARY CHART OF PRINCIPAL HYDRODYNAMIC CHARACTERISTICS

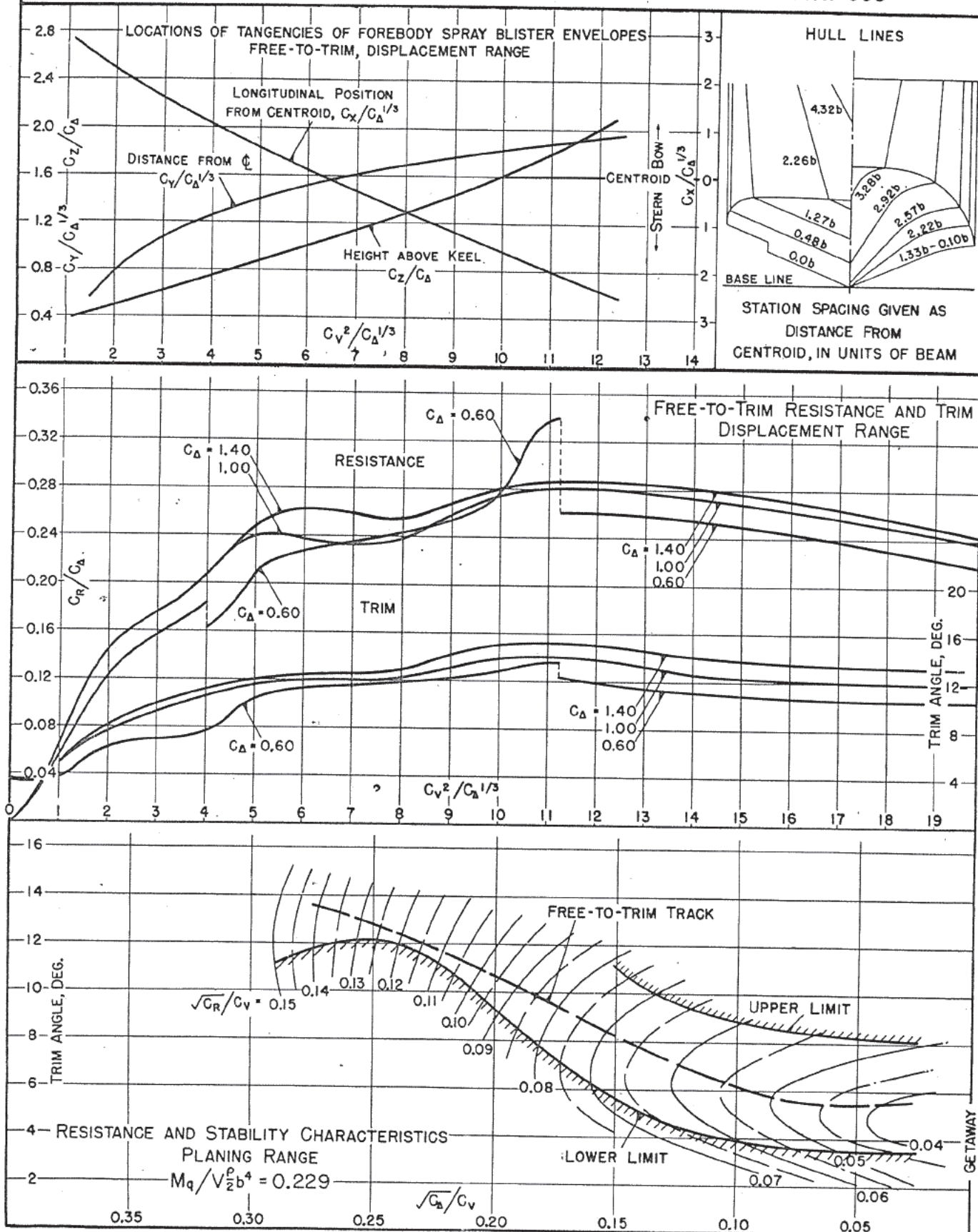
DATE: AUG. 21, 1945

MODEL BEAM: 5.40"

C.G. = 0.35 b FWD. OF CENTROID  $C_{\Delta} = 1.00$  (NOMINAL)  
0.90 b ABOVE KEEL  $k/L = 0.234$

DESIGNATION: 6-58-6

MODEL NO. 653



NATIONAL ADVISORY COMMITTEE FOR AERONAUTICS  
INVESTIGATION CONDUCTED BY  
EXPERIMENTAL TOWING TANK-STEVENS INSTITUTE OF TECHNOLOGY  
HOBOKEN, NEW JERSEY

### SUMMARY CHART OF PRINCIPAL HYDRODYNAMIC CHARACTERISTICS

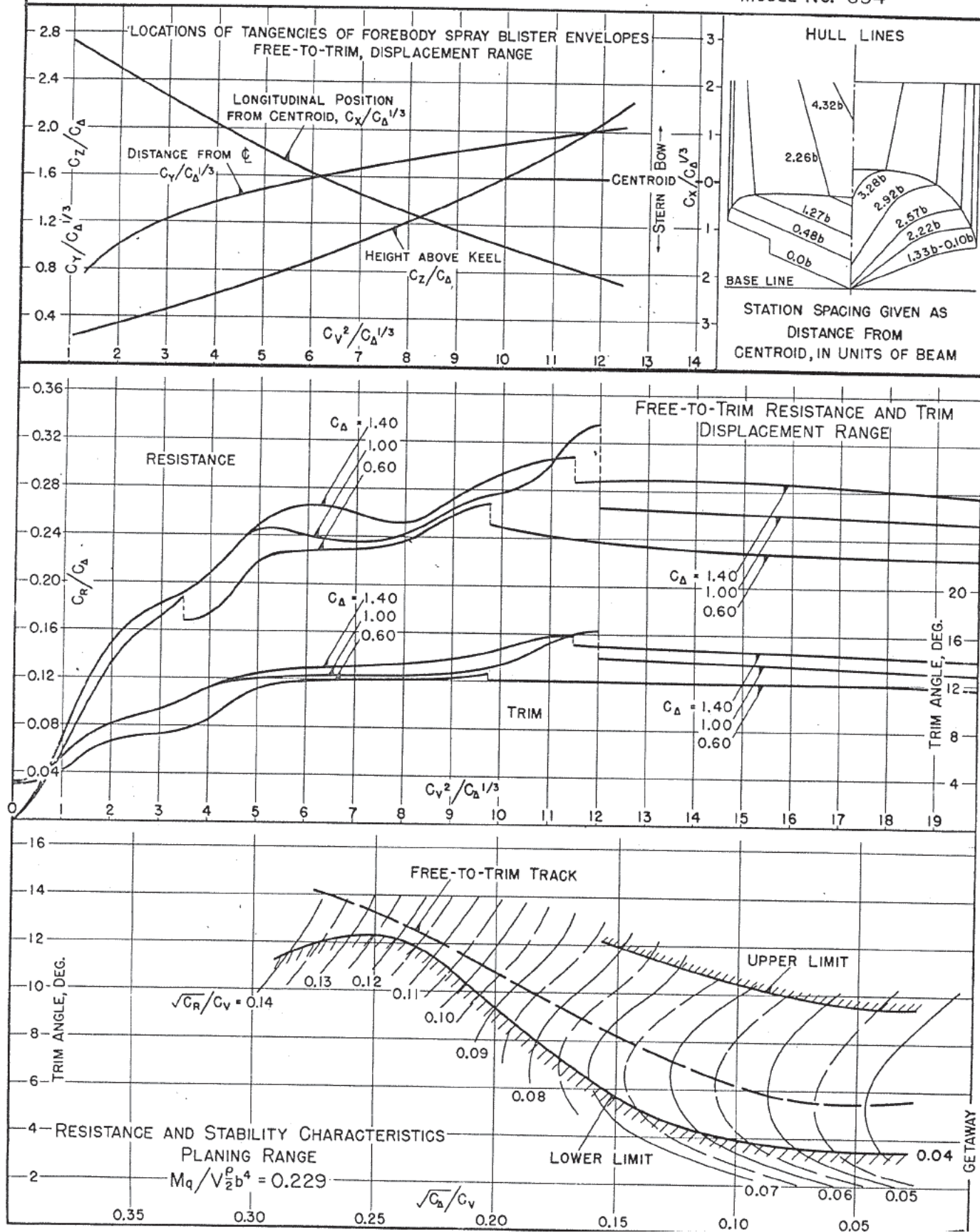
DATE: AUG. 24, 1945

MODEL BEAM: 5.40"

$C.G. = 0.35 b$  FWD. OF CENTROID  $C_{d_0} = 1.00$  (NOMINAL)  
 $0.90 b$  ABOVE KEEL  $k/L = 0.234$

DESIGNATION: 6-58-8

MODEL NO. 654



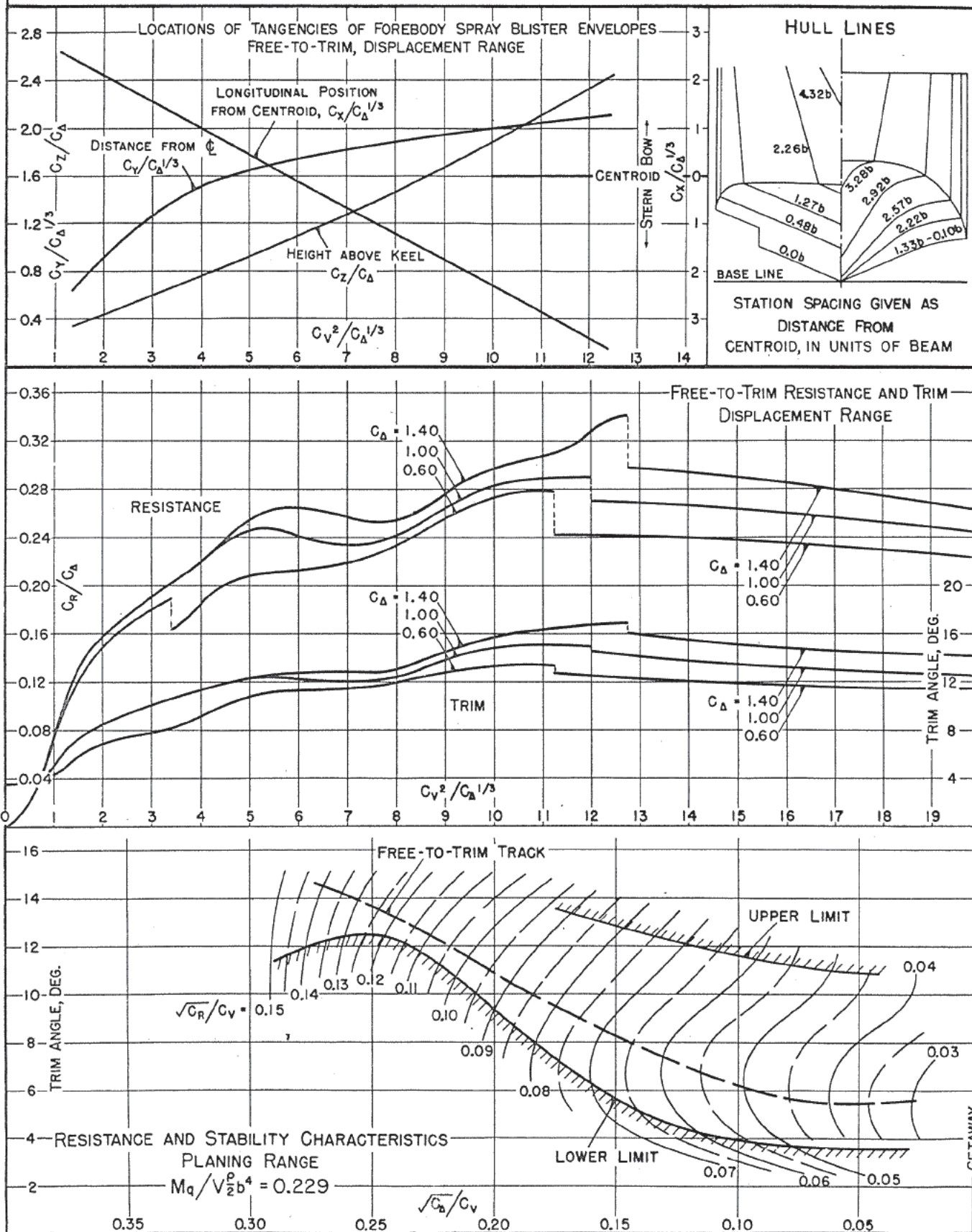
NATIONAL ADVISORY COMMITTEE FOR AERONAUTICS  
INVESTIGATION CONDUCTED BY  
EXPERIMENTAL TOWING TANK-STEVENS INSTITUTE OF TECHNOLOGY  
HOBOKEN, NEW JERSEY

SUMMARY CHART OF PRINCIPAL HYDRODYNAMIC CHARACTERISTICS

DATE: SEPT. 1, 1945  
MODEL BEAM: 5.40"

C.G. = 0.35b FWD. OF CENTROID  $C_{d_s} = 1.00$  (NOMINAL)  
0.90b ABOVE KEEL  $k/L = 0.234$

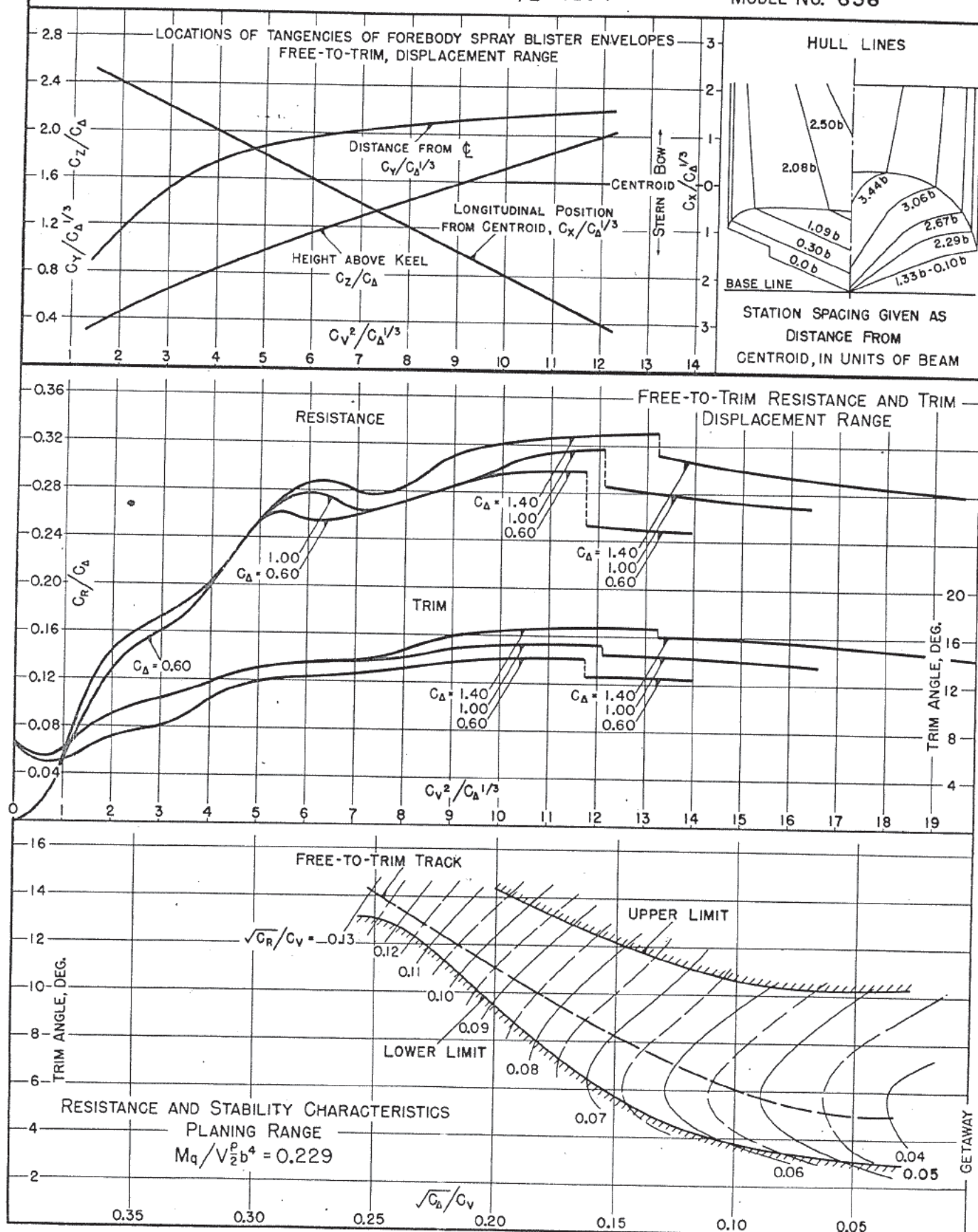
DESIGNATION: 6-58-10  
MODEL NO. 655





## SUMMARY CHART OF PRINCIPAL HYDRODYNAMIC CHARACTERISTICS

MODEL NO. 658



NATIONAL ADVISORY COMMITTEE FOR AERONAUTICS  
INVESTIGATION CONDUCTED BY  
EXPERIMENTAL TOWING TANK-STEVENS INSTITUTE OF TECHNOLOGY  
HOBOKEN, NEW JERSEY

SUMMARY CHART OF PRINCIPAL HYDRODYNAMIC CHARACTERISTICS

DATE: JUNE 28, 1945

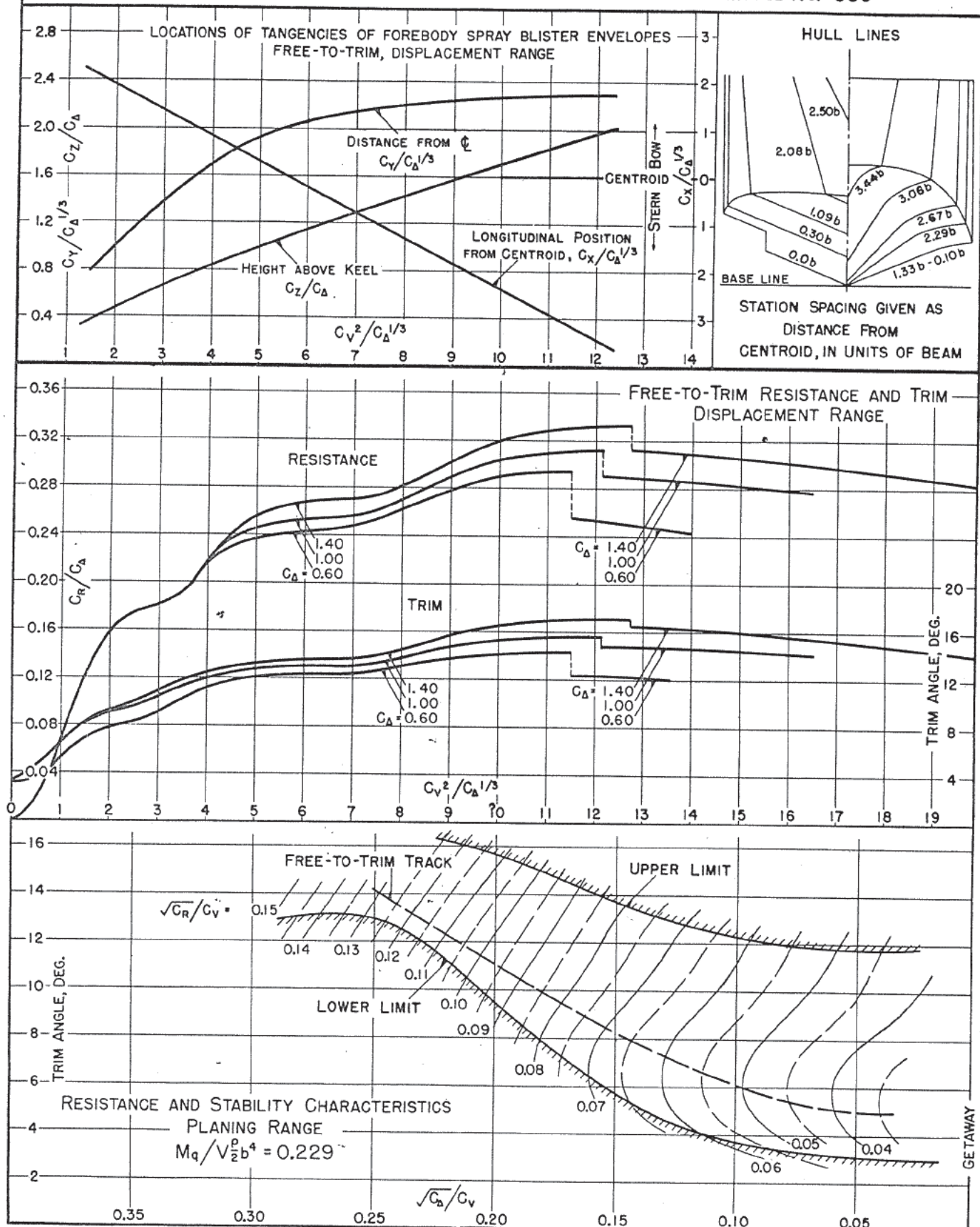
MODEL BEAM: 5.40"

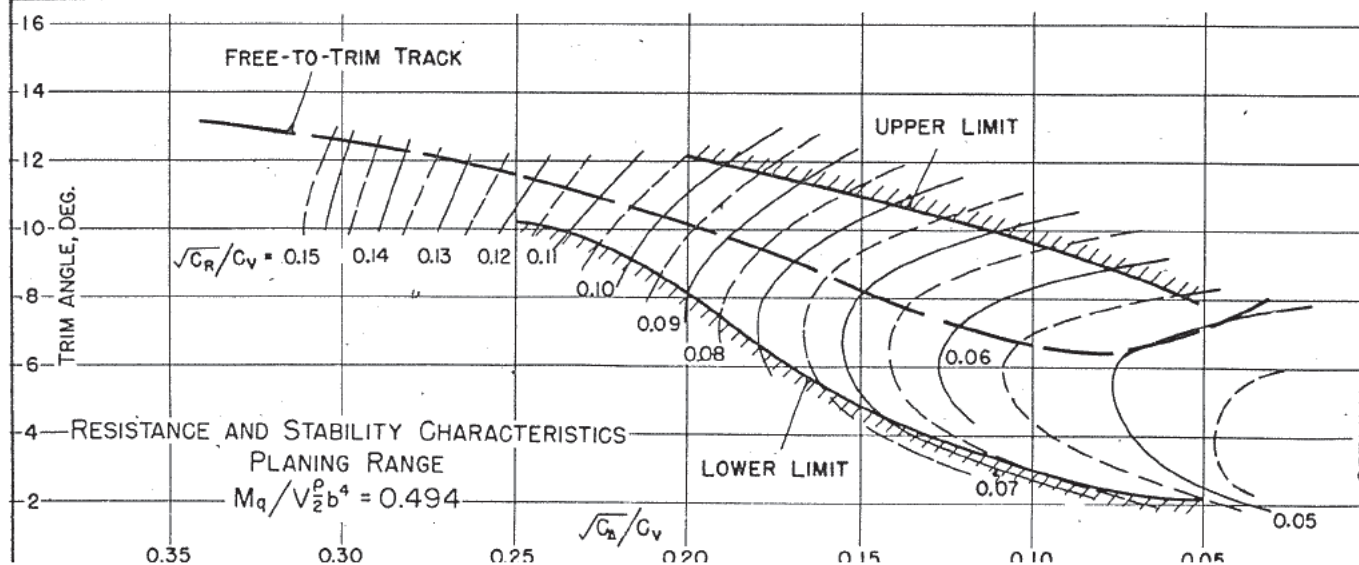
$C.G. = 0.35 b$  FWD. OF CENTROID  
 $0.90 b$  ABOVE KEEL

 $C_{D0} = 1.00$  (NOMINAL) $k/L = 0.234$ 

DESIGNATION: 6-61-10

MODEL NO. 659







NATIONAL ADVISORY COMMITTEE FOR AERONAUTICS  
INVESTIGATION CONDUCTED BY  
EXPERIMENTAL TOWING TANK-STEVENS INSTITUTE OF TECHNOLOGY  
HOBOKEN, NEW JERSEY

R-311

-74-

N-24

-27-

### SUMMARY CHART OF PRINCIPAL HYDRODYNAMIC CHARACTERISTICS

DEC. 12, 1945 (REVISED)

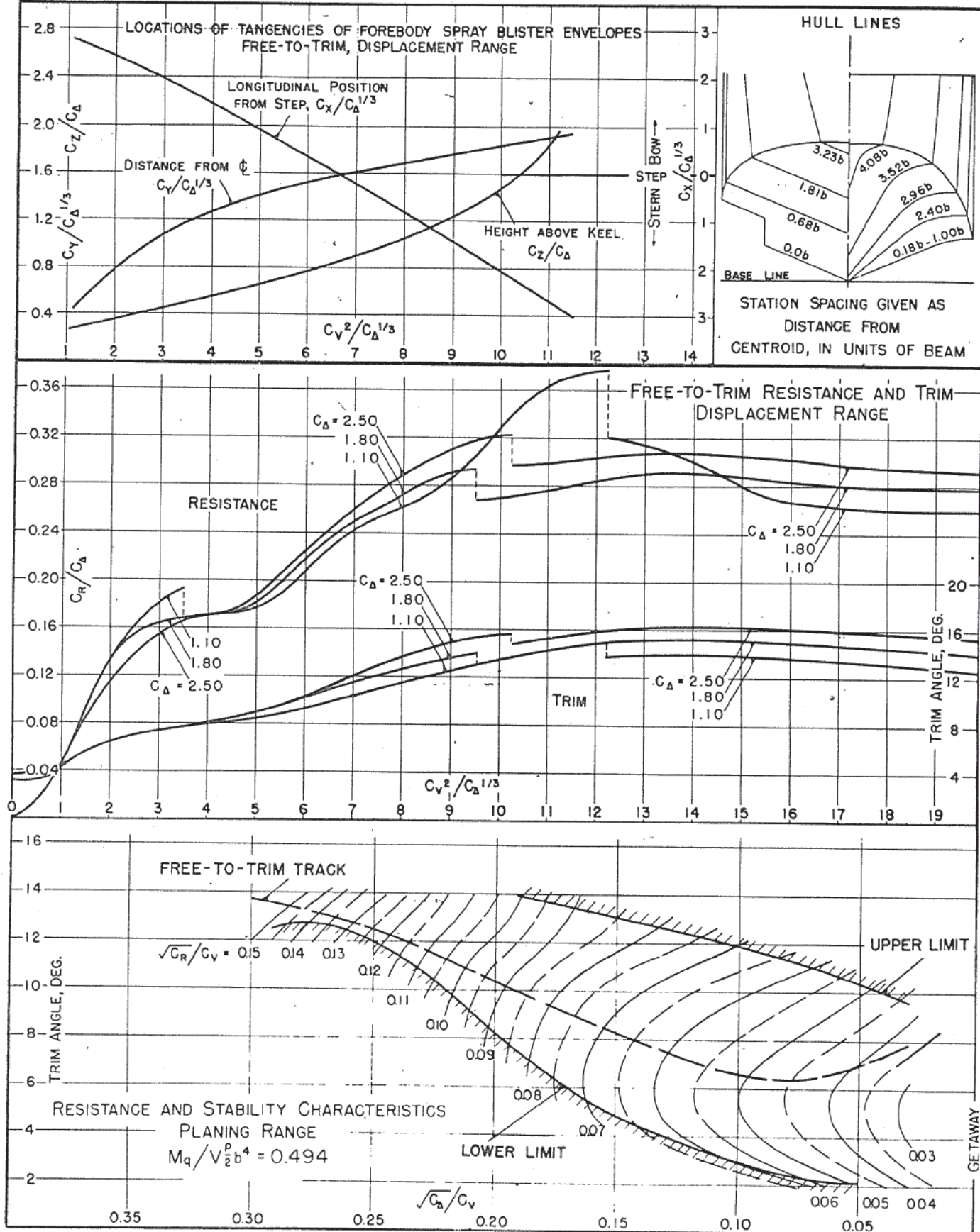
DATE: APRIL 19, 1945

MODEL BEAM: 5.4"

C.G. = 0.35b FWD. OF CENTROID  $C_{D_0} = 1.80$  (NOMINAL)  
0.90b ABOVE KEEL $k/L = 0.220$ 

DESIGNATION: 8-55-13.33

MODEL NO. 643



NATIONAL ADVISORY COMMITTEE FOR AERONAUTICS  
INVESTIGATION CONDUCTED BY  
EXPERIMENTAL TOWING TANK-STEVENS INSTITUTE OF TECHNOLOGY  
HOBOKEN, NEW JERSEY

R-31

-75-

N-2

-23

### SUMMARY CHART OF PRINCIPAL HYDRODYNAMIC CHARACTERISTICS

DEC. 12, 1945 (REVISED)

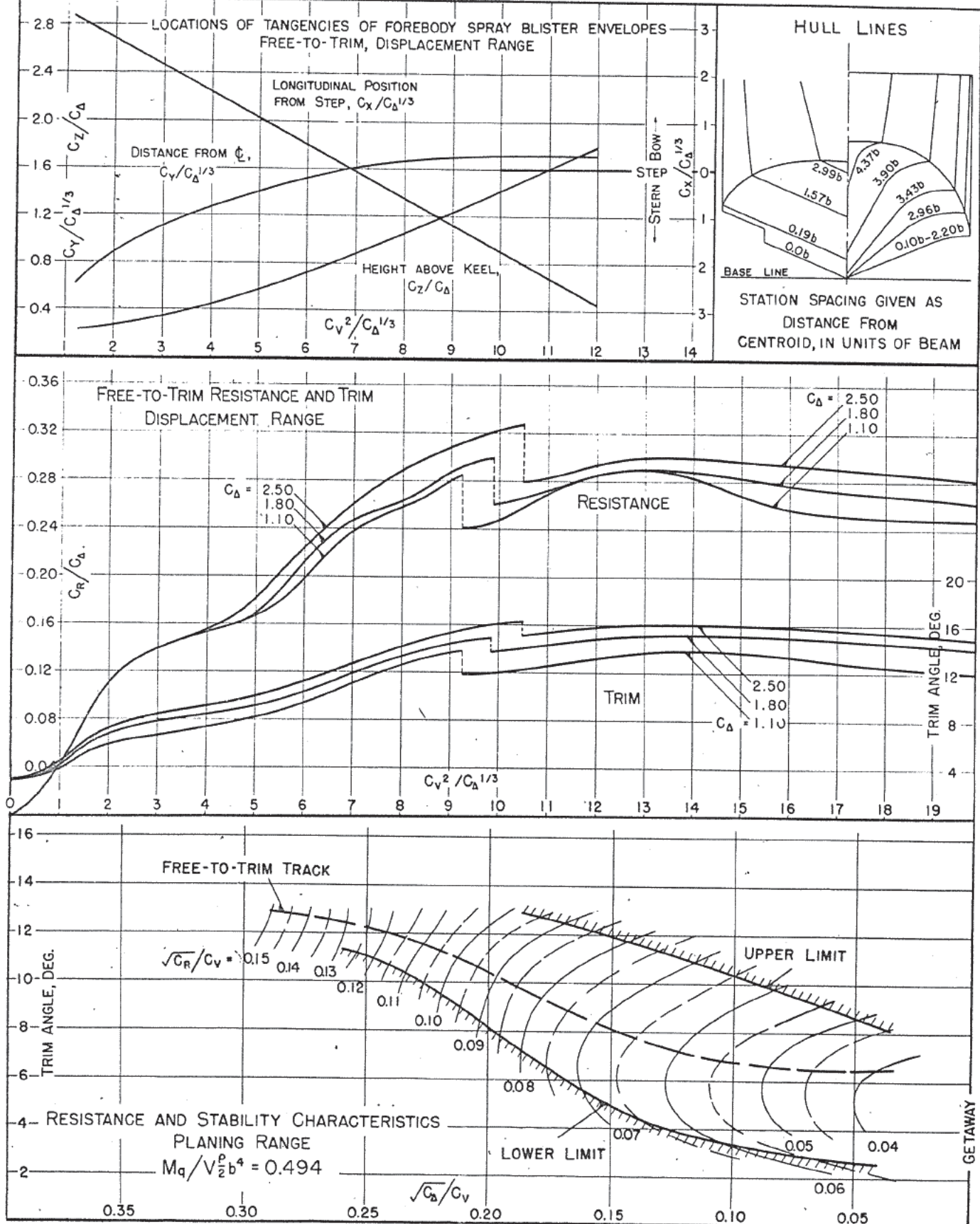
DATE: JAN. 25, 1945

MODEL BEAM: 5.40"

C.G. = 0.35b FWD. OF CENTROID  $C_{\Delta} = 1.80$  (NOMINAL)  
0.90b ABOVE KEEL  $k/L = 0.220$

DESIGNATION: 8-58-8

MODEL NO. 633-02



NATIONAL ADVISORY COMMITTEE FOR AERONAUTICS  
INVESTIGATION CONDUCTED BY  
EXPERIMENTAL TOWING TANK-STEVENS INSTITUTE OF TECHNOLOGY  
HOBOKEN, NEW JERSEY

### SUMMARY CHART OF PRINCIPAL HYDRODYNAMIC CHARACTERISTICS

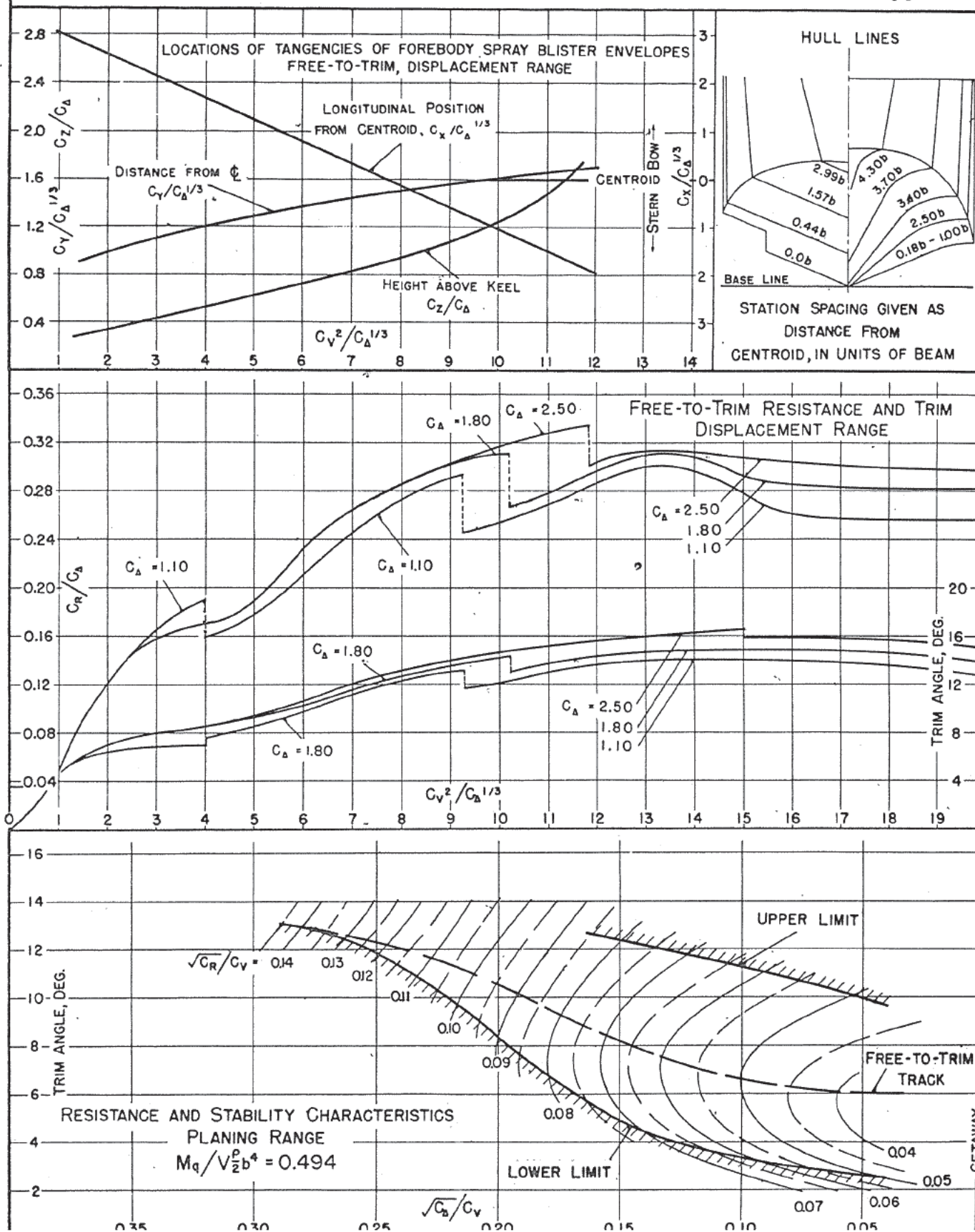
DATE: FEB. 28, 1946

MODEL BEAM: 5.40

C.G. = 0.35 b FWD. OF CENTROID  $C_{d_0} = 1.80$  (NOMINAL)  
0.90 b ABOVE KEEL  $k/L = 0.220$

DESIGNATION: 8-58-10.66

MODEL NO. 634-03





NATIONAL ADVISORY COMMITTEE FOR AERONAUTICS  
INVESTIGATION CONDUCTED BY  
EXPERIMENTAL TOWING TANK-STEVENS INSTITUTE OF TECHNOLOGY  
HOBOKEN, NEW JERSEY

R-3  
-77  
N-  
-2

### SUMMARY CHART OF PRINCIPAL HYDRODYNAMIC CHARACTERISTICS

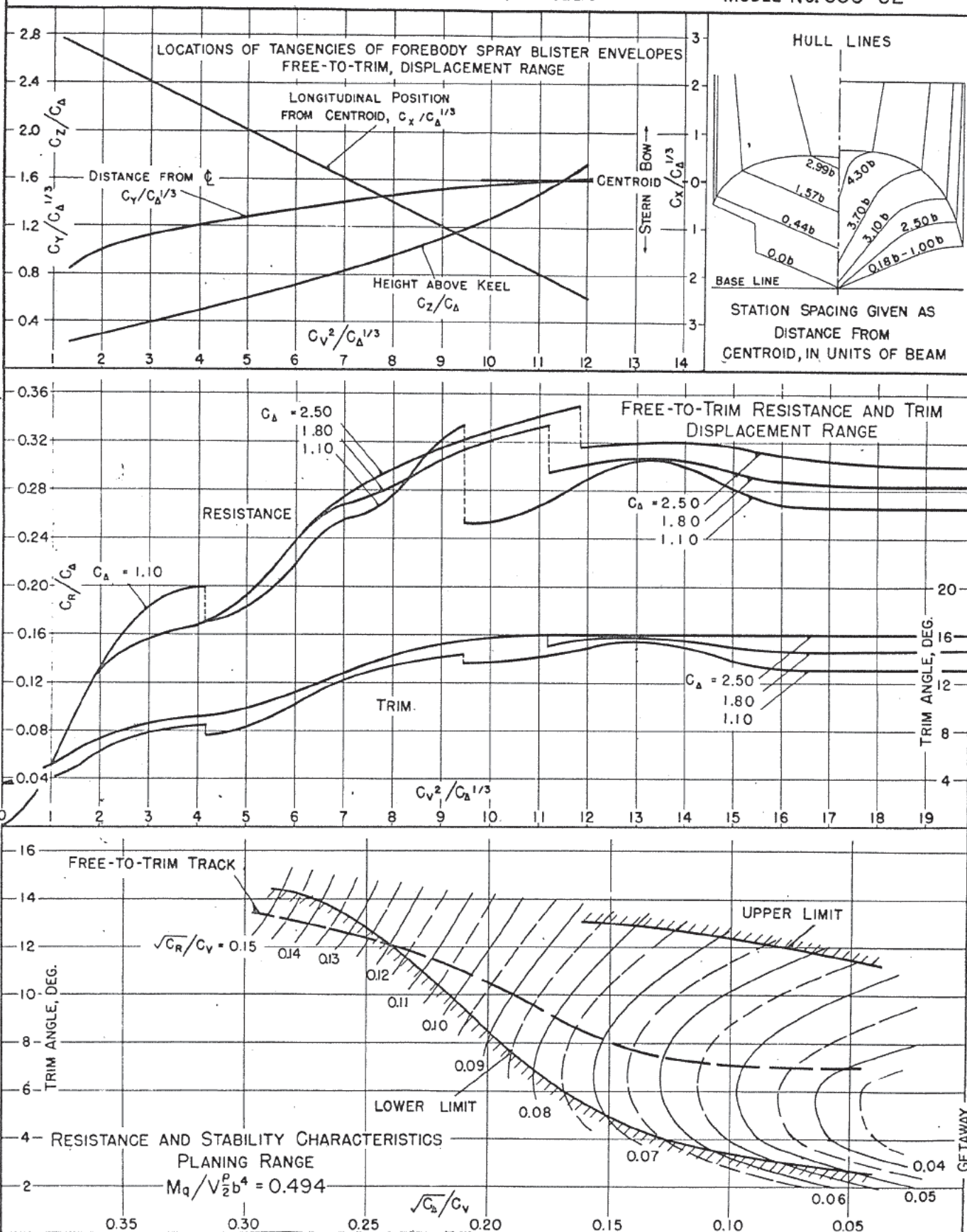
DATE: MAR. 27, 1946

MODEL BEAM: 5.40

C.G. = 0.35b FWD. OF CENTROID  $C_{d0} = 1.80$  (NOMINAL)  
0.90b ABOVE KEEL  $k/L = 0.220$

DESIGNATION: 8-58-13.33

MODEL NO. 635-02



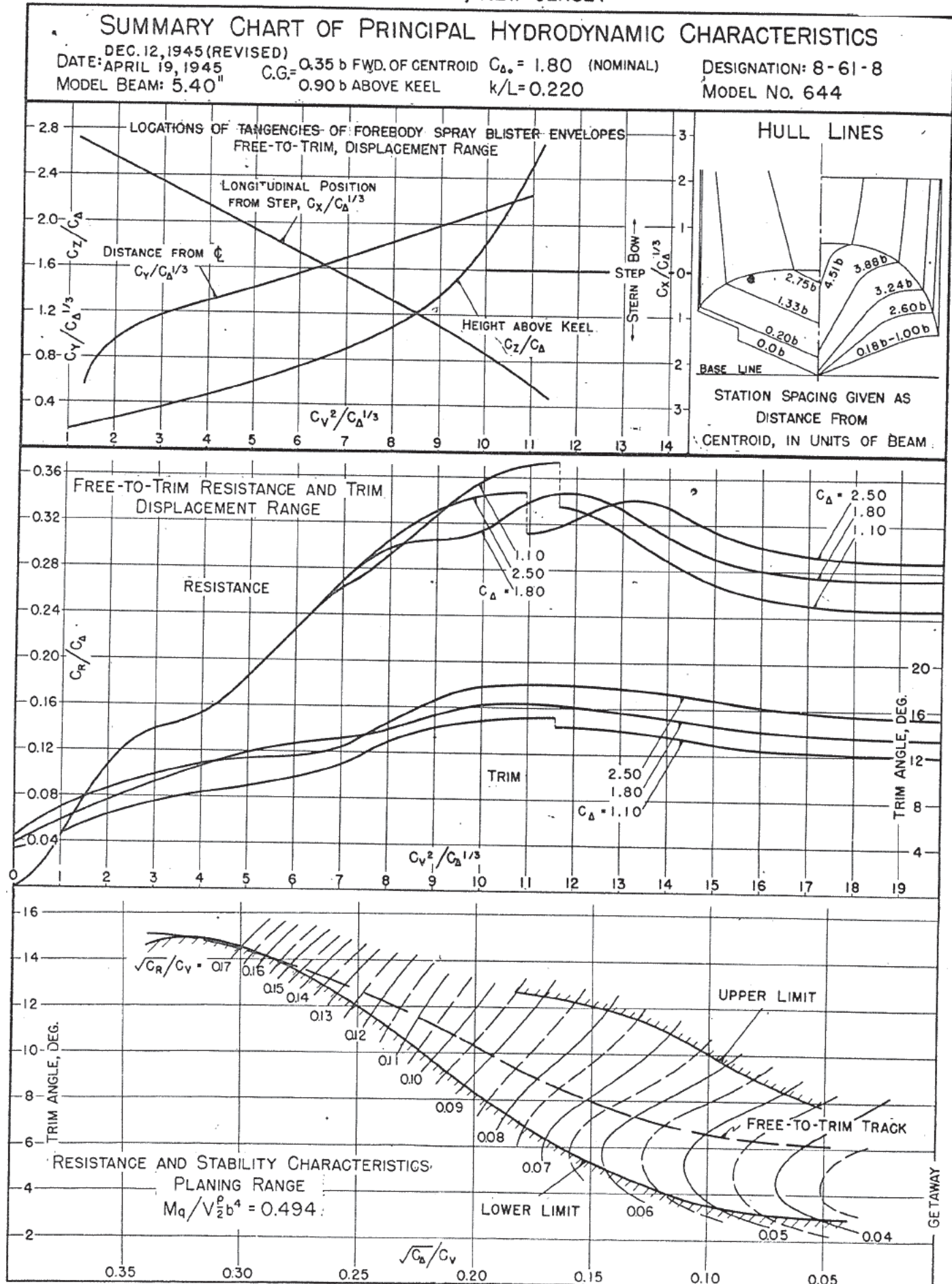
NATIONAL ADVISORY COMMITTEE FOR AERONAUTICS  
INVESTIGATION CONDUCTED BY  
EXPERIMENTAL TOWING TANK-STEVENS INSTITUTE OF TECHNOLOGY  
HOBOKEN, NEW JERSEY

R-31

-78-

N-2

-28





NATIONAL ADVISORY COMMITTEE FOR AERONAUTICS  
INVESTIGATION CONDUCTED BY  
EXPERIMENTAL TOWING TANK-STEVENS INSTITUTE OF TECHNOLOGY  
HOBOKEN, NEW JERSEY

R-31  
-79-  
N-24  
-29-

### SUMMARY CHART OF PRINCIPAL HYDRODYNAMIC CHARACTERISTICS

DEC. 12, 1945 (REVISED)

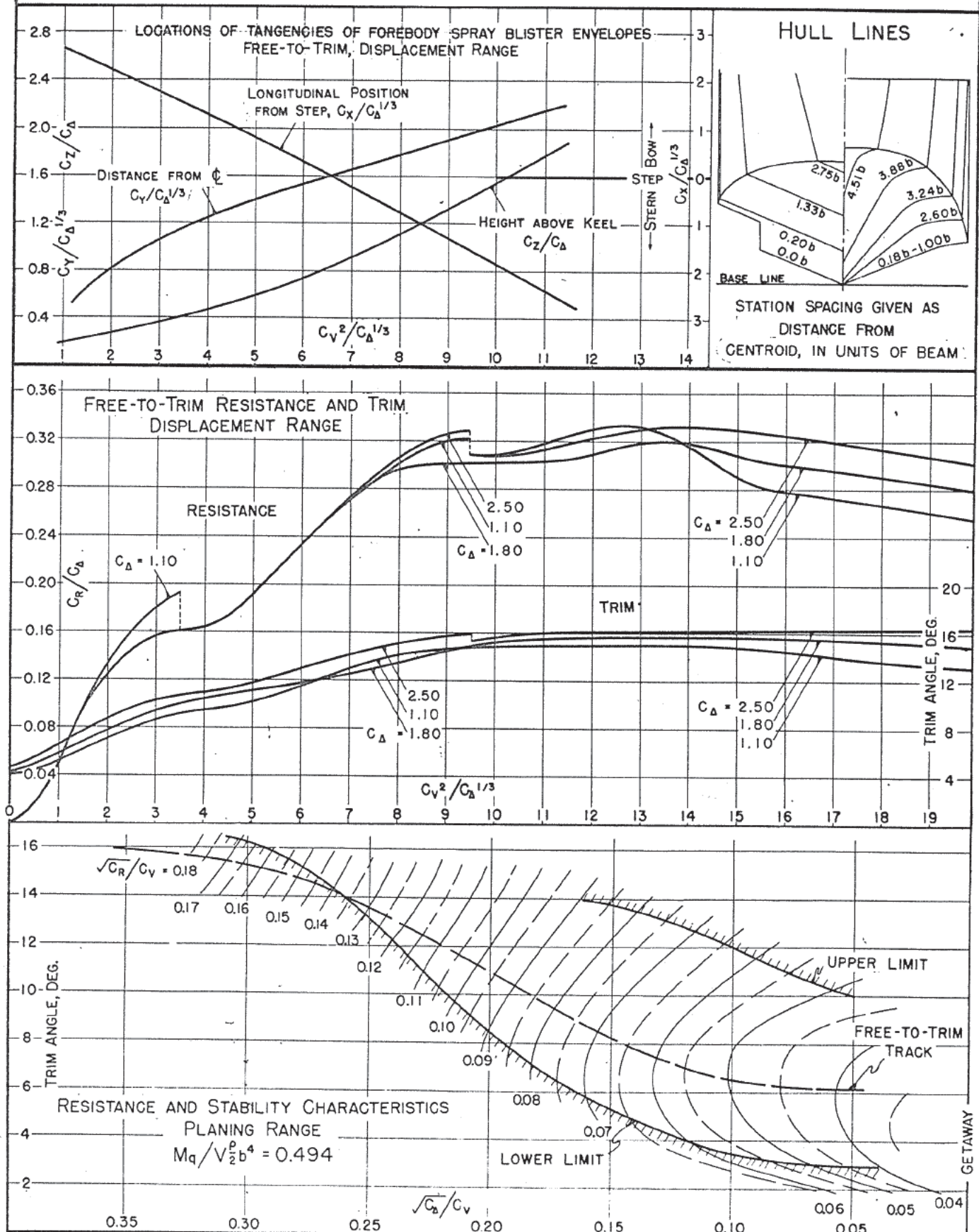
DATE: APRIL 19, 1945

MODEL BEAM: 5.40"

C.G. = 0.35 b FWD. OF CENTROID  $C_{D_0} = 1.80$  (NOMINAL)  
0.90 b ABOVE KEEL  $k/L = 0.220$

DESIGNATION: 8-61-13.33

MODEL NO. 645



NATIONAL ADVISORY COMMITTEE FOR AERONAUTICS  
 INVESTIGATION CONDUCTED BY  
 EXPERIMENTAL TOWING TANK-STEVENS INSTITUTE OF TECHNOLOGY  
 HOBOKEN, NEW JERSEY

-74-  
 R-312  
 -80-

### SUMMARY CHART OF PRINCIPAL HYDRODYNAMIC CHARACTERISTICS

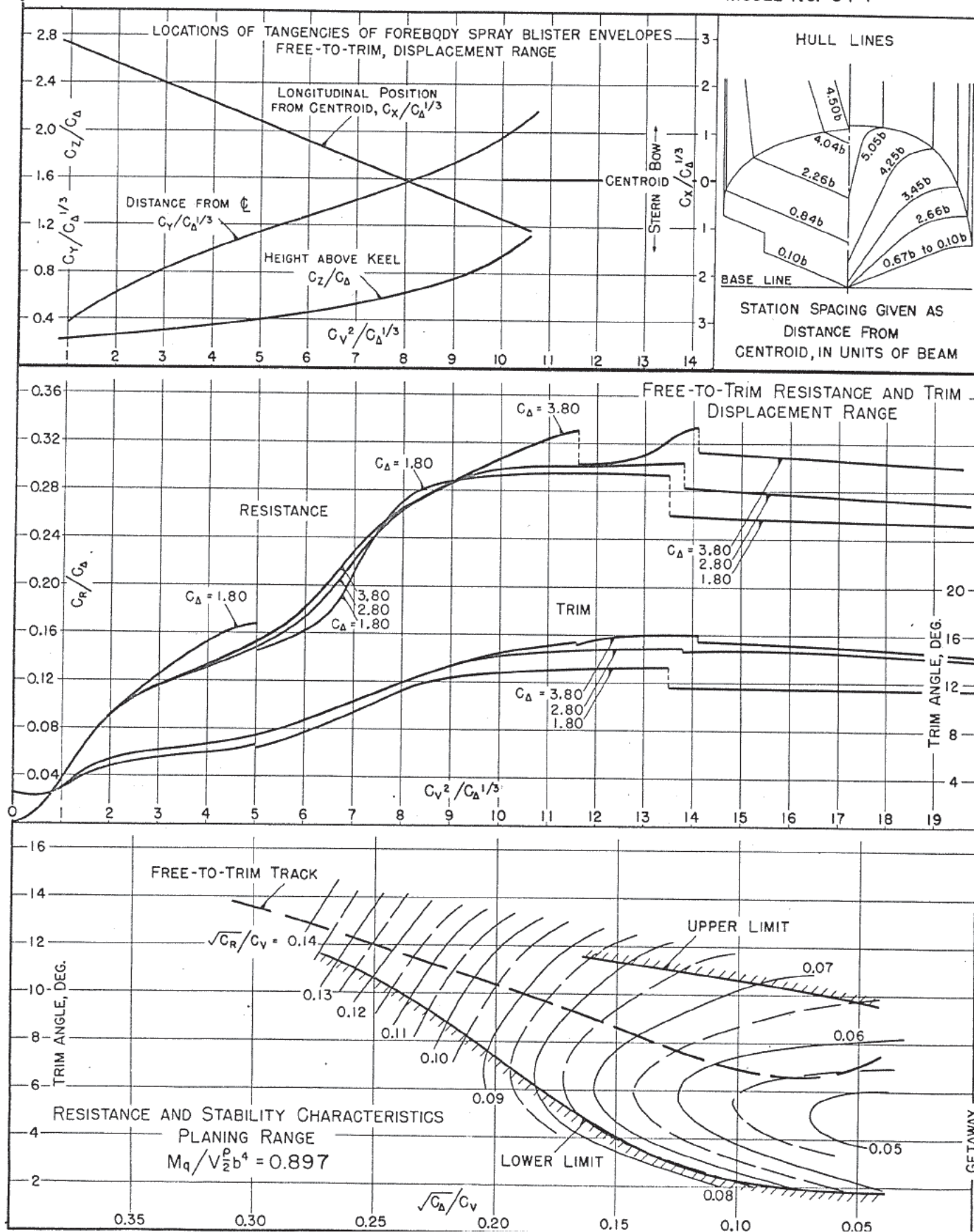
DATE: SEPT. 20, 1945

MODEL BEAM: 5.40"

C.G. = 0.35 b FWD. OF CENTROID  $C_{D_0} = 2.80$  (NOMINAL)  
 0.90 b ABOVE KEEL  $k/L = 0.211$

DESIGNATION: 10-55-10

MODEL NO. 674



NATIONAL ADVISORY COMMITTEE FOR AERONAUTICS  
INVESTIGATION CONDUCTED BY  
EXPERIMENTAL TOWING TANK-STEVENS INSTITUTE OF TECHNOLOGY  
HOBOKEN, NEW JERSEY

N-24

-75-

R-3

-81

## SUMMARY CHART OF PRINCIPAL HYDRODYNAMIC CHARACTERISTICS

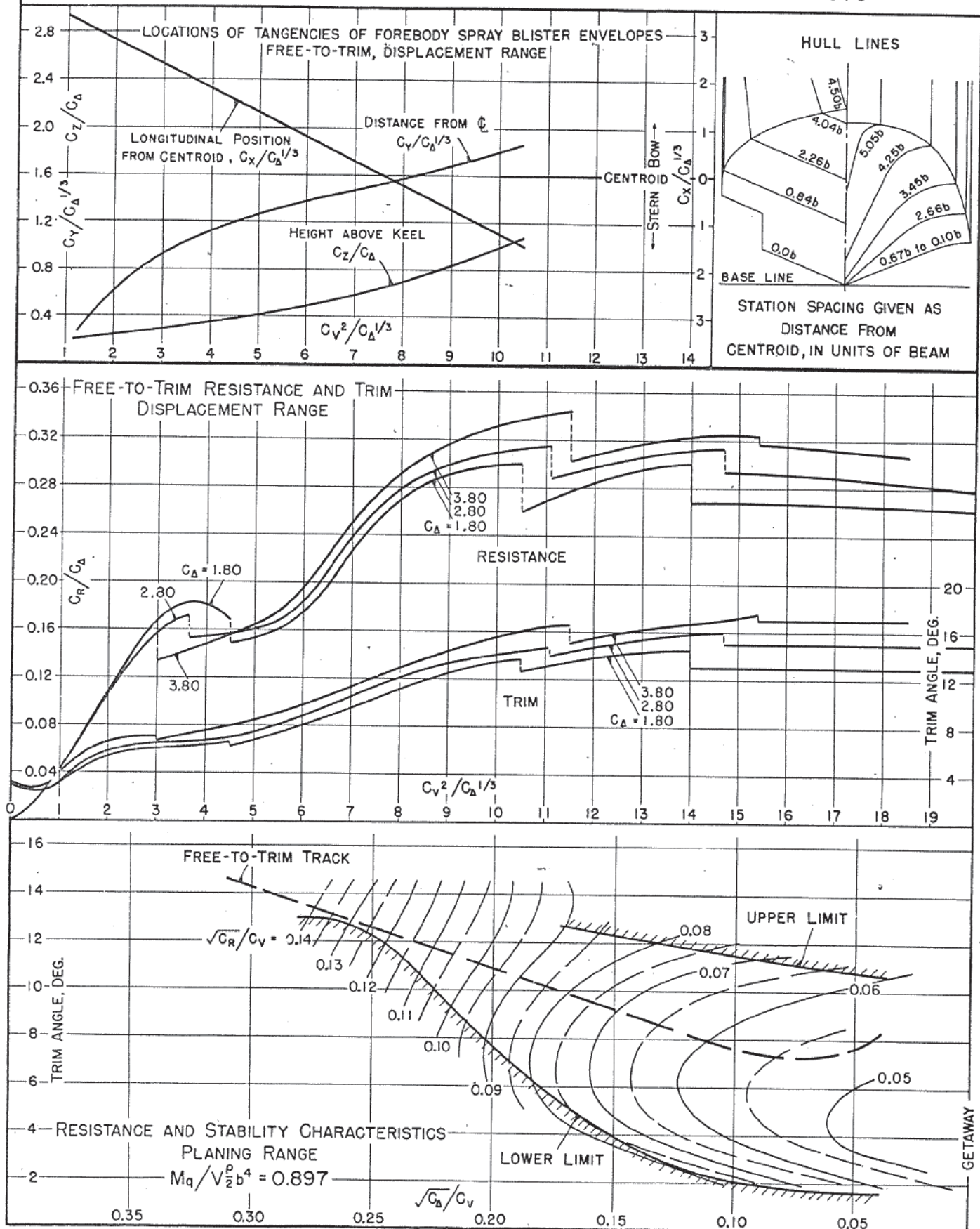
DATE: JUNE 5, 1945

MODEL BEAM: 5.40"

C.G. = 0.35 b FWD. OF CENTROID  $C_{\Delta} = 2.80$  (NOMINAL)  
0.90 b ABOVE KEEL  $k/L = 0.211$

DESIGNATION: 10-55-16.67

MODEL NO. 675





NATIONAL ADVISORY COMMITTEE FOR AERONAUTICS  
INVESTIGATION CONDUCTED BY  
EXPERIMENTAL TOWING TANK-STEVENS INSTITUTE OF TECHNOLOGY  
HOBOKEN, NEW JERSEY

M-24

-71-

R-3

-82

## SUMMARY CHART OF PRINCIPAL HYDRODYNAMIC CHARACTERISTICS

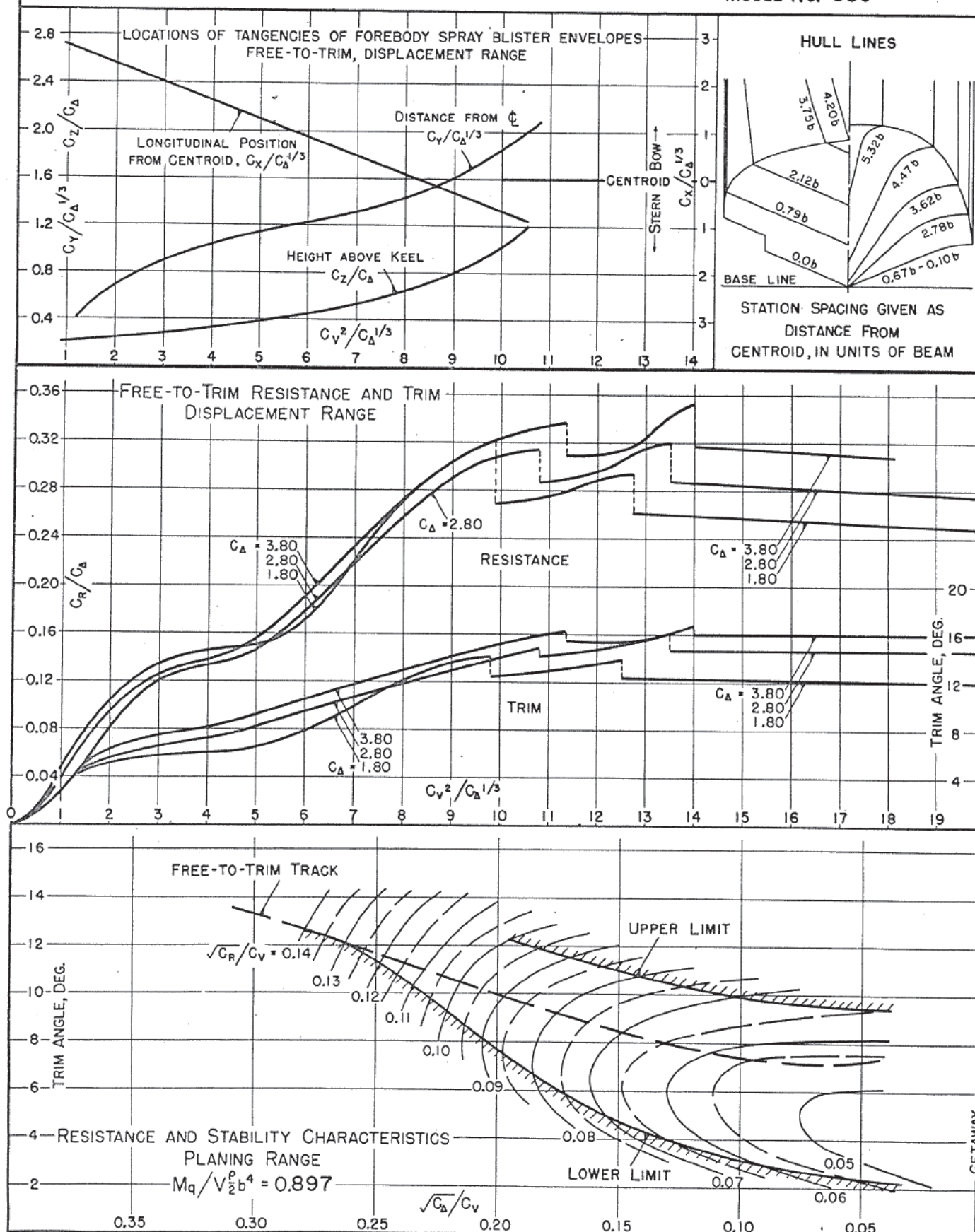
DATE: JULY 28, 1945

MODEL BEAM: 5.40"

C.G. = 0.35 b FWD. OF CENTROID  $C_{D,0} = 2.80$  (NOMINAL)  
0.90 b ABOVE KEEL  $k/L = 0.211$

DESIGNATION: 10-58-10

MODEL NO. 689



## SUMMARY CHART OF PRINCIPAL HYDRODYNAMIC CHARACTERISTICS

DATE: AUG. 18, 1945

MODEL BEAM: 5.40"

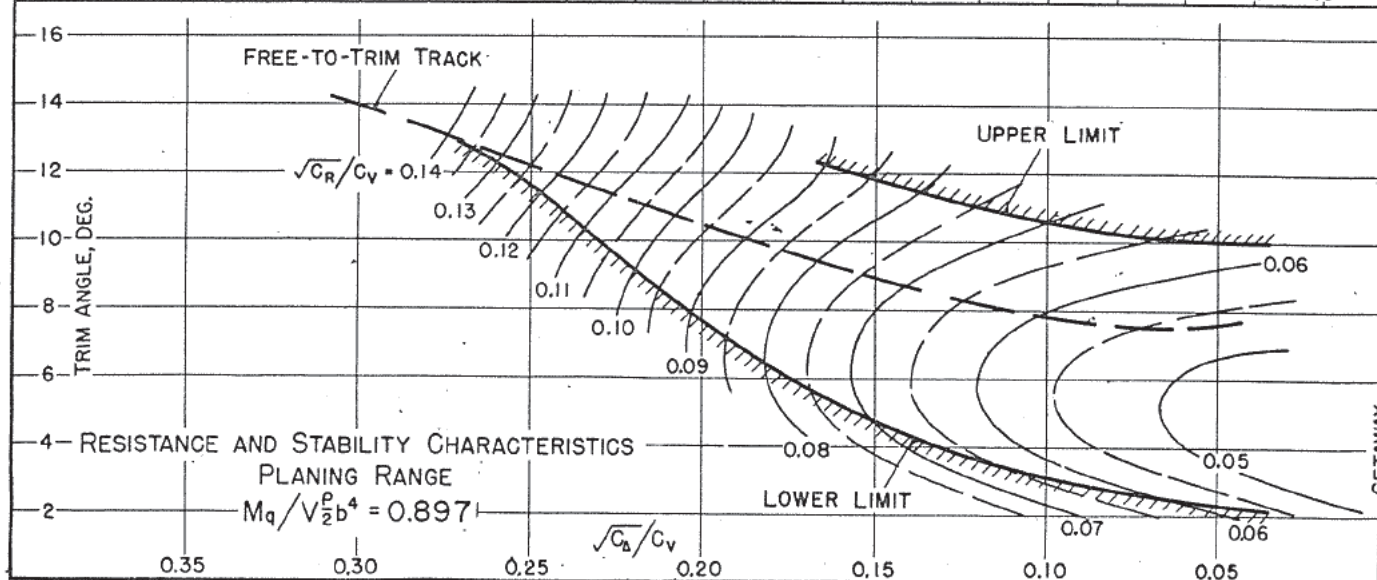
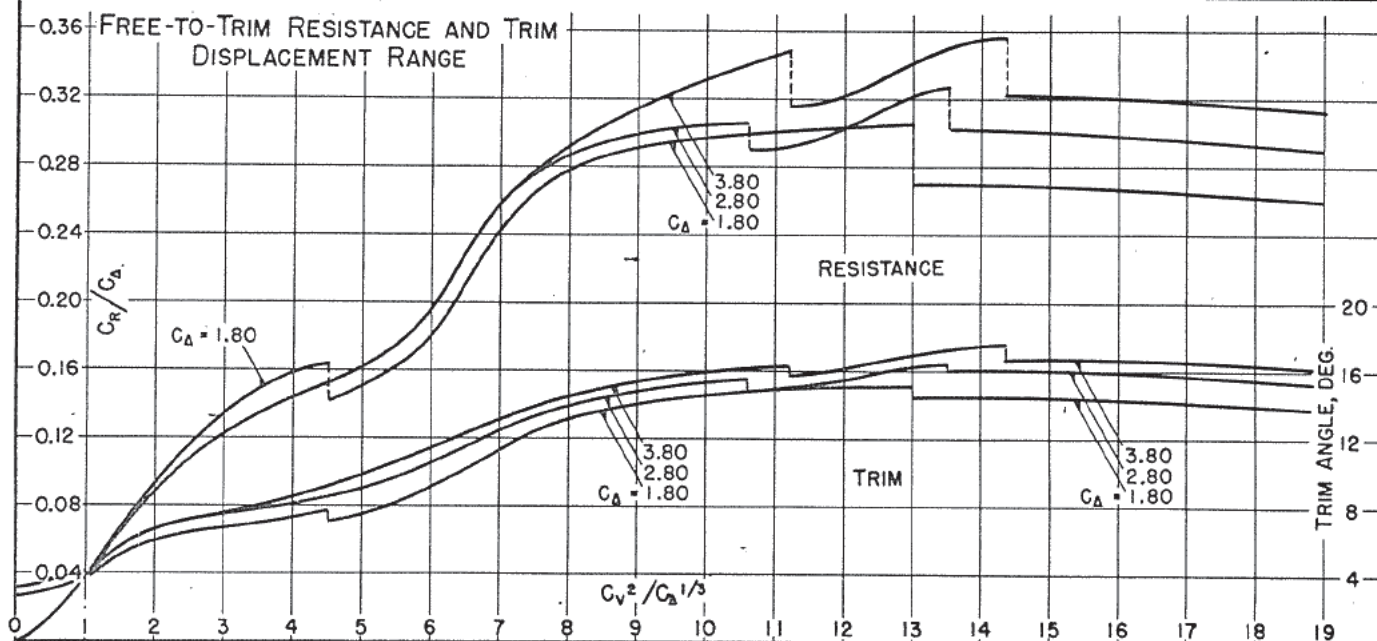
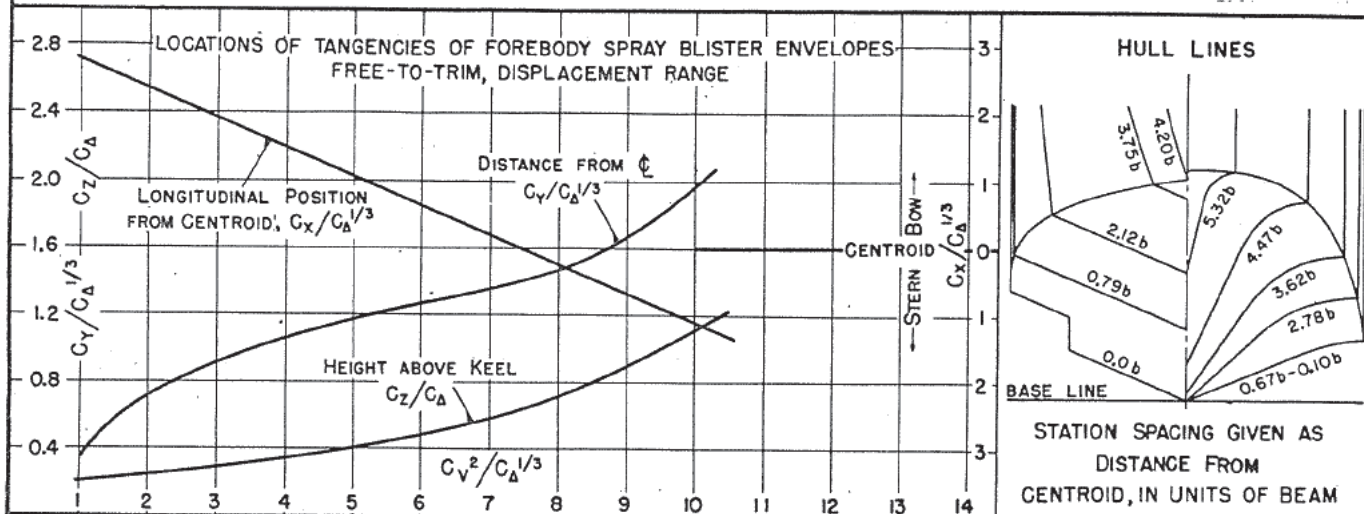
$C_G = 0.35b$  FWD. OF CENTROID  $C_{d_0} = 2.80$  (NOMINAL)

C.G. = 0.90b ABOVE KEEL

$$k/L = 0.211$$

DESIGNATION: 10-58-13.33

MODEL No. 685



NATIONAL ADVISORY COMMITTEE FOR AERONAUTICS  
 INVESTIGATION CONDUCTED BY  
 EXPERIMENTAL TOWING TANK-STEVENS INSTITUTE OF TECHNOLOGY  
 HOBOKEN, NEW JERSEY

N-24

-73-

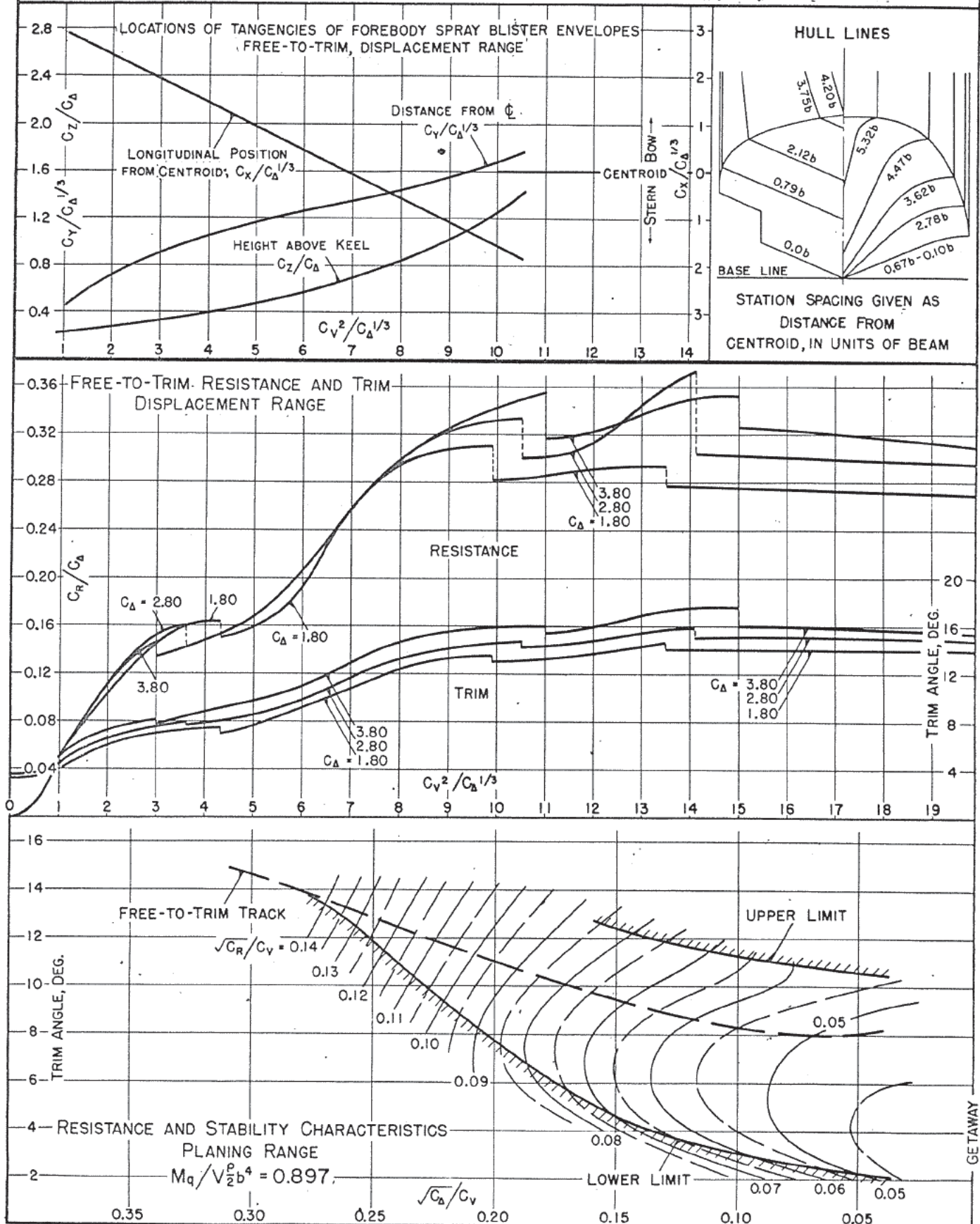
R-312

-84-

### SUMMARY CHART OF PRINCIPAL HYDRODYNAMIC CHARACTERISTICS

DATE: JULY 16, 1945 C.G. = 0.35 b FWD. OF CENTROID  $C_{d_0} = 2.80$  (NOMINAL)  
 MODEL BEAM: 5.40"  $C_G = 0.90$  b ABOVE KEEL  $k/L = 0.211$

DESIGNATION: 10-58-16.67  
 MODEL NO. 686



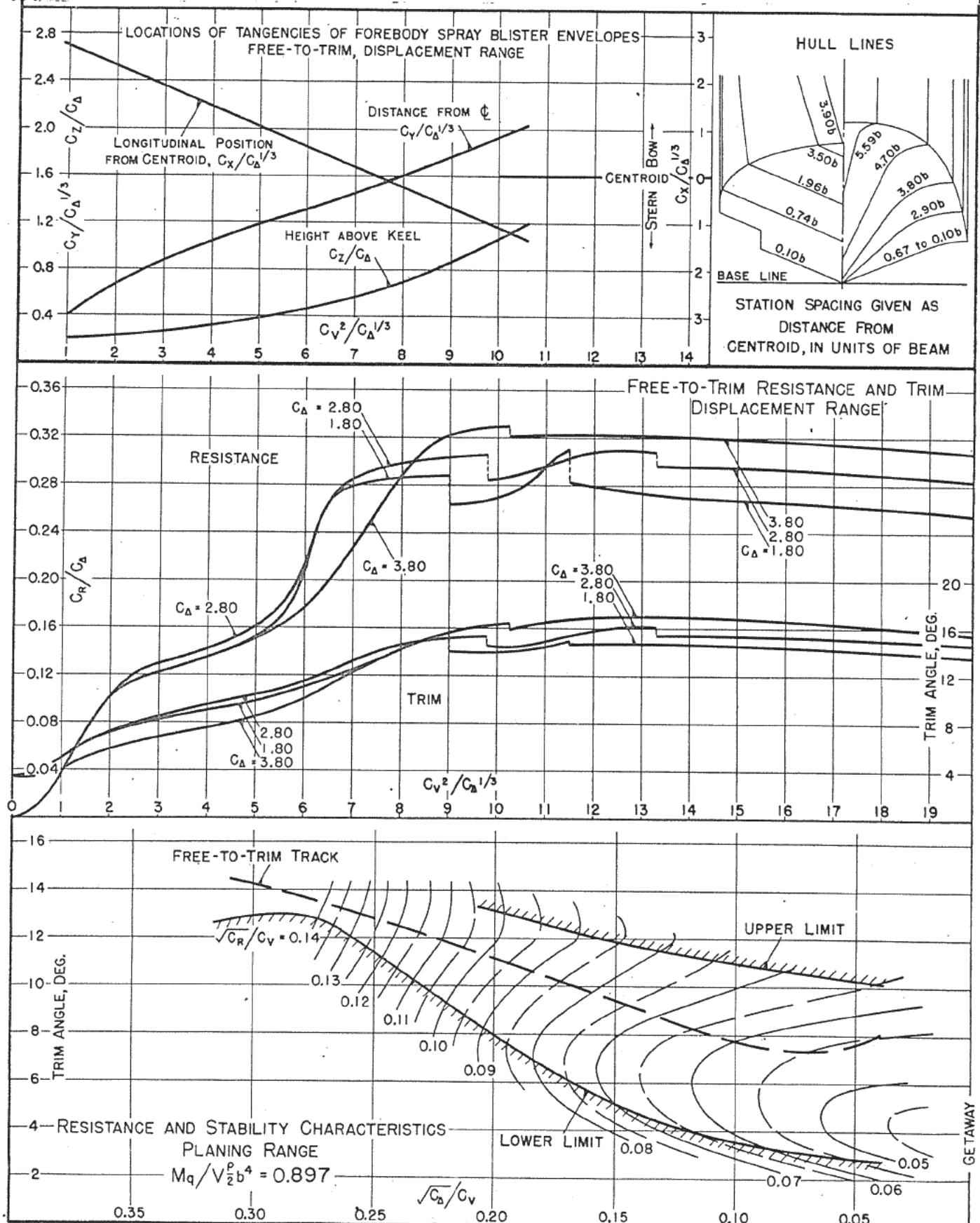


# SUMMARY CHART OF PRINCIPAL HYDRODYNAMIC CHARACTERISTICS

DATE: JULY 19, 1945  
 MODEL BEAM: 5.40"

C.G. = 0.35 b FWD. OF CENTROID  $C_{D0} = 2.80$  (NOMINAL)  
 0.90 b ABOVE KEEL  $k/L = 0.211$

DESIGNATION: 10-61-10  
 MODEL NO. 687



NATIONAL ADVISORY COMMITTEE FOR AERONAUTICS  
INVESTIGATION CONDUCTED BY  
EXPERIMENTAL TOWING TANK-STEVENS INSTITUTE OF TECHNOLOGY  
HOBOKEN, NEW JERSEY

N-24

-77-

R-3

-86

### SUMMARY CHART OF PRINCIPAL HYDRODYNAMIC CHARACTERISTICS

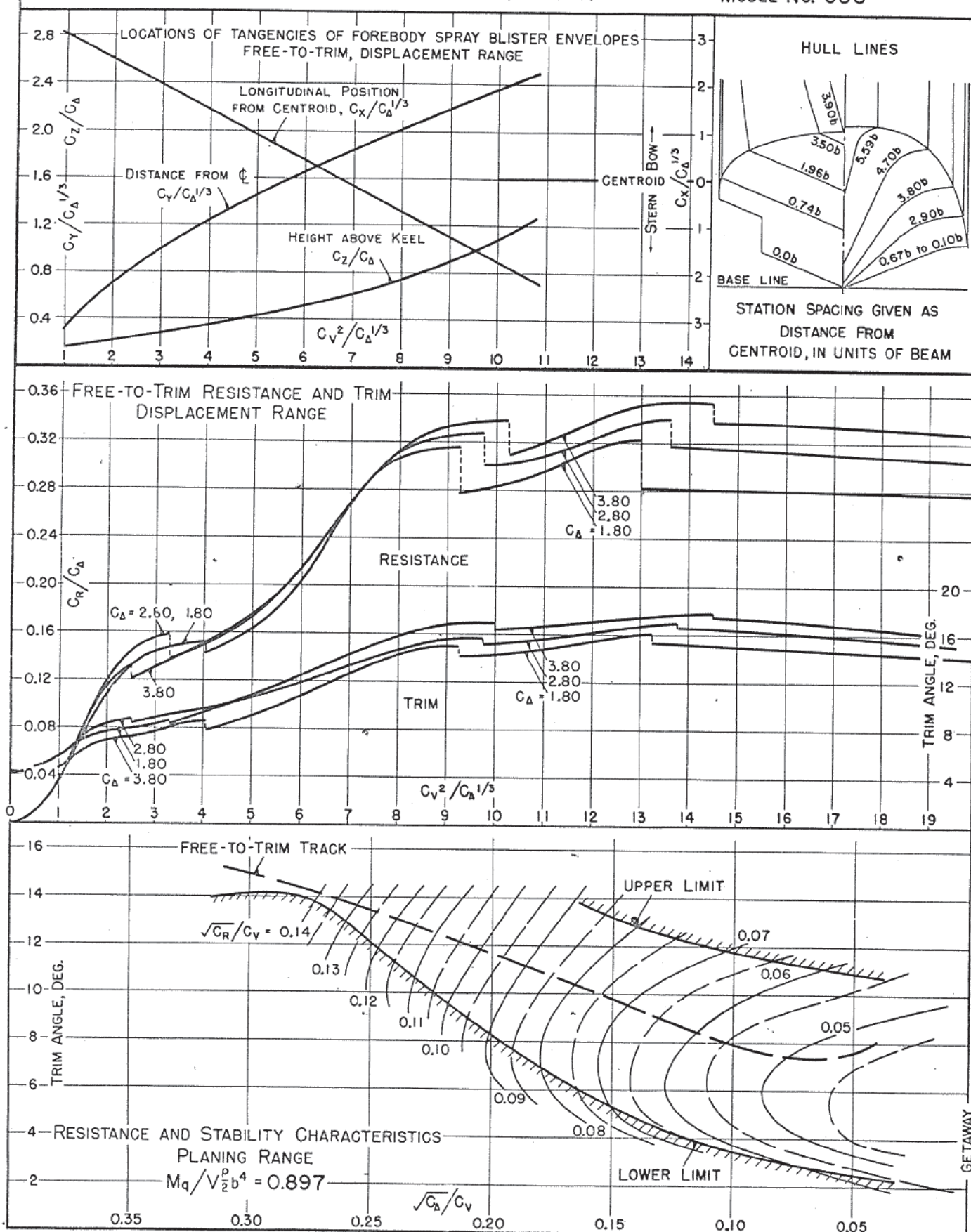
DATE: JULY 20, 1945

MODEL BEAM: 5.40"

C.G. = 0.35 b FWD. OF CENTROID  $C_{D_0} = 2.80$  (NOMINAL)  
0.90 b ABOVE KEEL  $k/L = 0.211$

DESIGNATION: 10-61-16.67

MODEL NO. 688







# NATIONAL ADVISORY COMMITTEE FOR AERONAUTICS

TECHNICAL NOTE

No. 1182

**CASE FILE  
COPY**

A COLLECTION OF THE COLLAPSED RESULTS  
OF GENERAL TANK TESTS OF MISCELLANEOUS  
FLYING-BOAT-HULL MODELS

By F. W. S. Locke, Jr.

Bureau of Aeronautics, Navy Department



Washington

March 1947

| Model No.   | Designation       |      |                | L/b  | L <sub>a</sub> /b | L <sub>T</sub> /L | h<br>φ b | α<br>(deg) | σ<br>(deg) | β <sub>a</sub> max | Center-of-gravity position |         | Model<br>beam<br>(in.) | Remarks                            | Source   | Fig. |
|-------------|-------------------|------|----------------|------|-------------------|-------------------|----------|------------|------------|--------------------|----------------------------|---------|------------------------|------------------------------------|----------|------|
|             | L <sub>T</sub> /b | h/σ  | P <sub>T</sub> |      |                   |                   |          |            |            |                    | Fwd/b                      | above/b |                        |                                    |          |      |
|             |                   |      |                |      |                   |                   |          |            |            |                    |                            |         |                        |                                    |          |      |
| NACA MODELS |                   |      |                |      |                   |                   |          |            |            |                    |                            |         |                        |                                    |          |      |
| 11          | 2.82              | 0.43 | 22.5           | 4.47 | 1.65              | 0.630             | 3.31     | 6.5        | 7.63       | 22.5               | 0.36                       | 1.19    | 17.00                  | Longitudinally concave forebody    | TN 464   | 1    |
| 11-A        | 2.82              | .43  | 22.5           | 4.47 | 1.65              | .630              | 3.31     | 6.5        | 7.63       | 22.5               | .36                        | 1.19    | 17.00                  |                                    | TN 470   | 2    |
| 11-B        | 2.82              | .32  | 22.5           | 4.47 | 1.65              | .630              | 3.31     | 9.0        | 10.13      | 22.5               | .47                        | .91     | 17.00                  |                                    | TN 545   | 3    |
| 11-C        | 2.82              | .43  | 22.5           | 4.47 | 1.65              | .630              | 3.31     | 6.5        | 7.63       | 22.5               | .47                        | .91     | 17.00                  |                                    | TN 535   | 4    |
| 11-C-7      | 2.82              | .76  | 22.5           | 4.47 | 1.65              | .630              | 3.31     | 3.5        | 4.35       | 22.5               | .47                        | .91     | 17.00                  |                                    | TN 541   | 5    |
| 11-C-8      | 2.82              | .55  | 22.5           | 4.47 | 1.65              | .630              | 3.31     | 5.0        | 6.00       | 22.5               | .47                        | .91     | 17.00                  |                                    | TN 541   | 6    |
| 11-C-9      | 2.82              | .36  | 22.5           | 4.47 | 1.65              | .630              | 3.31     | 8.0        | 9.13       | 22.5               | .47                        | .91     | 17.00                  |                                    | TN 541   | 7    |
| 11-C-10     | 2.82              | .30  | 22.5           | 4.47 | 1.65              | .630              | 3.31     | 10.0       | 11.10      | 22.5               | .47                        | .91     | 17.00                  |                                    | TN 541   | 8    |
| 11-C-11     | 2.82              | .11  | 22.5           | 4.47 | 1.65              | .630              | .74      | 6.5        | 6.73       | 22.5               | .47                        | .91     | 17.00                  |                                    | TN 535   | 9    |
| 11-C-12     | 2.82              | .26  | 22.5           | 4.47 | 1.65              | .630              | 1.84     | 6.5        | 7.12       | 22.5               | .47                        | .91     | 17.00                  |                                    | TN 535   | 10   |
| 11-C-13     | 2.82              | .69  | 22.5           | 4.47 | 1.65              | .630              | 5.88     | 6.5        | 8.50       | 22.5               | .47                        | .91     | 17.00                  | 30° Swallow-tail step              | TN 535   | 11   |
| 11-C-30° S  | 2.87              | .61  | 22.5           | 4.47 | 1.60              | .643              | 4.31     | 6.5        | 7.08       | 22.5               | .52                        | .91     | 17.00                  |                                    | TN 539   | 12   |
| 11-C-45° V  | 2.74              | .27  | 22.5           | 4.47 | 1.73              | .613              | 2.41     | 6.5        | 9.00       | 22.5               | .39                        | .91     | 17.00                  |                                    | TN 539   | 13   |
| 11-E        | 2.82              | .75  | 7.5            | 4.47 | 1.65              | .630              | 5.76     | 6.5        | 7.63       | 22.5               | .47                        | .91     | 17.00                  | Two longitudinal steps on forebody | TN 574   | 14   |
| 11-F        | 2.82              | .75  | 14.8           | 4.47 | 1.65              | .630              | 5.70     | 6.5        | 7.63       | 22.5               | .47                        | .91     | 17.00                  |                                    | TN 574   | 15   |
| 11-G        | 2.82              | .43  | 22.5           | 4.47 | 1.65              | .630              | 3.31     | 6.5        | 7.63       | 22.5               | .47                        | .91     | 17.00                  | Some chine flare on forebody       | TN 531   | 16   |
| 11-M        | 2.82              | .75  | 18.7           | 4.47 | 1.65              | .630              | 5.76     | 6.5        | 7.63       | 22.5               | .47                        | .91     | 17.00                  |                                    | TN 574   | 17   |
| 11-N        | 2.82              | .75  | 7.5            | 4.47 | 1.65              | .630              | 5.76     | 6.5        | 7.63       | 22.5               | .47                        | .91     | 17.00                  | One longitudinal step on forebody  | TN 574   | 18   |
| 12          | 3.00              | .44  | 22.5           | 4.75 | 1.75              | .630              | 3.31     | 6.5        | 7.57       | 22.5               | .39                        | 1.19    | 17.00                  |                                    | TN 491   | 19   |
| 13          | 2.64              | .43  | 22.5           | 4.18 | 1.54              | .630              | 3.31     | 6.5        | 7.73       | 22.5               | .34                        | 1.19    | 17.00                  | TN 491                             | 20       |      |
| 14          | 2.52              | .39  | 20.3           | 4.00 | 1.48              | .630              | 2.95     | 6.5        | 7.63       | 20.3               | .32                        | 1.07    | 19.00                  | TN 491                             | 21       |      |
| 15          | 3.20              | .49  | 25.1           | 5.07 | 1.87              | .630              | 3.73     | 6.5        | 7.63       | 25.1               | .41                        | 1.35    | 15.00                  | TN 491                             | 22       |      |
| 16          | 2.44              | .56  | 23.0           | 5.00 | 2.56              | .488              | 4.85     | 8.0        | 8.65       | 20.0               | 0                          | 1.03    | 15.42                  | TN 471                             | 23       |      |
| 18          | 2.84              | .51  | 22.5           | 4.67 | 1.83              | .608              | 3.8      | 6.25       | 7.5        | 22.5               | .49                        | .78     | 16.84                  | TN 681                             | 24       |      |
| 22          | 2.12              | 2.88 | 10.0           | 4.47 | 2.36              | .475              | 17.3     | 0          | 6.0        | 10.0               | -.23                       | .80     | 17.00                  | TN 488                             | 25       |      |
| 22-A        | 2.28              | 2.88 | 10.0           | 4.64 | 2.36              | .492              | 17.3     | 0          | 6.0        | 10.0               | 0                          | .80     | 17.00                  | Pointed step                       | TN 504   | 26   |
| 26          | 2.75              | .45  | 22.0           | 4.53 | 1.78              | .607              | 3.2      | 6.55       | 7.03       | 22.0               | .24                        | .82     | 17.86                  |                                    | TN 512   | 27   |
| 27          | ∞                 | ∞    | 0.0            |      |                   |                   |          |            |            |                    |                            |         | 16.00                  | Planing surface                    | TN 509   | 28   |
| 28          | ∞                 | ∞    | 10.0           |      |                   |                   |          |            |            |                    |                            |         | 16.00                  |                                    | TN 509   | 29   |
| 29          | ∞                 | ∞    | 20.0           |      |                   |                   |          |            |            |                    |                            |         | 16.00                  | -----do-----                       | TN 509   | 30   |
| 30          | ∞                 | ∞    | 30.0           |      |                   |                   |          |            |            |                    |                            |         | 16.00                  |                                    | TN 509   | 31   |
| 35          | 2.92              | 3.77 | 15.0           | 6.15 | 2.45              | .475              | 22.6     | 0          | 6.0        | 15.0               | .08                        | .97     | 13.00                  | Pointed step                       | TN 551   | 32   |
| 35-A        | 2.92              | 3.77 | 20.0           | 6.15 | 3.23              | .475              | 22.6     | 0          | 6.0        | 20.0               | .08                        | .97     | 13.00                  |                                    | TN 551   | 33   |
| 35-B        | 2.92              | 3.77 | 25.0           | 6.15 | 3.23              | .475              | 22.6     | 0          | 6.0        | 25.0               | .08                        | .97     | 13.00                  | -----do-----                       | TN 551   | 34   |
| 36          | 3.57              | .55  | 20.0           | 5.71 | 2.14              | .625              | 4.0      | 6.25       | 7.35       | 20.0               | .71                        | 1.00    | 14.00                  |                                    | TN 638   | 35   |
| 40-AC       | 3.12              | .44  | 20.0           | 5.57 | 2.45              | .560              | 3.7      | 7.5        | 8.5        | 20.0               | .30                        | 1.12    | 13.47                  | Rep. 543                           | Rep. 543 | 36   |
| 40-AD       | 3.12              | .44  | 20.0           | 5.57 | 2.45              | .560              | 3.7      | 8.5        | 8.5        | 20.0               | .30                        | 1.12    | 13.47                  |                                    | Rep. 543 | 37   |
| 40-AE       | 3.12              | .41  | 20.0           | 7.43 | 4.31              | .420              | 3.7      | 8.5        | 9.1        | 20.0               | .30                        | 1.12    | 13.47                  | Rep. 543                           | Rep. 543 | 38   |
| 40-BC       | 3.12              | .44  | 20.0           | 5.57 | 2.45              | .560              | 3.7      | 7.5        | 8.5        | 20.0               | .30                        | 1.12    | 13.47                  |                                    | Rep. 543 | 39   |
| 40-BE       | 3.12              | .41  | 20.0           | 7.43 | 4.31              | .420              | 3.7      | 8.5        | 9.1        | 20.0               | .30                        | 1.12    | 13.47                  | Rep. 543                           | 40       |      |

NACA TN No. 1182

13

| Model No.   | Designation       |      |                | L/p   | L <sub>R</sub> /b | L <sub>g</sub> /L | h/b  | α (deg) | σ (deg) | β <sub>max</sub> | Center-of-gravity position |         | Model beam (in.) | Remarks                       | Source     | Fig. |
|-------------|-------------------|------|----------------|-------|-------------------|-------------------|------|---------|---------|------------------|----------------------------|---------|------------------|-------------------------------|------------|------|
|             | L <sub>g</sub> /b | h/σ  | β <sub>f</sub> |       |                   |                   |      |         |         |                  | fwd/b                      | above/b |                  |                               |            |      |
| NACA MODELS |                   |      |                |       |                   |                   |      |         |         |                  |                            |         |                  |                               |            |      |
| 41-A        | 3.56              | 0.86 | 26.0           | 5.98  | 2.42              | 0.595             | 7.75 | 7.5     | 9.0     | 26.0             | 0.44                       | 2.04    | 12.00            |                               | TN 563     | 41   |
| 41-D        | 3.58              | .98  | 26.0           | 6.00  | 2.42              | .597              | 7.75 | 6.0     | 7.9     | 26.0             | .58                        | 2.04    | 12.00            |                               | TN 656     | 42   |
| 44          | 2.76              | .51  | 22.5           | 4.48  | 1.72              | .616              | 3.1  | 5.0     | 6.1     | 22.5             | .48                        | .97     | 17.00            |                               | TN 566     | 43   |
| 46          | 2.60              | .98  | -2.0           | 5.24  | 2.64              | .497              | 6.8  | 4.6     | 6.92    | 24.0             | 0                          | .80     | 14.24            |                               | TN 635     | 44   |
| 47          | 2.38              | .38  | 26.0           | 4.68  | 2.30              | .509              | 3.45 | 8.0     | 9.0     | 25.0             | .13                        | 1.31    | 16.26            |                               | TN 590     | 45   |
| 52          | 2.76              | .47  | 22.5           | 3.62  | .86               | .773              | 4.0  | 5.8     | 8.5     | 22.5             | .44                        | .88     | 17.00            |                               | TN 576     | 46   |
| 57-A        | 3.37              | .85  | 20.0           | 6.74  | 3.37              | .500              | 6.8  | 7.0     | 8.25    | 25.0             | .36                        | 1.93    | 12.45            |                               | TN 716     | 47   |
| 57-B        | 3.37              | .85  | 25.0           | 6.74  | 3.37              | .500              | 6.8  | 7.0     | 8.25    | 25.0             | .36                        | 1.93    | 12.45            |                               | TN 716     | 48   |
| 57-B-5      | 4.17              | .85  | 25.0           | 7.54  | 3.37              | .555              | 6.8  | 7.0     | 8.25    | 25.0             | .36                        | 1.93    | 12.45            |                               | TN 716     | 49   |
| 57-C        | 3.37              | .85  | 30.0           | 6.74  | 3.37              | .500              | 6.8  | 7.0     | 8.25    | 30.0             | .36                        | 1.93    | 12.45            |                               | TN 716     | 50   |
| 61-A        | 3.73              | 4.09 | 26.0           | 6.70  | 2.97              | .556              | 24.5 | 0       | 6.0     | 26.0             | .45                        | 2.04    | 12.00            | Pointed step                  | TN 656     | 51   |
| 62-AD       | 2.82              | .36  | 22.5           | 4.59  | 1.77              | .615              | 3.3  | 9.0     | 9.15    | 22.5             | .37                        | .91     | 17.00            |                               | TN 725     | 52   |
| 66          | 2.34              | .47  | 26.0           | 4.49  | 2.15              | .522              | 4.6  | 7.5     | 8.8     | 30.5             | .08                        | .96     | 21.60            | 30° V-step                    | TN 858     | 53   |
| 73          | 3.73              | 4.09 | 26.0           | 6.70  | 2.97              | .556              | 24.5 | 0       | 6.0     | 26.0             | .45                        | 2.04    | 12.00            | Paired pointed step           | TN 656     | 54   |
| 74-A        | 3.15              | .26  | R              | 5.24  | 2.09              | .601              | 1.95 | 6.8     | 7.5     | R                | .45                        | .93     | 15.92            | Circular bottom               | TN 668     | 55   |
| 75          | 2.87              | 2.44 | 20.0           | 5.42  | 2.55              | .530              | 19.5 | 1.5     | 8.0     | 20.0             | .17                        | .98     | 15.90            | Paired pointed step           | TN 668     | 56   |
| 83          | 3.09              | .63  | 25.0           | 4.58  | 1.49              | .675              | 2.6  | 2.2     | 4.15    | 37.0             | .42                        | .72     | 17.70            |                               | TN 836     | 57   |
| 84-AF       | 3.24              | .34  | 20.0           | 5.38  | 2.14              | .603              | 2.58 | 6.8     | 7.5     | 20.0             | .46                        | 1.16    | 15.92            |                               | ARR 3115   | 58   |
| 84-EF-1     | 3.24              | .34  | 20.0           | 5.38  | 2.14              | .603              | 2.58 | 6.8     | 7.5     | 20.0             | .46                        | 1.16    | 15.92            |                               | ARR 3115   | 59   |
| 84-EF-3     | 3.24              | .57  | 20.0           | 5.38  | 2.14              | .603              | 4.52 | 6.8     | 7.9     | 20.0             | .46                        | 1.16    | 15.92            |                               | ARR 3115   | 60   |
| 84-EF-4     | 3.24              | .47  | 20.0           | 5.38  | 2.14              | .603              | 4.52 | 8.5     | 9.6     | 20.0             | .46                        | 1.16    | 15.92            |                               | ARR 3115   | 61   |
| 126A-1      | 2.82              | .88  | 17.5           | 5.04  | 2.22              | .560              | 5.0  | 5.0     | 5.7     | 17.5             | .31                        | 1.17    | 14.00            |                               | ARR 3B23   | 62   |
| 126A-2      | 2.82              | .58  | 17.5           | 5.04  | 2.22              | .560              | 5.0  | 7.5     | 8.7     | 17.5             | .31                        | 1.17    | 14.00            |                               | ARR 3B23   | 63   |
| 126A-3      | 2.82              | .47  | 17.5           | 5.04  | 2.22              | .560              | 5.0  | 9.3     | 10.6    | 17.5             | .31                        | 1.17    | 14.00            |                               | ARR 3B23   | 64   |
| 126B-1      | 2.82              | .88  | 22.5           | 5.04  | 2.22              | .560              | 5.0  | 5.0     | 5.7     | 22.5             | .31                        | 1.17    | 14.00            |                               | ARR 3B23   | 65   |
| 126B-2      | 2.82              | .58  | 22.5           | 5.04  | 2.22              | .560              | 5.0  | 7.5     | 8.7     | 22.5             | .31                        | 1.17    | 14.00            |                               | ARR 3B23   | 66   |
| 126B-3      | 2.82              | .47  | 22.5           | 5.04  | 2.22              | .560              | 5.0  | 9.3     | 10.6    | 22.5             | .31                        | 1.17    | 14.00            |                               | ARR 3B23   | 67   |
| 126C-1      | 2.82              | .88  | 27.5           | 5.04  | 2.22              | .560              | 5.0  | 5.0     | 5.7     | 27.5             | .31                        | 1.17    | 14.00            |                               | ARR 3B23   | 68   |
| 126C-2      | 2.82              | .58  | 27.5           | 5.04  | 2.22              | .560              | 5.0  | 7.5     | 8.7     | 27.5             | .31                        | 1.17    | 14.00            |                               | ARR 3B23   | 69   |
| 126C-3      | 2.82              | .47  | 27.5           | 5.04  | 2.22              | .560              | 5.0  | 9.3     | 10.6    | 27.5             | .31                        | 1.17    | 14.00            |                               | ARR 3B23   | 70   |
| 144         | 3.14              | .74  | 20.0           | 5.23  | 2.09              | .601              | 6.28 | 6.8     | 8.45    | 20.0             | .45                        | 1.13    | 15.92            |                               | ARR 3J23   | 71   |
| 145         | 3.94              | .85  | 20.0           | 6.54  | 2.60              | .601              | 7.02 | 6.8     | 8.27    | 20.0             | .51                        | 1.26    | 14.24            |                               | ARR 3J23   | 72   |
| 146         | 4.71              | .95  | 20.0           | 7.84  | 3.13              | .601              | 7.70 | 6.8     | 8.14    | 20.0             | .55                        | 1.38    | 13.00            |                               | ARR 3J23   | 73   |
| 184         | 5.80              | .66  | 20.0           | 10.50 | 4.70              | .553              | 5.0  | 7.0     | 7.60    | 20.0             | .46                        | 1.40    | 11.81            |                               | ARR 15G19  | 74   |
| 185         | 5.80              | .66  | 24.5           | 10.50 | 4.70              | .553              | 5.0  | 7.0     | 7.60    | 24.5             | .46                        | 1.40    | 11.81            |                               | ARR 15G19  | 75   |
| 185-A       | 5.80              | 1.22 | 24.5           | 10.50 | 4.70              | .553              | 10.0 | 7.0     | 8.20    | 24.5             | .46                        | 1.40    | 11.81            | 45° V-step                    | ARR 15G19  | 76   |
| 207         | 3.78              | 1.10 | 25.0           | 7.00  | 3.22              | .540              | 9.0  | 8.3     | 9.90    | 35.0             | .31                        | .83     | 14.74            | With chine flare on afterbody | RMR 15H06a | 77   |
| 207A        | 3.78              | 1.06 | 25.0           | 7.00  | 3.22              | .540              | 9.0  | 8.3     | 9.57    | 35.0             | .31                        | .83     | 14.74            | Chine lowered near bow        | RMR 15H06a | 78   |
| 207C        | 3.78              | 1.06 | 25.0           | 7.00  | 3.22              | .540              | 9.0  | 8.3     | 9.57    | 35.0             | .31                        | .83     | 14.74            |                               | RMR 15H06a | 79   |

| Model No.   | Designation       |      |                | L/b  | L <sub>g</sub> /b | L <sub>T</sub> /L | h/b  | α (deg) | σ (deg) | β <sub>a</sub> max | Center-of-gravity position fwd/b | Model beam (in.) | Remarks   | Source      | Fig. |
|---|-------------------|------|----------------|------|-------------------|-------------------|------|---------|---------|--------------------|----------------------------------|------------------|---|-------------|------|
|   | RAE MODELS        |      |                |      |                   |                   |      |         |         |                    |                                  |                  |   |             |      |
|   | L <sub>f</sub> /b | h/a  | β <sub>r</sub> |      |                   |                   |      |         |         |                    |                                  |                  |   |             |      |
| L/b = 5.5<br>L/b = 7.0<br>L/b = 8.5<br>L/b = 10.5<br>Shetland | 2.31              | 0.38 | 20.0           | 4.47 | 2.16              | 0.516             | 3.07 | 7.3     | 8.11    | 20.0               | 0.18                             | 10.92            | Paired transverse step<br>-----do-----<br>Fully faired step<br>Parabolic step | BA 1350     | 80   |
|   | 2.94              | .48  | 20.0           | 5.70 | 2.76              | .516              | 3.91 | 7.3     | 8.11    | 20.0               | .23                              | 8.56             |   | BA 1350     | 81   |
|   | 3.57              | .58  | 20.0           | 6.91 | 3.34              | .516              | 4.75 | 7.3     | 8.11    | 20.0               | .28                              | 7.06             |   | BA 1350     | 82   |
|   | 4.20              | .69  | 20.0           | 8.14 | 3.94              | .516              | 5.58 | 7.3     | 8.11    | 20.0               | .32                              | 6.00             |   | BA 1350     | 83   |
|   | 3.69              | 1.06 | 27.0           | 7.29 | 3.67              | .497              | 10.0 | 7.2     | 9.0     | 37.0               | .24                              | 7.17             |   | Aero 1745   | 84   |
| N2/42-A1  | 2.85              | 1.30 | 21.5           | 6.40 | 3.55              | .445              | 11.0 | 6.5     | 8.5     | 26.0               | .16                              | 6.64             | Paired transverse step  | Aero 1858   | 85   |
| N2/42-Q   | 2.87              | 1.11 | 20.0           | 6.40 | 3.53              | .448              | 9.5  | 6.8     | 8.5     | 23.5               | .16                              | 6.56             | -----do-----  | Aero 1858   | 86   |
| OEH   | 4.02              | .98  | 27.5           | 8.28 | 4.26              | .485              | 8.6  | 7.0     | 8.8     | 42.0               | .10                              | 6.58             | Fully faired step   | Aero 2029   | 87   |
| FEH   | 4.02              | 1.09 | 27.5           | 8.28 | 4.26              | .485              | 9.9  | 7.3     | 9.1     | 42.0               | .10                              | 6.58             | Parabolic step  | Aero 2029   | 88   |
| 294-79  | 3.68              | 0.31 | 20.0           | 6.74 | 3.06              | 0.545             | 2.6  | 7.5     | 8.4     | 30.0               | 0.44                             | 5.10             |   | Unpublished | 89   |
| 339-1   | 3.32              | .62  | 20.0           | 6.07 | 2.75              | .547              | 5.0  | 7.0     | 8.00    | 20.0               | .35                              | 5.40             |   | ARR 4F15    | 90   |
| 339-15  | 3.32              | .64  | 20.0           | 6.57 | 3.25              | .505              | 5.0  | 7.0     | 7.75    | 20.0               | .35                              | 5.40             |   | Unpublished | 91   |
| 339-20  | 2.72              | .62  | 20.0           | 5.47 | 2.75              | .497              | 5.0  | 7.0     | 8.00    | 20.0               | .35                              | 5.40             |   | Unpublished | 92   |
| 339-22  | 2.72              | .61  | 20.0           | 4.97 | 2.25              | .547              | 5.0  | 7.0     | 8.25    | 20.0               | .35                              | 5.40             |   | ARR 4F15    | 93   |
| 339-23  | 3.93              | .64  | 20.0           | 7.18 | 3.25              | .547              | 5.0  | 7.0     | 7.75    | 20.0               | .35                              | 5.40             | ARR 4F15  | 94          |      |
| 339-46  | 4.54              | .67  | 20.0           | 8.29 | 3.75              | .547              | 5.0  | 7.0     | 7.50    | 20.0               | .35                              | 5.40             | ARR 4F15  | 95          |      |
| 339-49  | 3.93              | .67  | 20.0           | 7.68 | 3.75              | .513              | 5.0  | 7.0     | 7.50    | 20.0               | .35                              | 5.40             | Unpublished   | 96          |      |
| 439-1   | 3.32              | .62  | 20.0           | 6.07 | 2.75              | .547              | 5.0  | 7.0     | 8.00    | 20.0               | .43                              | 5.40             | ARR 3K11  | 97          |      |
| 439-2   | 3.32              | .62  | 10.0           | 6.07 | 2.75              | .547              | 5.0  | 7.0     | 8.00    | 10.0               | .43                              | 5.40             | ARR 3K11  | 98          |      |
| 439-3   | 3.32              | .62  | 30.0           | 6.07 | 2.75              | .547              | 5.0  | 7.0     | 8.00    | 30.0               | .43                              | 5.40             | ARR 3K11  | 99          |      |
| 406   | 3.28              | .59  | 20.0           | 6.02 | 2.74              | .545              | 5.0  | 7.5     | 8.50    | 30.0               | .37                              | 5.45             | 45° V-step  | Unpublished | 100  |
| 618-1   | 3.32              | .73  | 20.0           | 5.76 | 2.44              | .576              | 6.3  | 7.5     | 8.60    | 20.0               | .39                              | 5.40             | Straight step   | Unpublished | 101  |
| 621-2   | 3.36              | .87  | 20.0           | 6.12 | 2.76              | .549              | 8.0  | 7.5     | 9.20    | 20.0               | .40                              | 5.40             | Chine lowered fwd. afterbody warp   | Unpublished | 102  |
| 621-8   | 3.36              | .87  | 20.0           | 6.11 | 2.75              | .550              | 8.0  | 7.5     | 9.20    | 27.0               | .40                              | 5.40             |   | Unpublished | 103  |



Fig. 24

DESIGNATION: 2.84-0.51-22.5

NACA TN No. 1182

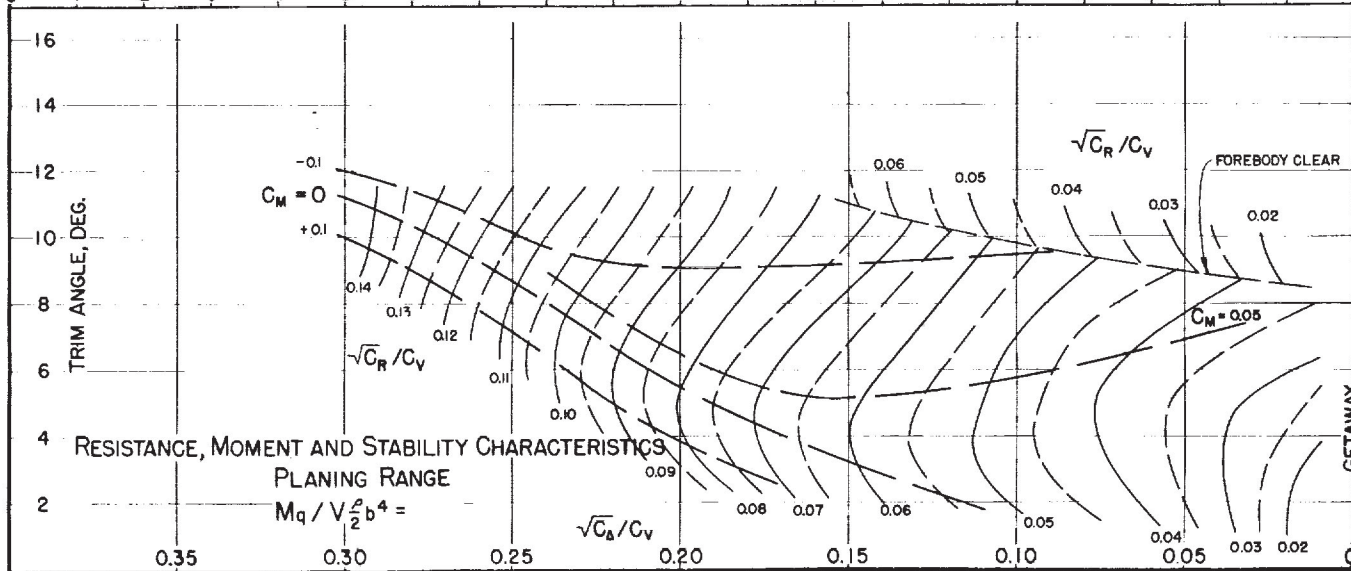
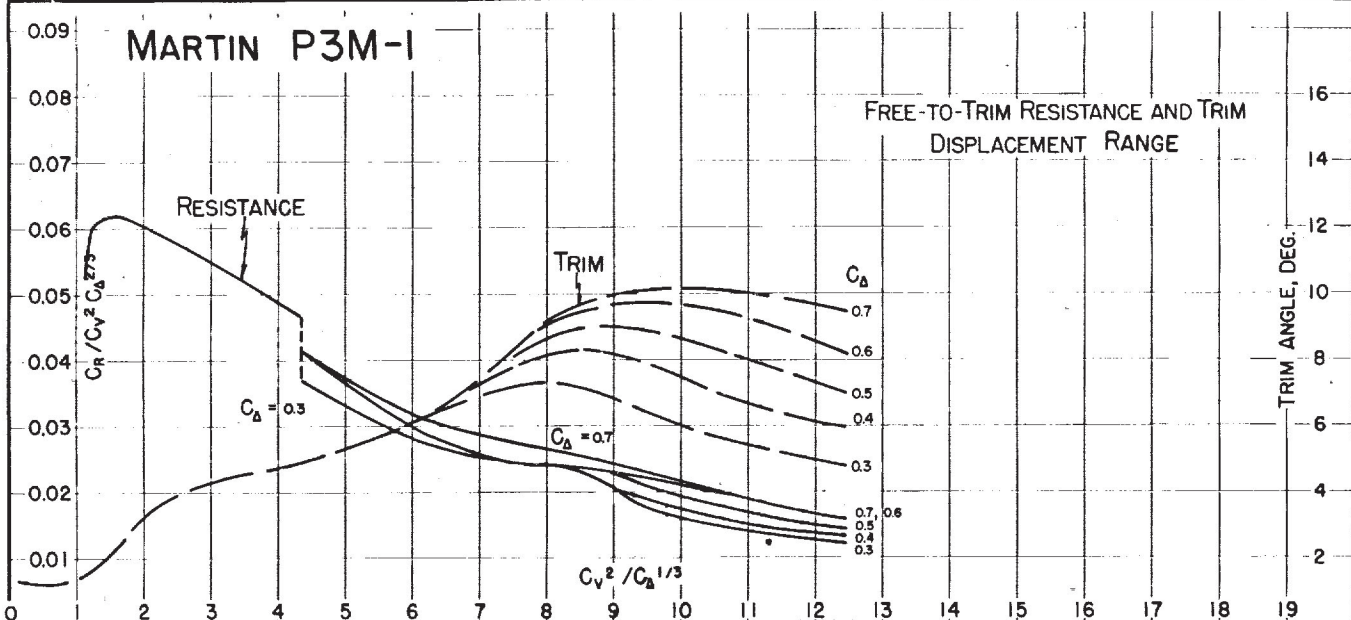
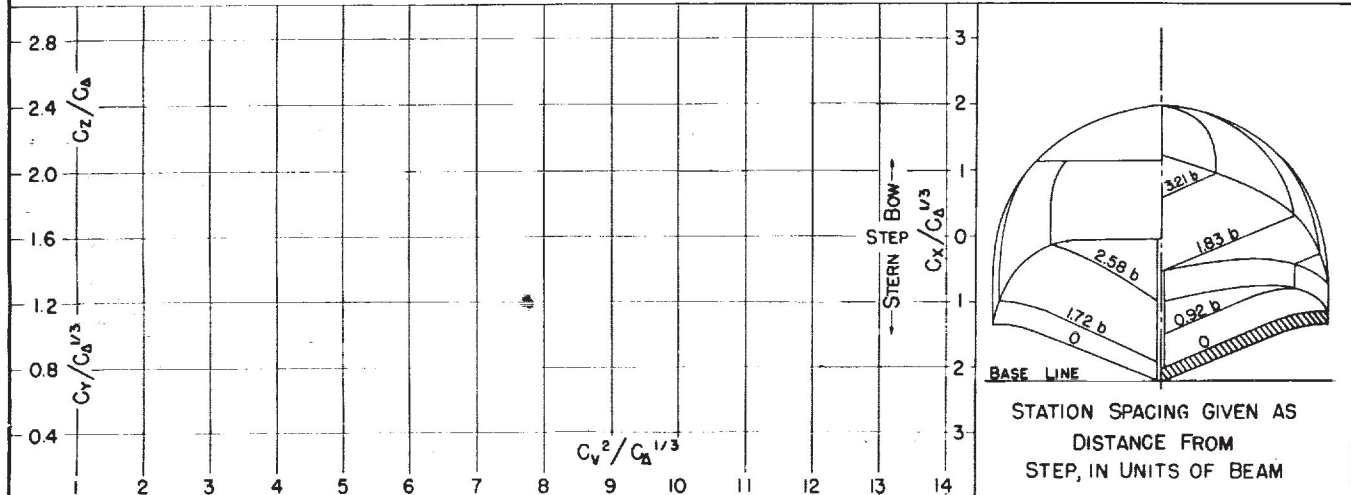
MODEL NO. 18

MODEL BEAM: 16.84"

C.G. = 0.49b FWD. OF STEP  
0.78b ABOVE KEEL $C_{d0} = 0.60$  (NOMINAL)  
 $k/L =$ 

TESTED AT NACA No. 1 TANK

DATE: 10/37



NACA TN No. 1182

DESIGNATION: 2.75-045-22.0

Fig. 27

MODEL No. 26

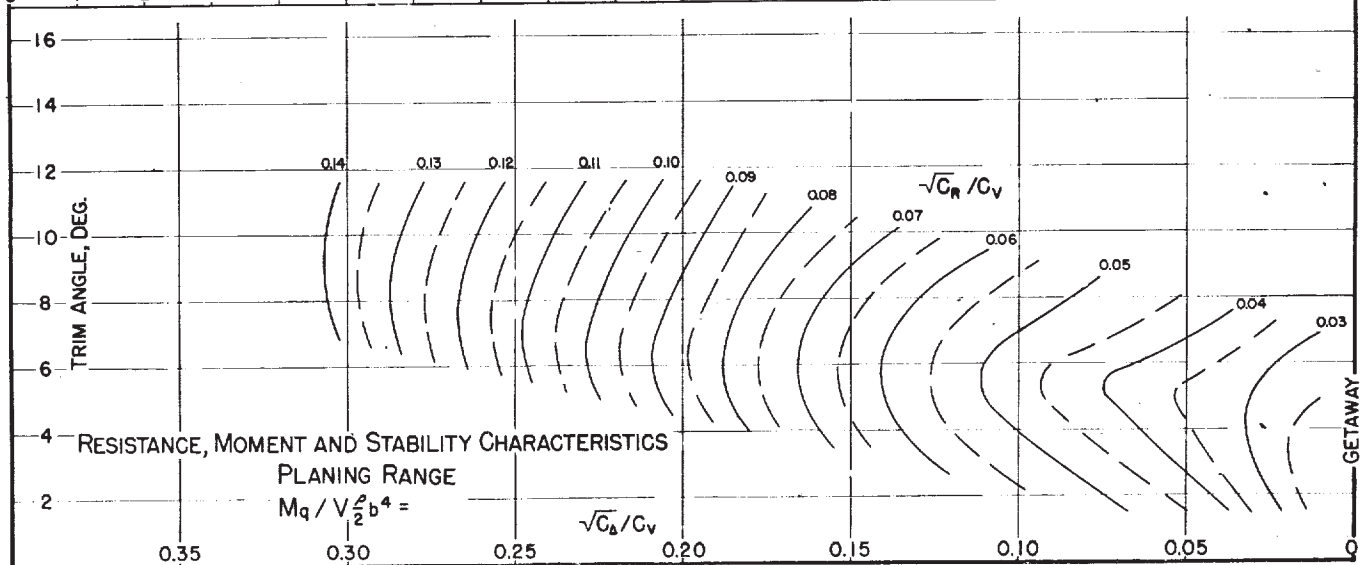
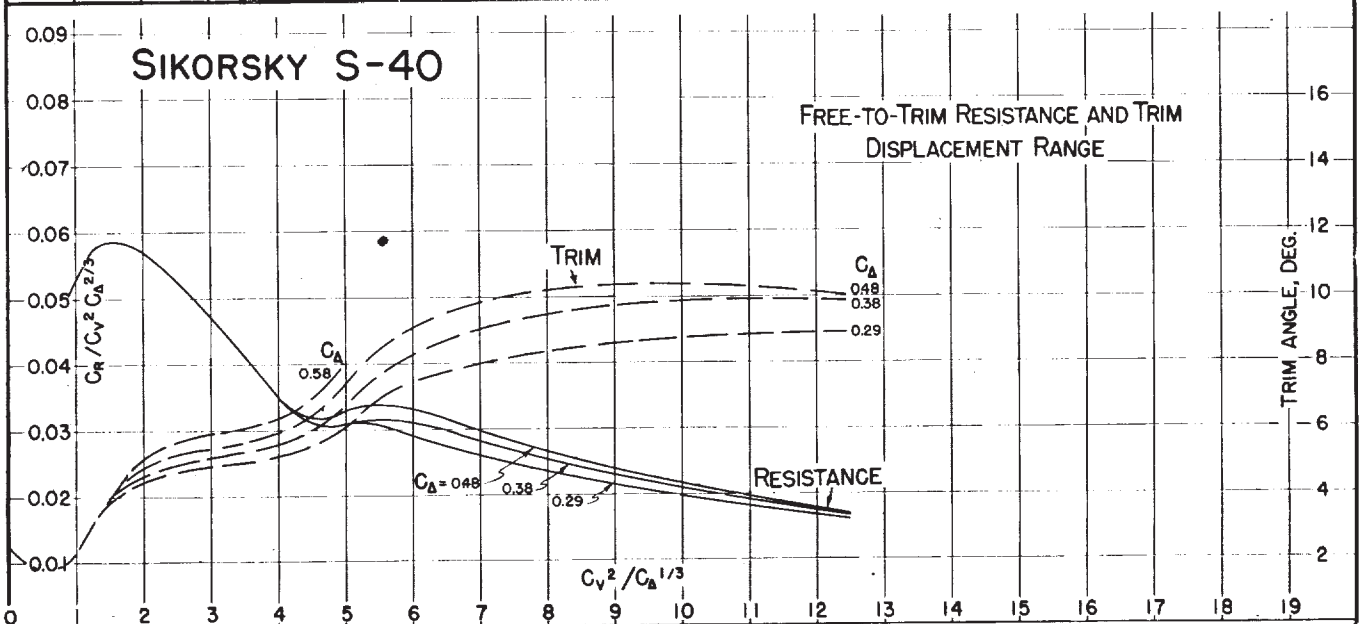
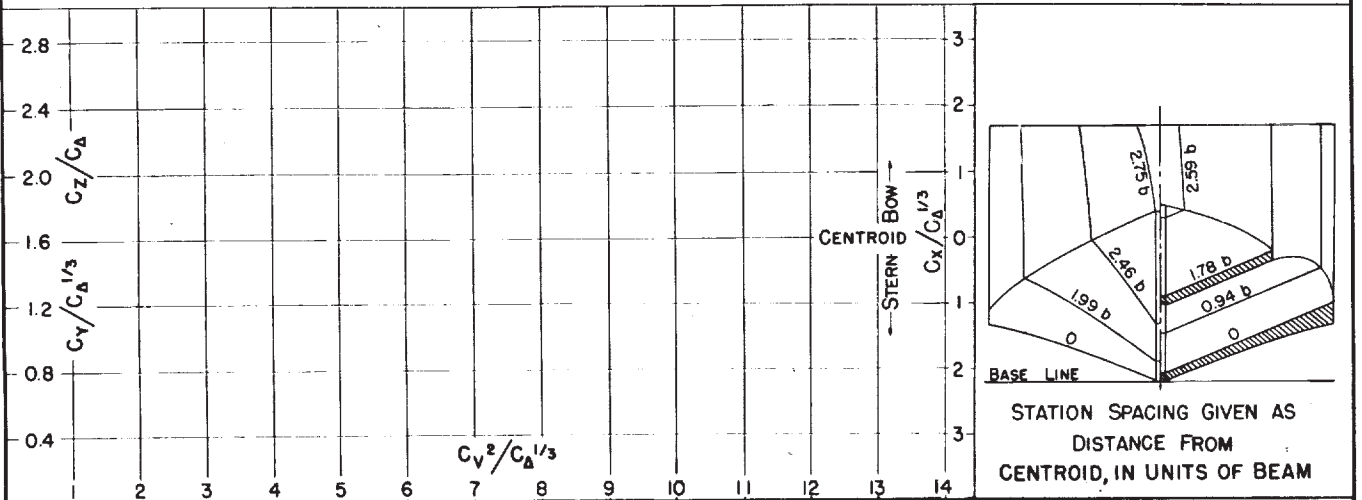
MODEL BEAM: 17.86"

 $C.G. = 0.24 b$  FWD. OF CENTROID  
 $0.82 b$  ABOVE KEEL
 $C_{d0} =$  $k/L =$ 

(NOMINAL)

TESTED AT NACA No. 1 TANK

DATE: 6/34



NACA TN No. 1182

DESIGNATION: 2.76-0.51-22.5

Fig. 43

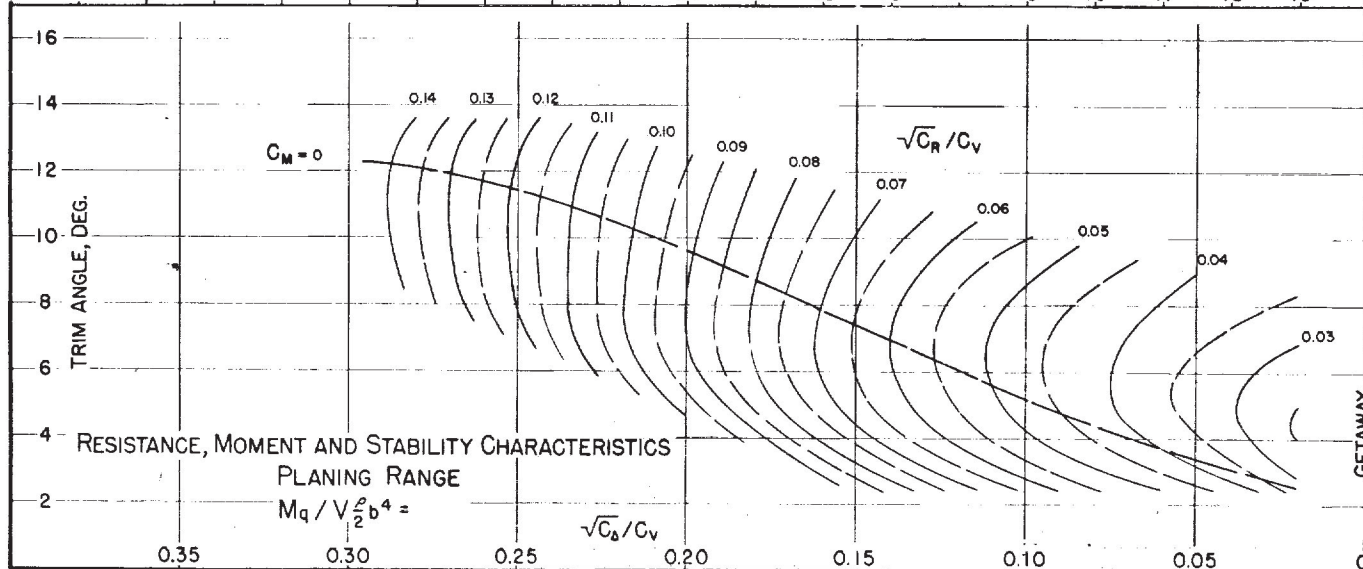
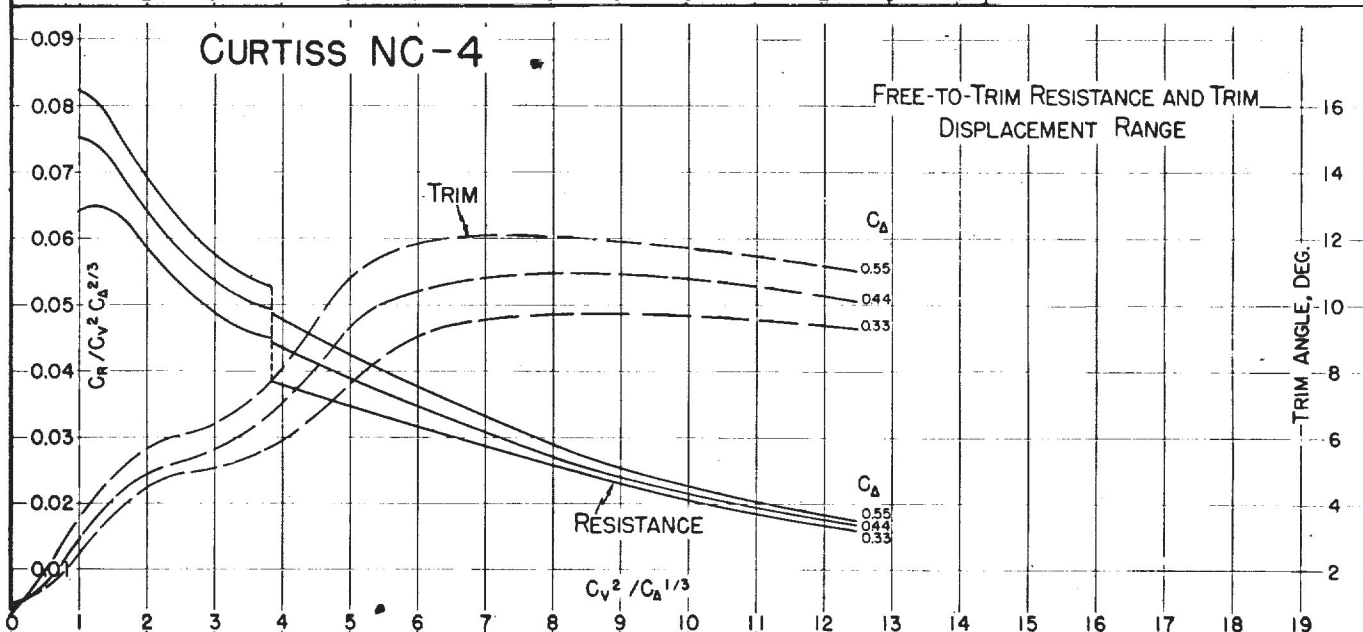
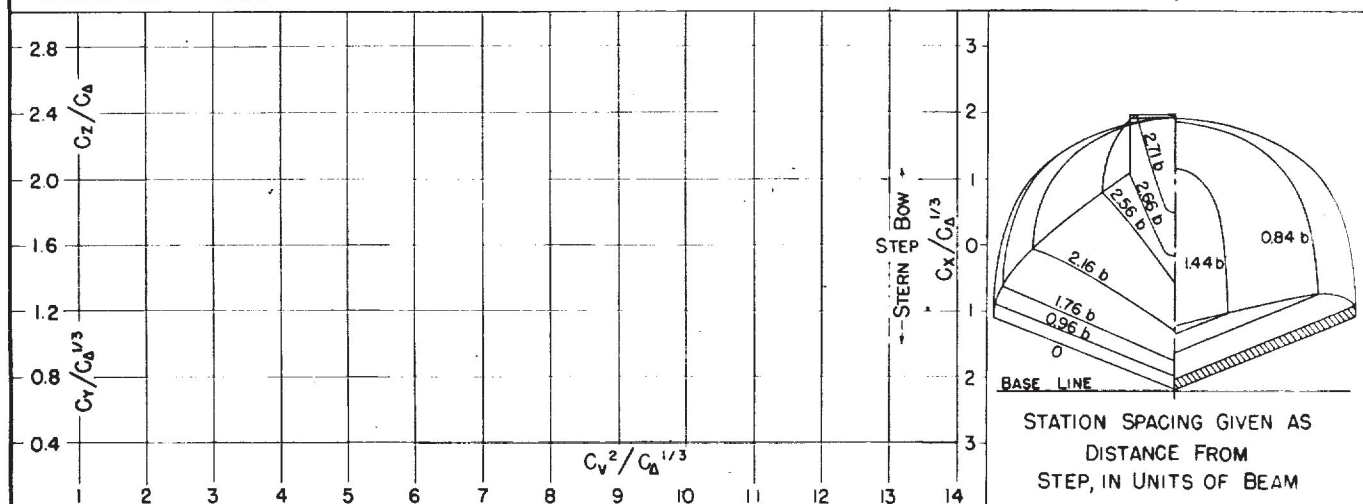
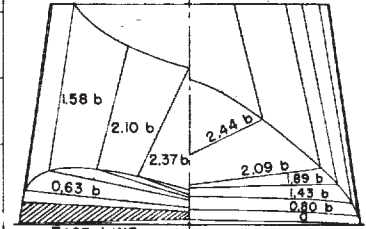
MODEL NO. 44  
MODEL BEAM: 1700"C.G. = 0.48 b FWD. OF STEP  
0.97 b ABOVE KEEL $C_{d_0} = 0.44$  (NOMINAL)  
 $k/L =$ TESTED AT NACA No. 1 TANK  
DATE: 6/35



Fig. 44

DESIGNATION: 2.60-0.98-2.0 NACA TN No. 1182

MODEL No. 46

C.G. = 0 b FWD. OF STEP  
0.80 b ABOVE KEEL $C_{d0} = 0.75$  (NOMINAL)  
 $k/L =$ TESTED AT NACA No. 1 TANK  
DATE: 2 / 35 $C_z/C_d$   
 $C_r/C_d^{1/3}$ BOW  
STEP  
STERN  
 $C_x/C_d^{1/3}$ STATION SPACING GIVEN AS  
DISTANCE FROM  
STEP, IN UNITS OF BEAM $C_v^2/C_d^{1/3}$ 

SAVOIA S-55-X

FREE-TO-TRIM RESISTANCE AND TRIM  
DISPLACEMENT RANGE

TRIM

RESISTANCE

TRIM ANGLE, DEG.

 $C_v^2/C_d^{1/3}$  $C_d$   
0.93, 0.74  
0.56  
0.37 $C_M = 0$  $\sqrt{C_R}/C_v$ RESISTANCE, MOMENT AND STABILITY CHARACTERISTICS  
PLANING RANGE $M_q / \sqrt{V} b^4 =$  $\sqrt{C_d}/C_v$ 

GETAWAY

NACA TN No. 1182

DESIGNATION: 2.38-Q38-26.0

Fig. 45

MODEL No. 47

MODEL BEAM: 16.26"

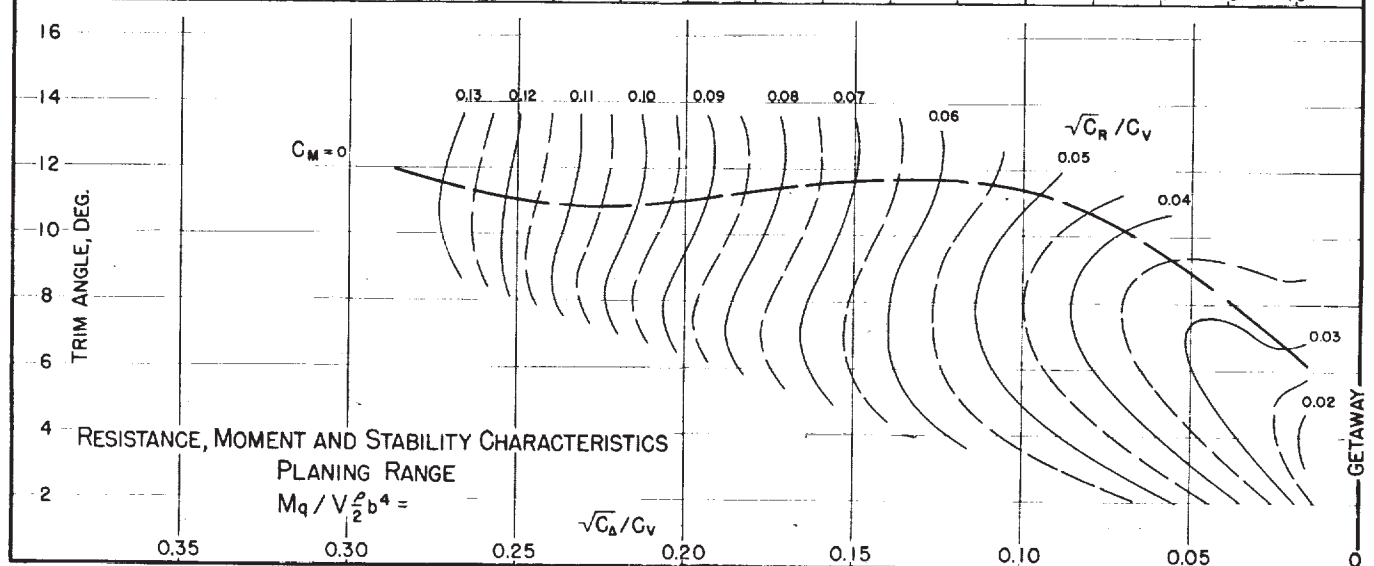
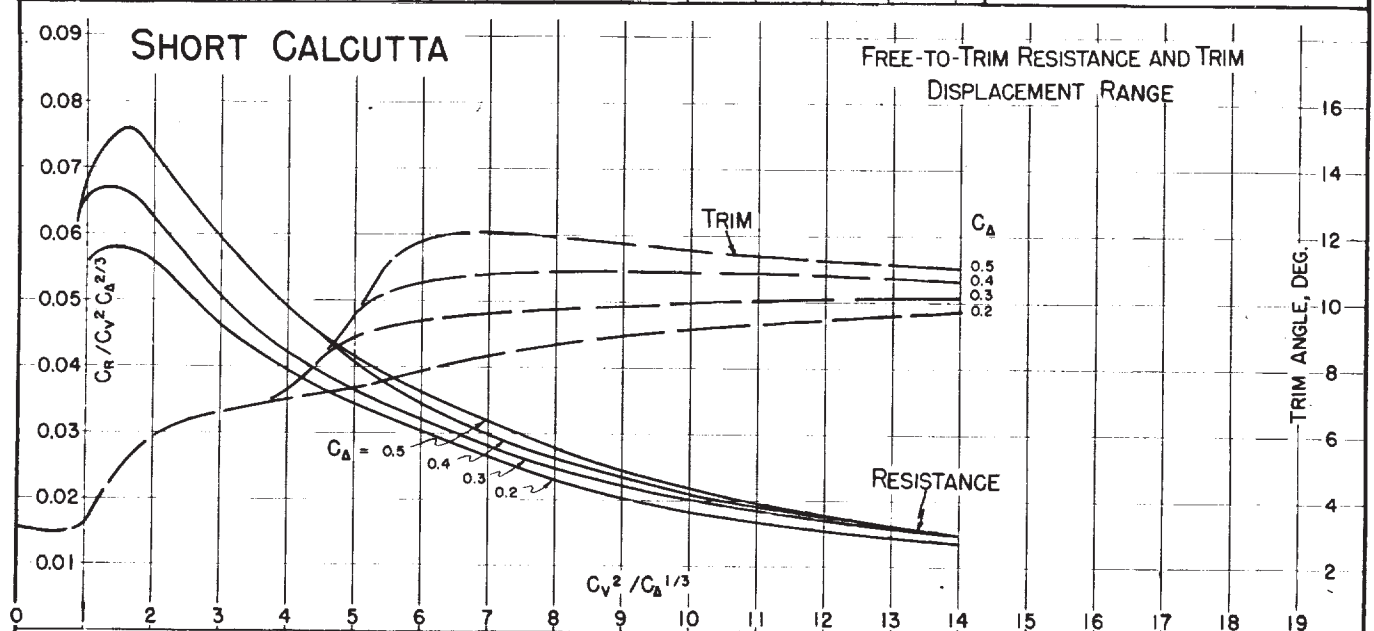
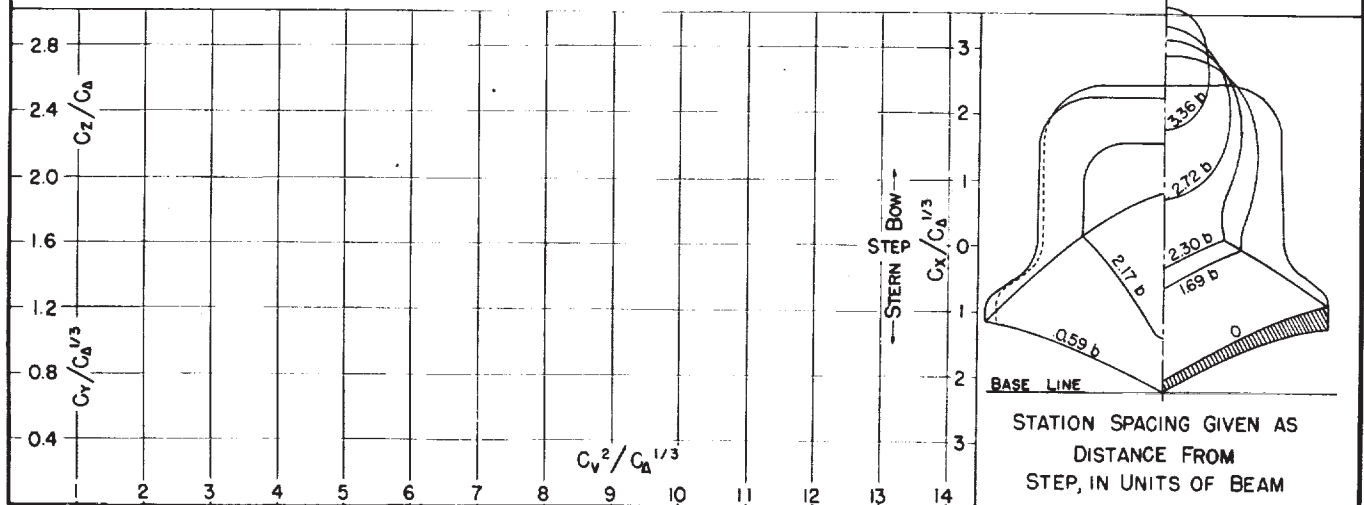
C.G. = 0.13 b FWD. OF STEP  
1.31 b ABOVE KEEL $C_{d,0} = 0.35$  (NOMINAL)  
 $k/L =$ TESTED AT NACA No. 1 TANK  
DATE: 10/35

Fig. 46

DESIGNATION: 2.76-047-22.5

NACA TN No. 1182

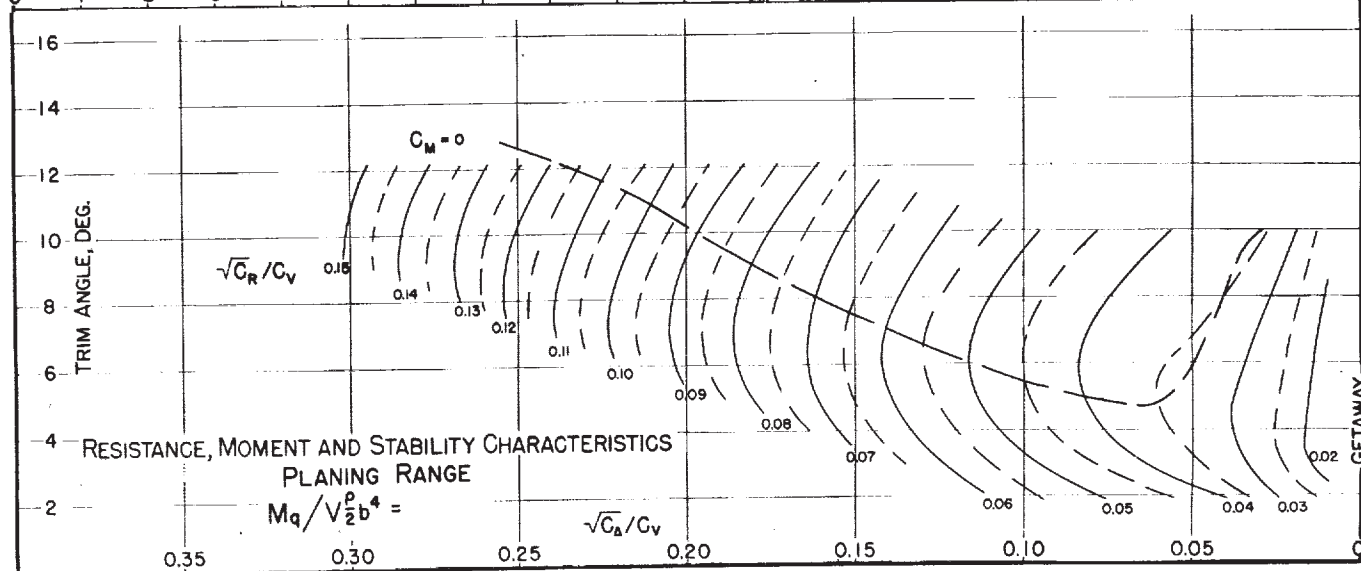
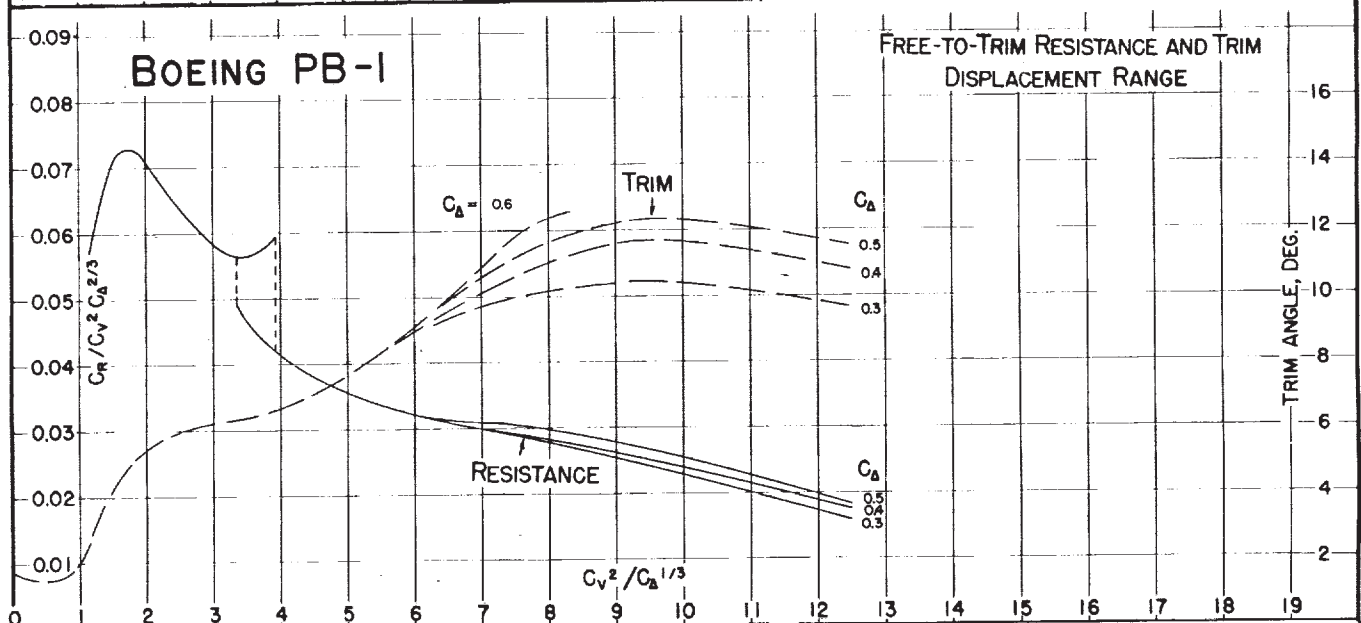
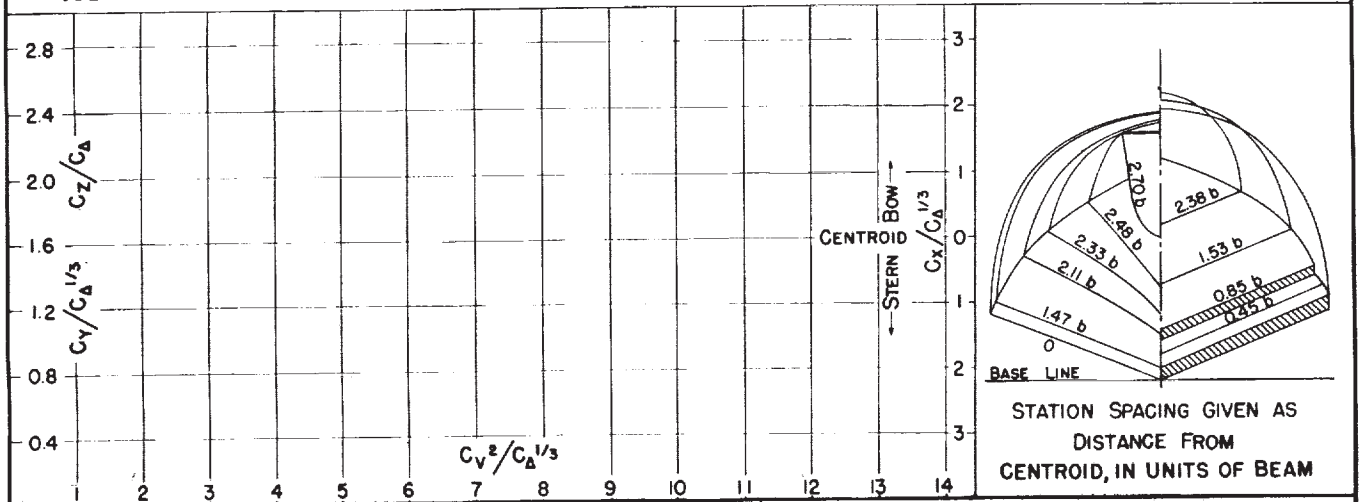
MODEL No. 52

MODEL BEAM: 1700"

C.G. = 0.44 b FWD. OF CENTROID  $C_{A_0} = 0.46$  (NOMINAL)  
 0.91 b ABOVE KEEL  $k/L =$

TESTED AT NACA No. 1 TANK

DATE: 6/35



NACA TN No. 1182

DESIGNATION: 2.34-0.47-26.0

Fig. 53

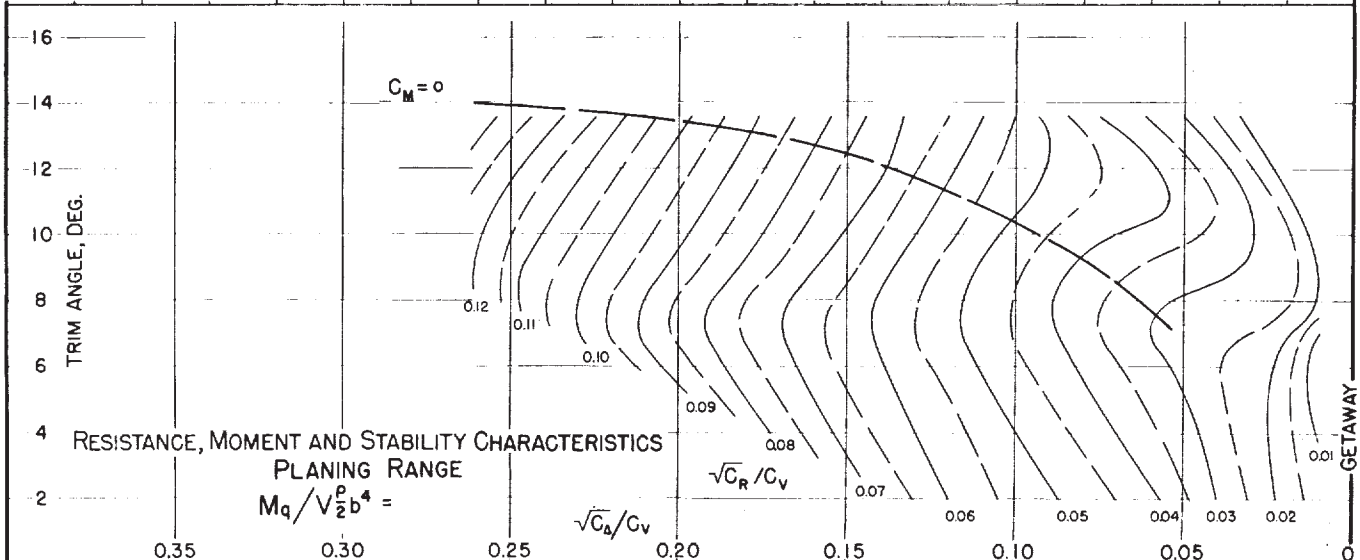
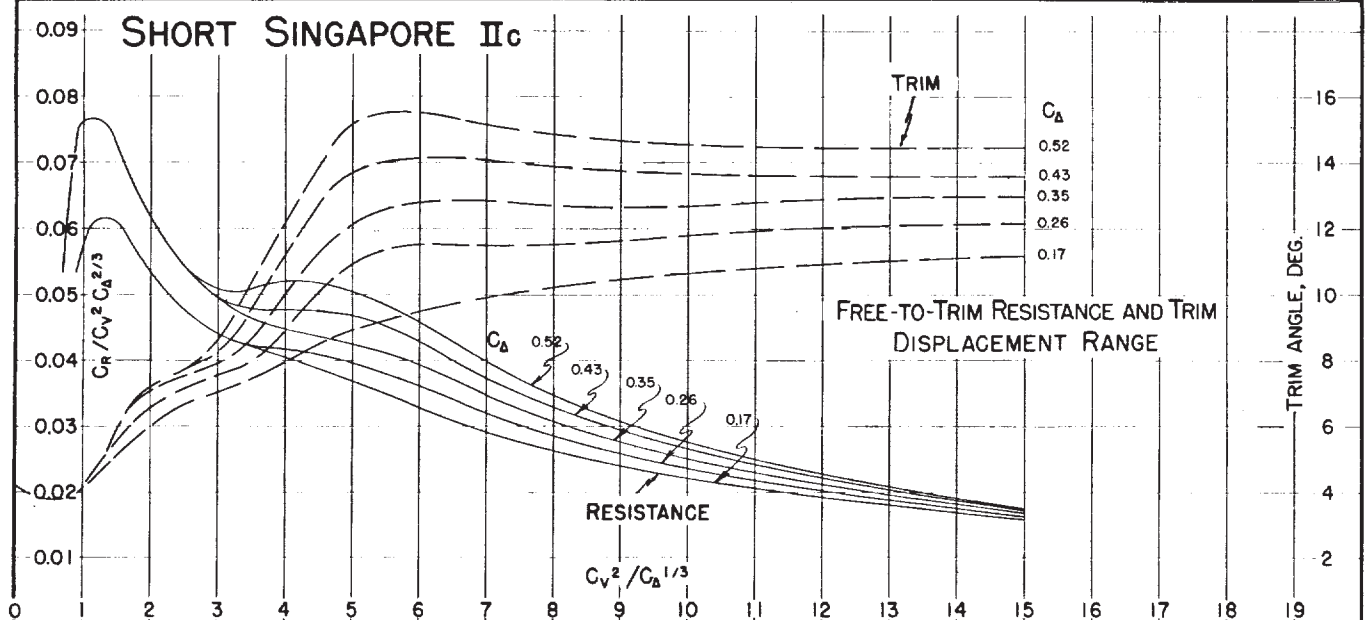
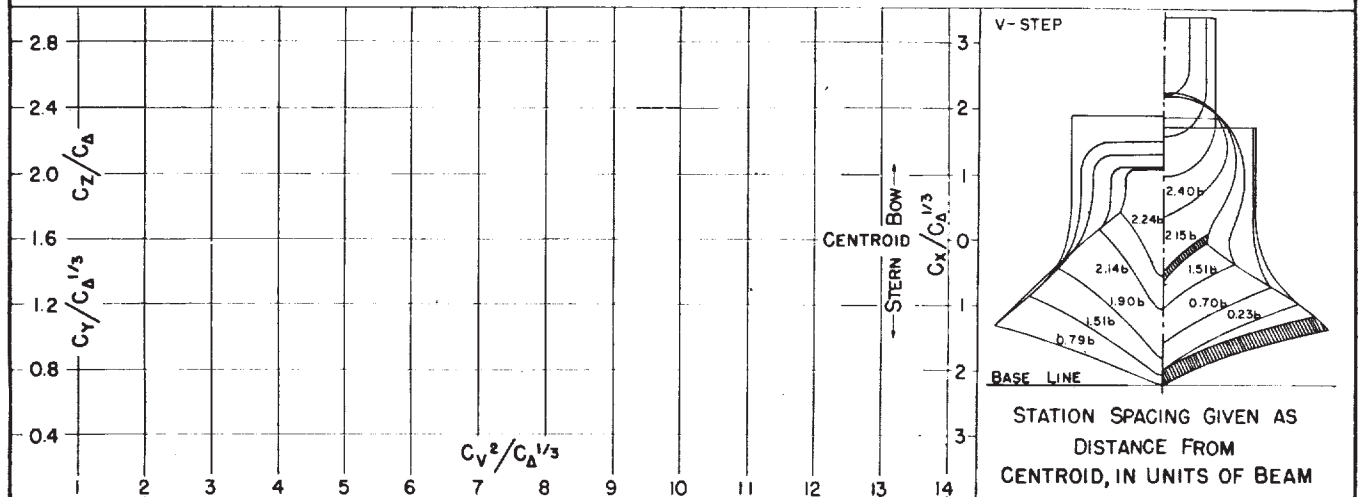
MODEL No. 66

MODEL BEAM: 21.60"

C.G. = 0.08 b FWD. OF CENTROID  $C_{d_0} = 0.32$  (NOMINAL)  
0.96 b ABOVE KEEL  $k/L =$ 

TESTED AT NACA No. 1 TANK

DATE: 36



NACA TN No. 1182

DESIGNATION: 3.09-0.63-25.0

Fig. 57

MODEL No. 83

MODEL BEAM: 17.70"

C.G. = 0.42 b FWD. OF STEP  
0.72 b ABOVE KEEL $C_{b_0} =$   
 $k/L =$ 

(NOMINAL)

TESTED AT NACA No. 1 TANK

DATE: 1/40

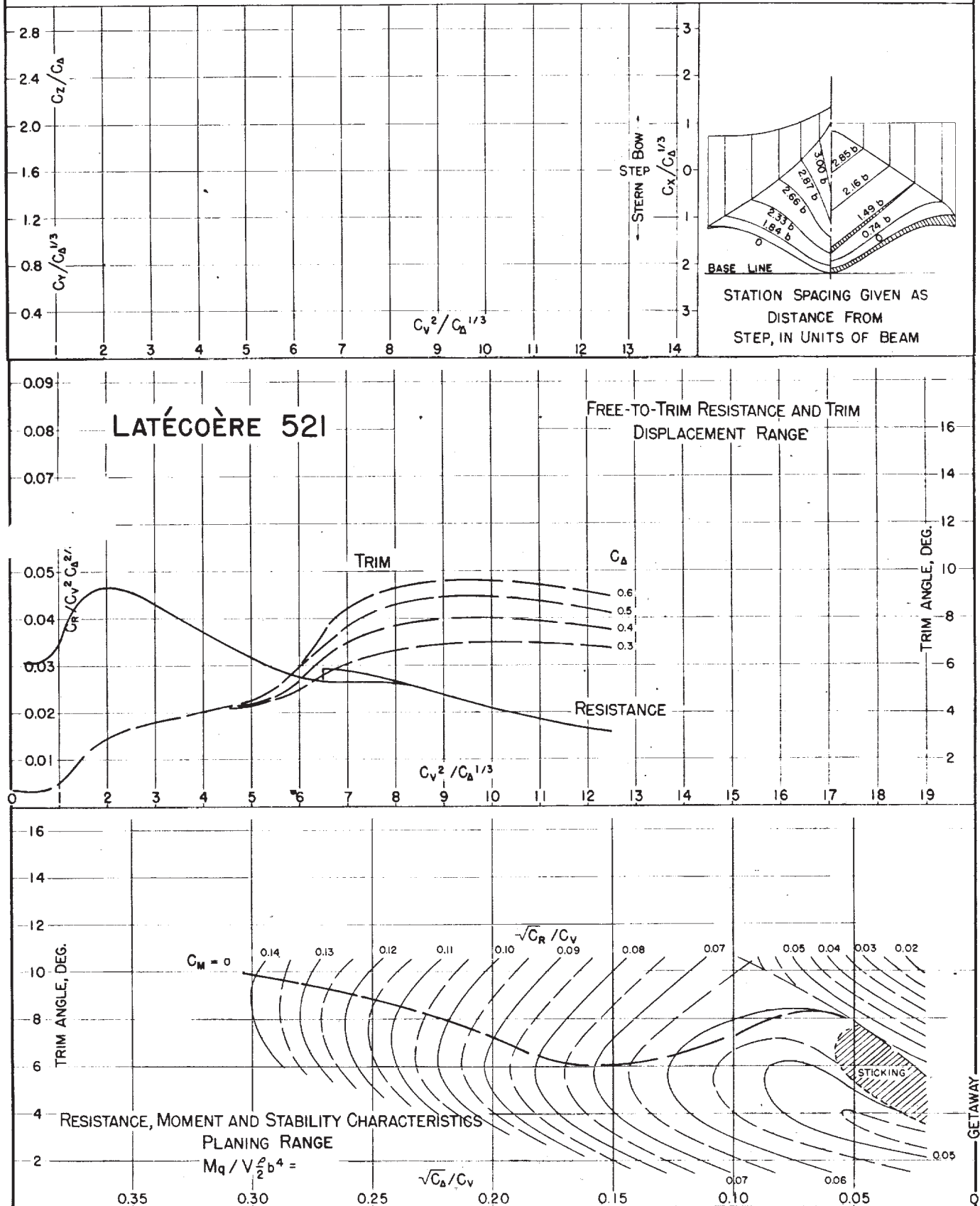


Fig. 84

DESIGNATION: 3.69-1.06-27.0 NACA TN No. 1182

MODEL No.

MODEL BEAM: 717 "

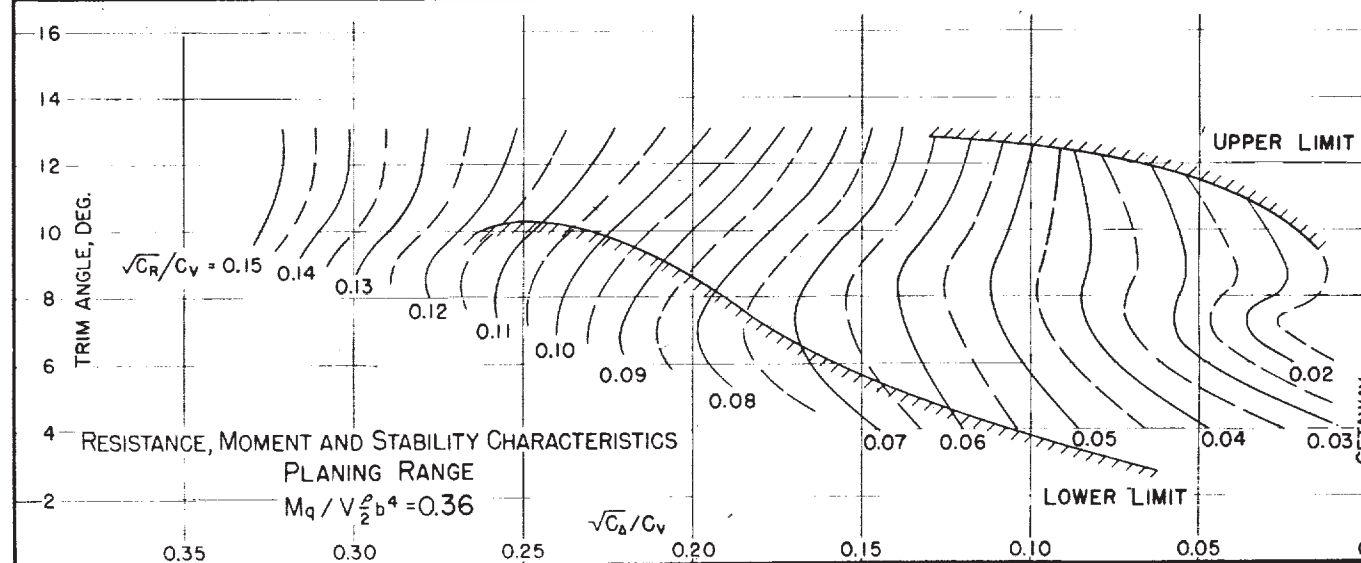
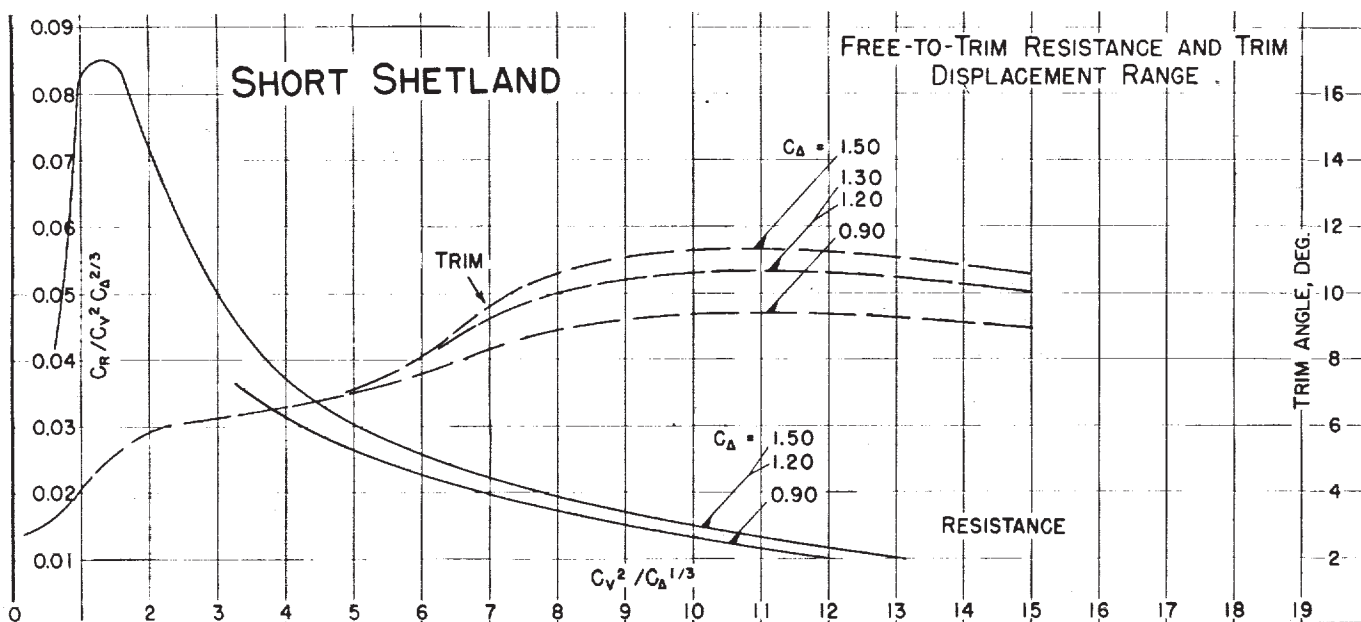
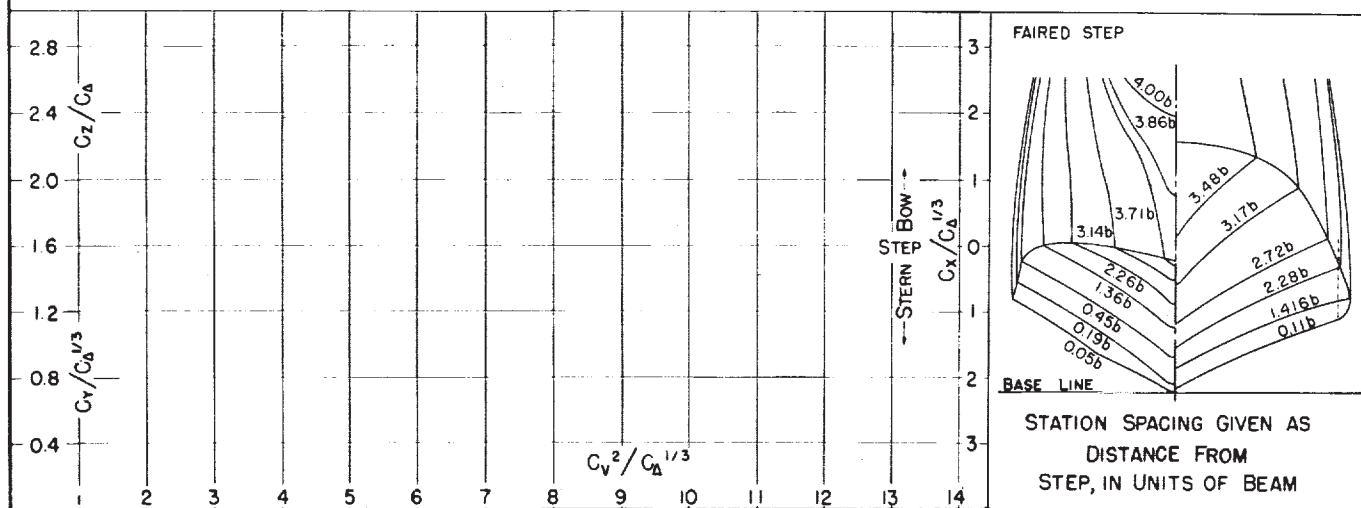
C.G. = 0.24 b FWD. OF STEP

1.32 b ABOVE KEEL

 $C_{d0} = 1.28$  (NOMINAL) $k/L = 0.228$ 

TESTED AT R.A.E. TANK

DATE: 2/42





NACA TN No. 1182

DESIGNATION: 2.85-1.30-21.5

Fig. 85

MODEL NO. N2/42-AI

MODEL BEAM: 6.64"

C.G. = 0.16 b FWD. OF CENTROID  $C_{A_0} = 1.35$  (NOMINAL)

1.92 b ABOVE KEEL

 $k/L = 0.218$ 

TESTED AT RAE TANK

DATE: '43

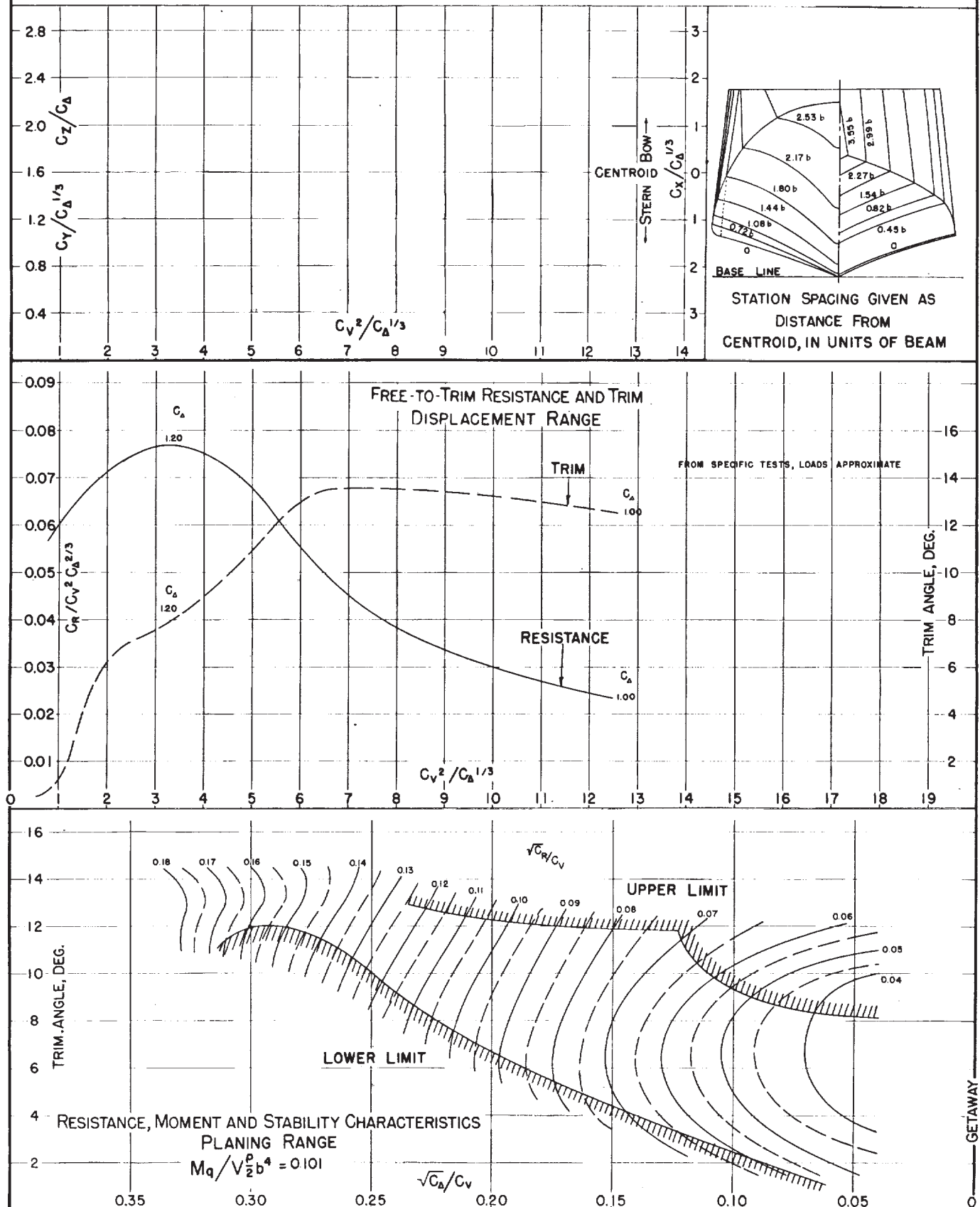


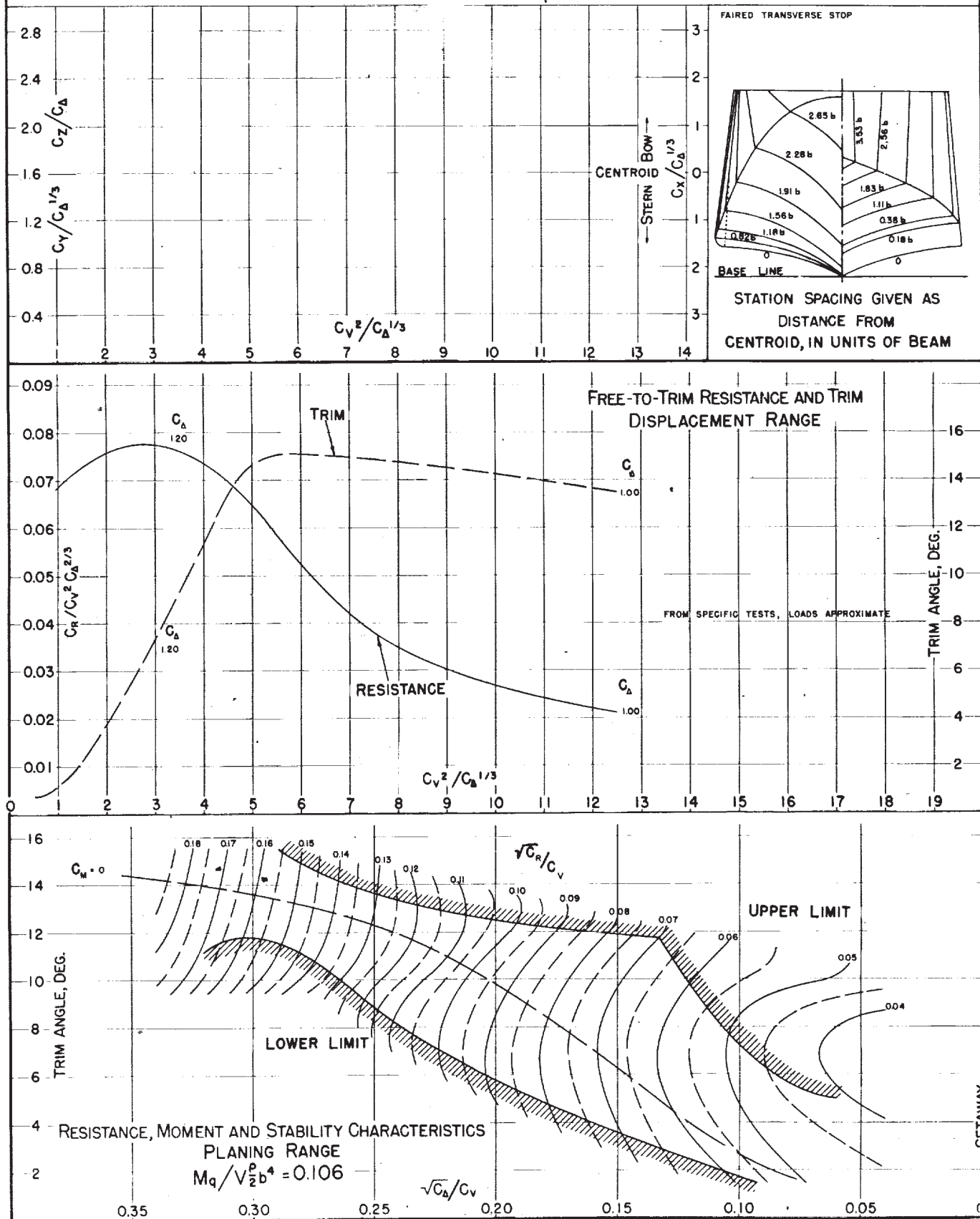
Fig. 86

DESIGNATION: 2.87-1.11-20.0 NACA TN No. 1182

MODEL NO. N2/42-Q  
MODEL BEAM: 6.56"

C.G. = 0.16 b FWD. OF CENTROID  $C_{A_0} = 1.40$  (NOMINAL)  
1.95 b ABOVE KEEL  $k/L = 0.218$

TESTED AT RAE TANK  
DATE: '43





NACA TN No. 1182

DESIGNATION: 4.02-0.98-27.5

Fig. 87

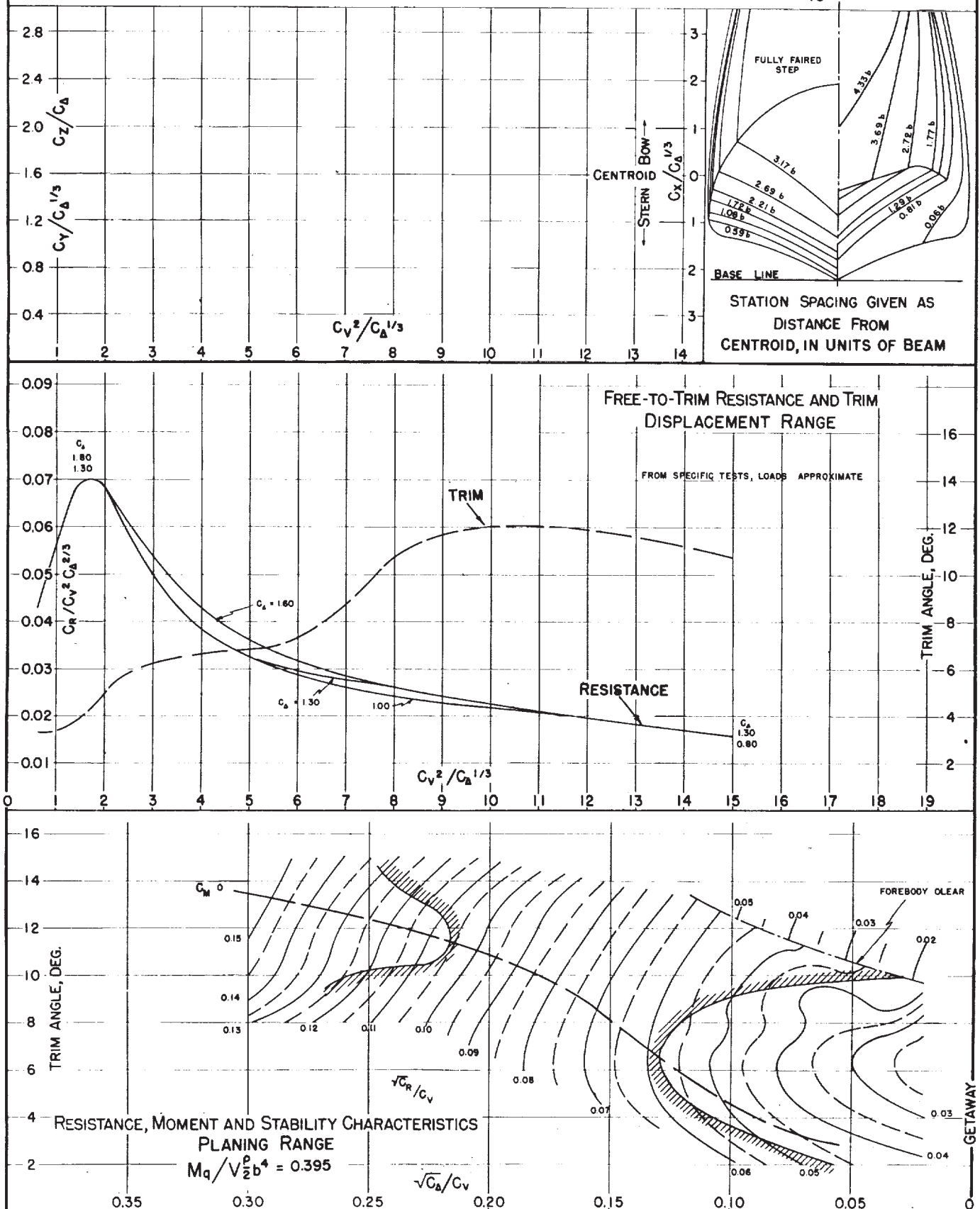
MODEL No. OEH  
MODEL BEAM: 6.58"C.G. = 0.10 b FWD. OF CENTROID  $C_{b_0} = 1.65$  (NOMINAL)  
1.29 b ABOVE KEEL  $k/L =$ TESTED AT RAE TANK  
DATE: 2/45

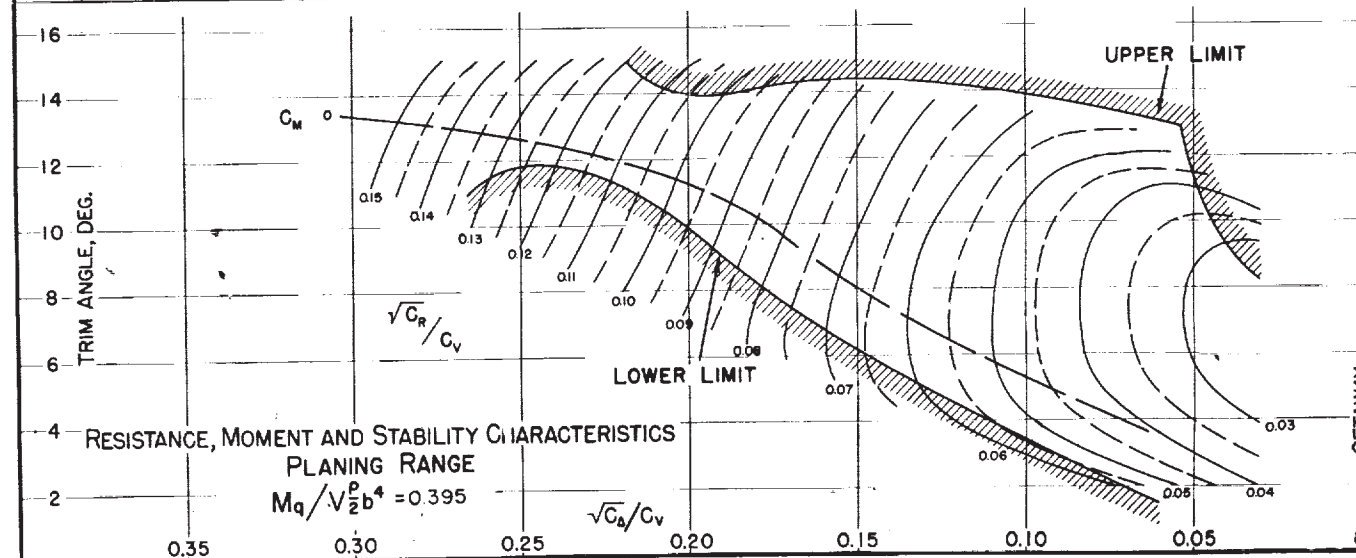
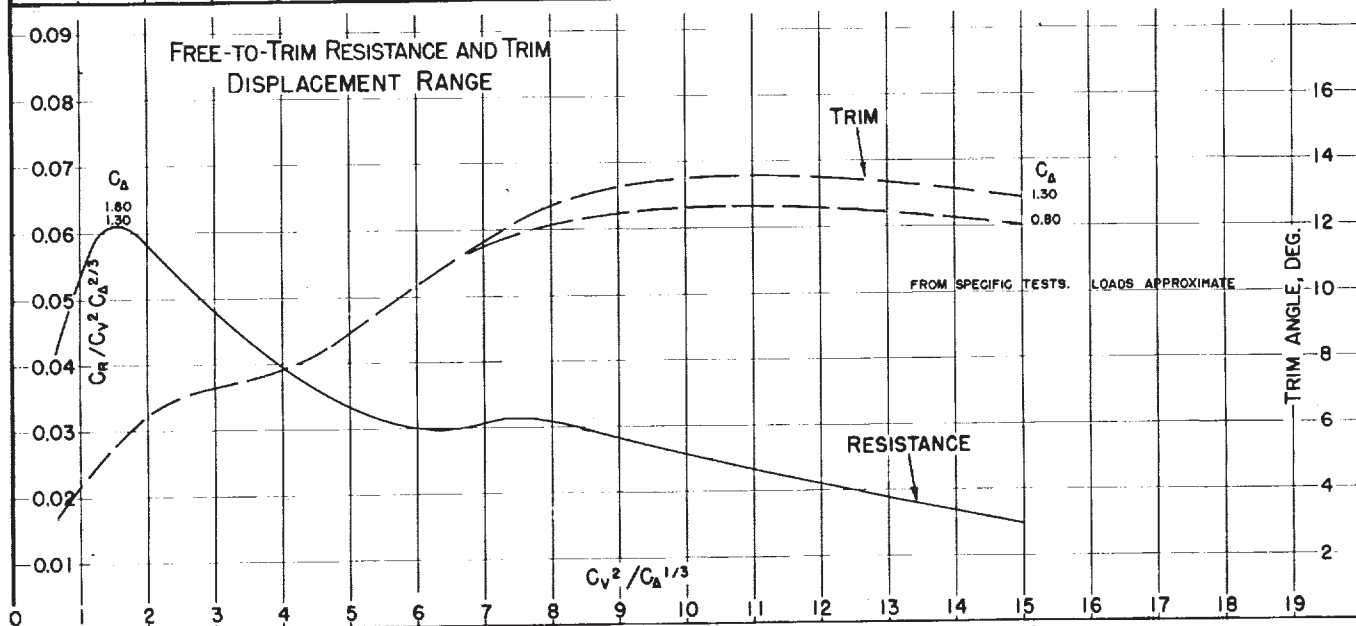
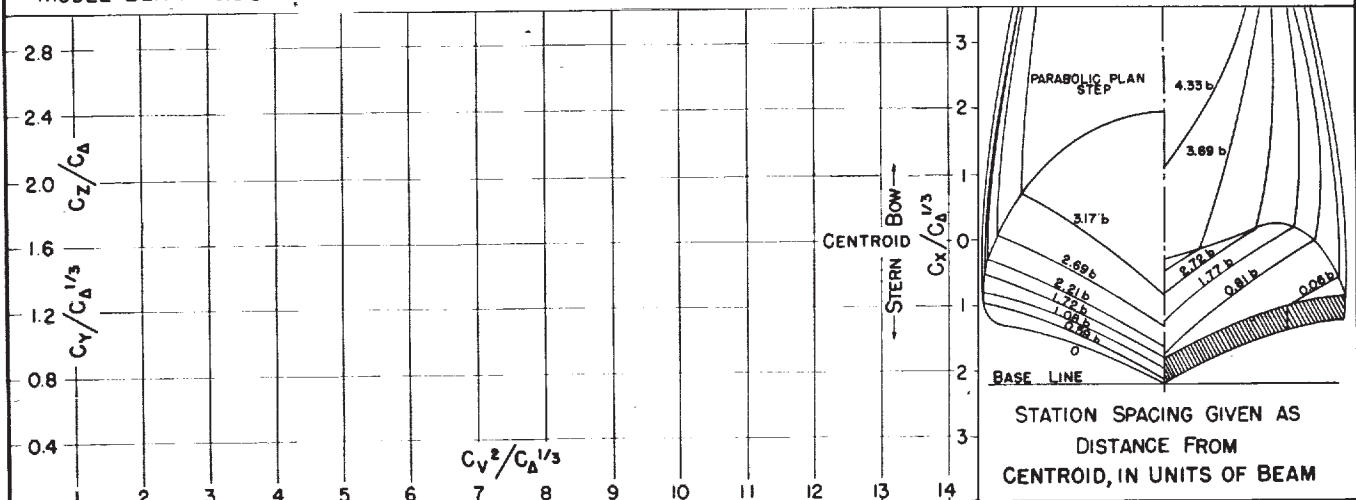
Fig. 88

DESIGNATION: 4.02-1.09-27.5 NACA TN No. 1182

MODEL No. FEH  
MODEL BEAM: 6.58"

C.G. = 0.10 b FWD. OF CENTROID  $C_{A_0} = 1.65$  (NOMINAL)  
1.29 b ABOVE KEEL  $k/L =$

TESTED AT RAE TANK  
DATE: 2/45





# NATIONAL ADVISORY COMMITTEE FOR AERONAUTICS

**TECHNICAL NOTE 2503**

HYDRODYNAMIC INVESTIGATION OF A SERIES OF HULL MODELS  
SUITABLE FOR SMALL FLYING BOATS AND AMPHIBIANS

By W. C. Hugli, Jr., and W. C. Axt

Stevens Institute of Technology



Washington

November 1951

TABLE II

PARTICULARS OF PARENT MODEL NO. 1024-01

| Item   | Full scale  | Model                       |
|--|---|-----------------------------|
| Scale  | 1   | 1/8                         |
| DIMENSIONS   |   |                             |
| Beam, maximum, in.                                   | 48.00   | 6.00                        |
| Beam at main step, in.                               | 47.72   | 5.96                        |
| Forebody length, in.                                 | 156.00  | 19.50                       |
| Afterbody length, in.                                | 162.00  | 20.25                       |
| Afterbody angle, deg                                 | 6.6   | 6.6                         |
| Step height, in.                                     | 4.00  | 0.50                        |
| Sternpost angle, deg                                 | 8.0   | 8.0                         |
| Length-beam ratio                                    | 7.63  | 7.63                        |
| Center-of-gravity location                           |   |                             |
| Forward of step, in.                                 | 12.00   | 1.50                        |
| Above forebody keel, in.                             | 52.00   | 6.50                        |
| Gross weight, $\Delta_0$ , lb                        | 3000  | 5.86                        |
| Gross load coefficient, $C_{\Delta_0}$ (fresh water) | 0.753   | 0.753                       |
| Pitching moment of inertia, lb sq in.                | $1.245 \times 10^7$                                 | 380                         |
| Wing span, ft  | 40.4  | 5.05                        |
| Wing incidence with forebody keel, deg               | 5.0   | 5.0                         |
| Horizontal tail area, sq ft                          | 36.9  | 0.577                       |
| Tail length (c.g. to 35-percent M.A.C. of tail), ft  | 15.63   | 1.954                       |
| AERODYNAMIC CHARACTERISTICS                          |   |                             |
| $C_L$ at $\tau = 6^\circ$ (take-off trim)            | 1.2   | 1.2                         |
| $dC_L/d\tau$ (wing), per deg                         | 0.073   | 0.073                       |
| $dC_L/d\tau$ (tail), per deg                         | 0.050   | 0.050                       |
| $dM/dq$ , lb ft sec/rad                              | $30.7V_B$   | $7.53 \times 10^{-3} V_m$   |
| $dM/d\theta$ , lb ft/deg                             | $0.0343V_B^2$                                       | $6.71 \times 10^{-5} V_m^2$ |
|  |   |                             |
| Item   | Ratio of full-scale dimension<br>to model dimension |                             |
| Speed  | $\lambda^{1/2} = 2.81$                              |                             |
| Length   | $\lambda = 8.00$                                    |                             |
| Area   | $\lambda^2 = 6.40 \times 10^1$                      |                             |
| Volume   | $\lambda^3 = 5.12 \times 10^2$                      |                             |
| Moment   | $\lambda^4 = 4.096 \times 10^3$                     |                             |
| Moment of Inertia                                    | $\lambda^5 = 3.277 \times 10^4$                     |                             |



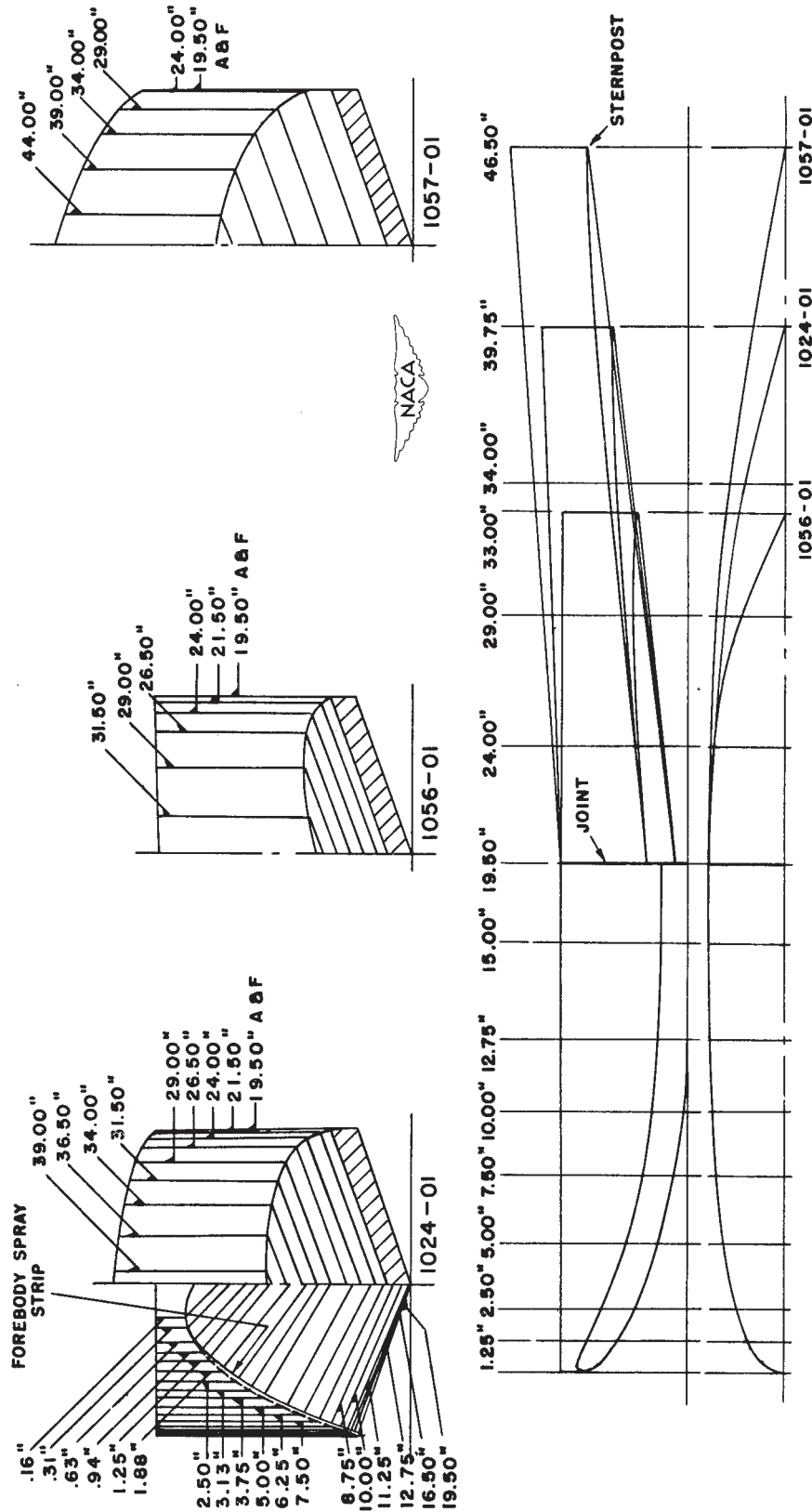


Figure 5.- E.T.T. series model hull lines with maximum beam of 6.00 inches.

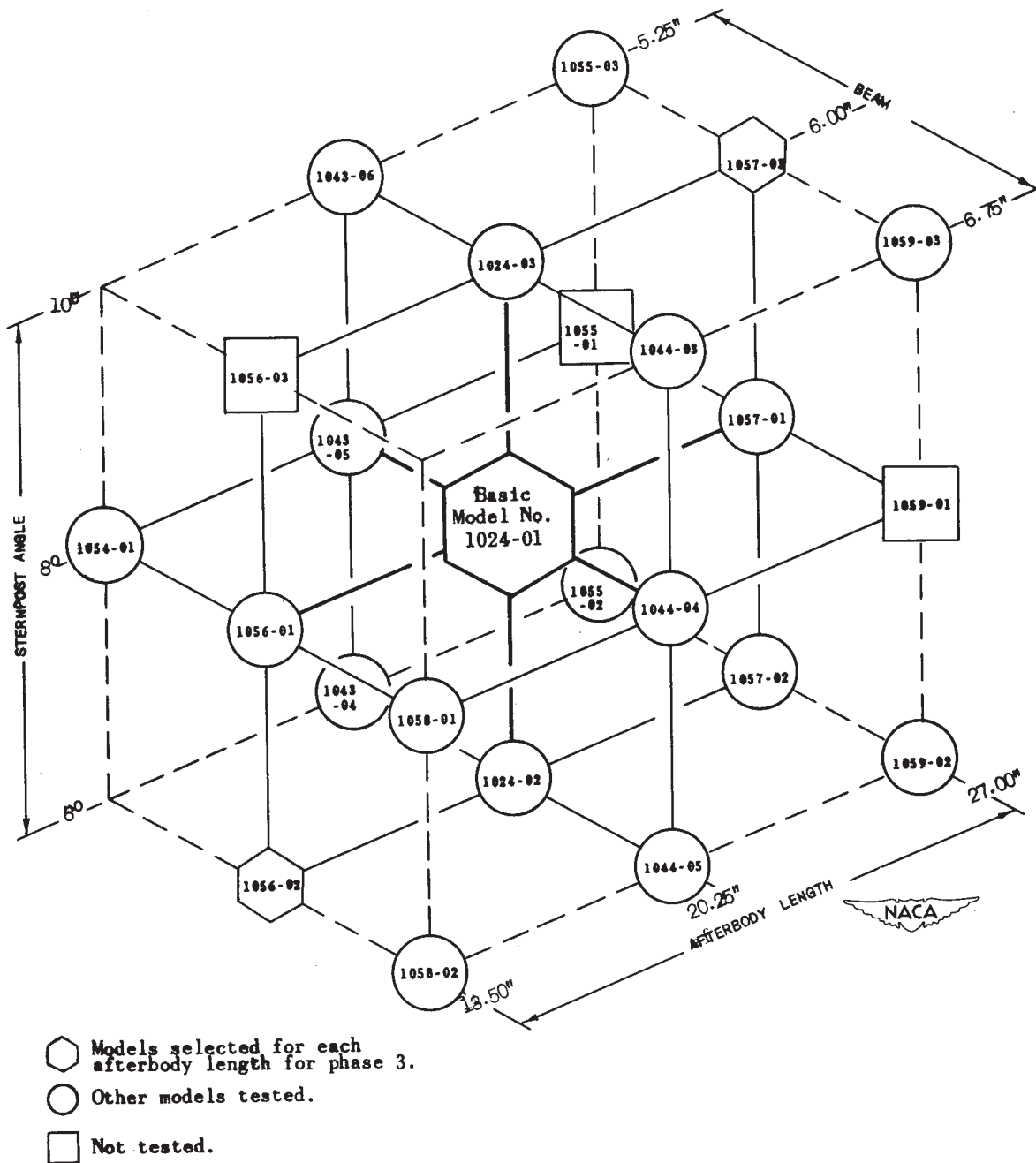


Figure 6.- E.T.T. series.

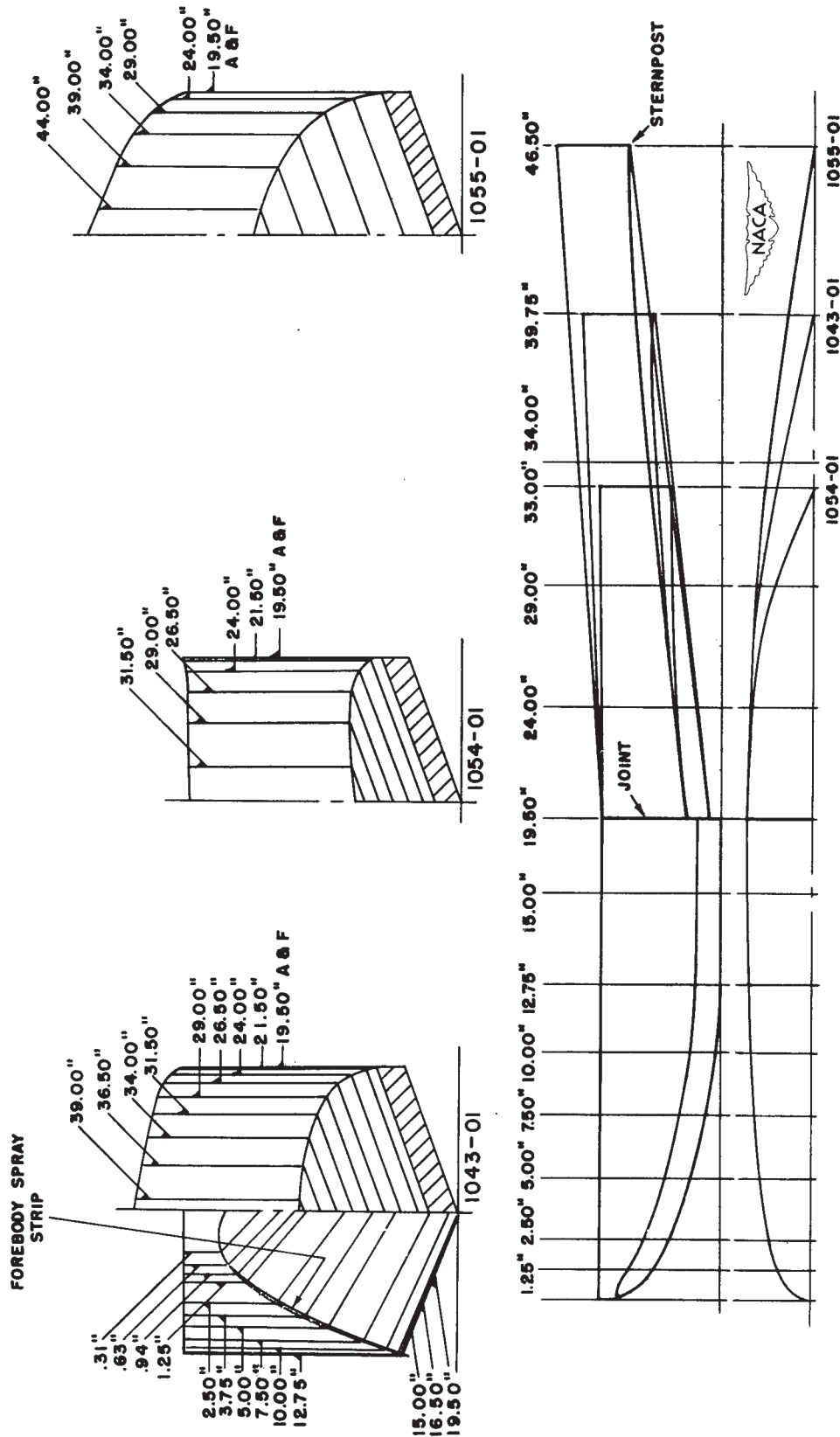


Figure 7.-- E.T.T. series model hull lines with maximum beam of 5.25 inches.



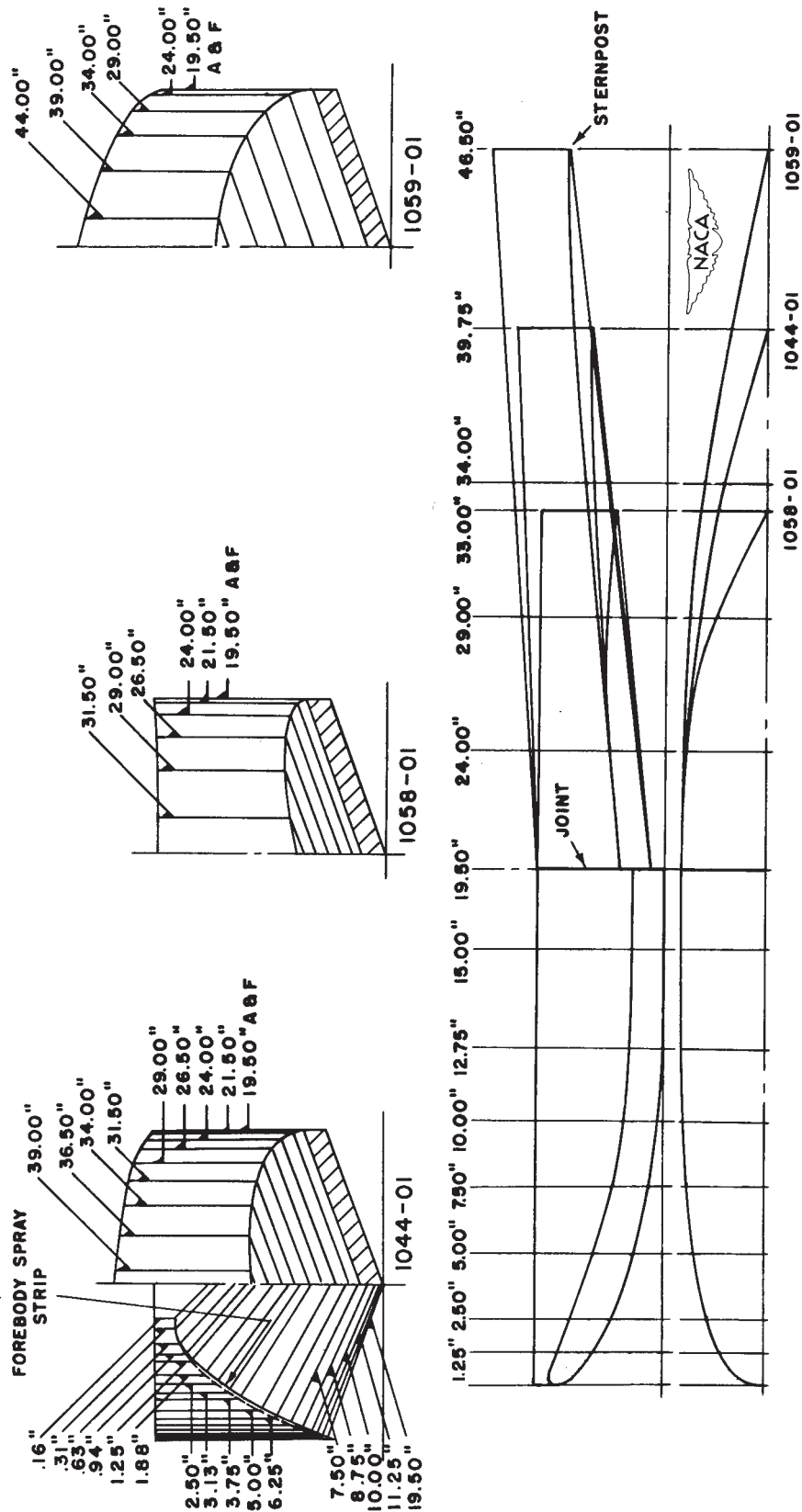


Figure 8.- E.T.T. series model hull lines with maximum beam of 6.75 inches.

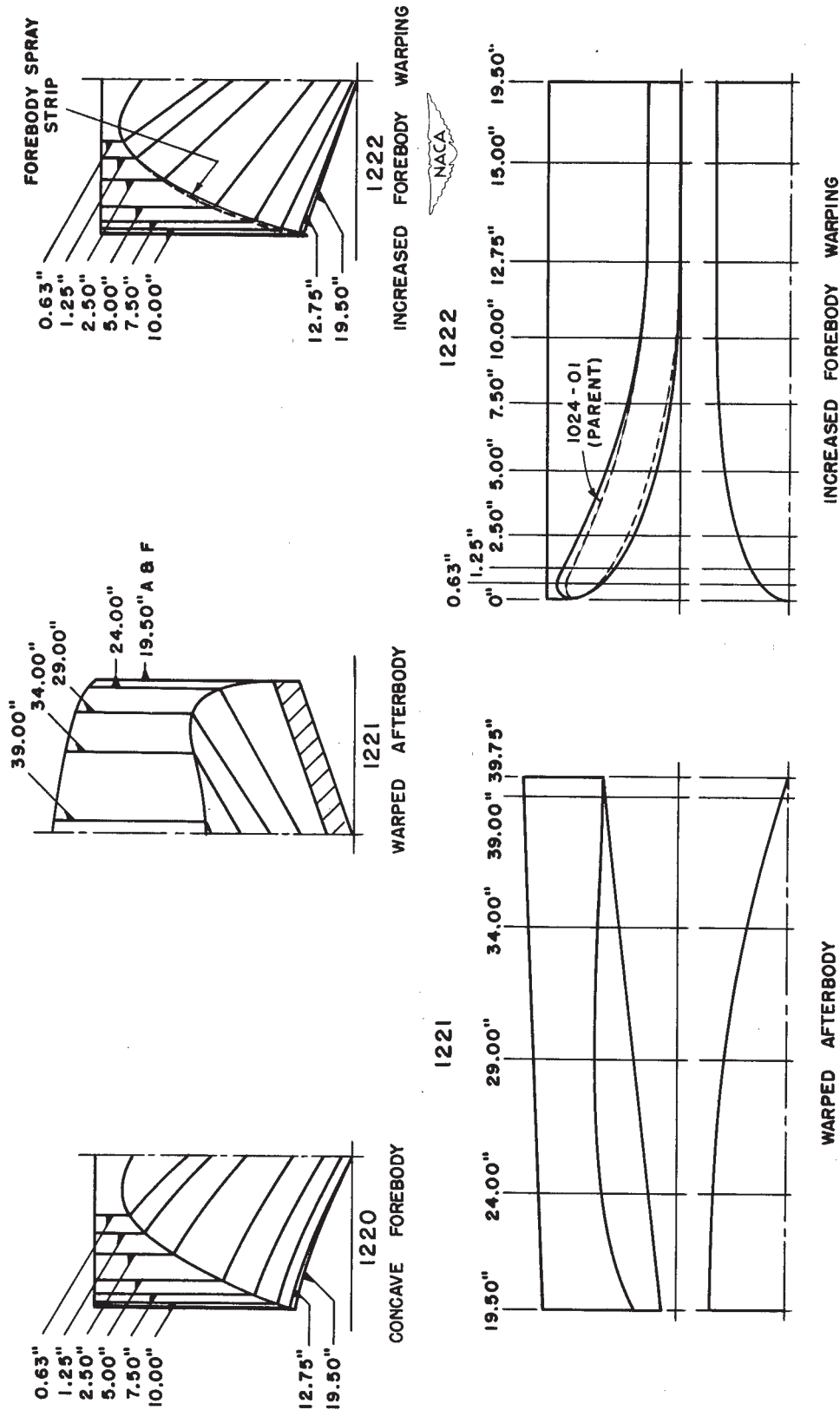


Figure 9.- E.T.T. series hull alterations. Maximum beam, 6.00 inches.

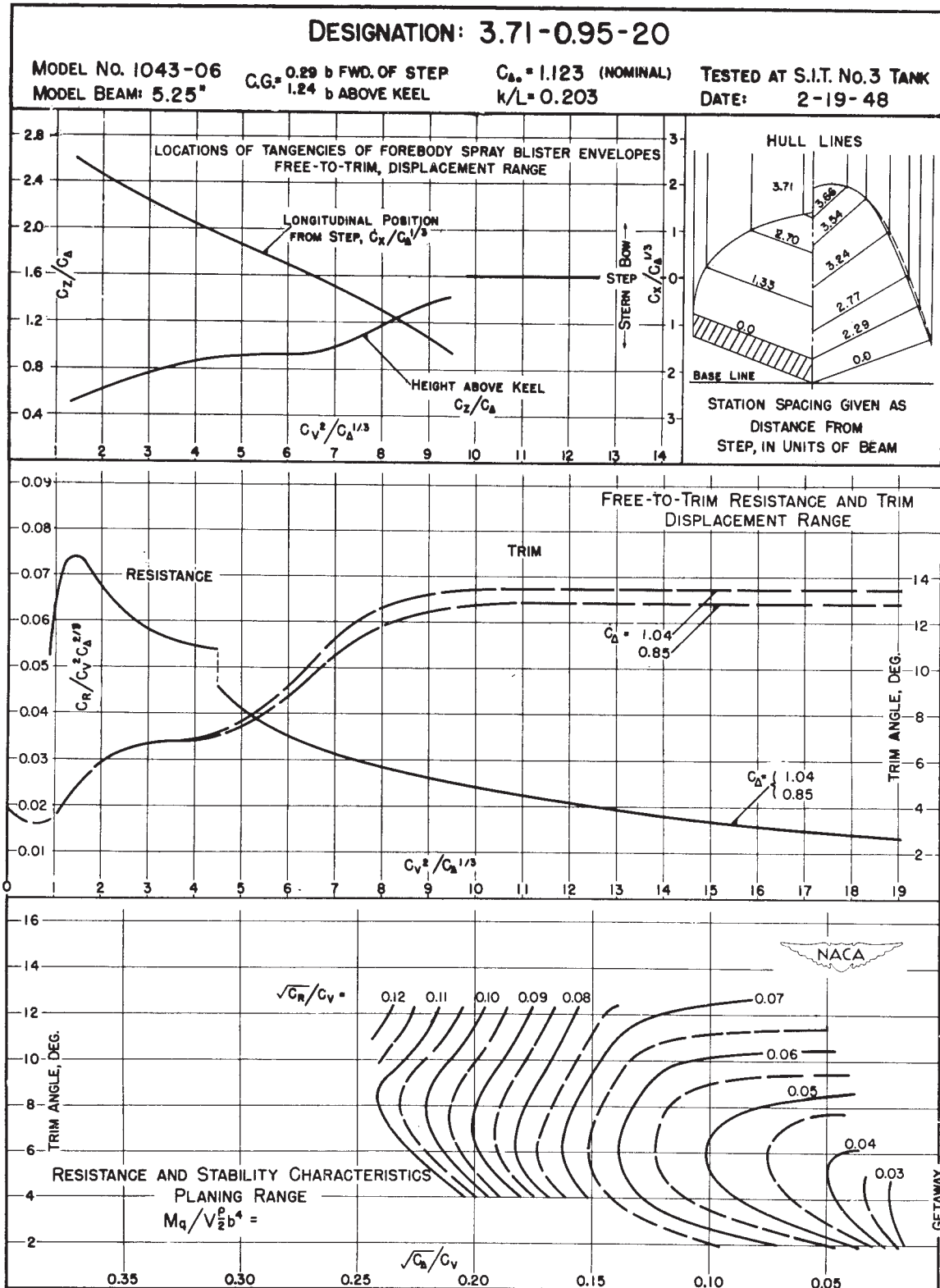


Figure 15.

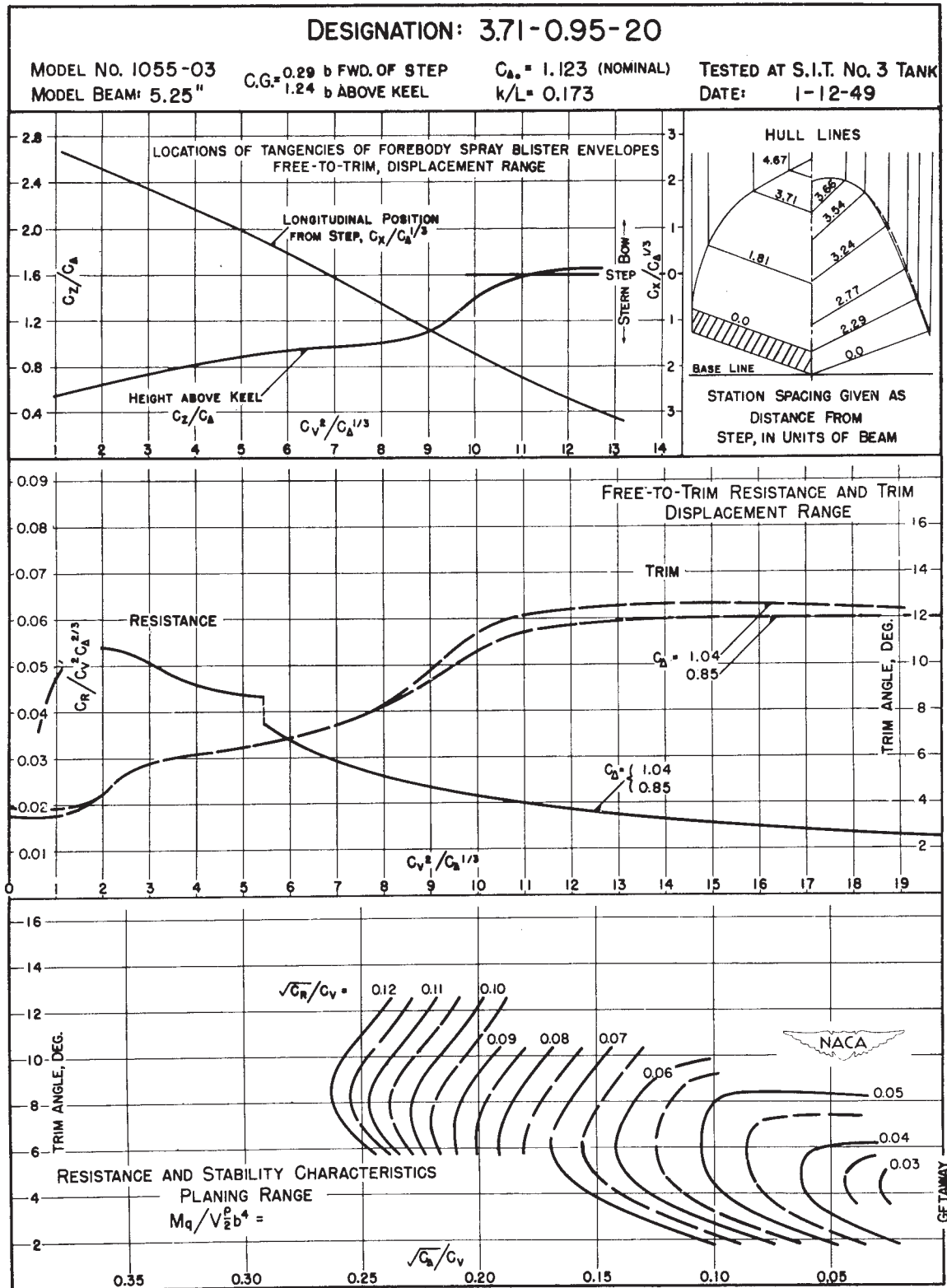


Figure 16.

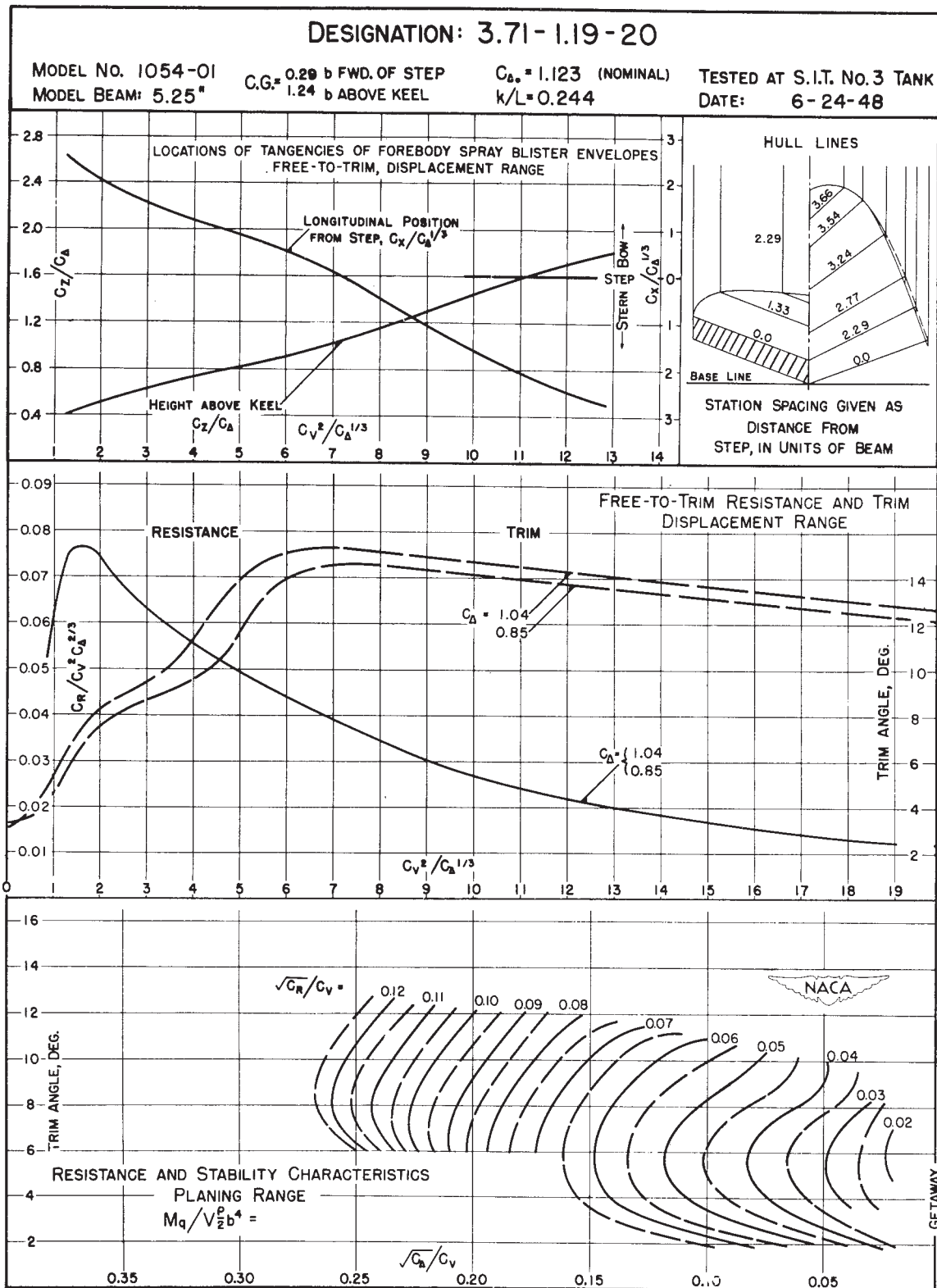


Figure 17.

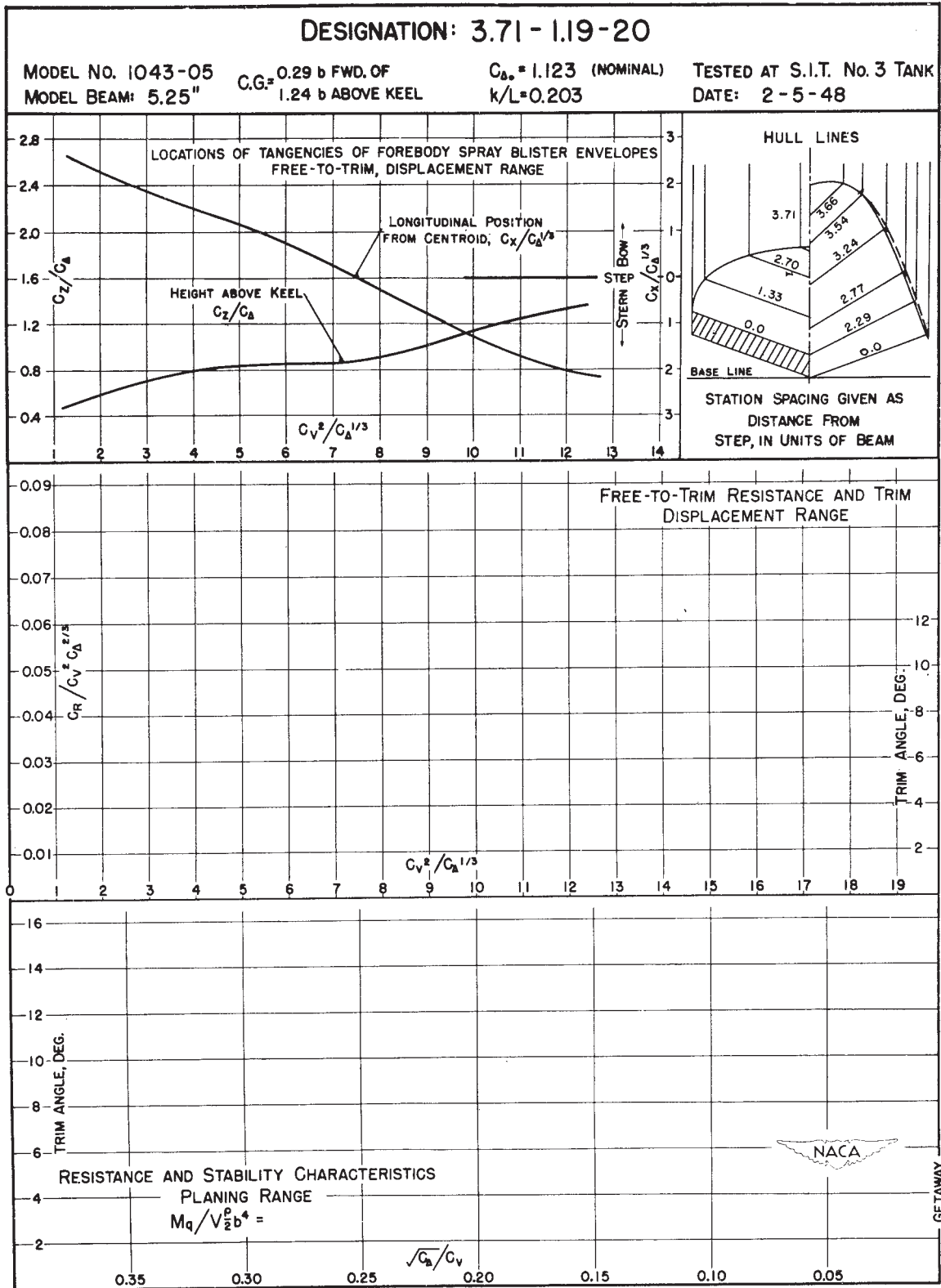


Figure 18.

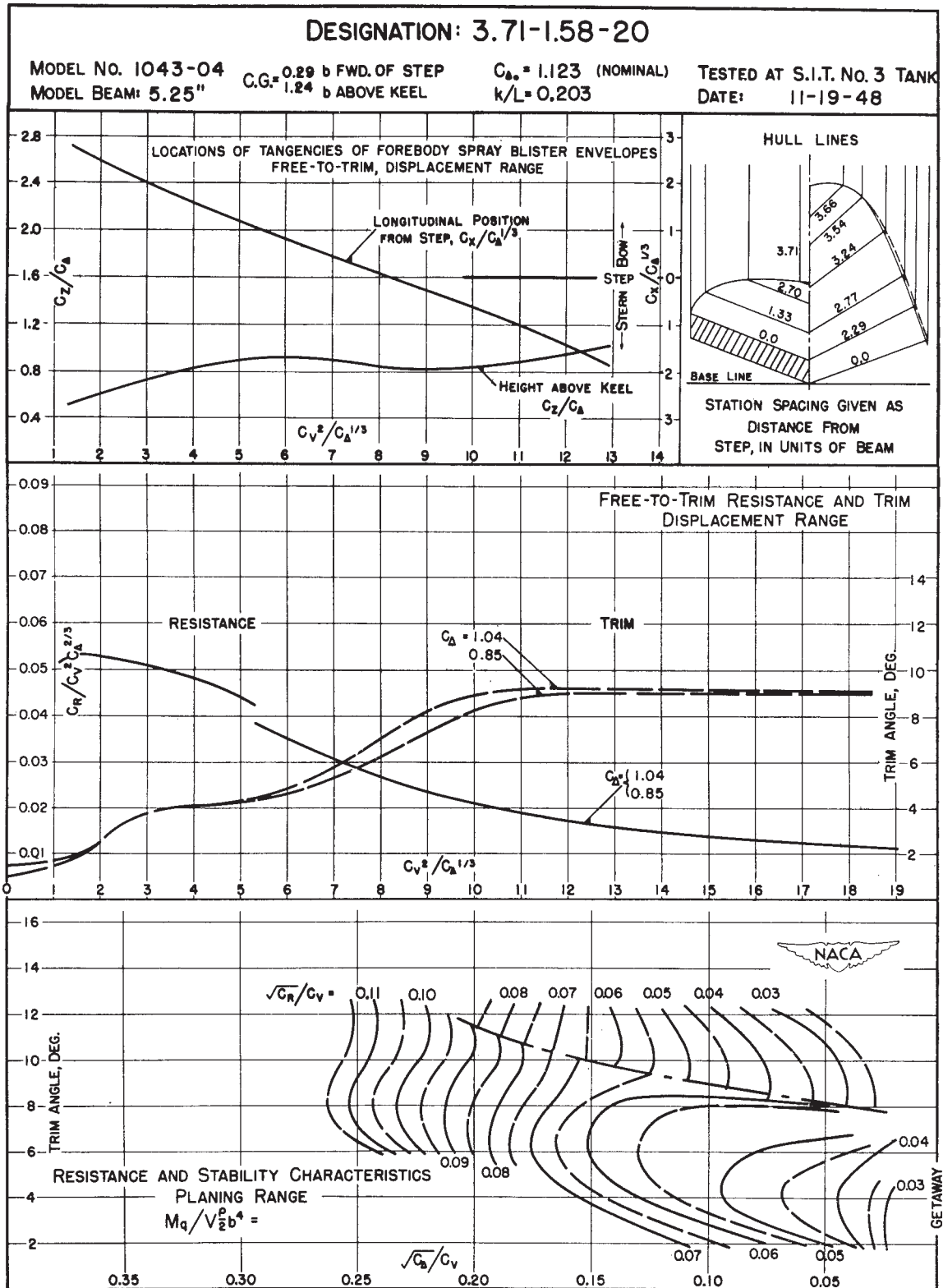


Figure 19.

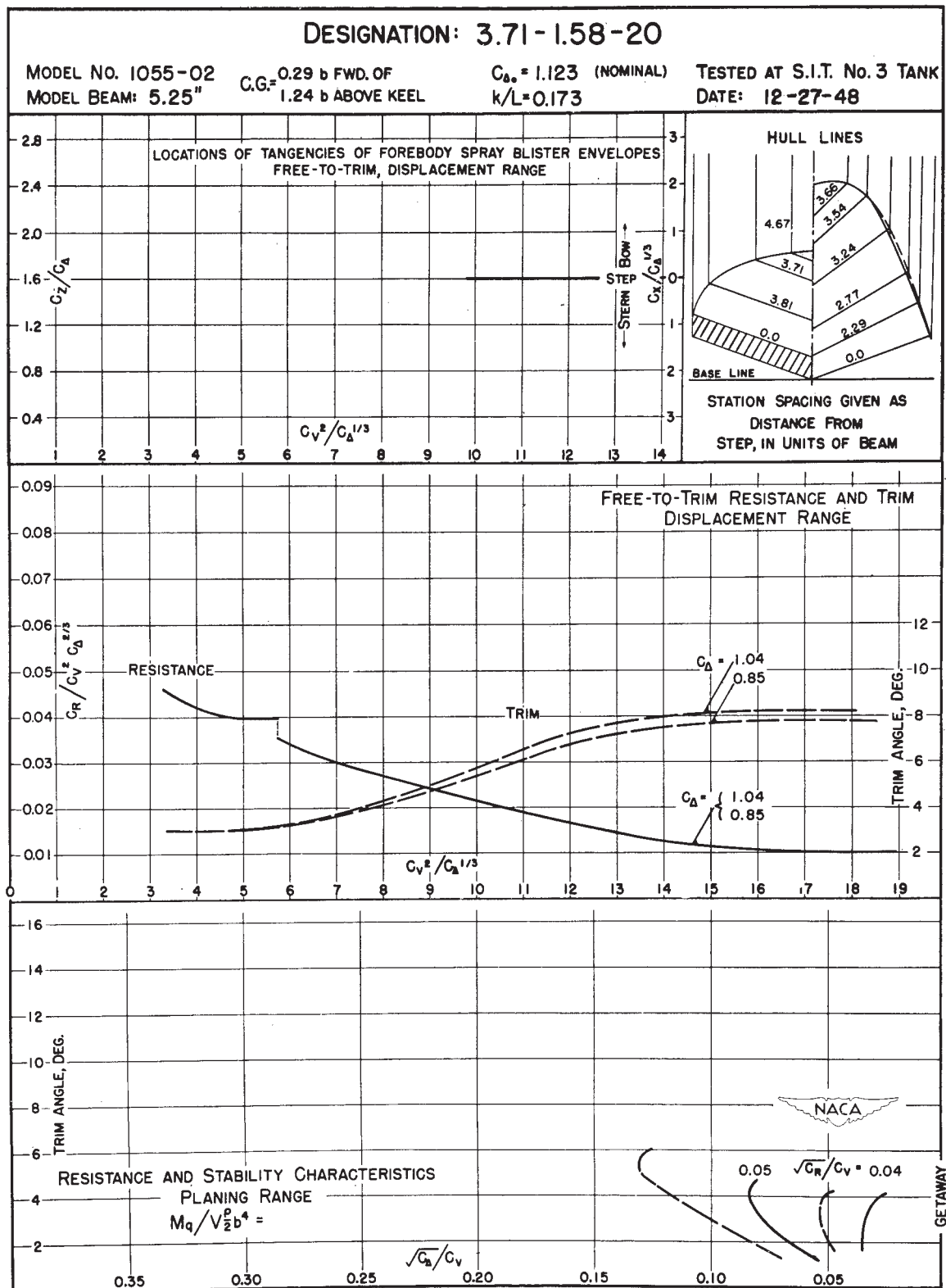


Figure 20.



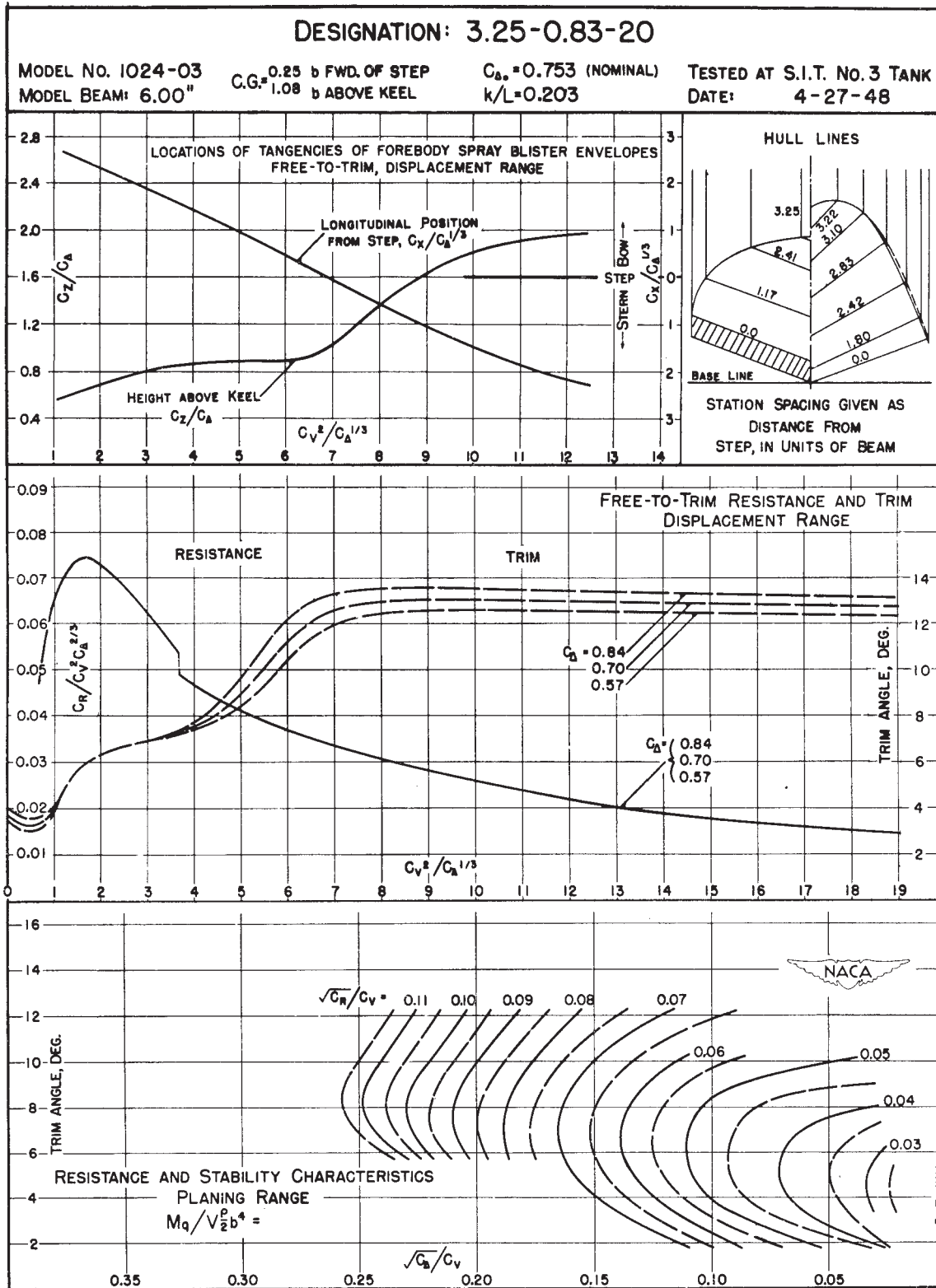


Figure 21.

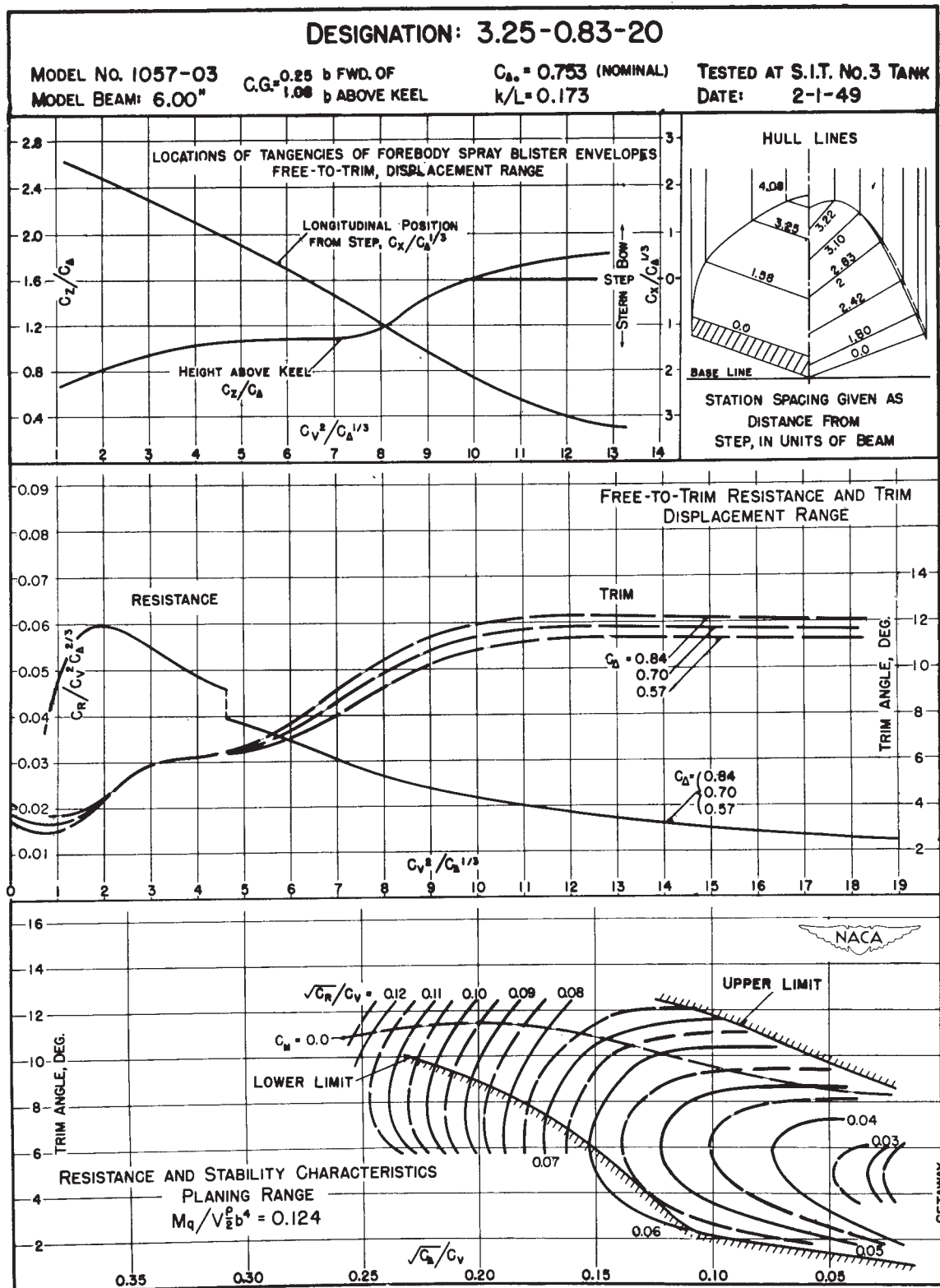


Figure 22.

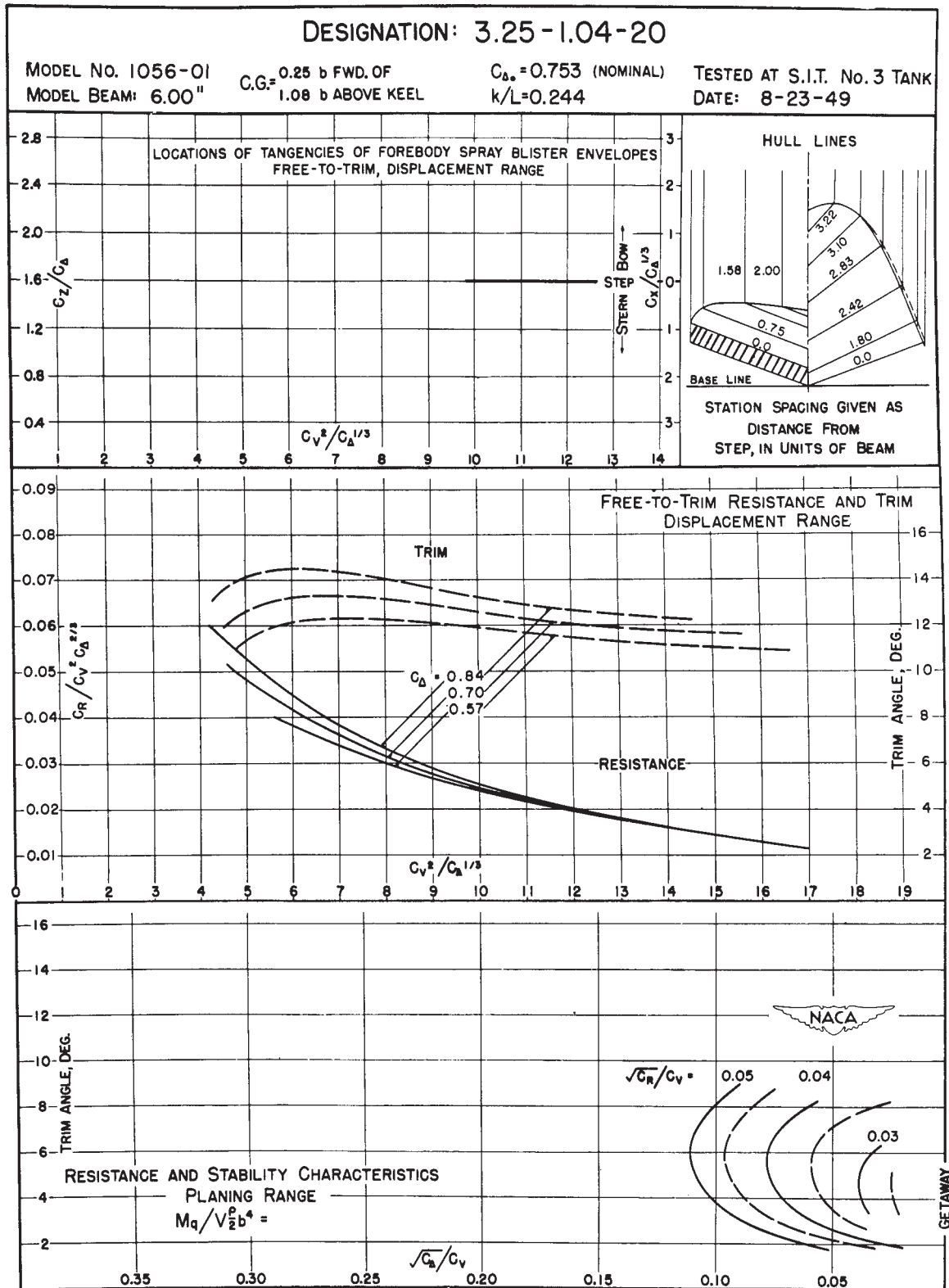


Figure 23.

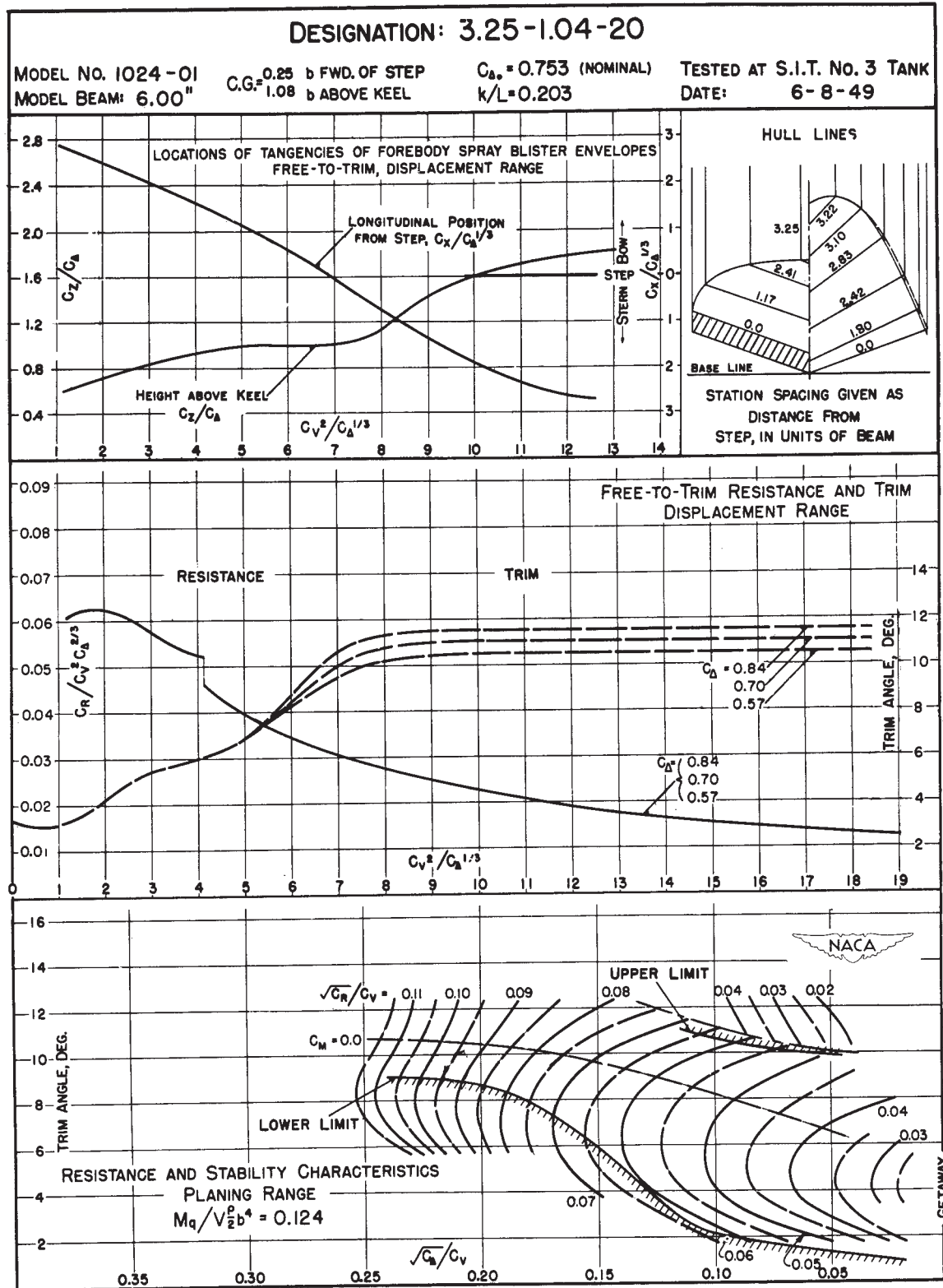


Figure 24.

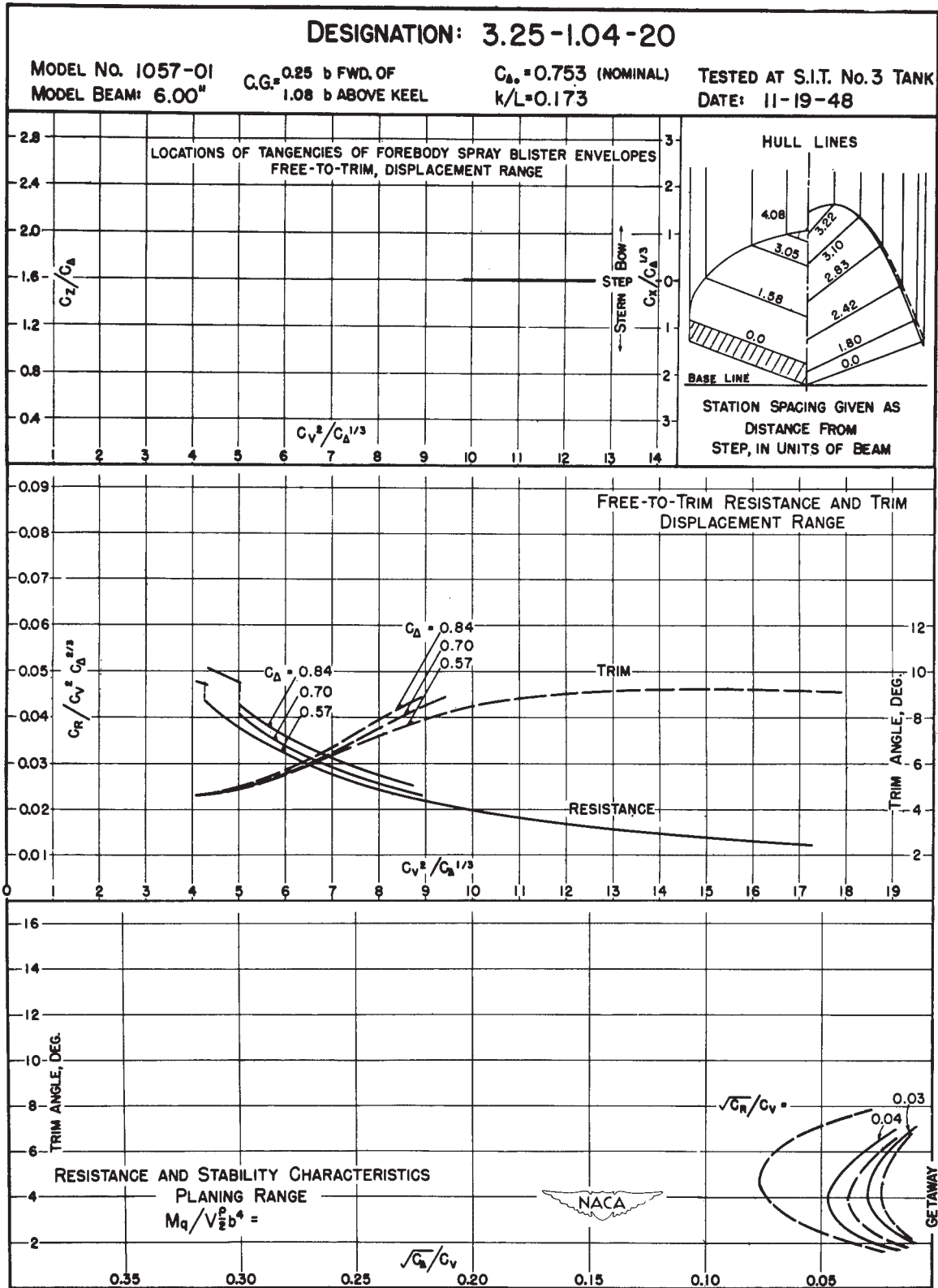


Figure 25.

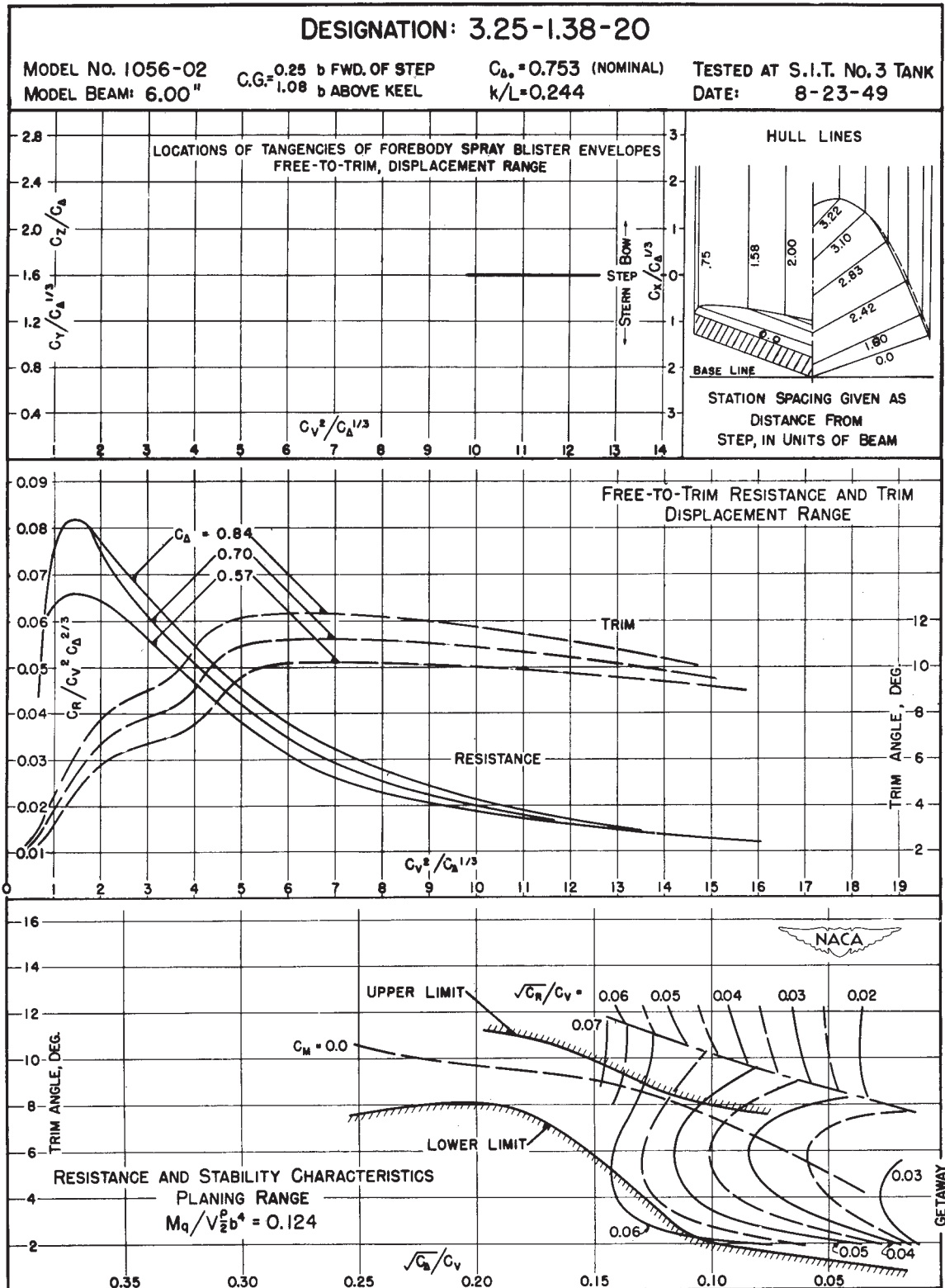


Figure 26

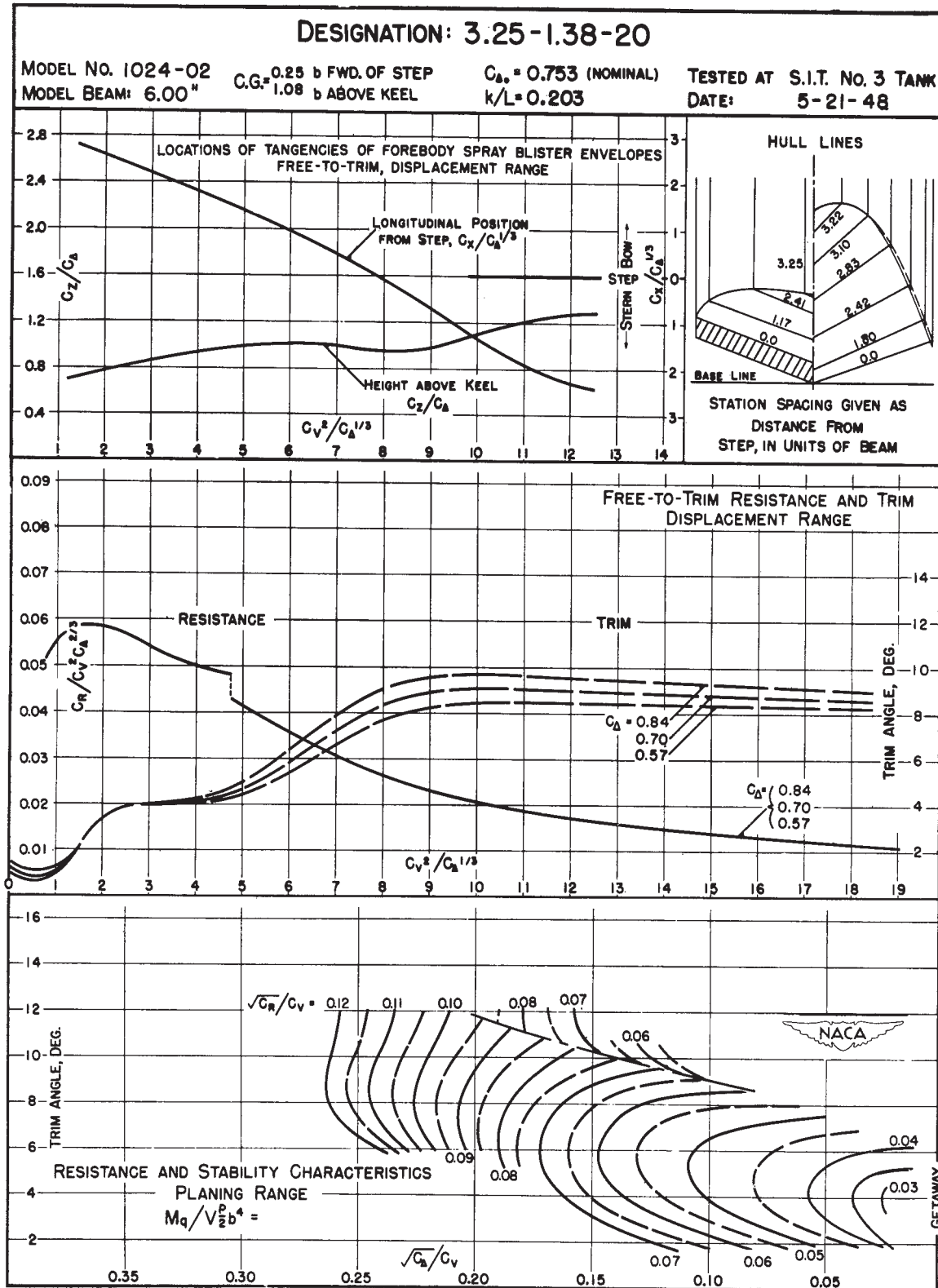


Figure 27.

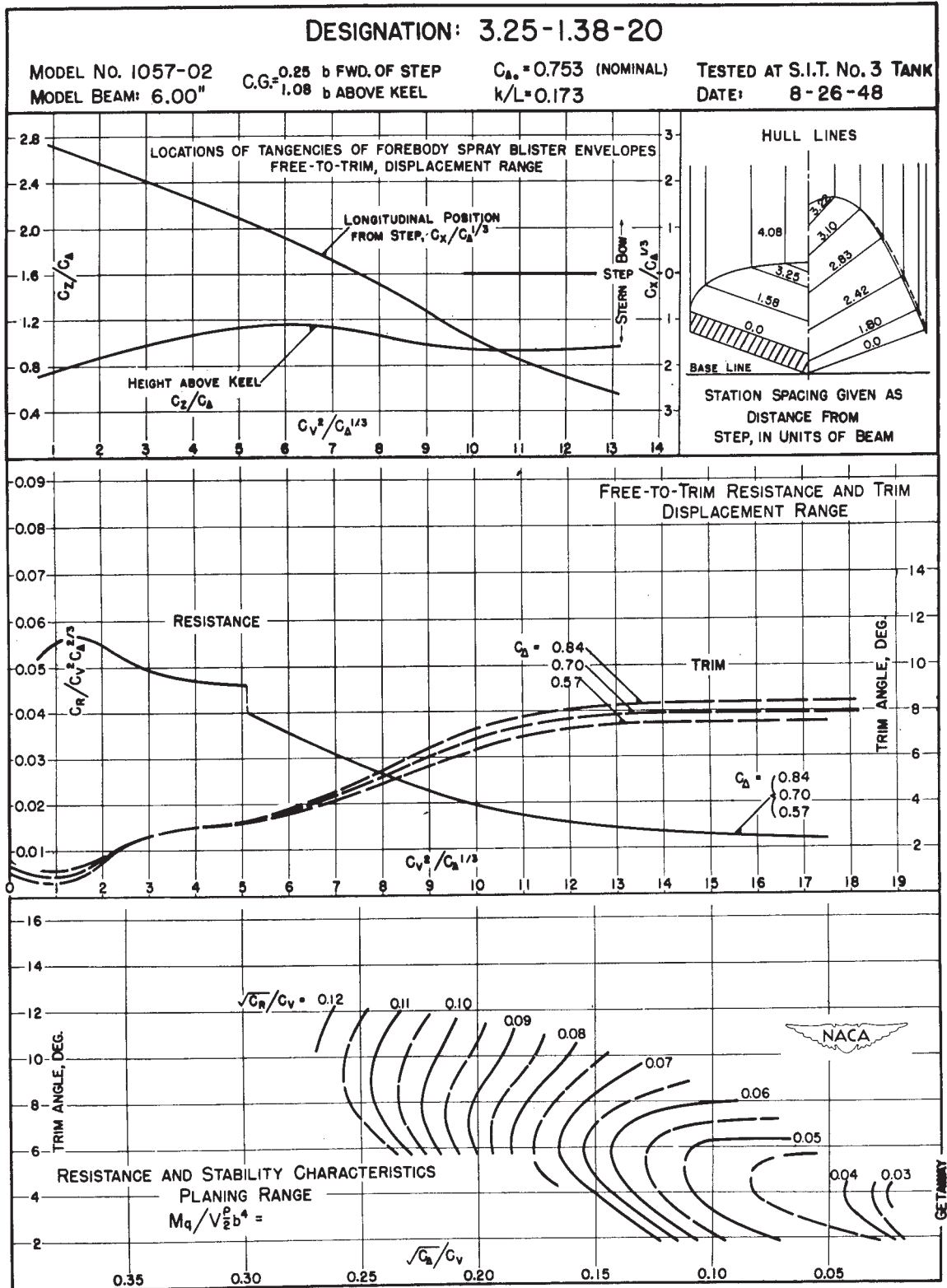


Figure 28.



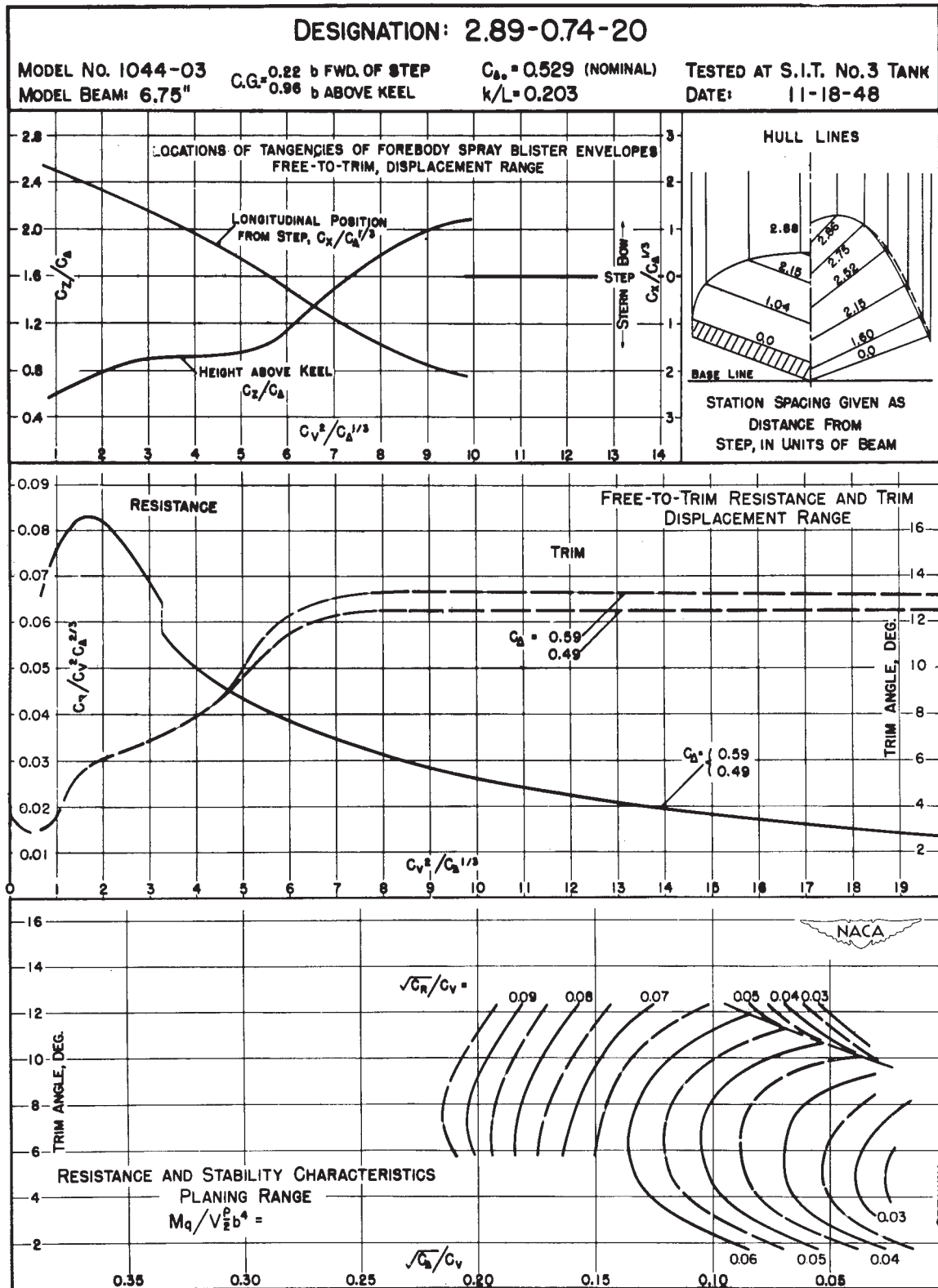


Figure 29.

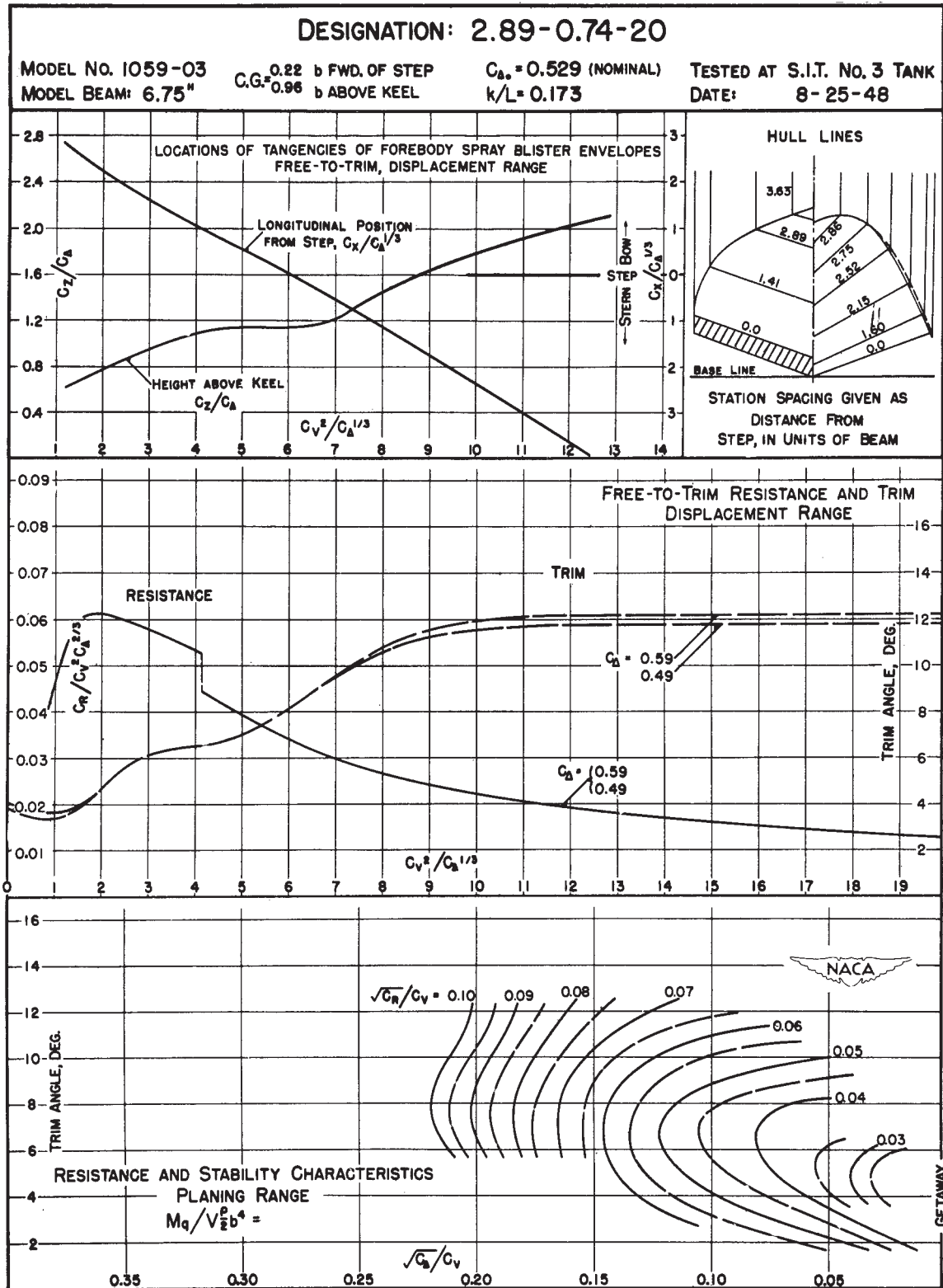


Figure 30.

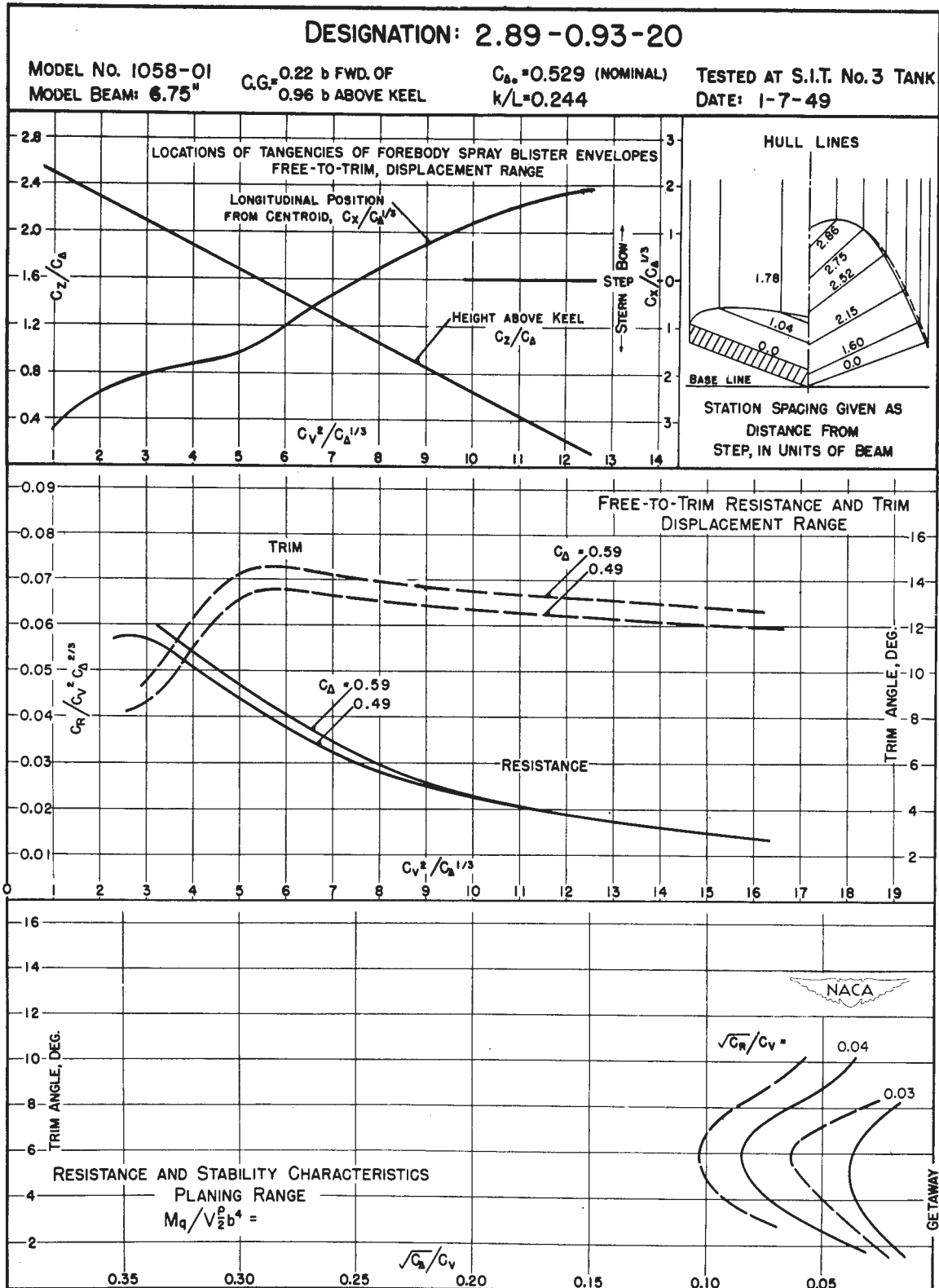


Figure 31.

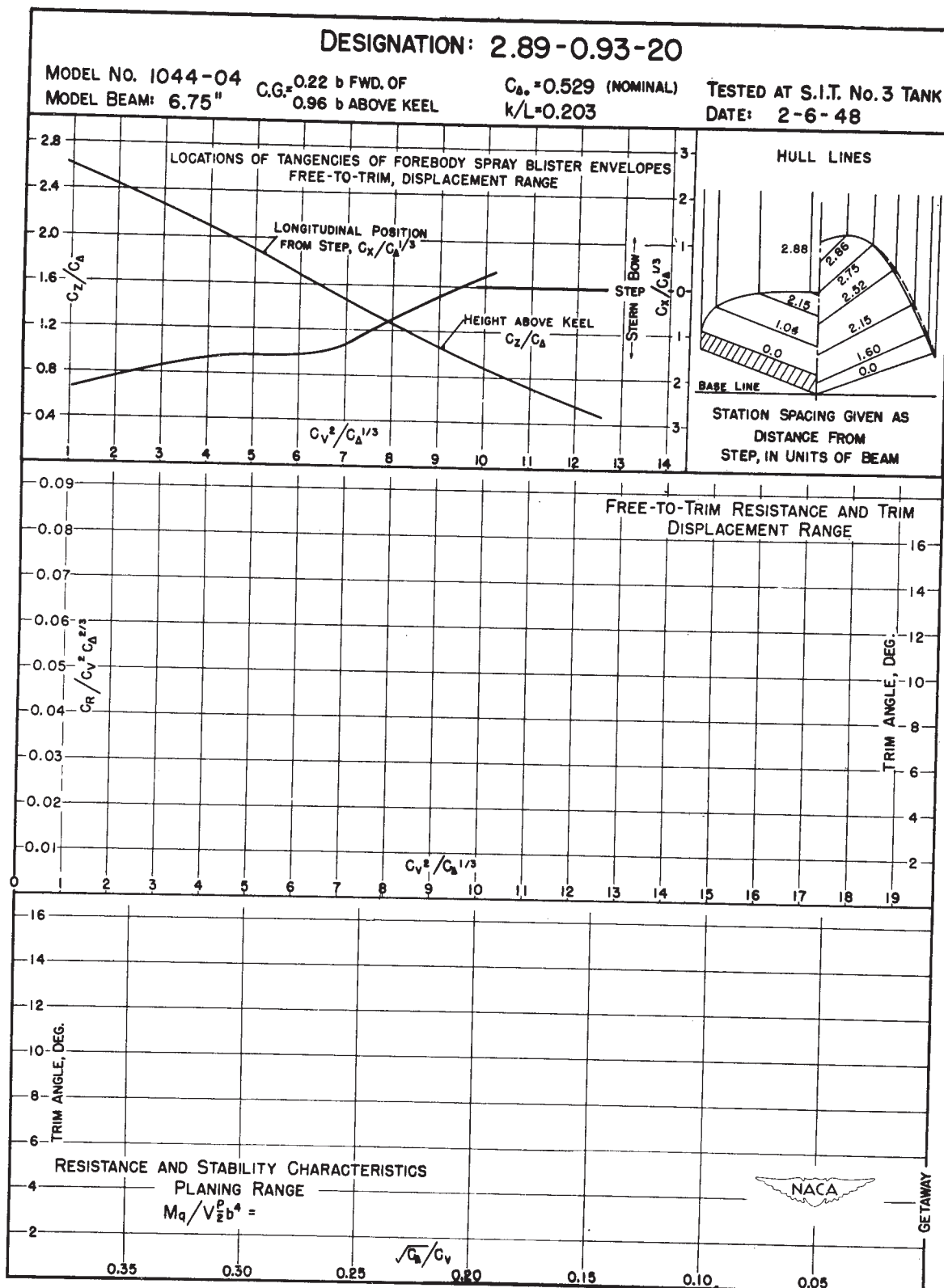


Figure 32.

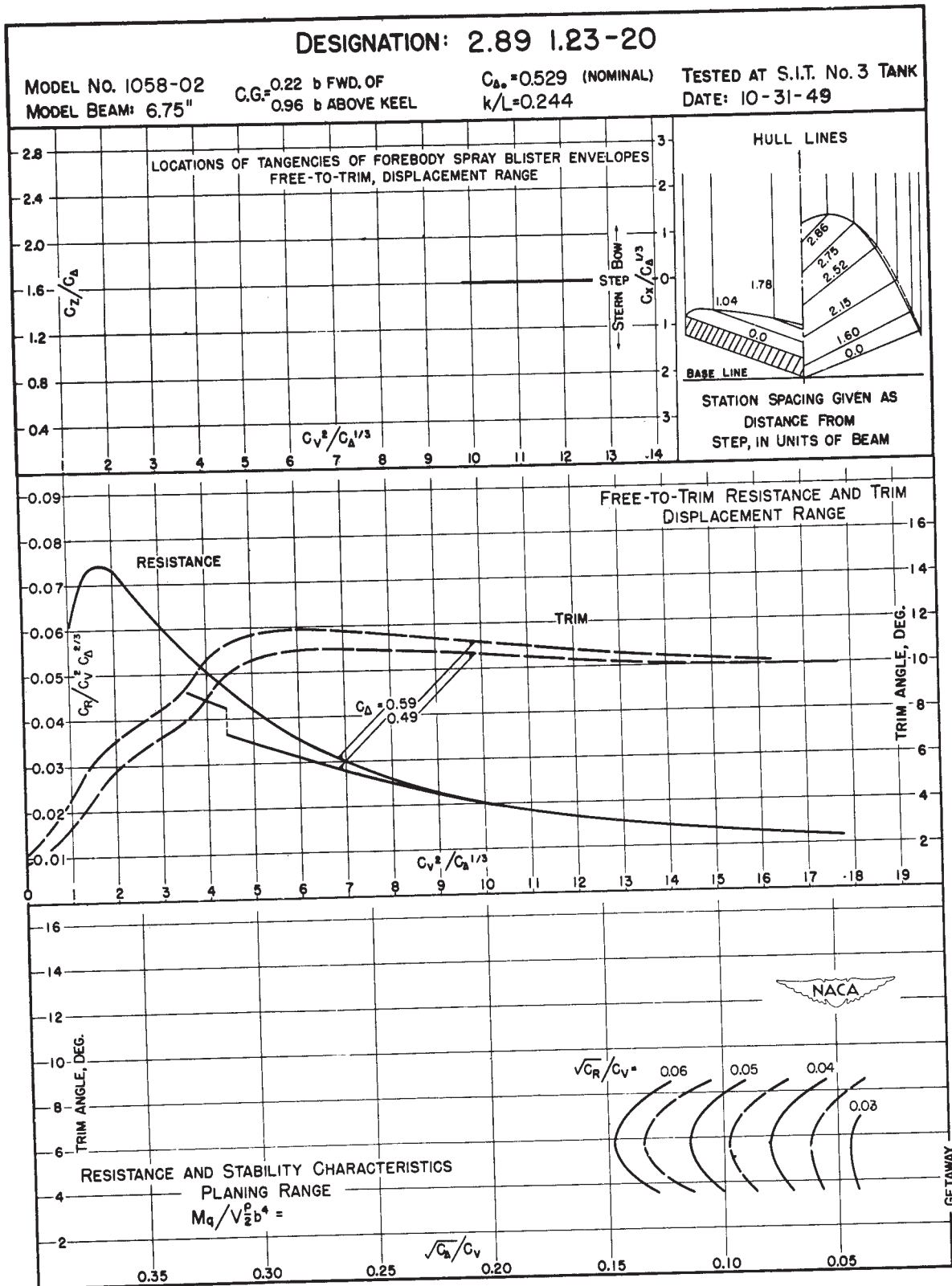


Figure 33.

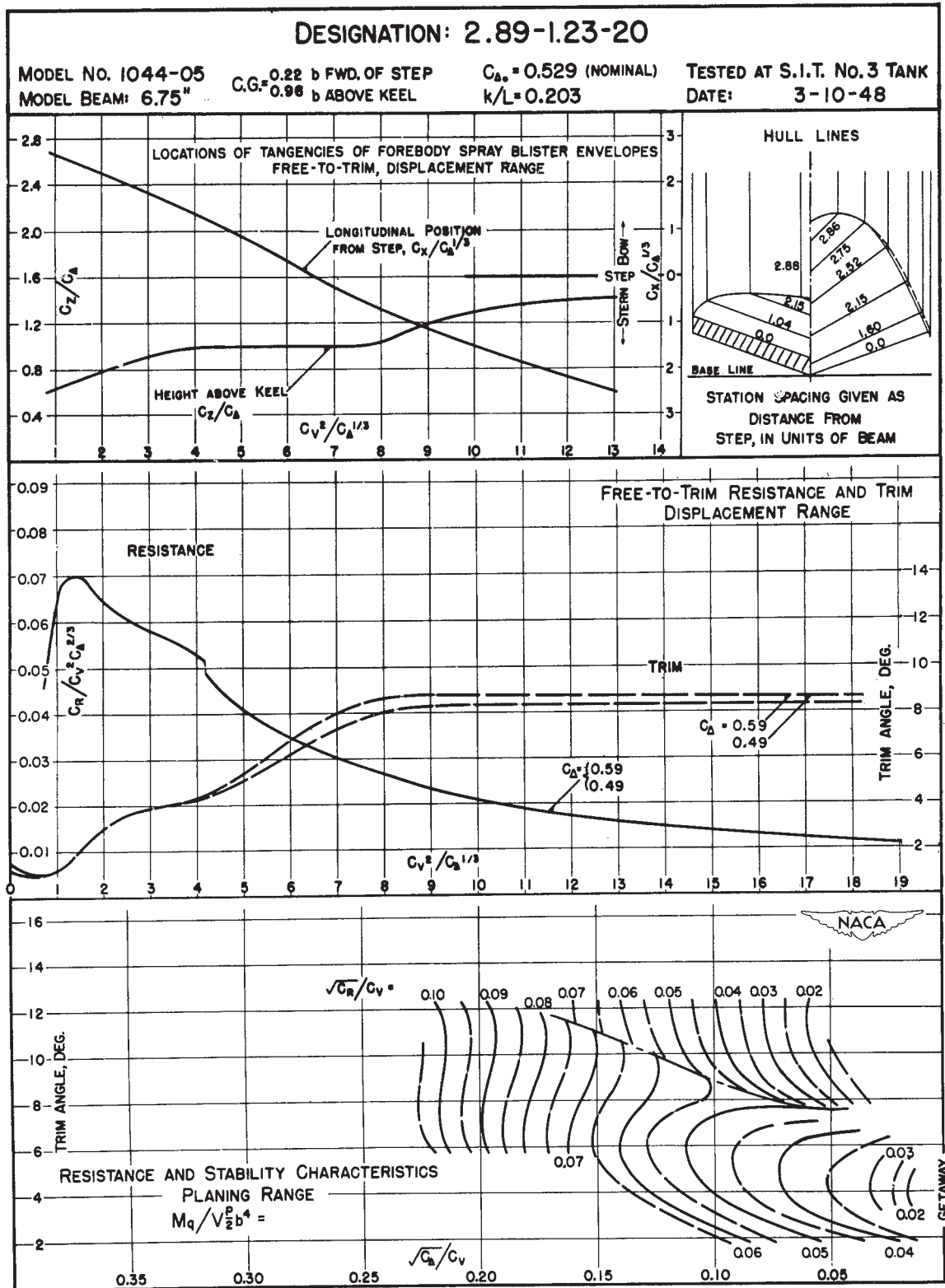


Figure 34.

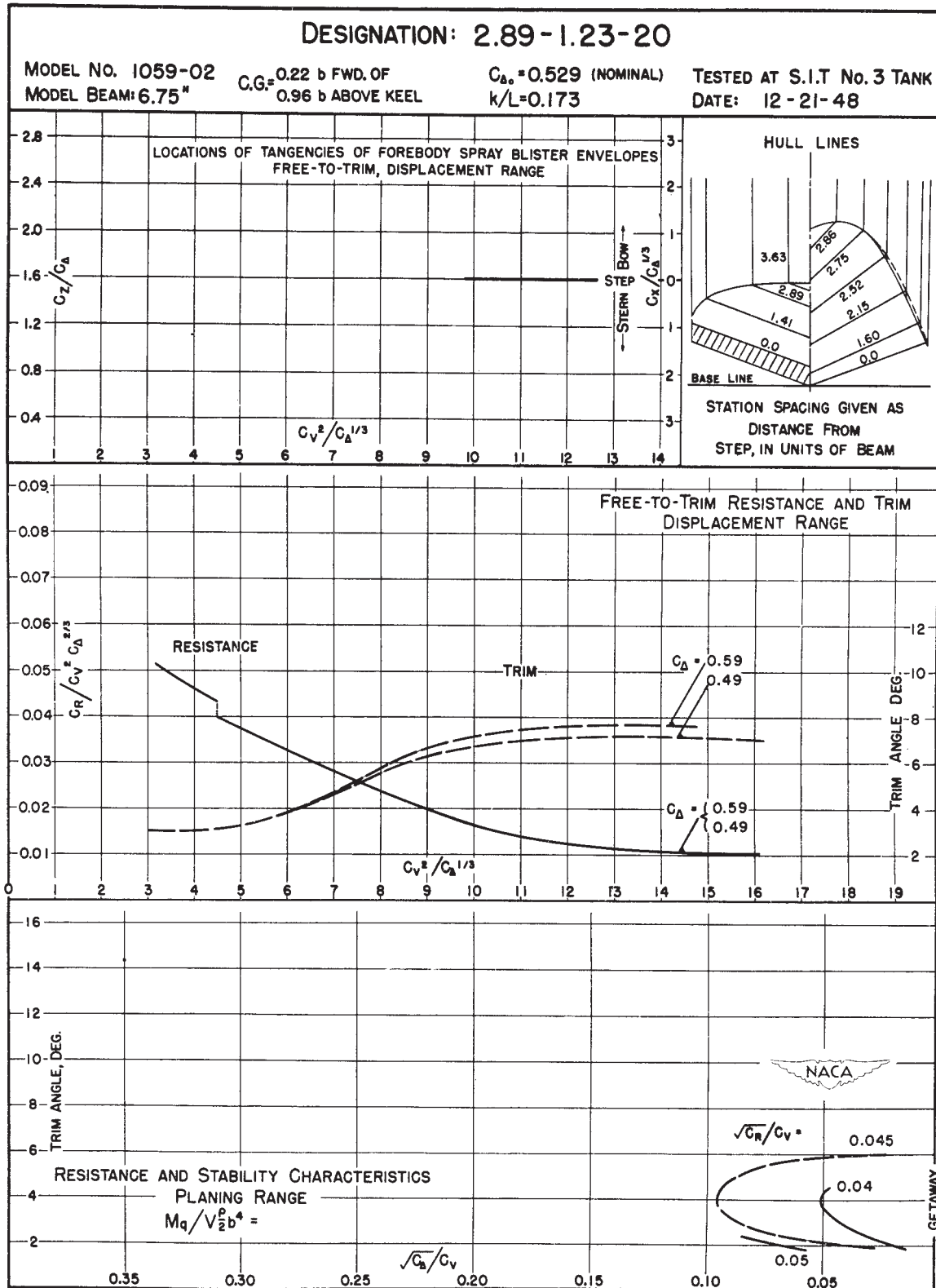


Figure 35.

*declassified by ONR letter dated 5 August 1957*

EFFECT OF FOREBODY-AFTERBODY PROPORTIONS  
AND LENGTH-BEAM RATIO  
ON THE HYDRODYNAMIC CHARACTERISTICS OF  
A SERIES OF FLYING-BOAT HULL MODELS

PREPARED FOR THE  
BUREAU OF AERONAUTICS  
DEPARTMENT OF THE NAVY

UNDER THE SPONSORSHIP OF THE  
OFFICE OF NAVAL RESEARCH  
CONTRACT NO. N6onr-247  
PROJECT NO. NR062-015

REPORT NO. 465

(E.T.T. PROJECT NO. CD1046, CD1047, CD1048)

October 1952

Prepared by: *Marvin I. Haar*  
Marvin I. Haar

Approved by: *W.C. Hugli, Jr.*  
W.C. Hugli, Jr.

EXPERIMENTAL TOWING TANK  
STEVENS INSTITUTE OF TECHNOLOGY  
HOBOKEN, NEW JERSEY



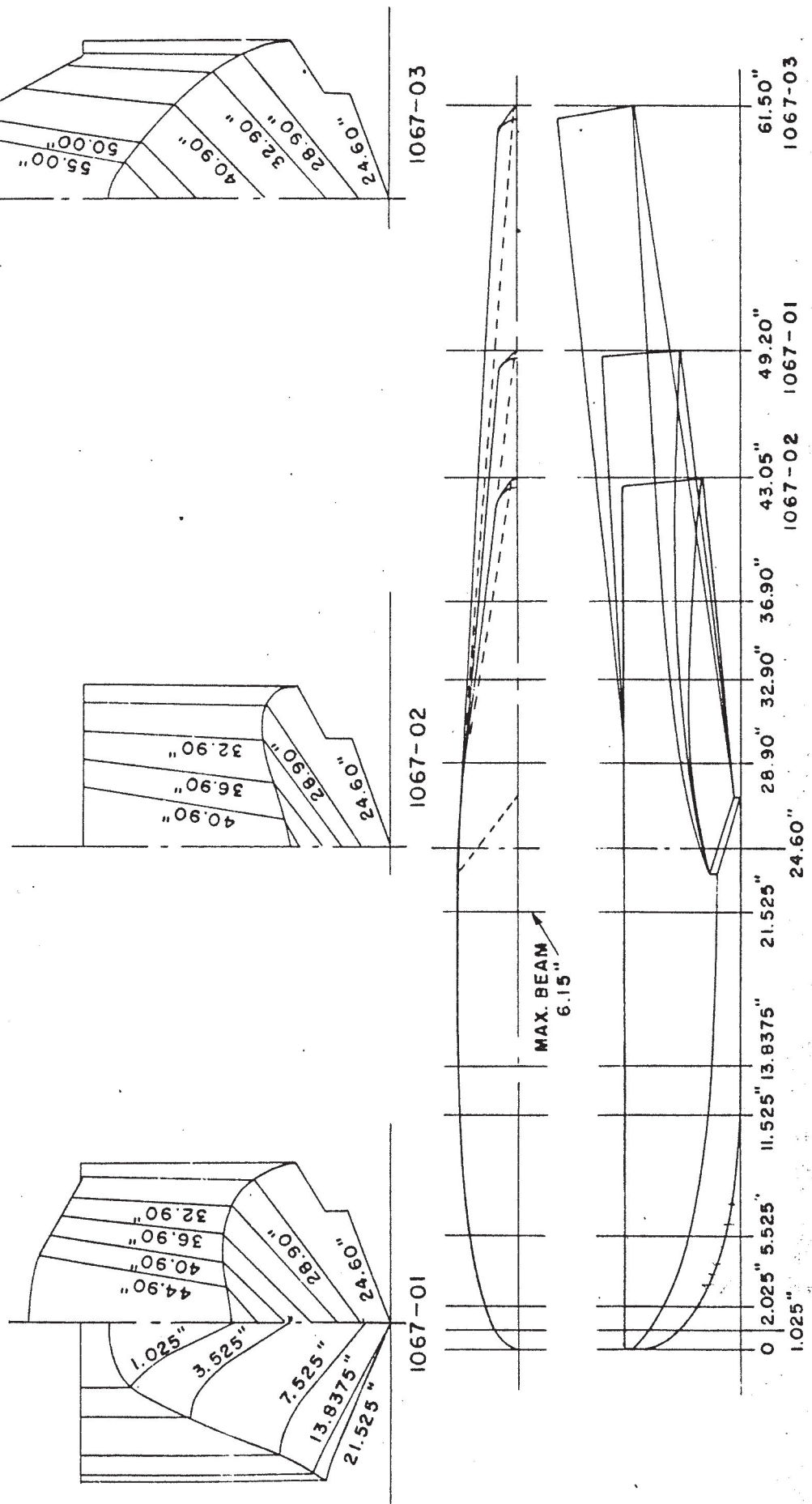
TABLE I  
MODEL DIMENSIONS

|   | Model No. |         |         |         |         |         |         |         |         |
|---|-----------|---------|---------|---------|---------|---------|---------|---------|---------|
|   | 1067-02   | 1067-01 | 1067-03 | 1068-02 | 1068-01 | 1068-03 | 1069-02 | 1069-01 | 1069-03 |
| Forebody Designation                          | short     | short   | short   | medium  | medium  | medium  | long    | long    | long    |
| Afterbody Designation                         | short     | medium  | long    | short   | medium  | long    | short   | medium  | long    |
| Over-all Length-Beam Ratio                    | 7.0       | 8.0     | 10.0    | 10.0    | 12.0    | 16.0    | 14.0    | 18.0    | 24.0    |
| Beam, Maximum, in.                            | 6.15      | 6.15    | 6.15    | 5.02    | 5.02    | 5.02    | 4.10    | 4.10    | 4.10    |
| Forebody Length-Beam Ratio                    | 4.0       | 4.0     | 4.0     | 6.0     | 6.0     | 6.0     | 8.0     | 8.0     | 8.0     |
| Forebody Length (to Step Centroid), in.       | 24.60     | 24.60   | 24.60   | 30.12   | 30.12   | 30.12   | 32.80   | 32.80   | 32.80   |
| Afterbody Length-Beam Ratio                   | 3.0       | 4.0     | 6.0     | 4.0     | 6.0     | 10.0    | 6.0     | 10.0    | 16.0    |
| Afterbody Length (from Step Centroid), in.    | 18.45     | 24.60   | 36.90   | 20.08   | 30.12   | 50.20   | 24.60   | 41.00   | 65.60   |
| Step Depth (at Keel), in.                     | 0.37      | 0.37    | 0.37    | 0.30    | 0.30    | 0.30    | 0.25    | 0.25    | 0.25    |
| Distance from Step Centroid to Step Apex, in. | 2.43      | 2.43    | 2.43    | 2.00    | 2.00    | 2.00    | 1.63    | 1.63    | 1.63    |

# HULL MODELS

GROUP I MAX. BEAM = 6.15" ;  $L_f/b = 4$

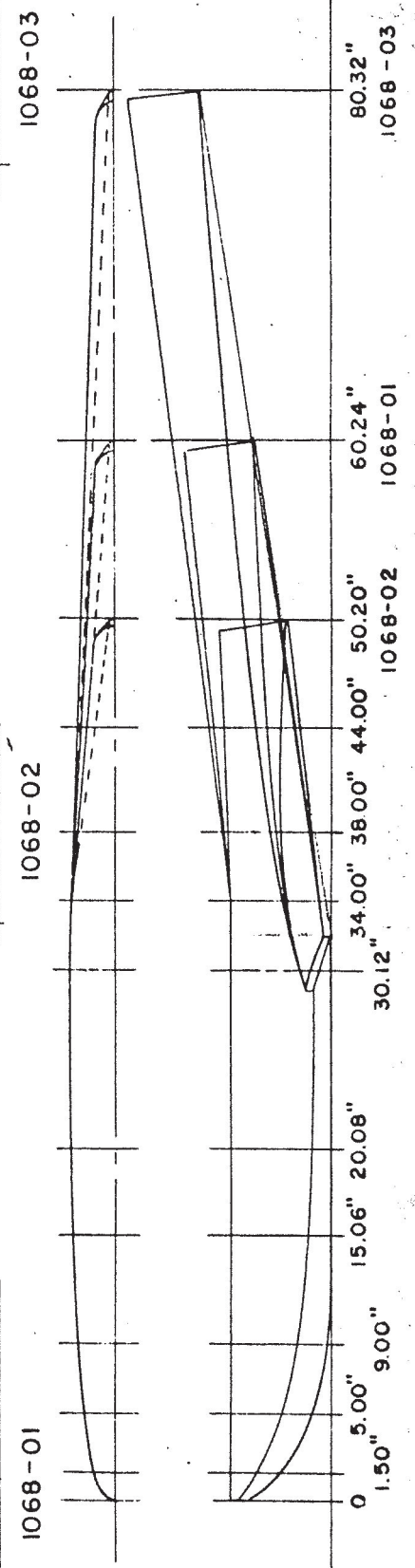
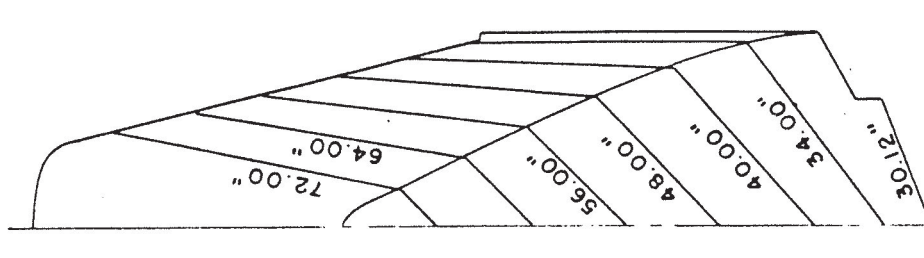
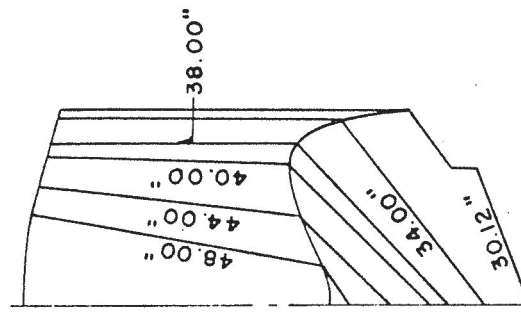
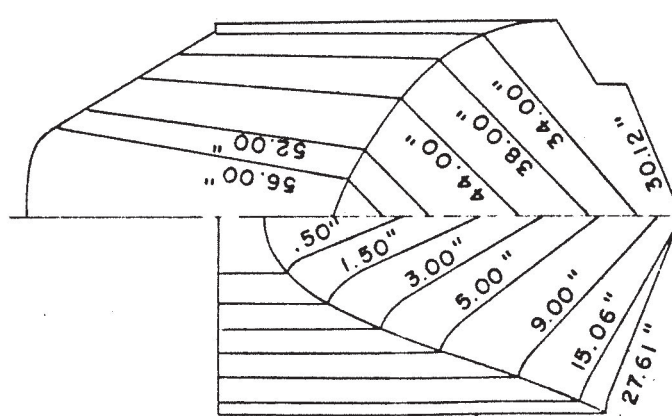
| MODELS NO. | DES.     | $L_a/b$ |
|------------|----------|---------|
| 1067-01    | 6.15-4-4 | 4       |
| 1067-02    | 6.15-4-3 | 3       |
| 1067-03    | 6.15-4-6 | 6       |



# HULL MODELS

GROUP II      MAX. BEAM = 5.02" ;  $L_f/b = 6$

| MODELS NO. | DES.      | $L_d/b$ |
|------------|-----------|---------|
| 1068-01    | 5.02-6-6  | 6       |
| 1068-02    | 5.02-6-4  | 4       |
| 1068-03    | 5.02-6-10 | 10      |



# HULL MODELS

GROUP III      MAX. BEAM = 4.10" ;  $L_f/b = 8$

| MODELS NO. | DES.      | $L_a/b$ |
|------------|-----------|---------|
| 1069-01    | 4.10-8-10 | 10      |
| 1069-02    | 4.10-8-6  | 6       |
| 1069-03    | 4.10-8-16 | 16      |

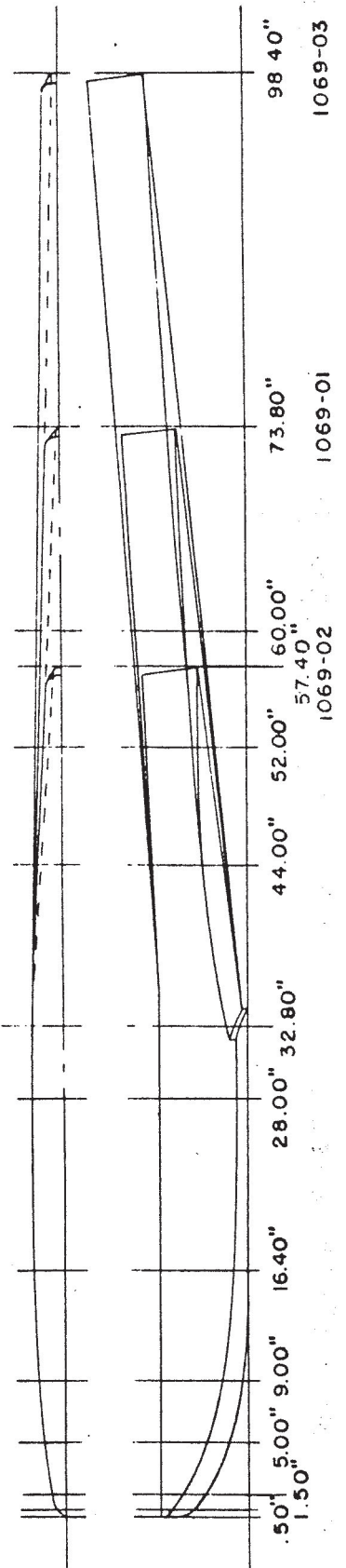
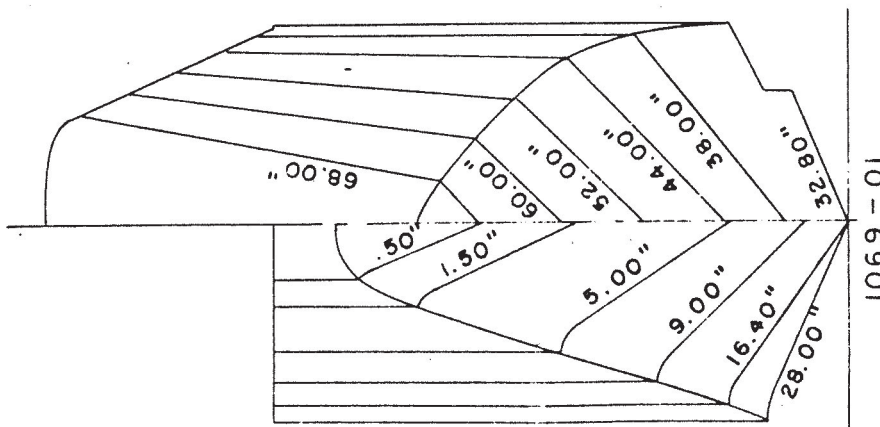
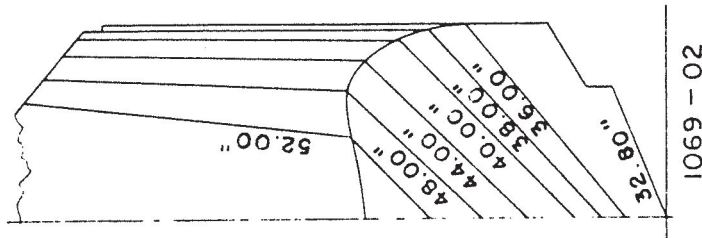
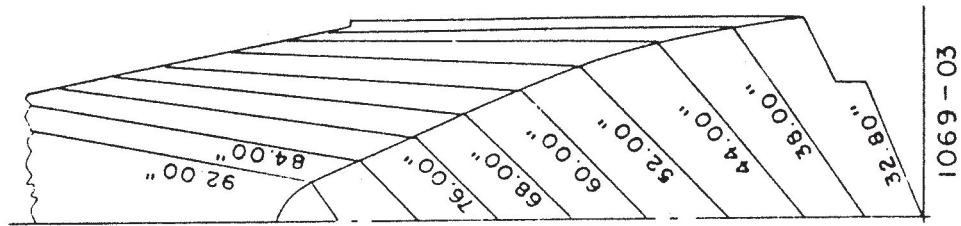




FIGURE 6

DESIGNATION: 4-3-1.18-22

MODEL NO. 1067-02-06

MODEL BEAM: 6.15"

C.G. = 0.27 b FWD. OF CENTROID  $C_{\Delta} = 1.17$  (NOMINAL)  
1.06 b ABOVE KEEL  $k/L =$ 

TESTED AT E.I.T. No. 3 TANK

DATE: SEPT. 19, 1951

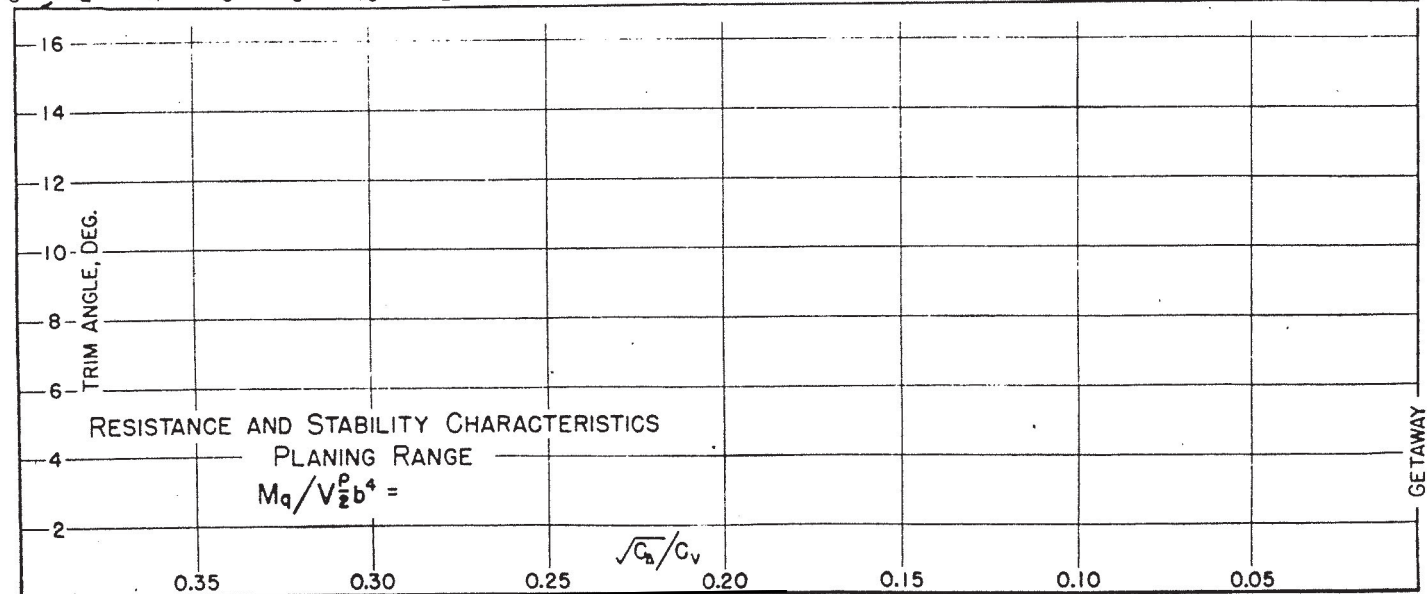
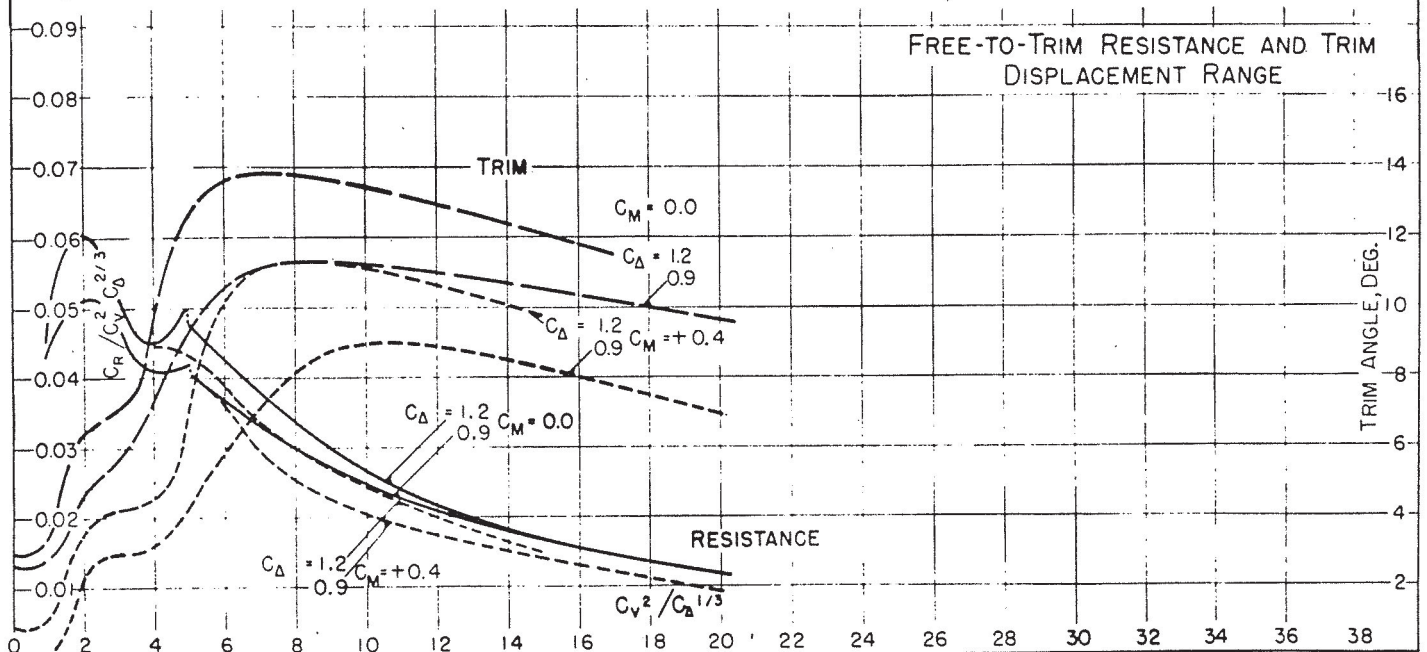
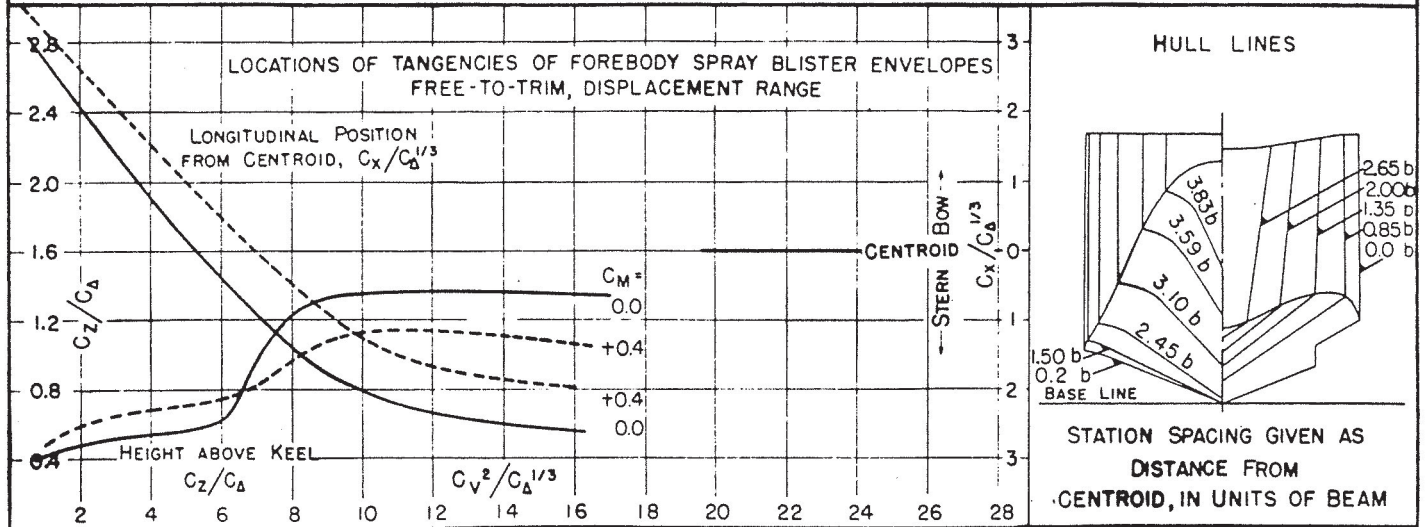


FIGURE 7

## DESIGNATION: 4-3-0.71-22

MODEL NO. 1067-02-10  
MODEL BEAM: 6.15 "

C.G. = 0.27 b FWD. OF CENTROID  $C_{\Delta} = 1.17$  (NOMINAL)  
1.06 b ABOVE KEEL  $k/L =$

TESTED AT E.T.T. No. 3 TANK  
DATE: SEPT. 24, 1951

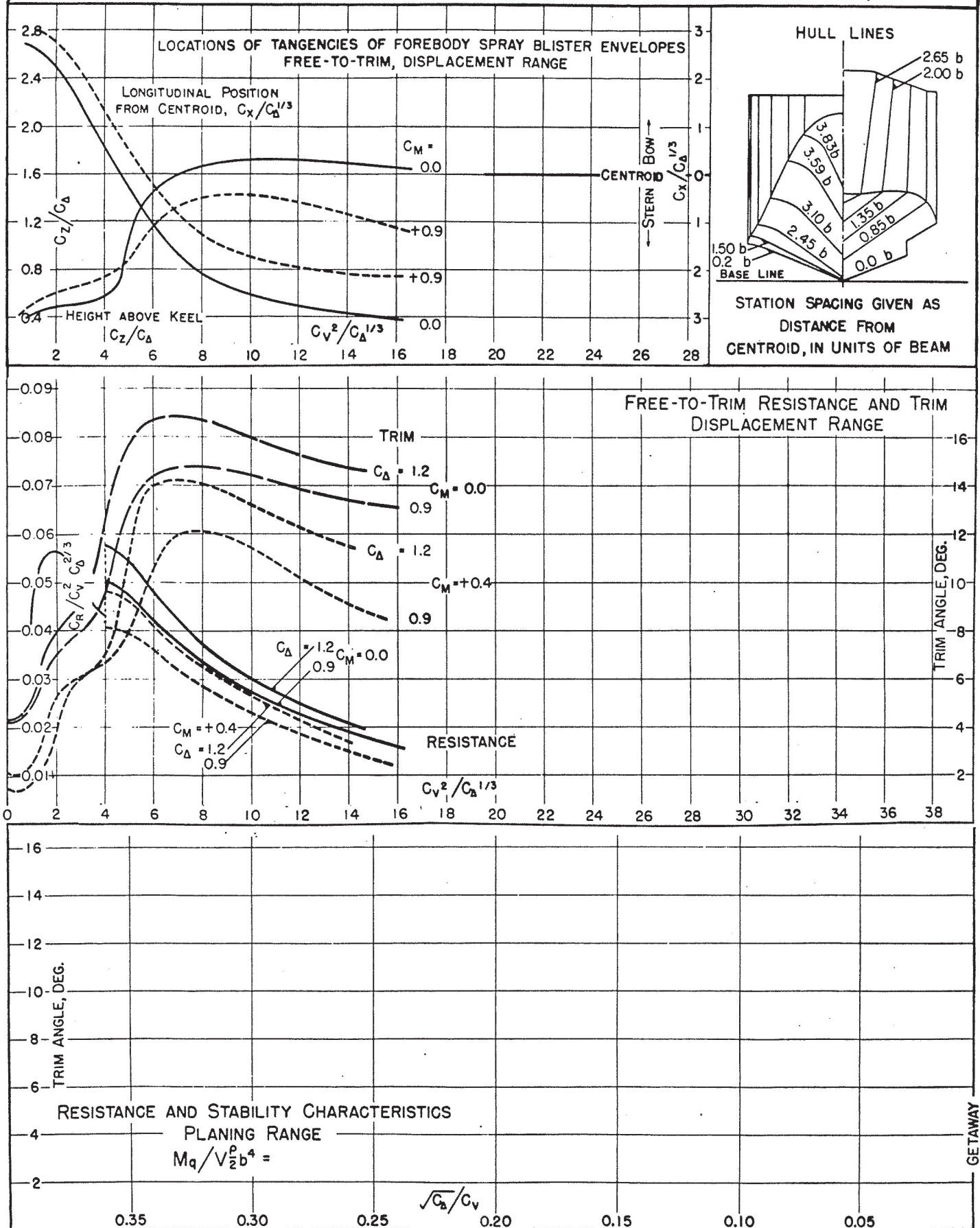




FIGURE 8

DESIGNATION: 4-4-1.18-22

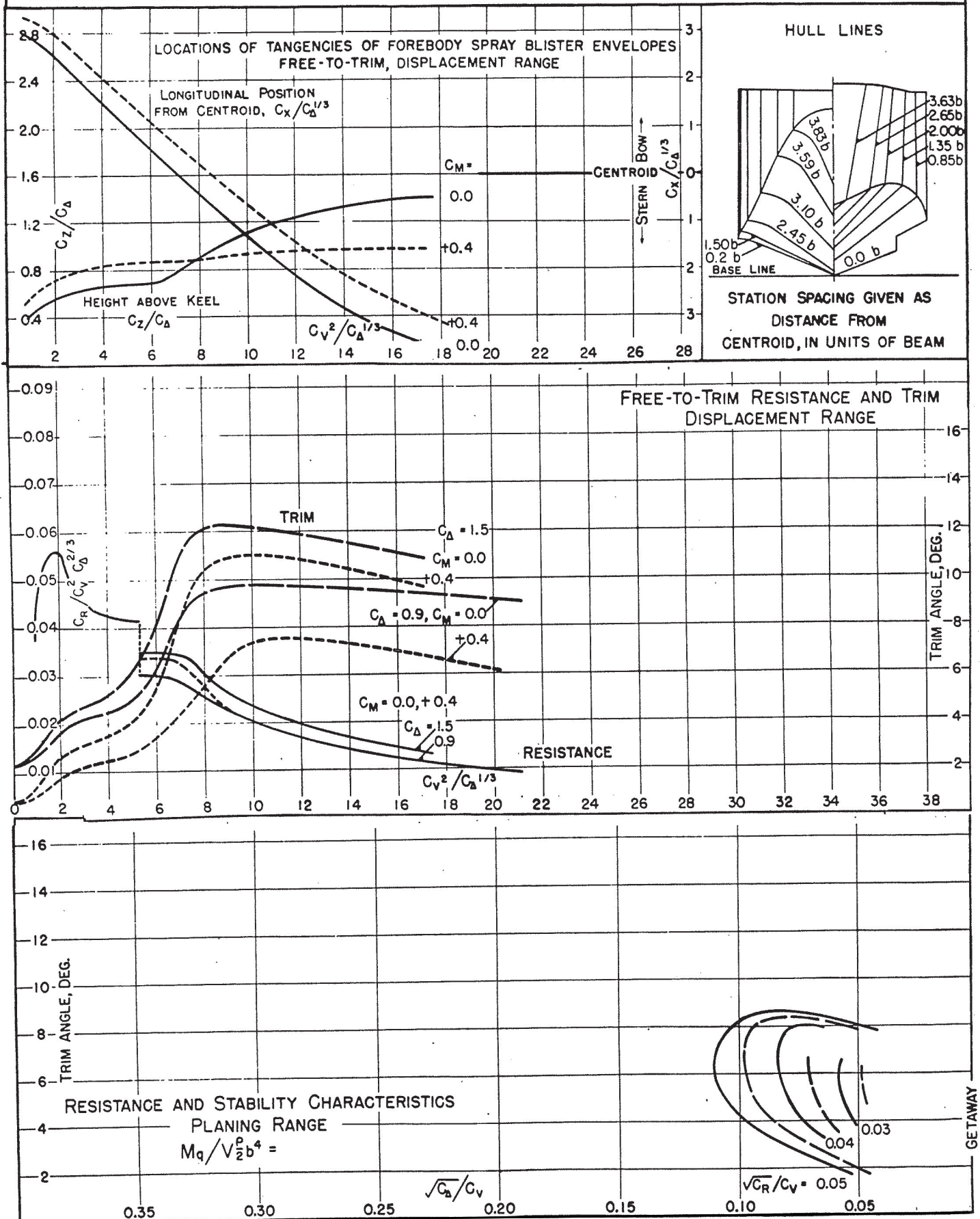
MODEL NO. 1067-01-06  
MODEL BEAM: 6.15"C.G. = 0.27 b FWD. OF CENTROID  $C_{A.} = 1.43$  (NOMINAL)  
1.06 b ABOVE KEEL  $k/L =$ TESTED AT E.T.T. No.3 TANK  
DATE: SEPT. 6, 1951

FIGURE 9

DESIGNATION: 4-4-0.71-22

MODEL NO. 1067-01-10

C.G. = 0.27 b FWD. OF CENTROID  $C_{\Delta} = 1.43$  (NOMINAL)

TESTED AT E.I.T. No. 3 TANK

MODEL BEAM: 6.15"

1.06 b ABOVE KEEL

 $k/L =$ 

DATE: SEPT. 11, 1951

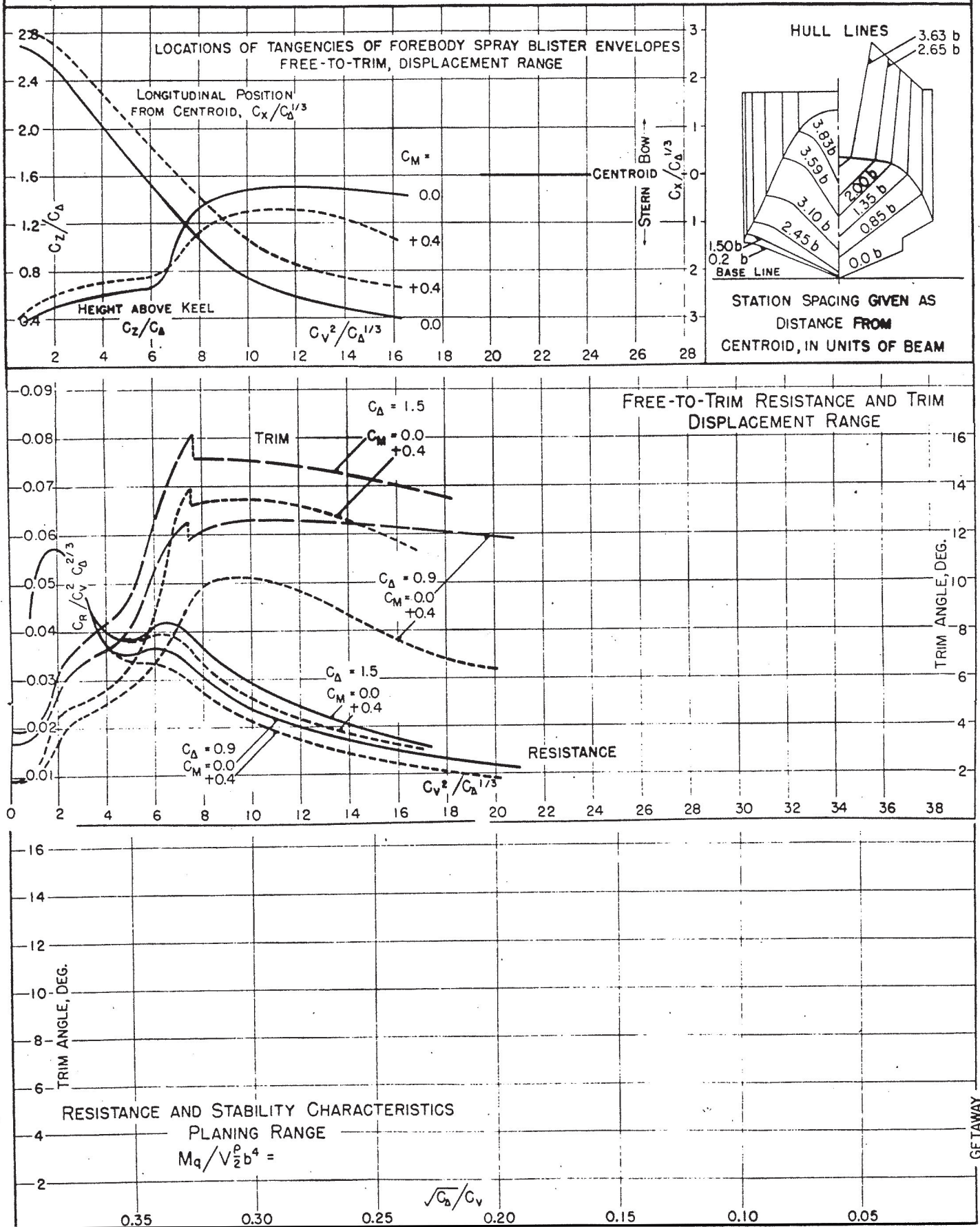




FIGURE 10

DESIGNATION: 4-6-1.18-22

MODEL NO. 1067-03-06

MODEL BEAM: 6.15"

C.G. = 0.27 b FWD. OF CENTROID

 $C_{A_0} = 2.00$  (NOMINAL)

1.06 b ABOVE KEEL

 $k/L =$ 

TESTED AT E.T.T. No. 3 TANK

DATE: SEPT. 14, 1951

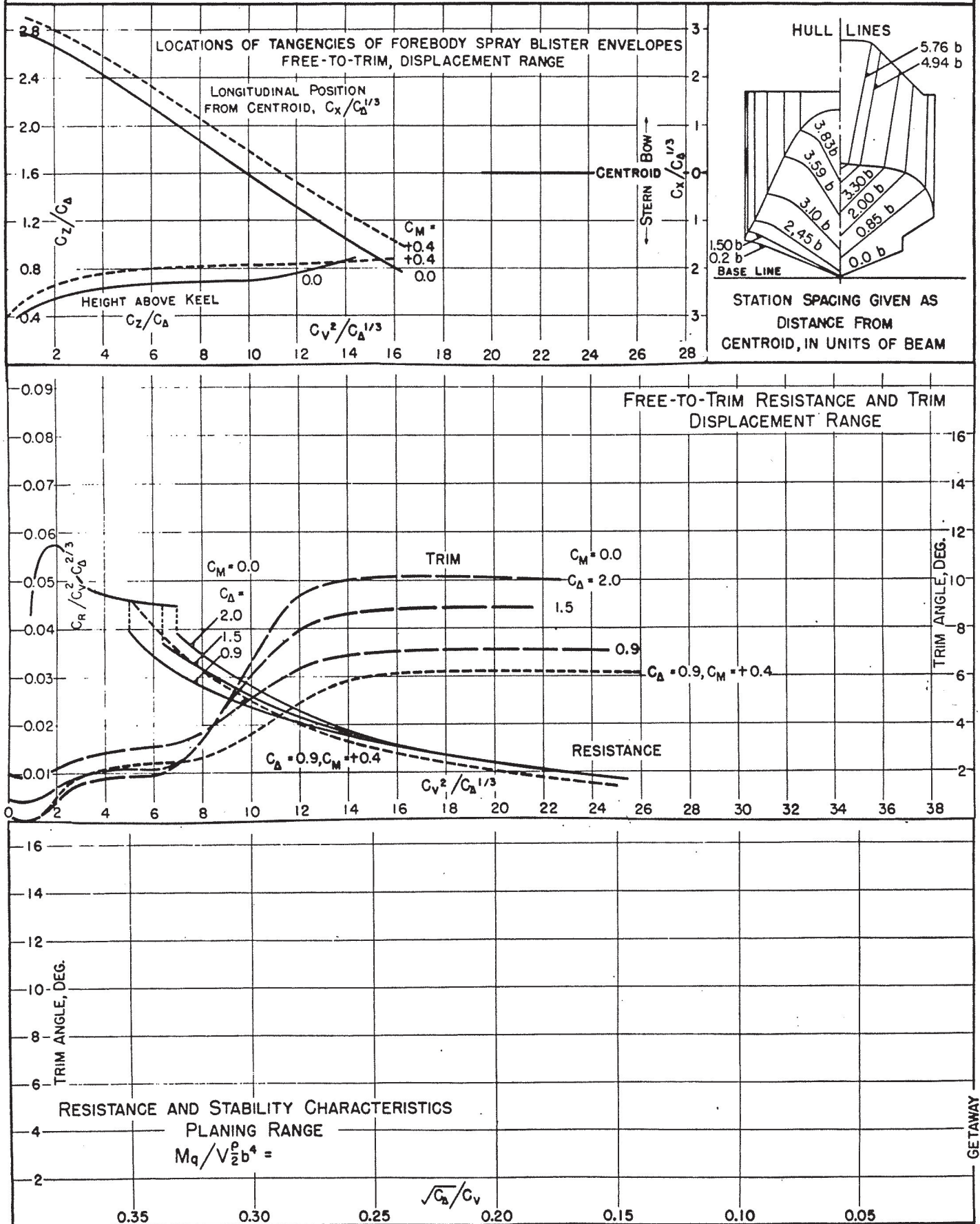


FIGURE 11

## DESIGNATION: 4-6-0.71-22

MODEL NO. 1067-03-10

MODEL BEAM: 6.15"

 $C.G. = 0.27 b$  FWD. OF CENTROID  
 $1.06 b$  ABOVE KEEL
 $C_{\Delta} = 2.00$  (NOMINAL) $k/L =$ 

TESTED AT E.I.T. No. 3 TANK

DATE: SEPT. 25, 1951

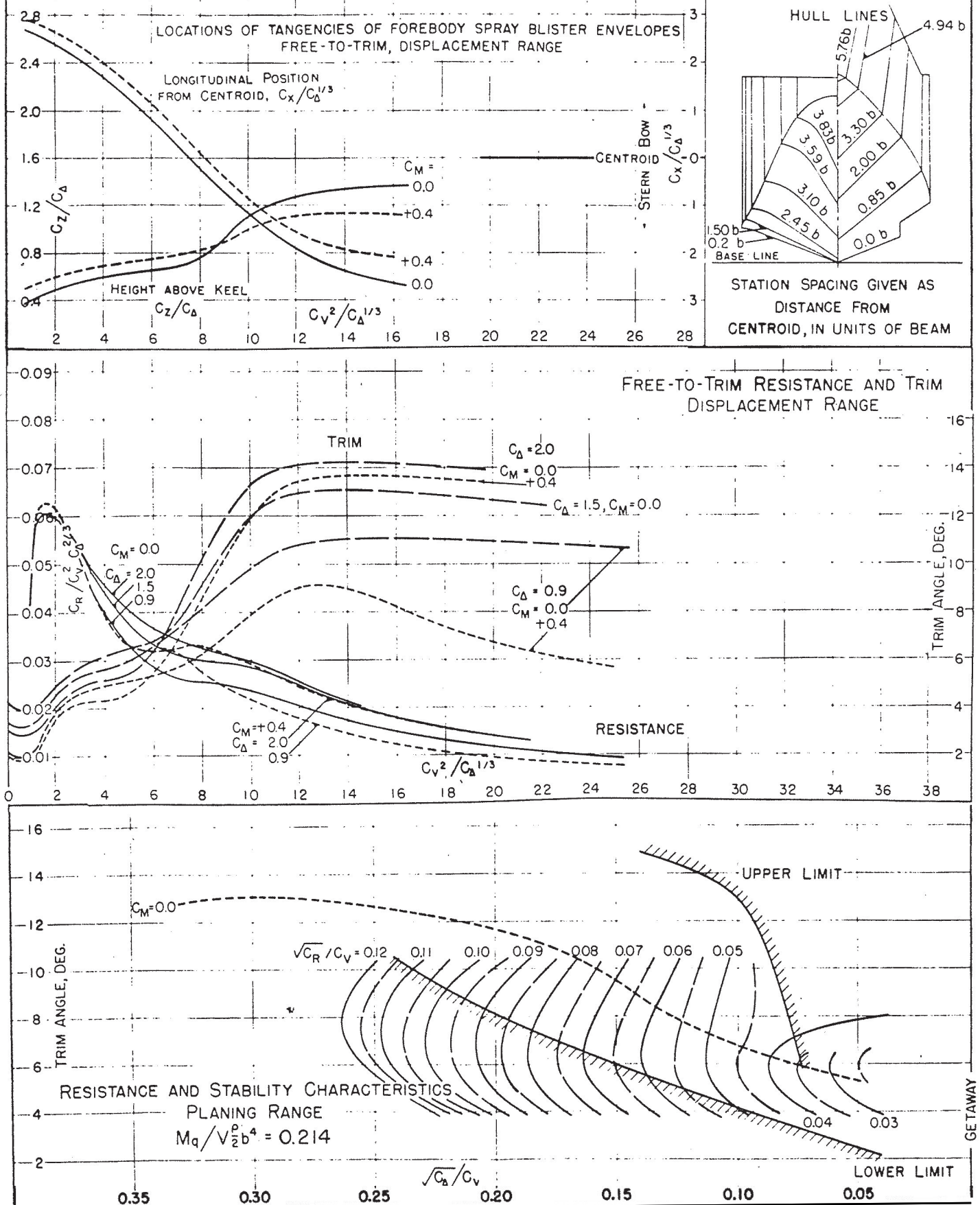




FIGURE 12

DESIGNATION: 6-4-1.33-22

MODEL NO. 1068-02-06  $C.G. = 0.32 b$  FWD. OF CENTROID  $C_{A_0} = 2.00$  (NOMINAL)  
 MODEL BEAM: 5.02"  $1.29 b$  ABOVE KEEL  $k/L =$

TESTED AT E.T.T. No.3 TANK  
 DATE: OCT. 23, 1951

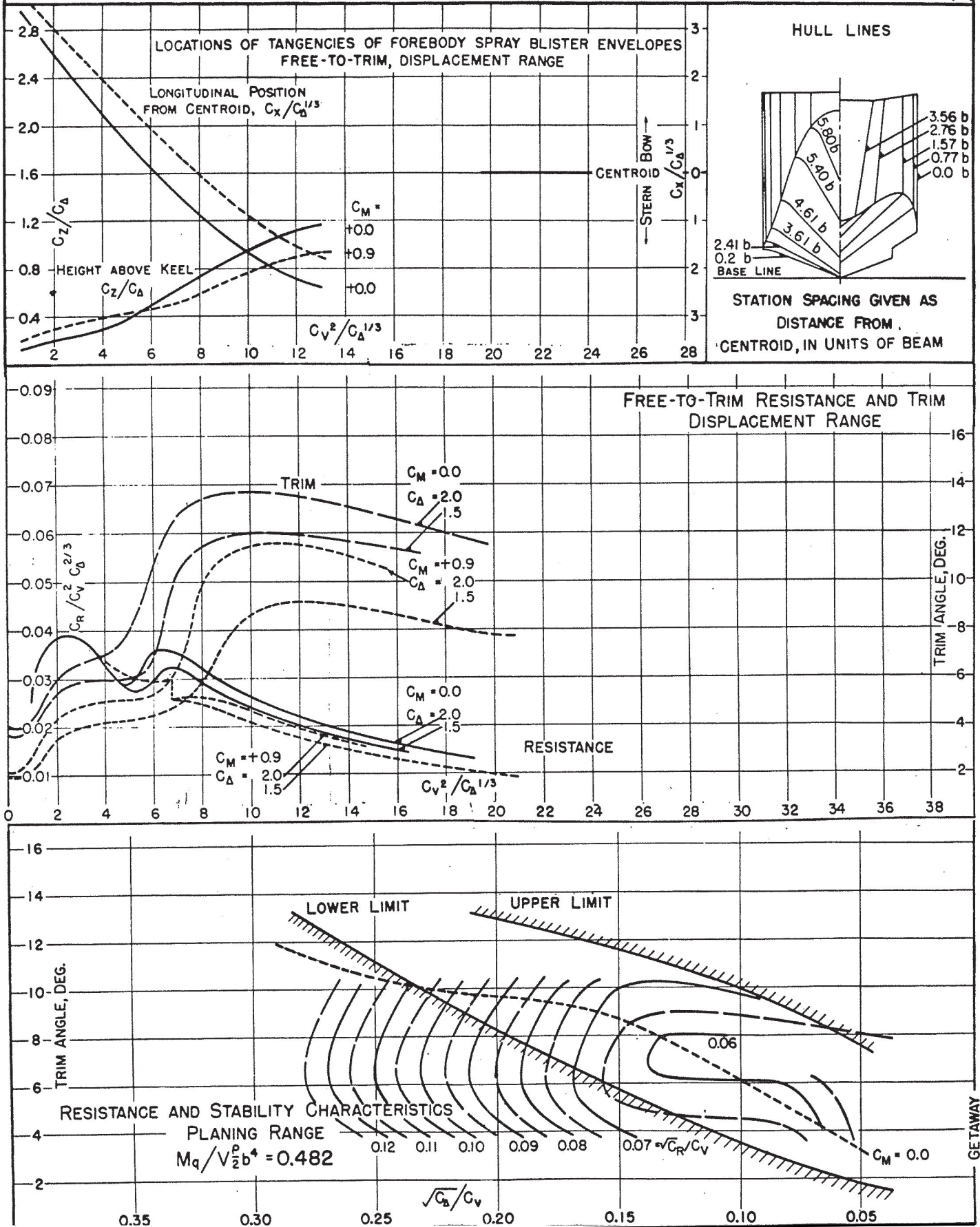


FIGURE 13

## DESIGNATION: 6-4-0.80-22

MODEL NO. 1068-02-10

MODEL BEAM: 5.02"

C.G. = 0.32 b FWD. OF CENTROID  $C_{A_0} = 2.00$  (NOMINAL)  
1.29 b ABOVE KEEL  $k/L =$ 

TESTED AT E.T.T. No. 3 TANK

DATE: NOV. 10, 1951

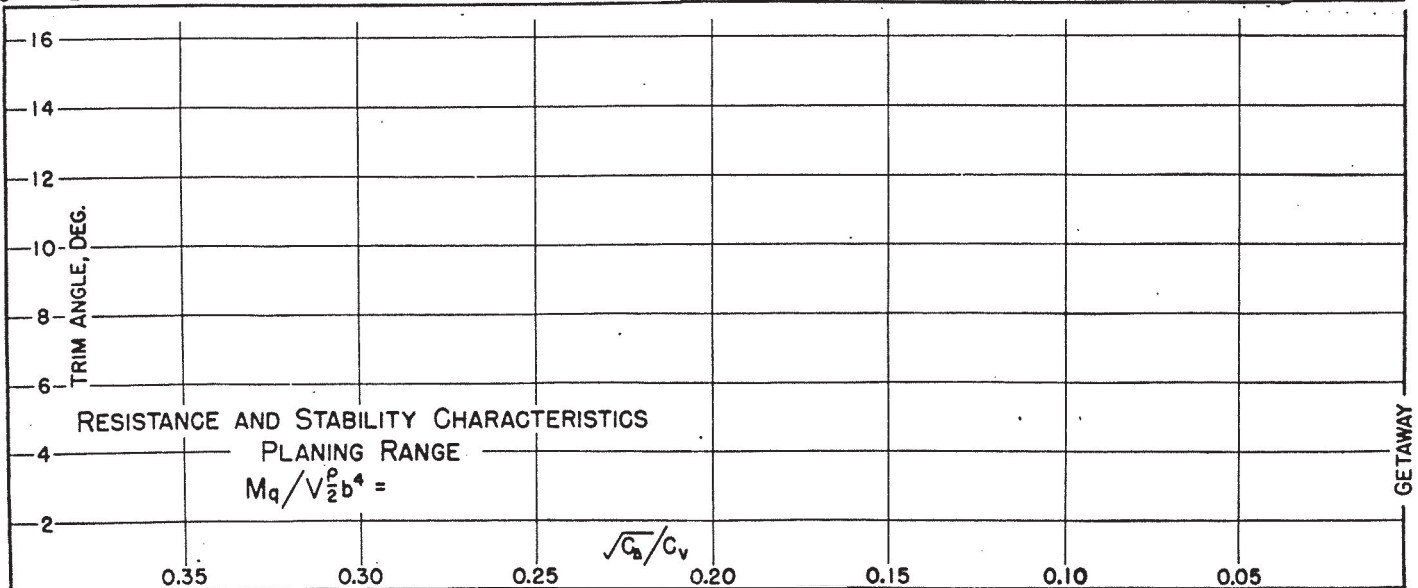
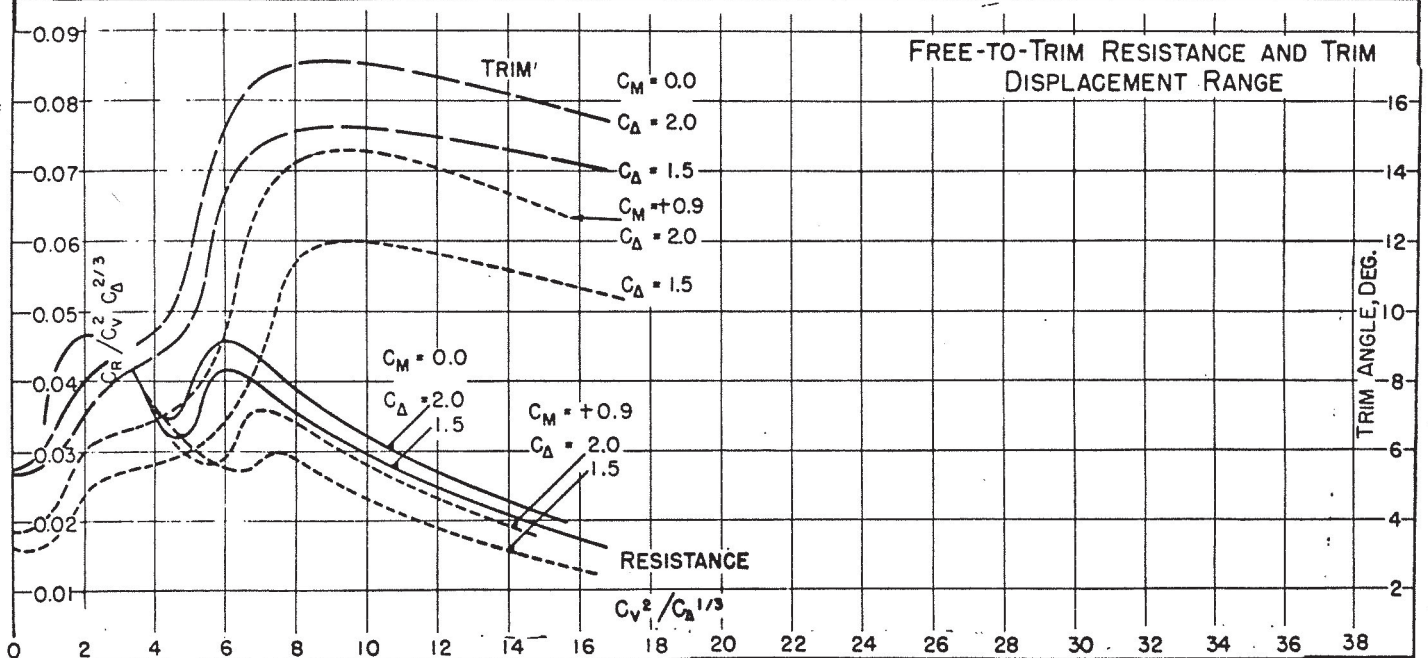
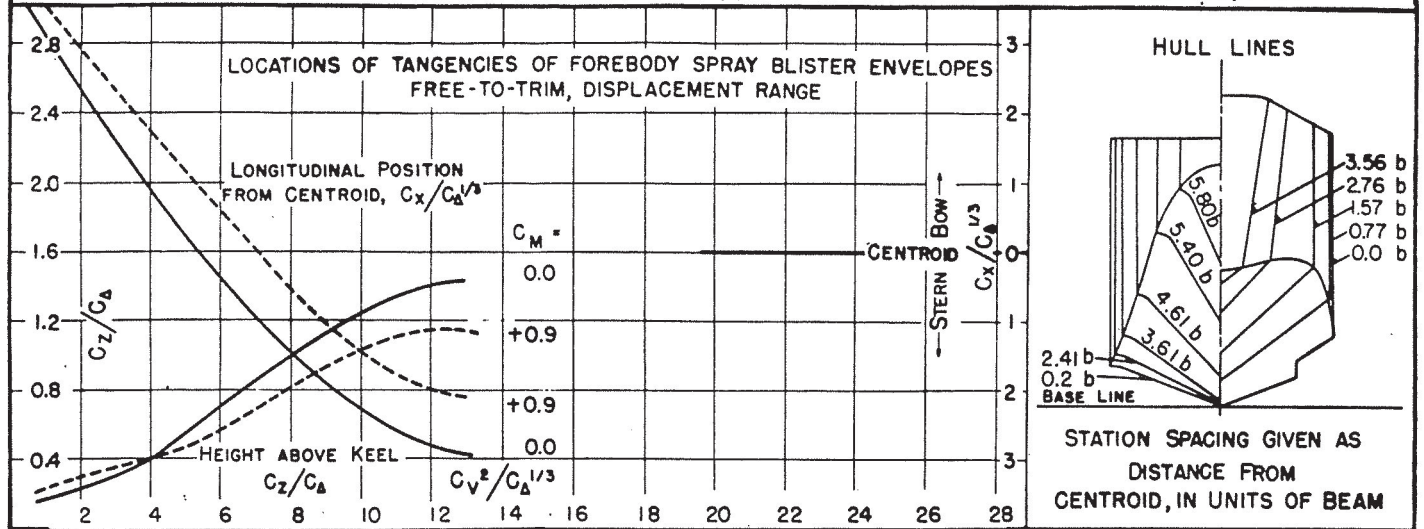




FIGURE 14

## DESIGNATION: 6-6-1.33-22

MODEL NO. 1068-01-06

MODEL BEAM: 5.02 "

C.G. = 0.32 b FWD. OF CENTROID  
1.29 b ABOVE KEEL $C_{A.} = 2.64$  (NOMINAL) $k/L =$ 

TESTED AT E.T.T. No. 3 TANK

DATE: OCT. 17, 1951

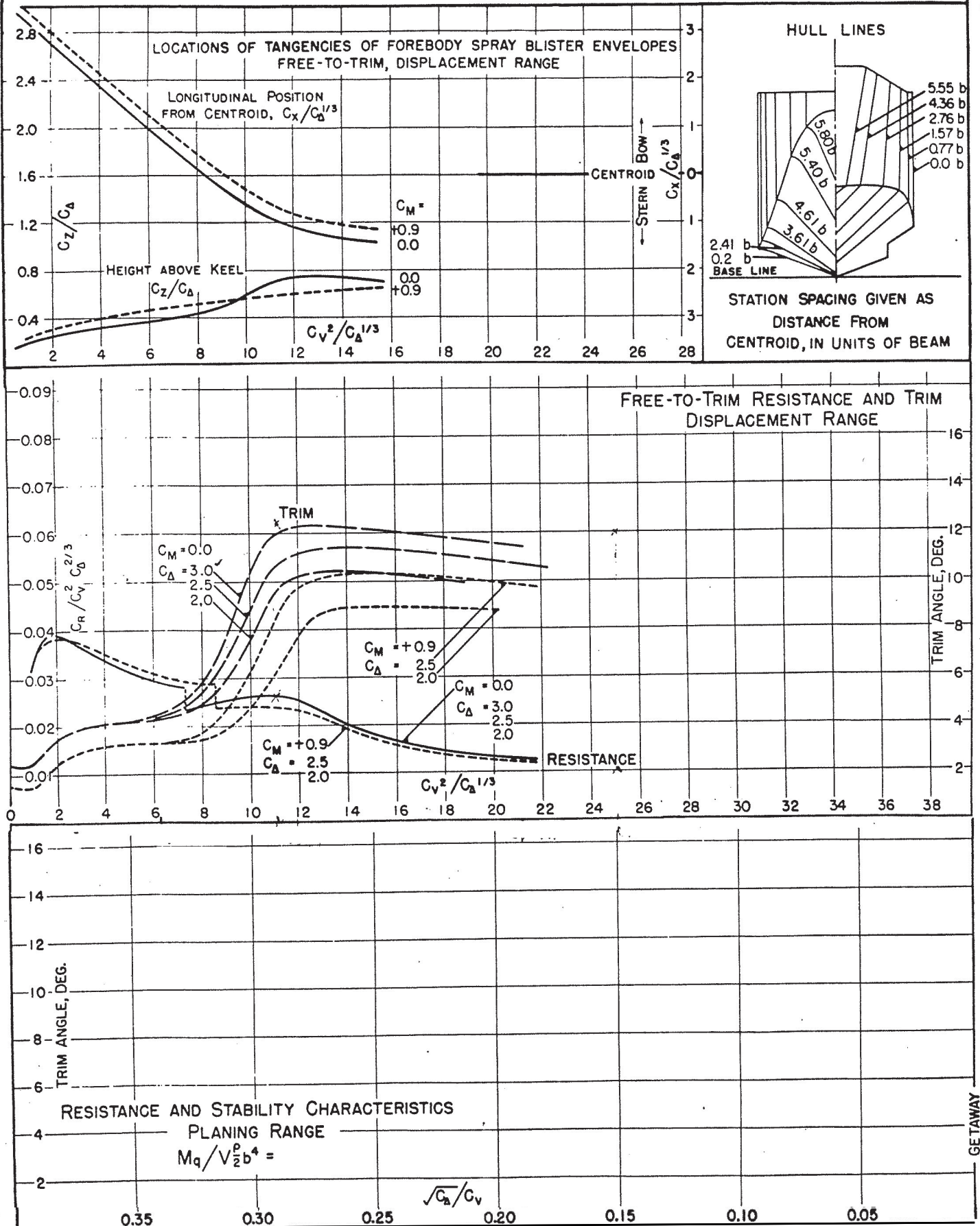


FIGURE 15

DESIGNATION: 6-6-0.80-22

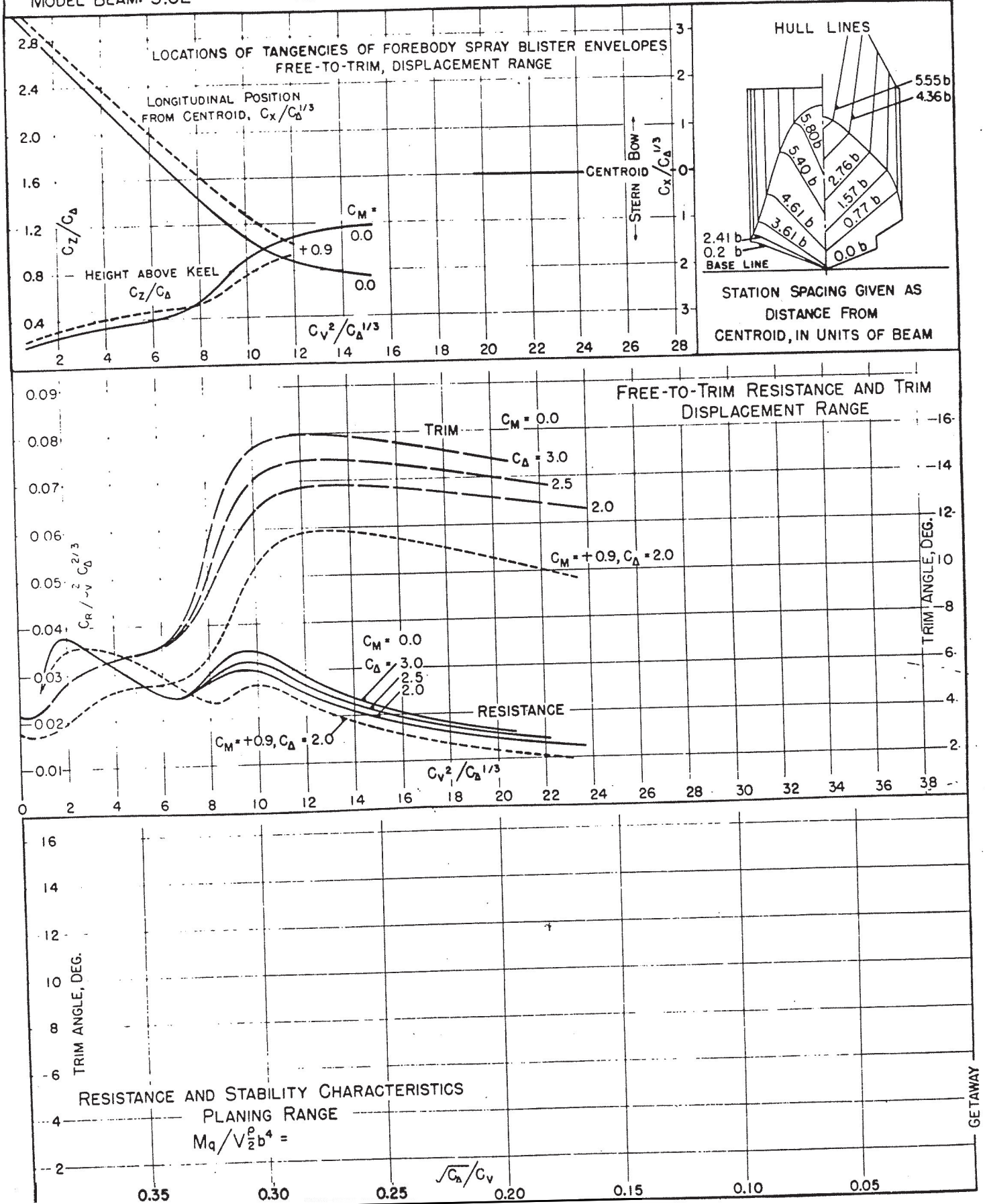
MODEL NO. 1068-01-10  
MODEL BEAM: 5.02"C.G. = 0.32 b FWD. OF CENTROID  $C_{A_0} = 2.64$  (NOMINAL)  
1.29 b ABOVE KEEL  $k/L =$ TESTED AT E.T.T. No.3 TANK  
DATE: OCT. 9, 1951



FIGURE 16

DESIGNATION: 6-10-1.33-22

MODEL NO. 1068-03-06

MODEL BEAM: 5.02"

C.G. = 0.32 b FWD. OF CENTROID  $C_{A_0} = 4.05$  (NOMINAL)  
1.29 b ABOVE KEEL  $k/L =$ 

TESTED AT E.T.T. No.3 TANK

DATE: NOV. 9, 1951

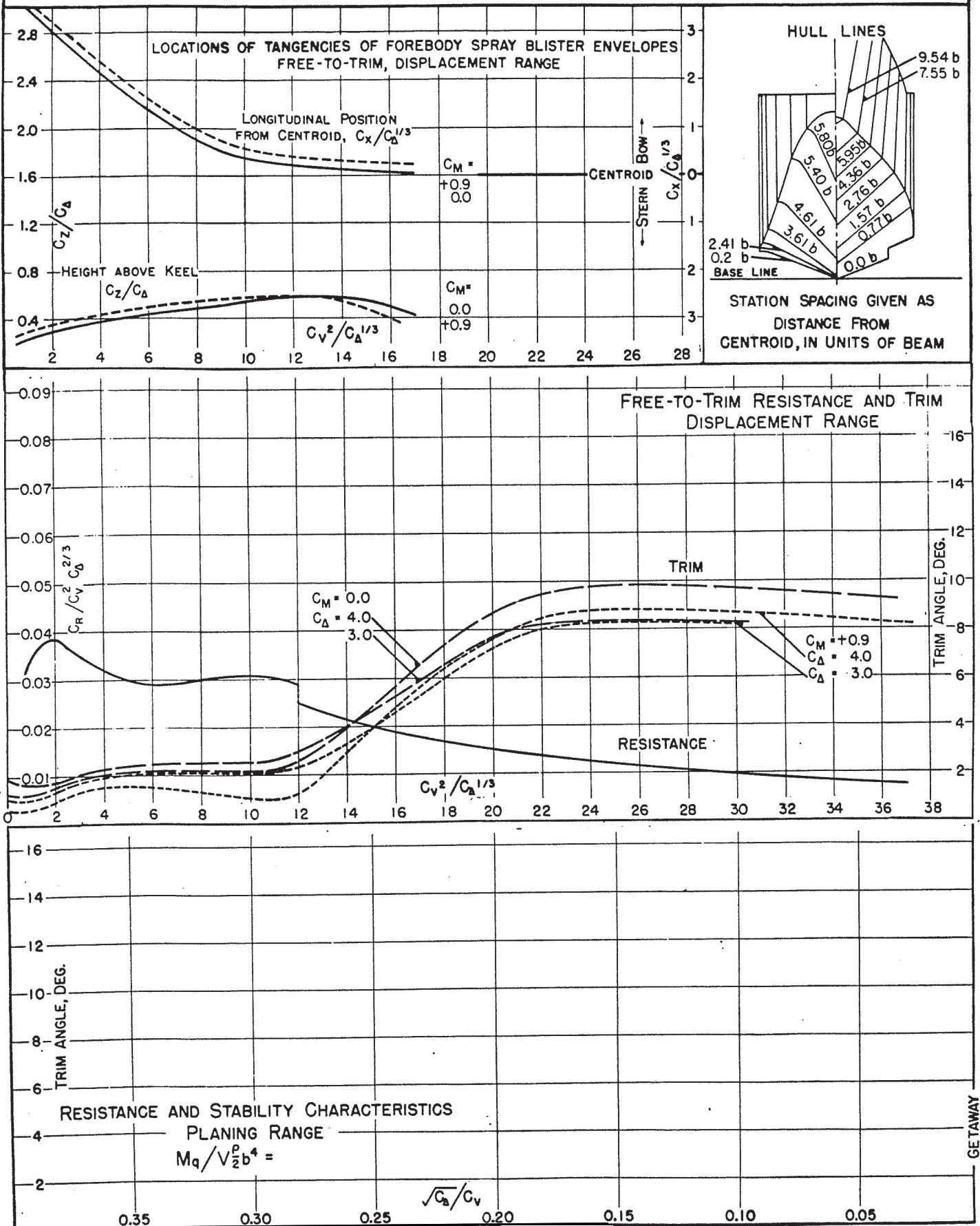


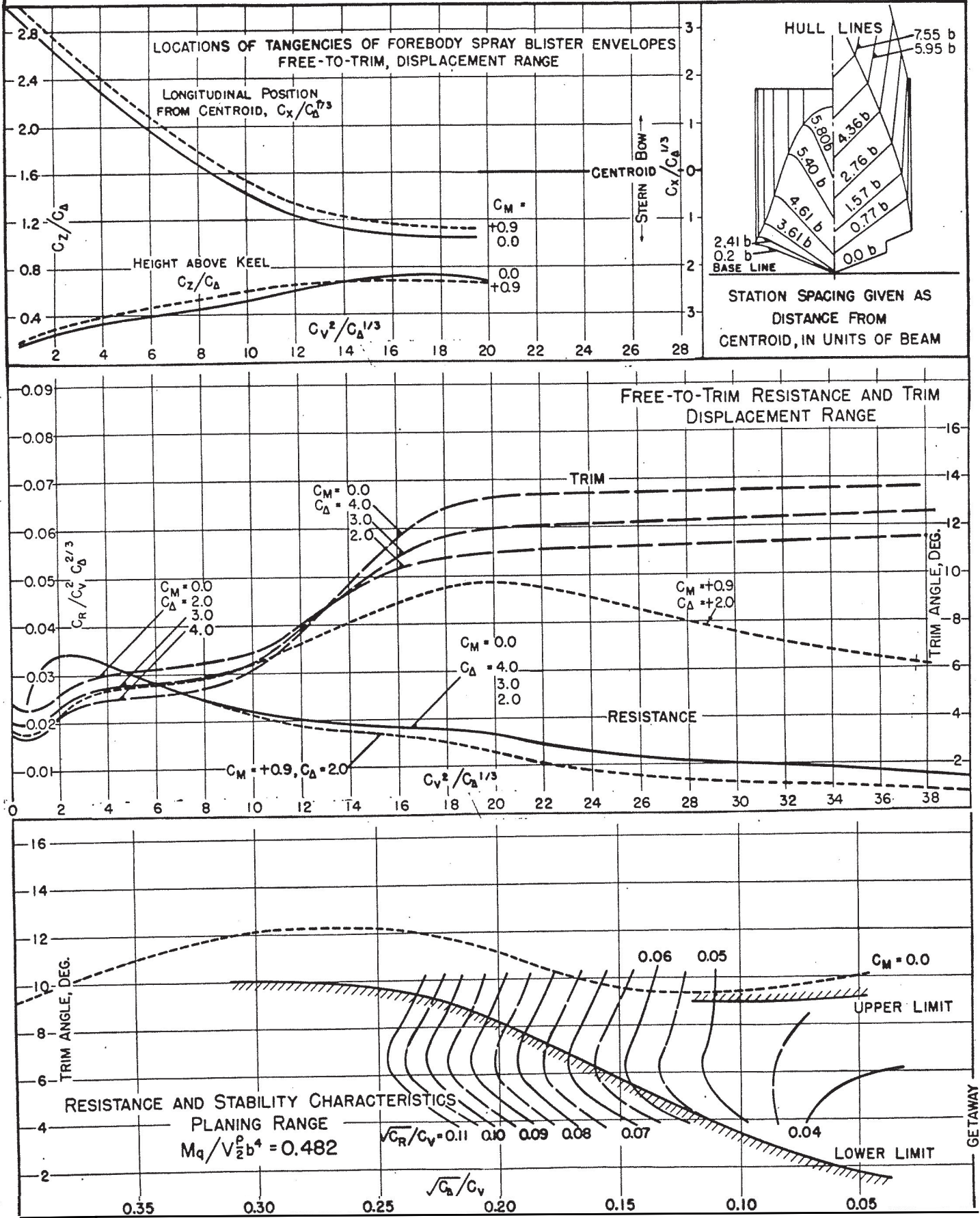
FIGURE 17

## DESIGNATION: 6-10-0.80-22

MODEL NO. 1068-03-10  
MODEL BEAM: 5.02"

C.G. = 0.32 b FWD. OF CENTROID  $C_{A_0} = 4.05$  (NOMINAL)  
1.29 b ABOVE KEEL  $k/L =$

TESTED AT E.T.T. No.3 TANK  
DATE: OCT. 22, 1951





DESIGNATION: 8-6-1.12-22

TESTED AT E.T.T. No. 3 TANK  
DATE: NOV. 21, 1951

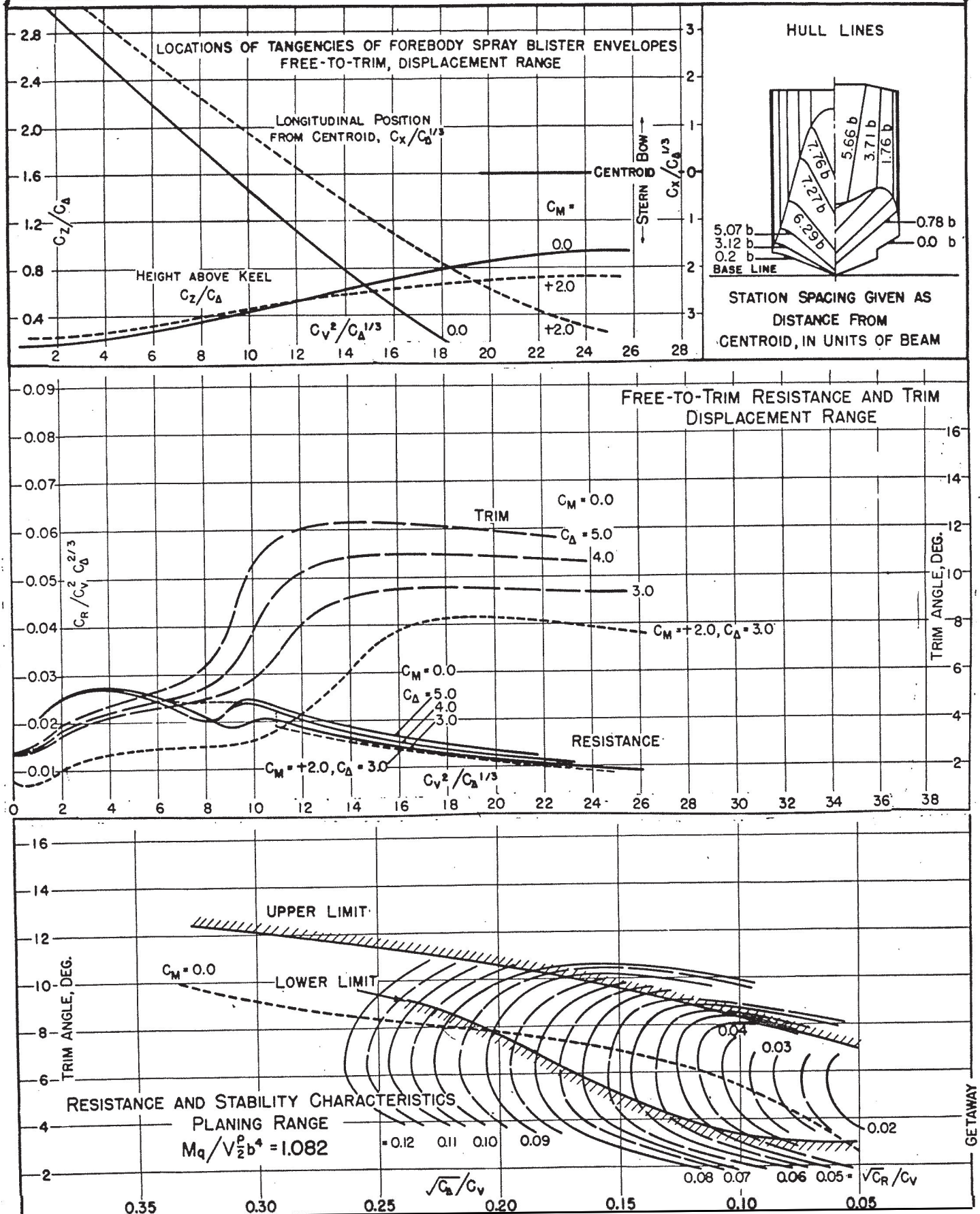


FIGURE 19

DESIGNATION: 8-6-0.67-22

MODEL NO. 1069-02-10

C.G. = 0.44 b FWD. OF CENTROID  $C_{\Delta} = 3.32$  (NOMINAL)

TESTED AT E.T.T. No. 3 TANK

MODEL BEAM: 4.10 "

1.59 b ABOVE KEEL

 $k/L =$ 

DATE: NOV. 15, 1951

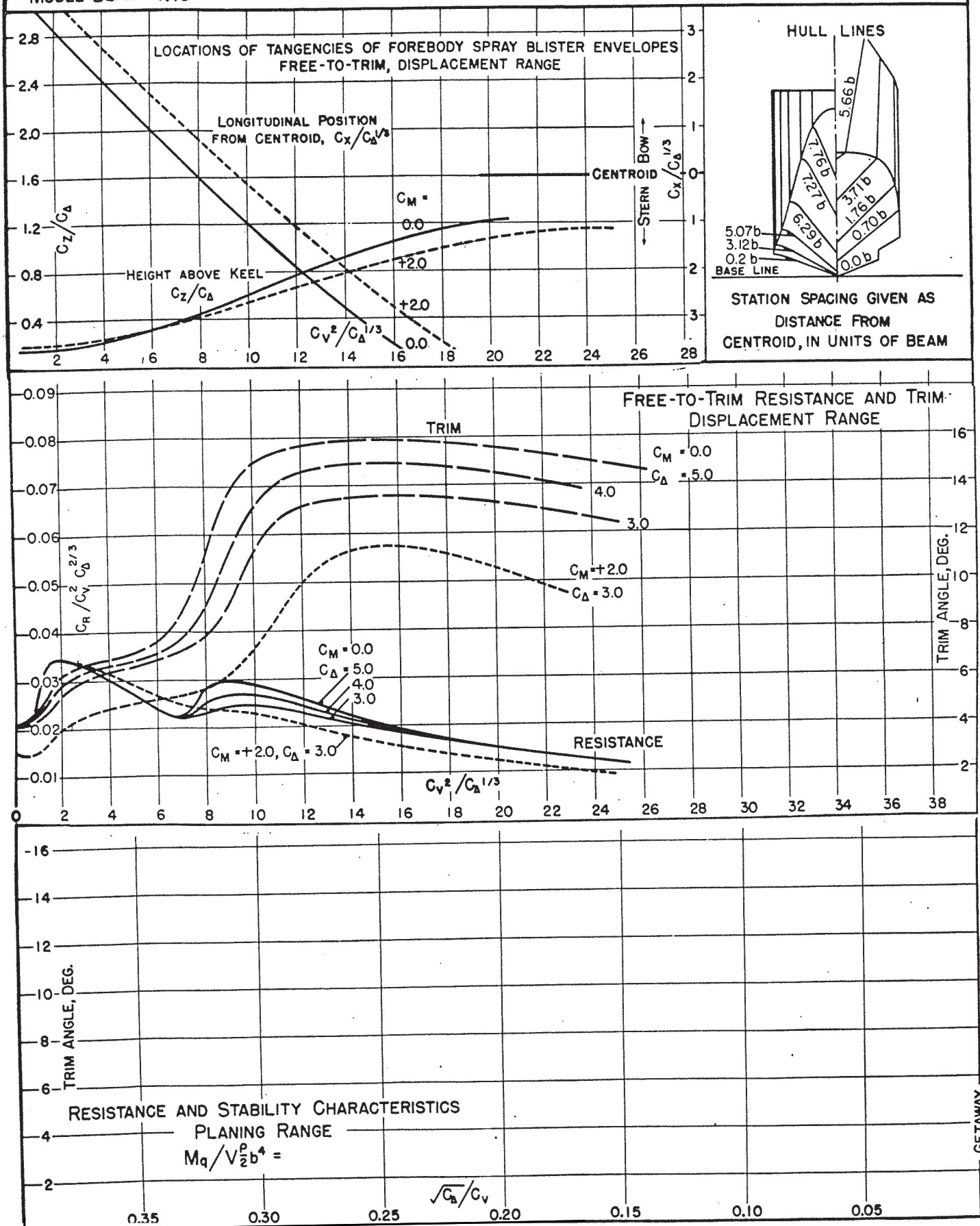




FIGURE 20

DESIGNATION: 8-10-1.12-22

MODEL NO. 1069-01-06

MODEL BEAM: 4.10"

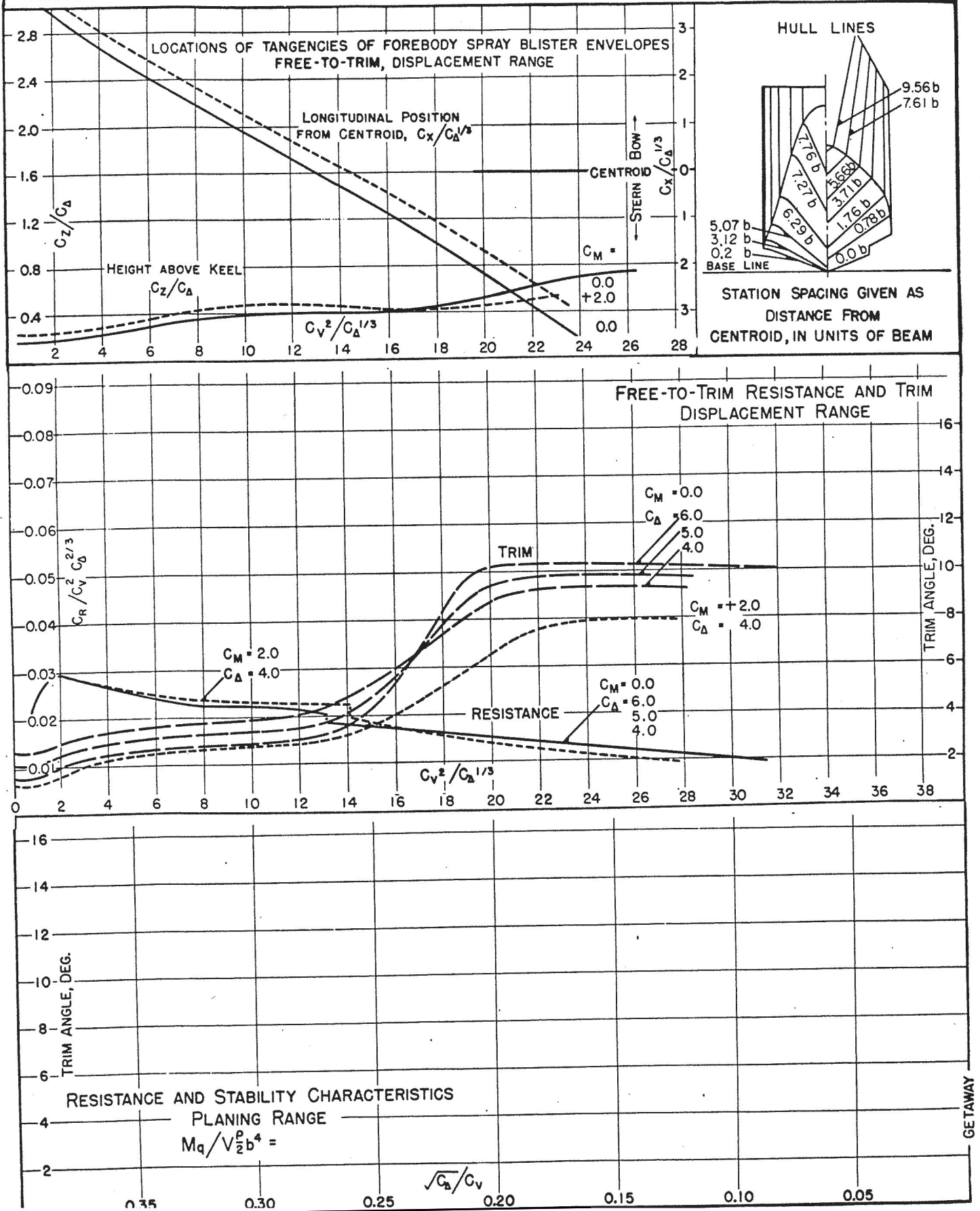
C.G. = 0.44 b FWD. OF CENTROID  
1.59 b ABOVE KEEL $C_{\Delta} = 4.84$  (NOMINAL)  
 $k/L =$ TESTED AT E.T.T. No. 3 TANK  
DATE: NOV. 22, 1951

FIGURE 21

DESIGNATION: 8-10-0.67-22

MODEL NO. 1069-01-10

MODEL BEAM: 4.10"

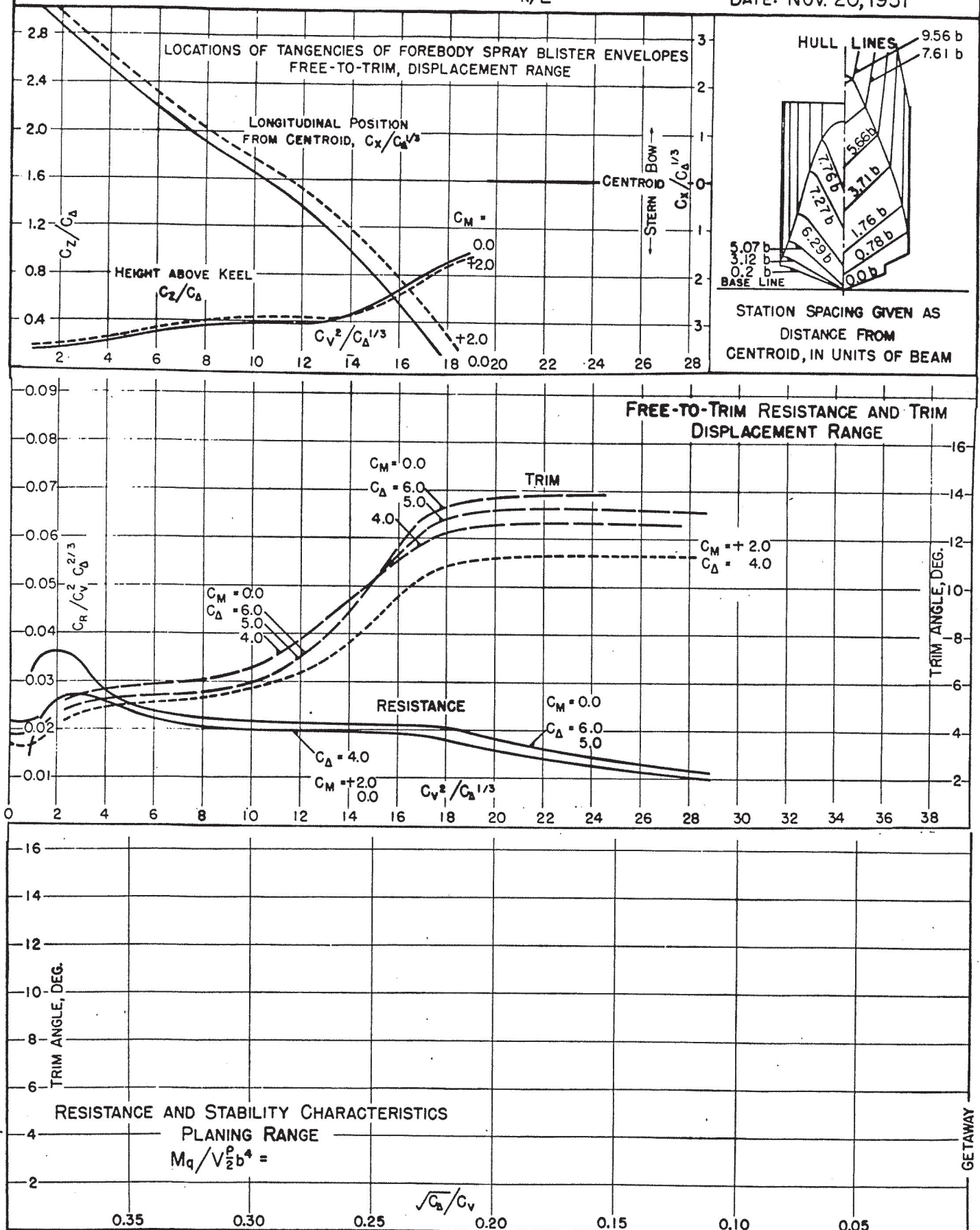
C.G. = 0.44 b FWD. OF CENTROID  $C_{A_0} = 4.84$  (NOMINAL)  
1.59 b ABOVE KEEL  $k/L =$ TESTED AT E.I.T. No. 3 TANK  
DATE: NOV. 20, 1951



FIGURE 22

DESIGNATION: 8-16-1.12-22

MODEL NO. 1069-03-06 C.G. = 0.44 b FWD. OF CENTROID  $C_{A_0} = 7.44$  (NOMINAL)  
 MODEL BEAM: 4.10"  $C_G = 1.59$  b ABOVE KEEL  $k/L =$

TESTED AT E.T.T. No. 3 TANK  
 DATE: NOV. 27, 1951

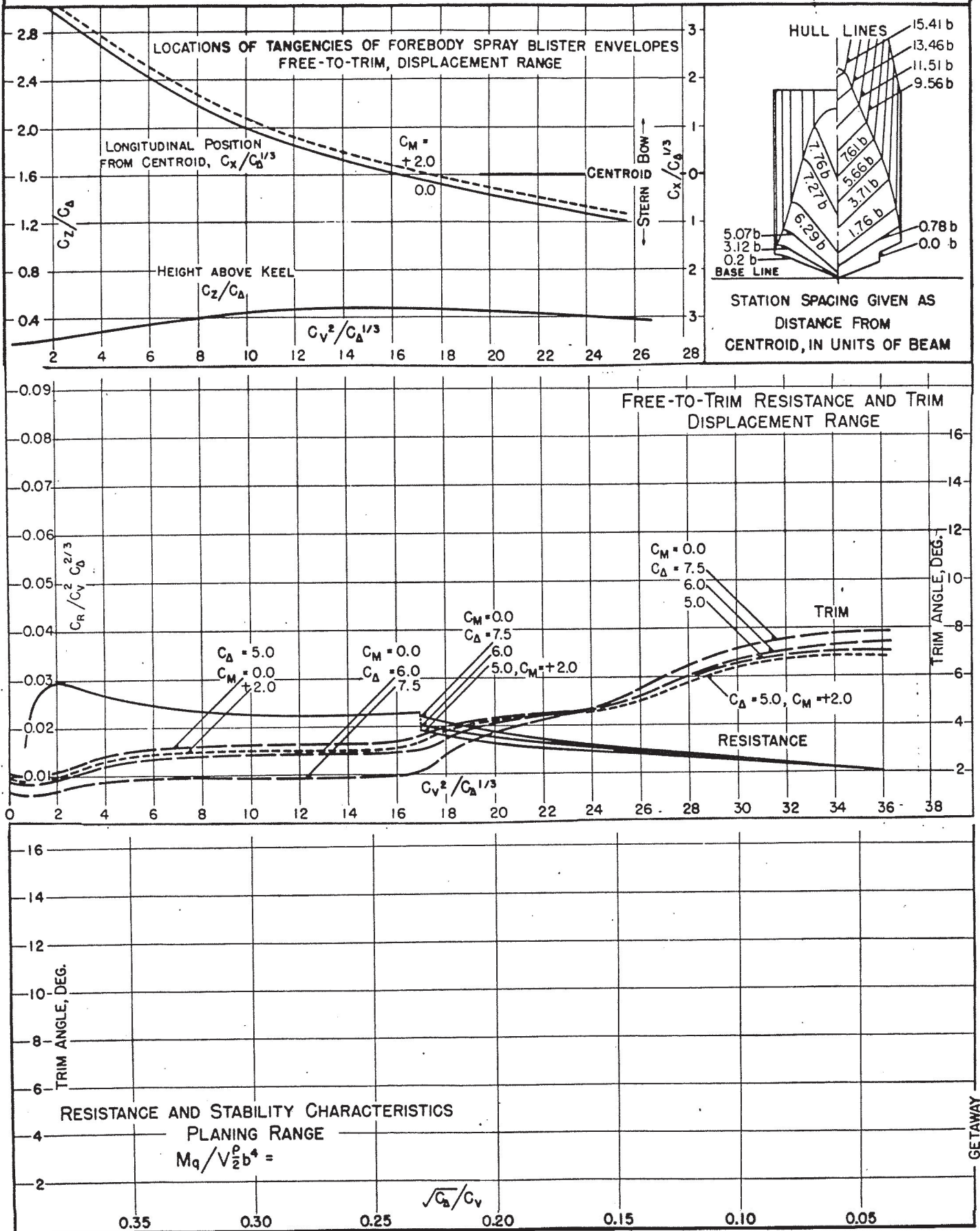


FIGURE 23

DESIGNATION: 8-16-0.67-22

MODEL NO. 1069-03-10

MODEL BEAM: 4.10"

C.G. = 0.44 b FWD. OF CENTROID  
1.59 b ABOVE KEEL $C_{\Delta} = 7.44$  (NOMINAL) $k/L =$ 

TESTED AT E.T.T. No. 3 TANK

DATE: NOV. 14, 1951

